FINAL REPORT

2014 Georgiana Slough Floating Fish Guidance Structure Performance Evaluation Project Report

California Department of Water Resources

October 2016

Final Report

2014 Georgiana Slough Floating Fish Guidance Structure Performance Evaluation Project Report

Prepared by:

California Department of Water Resources

1416 9th Street

Sacramento, CA 94236-001

Contact: Ryan Reeves, P.E.

916.653.6868

October 2016

State of California
Edmund G. Brown Jr., Governor

Natural Resources Agency
John Laird, Secretary for Resources

Department of Water Resources
Mark W. Cowin, Director

Chief Deputy Director
Carl Torgersen

Assistant Chief Deputy Director
Cindy Messer

Kasey Schimke Asst. Director Legislative Affairs	Ed Wilson Director of Public Affairs	Cathy Crothers Chief Counsel
Gary Bardini Deputy Director	William Croyle Deputy Director	Kathie Kishaba Deputy Director
John Pacheco Deputy Director		

Bay-Delta Office

Paul Marshall.....Chief

South Delta Branch

Mark Holderman .....Branch Chief, South Delta Branch

This report was prepared under the supervision of

Jacob McQuirk .....Chief, Temporary Barriers and Lower San Joaquin

Ryan Reeves .....Senior Engineer, Water Resources

This page intentionally left blank.

ACKNOWLEDGMENTS

The following individuals, agencies, and organizations contributed to the 2014 Georgiana Slough Floating Fish Guidance Structure Study and Report.[1]

Key Report Contributors	
Ryan Reeves, P.E.	California Department of Water Resources
Jacob McQuirk, P.E.	California Department of Water Resources
Mike Cane	California Department of Water Resources
Noah Adams	U.S. Geological Survey
Russell Perry, Ph.D.	U.S. Geological Survey
Jason Romine, Ph.D.	U.S. Geological Survey
Theresa Liedtke	U.S. Geological Survey
Jon Burau	U.S. Geological Survey
Aaron Blake	U.S. Geological Survey
Adam Pope	U.S. Geological Survey
Mike Horn, Ph.D.	U.S. Bureau of Reclamation
Chris Fitzer	Environmental Science Associates
Steve Pagliughi	AECOM Technical Services, Inc.
Roy Leidy	AECOM Technical Services, Inc.
Chuck Hanson, Ph.D.	Hanson Environmental, Inc.
Sam Johnston	Hydroacoustic Technologies, Inc.
Kevin Kumagai	Hydroacoustic Technologies, Inc.
Marin Greenwood, Ph.D.	ICF International, Inc.
Kenneth Cash	Normandeau Associates, Inc.

Project Collaborators	
California Department of Water Resources	Project Sponsor, Lead Project Manager/Implementing Agency, Data Analysis, and Report Contribution and Review
U.S. Bureau of Reclamation	Field Implementation, Data Analysis, and Report Contribution
U.S. Geological Survey	Field Implementation, Data Analysis, and Report Contribution
California Department of Fish and Wildlife	Field Implementation
AECOM Technical Services, Inc.	Consultant Team Project Manager, Field Implementation, Data Analysis, and Report Contribution
Cramer Fish Sciences	Data Analysis, Field Implementation, Report Contribution and Coordination
Environmental Science Associates	Field Implementation, Data Analysis, and Report Contribution
Hydroacoustic Technologies, Inc.	Field Implementation, Data Analysis, and Report Contribution
Hanson Environmental, Inc.	Field Implementation, Data Analysis, and Report Contribution
Normandeau Associates, Inc.	Data Analysis, and Report Contribution
Turnpenny Horsfield Associates	Field Implementation Support
Professional Aquaculture Services	Data Analysis, and Report Contribution
ICF International, Inc.	

[1] Any use of trade, firm, or product names is for descriptive purposes only and does not imply endorsement by the U.S. Government or State of California.

Additional Acknowledgments

The project team also would like to acknowledge and thank the many people who provided valuable input on the project study plan, construction support, field support, data analysis, report review, and document production. These individuals and organizations include: Bill McLaughlin, Ben Geske, Genny Schrader, Khalid Ameri, John Personeni, and numerous additional staff at DWR, the U.S. Geological Survey's Columbia River Research Laboratory, Worthington Waterway Barriers, Cal-Neva Construction Services, Inc., and CS Marine Constructors, Inc. for providing barrier construction and maintenance support. We also would like to thank the U.S. Fish and Wildlife Service's Coleman National Fish Hatchery and California–Nevada Fish Health Center for providing the late fall-run Chinook salmon used in the study and laboratory facilities for the tag retention and fish health evaluation. The difficult assignment of peer review of the draft report was completed by Cynthia LeDoux-Bloom (AECOM Technical Services, Inc.) and Brad Cavallo (Cramer Fish Sciences).

Project Report Reviews

To date, the 2014 Georgiana Slough Floating Fish Guidance Structure Performance Evaluation Project Report has gone through several review processes. These include:

1) Review of the first draft of the report (Contributors Draft) from May 2015 to July 2015;
2) Review of the second draft of the report (Peer Review Draft) from July 2015 to September 2015;
3) Review of the third draft of the report (Initial Management Draft) from September 2015 to July 2016;
4) Review of the fourth draft of the report (Final Management Draft) from July 2016 to September 2016; and
5) Review and issuance of the Final Project Report in October 2016.

Reviewed and Approved by:

Roy Leidy
AECOM Task Order Manager

Ryan Reeves, P.E.
DWR Task Order Manager

Suggested Report Citation

California Department of Water Resources. 2016. 2014 Georgiana Slough Floating Fish Guidance Structure Performance Evaluation Project Report. Bay-Delta Office, Sacramento, California.

TABLE OF CONTENTS

Figures

Note: Figures not attributable to a source are original to this report

Tables

Appendices

ACRONYMS AND OTHER ABBREVIATIONS

≥	greater than or equal to
≤	less than or equal to
<	less than
>	greater than
°C	degrees Celsius
°	degrees (angle)
2D	two-dimensional
%	percent
AADAP	Aquatic Animal Drug Approval Partnership
AC	AECOM
AC	alternating current
ADCP	acoustic Doppler current profiler
AIC	Akaike Information Criterion
ANOVA	analysis of variance
ATR	acoustic tag receiver
ATTS	acoustic tag tracking system
ACV	average channel velocity
AWS	Amazon Web Services
BAFF	bio-acoustic fish fence
BGS	behavioral guidance structure
BL/s	body lengths per second
BiOp	Biological and Conference Opinion for the Long-Term Operations of the Central Valley Project and State Water Project
CCF	Clifton Court Forebay
CDL	complete data likelihood
CDF	cumulative distribution function
cfs	cubic feet per second
CI	confidence interval
CIMIS	California Irrigation Management Information System
cm	centimeter
cm/s	centimeters per second
cms	cubic meter per second
CPUE	catch per unit effort
CSOT	convolved samples over threshold
.csv	comma-separated value (file)
CVP	Central Valley Project
dB	decibel
DC	direct current
DCC	Delta Cross Channel
Delta	Sacramento–San Joaquin Delta
df	degrees of freedom
DFG	California Department of Fish and Game
DFW	California Department of Fish and Wildlife
DIDSON	Dual-Frequency Identification Sonar

DR	California Department of Water Resources
DSM2	Delta Simulation Model II
DWR	California Department of Water Resources
e.g.	for example (*exempli gratia* in Latin)
ESA	federal Endangered Species Act
ESRI	Environmental Systems Research Institute, Inc.
FDA	U.S. Food and Drug Administration
FF	Fishery Foundation of California
FFGS	floating fish guidance structure
FIGS	floating impermeable guidance structure
FL	fork length
ft	foot/feet
FTP	File Transfer Protocol
ft/s	foot/feet per second
g	gram
GLM	generalized linear model (modeling)
GPS	global positioning system
GSFFGS	Georgiana Slough Floating Fish Guidance Structure
GSFFGS Study	Georgiana Slough Floating Fish Guidance Structure Study
GSNPB	Georgiana Slough Non-Physical Barrier
HIML	high intensity modulated light
HOR	Head of Old River
HTI	Hydroacoustic Technology, Inc.
ID	identification
i.e.	that is (*id est* in Latin)
in	inch
INAD	Investigational New Animal Drug
IPLW	inverse path-length weighted
IVM	index velocity method
JAGS	Just Another Gibbs Sampler
kHz	kilohertz
Km	kilometer
Km/d	kilometers per day
.kml	Keyhole Markup Language (file)
lb	pound
LPT	Lagrangian particle tracking
MCMC	Markov Chain Monte Carlo
mi	mile
mi/d	miles per day
MLE	Maximum Likelihood Estimation
mm	millimeter
m	meter
m/s	meters per second
ms	millisecond
N or n	number or sample size
NAD83	North American Datum of 1983
NAVD 88	North American Vertical Datum of 1988

NCRO	North Central Region Office (DWR)
NMFS	National Marine Fisheries Service
NTU	nephelometric turbidity unit
ODL	observed data likelihood
Off	BAFF or FFGS was not operational
On	BAFF or FFGS was operational
P	probability
PCC	percent correctly classified
PDAT	Predator Detection Acoustic Tag
PMF	probability mass function
pps	pings per second
PST	Pacific Standard Time
PVC	polyvinyl chloride
QA/QC	quality assurance/quality control
$QAIC_c$	glmulti with the quasi-likelihood equivalent of AIC corrected for small sample sizes
R^2	coefficient of determination
*.RAT	Raw Acoustic Tag (file)
®	registered trademark
Reclamation	U.S. Bureau of Reclamation
RMSE	root mean squared error
ROC	receiver operator characteristic
RPA	Reasonable and Prudent Alternative
RTK	real-time kinematic
S	critical streakline
SAA	standardized angling area
SC	surgery station
SD	standard deviation
SL-ADCP	sideward-looking acoustic Doppler current profiler
SL	standard length
SOP	standard operating procedure
SRWTP	Sacramento Regional Wastewater Treatment Plant
ST	single target
SWP	State Water Project
TL	total length
TM	trade mark
USFWS	U.S. Fish and Wildlife Service
USGS	U.S. Geological Survey
UTC	Coordinated Universal Time
VPM	velocity profile method
vs.	versus
W/m^2	Watts per square meter

ABSTRACT

Survival of out-migrating juvenile Chinook salmon *Oncorhynchus tshawytscha* in the Sacramento-San Joaquin River Delta (Delta), California, is determined by a number of factors including migration route. Survival of salmonids that enter the interior and southern Delta can be as low as half that of salmonids that remain in the main stem Sacramento River. Reducing entrainment into the higher mortality routes, such as Georgiana Slough, should increase overall through-Delta survival.

In the spring of 2014 a Floating Fish Guidance Structure (FFGS) designed to reduce entrainment into Georgiana Slough was constructed just upstream of the Georgiana Slough divergence from the Sacramento River. The effectiveness of the FFGS was tested by switching it between On (oriented away from the river bank at approximately 24 degrees into the downstream flow) and Off (oriented parallel and close to the river bank) positions every diel tidal cycle (approximately 25 hours). This evaluation used acoustic telemetry and other techniques to evaluate the effect of the FFGS on hatchery-reared juvenile late fall-run Chinook salmon. The effects of the FFGS on survival, entrainment rates, and behavioral responses were evaluated by investigating 23 hypotheses which resulted in the following four primary findings:

1. The effect of the FFGS on juvenile Chinook salmon entrainment into Georgiana Slough

At intermediate discharges (7,062-14,125 cubic feet per second), the FFGS reduced Chinook salmon entrainment into Georgiana Slough by approximately 20 percent, or a five percentage point reduction between the On and Off positions (19.1% On; 23.9% Off). The FFGS did not provide Chinook salmon entrainment reduction benefits at higher and lower discharges. Results show that the probability of being entrained into Georgiana Slough was primarily a function of Sacramento River discharge, cross-stream fish position, time of day, and proportion of flow remaining in the Sacramento River.

2. The ability of the FFGS to affect juvenile Chinook salmon behavior in the junction

Spatial analysis of the 2014 fish tracks showed that the FFGS was effective at changing Chinook salmon behavior in the area between the barrier-Off position and the barrier-On position: moving the barrier from the Off position to the On position reduced fish density behind the barrier by 40 to 50 percent. This reduction occurred because fish that approach the barrier in the On position consistently reversed their direction and swam away from Georgiana Slough which resulted in a 20-meter (66-foot) shift in the cross-stream location of these turning points at the tip of the barrier when the barrier was moved from the Off position to the On position. However, these behavioral changes did not reduce overall entrainment into Georgiana Slough because the 2014 ebb tide water velocities were low enough that often the fish's normal swimming behavior would still result in Georgiana Slough entrainment after they had responded to the FFGS. The analyses suggest that the 2014 barrier design may have been more effective under the high velocity conditions observed in 2011 and 2012.The flow conditions observed in 2014 may have required an FFGS extending 110 meters (361 feet) farther downstream to substantially increase the entrainment reduction into Georgiana Slough.

3. The effect of the FFGS on juvenile Chinook salmon route-specific and through-Delta survival

Ten groups of late-fall Chinook salmon were released over five-day periods during FFGS On and Off treatments were used to estimate the salmon entrainment rates into Georgiana Slough and route-specific survival. The

influence of the FFGS on salmonid survival could not be estimated because the tested configuration and operation of the FFGS did not provide entrainment reduction into Georgiana Slough over the entire range of river discharges. However, considerable variation in route-specific survival among release groups was found, with overall survival through the Delta varying markedly, from 0.22 to 0.62. Survival was positively correlated with Sacramento River discharge and turbidity (which are autocorrelated) and negatively with water temperature. In addition, survival of fish entering Georgiana Slough was lower than survival of fish remaining in the Sacramento River for every release group. This result confirms that through-Delta salmonid survival could be increased using a properly designed, located, and operated FFGS to either reduce/increase entrainment into lower/higher survival routes, respectively.

4. The effect of the FFGS on predatory fish behavior and predation success

There was little evidence of a relationship between the FFGS and predation or predatory fishes. The FFGS did not affect the probability of predation of juvenile Chinook salmon in the study area and the probability of predation was not related to proximity to the FFGS. There was no evidence to suggest a broad-scale effect on predation rates in response to the FFGS because: the residence time of tagged predatory fishes was unchanged with the FFGS turned On, there was no significant change in predator occupancy near the FFGS, and the standardized angling catch rate near the FFGS was similar to adjacent reference areas. However, there was some evidence of a localized effect of the FFGS because the predatory fish density was greater near the FFGS and a relatively high proportion of predation events occurred near pilings associated with the downstream anchorage of the FFGS.

The present study indicates that, with some modifications, the FFGS technology does provide the ability for managers to modify juvenile Chinook salmon entrainment at river junctions and, therefore, to affect through-Delta survival. However, the response of Chinook salmon to the FFGS relative to all the river flow characteristics must be carefully evaluated and understood during design to ensure that the desired Chinook salmon entrainment modification occurs. It is recommended that reduction of entrainment into Georgiana Slough be considered in the context of the potential to increase entrainment into two more northerly junctions (Sutter and Steamboat sloughs): barriers at these junctions could provide more consistent positive effects on through-Delta survival because of the more predictable river characteristics at these areas which should make barrier design optimization more straightforward. Additionally, their location upstream of Georgiana Slough (which results in a greater proportion of the juvenile salmonid population encountering these junctions), may increase the ability of barriers at these sites to produce a positive population-scale effect.

EXECUTIVE SUMMARY

ES.1 INTRODUCTION

Listed Chinook salmon (*Oncorhynchus tshawytscha*) and steelhead (*O. mykiss*) spawn and rear in the Sacramento River and its tributaries; adult fish use the mainstem Sacramento River for upstream migration to spawning sites and juvenile fish use the river for downstream outmigration to the Pacific Ocean in winter and spring. During their outmigration, juvenile salmonids encounter alternative migration pathways through the Sacramento–San Joaquin Delta (Delta), e.g., Sutter and Steamboat sloughs, the Delta Cross Channel (DCC) to Snodgrass Slough and the North and South forks of the Mokelumne River, Georgiana Slough to the North Fork Mokelumne River, and Threemile Slough. **Figure ES-1** shows the migration pathways in the north and east Delta for outmigrating salmonids, the location of the DCC, and the locations of the pumping facilities of the State Water Project (SWP) and the federal Central Valley Project (CVP) in the south Delta.

The National Marine Fisheries Service's (NMFS) 2009 *Biological and Conference Opinion for the Long-Term Operations of the Central Valley Project and State Water Project* (BiOp) requires the California Department of Water Resources (DWR) and the U.S. Bureau of Reclamation (Reclamation) consider engineering solutions to reduce the diversion of salmonids from the Sacramento River into the central (also called the 'interior' Delta) and south Delta where the potential for entrainment at the SWP and CVP pumping facilities increases. One of several locations identified in the BiOp for engineering solutions evaluation is Georgiana Slough, a natural distributary of the Sacramento River. The outmigration of salmonids into the interior Delta through pathways such as Georgiana Slough has been shown to contribute to greater mortality.

In an effort to identify potential engineering approaches to reduce the percentage of salmonids that migrate from the Sacramento River into Georgiana Slough, DWR implemented a large-scale testing program in 2011 and 2012 to assess the effectiveness of a non-physical barrier design (i.e., a Bio-Acoustic Fish Fence, or BAFF). The experimental design of the 2011 and 2012 tests used acoustically tagged juvenile Chinook salmon and steelhead (2012 only), released upstream of the BAFF when the barrier was 'On' and 'Off' (i.e., in operation or not in operation, respectively), to determine the effectiveness of the barrier. In 2014, a physical barrier called a Floating Fish Guidance Structure (FFGS) was tested, with methods similar to those used during the testing of the BAFF barriers in 2011 and 2012. This report presents the results of the tests conducted in 2014 using the FFGS (2014 GSFFGS Study).

ES.2 PURPOSE, OBJECTIVES, AND OVERVIEW

The primary objectives of the 2014 GSFFGS Study were to:

- Assess reach-scale route selection and survival of outmigrating Chinook salmon;
- Assess temporal distribution of Chinook salmon at arrival in FFGS area;
- Assess predation and predatory fish behavior in the vicinity of the FFGS;
- Assess far-field movements of predatory fishes and Chinook salmon;
- Assess alternative hypotheses specific to barrier function; and
- Compare effectiveness of the FFGS and the BAFF technologies.

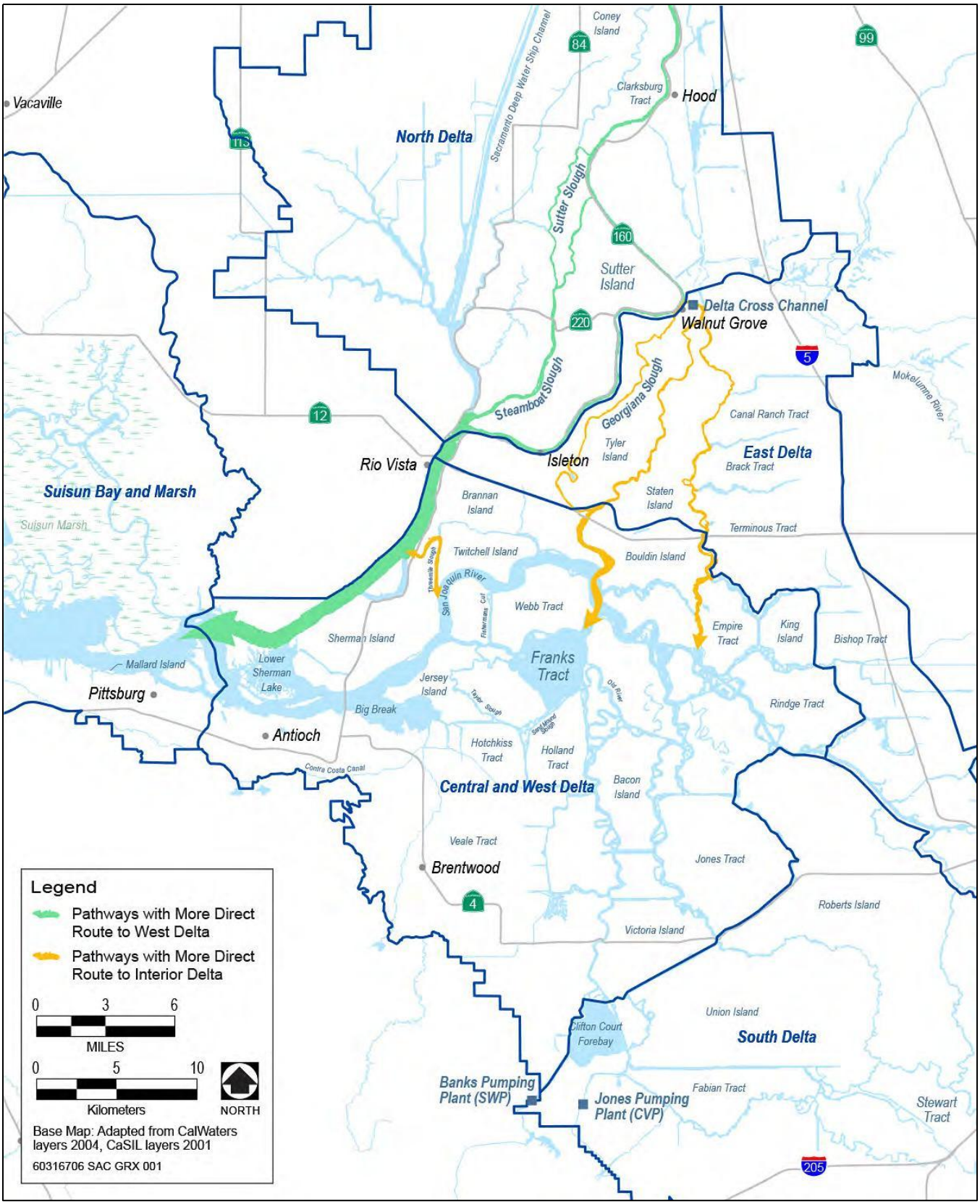

Figure ES-1 Lower Sacramento River and North Delta Migration Pathways

The basic study design of the 2014 GSFFGS Study was similar to that of the 2011 and 2012 BAFF studies: to release acoustically tagged hatchery-raised juvenile late fall–run Chinook salmon into the Sacramento River, and then to monitor the proportion of fish entering the study area that outmigrated downstream via the Sacramento River when the FFGS was On compared to when it was Off under a range of environmental conditions (e.g., tidal conditions, day and night, turbidity, water temperature, Sacramento River flows, and rate of flow entering Georgiana Slough).

Figure ES-2 shows the immediate study area at the community of Walnut Grove, Sacramento County, California. **Figure ES-3** provides an overview of the greater study area in the Delta, including the release locations for tagged juvenile Chinook salmon; the location of the FFGS; and the acoustic tag detection and monitoring sites, where the peripheral hydrophone arrays were located. **Figure ES-4** illustrates the conceptual design components of the FFGS.

The key elements of the 2014 GSFFGS Study were as follows:

- A total of 5,461 late fall-run juvenile Chinook salmon produced at the Coleman National Fish Hatchery, Anderson, California, were surgically implanted (tagged) with acoustic transmitters during the study. Of this total, 4,635 fish were released into the Sacramento River at the City of Sacramento, California, and their outmigration past the FFGS and Georgiana Slough was monitored. In addition, 826 fish were released into Georgiana Slough to supplement the sample size to assess fish survival through the interior Delta).
    - Chinook salmon were released from March 1 through April 15, 2014, during their outmigration ocean-phase period.
    - Releases into the Sacramento River were made approximately 53 kilometers (km) (35 miles; mi) upstream from the FFGS to allow the Chinook salmon time to adjust to the river conditions and disperse into the channel before reaching Georgiana Slough. Releases into Georgiana Slough were made approximately 5 km (3 mi) downstream from the divergence with the Sacramento River.
    - Passage of tagged Chinook salmon was monitored at and downstream of the FFGS in the Sacramento River, Georgiana Slough, and other Delta channels, when the FFGS was both On and Off.
- One hundred and ninety-five predatory fish were captured, implanted with acoustic tags, released, and monitored, to evaluate behavior, movement patterns, and potential predation on tagged Chinook salmon in association with the operation of the FFGS.
- A multiple-hydrophone array was installed in the Sacramento River immediately upstream from, downstream from, and adjacent to the FFGS, to monitor two-dimensional movements of tagged predatory fish and Chinook salmon as they encountered and responded to the FFGS. Additional hydrophones, referred to as the peripheral hydrophone arrays, were installed to detect tagged fish in channels upstream and downstream from the study array throughout the Delta.
- Multiple acoustic Doppler current profilers were installed in the Sacramento River in the vicinity of the FFGS to monitor local currents, water velocities, and general hydrodynamics.
- Active multibeam hydroacoustic devices, including dual frequency identification sonar (DIDSON), were installed to monitor fish densities in the immediate vicinity of the FFGS.

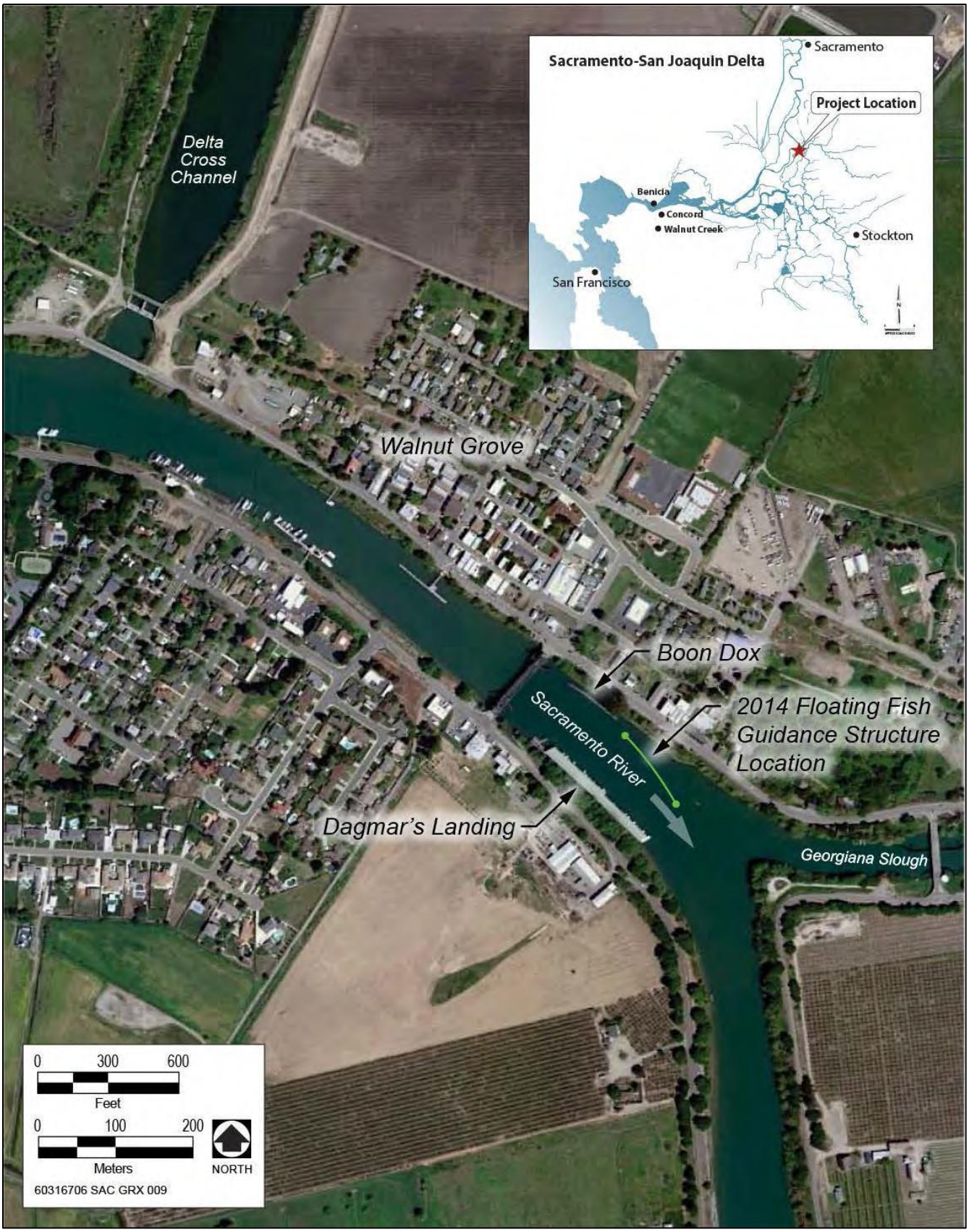

Figure ES-2 Floating Fish Guidance Structure Performance Evaluation Study Area

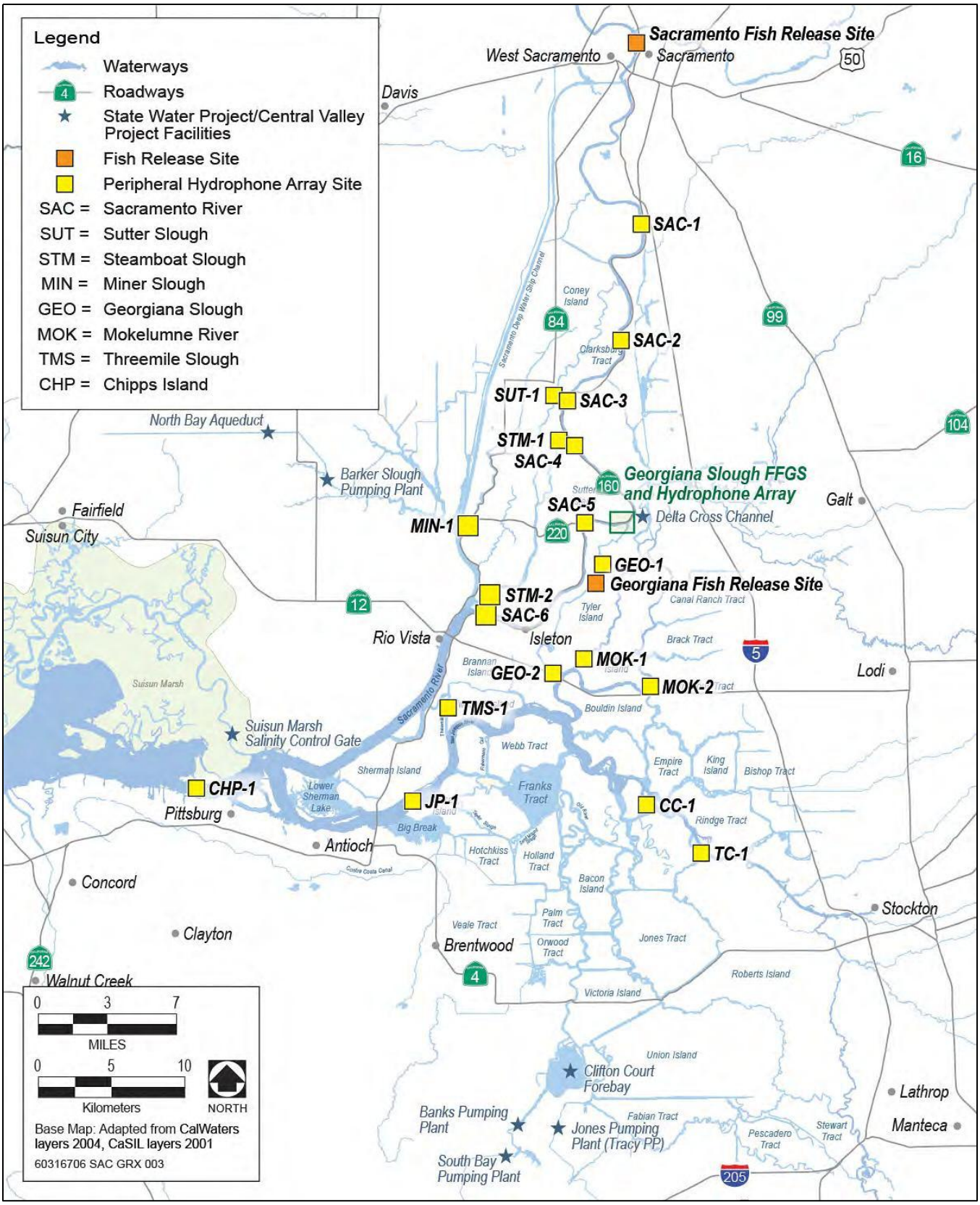

Source: Data provided by California Department of Water Resources and adapted by AECOM in 2014

Figure ES-3 Overview of the 2014 Georgiana Slough Floating Fish Guidance Structure Greater Study Area

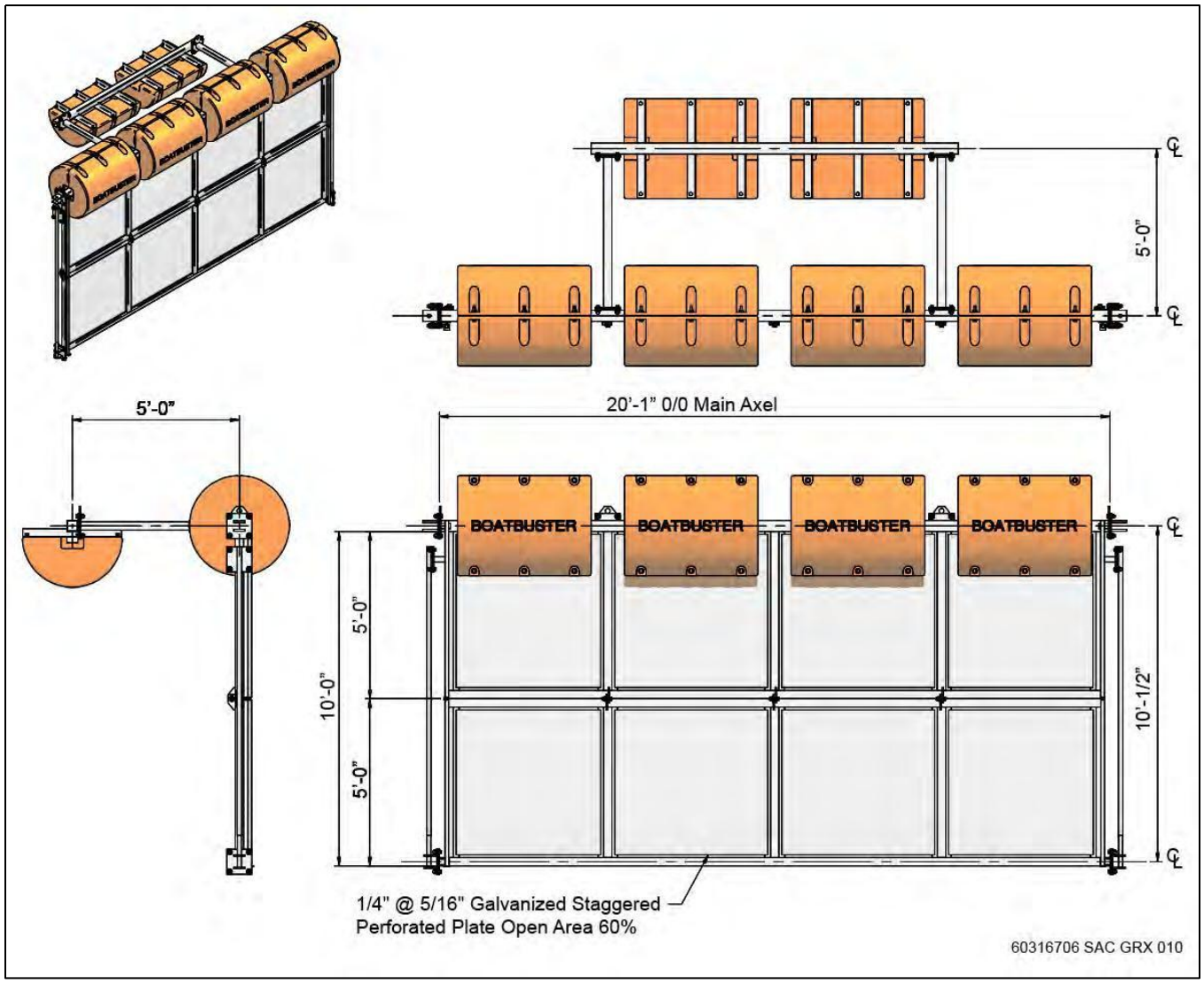

Source: Worthington Waterway Barriers 2013. Note: The 2014 deployment at Georgiana Slough was only one panel (5 feet) deep.

Figure ES-4 Three Sections of a Typical Floating Fish Guidance Structure

ES.3 STUDY RESULTS AND FINDINGS

The results and findings of the 2014 GSFFGS Study are summarized in the following sections. A key concept throughout much of the findings is the position of the *critical streakline*, i.e., the line separating parcels of water that either remain in a main river channel (the Sacramento River in the case of this study; green region in **Figure ES-5**) or else enter a side channel (Georgiana Slough; green region in **Figure ES-5**). The distribution of fish in relation to the critical streakline influences the risk of entrainment into the side channel (**Figure ES-5**).

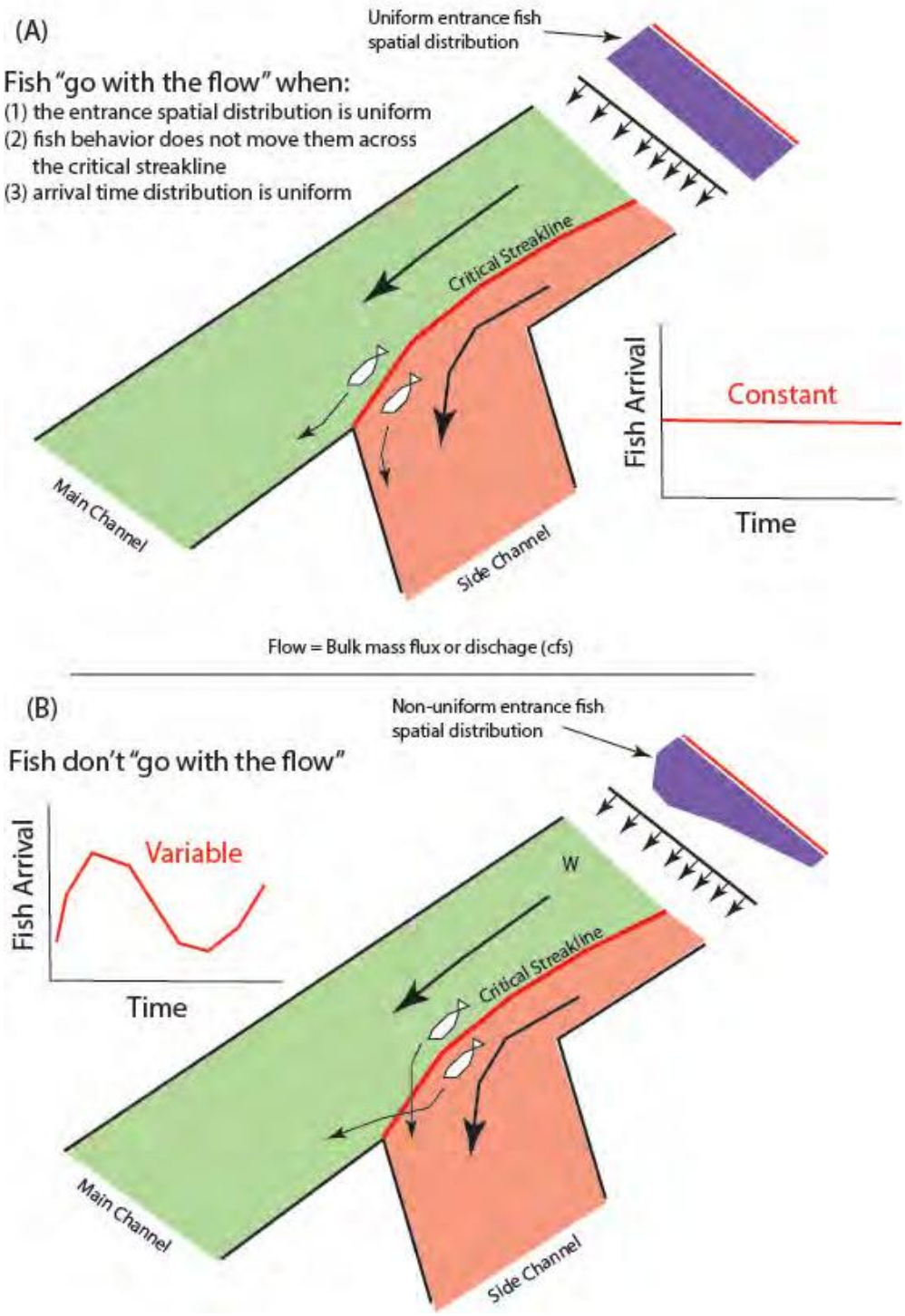

Note: Red regions denote the entrainment zone for the side channel, whereas the green regions show the region where fish continue along the main channel. The red line between these regions is the critical streakline. The top panel shows the required conditions for fish to "go with the flow"—in this case, the bulk as measured discharge in each channel. These conditions include the uniform entrance, fish spatial distribution that is shown and behaviors that do not result in fish crossing the critical streakline. The bottom panel shows those conditions that create conditions where fish are not distributed in proportion to the flows in each channel. These conditions include a non-uniform entrance fish distribution and behaviors that cause fish to transit the critical streakline.

Figure ES-5. Conceptual Diagram of Entrainment at a Junction Including the Critical Streakline

ES.3.1 STUDY FISH RELEASES AND RIVER CONDITIONS

- During the March 1 through April 15 period of the 2014 study, a total of 5,461 late fall-run juvenile Chinook salmon were surgically implanted (tagged) with acoustic transmitters during the study period:
    - Of this total, 4,635 fish were released into the Sacramento River, and their outmigration past the FFGS and Georgiana Slough was monitored; 1,651 arrived at the study area and were determined to have survived (i.e., not eaten by a predator); and
    - 826 fish were released in Georgiana Slough (Georgiana Slough was designed as a supplemental release location because fish released at this site would not encounter the FFGS but would be needed to support the analysis of fish survival through the Delta).
    - Chinook salmon were released at the City of Sacramento in order to allow greater development of more typical low light/nocturnal outmigration behavior than occurred during the 2011/2012 BAFF studies. Fish released at the City of Sacramento were confirmed to be positively biased toward moving during crepuscular and low light periods and consistently negatively biased toward moving in full daylight conditions.

- During the study period, **Sacramento River flows at the junction with Georgiana Slough were abnormally low** and ranged from -4,350 cubic feet per second (cfs) to 21,090 cfs. The majority of Chinook salmon (61%) arrived at the junction when flows were between 7,063 and 14,125 cfs. The highest flows occurred during the first three weeks of the study and during the first week of April. Aside from these time periods, the flow remained below 7,063 cfs. At this level of discharge, flows typically reverse twice daily on flood tides: these hydrodynamic conditions resulted in over half of the Sacramento River water flowing into Georgiana Slough, on a tidally averaged time scale, for the majority of the study period (70% of the time).

ES.3.2 BARRIER EFFICIENCY AND ENTRAINMENT PROBABILITY

Evaluating the effectiveness of the FFGS in altering fish routing is a central element of the 2014 GSFFGS Study. Analyses were conducted based on grouping fish into samples, or assessing effects on individuals to assess entrainment. Three types of barrier efficiencies were investigated for the sample-based approach: deterrence, protection, and overall.

- **Deterrence efficiency** is defined as the proportion of tagged Chinook salmon that were guided or deterred by the FFGS (i.e., that moved at a greater than 24° angle away from the FFGS).

- Deterrence efficiency was determined to be 9.5 percentage points greater with FFGS On than FFGS Off, but this difference was not statistically significant.

- **Protection efficiency** is the proportion of tags detected in the Sacramento River downstream of the FFGS relative to the total number of tagged fish outmigrating via the Sacramento River and Georgiana Slough combined (excluding tags that were assessed to represent fish that were preyed upon).

- The deterrence improvement contributed to a statistically significant improvement in protection efficiency with FFGS On compared to FFGS Off ($P = 0.0085$).

- The significant effect of the FFGS on protection efficiency was driven by the significant 18.2 percentage point increase that occurred under high velocity conditions (greater than 0.25 meters per second; m/s [0.08 feet per second; ft/s]).

- **Overall efficiency** was determined as the proportion of tags that remained in the Sacramento River relative to those tags deemed not to be eaten by a predatory fish that arrived at the study area.

- Overall efficiency was not significantly different between FFGS On and FFGS Off, but the statistical significance was less than 0.1 (as it also was for deterrence efficiency), and suggests that **further testing with larger sample sizes could demonstrate statistically significant differences for FFGS On versus FFGS Off**.

- A significant 6.2 percentage point increase in overall efficiency occurred with the FFGS On versus FFGS Off under high water velocity conditions, possibly because at higher water velocities Chinook salmon have insufficient time or are reluctant to swim beneath the FFGS and the upstream water deceleration caused by the FFGS structure may be detectable at a greater distance.

The individual-based approach to assessing barrier efficacy examined Chinook Salmon entrainment into Georgiana Slough in relation to FFGS position (On vs. Off) and other important environmental variables.

- Overall entrainment at low flows (less than 7,062 cfs) was two times or more the entrainment rate at intermediate (7,062-14,125 cfs) and high (>14,125 cfs) flows.

- The FFGS reduced Chinook salmon entrainment into Georgiana Slough at intermediate flows by 20 percent, or 5 percentage points (FFGS On: 19.1%; FFGS Off: 23.9%).

- At high flows, entrainment was greater with FFGS On (19.3%) than FFGS Off (9.7%); whereas at low flows entrainment was not greatly different between FFGS On (43.7%) and FFGS Off (47.3%).

- The probability of entrainment was modeled as a function of a FFGS On vs. Off, day vs. night, flow entering the junction, cross-stream position of the fish, and location of the critical streakline in the channel cross-section.

- The best model included all covariates plus interactions of FFGS state with quadratic effects of flow and provided a good fit to the data and had good predictive power.

- The effect of the FFGS varied across flow, revealing that the FFGS reduced entrainment at an intermediate range of flows (7,062 to 14,125 cfs), but not at higher or lower flows.

- As flow increased, the critical streakline became closer to the Georgiana Slough side of the junction, i.e. the left bank (looking downstream) of the Sacramento River, and the probability of entrainment decreased. However, the rate of decrease in entrainment was greater when the FFGS was Off at high flows, rather than when the FFGS was On.

- In general, entrainment to Georgiana Slough increased as flow decreased, until the point at which flows reversed.

- At the lowest positive flows, the critical streakline was located 15 to 20 meters (m) (49-66 feet [ft]) closer to the right bank of the Sacramento River, which translated into higher entrainment rates.

- As the critical streakline moved closer to the right bank of the Sacramento River with lower flows, a greater percentage of Chinook salmon were on the Georgiana Slough side of the streakline (i.e., closer to the left bank of the Sacramento River), leading to a higher probability of entrainment into Georgiana Slough. The mean location of the streakline during low flows intersected the FFGS in the On position. If Chinook salmon were guided by the FFGS during these conditions, their cross-stream location at the end of the FFGS would have been on the right side (Sacramento River side) of the streakline, resulting in a lower entrainment probability; but relatively few fish encountered the FFGS during these conditions.

ES.3.3 Spatial Analysis of Juvenile Chinook Salmon Distribution and Behavior

- A spatial analysis of Chinook salmon distribution and behavior suggested that overall entrainment rates and fish response to the FFGS was due to a combination of multiple modes of fish behavior in the vicinity of the FFGS, and multiple modes of response for Chinook salmon that encountered the FFGS or buoy line (in front of the FFGS).

- Automated track classification suggests that the majority of the Chinook salmon transiting the junction on ebb tides in 2014 and during a previous study in 2008 engaged in sustained, periodic cross-stream movements in the study area, and that their behavior was not consistent with the assumptions underlying the FFGS's design.

- Additionally, spatial analysis of track data and turning point data indicate that many fish responded to physical or hydrodynamic cues in the area near the FFGS, which produced a behavioral response when the FFGS was in the Off position that was similar to the response produced by the FFGS in the On position, reducing the overall effect of the FFGS on entrainment.

- Finally, it appears that some Chinook salmon did not initiate a cross-stream excursion at the FFGS but instead guided along the buoy line and became entrained in Georgiana Slough.

- Although operations did not result in a large decrease in overall entrainment, the reduction in the number of Chinook salmon between the FFGS On and Off positions during ebb tides indicates that **few fish passed under or through the FFGS** during this time.

- The greatest density of Chinook salmon 'turning points' (sustained cross-stream excursion initiation points) switched when the FFGS was Off from downstream of where the FFGS was located had it been in the On position, to the area immediately upstream of the FFGS when it was in the On position.

- This finding supports the hypothesis that the FFGS (or its hydrodynamic signature) triggered a sustained change in the cross-stream movement direction of Chinook salmon away from the FFGS.

- A structure similar to the FFGS that extended farther downstream in the Sacramento River could be used to successfully guide Chinook salmon away from Georgiana Slough, or a similar structure could be installed in other river junctions to move fish towards low-risk migration corridors.

- Although the FFGS did not reduce entrainment overall, it appears to have consistently initiated sustained cross-stream motion away from Georgiana Slough.

ES.3.4 Comparison of BAFF and FFGS Efficiency

- The 2011/2012 BAFF had significantly higher protection efficiency (89.2%) and overall efficiency (89.4%) than the FFGS in 2014 (protection efficiency: 72.8%; overall efficiency: 77.7%), possibly because a high number of Chinook salmon that travelled past the FFGS' downstream end were subsequently entrained into Georgiana Slough in 2014. This guidance past the barrier then entrainment into Georgiana Slough was less commonly seen with the BAFF compared to the FFGS.

- For both low (< 0.25 m/s) and high approach velocities (≥ 0.25 m/s), deterrence efficiency was not significantly different between the FFGS and the BAFF.

- In high velocity conditions (≥ 0.25 m/s), the FFGS protection and overall efficiency were greater than for the BAFF which, although not statistically significant, was consistent with the good performance of the FFGS under high velocity conditions. **Protection and overall efficiency of the BAFF was significantly higher than the FFGS when approach velocities were low** (< 0.25 m/s).

ES.3.5 2014 Delta-wide Survival

- Chinook salmon travel times from Freeport to Chipps Island in 2014 were remarkably short compared to other Delta studies.

- Travel times varied by route and were longer for fish traveling via the interior Delta/Georgiana Slough (modes of 4.59 to 7.44 days) than fish travelling via the Sacramento River, Sutter Slough, or Steamboat Slough (2.33 to 5.56 days), for which modes generally were within a day among these three routes for any given release group.

- Short travel times of Chinook salmon resulted in a high probability of fish arriving at Chipps Island with operational tags, despite unexpected premature tag failure for both tag types (i.e., HTI and VEMCO).

- Survival of Chinook salmon from Freeport to Chipps Island in 2014 varied considerably among outmigration routes and release groups.

- Survival was consistently lower for Chinook salmon traveling through the interior Delta (0.076 to 0.42) compared to survival of fish remaining in the Sacramento River (0.216 to 0.704).

- Delta-wide survival varied from 0.221 to 0.624, and higher survival was associated with higher flow, higher turbidity, and lower water temperature.

ES.3.6 Predation and Predatory Fish

- There was little evidence to suggest that the FFGS operations (On vs. Off) affected predation rates in the Sacramento River near the divergence with Georgiana Slough.

- There was no significant difference in the mean proportion of Chinook salmon eaten by predatory fish with the FFGS On (0.15) versus the FFGS Off (0.17).
- The proportion of Chinook salmon eaten was either not significantly different between distances from the FFGS, or was greater farther from the FFGS, contrary to the hypothesis that the probability of predation would be greater closer to the FFGS.
- Of the environmental factors examined, including FFGS operation, the probability of predation significantly decreased as turbidity increased; no other factors were statistically important.
- There was no change in the spatial distribution of predation events between FFGS On and FFGS Off; however a relatively high proportion of predation events occurred near the three-pile dolphin to which the FFGS was moored at its downstream end.
- The lack of effect of the FFGS on predation is consistent with the lack of effect for the 2011/2012 BAFF.
- There was no broad-scale effect of the FFGS on predatory fish behavior in the study area.
- Predatory fish did not reside in the study area longer with the FFGS On than with the FFGS Off.
- Predatory fish standardized angling catch rate in areas hypothesized to be influenced by the FFGS relative to reference areas did not differ between FFGS On and FFGS Off.
- Habitat zones near the FFGS were not occupied frequently relative to other areas by striped bass, whereas the nearshore habitat in the vicinity of the FFGS was occupied frequently by *Micropterus* species (black basses), although this may have been the result of homing to initial capture areas.
- The only evidence of a localized effect of the FFGS was the relatively higher density of predatory fish near the FFGS compared to areas just beyond the FFGS.

ES.4 STUDY CONCLUSIONS

- The FFGS was partially effective at reducing Chinook salmon entrainment into Georgiana Slough.
- The ~20 percent (five percentage point) reduction in entrainment at intermediate flows was modest, and was not evident at lower or higher flows.
- The limited effectiveness of the FFGS was the result of flows being considerably lower than anticipated.
- Lower flows resulted in the critical streakline extending farther into the Sacramento River channel, resulting in Chinook salmon remaining susceptible to entrainment once they had passed the downstream end of the FFGS.
- The FFGS was not designed to reduce entrainment during reverse flows, which occurred frequently in 2014.
- An FFGS extending farther into the Sacramento River channel could have been more effective over a broader range of flows.

- The FFGS *did* affect fish distribution: fish density was 40-50 percent lower behind the FFGS when it was On compared to Off, as a result of fish moving away from the FFGS.
- The 2014 barrier design may have been more effective under the high velocity conditions observed in 2011 and 2012.
- The observed 2014 conditions required a barrier extending 110 m (361 ft) farther downstream for higher efficacy.
- Through-Delta survival probability was consistently greater for fish not entering the interior Delta through Georgiana Slough.
- The FFGS did not increase through-Delta survival because of its limited overall effectiveness for the range of observed flows.
- Relatively high survival occurred in the Sacramento River and Sutter/Steamboat Slough routes, suggesting that greater use of these routes would increase overall through-Delta survival.
- FFGS operation did not affect predation or predatory fish.
- However, as with the BAFF studies in 2011 and 2012, there was not a true control condition, because the FFGS was always physically present (either On or Off).

ES.5 RECOMMENDATIONS

- Test additional FFGS configurations and consider adaptive deployment of the FFGS as part of a cost-benefit analysis.
- Only one configuration of the FFGS was tested, and it is recommended that additional study be made of different lengths, depths, and angles of FFGS.
- Placement of a longer FFGS that extends further downstream in the Sacramento River could be effective over a broader range of flows.
- An analysis is recommended to determine the optimal distance the FFGS should extend from the left bank versus the added cost that would be incurred for the benefit gained from a longer barrier.
- A deeper FFGS (two five-foot panels instead of one) is recommended for consideration because over 20 percent of Chinook salmon entrained into Georgiana Slough were observed to pass under the FFGS.
- Test a combination of FFGS and BAFF.
- Results of the 2011/2012 BAFF studies and the 2014 FFGS study suggests that it could be worthwhile testing a combination of the FFGS and BAFF, e.g., with the FFGS upstream of the BAFF, in order to provide entrainment reduction over a broader range of flows.
- Use critical streakline analysis to assess optimal engineering solutions at multiple junctions.

- Barriers should be considered at Sutter Slough and Steamboat Slough to guide Chinook salmon into these channels: optimization of barriers at these locations should be more straightforward than at Georgiana Slough because the location of critical streaklines is more predictable.
- Barriers at these junctions, possibly in combination with a barrier at Georgiana Slough, could increase through-Delta survival.
- Assess predation and predatory fish with no barrier and over a long-term deployment, while limiting in-water structure size.
- Study predation and predatory fish at the Georgiana Slough junction with no barrier present in order to provide a true control with which to compare to barrier conditions.
- Study predation and predatory fish with a long-term barrier On deployment, in order to assess whether predatory fish habituation to the barrier occurs.
- Limit in-water structure size associated with barriers, e.g., avoid having large dolphin-type structures if possible, in order to limit habitat with which predatory fish could be associated.

1 INTRODUCTION

1.1 BACKGROUND

The Sacramento River and its tributaries support populations of anadromous salmonid species, including: winter-run, spring-run, fall-run, and late fall-run Chinook salmon (*Oncorhynchus tshawytscha*); and Central Valley steelhead (*O. mykiss irideus*). Three of these taxa (winter-run Chinook salmon, spring-run Chinook salmon, and Central Valley steelhead) are listed as threatened or endangered under the California Endangered Species Act (California Fish and Game Code Sections 2050-2069), the federal Endangered Species Act (ESA; 16 United States Code Sections 1531-1544), or both (California Department of Fish and Wildlife 2015). Both Chinook salmon and steelhead spawn and rear in Sacramento River and its tributaries; adult fish use the mainstem Sacramento River for upstream migration to spawning sites and juvenile fish when rearing is completed use the river for downstream outmigration to the Pacific Ocean. Juvenile Chinook salmon and steelhead migrate through the lower Sacramento River during winter and spring. During their outmigration, juvenile salmonids encounter alternative migration pathways through the Sacramento–San Joaquin Delta (Delta), for example, Sutter and Steamboat sloughs, the Delta Cross Channel (DCC) to Snodgrass Slough and the North and South forks of the Mokelumne River, Georgiana Slough to the North Fork Mokelumne River, and Threemile Slough. **Figure 1-1** shows the migration pathways in the north and east Delta for outmigrating juvenile salmonids,[2] the location of the DCC, and the locations of the pumping facilities of the State Water Project (SWP) and the federal Central Valley Project (CVP) in the south Delta.

Pursuant to the ESA, the National Marine Fisheries Service (NMFS) issued the 2009 *Biological and Conference Opinion for the Long-Term Operations of the Central Valley Project and State Water Project* (BiOp) for winter-run and spring-run Chinook salmon, Central Valley steelhead, North American green sturgeon (*Acipenser medirostris*), and southern resident orca (*Orcinus orca*) (NMFS 2009). Reasonable and Prudent Alternative (RPA) Action IV.1.3 of the BiOp required the California Department of Water Resources (DWR) and the U.S. Bureau of Reclamation (Reclamation) to consider engineering solutions to reduce the diversion of juvenile salmonids from the Sacramento River into the central (also called the 'interior' Delta) and south Delta where the potential for entrainment at the SWP and CVP pumping facilities increases. One of several locations identified in the BiOp for engineering solutions evaluation was Georgiana Slough, a natural distributary of the Sacramento River.

Results from survival studies have demonstrated significantly higher mortality for juvenile Chinook salmon that outmigrate through the interior Delta than for those that remain in the Sacramento River (Brandes and McLain 2001; Perry et al. 2010). Also, studies conducted in December 2009 and January-February 2010, found that outmigrating juvenile Chinook salmon remaining in the Sacramento River had survival rates ranging from 48.5 percent to 58.4 percent, while fish entering the Sutter Slough/Steamboat Slough route had survival rates ranging from 34.5 percent to 55.0 percent, and fish using the Georgiana Slough route had survival rates ranging from 17.9 percent to 31.4 percent (Perry et al. 2012). Based upon these studies, it appears that survival rates for outmigrating juvenile Chinook salmon in the Delta are highest when routed through the Sacramento River, followed by the Sutter/Steamboat sloughs, and lowest via Georgiana Slough.

[2] During periodic periods of high Sacramento River discharge when water is spilling over the Fremont Weir, juvenile Chinook salmon may outmigrate via the Yolo Bypass floodway (not shown on **Figure 1-1**).

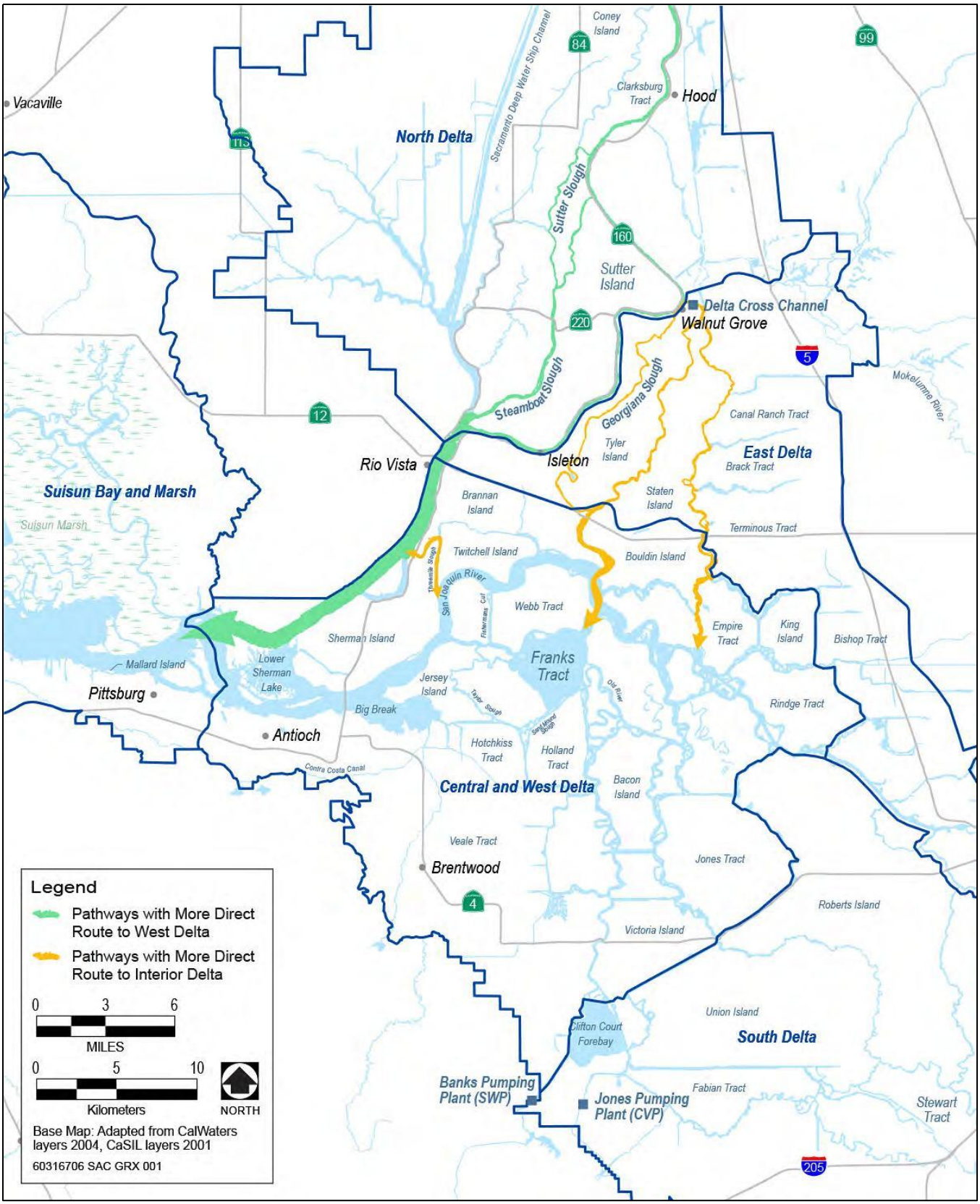

Figure 1-1 Lower Sacramento River and North Delta Migration Pathways

Movement of fish into the interior Delta is thought to increase risk of predation mortality and also increases potential exposure to agricultural, municipal, and industrial water diversions, as well as the SWP and CVP pumping facilities in the south Delta (Perry 2010; Perry et al. 2010; Perry et al. 2012; Singer et al. 2013; Zeug and Cavallo 2014). Other sources of fish mortality may also influence survival through the interior Delta. In an effort to identify potential engineering approaches to reduce the percentage of the juvenile salmonids that migrate from the Sacramento River into Georgiana Slough, DWR implemented a large-scale testing program in 2011 and 2012 to assess the effectiveness of a non-physical barrier design (i.e., a Bio-Acoustic Fish Fence, or BAFF) as a method for guiding outmigrating juvenile salmonids away from the divergence of Georgiana Slough. The experimental design of the 2011 and 2012 tests used acoustically tagged late fall-run juvenile Chinook salmon and steelhead (2012 only), released upstream of the BAFF when the barrier was 'On' and 'Off' (i.e., in operation or not in operation, respectively), to determine the effectiveness of the barrier. In 2014, a physical barrier called a Floating Fish Guidance Structure (FFGS) was tested, with methods similar to those used during the testing of the BAFF barriers in 2011 and 2012. This report presents the results of the tests conducted in 2014 using a FFGS (i.e., 2014 Georgiana Slough Floating Fish Guidance Structure Study [GSFFGS Study]).

1.2 PREVIOUS TECHNOLOGIES STUDIED AT GEORGIANA SLOUGH

This section of the report summarizes two technologies that have been previously tested at the Sacramento-Georgiana Slough divergence with the goal of guiding the outmigration of juvenile salmonids to the Sacramento River route instead of the Georgiana Slough route (San Luis & Delta-Mendota Water Authority and Charles H. Hanson 1996; DWR 2012, 2015b). This section is not intended to be a detailed review or comparison of these technologies but, rather, an overview. The interested reader should consult the original reports for full details and results.

1.2.1 ACOUSTIC BARRIER - 1994

In 1994, an acoustic system developed by Energy Engineering Services Company was tested in the Sacramento River immediately upstream from the divergence of Georgiana Slough (San Luis & Delta–Mendota Water Authority and Charles H. Hanson 1996). The objective of the test was to prevent juvenile fall-run Chinook salmon (as a surrogate for winter-run fish) from entering Georgiana Slough from the Sacramento River. The acoustic barrier was approximately 192 meters (m) (630 feet [ft]) in length comprised of 21 transducers spaced about 9 m (30 ft) apart. The sound array generated a low frequency of 300-400 Hertz. Testing was conducted from April 5 through June 10, 1994. During this period, the instantaneous discharge in the Sacramento River ranged from -6,000 cubic feet per second (cfs) during flood tide to 12,000 cfs during ebb tide. A Kodiak trawl was used to net juvenile Chinook salmon to quantify the "guidance" efficiency of the acoustic barrier. Guidance efficiency was defined as the ratio of mean catch per unit effort (CPUE) of juvenile Chinook salmon in the trawl collected in Georgiana Slough and downstream in the Sacramento River when the barrier was On and when it was Off. Overall, the acoustic barrier guidance efficiency averaged 57.2 percent (95% confidence interval [CI] 47.7–65.0%) when activated (On) and this efficiency was statistically significant ($p<0.001$) (San Luis & Delta–Mendota Water Authority and Charles H. Hanson 1996). Guidance efficiency was found to be greater during ebb tide (60.0%) than during flood tide (39.2%) and greater during the daytime (58.5%) than at night (26.6%). However, the day/night analyses were confounded by observations showing a statistically significant decrease in juvenile Chinook salmon collections using Kodiak trawls at night when compared with daytime collections. Because the guidance efficiency observed during the 1994 tests was less than the 95 percent level of performance desired for a physical barrier, additional testing of the acoustic barrier was discontinued.

1.2.2 BIO-ACOUSTIC FISH FENCE – 2011-2012

The BAFF was developed by Fish Guidance Systems Limited of Southampton, United Kingdom, and field tests produced promising results in Europe and the United States (Maes et al. 2004; Ruebush et al. 2012). The BAFF design combines three stimuli to deter the movement of juvenile salmonids: 1) acoustics; 2) high intensity modulated light (HIML); and 3) an air bubble curtain. All three stimuli work synergistically, with sound being the primary deterrent. A signal generator located near the location where fish deterrence is desired emits chirps at varying intervals and sound levels, depending on the target fish species. The bubble curtain keeps the sound enclosed into a well-defined area, and the strobe lights allow the fish to perceive where the sound source originates, so that they can swim away from it. The BAFF technology was evaluated at the divergence of Georgiana Slough from the Sacramento River in 2011 and 2012.

During the 2011 study period, the BAFF changed the percentage of juvenile Chinook salmon passing into Georgiana Slough from 22.1 percent (Off) to 7.4 percent (On), a reduction of approximately two-thirds that otherwise may have been entrained into the Georgiana Slough (DWR 2012). Statistical analysis of the 2012 data showed that the percentage of juvenile Chinook salmon migrating into Georgiana Slough was changed from 24.1 percent (Off) to 11.4 percent (On), a reduction of just over one-half (DWR 2015b). Results of a comparison of 2011 and 2012 studies for juvenile Chinook salmon found no statistically significant differences in deterrence efficiency, protection efficiency, or overall efficiency when the BAFF was On between the two years, despite substantially higher river flows in 2011 than in 2012. The magnitude of juvenile Chinook salmon migration into Georgiana Slough when the BAFF was Off was similar between the two years, as was the percentage reduction in the risk of entrainment into Georgiana Slough when the BAFF was On (a reduction of 14.7 percentage points in 2011 and 12.7 percentage points in 2012). In both years, the BAFF contributed to a reduction in the movement of juvenile Chinook salmon from the Sacramento River into Georgiana Slough. A total of 23.4 percent of the juvenile steelhead were entrained into Georgiana Slough when the BAFF was Off, compared to 10.5 percent when the BAFF was On, representing a 12.9 percentage point overall reduction of entrainment into Georgiana Slough. These findings demonstrated that an integrated multi-sensory (i.e., light, sound, and air bubbles) non-physical barrier reduced, but did not eliminate, juvenile salmonid entrainment into Georgiana Slough.

1.3 2014 GEORGIANA SLOUGH FLOATING FISH GUIDANCE STRUCTURE STUDY

1.3.1 BACKGROUND

Floating Fish Guidance Structures[3] (FFGSs) evolved from technologies that protect dams, diversions, and intake areas from trash, ice, debris, and other floating hazardous materials. To protect dams, water intakes, and other safety-related areas, cables with log-shaped floats that were tied together were assembled and arranged in an alignment to catch or deflect hazardous materials. To create an effective debris barrier, some systems were designed with metal plates or nets to form a wall, hanging from the floats, to deflect submerged debris. This made it possible to provide protection in the upper portion of the water column where floating debris exists.

These types of debris barriers were modified to act to guide adult and juvenile anadromous fishes away from water intakes, particularly at power plants. The design concept is based on: 1) juvenile anadromous salmonids

[3] Some studies refer to FFGSs as Floating Impermeable Guidance Structures (FIGSs) or Behavioral Guidance Structures (BGSs). For example, see Mulligan (2014) and Cash et al. (2002).

tend to swim in the top portion of the water column (Whitney et al. 1997; Buckley and Kynard 1985; Faber et al. 2011); 2) some juvenile salmonids have been shown to select a shallow rather than deep passage route when given the choice (Johnson et al. 1997); and 3) anadromous salmon juveniles tend to migrate downstream in the river thalweg (Whitney et al. 1997).

In 1998, a behavioral guidance structure (BGS) was constructed in the forebay of Lower Granite Dam on the Snake River, Washington. The BGS was constructed similarly to the FFGS which included a relatively large floating steel wall, measuring over 330 m (1,083 ft) long and between 17-24 m (56-79 ft) deep. The purpose of this installation was to alter the horizontal distribution of emigrating juvenile salmonids and to guide them into the surface bypass and collector. To prevent harmful debris from entering the turbines, a debris boom was installed upstream from the BGS, turbines, and surface bypass and collector (Cash et al. 2002). Using acoustic telemetry and passive hydro-acoustics, BGS study results indicated that juvenile salmonids were guided along the debris boom to a greater extent than by the BGS. Based on these results and other experiments and applications using floating fish guidance walls, manufacturers started designing walls with the specific intent of guiding fish. The relative simplicity of the floating barriers made the cost of manufacturing, installing, and maintaining more economical than other methods.

Other installations of FFGSs have achieved varying degrees of effectiveness. Some reports show guidance efficiencies ranging between 53 percent and 92 percent, depending on location and target species (Scott 2011; Mulligan 2014). These reports present study data for installations at dams in Vermont, Washington, Maine, and Oregon. The targeted species in these studies included Chinook salmon, hatchery and wild steelhead, coho salmon (*Oncorhynchus kisutch*), and Atlantic salmon (*Salmo salar*).

The FFGS can be designed and constructed in many different ways to optimize effectiveness in specific applications. When designing an FFGS barrier, many variables need to be considered which include buoyancy, strength, depth of vertically submerged guidance wall, length of the barrier, and shape of the alignment to utilize existing hydraulics. The structural design must be flexible to accommodate site and target species characteristics. Site geometry, vertical distribution of target species in the water column by life stage, water velocity, and other site-specific details help determine the optimal FFGS design.

1.3.2 STUDY LOCATION AND STUDY AREAS

The 2014 GSFFGS Study was comprised of two large-scale elements: 1) the FFGS barrier performance evaluation study; and 2) the juvenile Chinook salmon outmigration survival study. These elements were linked and data use overlapped. The regional location of the 2014 GSFFGS Study encompassed the entire Delta, except for the south Delta (**Figure 1-1**).

The FFGS barrier was located in the northeast Delta, in unincorporated Sacramento County, approximately 53 kilometers (km) (35 miles [mi]) southwest of the City of Sacramento at the community of Walnut Grove (**Figure 1-2**). The primary FFGS barrier evaluation "study area" extended along the Sacramento River from the divergence of the DCC[4] downstream past the divergence of Georgiana Slough (approximately Sacramento River Miles[5] 26-27) (California State University Chico 2015). **Figure 1-3** illustrates the location of the FFGS in the On and Off operating and non-operating positions, respectively, located across the Sacramento River from Dagmar's Landing.

[4] The DCC was closed during the 2014 GSFFGS Study.

[5] Sacramento River Miles as measured in an upstream direction from the confluence of the Sacramento and San Joaquin rivers near Point San Joaquin (River Mile 0).

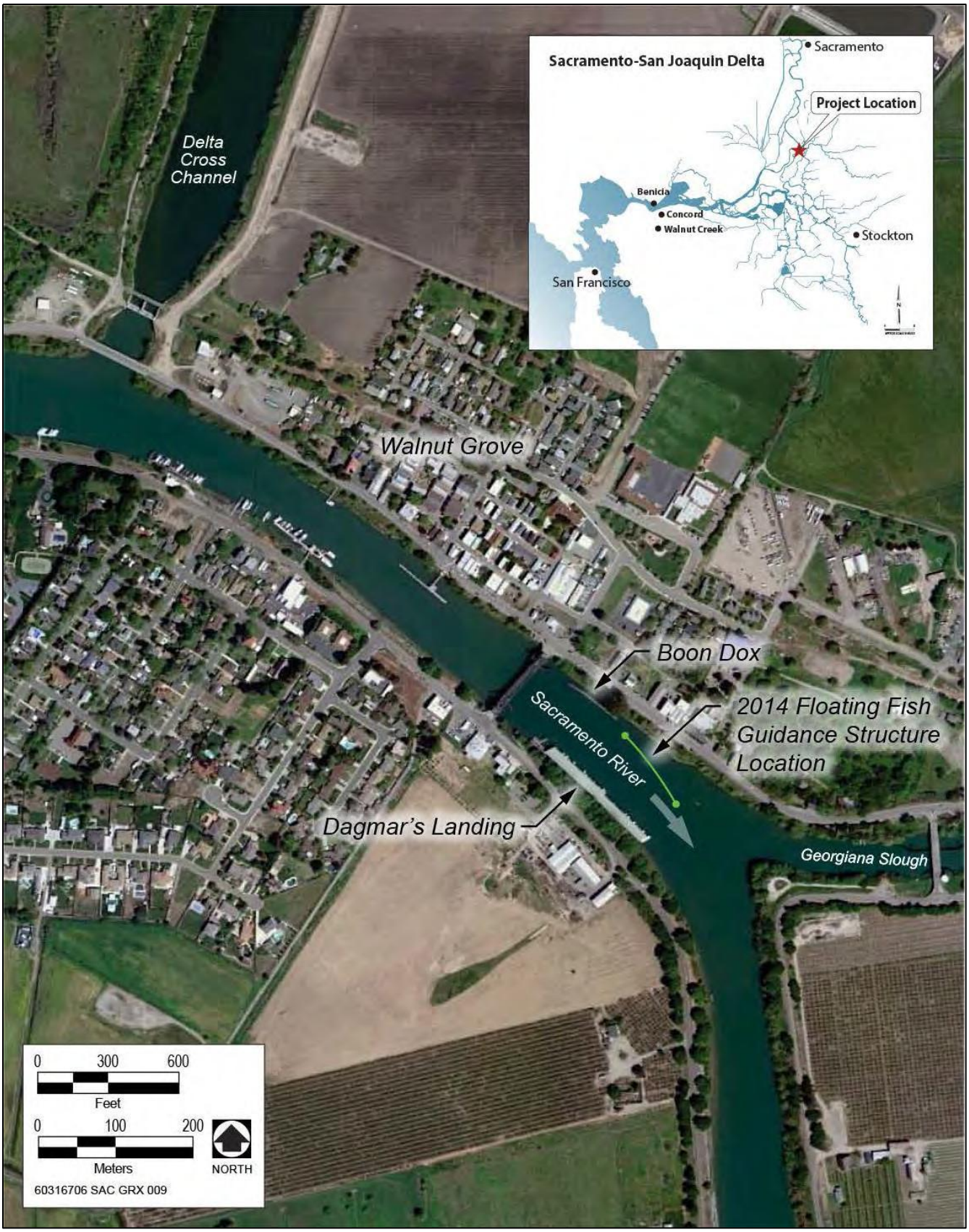

Figure 1-2 Floating Fish Guidance Structure Performance Evaluation Study Area

The larger "study area" for the outmigration survival study extended from the juvenile Chinook salmon release site at the City of Sacramento (approximately Sacramento River Mile 59) to the final fish monitoring location at Mallard Island in Suisun Bay downstream of the confluence of the Sacramento and San Joaquin rivers (California State University Chico 2015).

1.3.3 GOALS, OBJECTIVES, AND OVERVIEW

There were two primary goals of the 2014 GSFFGS Study: 1) test the effectiveness of an FFGS in preventing outmigrating juvenile Chinook salmon in the Sacramento River from entering Georgiana Slough; and 2) determine if the FFGS increased the overall survival of juvenile Chinook salmon past Georgiana Slough and through the Delta to Mallard Island. The tests conducted as part of the 2014 GSFFGS Study provide additional data to address RPA Action IV.1.3 of the NMFS BiOp. The study results also inform decision makers considering adaptive management actions that may be necessary to ensure that the long-term operations of the SWP and CVP are in compliance with the ESA.

The six primary objectives of the 2014 GSFFGS Study were to:

- Assess reach-scale route selection and survival of juvenile Chinook salmon;
- Assess temporal distribution of juvenile Chinook salmon at arrival in FFGS area;
- Assess predation and predatory fishes behavior in the vicinity of the FFGS;
- Assess far-field movements of predatory fishes and juvenile Chinook salmon;
- Assess alternative hypotheses specific to barrier function; and
- Compare effectiveness of the FFGS and the BAFF technologies.

The basic design of the 2014 GSFFGS Study was similar to that of the 2011 and 2012 BAFF studies: to release acoustically tagged hatchery-raised juvenile late fall-run Chinook salmon into the Sacramento River, and then to monitor the proportion of fish entering the study area at Walnut Grove that outmigrated downstream in the Sacramento River when the FFGS was On compared to when it was Off under a range of environmental conditions (e.g., tidal conditions, day and night, Sacramento River flows, rate of flow entering Georgiana Slough).

Similar to the previous studies, the FFGS was tested for its effectiveness as both a behavioral and physical deterrent to prevent outmigrating juvenile Chinook salmon from entering into Georgiana Slough. To evaluate the efficacy of the FFGS, a network of approximately 200 fixed-location hydrophones were deployed in the Sacramento River, Georgiana Slough, and other Delta channels to record acoustic signals from the tagged juvenile Chinook salmon.

The 2011, 2012, and 2014 tests included the same key components, with some 2014 modifications to the technical design of the components.

- **Barrier/Guidance Structure Design.** The 2011 and 2012 studies evaluated the performance of the BAFF technology. The 2014 GSFFGS Study evaluated the performance of an FFGS. All studies used piles to support the barrier/guidance structure. The 2011 BAFF barrier was 192 m (630 ft) long mounted on 15 piles. The 2012 BAFF barrier was also 192 m long mounted on 19 piles. The 2014 FFGS barrier was 110 m (361 ft) long mounted on 12 piles.

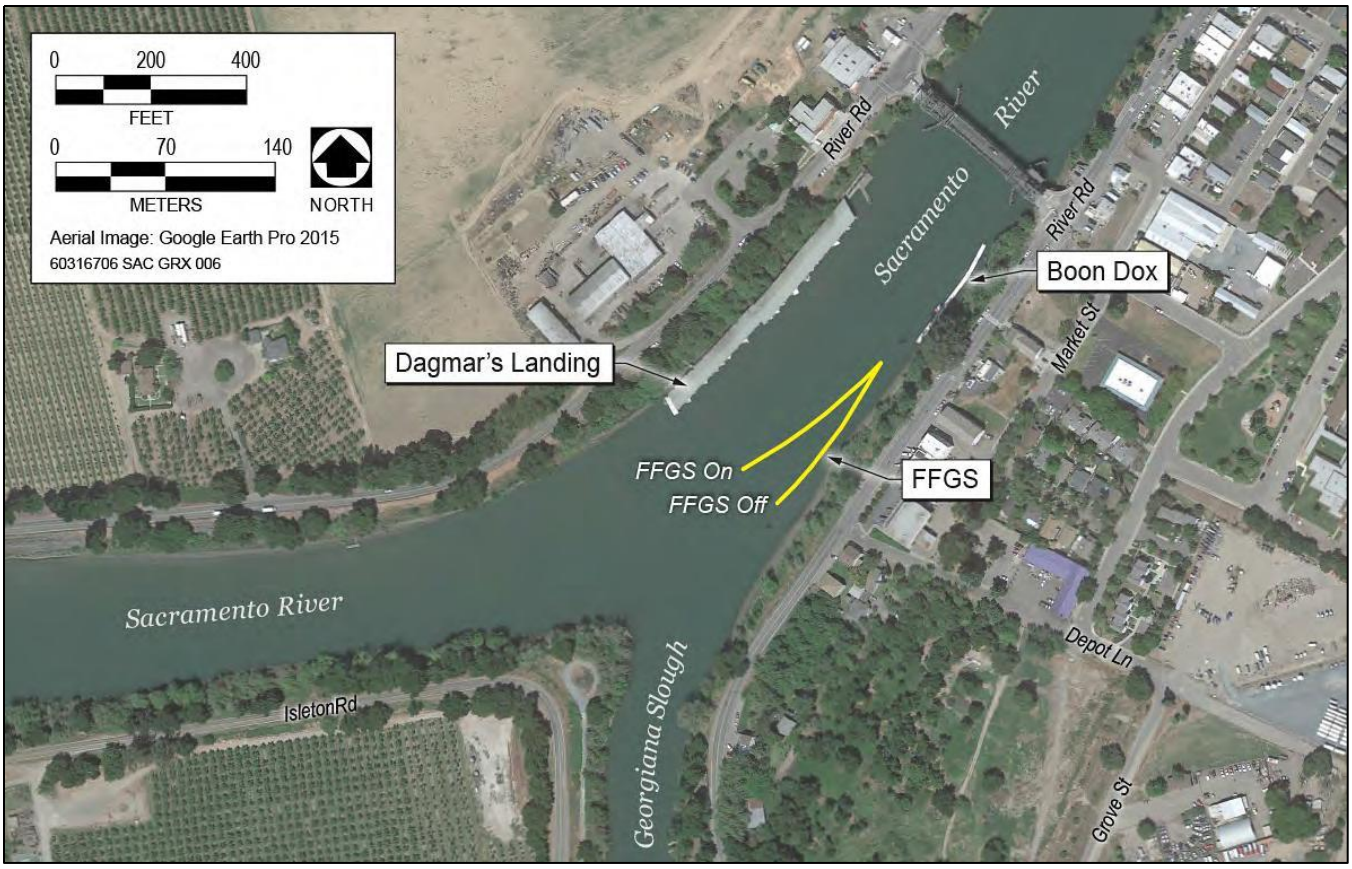

Figure 1-3 **Location of the FFGS in the On Position (mid-channel) and Off Position (along left river bank)**

- **Fish Tracking and Other Data Collection Equipment Deployment.** All studies monitored juvenile Chinook salmon movement with scientific data collection equipment mounted on piles. The 2011 study used three piles for fish tracking and data collection equipment. The 2012 study used seven piles for tracking and data collection equipment. The 2014 study used 14 piles for fish tracking and data collection equipment. Additional hydroacoustic equipment was attached to docks and/or deployed in-stream using anchors.

- **Study Fishes.** Studies included the release of tagged late fall-run juvenile Chinook salmon, steelhead (2012 only), and predatory fishes to test the effectiveness of the guidance structure. The 2011 study tagged and released 1,500 juvenile Chinook salmon and 50 predatory fishes. The 2012 study tagged and released 1,501 juvenile Chinook salmon, 299 juvenile Central Valley steelhead, and 50 predatory fishes. The 2014 study tagged and released approximately 5,461 juvenile Chinook salmon and 195 predatory fishes.

- **Study Fish Release Location.** All studies included release locations in the Sacramento River. During the 2011 and 2012 studies, juvenile Chinook salmon and steelhead (2012) were released immediately downstream from the divergence of Steamboat Slough, about 10 km (6 mi) upstream from the BAFF. During the 2014 study, fish were released at one location in the Sacramento River approximately 56 km (35 mi) upstream at the City of Sacramento (Old Sacramento) and at one location in Georgiana Slough approximately 5 km (3 mi) downstream from the divergence with the Sacramento River. The change in the upstream release point in 2014 was implemented to allow juvenile Chinook salmon additional time to acclimate to the Sacramento River following their release.

- **Barrier/Guidance Structure Operation Timeline.** All studies included late winter and spring operations of the BAFFs or FFGS. The 2011 BAFF construction took 35 days from mid-February to mid-March. The BAFF was operated in 2011 from mid-March to mid-May. The 2012 BAFF construction required approximately 30 days from early February to mid-March. The 2012 BAFF was operated from mid-March to late April. The 2014 FFGS construction required approximately 32 days from mid-February to mid-March. The 2014 FFGS operated from March 10 to June 15. Deployment of monitoring equipment began in January before the start of the 2014 GSFFGS Study.

1.4 ORGANIZATION OF THE REPORT

The 2014 GSFFGS Performance Evaluation Project Report is organized as follows:

- **Chapter 1, Introduction** provides a brief summary background on outmigrating anadromous juvenile Chinook salmon in the Sacramento River, including route selection and survival; summarizes past studies of behavioral fish barriers at Georgiana Slough; and describes the study goals, objectives, and provides an overview.

- **Chapter 2, Experimental Design and Implementation** provides an overview of the experimental design and includes a detailed description of its components.

- **Chapter 3, Analysis Methods, Results, and Discussion** describes the methods used, results achieved, and analyses conducted as part of the overall project. The various analyses are presented in the following sections:

    - Section 3.1, Floating Fish Guidance Structure Performance;
    - Section 3.2, Survival Model;
    - Section 3.3, Hydrodynamics and Critical Streakline;
    - Section 3.4, Generalized Linear Modeling of Fish Fates;
    - Section 3.5, Spatial Analysis of Fish Distribution and Behavior;
    - Section 3.6, Analysis of Predatory Fishes and Predation; and
    - Section 3.7, Analysis of Diel Arrival Distribution.

- **Chapter 4, Integration and Synthesis of Results** provides a summary integration and synthesis of the results from the analyses related to the barrier performance evaluation. This chapter also provides a comparison of the 2011, 2012, and 2014 test results. The chapter also highlights the key findings and conclusions of the 2014 study.

- **Chapter 5, Recommendations** provides a suite of management-level recommendations.

- **Chapter 6, References** provides sources cited in the report.

- The **Appendices** contain the following technical information supporting the report:

    - **Appendix A**, Fish Summary Statistics
    - **Appendix B**, Summary of Standard Operating Procedures
    - **Appendix C**, Fish Tagging Effects Study
    - **Appendix D**, Conference on Fates – Predation and Guidance Rules

- **Appendix E**, Focal Predatory Fish Species
- **Appendix F**, Survival Modeling – Predator Transitions

2 EXPERIMENTAL DESIGN AND IMPLEMENTATION

2.1 OVERVIEW OF EXPERIMENTAL DESIGN

As summarized in **Chapter 1 Introduction**, Subsection 1.3.3, the 2014 GSFFGS Study experimental design was based, in part, on the designs and results gathered during the 2011 and 2012 BAFF testing. The basic 2014 GSFFGS Study design matched the 2011 and 2012 design concepts with regard to: 1) use of in-water monitoring equipment including hydrophones, acoustic Doppler current profilers (ADCPs), split-beam transducer echosounders, and dual-frequency identification sonar (commonly called DIDSON cameras); 2) the surgical implanting of acoustic tags and release of hatchery-raised juvenile late fall-run Chinook salmon into the Sacramento River and wild fish predators in the vicinity of the FFGS; 3) the monitoring and comparison of the proportion of tagged juvenile Chinook salmon entering the study area that successfully outmigrated in the Sacramento River when the barrier was On to the proportion that entered Georgiana Slough when the barrier was Off; and 4) the monitoring of the behavior of the tagged predatory fishes and their densities.

Like the 2011 and 2012 studies, one goal of the 2014 GSFFGS Study was to test the effectiveness of the FFGS in preventing juvenile Chinook salmon in entering Georgiana Slough from the Sacramento River when the barrier was On and Off under a range of environmental conditions. Unlike the 2011 and 2012 studies, a second goal of the 2014 GSFFGS Study was to determine if the FFGS increased the overall survival of juvenile Chinook salmon past Georgiana Slough and through the Delta to Mallard Island.

2.2 KEY ELEMENTS OF THE 2014 GSFFGS STUDY

The 2014 GSFFGS Study included the following key elements:

- A total of 5,461 late fall-run juvenile Chinook salmon, produced at the Coleman National Fish Hatchery located near Anderson, California, were surgically implanted (tagged) with acoustic transmitters during the study period. Of this total, 4,635 fish were released into the Sacramento River at the City of Sacramento California, and their outmigration past the FFGS and Georgiana Slough at Walnut Grove, California, was monitored. In addition, 826 fish were released into Georgiana Slough. Georgiana Slough was designed as a supplemental release location because fish released at this site would not encounter the FFGS but would support the analysis of fish survival through the Delta.

- Juvenile Chinook salmon were released daily from March 1 through April 15, 2014, during their outmigration ocean-phase.

- Releases into the Sacramento River were made approximately 53 km (35 mi) upstream from the FFGS to allow juvenile Chinook salmon time to adjust to the river conditions and disperse into the channel before reaching Georgiana Slough. Releases into Georgiana Slough were made approximate 5 km (3 mi) downstream from the divergence with the Sacramento River.

- Passage of tagged juvenile Chinook salmon was monitored at and downstream from the FFGS in the Sacramento River, Georgiana Slough, and other Delta channels, both when the FFGS was both On and Off.

- 195 predatory fishes of four species were captured, acoustically tagged, released into the study area, and monitored to evaluate behavior, movement patterns, and potential predation on tagged juvenile Chinook salmon in association with the operation of the FFGS.

- 60 hydrophones were installed in the Sacramento River immediately upstream from, downstream from, and adjacent to the FFGS, to monitor movements of tagged fishes as they encountered and responded to the FFGS. These hydrophones are referred to as the "behavioral array" or "study array" at the FFGS. The path tagged fish swam was determined as they passed through the study array. Additional hydrophones, referred to as the "peripheral hydrophones" were installed to detect tagged fishes in channels upstream and downstream from the study array throughout the Delta.

- Multiple ADCPs were installed in the Sacramento River in the vicinity of the FFGS to monitor local currents, water velocities, and general hydrodynamics.

- Active hydroacoustic devices, including split-beam transducers and DIDSON cameras, were installed to monitor fish densities in the immediate vicinity of the FFGS.

Figure 2-1 shows an overview of the 2014 GSFFGS Study location, including: the release locations (i.e., Sacramento River near the City of Sacramento and Georgiana Slough) for tagged juvenile Chinook salmon; the location of the FFGS; and the locations of peripheral hydrophone arrays.

2.3 STATISTICAL BASIS AND SAMPLE SIZES FOR THE EXPERIMENTAL DESIGN

Data were analyzed in the 2014 GSFFGS Study using two statistical approaches. In the first approach, hypotheses were explicitly stated *a priori* (see **Table 2-1**) and tested using univariate methods with predefined critical alpha values. For the second approach, generalized linear modeling (GLM) was used to examine the relative importance of the presence of the FFGS (compared to other independent variables that also were hypothesized to be of importance) in influencing juvenile Chinook salmon to continue outmigration in the Sacramento River instead of entering Georgiana Slough or being preyed on in the vicinity of the FFGS.

Evidence suggests that the movement and survival fate of outmigrating juvenile salmon are affected by a minimum of three generalized variables (i.e., day-night phase, Sacramento River discharge, and tidal phase) (Horn and Blake 2004; Blake and Horn 2006; Perry 2010; Steel et al. 2013; Perry et al. 2015; Cavallo et al. 2015). Changing flows, tides, and day/night cycles produce varying combinations of light, water velocity, and the angle of approach of the water velocity vector relative to the face of the FFGS. The effectiveness of the FFGS was tested across different combinations of light levels measured underwater and water velocities measured with ADCPs. The water velocity variables consisted of along-FFGS velocity (i.e., sweeping velocity), cross-FFGS velocity (i.e., approach velocity), and upstream secondary circulation (i.e., main channel velocity). Results of the independent variables (i.e., light and water velocity) were partitioned into categories based on thresholds derived for the BAFF evaluations of 2011 and 2012 (DWR 2012, 2015b): 5.4 lux (underwater light) and 0.25 meters per second (m/s) (0.82 feet per second [ft/s]; water velocity). Light values less than (<) 5.4 lux were representative of dark conditions and values greater than or equal to (≥) 5.4 lux were representative of high light conditions (Anderson et al. 1988). Similarly, based on the work of Swanson et al. (2004), a sustained swimming speed for juvenile Chinook salmon was determined to be 3.6 body lengths per second (BL/s). Based on this

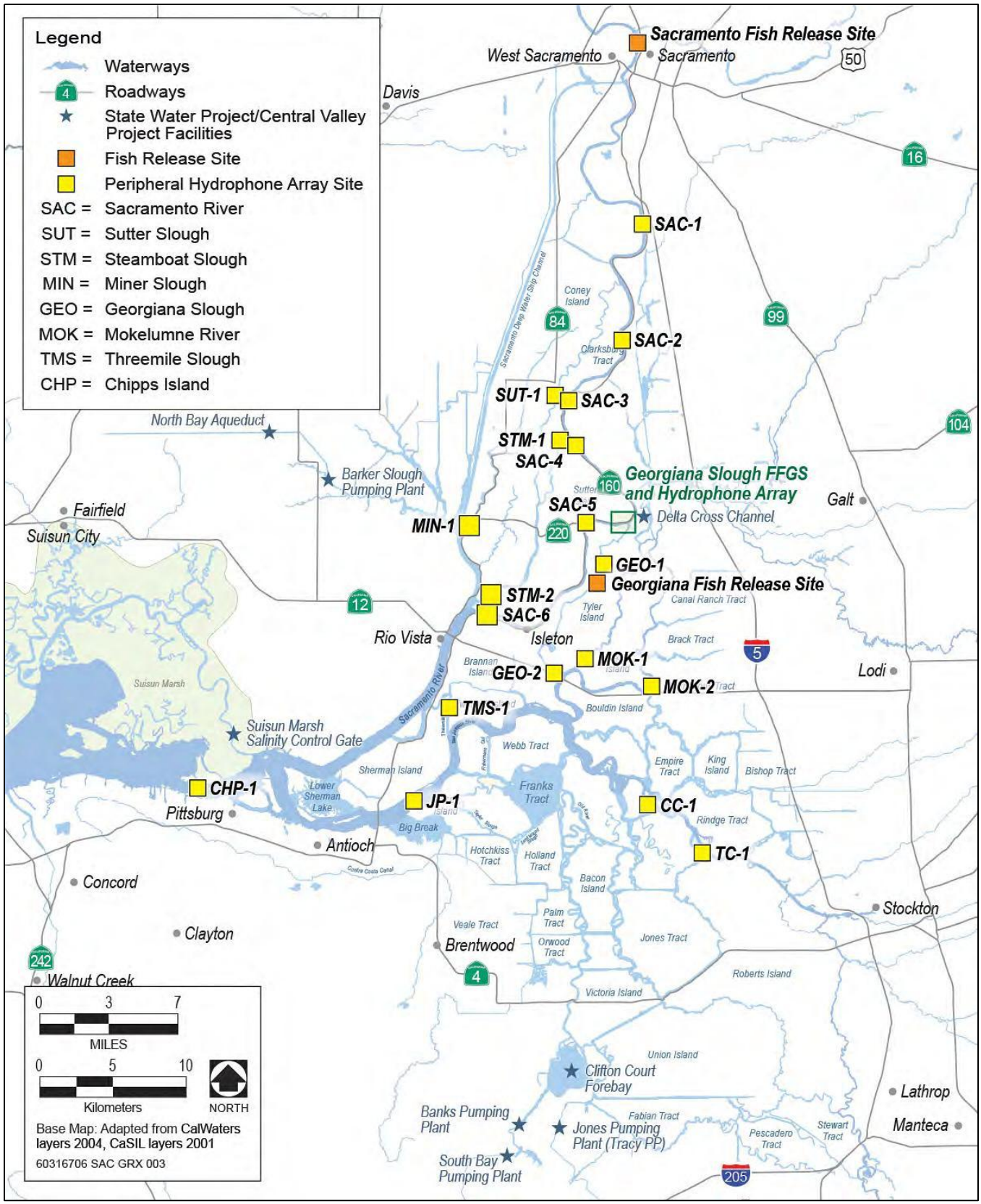

Source: Data provided by California Department of Water Resources and adapted by AECOM 2014

Figure 2-1 Location of the FFGS, Fish Release Locations, and Peripheral Hydrophone Arrays

information and the angle of the barrier to river flow of 24 degrees (°), a threshold approach velocity of 0.25 m/s (0.82 ft/s) was chosen to categorize low and high velocities. These threshold levels were used so that direct statistical comparisons of barrier efficiency could be made between the FFGS and the BAFF.

For the hypothesis testing based on univariate methods, a single "sample" was defined because all the tagged juvenile Chinook salmon passed by the FFGS study area during a period in which: 1) the FFGS (On/Off) state did not change; 2) light did not cross the threshold level (5.4 lux); and 3) water velocity did not cross the threshold level (0.25 m/s [0.82 ft/s]).

Hypotheses which focus on the deterrence, protection, and overall efficiencies of the FFGS (i.e., Hypotheses 16, 22a, and 23a in **Table 2-1**) were tested with all samples combined for light level and water velocity in an overall test. In addition, these same hypotheses were tested separately under low light (< 5.4 lux), high light (≥ 5.4 lux), low water velocity (< 0.25 m/s [0.82 ft/s]), and high water velocity (≥ 0.25 m/s [≥ 0.82 ft/s]) conditions.

In addition to this univariate hypothesis testing approach, an exploratory approach based on combining multiple independent variables in a GLM was used. This approach was similar to the approach used by Perry et al. (2014). Previous research (Bowen and Bark 2010; Bowen et al. 2012; DWR 2012, 2015b) suggested that several variables, for example, cross-stream location of fish, river discharge, and critical streakline location, not included in the hypothesis testing framework, may influence fish behavior and barrier effectiveness. To consider these variables, the study investigators used a GLM to answer: Does the operation of the FFGS significantly increase the probability of a juvenile Chinook salmon outmigrating via the Sacramento River as opposed to entering Georgiana Slough? The GLM assessed the relative importance of different independent variables (including FFGS On/Off) influencing route selection of juvenile Chinook salmon in the Sacramento River.

The experimental design was strengthened by the use of continuous monitoring of water velocity and day/night conditions immediately upstream from the FFGS location to record the range of environmental conditions likely to affect the movement and fate of tagged juvenile Chinook salmon entering the study area. Results provided a strong technical basis for assessing the performance of the FFGS as a method for improving survival of juvenile Chinook salmon outmigrating from the Sacramento River, as well as a statistical basis for further refining and optimizing the experimental design of any subsequent tests and/or evaluations.

Table 2-1 defines the specific objectives and associated hypotheses identified for testing during the 2014 GSFFGS Study. Hypotheses are grouped according to the main objectives. Further discussion of statistical testing methods is provided in the Study Plan for the 2014 GSFFGS Study (DWR 2014).

In addition to these specific objectives and hypotheses, the study linked the detailed juvenile Chinook salmon acoustic tag tracking data/river hydraulic data at the Sacramento River–Georgiana Slough divergence to model factors influencing their navigation through the study area.

2.3.1 REACH-SCALE ROUTE SELECTION AND SURVIVAL

Three hypotheses were identified for testing, related to reach-scale route selection and survival of juvenile Chinook salmon, as part of the 2014 GSFFGS Study: H1, H2, and H3 (**Table 2-1**). These hypotheses relate to study objectives, including understanding through-Delta survival, reach-specific survival, and barrier effectiveness that were analyzed using the hydroacoustic data with the mark-recapture survival models and GLMs.

Table 2-1 Objectives and Hypotheses Related to the 2014 Georgiana Slough Floating Fish Guidance Structure

Primary Objective	Specific Objective	Hypothesis Number	Hypothesis
Assess reach-scale route selection and survival of juvenile Chinook salmon	Determine whether through-Delta survival of juvenile Chinook salmon differs between migration routes	H1	The survival of juvenile Chinook salmon is higher from a specified starting point (e.g., Freeport, California) through the Sacramento River route to Chipps Island, compared to routes through the interior Delta.
	Determine whether juvenile Chinook salmon survival from Steamboat Slough to the FFGS area differs between years (e.g., because of environmental conditions or fish acclimation) (upstream releases in 2014)	H2	The survival of tagged juvenile Chinook salmon between the Steamboat Slough junction and the Sacramento River-Georgiana Slough divergence is different in 2011, 2012, and 2014.
	Determine whether the FFGS is effective at reducing juvenile Chinook salmon entry into Georgiana Slough	H3	The FFGS reduces the probability of juvenile Chinook salmon entering Georgiana Slough.
Assess temporal distribution of juvenile Chinook salmon at arrival in FFGS area	Determine whether juvenile Chinook salmon arrival in the FFGS area differs depending on release location (e.g., because of different acclimation time to establish diel cycles of migration activity)	H4	The diel distribution of juvenile Chinook salmon arriving at the Georgiana Slough hydrophone array released at Steamboat Slough is different from the fish released at the City of Sacramento.
Assess predation and predatory fish behaviors in the vicinity of the FFGS	Assess whether predation risk increases with FFGS On	H5	The probability of experimentally released juvenile Chinook salmon being eaten within the Georgiana Slough hydrophone array is greater with the FFGS On than with the FFGS Off.
	Assess whether predation risk of juvenile Chinook salmon changes in relation to the proximity to the FFGS (i.e., because the FFGS harbors predatory fishes or increases their predation effectiveness)	H6	The probability of juvenile Chinook salmon being eaten within the Georgiana Slough hydrophone array increases with decreasing distance from the FFGS.
	Assess whether the physical structure of the FFGS and its effect on study area hydrodynamics results in changes in predatory fishes density and the proportion of predatory fish density near the FFGS (e.g., by providing structure for ambushing prey or resting near the structure, or by changing the hydrodynamics of the study area so that changes in predator behavior are evident further from the FFGS)	H7	The density of predatory fishes in the vicinity of the FFGS footprint is greater with the FFGS On than with the FFGS Off.
	Assess whether the physical structure of the FFGS and its effect on study area hydrodynamics results in changes in the amount of time spent near the FFGS footprint by individual predatory fishes (e.g., by providing more structure for ambushing prey or resting)	H8	Predatory fishes released in the vicinity of the FFGS footprint reside there longer when the FFGS is On than when the FFGS is Off.

Table 2-1 Objectives and Hypotheses Related to the 2014 Georgiana Slough Floating Fish Guidance Structure

Primary Objective	Specific Objective	Hypothesis Number	Hypothesis
	Assess whether predation risk of juvenile Chinook salmon changes with FFGS position (i.e., because the FFGS harbors predatory fishes or increases their predation effectiveness)	H9	The standardized angling catch rate of predatory fishes in the vicinity of the FFGS footprint is greater when the FFGS is On compared to when the FFGS is Off.
	Assess whether the physical structure of the FFGS and its effect on study area hydrodynamics results in changes in predatory fish density and the proportion of predatory fish density near the FFGS (e.g., by providing structure for ambushing prey or resting near the structure, or by changing the hydrodynamics of the study area so that changes in predator behavior are evident further from the FFGS)	H10	The proportion of predatory fishes in the study area that is in the vicinity of the FFGS footprint is greater with the FFGS On than with the FFGS Off
	Assess the use of different habitat types (e.g., open water, mud bank, riprap) by predatory fishes	H11	The percentage of time that predatory fishes spend within different habitat types in the study area is not equal.
	Assess the use of different water velocities by predatory fishes in relation to those available	H12	The percentage of time that predatory fishes spend in different water velocities in the study area is not equal.
Assess far-field movements of predatory fishes and Chinook salmon juveniles	Assess whether the through-Delta travel time of predatory fishes differs from the travel time of juvenile Chinook salmon	H13	Travel times of predatory fishes are different than juvenile Chinook salmon.
	Assess whether the through-Delta travel rate of predatory fishes differs from the travel time of juvenile Chinook salmon	H14	Travel rates of predatory fishes are different than juvenile Chinook salmon.
	Assess whether a difference exists in the direction of movement of predatory fishes and juvenile Chinook salmon (e.g., do predatory fishes primarily move upstream, whereas juvenile Chinook salmon primarily move downstream?)	H15	The direction of movements of predatory fish is different than that of juvenile Chinook salmon.
Assess alternative hypotheses specific to barrier function	Assess whether the FFGS is effective at deterring juvenile Chinook salmon or routing them away from Georgiana Slough, while accounting for predation in the vicinity of the FFGS	H16	The deterrence, protection and overall efficiencies are higher when the FFGS is in place compared to when the FFGS is not in place.
	Assess whether portions of the FFGS have a relatively high tendency for juvenile Chinook salmon to pass beneath them	H17	The proportion of juvenile Chinook salmon that pass under the FFGS is not uniform along the length of the structure.
	Assess whether the tendency for juvenile Chinook salmon to pass beneath the FFGS is related to the hydrodynamics at the FFGS (e.g., greater downward water velocity may push fish under the barrier more frequently than lower downward velocity)	H18	The probability that a juvenile Chinook salmon will pass under the FFGS is dependent on the vertical component of velocity within the near-field of the structure.

Table 2-1 Objectives and Hypotheses Related to the 2014 Georgiana Slough Floating Fish Guidance Structure

Primary Objective	Specific Objective	Hypothesis Number	Hypothesis
	Assess whether the tendency for juvenile Chinook salmon to pass beneath the FFGS is related to water temperature (e.g., higher water temperature may facilitate better FFGS avoidance through increased swimming ability)	H19	The probability that a juvenile Chinook salmon will pass under the FFGS is dependent on water temperature.
	Assess whether the FFGS increases the probability of juvenile Chinook salmon occurring to the right of the critical streakline	H20	At the downstream end of the FFGS, the proportion juvenile Chinook salmon fish to the right of the critical streakline is greater when the FFGS is in place than when the FFGS is not present.
Compare effectiveness of the FFGS and the BAFF technologies and years	Assess deterrence efficiency and whether effectiveness in keeping juvenile Chinook salmon out of the interior Delta differed between the FFGS and BAFF (grouping the BAFF data from 2011 and 2012)	H22a	The deterrence, protection overall efficiencies are different with the FFGS in place compared to when the BAFF was in place.
	Assess whether effectiveness in keeping juvenile Chinook salmon out of the interior Delta differed between the FFGS and BAFF (grouping the BAFF data from 2011 and 2012)	H22b	The probability of entrainment into Georgiana Slough is different with the FFGS in place compared to when the BAFF was in place.
	Assess deterrence efficiency and whether effectiveness in keeping juvenile Chinook salmon out of the interior Delta differed between the FFGS and BAFF (using the BAFF data from 2011 and 2012 as separate treatments)	H23a	The deterrence, protection, overall efficiencies are different with the FFGS in place in 2014 compared to when the BAFF was in place in 2011 and compared to when the BAFF was in place in 2012.
	Assess whether effectiveness in keeping juvenile Chinook salmon out of the interior Delta differed between the FFGS and BAFF (using the BAFF data from 2011 and 2012 as separate treatments)	H23b	The probability of entrainment into Georgiana Slough is different with the FFGS in place in 2014 compared to when the BAFF was in place in 2011 and compared to when the BAFF was in place in 2012.

2.3.2 TEMPORAL DISTRIBUTION OF FISH AT ARRIVAL

Differences in the arrival time of juvenile Chinook salmon into the FFGS study area based on their release location were investigated to determine if those released further upstream had a greater tendency toward diel activity patterns (H4). Previous research suggested that fish released further upstream may have a greater tendency to exhibit nocturnal migration because of a longer acclimation period in the Sacramento River (Chapman et al. 2013). This knowledge would be important in relation to assessing the likely diel distribution of individuals encountering the FFGS during future operations, if the FFGS (or other barriers) were implemented to deter juvenile salmonids away from the interior Delta.

2.3.3 PREDATION AND PREDATORY FISHES

Eight hypotheses (H5 to H12) were tested in relation to predation and predatory fishes during the 2014 GSFFGS Study. Collectively, these hypotheses assessed the influence of the FFGS on behavior of predatory fishes and predation risk to juvenile Chinook salmon (**Table 2-1**).

2.3.4 FAR-FIELD MOVEMENTS OF PREDATORY FISHES AND JUVENILE CHINOOK SALMON

Three hypotheses (H13-H15) were proposed for testing related to the far-field movements of predatory fishes and juvenile Chinook salmon. These hypotheses were tested to provide more knowledge regarding different migratory behavior of predatory fishes and juvenile Chinook salmon in the broader Delta ecosystem (**Table 2-1**).

2.3.5 ALTERNATIVE HYPOTHESES SPECIFIC TO BARRIER FUNCTION

Two objectives related to the detailed assessment of FFGS functioning were proposed for investigation by testing hypotheses H16 and H17 (**Table 2-1**). Hypothesis H16 was tested via analysis of variance (ANOVA); or if the assumptions of ANOVA were not met, the Kruskal-Wallis test was used (Sokal and Rohlf 1995). H17 was tested via a chi-squared goodness of fit test. Hypothesis H20 tested the ability of the FFGS to move juvenile Chinook salmon to the right of the critical streakline. The failures of the FFGS (defined as juvenile Chinook salmon that passed the FFGS and continued down Georgiana Slough) were investigated via hypothesis H21. The hypothesis was tested by chi-squared goodness of fit (Sokal and Rohlf 1995). Hypothesis H21 specifically addresses six possible failure modalities.

2.3.6 ALTERNATIVE HYPOTHESES SPECIFIC TO COMPARING TECHNOLOGIES

Of considerable interest was a comparison of the effectiveness of the two alternative technologies (FFGS and BAFF). The objectives of assessing differences in effectiveness between these technologies were addressed by hypotheses H22a and H22b (**Table 2-1**). Differences between years (i.e., 2011 versus [vs.] 2012 vs. 2014) were addressed by testing hypotheses H23a and H23b (Section 2.3.7). Care was taken when executing this approach because the experiments were not designed to directly compare the BAFF and FFGS.

2.3.7 ALTERNATIVE HYPOTHESES SPECIFIC TO COMPARING YEARS

Comparisons of barrier effectiveness between years were investigated further by testing hypothesis H23a and H23b. These hypotheses compared barrier efficiency or probability of entrainment treating the BAFFs of 2011 and 2012 as separate treatments (**Table 2-1**).

2.3.8 SAMPLE SIZE POWER ANALYSIS

A power analysis is a statistical planning tool that explicitly acknowledges different types of errors resulting from application of statistical tests and attempts to inform the design of the study to minimize the chances of committing such errors. For the 2014 GSFFGS Study, power analyses were conducted to ensure an adequate number of study fish were being tagged and released to meet the statistical requirements of each of the analyses. All of the power analyses used predefined confidence levels to detect a percent change when testing each of the hypotheses for the FFGS On and Off treatments over the expected range of environmental conditions. A detailed description of the different power analyses that were conducted for the 2014 GSFFGS Study is provided in the Study Plan (DWR 2014).

2.4 EXPERIMENTAL METHODS

2.4.1 FLOATING FISH GUIDANCE STRUCTURE

DESCRIPTION

The FFGS is a physical fish deterrence system designed to induce behavioral guidance. A typical FFGS is made up of floating buoys that support vertically submerged solid metal plates. The structure is formed by separate plate sections that are linked together with heavy-duty hardware and a flexible rubber material attached between the plates to prevent gaps (**Figure 2-2**). The sectioning provides flexibility for transporting, installing, aligning, and storing the FFGS, as well as for guiding fish and debris. This technology is designed to have a relatively small in-water footprint to minimize changes to the existing hydraulic conditions.

Source: Worthington Waterway Barriers 2013

Figure 2-2 Three Sections of a Typical Floating Fish Guidance Structure

INFRASTRUCTURE

The FFGS used at Georgiana Slough was about 110 m (361 ft) long and was made up of steel sections 6.1 m (20 ft) wide and 1.5 m (5 ft) deep (vertical) (**Figure 2-3** and **Figure 2-4**). Historical water stage elevation and bathymetry data were analyzed to calculate the depth of the submerged panels. A 3 m (10 ft) depth was considered optimal during average and above-average flows in the Sacramento River, but stage was predicted to be much lower because of drought conditions in California; therefore, the FFGS was deployed using only the

upper panel sections 1.5 m (5 ft). This ensured that the panel submergence depth relative to the water depth never exceeded 50 percent, which is explained in further detail later in this section. This criterion was developed during physical modeling done by DWR on scaled-down FFGSs in a laboratory flume.

The barrier was made up primarily of modular components (e.g., FFGS panels and floats), and anchored by three dolphin pile clusters. Each pile cluster consisted of three 24-inch piles (i.e., one vertical [plumb pile] and two angled [batter piles] into the vertical pile). The pile clusters were attached to each other at the top of the piles with a welded gusset. Nine additional individual 12-inch piles also were installed to support scientific instruments. Geotechnical data were gathered and analyzed to verify that the piles were driven sufficiently to support the forces applied to the structure. Design details are provided in the report *Georgiana Slough Floating Fish Guidance Structure Basis of Design* (Moffatt & Nichol 2014).

The depth of the barrier was limited so it would not occlude more than 50 percent of the depth of the water column. FFGS barriers that occlude more than 50 percent of the water column can cause undesirable turbulence which could impact the desired guidance effect. Each steel section included a float at the top of the barrier to facilitate adjustments to the changes in the stage of the Sacramento River. This was necessary because the area around the Georgiana Slough divergence experiences regular changes in stage, velocity, and flow as a result of tidal influences and flows in the Sacramento River. It was not uncommon for the combination of events to result in reverse river discharges in the Sacramento River immediate downstream of the Georgiana Slough divergence. Because the FFGS floats, it self-adjusts vertically to the changes in river elevation, thereby keeping the depth of the barrier at a constant 1.5 m below the surface over all variable conditions.

Figure 2-3 Georgiana Slough Floating Fish Guidance Structure Being Installed

A system of winches and cables was designed to move the barrier between "barrier On" and "barrier Off" positions. The deck-mounted winches were connected by cable to the downstream pile clusters, which worked in conjunction to pull the FFGS into the On and Off positions on a specific schedule. The structural design criteria constrained the operation of the FFGS to a maximum water velocity of 1.4 m/s (4.5 ft/s). A contingency plan was developed, but not executed during the 2014 operational period, to move the barrier to the FFGS Off position, to decrease drag force and ensure safety, if the maximum water velocity occurred. The contingency plan did not need to be implemented during the study period.

GUIDANCE STRUCTURE ALIGNMENT

The FFGS was designed to guide fish across the critical streakline[6] toward the right bank of the Sacramento River. This intended design feature was based on the observation from the 2011 and 2012 studies that fish with a cross-stream position farthest to the right of the critical streakline had the highest probability of guiding past the Georgiana Slough divergence and continue their outmigration in the Sacramento River. The upstream end of the barrier was about 213.4 m (700 ft) from the point of divergence between the Sacramento River and Georgiana Slough. The barrier started at the downstream end of the Boon Dox public dock to provide study fish enough time to sense and react to the barrier before they reached the divergence point. Having the upstream end of the barrier near the dock also simplified the installation of the barrier by taking advantage of the existing dock. The barrier extended out into the river about 76.2 m (250 ft) from the left bank, across the critical streakline to maintain what was estimated to be an optimum angle-to-flow throughout the entire alignment.

The FFGS was aligned so that it had a relatively shallow angle relative to the flow orientation (24°). This configuration was designed based on the assumption that study fish would be guided while minimizing the effects of the river's hydrodynamic forces. Citing the results of the barrier study at the Head of Old River in 2010, which included a relatively steep BAFF angle and higher flows (Bowen and Bark 2010) suggested that such influences can reduce deterrence efficiency. The downstream end of the barrier was placed just upstream of the junction of the Sacramento River and Georgiana Slough.

[6] The critical streakline defines the streamwise division of flow vectors entering each channel (i.e., Sacramento River or Georgiana Slough).

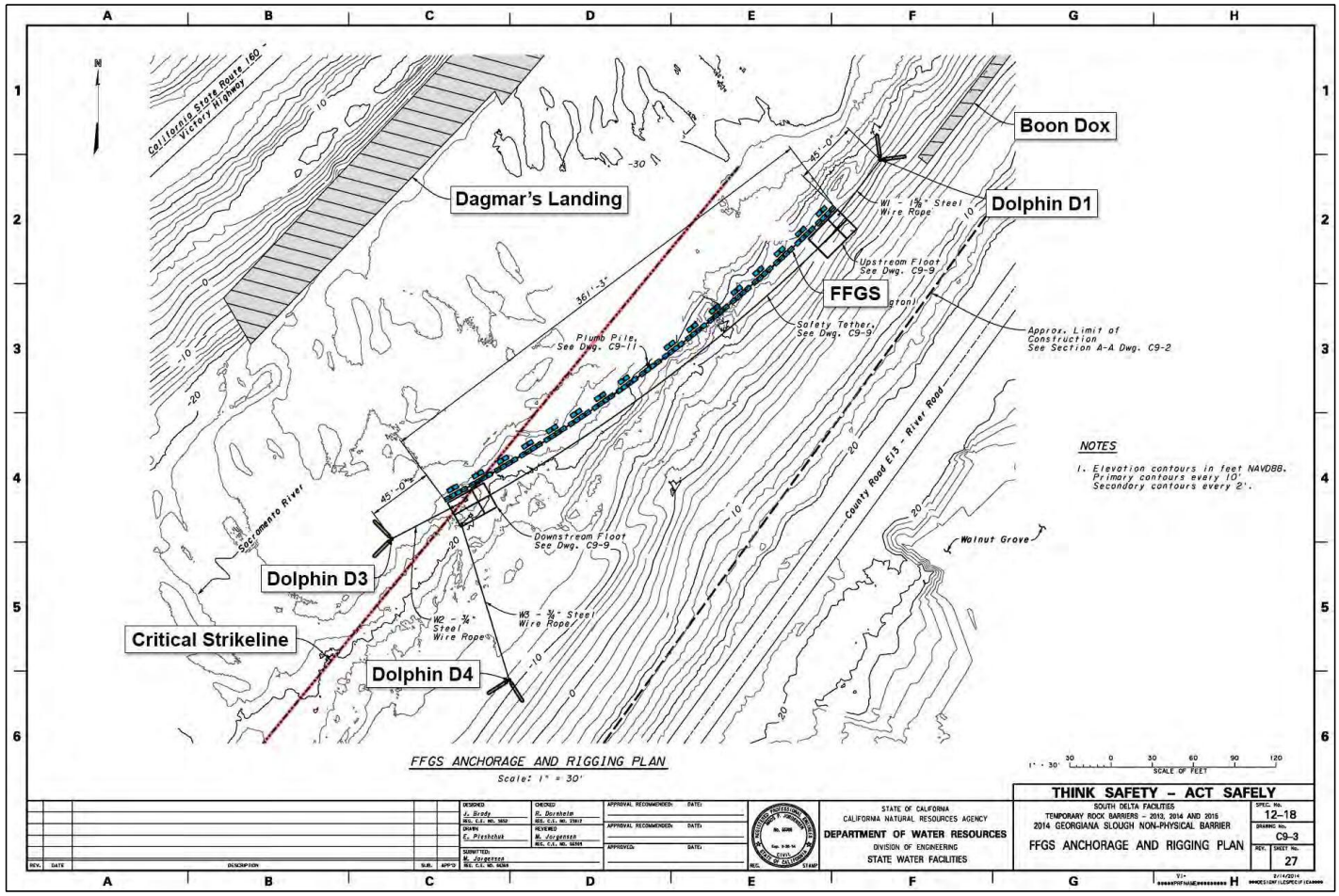

Figure 2-4 2014 Floating Fish Guidance Structure Layout Plan

The alignment, and in particular the angle-to-flow of the river, was a critical element of barrier design. The general principle of angled barrier design (as used, for example, in louver screen arrangements) is that when flow meets the barrier at an acute angle, fish need to make only a relatively small turn to be guided along the face of the barrier. This alignment also ensures that fish swimming at a relatively low sustained speed can avoid passing through the barrier (Rainey 1985; Turnpenny and O'Keeffe 2005). The swimming direction requiring the lowest escape velocity is at 90° to the line of the barrier; thus, the design should ensure that this velocity component is kept below the maximum sustainable swimming speed of the fish over the range of river flows for which the barrier is designed. **Figure 2-5** shows the relevant velocity components for an angled fish barrier.

The main channel velocity is denoted as *Ua*. The velocity perpendicular to the barrier face is the fish's escape velocity, *Ue*. For a barrier angle φ, escape velocity is calculated as:

$$Ue = Ua \sin \varphi$$

The sweeping velocity, *Us*, is the component parallel to the barrier face. It is used to calculate the time taken for a fish to traverse the screen from any given point when swimming at velocity *Ue*. It is calculated as:

$$Us = Ua \cos \varphi$$

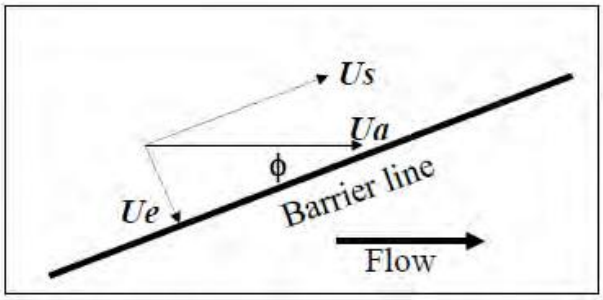

Note: *Ua* is the channel velocity, *Ue* is the fish escape velocity, and *Us* is the sweeping velocity component along the face of the barrier.

Source: Turnpenny and O'Keeffe 2005

Figure 2-5 Flow Velocity Components in Front of an Angled Fish Barrier

The swimming ability of juvenile Chinook salmon was determined by Swanson, Young, and Cech (2004), who reported a sustained swimming velocity of 20 centimeters per second (cm/s) (0.77 ft/s) (**Figure 2, Panel a**) at a sweeping velocity of 31cm/s (1.02 ft/s) for fish 4.4-6.4 centimeters (cm) (1.7-2.5 inches) standard length (SL) (mean: 5.6 cm SL [2.2 inches]). This swimming velocity, 20 cm/s, provided a sustained swimming speed of 3.6 BL/s for a 5.6 cm SL Chinook salmon. The minimum standard length of juvenile fall-run Chinook salmon used in the design calculation was 60 mm (2.4 inches) fork length (FL) (based on the selection of a conservatively small size relative to the size of outmigrating juvenile Chinook salmon in the north Delta, and the maximum design river velocity was 0.5 m/s (1.6 ft/s) (based on design parameters for a BAFF). **Table 2-2** shows the derivation of the barrier angle for these design parameters, which resulted in a barrier angle to flow of 24°. Based on the design assumptions, the maximum approach velocity perpendicular to the barrier was calculated to be 0.204 m/s (0.669 ft/s) (within the design discharge range). Use of sustained swimming speed values in this calculation provides a margin of safety because fish are capable of significantly higher prolonged and burst speeds for short periods (Beamish 1978). The margin of safety was built into the maximum design approach velocity perpendicular to the

barrier, so for a threshold, a slightly higher value was chosen, 0.25 m/s (0.820 ft/s), to categorize low and high velocities. For the samples of deterrence, protection, and overall efficiency, the definition of high velocities used was ≥ 0.25 m/s (≥ 0.820 ft/s), and low velocities were < 0.25 m/s (< 0.820 ft/s) (see Section 3.2, "Survival Model" for additional information).

Table 2-2 Design Angle Parameters for a Barrier Capable of Deflecting or Guiding Juvenile Chinook Salmon

Attribute		Value
Minimum size of fish (FL)		60 mm
Sustained swimming speed		3.6 BL/s
Swimming speed (prolonged)		0.204 m/s
Maximum design channel velocity		0.5 m/s
Approximate barrier angle		24°
Angle and Velocity		
Escape velocity	24°	0.203 m/s
Sweeping velocity	24°	0.457 m/s

Notes: BL/s = body lengths per second; mm = millimeter(s); m/s = meter(s) per second; FL = fork length.

2.4.2 ACOUSTIC TAG SYSTEM OVERVIEW

Study fish movements in the vicinity of the FFGS were monitored with an acoustic tag tracking system. The project incorporated a Hydroacoustic Technology, Inc. (HTI) Acoustic Tag Tracking System (ATTS), which used a fixed array of underwater hydrophones to track movements of fish implanted with acoustic tags. As the study fish approached the array, the signal transmitted from each tag was detected and the arrival time was recorded at several hydrophones. The differences in tag signal arrival times at each hydrophone were used to calculate two-dimensional (2D) positions. These positions were assembled into tracks that measured behavioral responses of the study fish to the FFGS. The ATTS included the following hardware and software components:

- A tag programmer to activate and program the tag;
- Acoustic tags that transmitted a pulse of sound at regular intervals;
- Hydrophones that functioned like underwater microphones, capturing sound in a defined volume of water;
- Cables connecting the hydrophones to the tag receivers; and
- Tag receivers that received the tag signals from the hydrophones were connected to computers that used specialized software to output the tag signal data in a format that could be stored in data files.

ACOUSTIC TAGS

All tags used in this study operated at a frequency of 307 kilohertz (kHz) and were encapsulated with a nonreactive, inert, low-toxicity resin compound. The tags used "pulse-rate encoding," which provided an increased detection range, an improved signal-to-noise ratio and pulse-arrival resolution, and decreased position variability when compared to other types of acoustic tags (Ehrenberg and Steig 2003). Pulse-rate encoding uses

the interval between each transmission to detect and identify the tag. Each tag was programmed with a unique pulse rate to track movements of individual tagged fish.

The pulse rate is measured from the peak amplitude of one pulse to the peak amplitude of the next pulse in sequence. Because the tags had slightly different pulse rates, they could be individually identified. The timing of the start of each transmission was precisely controlled by a microprocessor in the tag. Test tag frequency periods ranged between 2.014 and 4.997 milliseconds (ms). The amount of time that the tag actively transmitted is the pulse length (or pulse duration). For this study, the transmit pulse length was 2.0 ms.

In addition to the tag period, the HTI tag double-pulse mode or "subcode" option was used to increase the number of unique tag identification (ID) codes available. When this tag coding option is used, each tag is programmed with a defined primary tag period, and also with a defined secondary transmit signal, called the subcode. This subcode defines the precise elapsed period between the primary and secondary tag transmit signals. Thirty-one different subcodes are possible for each tag period, which resulted in more than 100,000 total unique tag ID codes being available for use in the 2014 GSFFGS Study.

HYDROPHONES

HTI Model 590 hydrophones were installed for this study, and they also were used for pre-release tag testing operations. Model 590 hydrophones operate at 307 kHz and include a low-noise preamplifier. Hydrophone directional coverage was about 330°, with equivalent sensitivity in all directions except for a 30° limited sensitivity cone directly behind the hydrophone where the cable was attached. The hydrophone sensor element tip was encapsulated in specially treated rubber, for long-term reliability with acoustic impedance close to that of water. The hydrophone and connector housing were made of a corrosion-resistant aluminum-bronze alloy. Cables used to connect the hydrophones to the shore-based receivers were twisted pair wire and double shielded for noise reduction.

The hydrophone preamplifier circuit provided signal conditioning and background noise filtering for transmission over long cable lengths and in acoustically noisy environments. A calibration circuit in the preamplifier provided a method for field testing hydrophone operation and was used to measure the signal time delays between hydrophones in the array. The Model 590 hydrophones included temperature sensors to measure changes in water temperature and the effect these changes had on the velocity of the signal in water.

ACOUSTIC TAG RECEIVER

Four HTI Model 290 Acoustic Tag Receivers (ATRs), one HTI Model 291 ATR, and twelve HTI Model 395 dataloggers were used to record hydrophone data in the array between the DCC and the FFGS. The Model 290 ATR is designed to record signals from up to 16 separate channels; Model 291 ATRs receive up to four channels, and Model 395 dataloggers receive one channel. In all cases, one channel is assigned to each hydrophone. Each ATR was connected to a personal computer that was used to analyze and store the acoustic data. Dataloggers contain embedded computers for this purpose. All receivers were synchronized, using an internal global positioning system (GPS) receiver that was embedded within each of the ATRs. An individual raw data file was created for each sample hour. Filters in all receivers were set to identify the acoustic tag sound pulse and discriminate tags from the ambient background noise.

When the tag signal was received by the ATR, a series of signal processing steps were completed. The envelope detector received the signal and output the positive "envelope" with the carrier frequency removed. This detected echo envelope was then digitized at a rate of 12 kHz. A real-time adaptive noise threshold was set, based on a 1-second window of the background noise level for each hydrophone independently, which was updated every 0.083 ms. The pulse length (or duration) of each pulse that exceeded a predetermined threshold was measured at the -3-, -6-, and -12-decibel points, and the pulse peak amplitude was located and measured.

The ATR pulse measurements were reported for each single echo from each hydrophone and written to Raw Acoustic Tag (*.RAT) files. Each *.RAT file contained header information for data acquisition settings, followed by the raw echo data. Each *.RAT file contained all acoustic signals detected during the period, including signals from tagged fish and additional unfiltered acoustic noise.

The *.RAT files from all receivers were compressed and automatically uploaded to a cloud-based server each hour by way of cell phone modems at each receiver site. Access to the server data was made possible by an Internet connection so researchers could view or process the data from any location with Internet access. Data was available for review and quality assurance/quality control (QA/QC) approximately 15 minutes after each hourly file was collected.

TAG PROGRAMMER

Each of the acoustic transmitters was activated and programmed with unique properties (e.g., tag code) before being implanted in a study fish. The HTI Tag Programmer application running on a computer and attached to the HTI Model 490-LP tag programmer unit was used to set individual settings for each tag used in the study.

HYDROPHONE PLACEMENT GEOMETRY AND POSITION CALCULATION

The principle used to determine acoustic tag positions is similar to the principle used to determine positions using a GPS. The acoustic tag transmits a signal that is received by at least four hydrophones. Because the positions of the four hydrophones are known and the relative signal arrival times at the hydrophones can be measured, the locations of tagged fish can be estimated. In particular, if h_{ix},h_{iy},h_{iz} specify the x,y,z location of the i^{th} hydrophone and F_x,F_y,F_z specify the unknown x,y,z locations of the tagged fish, then the travel time from the tagged fish to the i^{th} hydrophone, t_i, is given by:

$$t_i = \frac{1}{c}\sqrt{(h_{ix} - F_x)^2 + (h_{iy} - F_y)^2 + (h_{iz} - F_z)^2}$$

where: c is the velocity of sound.

Because tags in free swimming fish necessarily transmitted at times not controlled by a tag receiver, the absolute travel time could not be measured directly. However, the differences between the arrival times of the signal at the various hydrophones (t_i - t_j) could be measured by:

$$t_i - t_j = \frac{1}{c}\left[\sqrt{(h_{ix} - F_x)^2 + (h_{iy} - F_y)^2 + (h_{iz} - F_z)^2} - \sqrt{(h_{jx} - F_x)^2 + (h_{jy} - F_y)^2 + (h_{jz} - F_z)^2}\right]$$

With four hydrophones, three distinct signal-arrival time-difference equations exist. The system of nonlinear equations is determined by solving the tagged fish coordinates, F_x,F_y,F_z, so that the mean-squared difference

between the measured (left side of the equation above) and calculated (right side of the equation above) time differences are minimized.

MONITORING EQUIPMENT DEPLOYMENT AND HYDROPHONE ARRAY DESIGN

Monitoring equipment was deployed in the study area at the Sacramento River/Georgiana Slough divergence starting in January 2014 and installation was completed in late February 2014. A total of 60 hydrophones were installed in the Sacramento River immediately upstream from, downstream from, and adjacent to the barrier, to monitor behavior of tagged fish as they encountered and responded to the barrier. These hydrophones are referred to as the "behavioral array" or "study array." Model 590 hydrophones were installed on bottom or surface mounts, designed for the environmental and river discharges at each location. Cables attached to the hydrophones ranged in length from 15 to 150 m (49-492 ft). Hydrophone cables were paired with tensioned stainless steel cable to relieve the strain on the signal cables during deployment, retrieval, and in flow.

Additional hydrophones, referred to as the peripheral hydrophones, were installed to detect tagged fish outside the area in the immediate vicinity of the barrier (**Figure 2-1**). Hydrophones installed throughout the larger north Delta at important passage route junctions and endpoints were part of the larger survival array. Each of the peripheral and survival hydrophones was combined with a Model 395 Datalogger and was operated independently using air card modems for communication access and remote data downloading.

The behavioral array hydrophones, peripheral hydrophones, and survival hydrophones with cable assemblies were deployed and tested before study fish were released. All equipment was bench-tested and calibrated before installation. Hydrophones were installed and cables were routed to electronic equipment, housed either in secure, climate-controlled structures supplied with 110-volt alternating current (AC) power or in locked, steel 'job' boxes located on-shore.

Hydrophone Array at the FFGS

The FFGS behavioral hydrophone array was installed near the FFGS. Hydrophones were positioned on both the Sacramento River side and the Georgiana Slough side of the barrier, as well as upstream from the barrier, starting above the DCC. They were placed so that high-quality 2D) tracks could be obtained throughout this approximately 1.2 km (0.75 mi) reach.

FFGS behavioral array hydrophones were positioned as part of barrier deployment and were monitored on-site for use in documenting the response of tagged juvenile Chinook salmon and tagged predatory fishes to the barrier when it was either in the On position or along shore in the Off position. This monitoring system allowed on-site, real-time detection and monitoring of movement by tagged fish into and through the study area. The system was maintained throughout the study.

The precise locations of hydrophones in the array were measured in situ, using a GPS unit. The positions were checked and refined using a procedure for calculating hydrophone placement geometry and positioning known as the "Ping-around™." The Ping-around procedure uses time delays to estimate relative locations of hydrophones in a close proximity grid such as the FFGS behavioral array. To measure signal time delays, the calibration circuit for each hydrophone was rotationally set to transmit ("ping"), whereas all other hydrophones were set to receive. This procedure was repeated for all hydrophones in the array. Data from each hydrophone were processed to measure the time delay and water temperature. Accurate measurement of signal time delays between hydrophones

provided the position data to locate the array in Universal Transverse Mercator or Latitude/Longitude coordinates and provided the resolution necessary for sub-meter 2D positioning.

The effective range of detection and overlap of hydrophones in the array also was examined in situ by actively moving a transmitting tag throughout the array and verifying consistent detection and positioning of the tag (termed the "tag drag" procedure). An automated data downloading and storage system for the hydrophone array was set up, operated, and maintained over the duration of testing. Hydrophone array locations for the FFGS behavioral array are shown in **Figure 2-6**.

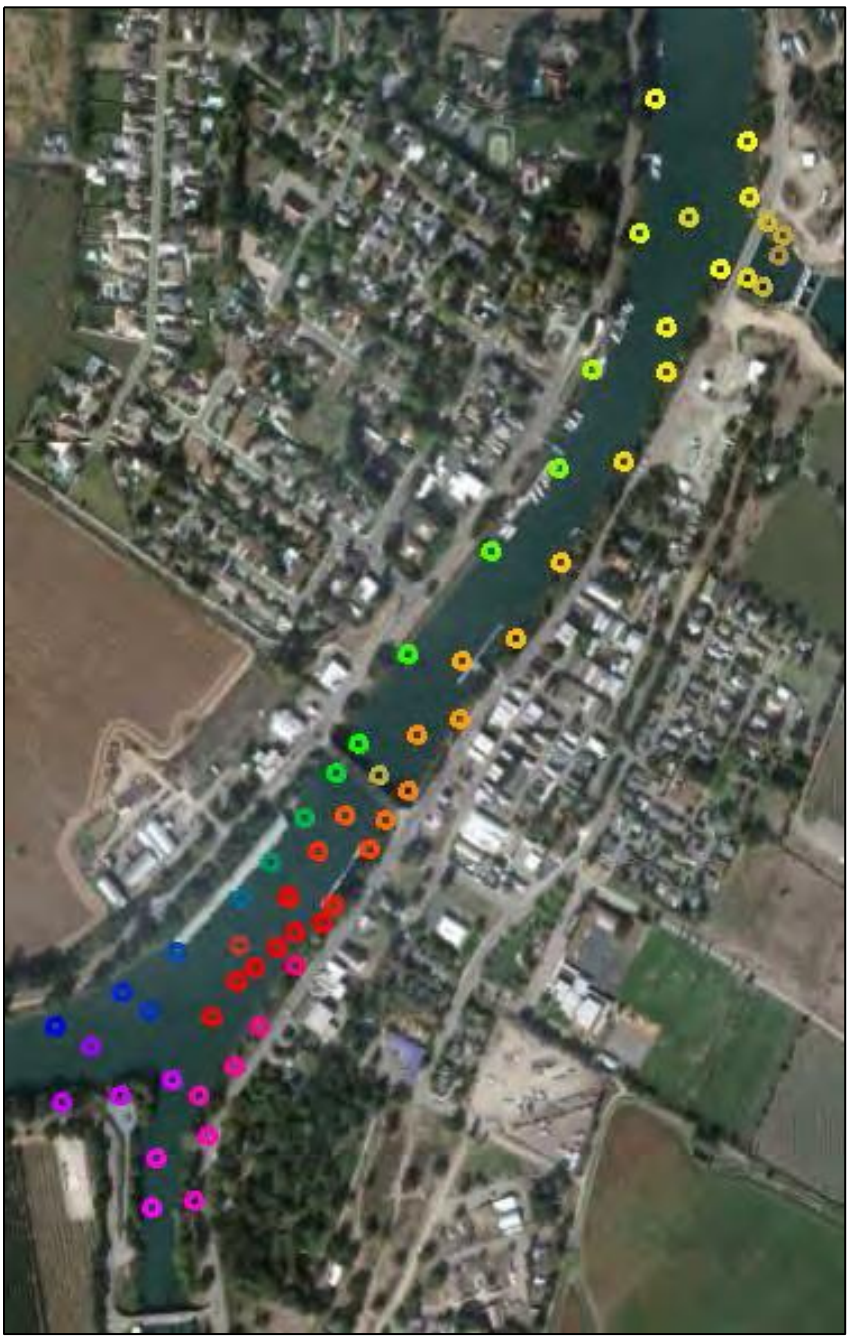

Note: The colors are only used to identify individual hydrophones and have no other significance. One location has two hydrophones (shallow and deep). N=60.

Figure 2-6 Behavioral Array Hydrophone Locations in the Georgiana Slough Study Area

Hydrophone Array at Sutter Slough

An additional 15-hydrophone behavioral array was deployed at the junction of Sutter Slough and the Sacramento River. Hydrophone locations extended upstream and downstream from the junction in the main Sacramento River and also into Sutter Slough. The Sutter Slough array was deployed with similar mounts, hydrophones, and cabling to the Georgiana FFGS array. One Model 290 ATR was housed in a cargo container on the southwest corner of the junction. An automated data downloading and storage system was installed at this location. Hydrophone array locations for the Sutter Slough array are shown in **Figure 2-7**.

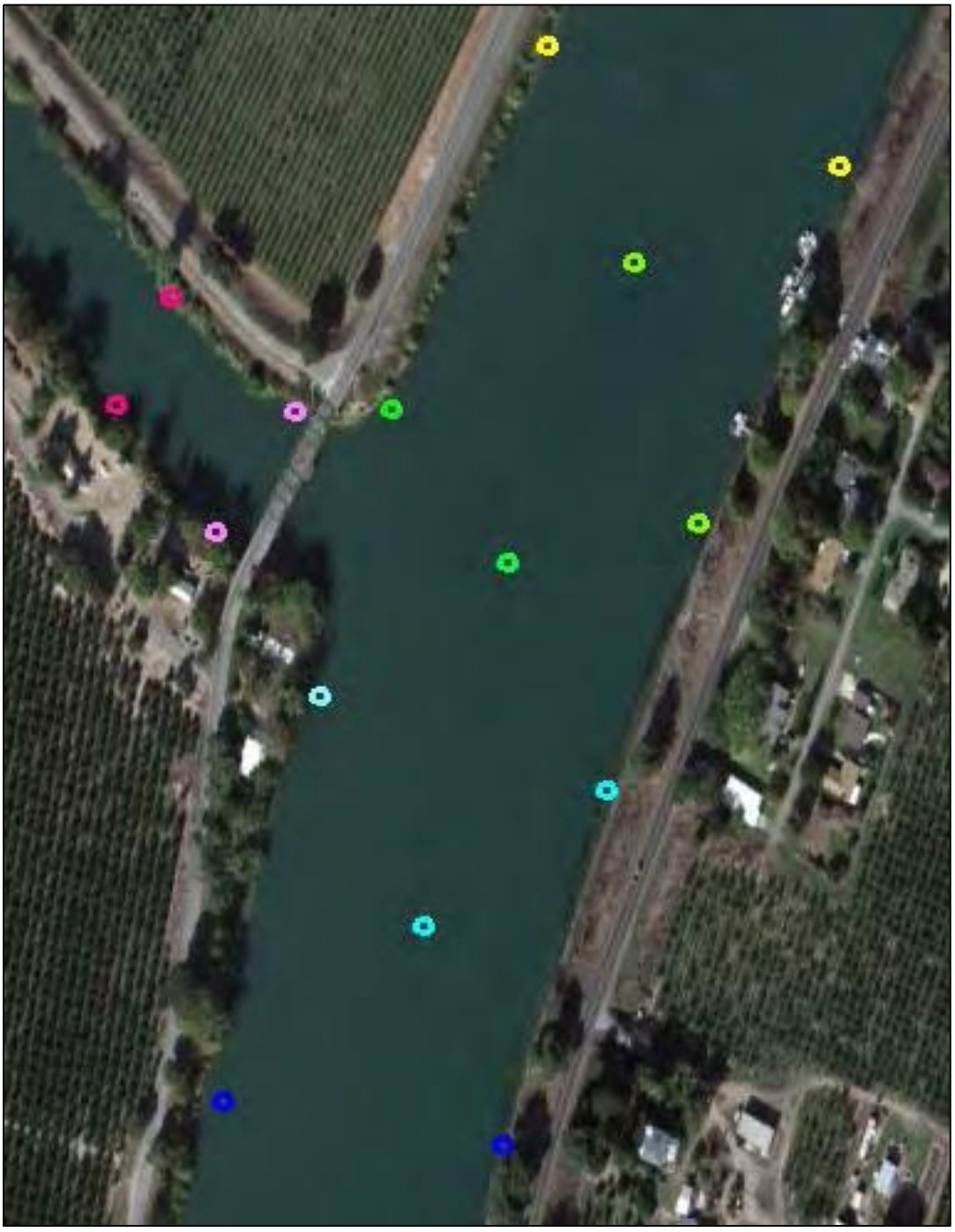

Note: The colors are only used to identify individual hydrophones and have no other significance. N=15.

Figure 2-7 Peripheral Array Hydrophone Locations in the Sutter Slough Study Area

Bottom-Mounted Hydrophones

Several hydrophones in the behavioral arrays and also at peripheral sites were deployed on the river bottom. The type of bottom mount used was dependent on flow velocities and the position of the hydrophone relative to the shore. Tower mounts are large, heavy mounts that are used to minimize hydrophone movement after positioning (**Figure 2-8**). These types of mounts were used in offshore areas or other areas of high flow. Pound-in mounts are mounts with large stakes. They were used to mount hydrophones near shore (**Figure 2-9**). Hydrophones were attached to bracket plates, and then bolted to the mount frame. Cables were attached to the hydrophones and were secured to the mount frame with cable ties. Offshore tower mounts were deployed from a boat, using a winch (**Figure 2-8**). Near-shore pound-in mounts also were deployed from a boat.

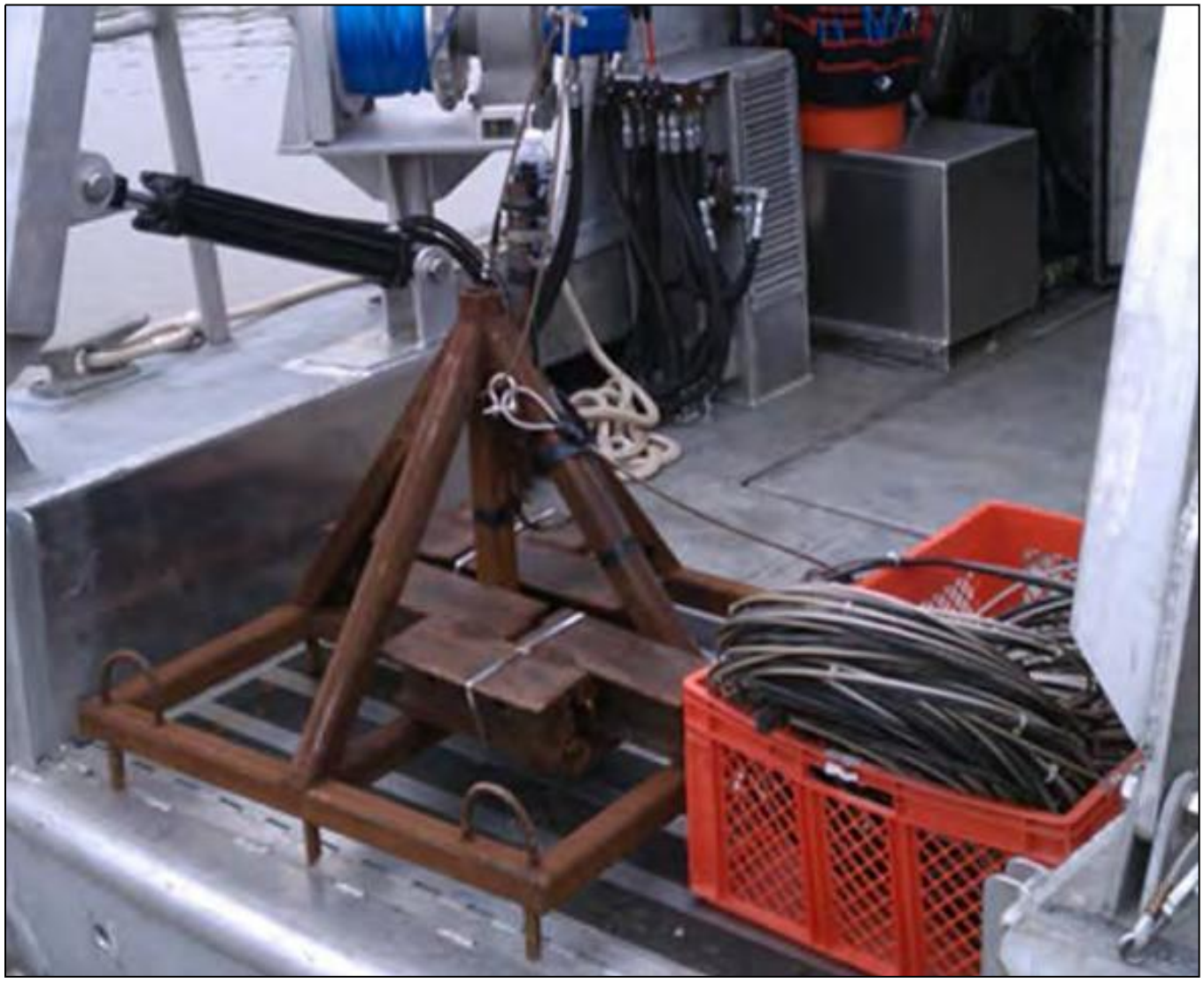

Source: HTI 2011

Figure 2-8 Typical Tower Mount

Source: HTI 2011

Figure 2-9 Typical "Pound-In" Bottom-Mount

Surface-Mounted Hydrophones

Surface-mounted hydrophones were attached to existing underwater structures, such as docks and pilings. Dock mounts were used and were attached to underwater structures where available (**Figure 2-10**). Floating pile mounts also were used at selected piles, to allow varying surface positions associated with changes in water stage elevation (**Figure 2-11**).

Source: HTI 2011

Figure 2-10 Typical Dock Mount

Source: USGS 2011

Figure 2-11 Typical Floating Pile Mount

Peripheral Hydrophones

Peripheral hydrophones were attached to self-contained receivers that could be accessed remotely using cell modems and an Internet-based file upload and storage system. Receivers for the peripheral hydrophones were housed in secure structures, supplied with 12-volt direct current (DC) power from deep-cycle batteries. Batteries were charged with solar panels or 120-volt AC battery chargers where available. **Figure 2-1** shows the locations of the peripheral hydrophone sites (yellow boxes). An automated data downloading and storage system for the peripheral hydrophone sites was set up, operated, and maintained over the duration of the study period.

2.4.3 STUDY JUVENILE CHINOOK SALMON AND TAGGING

EXPERIMENTAL DESIGN OF FISH RELEASES

Juvenile Chinook salmon implanted with acoustic tags were released at two locations: the Sacramento River just downstream of the Tower Bridge in Sacramento; and Georgiana Slough at the Georgiana Slough Fishing Access located 5 km (3 mi) downstream from the Sacramento River and Georgiana Slough divergence (**Figure 2-1**). Two release locations were used to balance the study objectives of monitoring fish response to the FFGS and evaluating survival through the system. The Sacramento River release site at the Tower Bridge was the primary release location, where the majority of juvenile Chinook salmon were released. Georgiana Slough was designed as a supplemental release location, because fish released at this site would not encounter the FFGS but would allow the analysis of juvenile Chinook salmon survival through the Delta via this route.

Tagged juvenile Chinook salmon were released throughout day and night periods at both release locations. As previously described, a variety of factors may affect the behavior of juvenile Chinook salmon released into the Sacramento River. Among these factors are river flows and tidal hydrodynamics that vary daily, in response to ebb and flood tidal conditions and the magnitude of Sacramento River flows. The migratory behavior of juvenile Chinook salmon also may vary throughout the day/night cycle. To address these factors, tagged juvenile Chinook salmon were released at regular intervals throughout the day/night cycle and the study period. Small subgroups of about 12 to 14 tagged juvenile Chinook salmon were released every 3 hours at the Tower Bridge location on each study release date, resulting in eight subgroups daily (i.e., midnight, 3 a.m., 6 a.m., 9 a.m., noon, 3 p.m., 6 p.m., and 9 p.m.). Four subgroups, with 3 to 4 tagged juvenile Chinook salmon each, were released at 9 a.m., 3 p.m., 9 p.m., and 3 a.m. daily at Georgiana Slough. The continuous release of tagged fish allowed study fish to be exposed to day and night conditions, and to flood and ebb tidal conditions, under a variety of Sacramento River discharges throughout the study period.

STUDY FISH

The 2014 GSFFGS Study used juvenile late fall-run Chinook salmon that were reared at the U.S. Fish and Wildlife Service's (USFWS) Coleman National Fish Hatchery located in Anderson, California. Ration level and holding conditions in the hatchery before tagging were managed, to the extent possible, to produce Chinook salmon ranging in size from 110 to 140 mm FL. Late fall-run Chinook salmon had a size range greater than that of the fall-run, winter-run, and spring-run Chinook salmon that migrate past the mouth of Georgiana Slough in spring (Vogel and Marine 1991). Study fish were held at the hatchery compound throughout the study, and small groups were transported (typically 160 fish for regular tagging operations; 250 when additional fish were transported for tagging as part of the fish tagging effects study) to the tagging location daily to meet tagging requirements.

TAGGING LOCATION

Study fish holding and tagging operations were conducted on a houseboat moored in Sacramento, directly downstream from the Tower Bridge on the Sacramento River upstream from the FFGS. All study fish, regardless of release site, were tagged at the Sacramento site. The location and configuration of the tagging operation were selected to: 1) allow fish to be held in Sacramento River water both before and after tagging; 2) facilitate the delivery of untagged fish from the hatchery; 3) facilitate the loading and transport of tagged study fish to the Georgina Slough release site; and 4) facilitate the release of tagged fish at the Sacramento release site with minimal handling. The houseboat and the supporting dock structure to which it was moored met these objectives and provided an effective and safe work platform (**Figure 2-12**).

Figure 2-12 **Study Fish Holding and Tagging Facility on the Sacramento River, downstream from the Tower Bridge, City of Sacramento**

TAGGING SCHEDULE

Releases of tagged juvenile Chinook salmon began on March 1, after the FFGS and monitoring equipment had been installed and tested. Juvenile Chinook salmon releases continued daily until April 15 (**Appendix A**, "Fish Summary Statistics"). The daily tagging schedule was designed to minimize the variability in holding times for both the period before tagging (hereafter referred to as pre-tag holding) and the period after tagging (hereafter referred to as post-tag holding) for the twelve subgroups of study fish released within each 24-hour period at the two study release sites. The limits of pre-tag and post-tag holding times were defined by the standard operating procedure (SOP) used for fish handling and tagging (**Appendix B**, "Summary of Standard Operating Procedures"). Two tagging sessions (six subgroups per session) were implemented each day to minimize variability in holding times. A morning session (between 8 a.m. and about 1 p.m.) was used to tag the 9 a.m., noon, 3 p.m., and 6 p.m. Sacramento release groups, and the 9 a.m. and 3 p.m. Georgiana Slough release groups.

An afternoon session (between 2 and about 7 p.m.) was used to tag the 9 p.m., midnight, 3 a.m., and 6 a.m. Sacramento release groups, and the 9 p.m. and 3 a.m. Georgiana Slough groups.

TRANSPORT TO TAGGING LOCATION AND FISH HOLDING

Groups of juvenile Chinook salmon were transported daily from the hatchery to the tagging location. The transport system consisted of 2-3 portable, 265-liter insulated tanks, mounted on frames with dollies. The tanks were secured in the bed of a truck, and oxygen cylinders, regulators, and diffusers provided aeration to the fish during transport.

Transport operations began at approximately 7 a.m. at the hatchery, in an effort to complete the 3 to 4-hour transport to the tagging location to minimize risk of increased water temperatures. The insulated tanks were filled with water from the hatchery (mean temperature of 10.7 degrees Celsius [°C]) located along the Sacramento River, and non-iodized salt was added to achieve a working concentration of 5 to 7 parts per thousand, to reduce osmotic stress. Oxygen was supplied to each tank through diffusers, to maintain dissolved oxygen concentration near saturation throughout the transport. Approximately 80 fish were loaded into each of the 265-liter (70 gallon) tanks at a conservative loading density (less than 20 grams per liter), based on accepted hatchery transport guidelines for the transport of hatchery-produced juvenile salmonids and the fish transport SOP (Piper et al. 1982).

Rations were withheld from fish on the day before transport, to reduce stress during transport, handling, and subsequent surgical implantation procedures (Liedtke and Wargo-Rub 2012). To allow the bulk of the study fish to maintain a normal feeding regime, groups of fish to be transported were isolated in perforated 76-liter containers at the head of the raceway about 24 hours before transport. Approximately 150 to 160 juvenile Chinook salmon were transported daily, distributed approximately equally across the 2-3 transport tanks. The number of study fish transported on each date was based on the requirements of the tagging operation for the following day, with additional fish to allow selection based on condition and/or size.

Water temperature, salinity, and dissolved oxygen concentrations in the transport tanks were monitored at the hatchery, during the transport, and on arrival at the tagging location, as directed by the SOP for fish transport operations.

On arrival at the tagging location, the transport tanks were unloaded from the truck and were rolled down to the dock next to the moored houseboat. Water temperatures in the tanks were measured and were compared to the water temperature of the Sacramento River at the tagging location. If the difference in water temperature between the tanks and the Sacramento River was more than 2°C, a tempering procedure was initiated. Sacramento River water was added to the tanks to adjust the water temperature at a rate of about 5°C per hour until the water temperature differential was within 2°C. After the water temperature in the tanks was within 2°C of the river temperature a hose was attached to the inflow valve of each tank and river water was pumped through the tank to maintain water quality conditions (**Figure 2-13**).

Fish were held for 18 to 24 hours before tagging, to allow them to adjust to Sacramento River conditions and recover from handling and transport stress. Water temperature and dissolved oxygen concentration adjacent to the transport tanks were monitored regularly. The SOP for study fish transportation is provided in **Appendix B**, "Summary of Standard Operating Procedures."

Note: A hose was connected to the inflow valve to provide flow-through river water during the pre-tag holding period.

Figure 2–13 Insulated 265-liter Transport Tanks Containing Untagged Fish Delivered from Coleman National Fish Hatchery

A total of 45 study fish transport events occurred during the study period. The mean change in water temperature in the transport tanks that occurred between the hatchery and the tagging location was less than or equal (≤) 0.3°C. The mean difference in water temperature between the transport tanks and the Sacramento River at the tagging location was 3.9°C, and 41 of the 45 transport events (91.1%) required some tempering to adjust water temperatures before allowing Sacramento River water to circulate through the tanks.

ACOUSTIC TAGS

Juvenile Chinook salmon were surgically implanted with one of two acoustic transmitters: HTI Model 900-LD or VEMCO V5 micro-acoustic tags (see also Section 2.5.2). The HTI tags had a dry weight of about 0.96 grams (g), and the VEMCO tags weighed 0.65 g in air. Study fish that weighed at least 13.0 g were implanted with VEMCO tags, and those that weighed at least 22.4 g were implanted with HTI tags. These minimum weight criteria were established so that the anticipated tag burden (defined as transmitter weight in air relative to fish weight in air) would be less than 5 percent of the fish body weight before tagging, following published recommendations (Adams et al. 1998; Martinelli et al. 1998; Liedtke et al. 2012). The mean tag burden for fish tagged with HTI tags was 2.9 percent (range: 2.4-3.5%). Fish tagged with VEMCO tags had a mean tag burden of 1.8 percent (range: 1.4-2.1%). Transmitters were activated and programmed on the morning of each tagging operation to maximize usable tag life. Before the tags were implanted into the study fish, each was checked to ensure that it was functioning properly.

SURGICAL IMPLANTATION PROCEDURES

Fish handling, holding, and tagging procedures were based on a well-established SOP developed for juvenile salmonids in the Columbia River Basin (Liedtke et al. 2012) and were modified to meet the experimental design of this evaluation. To limit the potential influence of individual taggers, three proficient taggers were used throughout the study period, rotating regularly to balance their contributions to the overall number of tagged study fish for each release site, tag type, and release time.

Aseptic procedures were used throughout the surgical implantation process (Liedtke and Wargo-Rub 2012). Following activation and programming, transmitters were disinfected in chlorhexidine diacetate solution for 20 minutes and were rinsed thoroughly with distilled water before being implanted. Following disinfection, transmitters were handled only with clean instruments or gloved hands. Surgical instruments were sterilized daily and were disinfected between individual surgical procedures. Taggers wore surgical gloves whenever handling study fish.

Study fish were anesthetized in 25 to 30 milligrams per liter AQUI-S® 20E to stage 4 anesthesia (Liedtke et al. 2012). The time in anesthesia was monitored for each fish and did not exceed 5 minutes. Fish were removed from anesthesia and weighed (to the nearest 0.1 g), were measured (FL to the nearest mm), and quickly were evaluated for general condition. Fish with obvious deformities or significant (greater than [>] 20% per side) scale loss were not selected for tagging. A surgical platform (i.e., V-shaped foam trough) was used to support fish with the ventral surface exposed while the gills were perfused with a maintenance dose of AQUI-S® 20E via a gravity feed system (**Figure 2-14**). An incision was made 2 to 3 mm anterior to the pelvic girdle and 2 to 3 mm away from and parallel to the midventral line, using a microsurgical scalpel. The incision was long enough to allow insertion of the transmitter without tearing the surrounding tissue (i.e., slightly longer than the diameter of the transmitter). The disinfected acoustic transmitter was inserted into the body cavity through the incision and the incision was closed using two simple interrupted sutures with 5/0 Vicryl® Plus suture material.

Figure 2-14 Foam Surgical Platform Supports Fish during Surgical Implantation of the Transmitter

Following the surgical procedure, study fish were transferred to a recovery container with a high concentration of dissolved oxygen (120 to 130%) to aid recovery from anesthesia. Study fish were held in recovery containers for a minimum of 10 minutes. The mean amount of air exposure time (from removal from anesthesia until placement in a recovery container) was less than 2 minutes. Full details of the fish handling and surgical procedures are provided in the SOP (see **Appendix B**, "Summary of Standard Operating Procedures").

POST-TAG HOLDING AND RECOVERY

After a minimum of 10 minutes in a recovery container, exposed to high concentration oxygen, study fish were transferred from the recovery container into a post-tag holding and release container (i.e., a 120-liter [32 gallon] perforated container). Following stocking, the holding and release containers were positioned in the Sacramento River to allow water exchange, and were secured to the dock near the houseboat. Each 3-hour release group was held in a separate container to facilitate release. The containers were supported by floating frames made of PVC pipe so that the upper quarter of the container was above the water. This configuration reduced the risk of study fish escape and provided access to the air-water interface which facilitates regaining neutral buoyancy prior to released (Liedtke and Wargo-Rub 2012; Liedtke et al. 2012). After placement into holding container, the fish were not handled again before release. Fish remained in the release containers for 18 to 30 hours after tagging.

TAG VERIFICATION

Two approaches were used to confirm that all study tags implanted into fish were functioning properly before fish release. The first approach involved using a hydrophone, positioned near the release containers. The hydrophone and corresponding receiver recorded the acoustic signals from the HTI and VEMCO transmitters in study fish held at the tagging location for the 18 to 30-hour, post-tag holding period. The second approach involved using two additional hydrophones, which were mounted in a trough on the dock. An individual release container was placed into the trough within 30 minutes of the planned release time, to confirm the operation of all (HTI and VEMCO) transmitters for that release (**Figure 2-15**). This redundant approach to tag verification allowed the detection of non-functioning tags before release.

Figure 2-15 Confirming Operation of Acoustic Transmitters before Release

STUDY FISH RELEASES

Immediately before release, the container holding the release subgroup was partially dewatered to visually observe the study fish. As part of the SOP, dead or moribund fish were removed from the release container, and transmitters were recovered and stored for evaluation and possible reuse.

For releases of study fish at Sacramento, release containers were lifted out of the tag verification trough and transferred into a boat for transport to the release site. The release location was immediately upstream from the Tower Bridge at the center of the Sacramento River channel. After the boat was in position at the release location, the container was positioned near the water's surface and was tipped so that the study fish could swim out of the container (**Figure 2-16**).

Study fish to be released in Georgiana Slough were transported by road from the Sacramento tagging location to the Georgiana Slough Fishing Access release site located 5 km (3 mi) downstream from the divergence from the Sacramento River. Tag verification was performed at the Sacramento site approximately 3 hours before the planned release time for these groups to accommodate the transit. Following tag verification, the release containers were loaded into an insulated 1,135 liter-capacity (300 gallon) transport tank filled with Sacramento River water that was mounted on a trailer (**Figure 2-17**). During the approximately 1-hour transport, the tank was aerated using oxygen cylinders, regulators, and diffusers to maintain dissolved oxygen levels near saturation. Immediately before the scheduled release time, the container was removed from the insulated tank and placed into the Sacramento River, near the shoreline, and was tipped to allow study fish to exit the container. Transfers of study fish between water sources (i.e., between the Sacramento River and the transport tank, between the transport tank and Georgiana Slough) were managed by tempering when the differences in water temperature were more than 2°C. Study fish were transported between the Sacramento tagging barge and Georgiana Slough four times each study day so that each release group experienced similar pre-tag and post-tag holding at the tagging location.

Figure 2-16 **Releasing Tagged Study Fish on the Sacramento River Upstream from the Tower Bridge, Sacramento, California**

Figure 2-17 Insulated Transport Tank

SUMMARY OF RELEASED TAGGED STUDY FISH

In total, 46 groups of juvenile Chinook salmon (5,461) were surgically implanted with acoustic transmitters during the study period. The 4,635 study fish released in the Sacramento River had a mean FL of 157 mm (range: 109-213 mm) and a mean weight of 41.8 g (range: 13.3-112.0 g) (**Appendix A**, "Fish Summary Statistics"). The 826 study fish released in Georgiana Slough had a mean FL of 157 mm (range: 113-204 mm) and a mean weight of 41.7 g (range: 14.2-93.1 g) (**Appendix A**, "Fish Summary Statistics").

TAG RETENTION AND FISH HEALTH STUDIES

To evaluate tag retention, tagger proficiency, and potential transmitter effects on fish performance, groups of tagged study fish were held in tanks and evaluated 30 days post-tagging. The tank studies were conducted at the California–Nevada Fish Health Laboratory. Detailed procedures and findings are provided in **Appendix C**, "Fish Tagging Effects Study."

2.4.4 STUDY PREDATORY FISHES AND TAGGING

A number of predatory fish species are known to reside year-round in the vicinity of the study area, including striped bass *(Morone saxatilis*), smallmouth bass (*Micropterus dolomieu*), largemouth bass (*Micropterus salmoides*), and spotted bass (*Micropterus punctulatus*). Previous field studies have shown evidence of predation on juvenile salmonids in the Delta, including predation at the non-physical barrier in the lower San Joaquin River at the Head of River (Nobriga and Feyrer 2007; Hanson 2009; Bowen and Bark 2010; Bowen et al. 2012). Details of the study of predatory fishes and predation in relation to the FFGS are provided in Section 3.6, "Predatory Fishes and Predation".

TARGET SPECIES AND SAMPLE SIZE

Based on results from the 2011 and 2012 Georgiana Slough BAFF predatory fishes studies (DWR 2012, 2015b), the target species for acoustic tagging in 2014 were striped bass, smallmouth bass, and spotted bass. Given the particular statistical analyses to be undertaken for the 2014 predatory fishes investigations, it is more desirable to have tags concentrated within a few more commonly collected predatory species in order to make stronger inferences for these species rather than applying tags to more uncommon species for which the ultimate sample size may be insufficient to generate useful information. The target tagging sample size was 200 predatory fishes. Current information and data describing predatory fish community structure within the study area were unavailable. Historical sampling data were used to determine tagging proportions among target species such that the tagged sample approximates the natural predator community structure within the study area. Tagging proportions were based on sampling data collected by the California Department of Fish and Game (DFG) from 1995-1999 in Taylor Slough, Steamboat Slough, the Sacramento River at Threemile Slough and at Paintersville, and the San Joaquin River at Bradford Island. Based on these data, the target tagging sample size for each target species was selected (**Table 2-3**).

Table 2-3 Target Tagging Proportions for each Predatory Fish Species for the 2014 Georgiana Slough Floating Fish Guidance Structure Performance Evaluation Predatory Fishes Study

	Striped Bass	Smallmouth Bass	Spotted Bass	Target Sample Size
Target Proportions	40% (80)	30% (60)	30% (60)	200

Sampling and tagging of predatory fishes occurred throughout the study period to account for: 1) the potential of tagging fish that may migrate outside of the study area; and 2) the wide range of environmental conditions study fish will encounter. A small group of predatory fishes was tagged, released, and monitored prior to the first release of tagged juvenile Chinook salmon. The pre-project sampling and tagging schedule provided a broad framework for the study duration. However, under an adaptive approach the schedule was flexible and changed based on various factors including: weather conditions, the number of tagged predators within the study area at any one point in time, sampling and tagging success, and the amount of time tagged fish stayed within the detection range of the acoustic detection and monitoring arrays. There were a total of 27 predatory fishes sampling days. Twenty of these days included both roving hook-and-line angling and standardized angling (each approximately 4 hours long for an approximate 8 hours of on-water angling). The remaining 7 sampling days consisted strictly of roving hook-and-line angling (approximately 8-hours of on-water angling).

PREDATORY FISHES CAPTURE METHODOLOGY

There were two components to the predatory fishes sampling: 1) standard roving hook-and-line angling; and 2) standardized angling. During both components, predatory fishes were captured via hook-and-line using bait

and artificial lures; every capture was a candidate for acoustic tagging. Circle hooks were used during bait fishing to minimize hooking injuries. Landing nets were not used to avoid associated injuries and maintain tagging candidates in the best possible condition. Captured predatory fishes having hooking or other injuries and/or displaying obvious abnormal behavior were immediately released and were not tagged. Sampling was confined to a one-mile radius (**Figure 2-18**) from the behavioral study array. However, every effort was made to capture predators within the study area to address concerns of introducing predators to the study area. Predatory fishes were collected outside of the one-mile radius only if a sufficient number of predatory fishes were not collected in a one-mile radius of the study area.

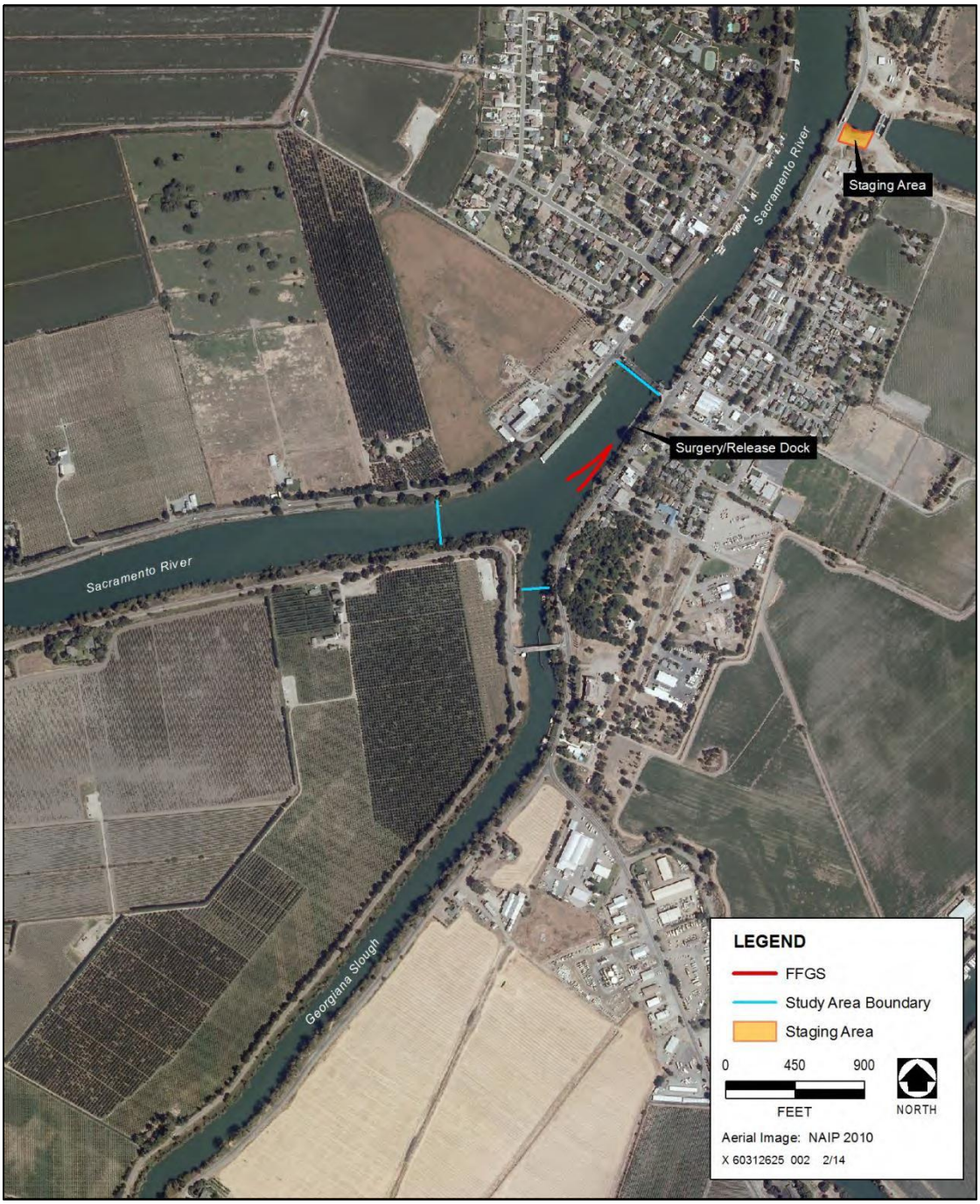

Figure 2-18 **One-mile Sampling Boundaries for the 2014 Georgiana Slough Floating Fish Guidance Structure Performance Evaluation Predatory Fishes**

Eight crew members participated during each sample day. AECOM, Fishery Foundation of California, and DWR each provide one boat and two anglers on each sample day. In addition, AECOM and Cramer Fish Sciences each provide one person to staff the surgery station which was located at the release dock (i.e., Boon Dox) (**Figure 2-19**). The two crew members stationed at the release dock were responsible for receiving and caring for fish, surgeries, post-surgery care and release, and hook-and-line sampling when other responsibilities allowed. The roving fishing crews were responsible for capturing predatory fishes and transporting them to the release dock (except when angling during standardized angling efforts), and assisting the release dock crew when appropriate.

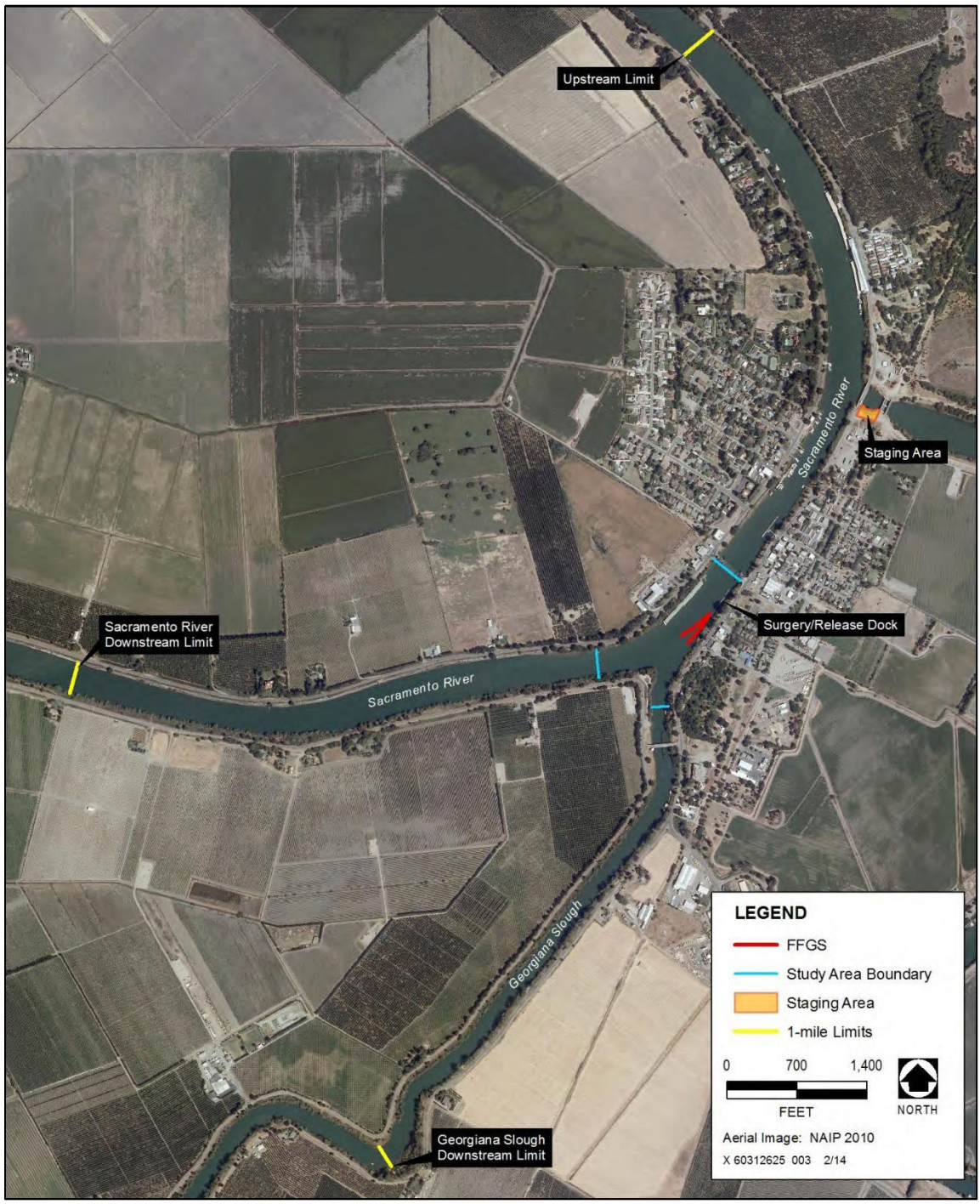

Figure 2-19 **Points of Interest for the 2014 Georgiana Slough Floating Fish Guidance Structure Performance Evaluation Predatory Fishes**

Capture datasheets were filled out immediately after a predatory fish was captured, including logging capture location using GPS. Each predator was given a capture number on the capture datasheet and this number was used to name the point file for capture location. Each crew sequentially numbered their captures among all sample days, and this applied regardless of whether conducting roving hook-and-line angling or standardized angling. For example, if the AECOM crew ended a sample day by catching fish number 72, the first capture on the next sample day will be capture number 73. The format of the capture location point file was GS14***** where the first three placeholders represent associated capture number and the last two placeholders represent the capture crew. AECOM capture crews used AC, Fishery Foundation crews used FF, and DWR used DR. For example, the point file for the first fish of the study captured by the DWR sampling crew will be named GS14001DR, and the capture number assigned was 001DR. Captures that occur from the surgery/release dock did not require a GPS point file for capture location, but the capture numbering scheme was identical, as described previously, with the acronym SC used. Additional information was filled out on the capture datasheets for each predator selected for tagging, including sample number (this number was provided by the crew staffing the surgery station). This approach provided information for all captures and allowed capture crews to monitor the number and species composition of all tagged fish. After a predator was implanted with an acoustic tag at the surgery station the tag code and sample number was logged in the capture datasheet linking tag code to capture location. Therefore, it was necessary to be able to identify each individual between the time of capture and the time of tagging. Total length (TL) and FL (mm), weight in pounds (lb) to two decimal places, and species were recorded immediately after capture to identify individuals. This approach eliminated having to mark or attach a numbered culling buoy to each individual thus avoiding marking injuries that may affect post-release survival and normal behavior. The assumption was that it was highly unlikely that the same predatory fish having identical lengths and weights would be recaptured prior to having to take all captures being held in the capture boats livewells to the surgery station. All tagged predatory fishes were released within the study area at the most upstream tip of the release dock (**Figure 2-19**). All predatory fishes of sufficient size to effectively prey on the juvenile Chinook salmon were eligible for tagging. Gape size and not fish length generally dictates the size range of prey a predatory fish is able to prey upon. The length based tagging criterion differs among predatory species because gape limitations differ among species. The minimum tagging length for target species was approximately 300 mm TL for smallmouth and spotted basses and approximately 360 TL mm for striped bass. An effort was made to capture and tag fish throughout a range of lengths such that the length range of the tagged sample approximates the length range of predatory fish species utilizing the study area.

Each roving boat was equipped with a large 568 liter (150 gallon) cooler modified to function as a livewell (i.e., large enough to accommodate a large striped bass comfortably; manufacturer provided livewells do not meet this criterion) and outfitted with a re-circulating pump and spray bar. The livewell was filled with river water using a bilge pump and hose. On each sample day, a minimum of six in-river livewells were also attached to the release dock. These livewells were used to hold fish before and after surgery, and to keep track of individual fish. The in-river livewells consisted of uniquely numbered, large, plastic storage containers modified with a polyvinyl chloride (PVC) collar for flotation. Holes were drilled in the sides of the containers to allow water to flow through them when they were placed in the Sacramento River.

SURGICAL TAG IMPLANTATION METHODOLOGY

A mobile surgery station was assembled on each sample day on the surgery/release dock. The location was stable, provided shade, was easily accessible from land, provided adequate parking, and provided crew members access to food, beverages, and a restroom. An HTI representative delivered approximately 30 activated acoustic tags and code out datasheets to the surgery station once per week the morning of the first sample day of each sample week and prior to the beginning of predatory fishes capture efforts. Captured predatory fishes were transferred from the fishing boat livewell in a 18.9 liter (5 gallon) bucket of water and placed in one of the in-river livewells that

received a continuous supply of water from the Sacramento River. Each floating livewell was attached to the release dock and was clearly marked with a unique number to identify individual fish.

The physical environment implantation surgeries are performed is an important component that determines the quality and success of the procedure. The surgical environment was maintained in a sterile condition throughout all procedures. The surgical station was intermittently cleaned and wiped down with a solution of disinfectant; surgical instruments were placed in a disinfectant bath (i.e., dilute Novalsan S, chlorhexidine solution) before and after surgical procedures. Surgical instruments were transferred to a freshwater rinse bath before surgery. All equipment used for capture, holding, anesthesia, surgery, recovery, and movement of fish during the project were thoroughly cleaned and disinfected to minimize the potential for pathogen transfer among fish populations.

Predatory fishes were transported from the in-river livewells to the surgery station in 18.9 liter (5 gallon) buckets containing fresh water and placed in a large, surgery station livewell (identical to the fishing boat livewell) containing aerated water and AQUI-S® 20E. The oxygen level within the surgery station livewell was maintained near saturation via a diffuser and approximately 7-10 g of salt was added per liter of water. Maintaining the oxygen level near saturation in the surgery station livewell potentially results in higher blood oxygen levels during anesthesia which aids in post- surgery recovery (Itazawa and Takeda 1982). Iwama and Ackerman (1994) suggested adding small amounts of salt to reduce gill irritation and help control blood hematology and chemistry. There are five commonly defined stages of anesthesia including: 1) onset; 2) sedation; 3) general anesthesia; 4) induction (surgical anesthesia); and 5) death (Sladky et al. 2001; Coyle et al. 2004). Complete induction is attained within 3 to 5 minutes following immersion in the AQUI-S® 20E bath. Anesthetized fish were removed from the immersion bath shortly after attaining full surgical anesthesia and placed in a wet fish holding cradle. Each fish was inspected for anomalies (e.g., general condition of eyes, scales, and fins) and general health; unfit individuals were rejected for tagging. Surgical tag implantation was begun immediately after placement in the fish cradle and lasted approximately 2 to 3 minutes. During the first two minutes of surgery, anesthetic solution was continuously flushed across the gill membranes to maintain induction, provide oxygen, and remove metabolic wastes. After two minutes, fresh water was introduced and flushed across gill membranes to facilitate rapid recovery before fish transfer to a freshwater recovery bath and in-river livewells.

A 10- to 12-mm (0.4-0.5 in) incision was made parallel to but offset by approximately 2 mm (0.08 in) from the ventral midline anterior to the pelvic girdle (**Figure 2-20**). The incision was made under the scale plating to ensure the incision is made with a single fluid motion. Incisions made by repeatedly scoring tissue results in scar tissue formation and prolonged healing. A sterilized HTI Model 795 Lg Micro Acoustic tag (tag life is approximately 90 to 130 days) was inserted into the peritoneal cavity of the fish and positioned immediately under the incision. The incision will be closed with two simple interrupted sutures using a 26-mm (1.0-in) (FS-1) reverse cutting, 3/8” circle needle with 3/0 monofilament suture material. Placing the needle under the scale plating before puncturing the skin will aid with suture placement and improve efficacy. Following completion of the sutures, slime will be introduced to the wound from adjacent areas of the fish as a disinfecting measure. Iodophores and other disinfectants can damage cells and inhibit localized healing; the natural slime coat can effectively promote wound healing without the use of pharmaceuticals.

Figure 2-20 **Image Shows Incision Location for Acoustic Tag Insertion for the 2014 Georgiana Slough Floating Fish Guidance Structure Performance Evaluation Predatory Fish Study**

Immediately after surgery completion, fish were placed in PVC recovery tubes submerged in post-surgery livewells (identical to the fishing boat livewell) containing fresh water saturated with oxygen. The post-surgery recovery livewells were located adjacent to the surgery station. Fish were removed from the recovery tubes after approximately 10 minutes, but kept in the post-surgery recovery livewell until they exhibit normal behavior. Individuals exhibiting normal behavior were transferred to an in-river livewell for approximately 30 minutes to be monitored before being released into the Sacramento River. At any time during the recovery period, individuals exhibiting impaired behavior were dispatched for tag retrieval. Post-surgery datasheets were carefully filled out with particular attention paid to the time each tagged fish was placed in the in-river livewell and the time they are released into the Sacramento River; these data are important for post-project data analysis.

FISH ANESTHETIC

AQUI-S® 20E was used as a fish anesthetic for surgery procedures. The U.S. Food and Drug Administration (FDA) has granted amended authorization for the use of AQUI-S®20E, a sedative drug, to allow for the immediate release of freshwater finfish sedated as part of field-based fisheries studies. The amended authorization comes under the USFWS's Aquatic Animal Drug Approval Partnership (USFWS-AADAP) Investigational New Animal Drug (INAD) 11-741. The 2014 GSFFGS Study is enrolled in the AQUI-S® 20E INAD program. As a program participant, all project personnel involved in the use of AQUI-S® 20E must comply with the requirements as set forth in the INAD Study Protocol for AQUI-S® 20E. More information on this protocol is found at http://www.fws.gov/fisheries/aadap/aquis-e.

2.5 STANDARDIZED ANGLING

The objective of standardized angling is to compare catch rates of predatory fish species (i.e., striped bass, smallmouth bass, and spotted bass) within the vicinity of the FFGS study area between the FFGS On/operating and the FFGS Off/not operating conditions. The study design accounts for temporal differences in catch rate, as influenced by many factors, by sampling throughout the study period. Standardized angling areas (SAA) were established within the study area. The FFGS footprint constitutes the main area of interest. The FFGS SAA consists of a polygon encompassing an area within 6.1 m (20 ft) of the offshore side of the FFGS and encompassing all water between the FFGS and the left bank of the Sacramento River. Waters within this polygon are likely to have changed velocity fields as a result of installation of the FFGS. Three reference SAAs were also be established within the study area. The FFGS footprint, which includes the FFGS SAA, has high catch rates of predatory fishes based on hook-and-line sampling from the 2011 and 2012 studies. Therefore, reference SAA locations were selected based on high catch rates during prior sampling to control for differences in predatory fish densities throughout the study area. The four SAAs are shown in **Figure 2-21**.

Twenty standardized angling events were conducted throughout the study period. A sampling event consists of one 4-hour hook-and-line sampling period. Two fishing boats, each having two crew members, were responsible for hook-and-line angling during each standardized angling event (i.e., fishing within the designated SAA polygon). A third fishing boat staffed with two anglers was present during each standardized angling event with the responsibility of roving hook-and-line angling and transporting fish caught within the SAA polygons to the surgery station at the release dock. To the extent possible, sampling events were evenly spread throughout the duration of the study period. Each 4-hour standardized angling sampling event was divided into 2 two-hour angling sessions. During each session, one crew (consisting of two anglers in one boat) fished one SAA polygon while the second crew simultaneously fished another SAA polygon. SAA 3 and SAA 1 were always be fished simultaneously and the FFGS SAA and SAA 2 were always be fished simultaneously. A total of 20 standardized angling events were conducted: 10 during the FFGS On/operating treatment and 10 during the FFGS Off/not operating treatment. Prior to and/or after each standardized angling event, crews in the three boats conducted roving hook-and-line sampling.

Appropriate time periods to conduct standardized angling were based on maximizing catch rates. Fish behavior and activity periods, including feeding, are influenced by many factors, particularly in lotic, tidally-influenced systems like the study area. However, activity levels in the study area, as reflected by hook-and-line catch rates in prior studies, are most influenced by tidal stage. In particular, fish activity and catch rates appear to be highest from approximately one hour after high tide to slack low tide (S. Pagliughi, AECOM, personal observations).

Therefore, in an attempt to maximize catch rates, standardized angling events were scheduled to occur within the period from one hour after high tide to slack low tide. Standardizing the tidal stage sampled controls for the effects from tidal stage on fish activity. The study area experiences a mixed tide with two uneven tides per day. The amount of time between peak high tides is approximately 11 hours. Therefore, this interval provided ample opportunity for scheduling each 4-hour standardized angling event during approximately the same tidal stage. Tidal stage within the study area was determined by using tidal predictions from stage gauges on the Mokelumne River at the confluence with Georgiana Slough and at Clarksburg (http://www.deltaboating.com/tides/tidesac.html).

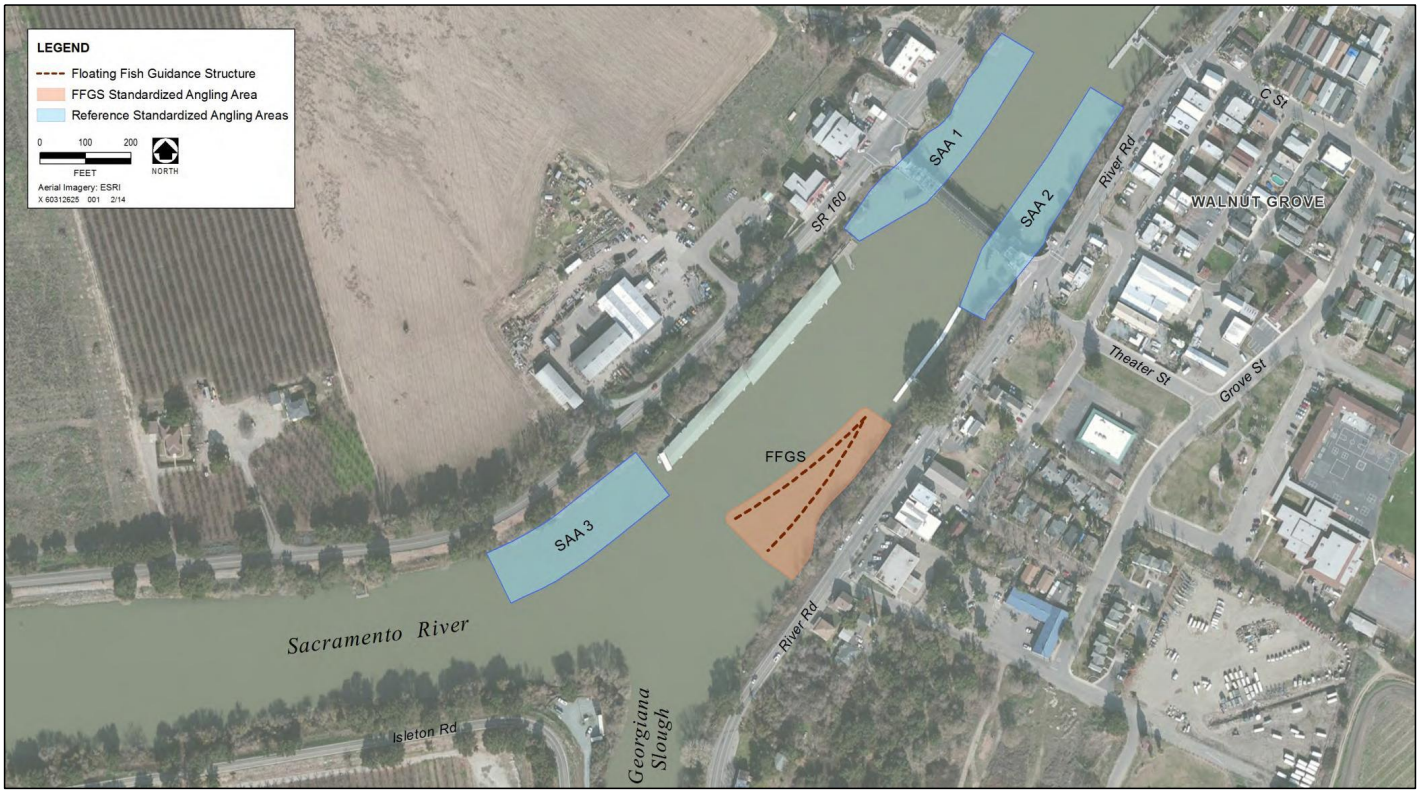

Figure 2-21 **Location of the Standardized Angling Areas (SAA) for the 2014 Georgiana Slough Floating Fish Guidance Structure Performance Evaluation Predatory Fishes Study**

Angling techniques were species-specific. Standardized techniques were employed during each 2 two-hour angling session to control for variation in catch rates among species resulting from angling technique. During each session, one hour was spent fishing artificial lures which targets striped bass, smallmouth bass, and spotted bass, and one hour was spent fishing dead bait which targets striped bass. The order in which each technique is employed was randomly selected for each angling session, but the same technique was employed at the same time in both polygons being fished.

A datasheet for standardized angling was developed and it was different than the datasheet used during the roving hook-and-line predatory fishes sampling events. Fish captured during standardized angling were retained for acoustic tagging and were transported to the surgery station by the third fishing boat or released following collection of capture data (i.e., species, length, weight, etc.). Effort (start and stop time for each session) and location (SAA), as well as other pertinent observations such as weather conditions and type of technique used also were recorded. A capture number and a tagging sample number (if retained for tagging) was assigned to predatory fishes captured during the hook-and-line sampling events (i.e., each fish captured received a capture number and each fish tagged received a sample number). During standardized angling events, capture number was consistent and sequential for each crew with the capture number from the hook-and-line sampling events; captured fish selected for tagging during standardized angling were assigned a tagging sample number that was consistent and sequential with the tagging sample numbers assigned during the hook-and-line sampling events. Fishing crews were not able to assign the tagging sample number to a capture; this number was provided by the surgery crew.

2.6 MONITORING AND DATA COLLECTION

This section describes the monitoring and data collection procedures.

2.6.1 ENVIRONMENTAL CONDITIONS MONITORING

Several variables were monitored during the GSFFGS Study to document environmental and other conditions that could influence the ultimate fate of the study fishes.

SACRAMENTO RIVER AND GEORGIANA SLOUGH HYDROLOGY AND WATER QUALITY

The U.S. Geological Survey (USGS) maintains a network of flow monitoring and water quality gauges in the Sacramento River and Georgiana Slough. A gauge is located in the Sacramento River upstream from Walnut Grove (Station SDC), in the Sacramento River below Georgiana Slough (Station GES), and in Georgiana Slough at the Sacramento River divergence (Station GSS). Data from these monitoring locations were used to characterize the hydrologic and water quality conditions in the study area throughout the study period. Information characterizing each station is provided in **Table 2-4**. Stage, discharge (flow), water temperature, turbidity, and conductivity data were collected at 15-minute intervals from March 1 through May 31, 2014.

HYDRODYNAMICS

Two types of complementary hydrodynamic measurements were made to document the temporal changes in the velocity field on the Sacramento River side of the FFGS: 1) Eulerian (fixed position) sideward-looking acoustic Doppler current profilers (SL-ADCPs); and 2) Lagrangian measurements (i.e., drifters).

Table 2-4	Discharge and Water Quality Stations Close to the GSFFGS Study Area		
Attribute	Station Code		
	SDC	GES	GSS
River Basin	Sacramento River	Sacramento River	Sacramento River
Hydrologic Area	Sacramento River	Sacramento River	Sacramento River
County	Sacramento	Sacramento	Sacramento
Nearby Town	Walnut Grove	Walnut Grove	Walnut Grove
Operator	USGS	USGS	USGS
Elevation	3 m (9.8 ft)	3 m (9.8 ft)	3 m (9.8 ft)
Latitude	38.257000°N	38.238900°N	38.237000°N
Longitude	121.518000°W	121.523400°W	121.518000°W
Full Name	Sacramento River Upstream of the DCC	Sacramento River Downstream of Georgiana Slough	Georgiana Slough at the Sacramento River Divergence

Eulerian Measurements

Six 600-kHz sideward-looking acoustic Doppler current profilers (SL-ADCPs) were deployed along the FFGS face. The pilings were driven in locations and SL-ADCPs were mounted in specific orientations to the flow to provide the maximum coverage under a variety of river discharges. All of the SL-ADCPs were mounted on buoys attached to pilings (**Figure 2-11**). These buoys allowed the SL-ADCPs to remain at a fixed depth below the water surface. Fixing the SL-ADCPs on the water-surface-following buoys allowed for continuous monitoring of the surface currents, where juvenile Chinook salmon outmigrants typically reside (Blake and Horn 2015a, b, in press) under a wide range of Sacramento River flows and surface water elevation levels.

Lagrangian Measurements

In collaboration with DWR, USGS documented the surface velocity field using surface-following drifters. These measurements were used to: 1) produce snapshots of surface current maps by interpolating velocities inferred from the drifter paths; and 2) calculate estimates of the location and shape of the critical streakline at the divergence (junction) of Georgiana Slough from the Sacramento River.

When Sacramento River flows were strongly uni-directional downstream, only a handful of drifter releases were made. However, during conditions where the flow field was substantially affected by the tides, drifters were deployed over an approximately 12-hour flood/ebb cycle to document a specific hydrologic condition (i.e., a specific Sacramento River flow).

For downstream flowing conditions, a number of drifters were placed across the upstream section as rapidly as possible (over an approximately 5 to 10-minute period). Releasing drifters rapidly is important because the velocity fields in waterway junctions can change rapidly with the tides and it is preferred to have all drifters experience, as near as possible, the same conditions (this is one of the reasons that the drifters used in this experiment were small). The spacing between drifters released was decreased near the critical streakline so that the position and shape of the critical streakline could be determined as accurately as possible. For converging river discharges, drifters were deployed in the Sacramento River both upstream and downstream from the

Georgiana Slough junction. Furthermore, for upstream flowing conditions, drifters were released downstream from the junction.

UNDERWATER LIGHT LEVELS

Continuous ambient light measurements were collected throughout the study at the houseboat stationed at Dagmar's Landing located on the right bank of the Sacramento River (**Figure 2-22**). The ambient light levels were collected to serve as representations of background light conditions occurring in the Sacramento River near the FFGS. Measurements were taken at a fixed 1-m (3.3 ft) depth below the water surface, using an LI-COR LI-192SA light sensor, and recorded using an LI-1400 datalogger. Data were recorded in photosynthetic photon flux units and then were converted manually to lux. Data values ≥5.4 lux were considered to represent light conditions, whereas data with values < 5.4 lux were considered representative of dark conditions. See Section 3.2, "Survival Model," for additional discussion on underwater light levels.

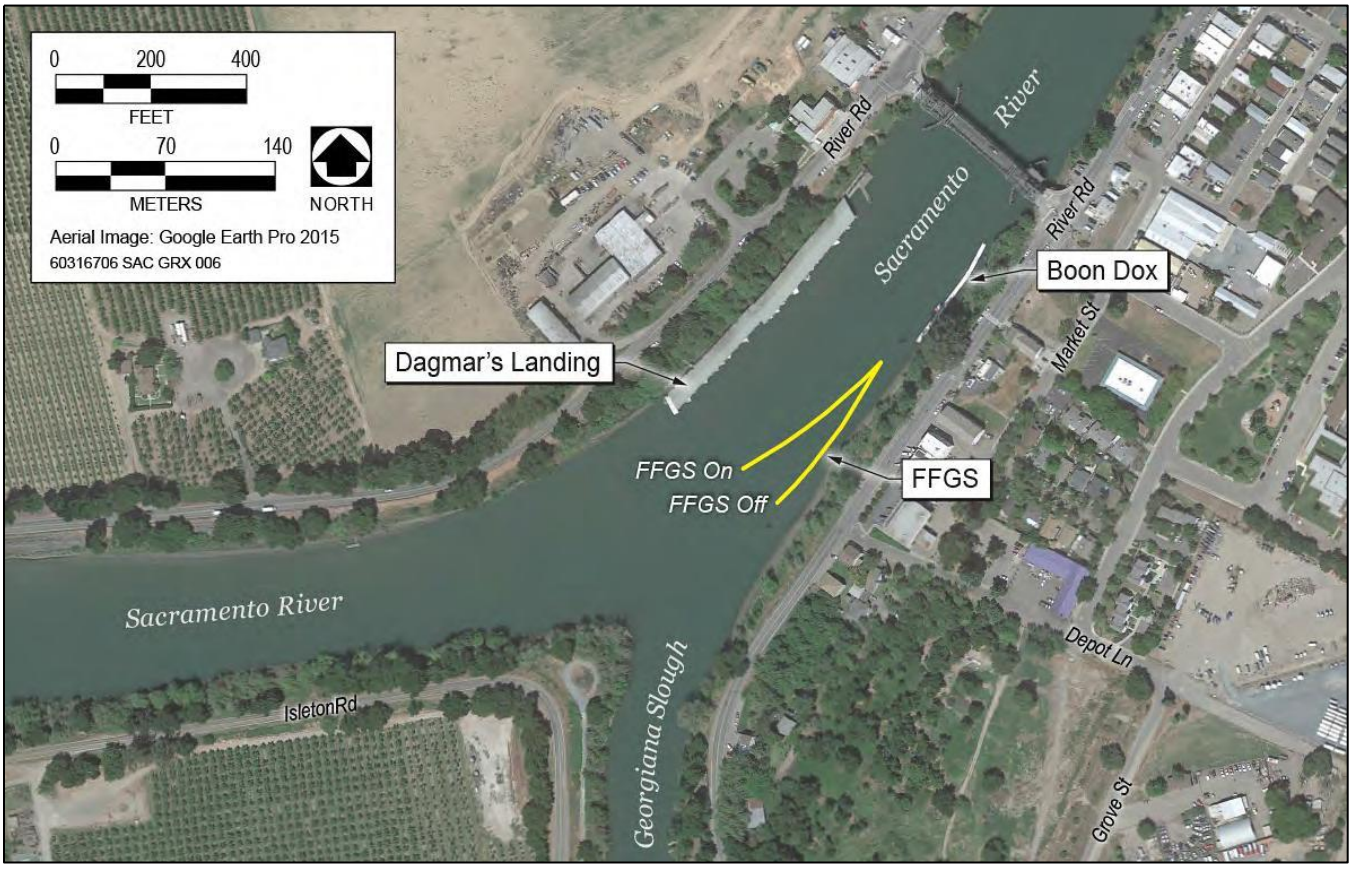

Figure 2-22 Dagmar's Landing

BATHYMETRIC DATA

In support of the 2014 GSFFGS Study DWR's North Central Region Office (NCRO) conducted two multibeam bathymetry data collection mini-projects of the Sacramento River and Georgiana Slough in the study area. The first survey was conducted on June 12 and July 3, 2013, prior to barrier construction. The second survey was conducted on June 16 and 17, 2014, after barrier deconstruction. Data were collected with equipment both on land and water and were positionally corrected with real-time kinematic (RTK) GPS to conform with the North

American Datum of 1983 (NAD83) California State Plane Zone II coordinate system and North American Vertical Datum of 1988 (NAVD 88).

Field calibration tests (including multibeam patch tests, sound velocity readings, and RTK GPS observations were regularly performed in order to ensure data quality and positional accuracy. Multibeam data were collected from a boat and recorded using Hypack® Hydrographic Survey software (Hypack, Inc.). Data were processed using either Caris or Hypack, exported as XYZ text files, and imported as a raster in a geodatabase using ArcGIS software. For more processing detail please refer to the "Data Quality Section" in the metadata associated with each data set.

NCRO's multibeam bathymetry and positioning systems are composed of the following items:

1. Multibeam Sonar Bathymetry System:

    - Sonic 2022 Broadband Multibeam Echosounder (R2Sonic, LLC);
    - POS MV™ Wavemaster II - Inertial Measurement Unit (Applanix™ Corporation);
    - Hydrographic Digibar Pro Profiling Sound Velocimeter (Teledyne Odom Hydrographic); and
    - Boat Model 2072 Flat (Oquawka Boats).

2. RTK Positioning System:

    - R-8 GNSS GPS System (Trimble Navigation Limited); and
    - Trimark™ 3 Radio Modem (Trimble Navigation Limited).

Data deliverables include geodatabases, XYZ text files, and the maps in Figures 2 thru 4 that detail channel bottom elevations. These datasets precisely describe the complex geometry of the channels and also provides an indication of the flow history, channel bottom material, and sediment movement. For instance, the relative lack of sand waves in the 2014 dataset near Georgiana Slough may be an indication of both low sediment supply and flow energy (both required for sand wave formation) from the ongoing drought conditions.

2.6.2 ACOUSTIC TAG DETECTION/MONITORING

During the study, acoustic data from tagged fish moving within study area were collected on four HTI 290 ATRs, one HTI 291 ATRs, and 12 HTI 395 dataloggers. To collect, process, and analyze the data in a timely manner, USGS used cloud computing services (Amazon Web Services [AWS]) to implement a series of automated computer processes. These processes enabled configuring each data collection device to automatically transmit data to central data collection servers via remote network connections using mobile broadband devices. The model 290 and 291 ATRs used USGS-developed software to automatically move data every hour to the collection servers. The model 395 dataloggers were configured as individual File Transfer Protocol (FTP) servers, with restricted access to prevent accidental data loss. The collection servers had USGS-developed software installed to continuously scan each datalogger and automatically pull data to the collection servers. Another USGS software application was used to automatically scan and compare data on the collection servers and duplicate all data to the AWS S3 data backup and recovery service. The AWS platform then was used to divide the processing burden among multiple detection events allowing much faster data processing. For example, at the peak of data processing and analysis, the AWS was used to run 500 simultaneous analyses of the USGS-developed software FishCount and GeneticFish.

QUALITY ASSURANCE/QUALITY CONTROL

A series of QA/QC steps were implemented to ensure data integrity. To achieve this, continuous monitoring for abnormalities was conducted for the structure of the incoming data files, power failures at the collection sites, and conductivity of the network used to transmit the data to the collecting servers. When a problem was detected, the software would send e-mail and text message notifications for alerts about the nature and severity of the problem. Although this automated process detected some of the potential problems that could lead to the loss of data, it was not able to detect all of the potential problems. Therefore, manual review of data collected at each of the sites was conducted approximately every 3 days. This review included determining whether the size of the data file was appropriate for the duration of time since the last manual inspection. A subsample of the data, usually a randomly selected 24-hour block, then was reviewed using HTI software MarkTags. This process was used to determine whether the signal detected from the tags had an acceptable number of quality detections that were in the proper voltage range for the tag. Whether the reference tag (also known as a beacon tag) that was deployed at the site was being detected and recorded in the data file was also determined. When problems in data quality and/or quantity were identified, they were corrected using remote access to the collection equipment via the broadband network, or field crews were dispatched as soon as possible to visit the site and correct the problems.

SYNCHRONIZING TIME BEFORE DATA PROCESSING

During the study period monitoring equipment was replaced periodically when hardware failed because of internal electronic problems, or when environmental conditions damaged the equipment. In addition, hardware was removed when software updates needed to be installed. During the replacement process it was necessary to adjust the internal central processing unit clocks so that they were synchronized with the other equipment deployed at other locations throughout the study area. Similarly, all of the clocks associated with the monitoring equipment needed to be set to account for daylight savings time. On several occasions the time was inadvertently set incorrectly when equipment was replaced. If the clocks were set incorrectly the data could not be merged automatically to form an accurate history of the moments of fish in the study area. To address this issue, a software process was developed to scan all *.RAT files and determine whether each file was within the correct time zone. This process compared the start and stop time at the beginning and end of the file (times that were generated by the computer clock) with the Coordinated Universal Time (UTC) GPS time stamp that was recorded every 30 seconds within the body of the *.RAT file. The start/stop time stamps and file names of data files that had incorrect times were adjusted to reflect the correct time zone and represent the correct local date and time. All of the raw data files were standardized to Pacific Daylight Time before echo selection; during the echo selection process all of the data were standardized to UTC and UTC was used for all data analyses.

All the monitoring equipment relied on the continuous GPS time stamp data recorded as a sync echo within the *.RAT files to synchronize the echo events received from the transmitters across multiple collection sites. Synchronizing detections across multiple individual monitoring sites allowed them to be merged into a single monitoring system. This enabled a more continuous history of the movements of fish to be recorded across the greater study area. Certain known conditions created drift within the accuracy of the sync echo to its representative GPS time stamp and this drift could cause diminished positioning accuracy when forming position estimates that used multiple systems. To help alleviate the effects of this drift a subroutine was added to the processing software (FishCount) that mitigated the effects of the drift before merging multiple system files. A linear regression calculation was performed on all sync echoes within a file that modeled the UTC time of each clock tick using the GPS sync echoes contained in each *.RAT file. If the R-squared value of the regression (i.e., the coefficient of determination) was less than 0.9999, then outlying points were removed until an R-squared

of 0.9999 was achieved. The slope of the regression then was used to calculate the most accurate time stamp to use in the merging process. If an R-squared value of 0.9999 or better could not be achieved, or if too much of the data had to be removed to achieve the desired R-squared value, then that file was not used in the merging process. The drift was not adjusted and the file was marked but not tracked. These marked files were used for determining presence or absence of the fish only and were not used to create fish tracks.

PROCESSING DATA

Files were processed using software developed by USGS (FishCount) to identify valid tag returns within the raw data. Additional USGS software (InstrumentFileCompile) was used to compile all valid detections into a single detection history for each fish. This detection history was processed further to identify false/positive events using the history to identify nonsensical events. An example of a nonsensical event is a detection history between two sites that would require the fish to move at speeds that are not possible. Events that were flagged as nonsensical were then proofed using USGS-developed software to remove the false event and update the detection history to reflect the changes.

On completion of proofing the data and ensuring that all events were marked properly, the data were ready to be used to create fish tracks. Creating position estimates and subsequent fish tracks required additional data. Fish positions were calculated by using the time of arrival of the tag signal at multiple hydrophones in the monitoring array. To accurately create position estimates based on the time of arrival of the signal at multiple hydrophones, it was imperative to know the exact physical location of each hydrophone. To accomplish this, the location of each hydrophone was surveyed using RTK GPS equipment. Each time a damaged hydrophone was replaced, the survey crew resurveyed the hydrophone's location. In addition, the locations of the four hydrophones mounted on the face of the FFGS were monitored continuously by RTK GPS antennas located directly above each hydrophone. Continuous monitoring was necessary for these hydrophones because the barrier was constantly being moved by currents in the river. A small number of hydrophones were mounted on docks in the study area. For these hydrophones, the Northing and Easting Cartesian coordinates were assumed to stay fixed and the elevation was adjusted as the river level changed by using the USGS gauging stations in the area. GeneticFish used estimates of individual hydrophone positioning errors to optimize the positioning process so all hydrophone locations were assigned a measure of uncertainty in the horizontal and vertical plane based on the difficulty of accurately surveying each hydrophone placement.

Before being able to use the hydrophone location data and the fish detection data to create fish tracks, it was necessary to determine the speed of sound through water in the study area. The speed of sound in water affected conversion of the time of arrival information into distances that were used to create the individual points making up a fish track. To calculate speed of sound, conductivity and salinity were assumed to be fixed at the values for pure fresh water. Water temperature data then was gathered from the three closest USGS gauging stations and the values were averaged over 5-minute intervals. The average of the temperature time series was used to calculate the speed of sound for each tracked tag ping, and the average standard deviation between the three temperature time series over the study period was used to develop a single estimate of speed of sound error for the entire study. USGS software (GeneticFish) used the speed of sound data, hydrophone position data, and the fish detection data to create individual fish tracks. The individual fish tracks then were merged into a single dataset and were used by various investigators to conduct spatial and temporal analyses.

2.6.3 FISH FATES CLASSIFICATION AND ASSIGNMENT

To determine the fates of a subset of study fish (e.g., deterred, undeterred, eaten; see **Figures 2-23a** and **2-23b**), fish tracks derived using the methods described previously were systematically reviewed by the project team over a week-long conference (November 17 through 19, 2014), referred to as the Fish Fates Conference. For all fish tracks, fish "fates" were determined for a total of seven possible "events." The events were grouped into categories of entering the array, exiting the array, and predation. Each fish was assigned a fate code that was entered into a spreadsheet for further analysis. A schematic showing the categories of events, responses, and fates (with fate codes) used during the conference is shown in **Figures 2-23a** and **2-23b**. A detailed description of the rules used in making determinations on fish fates is provided in **Appendix D**, "Conference on Fates – Predation and Guidance Rules."

2.6.4 ACTIVE HYDROACOUSTICS

Active hydroacoustics (split-beam transducers and DIDSON cameras), were used to detect and quantify predator-sized fish immediately adjacent to and in the vicinity of the FFGS during much of the study period. Details of the active hydroacoustics study are provided in Section 3.6.6. A brief summary of the methods is provided.

All split-beam acoustic data were collected using two fixed Biosonics® DT-X Digital Scientific Portable Echosounders operating at either 200 or 420 kHz, depending on the location. One transducer was just downstream from the FFGS on the left bank (Walnut Grove side) of the river. The other transducer was approximately midway down Dagmar's Landing on the right bank of the river across from the FFGS. The transducers were angled generally to be perpendicular to typical river flow, with the Walnut Grove transducer pointed towards the opposite bank, perpendicular to the shore, and the Dagmar's Landing transducer pointed slightly upstream. The Dagmar's Landing transducer was suspended on a metal pipe hanger about 1.5 m (4.9 ft) below the surface and was pitched down at 1.5-2.5°, depending on river discharges. The transducer beam was 7° and had a maximum effective range of 55 m (180 ft), beyond which the rising river bank on the far shore, and buoy and guy lines associated with the FFGS interfered with the beam. The Walnut Grove transducer was fixed to a metal tripod, set on the river bottom in about 3 m (10 ft) of water. The transducer itself was about 0.3 m (1 ft) off the bottom and was pitched at varying angles upward or downward, depending on river depth. The transducer beam angle was 6.5° and had a maximum effective range of 30 m (98 ft) before barrier anchors and pilings interfered with the beam.

DIDSON data were collected and analyzed using similar techniques to the split-beam transducer, with some differences related to the type of data collected. Unlike the split-beam transducers, the DIDSON sonar is a multibeam unit employing up to 96 beams (when run in high-frequency mode, as in the present study), with each beam having an angle of 0.3° in the horizontal and 14° in the vertical, producing an overall 29° by 14° beam. Two DIDSON units were used in the study, one mounted approximately 37 m (121 ft) from the upstream end of the FFGS (hereafter referred to as the mid-FFGS DIDSON) and the other mounted approximately 14 m (46 ft) from the downstream end of the DIDSON (hereafter referred to as the end-FFGS DIDSON). Both DIDSON units were mounted approximately 1.8 to 2.2 m (5.9-7.2 ft) below the water surface and were attached to the crossbars linking the smaller flotation devices boatbusters (flotation devices). The DIDSON units were operated in high-resolution mode and were set to provide data outputs every 30 minutes. The mid-FFGS DIDSON sampled 2.5 to 12.5 m (8.2-41.0 ft) from the unit, whereas the end-FFGS DIDSON sampled 4.5 to 14.5 m (14.8-47.6 ft) from the unit. Different sampling ranges were used for each unit because of differences in how each unit operated.

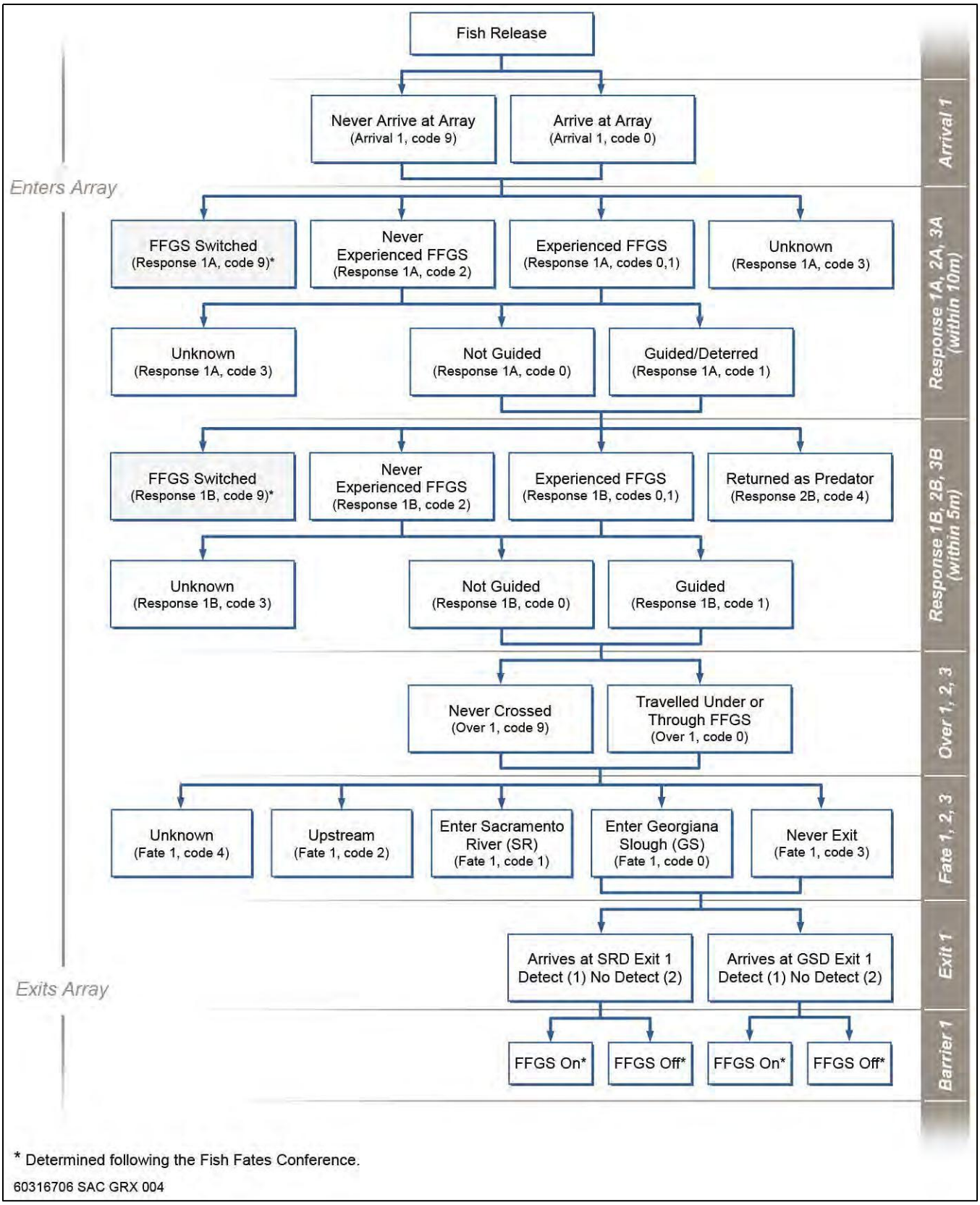

Figure 2-23a Fish Fates Determination Schematic (Array Events)

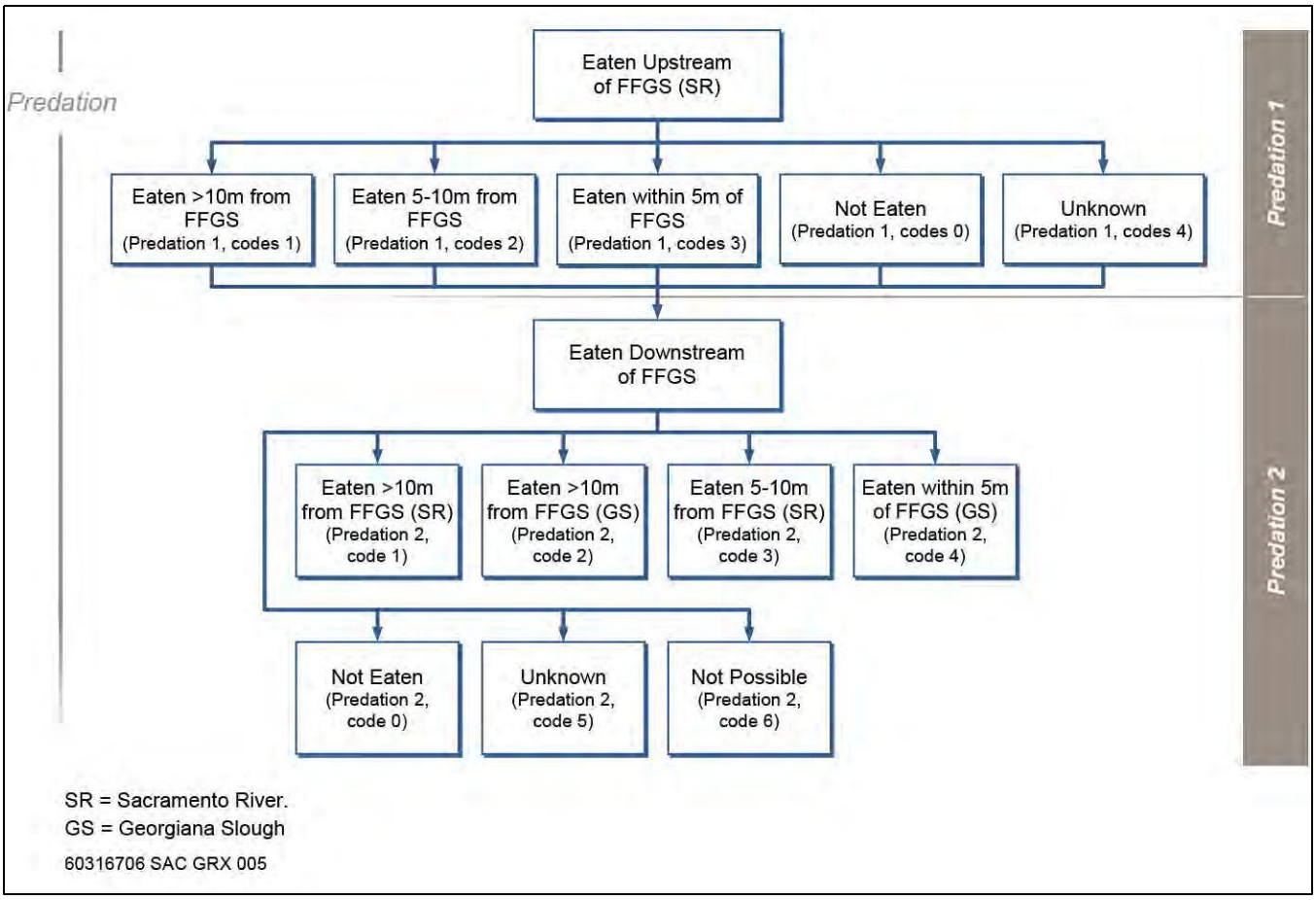

Figure 2-23b Fish Fates Determination Schematic (Predation Events)

2.7 EXPERIMENTAL BARRIER OPERATIONS

The experimental FFGS operations were designed to measure the responses of tagged juvenile Chinook salmon migrating downstream in the Sacramento River that encountered Georgiana Slough when the FFGS was On (deployed at an angle into the river) or when the FFGS was Off (set back adjacent to and parallel to the left bank) over a range of discharge, tidal, and diel conditions. The experiment began with the FFGS in the Off position. Thereafter, the FFGS was switched about every 25 hours (full tide cycle) on the minimum low tide. Switching the FFGS operation about every 25 hours on the minimum low tide resulted in FFGS On and FFGS Off conditions over a range of light and tidal cycles; two full tidal cycles were completed every 25 hours.

The FFGS On and FFGS Off operations are shown in **Table 2-5**. During the field study, observations of the FFGS operations were made routinely in order to assess that the desired positioning was being achieved and that the FFGS support systems were working properly. From approximately March 1 through March 7, 2014, the FFGS was tested and various repairs were implemented. Full operation of the FFGS (starting in the Off position) started on March 9, 2014.

Table 2-5 2014 Georgiana Slough Study FFGS Operation (all times Pacific Daylight Time)			
Date	**FFGS On**	**FFGS Off**	**Duration (HH:MM)/Notes**
1-Mar-14	1:17:00 - Testing and Repairs		Testing and Repairs
9-Mar-14	1:37:00 - Testing and Repairs		
9-Mar-14		13:00 - Start in Off	Start in Off
10-Mar-14	15:26		24:29:00
11-Mar-14		15:55	
12-Mar-14	16:56		24:49:00
13-Mar-14		17:45	
14-Mar-14	18:21		24:48:00
15-Mar-14		19:09	
16-Mar-14	20:05		24:35:00
17-Mar-15		20:40	
18-Mar-14	21:38		24:24:00
19-Mar-14		22:02	
20-Mar-14	22:57		1:03:00
22-Mar-14		0:00	
23-Mar-14	0:50		24:57:00
24-Mar-14		1:47	
25-Mar-14	3:29		24:48:00
26-Mar-14		4:17	
27-Mar-14	5:20		24:58:00
28-Mar-14		6:18	
29-Mar-14	7:05		24:43:00
30-Mar-14		7:48	
31-Mar-14	8:48		25:00:00
1-Apr-14		9:48	
2-Apr-14	9:10		24:48:00
3-Apr-14		9:58	
4-Apr-14	10:28		24:32:00
5-Apr-14		11:00	
6-Apr-14	13:07		25:59:00
7-Apr-14		15:06	
8-Apr-14	14:31		24:53:00
9-Apr-14		15:24	
10-Apr-14	16:18		24:42:00
11-Apr-14		17:00	
12-Apr-14	17:25		24:17:00
13-Apr-14		17:42	
14-Apr-14	18:55		26:00:00
15-Apr-14		20:55	
16-Apr-14	21:34		24:50:00
17-Apr-14		22:24	
18-Apr-14	22:58		24:57:00
19-Apr-14		23:55	

Table 2-5 2014 Georgiana Slough Study FFGS Operation (all times Pacific Daylight Time)			
Date	**FFGS On**	**FFGS Off**	**Duration (HH:MM)/Notes**
21-Apr-14	0:55		25:22:00
22-Apr-14		2:17	
23-Apr-14	3:02		24:55:00
24-Apr-14		3:57	
25-Apr-14	4:46		40 days, 06:44:00
4-Jun-14		11:30	

3 ANALYSIS METHODS, RESULTS, AND DISCUSSION

This chapter describes the analysis methods, results, and discussion of results for six key investigations that collectively comprise the 2014 GSFFGS Study. These investigations are all of importance to an understanding of the FFGS technology. The specific investigation topics were:

- Section 3.1: FFGS barrier efficiencies in fish guidance measured by deterrence efficiency, protection efficiency, and overall efficiency;
- Section 3.2: Migration route survival modeling using mark recapture methods;
- Section 3.3: Hydrodynamic influences and the critical streakline;
- Section 3.4: General linear modeling of juvenile Chinook salmon fates as influenced by FFGS operations and environmental factors;
- Section 3.5: Spatial analysis of juvenile Chinook salmon distribution in relation to a number of factors, including water velocity, light/dark conditions, and barrier operations;
- Section 3.6: Predatory fishes and their predation on juvenile Chinook salmon related to barrier operational condition and other environmental factors; and
- Section 3.7: Study fish releases and river conditions and the effects on diel Chinook salmon arrival at the study area.

3.1 FLOATING FISH GUIDANCE STRUCTURE PERFORMANCE

Evaluating the effectiveness of the FFGS in altering fish routing is a central element of the 2014 GSFFGS Study. In this subchapter, three types of barrier efficiencies are investigated: deterrence, protection, and overall.

- Deterrence efficiency is defined as the proportion of tagged juvenile Chinook salmon (i.e., tags that passed within 10 m (33 ft) of the FFGS) not determined to have been eaten by predators, that were guided or deterred by the FFGS when compared to the number of tags that came within 10 m (33 ft) of the FFGS (Equation 1 (Section 3.1.1) provided the mathematical definition). A juvenile Chinook salmon that changed direction within 10 m ft) of the FFGS line by turning away from the FFGS by more than 24° was deemed “deterred.” A turning angle of 21° to 24° was considered weak evidence of deterrence and, without any other evidence, would be deemed “unknown”. If the turning angle was less than 21°, then the juvenile Chinook salmon was deemed “not deterred;”
- Protection efficiency measures the incidence of juvenile Chinook salmon outmigrating in the Sacramento River, as measured by the proportion of tags detected approximately 3.3 km (2.1 mi) downstream of the FFGS relative to the total number outmigrating via the Sacramento River and Georgiana slough combined; and
- Overall efficiency was determined as the proportion of tags that remained in the Sacramento River relative to those tags deemed not to be eaten by a predatory fish that arrived at the study area.

3.1.1 METHODS

The efficiency of the FFGS was tested by releasing tagged juvenile Chinook salmon at the City of Sacramento upstream from the FFGS and monitoring the migration pathway of each fish as it passed through the hydroacoustic array in the study area at Walnut Grove. Based on acoustic tag tracking results for juvenile Chinook salmon that entered the array, estimates were derived for deterrence efficiency, protection efficiency, and overall efficiency by comparing results for fish passing through the array when the FFGS was On and Off (see Section 2.5.3). Some juvenile Chinook salmon were classified as eaten by predatory fish[7] within the study area based on changes in the characteristics of their acoustic tag track (see **Appendix D**, "Conference on Fates – Predation and Guidance Rules").

Four lines of evidence were used for determining if a juvenile Chinook salmon had been eaten:

1. Predator behavior was evident when the tag executed patrolling loops (**Figure 3.1-1**) in the study area, and/or changed speed or direction (see Rule 2) often, and/or held position for extended time periods. However, a tagged juvenile Chinook salmon may have moved into the study area, stopped, and waited for the next ebb tide, and then continued its seaward migration.

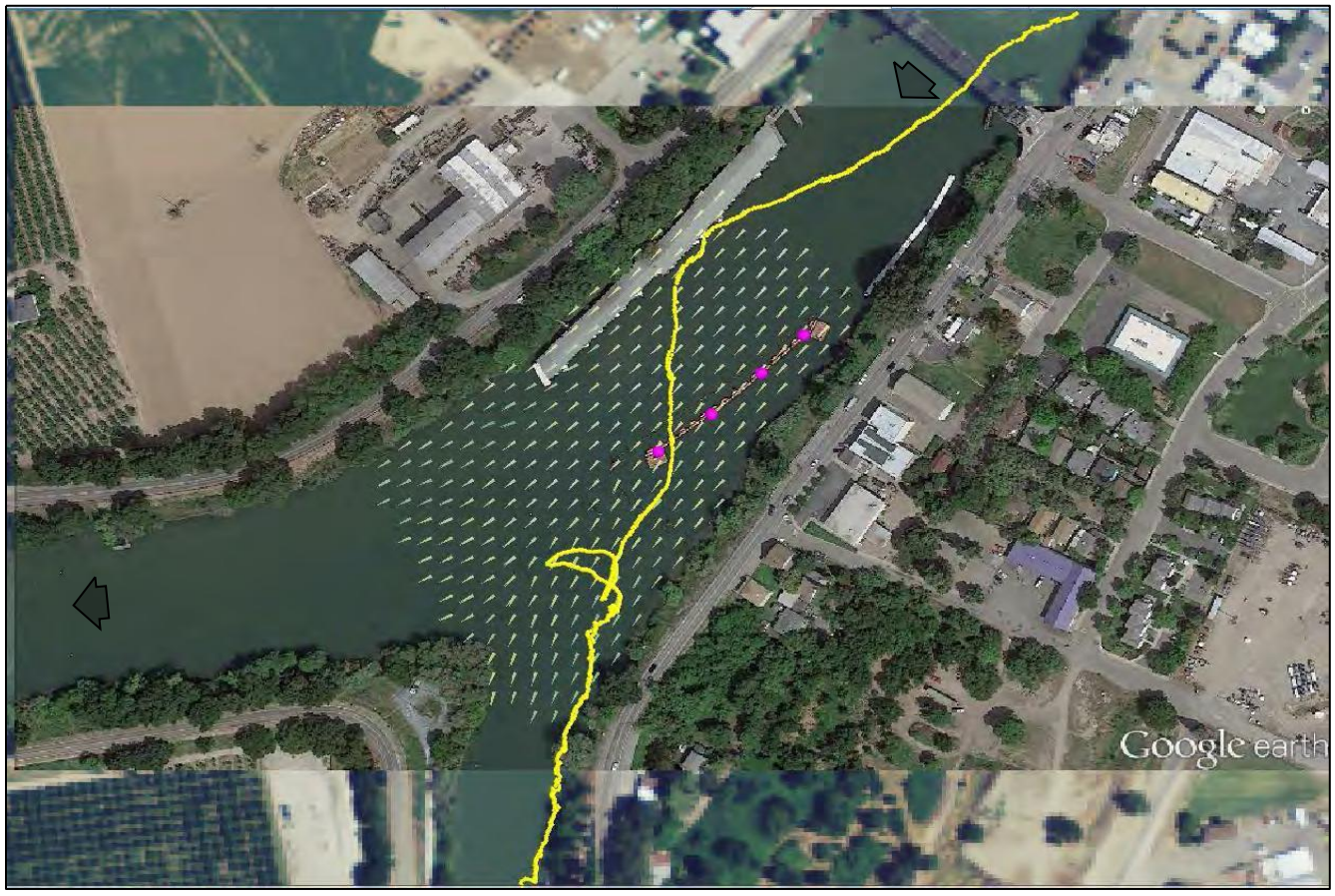

Note: This was the path of a striped bass (tagged 2897.381) that passed by the FFGS on March 25, 2014 between 1347 and 1425 hours, exhibited a loop and swam upstream against high downstream velocities. The FFGS was On as indicated by the purple spheres.

Figure 3.1-1 Path of a Striped Bass Tracked March 25, 2014

[7] It was assumed based on the pattern of acoustic tag tracks classified as indicating predation, that predation was due to predatory fishes and not due to other potential predators, e.g., sea lions, river otters, birds, or aquatic reptiles.

2. A single 90° turn was not definitive proof that a tagged fish was eaten by a predatory fish; three or more turns greater than 30° was one criterion used to classify a juvenile Chinook salmon as having been eaten. Low or negative water velocity in the area of a juvenile Chinook salmon may have made large turns greater than 30° more likely. If large turns occurred and the water velocity was low (less than 2 BL/s or negative), then five or more turns of ≥30° (**Figure 3.1-2**) were required before such turns were considered evidence of predation. These rules were developed from expert opinion upon review of the 2D tracks of tagged predatory fishes.

Note: This was the path of a striped bass (tagged 2533.365) on March 26, 2014, that executed loops, displayed upstream swimming behavior before reaching the FFGS hydrophone array, and made many acute turns, including more than five acute turns (greater than 30°) in the immediate vicinity of the FFGS. The FFGS was in the Off position indicated by the purple spheres.

Figure 3.1-2 Path of a Striped Bass Tracked on March 26, 2014

3. The following qualitative metrics were used to distinguish between juvenile Chinook salmon and predatory fishes behavior:

   a) Higher tortuosity[8] was evidence of predatory fishes behavior;

   b) Transit speed (within array and/or transit time to downstream node) of juvenile Chinook salmon was significantly faster than those deemed eaten by predatory fishes (DWR 2015a); and

   c) High residence time in the study area was evidence of behavior exhibited by predatory fishes. This rule was developed from expert opinion upon review of the 2D tracks of tagged *Micropterus* species.

4. Detection at downstream node (considered the weakest form of evidence):

   a) If a tag never reached a downstream node, this was suggestive evidence that the juvenile Chinook salmon was eaten by a predatory fish; and

[8] Tortuosity is the ratio of the 2D track's length to the length of a line segment from the first to the last point in that 2D track. tortuosity was estimated visually.

b) If a tag reached a downstream node in less than 3 hours and average channel velocity in the hydrophone array was greater than 0.25 m/s (0.82 ft/s) , then this was evidence that the juvenile Chinook salmon was not eaten and passed the downstream node uneaten.

During the Conference on Fates (**Appendix D**) teams of two researchers working together used the "preponderance of evidence" (i.e., greater weight of evidence) to make the determination of predation on juvenile Chinook salmon based on expert opinion. Quality assurance was performed on predation classifications. All predation determinations that exceeded 2 minutes on initial consideration, indicating some uncertainty by the original team, were reviewed later by other experts on the research team.

Tracks of tagged fish determined to be juvenile Chinook salmon, moved consistently in a downstream direction (DWR 2012, 2015b), but generally, more erratic behavior with more turns was observed in the 2014 tracks (**Figure 3.1-4**) than in the 2011 (**Figure 3.1-3**) or 2012 tracks. Tracks for juvenile Chinook salmon that were determined to have been eaten by a predatory fish (using the Predation Rules above) typically exhibited stronger turning angles, pathways that included upstream movement. For some tracks a large amount of movement occurred along the river margin, and for many tracks looping behavior was observed.

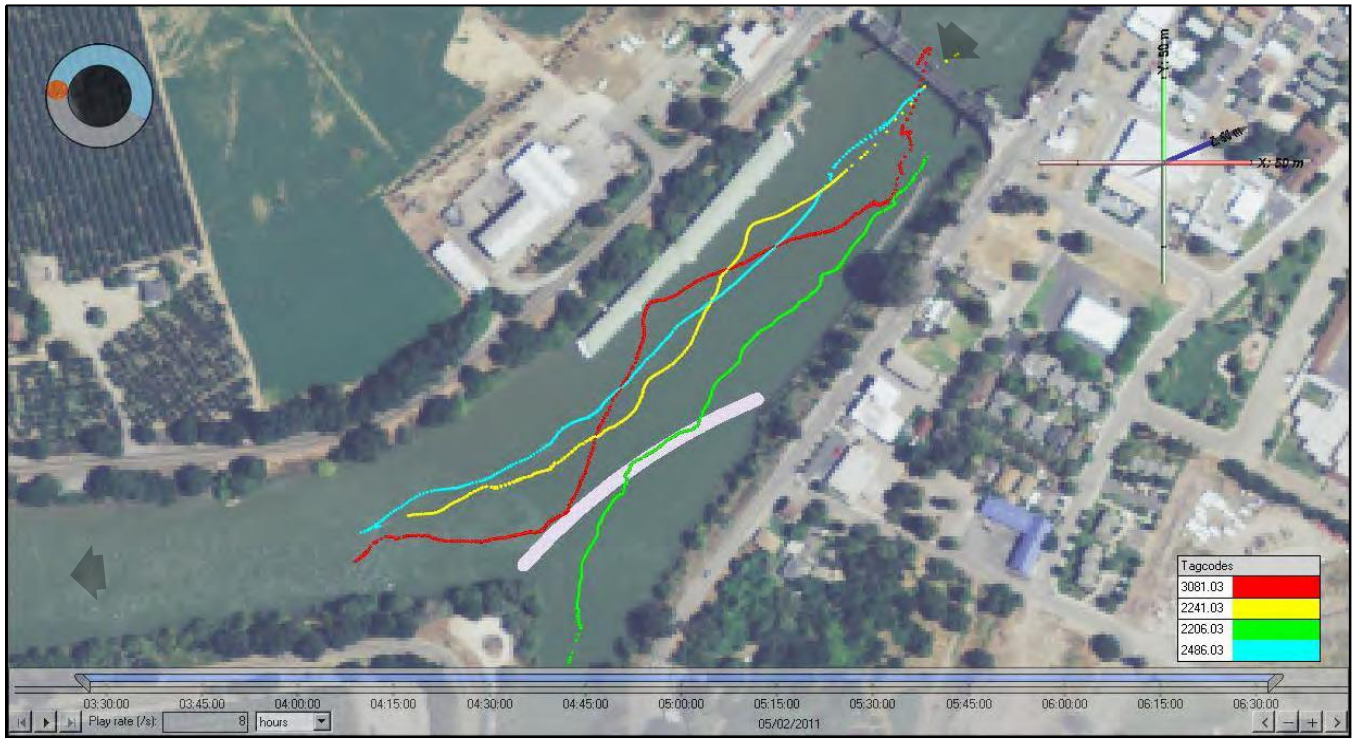

Note: All four juvenile Chinook salmon were released May 2, 2011 at 0000 hours. All four tracks passed by the divergence of the Sacramento River and Georgiana Slough on May 2, 2011 between 0317 and 0344 hours. 2206.03 was undeterred and entered Georgiana Slough. 3081.03 and 2241.03 were deterred into the Sacramento River. 2486.03 was determined to be undeterred because it made no movement away from the BAFF.

Source: DWR 2012

Figure 3.1-3 Two-Dimensional Tracks of Four Juvenile Chinook Salmon on May 2, 2011

The experimental design and data collection associated with the 2014 evaluation of FFGS performance efficiency included comparisons of results under the following conditions: 1) time periods when the FFGS was On and Off (i.e., it did not include FFGS states that were in a transitional phase between the On and Off positions); 2) time periods when the FFGS was On and Off under light conditions defined as dark (low light < 5.4 lux) or light (high light ≥5.4 lux); and 3) time periods when the FFGS was On and Off, when the approach velocity experienced by a

juvenile Chinook salmon was low (approach velocity was < 0.25 m/s [0.82 ft/s]) or high (approach velocity was ≥ 0.25 m/s [0.82 ft/s]). The criteria used for characterizing light and velocity were based on DWR studies (DWR 2012, 2015b), where sound, bubbles, and light were used as juvenile Chinook salmon deterrents at this same Delta junction.

Note: A juvenile Chinook salmon (tagged 619.225), determined to have not been eaten, passed by the FFGS on April 13, 2014, exhibiting many turns in the hydrophone array in the immediate vicinity of the FFGS. Only two of the turns were greater than or equal to 30° incident to the FFGS. The FFGS was in the On position indicated by the purple spheres.

Figure 3.1-4 Path of a Juvenile Chinook Salmon Tracked on April 13, 2014

A single "sample" was a period during which: 1) the FFGS state (On or Off) did not change; 2) light did not cross the threshold level (5.4 lux); and 3) the approach velocity did not cross the threshold level (0.25 m/s [0.82 ft/s]) (DWR 2012). All juvenile Chinook salmon that passed through the array during a single sample period were used to calculate deterrence efficiency, protection efficiency, overall efficiency, proportion eaten, and guidance time for that sample. A new sample was started when one of the three variables (i.e., FFGS state, light, or velocity) changed state or crossed a threshold value (light or velocity).

A single sample then had similar conditions for three variables, FFGS state, ambient light at 1 m (3 ft) below the surface (lux), and approach velocity. Samples that had contained only one tag were not included in calculations for deterrence efficiency, protection efficiency, or overall efficiency (e.g., Sample Number 28: **Table 3.1-1**).

The 2014 GSFFGS Study was designed to evaluate the barrier's performance by testing deterrence efficiency, protection efficiency, and overall efficiency. The hypotheses related to each of the evaluation metrics of barrier efficiency are described.

Table 3.1-1 A Selection of the Master Data Set Illustrating Sample Identification with Tagged Juvenile Chinook Salmon that Arrived at the Study Area Hydrophone Array in 2014

Record	Tagcode USGS	EXIT_1	FFGS 1	Array_Time	LUX_Value	Light_Code	A_Vel (m/s)	A_Vel code	Sample Number
354	2715.523	1	1	3/11/2014 7:46:20	23.98	1	0.296	1	27
355	3863.523	0	1	3/11/2014 7:58:25	23.98	1	0.298	1	27
356	4773.523	1	1	3/11/2014 8:52:13	188.74	1	0.287	1	27
357	4913.523	2	1	3/11/2014 9:06:31	558.74	1	0.286	1	27
358	2869.523	1	1	3/11/2014 9:40:56	558.74	1	0.278	1	27
359	4549.523	2	1	3/11/2014 10:18:57	915.84	1	0.184	0	28
360	3387.523	1	1	3/11/2014 10:41:41	915.84	1	0.291	1	29
361	3177.523	2	1	3/11/2014 11:13:12	1696.60	1	0.343	1	29
362	4199.523	1	1	3/11/2014 11:30:06	1696.60	1	0.333	1	29
363	3583.523	2	1	3/11/2014 13:00:23	4680.99	1	0.270	1	29
364	2631.523	1	1	3/11/2014 13:02:32	4680.99	1	0.375	1	29
365	3849.523	2	1	3/11/2014 14:03:04	5473.82	1	0.327	1	29
366	3289.523	1	1	3/11/2014 14:22:28	5473.82	1	0.459	1	29
367	2883.523	1	1	3/11/2014 14:40:54	5473.82	1	0.432	1	29
368	4241.523	1	1	3/11/2014 14:49:02	5473.82	1	0.364	1	29
369	3597.523	1	1	3/11/2014 15:22:39	4257.29	1	0.449	1	29
370	4885.523	1	1	3/11/2014 16:36:44	1913.75	1	0.462	1	29
371	3513.523	1	1	3/11/2014 16:42:51	1913.75	1	0.383	1	29
372	4311.270	2	1	3/11/2014 17:18:24	223.70	1	0.375	1	29
373	2771.523	1	1	3/11/2014 21:57:05	0.00	0	0.268	1	31
374	3079.523	2	0	3/12/2014 0:09:52	0.00	0	0.478	1	31
375	4983.523	1	0	3/12/2014 1:15:43	0.00	0	0.429	1	31
376	3485.523	2	0	3/12/2014 2:04:19	0.00	0	0.362	1	31
377	4353.523	2	0	3/12/2014 2:22:17	0.00	0	0.366	1	31

Table 3.1-1 A Selection of the Master Data Set Illustrating Sample Identification with Tagged Juvenile Chinook Salmon that Arrived at the Study Area Hydrophone Array in 2014									
Record	Tagcode USGS	EXIT_1	FFGS 1	Array_Time	LUX_Value	Light_Code	A_Vel (m/s)	A_Vel code	Sample Number
378	4129.523	1	0	3/12/2014 2:25:55	0.00	0	0.501	1	31
379	3107.647	2	0	3/12/2014 3:38:08	0.00	0	0.574	1	31
380	4759.523	1	0	3/12/2014 4:09:44	0.00	0	0.435	1	31
381	2729.647	2	0	3/12/2014 5:04:54	0.00	0	0.554	1	31
382	4577.523	1	0	3/12/2014 5:09:00	0.00	0	0.381	1	31
383	4381.523	2	0	3/12/2014 5:23:37	0.00	0	0.494	1	31
384	4829.647	0	0	3/12/2014 7:01:08	0.00	0	0.441	1	31
385	3695.647	2	0	3/12/2014 7:25:13	0.00	0	0.388	1	31

Notes: The tags are arrayed chronologically according to when that tag was closest to the FFGS. EXIT_1(0: Georgiana Slough; 1: Sacramento River; 2: Not Detected). FFGS (0: Off Position; 1: On Position). Array_Time (Time when tag was nearest the FFGS). LUX_Value (Ambient light at 1 m below surface (lux); Light_Code (0: Light < 5.4 lux; 1: Light ≥ 5.4 lux). A_Vel (m/s) (Approach Velocity (m/s)). A_Vel_Code (0: < 0.25 m/s; 1: ≥ 0.25 m/s). Sample Number (Sample Number assigned by rules described in report text).

Testing Hypothesis 16: Deterrence Efficiency

The efficiency of a barrier at deterring juvenile Chinook salmon from passing through or under was an important evaluation metric in other studies (DWR 2012, 2015b). In those studies, a distance of influence was established for the barriers of 5 m (16 ft). That is, if a juvenile Chinook salmon passed ≤ 5 m (≤16 ft) from the barrier it was deemed to have close contact with the barrier. In the present study, unanimous consensus of all researchers[9] working on this project was that juvenile Chinook salmon would not be able to sense the FFGS from more than 10 m (33 ft). Thus, 10 m (33 ft) was selected and if a juvenile Chinook salmon passed ≤10 m (≤33 ft) from the FFGS then it was deemed to have experienced the barrier.

In the present study, the deterrence efficiency was defined as the proportion of Chinook salmon juveniles that came within 10 m (33 ft) of the FFGS, and that were guided or deterred by the FFGS when compared to all the Chinook salmon juveniles that came within 10 m (33 ft) of the FFGS. A juvenile Chinook salmon that changed direction within 10 m (33 ft) of the FFGS line by turning away from the FFGS by > 24° (e.g., **Figure 3.1-5**, **Panel A**) was deemed "deterred." A turning angle of 21° to 24° was considered weak evidence of deterrence and, without any other evidence, would be deemed "unknown" (**Figure 3.1-5**, **Panel B**). If the turning angle was < 21°, then the juvenile Chinook salmon was deemed "not deterred" (**Figure 3.1-5**, **Panel C**).

[9] The 10 m (33 ft) threshold was defined as the maximum distance away from the FFGS that it would be possible for a Chinook juvenile to detect an effect of the FFGS via turbulence or a visual stimulus. This definition was agreed to by unanimous agreement of the research group by conference call in September, 2013, that included representatives from the U.S. Geological Survey, California Department of Water Resources, Hydroacoustic Technology, Inc., AECOM, Environmental Science Associates, and Turnpenny Horsfield Associates.

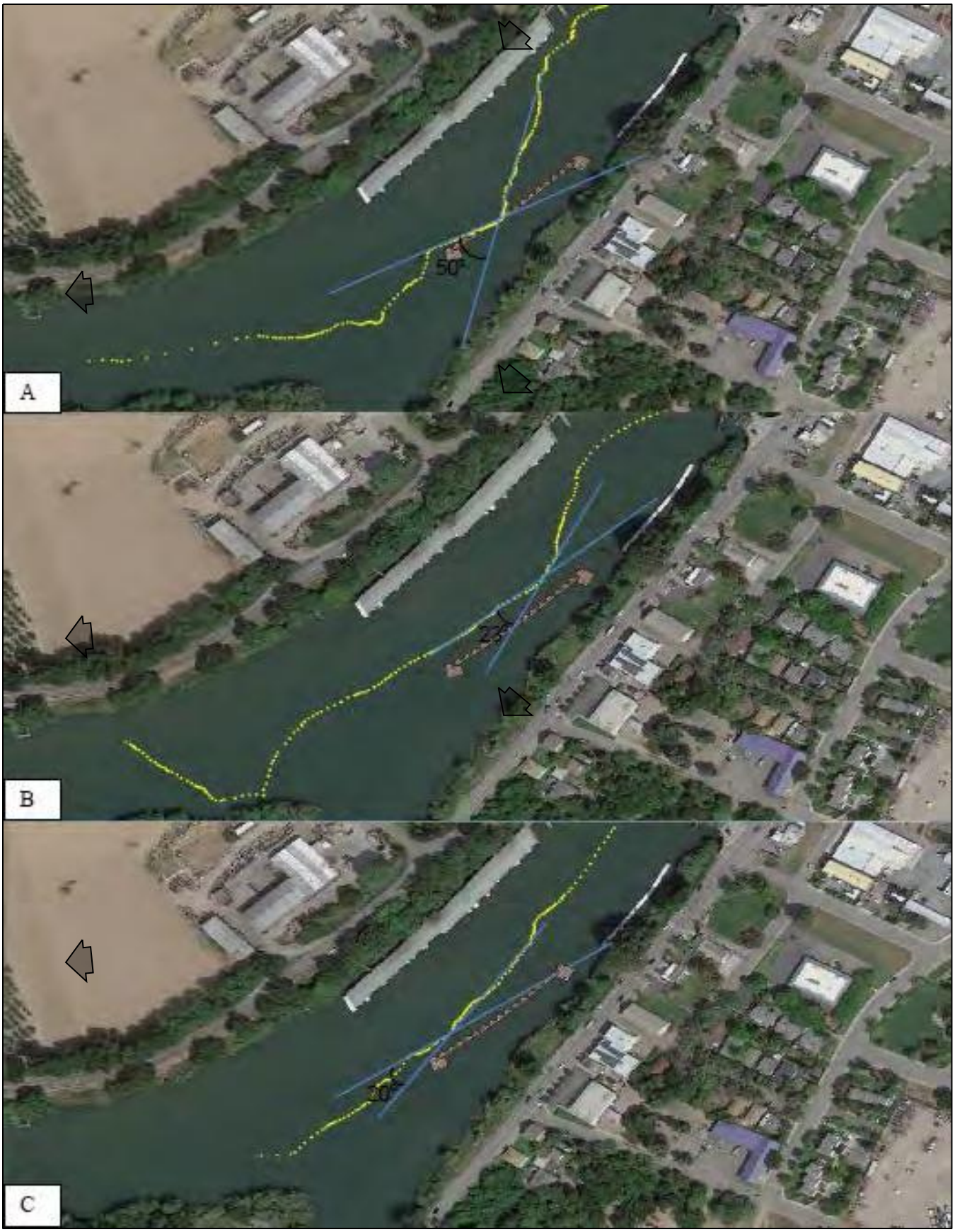

Figure 3.1-5 Examples of Turning Angles Made by Juvenile Chinook Salmon at the FFGS

The following *null hypothesis* was developed for Hypothesis H16:

$H16_0$: The deterrence, protection, and overall efficiencies are higher when the FFGS is in place compared to when the FFGS is not in place.

Deterrence efficiency was calculated as:

Equation 1. $E_D = B/(B + C)$

where:

E_D = deterrence efficiency;

B = the number of tagged juvenile Chinook salmon that: 1 were determined to have not been eaten; 2) came within 10 m (33 ft) of the FFGS; and 3) were deterred or guided by the FFGS (i.e., visibly changed direction by making a directed movement, ≥ 24°, away from the barrier (FFGS), or were guided by the barrier (changed direction and proceeded approximately parallel to the FFGS alignment); and

C = the number of tagged juvenile Chinook salmon that: 1) were determined to have not been eaten; 2) that came within 10 m (33 ft) of the FFGS; and 3) were undeterred or were not guided by the barrier.

Protection Efficiency

Protection efficiency describes the incidence of juvenile Chinook salmon successfully outmigrating in the Sacramento River, as measured by the proportion detected approximately 3.3 km (2 mi) downstream at hydrophone array SAC-5 (**Figure 2-1**) relative to the total number detected in the Sacramento River and Georgiana Slough combined. This metric excludes juvenile Chinook salmon that were determined to have been eaten in the FFGS study area and, therefore, is a measure of the efficacy of *routing* by the FFGS.

Protection efficiency was calculated (Equation 2) in exactly the same manner as that used for evaluation of a non-physical barrier at Georgiana Slough in previous DWR studies (DWR 2012, 2015b). The monitoring location was selected to be a sufficient distance downstream so that a juvenile Chinook salmon was completely out of the FFGS's potential area of influence and free from any associated increased risk of predation mortality. It was possible that a juvenile Chinook salmon could have exited the FFGS hydrophone array and been eaten before it reached either the SAC-5 or GEO-1 hydrophone arrays. The selected downstream monitoring location represented a distance of greater than one tidal excursion from the FFGS.

Barrier protection efficiency was calculated as:

Equation 2. $E_P = F/(F + G)$

where:

E_P = protection efficiency;

F = number of tagged juvenile Chinook salmon, determined to have not been eaten, that passed the downstream Sacramento River hydrophone array (i.e., SAC-5); and

G = the number of tagged juvenile Chinook salmon, determined to have not been eaten, that passed the downstream Georgiana Slough hydrophone array (i.e., GEO-1).

Overall Efficiency

Overall efficiency was determined as the proportion of tagged juvenile Chinook salmon that continued down the Sacramento River relative to the tags deemed not to be in a predator when that tag arrived at the study area. Tagged juvenile Chinook salmon that were eaten in the FFGS study area were not excluded from the overall efficiency calculation.

Barrier overall efficiency was calculated as:

Equation 3. $E_O = H/(H + I)$

where:

E_O = overall efficiency;

H = the number of tagged juvenile Chinook salmon that passed the downstream Sacramento River hydrophone array (i.e., SAC-5); and

I = the number of tagged juvenile Chinook salmon that entered the study array.

All the tagged juvenile Chinook salmon that moved 3.3 km (2.2 mi) downstream in the Sacramento River past SAC-5 were included in the overall efficiency calculation. This metric is a measure of routing efficacy of the FFGS and included all tagged juvenile Chinook salmon that arrived at the study area including those determined to have been eaten by behavioral analysis by predatory fishes. Thus, E_O is not dependent on expert interpretation of 2D track data for determination of predation events in the FFGS study area. This dependent variable also provided information on the behavioral response of juvenile Chinook salmon encountering the FFGS over a range of environmental conditions (i.e., tidal conditions, day and night, Sacramento River flows, and proportion of flow entering Georgiana Slough).

It should be noted that overall efficiency did include only those tags that were determined to have arrived at the array in a Chinook juvenile. Expert opinion was used to determine which tags arrived at the FFGS hydrophone

array in a juvenile Chinook salmon and not in a predatory fish. Thus, it was assumed that the removal from consideration of tags that were deemed to have arrived in a predatory fish would yield the most precise estimates of deterrence, protection, and overall efficiency.

Hypotheses H16, H22a, and H23a Testing

For detection, protection, and overall efficiency, following assignment of deterrence (if a tag passed within 10 m (33 ft) of the FFGS), predation, and fish exit location, each tag was placed into samples according to the method outlined by DWR (2012) (examples in **Table 3.1-1**). Then, for each of the three dependent variables, E_D, E_P, and E_O, a hypothesis test followed these four steps:

1. The data were tested to determine if they met the assumptions of ANOVA: independence of observations, homogeneity of variance, and normality;

2. If the data met these three criteria, a One-Way ANOVA was conducted for all light and velocity conditions combined;

3. Then, One-Way ANOVAs were conducted for each of the unique combinations of light and velocity defined previously; and

4. If the data did not meet the assumptions of ANOVA, nonparametric techniques were used (e.g., Wilcoxon Two-Sample test, or a Kruskal-Wallis test for more than two samples).

The first hypothesis tested was deterrence efficiency for hypothesis H16. If the one-sided P-value obtained was less than or equal to the critical alpha, the null of hypothesis H16 was rejected. A one-sided P-value was used because the only result of interest was that the FFGS significantly improved barrier efficiency. Then, the deterrence data were partitioned by light level, using a threshold value of 5.4 lux. At each light level, Hypothesis 16 was tested—this was the second test using the deterrence data. Then, the deterrence data were partitioned by approach velocity level, using a threshold value of 0.25 m/s (0.82 ft/s). At each light level, Hypothesis 16 was tested—this was the third and final test using the deterrence data.

Three tests were conducted using each sample. Thus, a Bonferroni method adjustment (Sokal and Rohlf 1995) to the critical alpha was required to maintain the experiment-wise error rate at the accepted level of 0.05. Three tests were conducted with each data sample, so 0.0167 (0.05/3) was the critical alpha value for these comparisons. The P-value of a test had to be equal to or smaller than this critical alpha value to reject the null hypothesis.

Similarly, protection and overall efficiency were tested (Hypothesis H16) for all samples, then partitioned by light, and then partitioned by velocity. Therefore, the E_P and E_O hypothesis tests used the same critical alpha 0.0167 (0.05/3) to control the experiment-wise error rate.

Hypothesis 22a (i.e., the deterrence, protection and overall efficiencies are different with the FFGS in place compared to when the BAFF was in place) provided the clearest possible test of the performance of the BAFF compared to the FFGS. The BAFF-On data in 2011 and the BAFF-On data in 2012 were grouped together for E_D. The grouped BAFF-On E_D samples were compared to the FFGS-On E_D samples using ANOVA. If the data did not meet the assumptions of ANOVA, nonparametric methods were employed, as previously described. After the H22a hypothesis test for deterrence efficiency was completed, the E_P and E_O were tested in the same manner.

A treatment-year effect like that seen at the Head of Old River may have been possible (DWR 2015a). That is, certain factors (e.g., flow) could have co-varied with the application of a particular technology treatment. To partially address this, BAFF On-2011, BAFF On-2012, and FFGS On-2014 were compared for E_D, E_P and E_O. Thus, a particular set of samples (e.g., BAFF On-2011), for all light and velocities levels combined, were used twice: once in the H22a test and once in the Hypothesis 23a test. Then, the samples were partitioned by light, and H22a and H23a were tested at low and high light conditions; this resulted in two more tests for each set of samples. Next, the samples were partitioned by velocity, and H22a and H23a were tested at low and high velocity conditions; this resulted in two more tests for each set of samples. So, the Bonferroni method adjustment (Sokal and Rohlf 1995) to the critical alpha was applied to maintain the experiment-wise error rate at the accepted level of 0.05. Six tests were conducted with each data sample, and thus 0.0083 (0.05/6) was the critical alpha value for these comparisons. The P-value of a test had to be equal to or smaller than this value to reject the null hypothesis.

Segment Intersection (Hypothesis H17)

Hypothesis 17 was "The proportion of juvenile Chinook salmon that pass under the FFGS is not uniform along the length of the barrier structure." This hypothesis was designed to assess where the FFGS failed to deter fish from entering Georgiana Slough.

Eight Segments

The FFGS was divided into eight equal segments, each approximately 15 m (49 ft) in length. The upstream segment was Segment 1, and the segments were numbered sequentially downstream to the end with the final

segment being Segment 8 (**Figure 3.1-6**). All juvenile Chinook salmon that were determined to have been eaten were removed. Then, the number of juvenile Chinook salmon that passed under each of the eight segments was tallied.

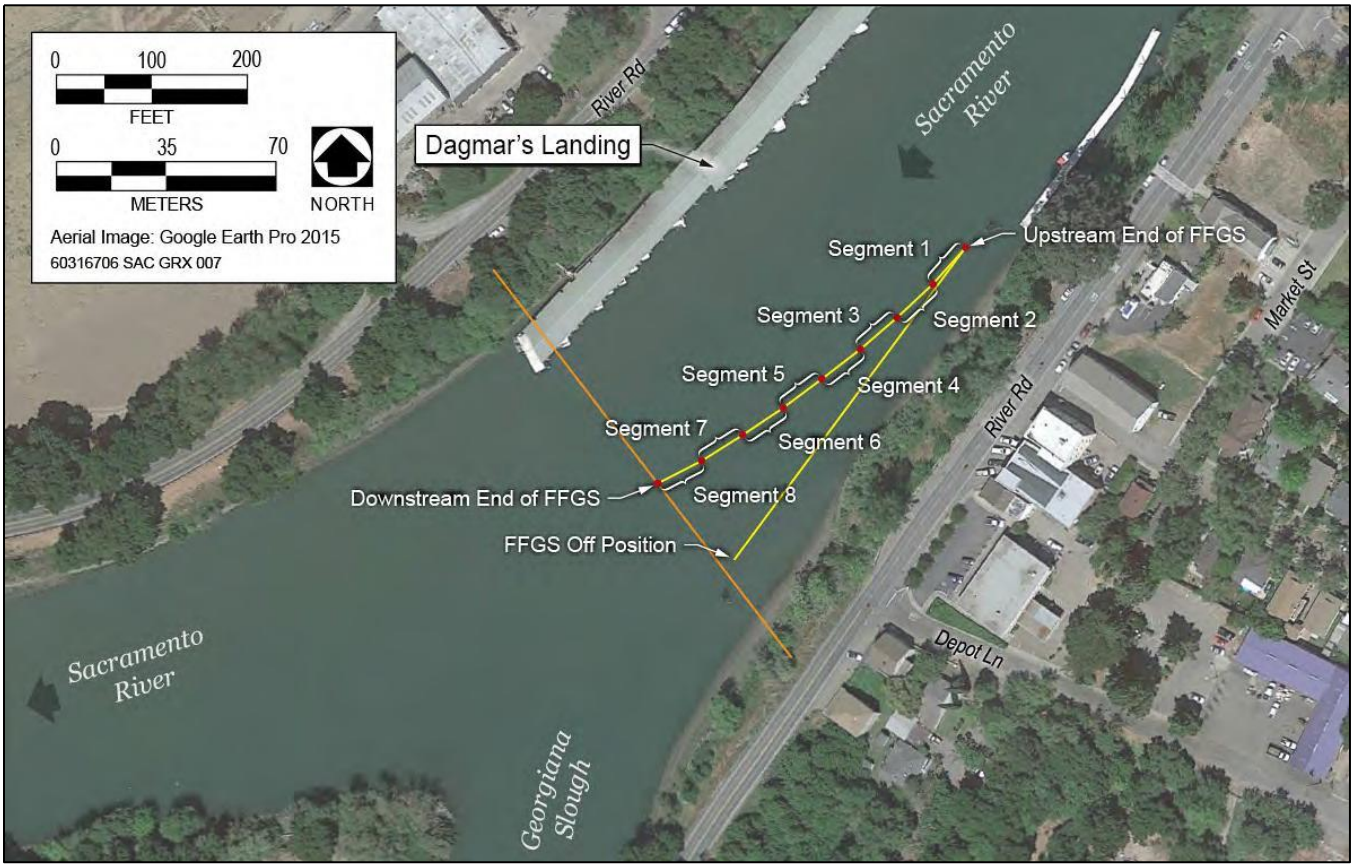

Note: Each segment is approximately 15 m (49 ft) in length.

Figure 3.1-6 Floating Fish Guidance Structure Divided into Eight Segments

After tallying was completed, a goodness of fit test was conducted with the juvenile Chinook salmon that passed the FFGS line when the FFGS was Off. The "FFGS line" is the location where the FFGS structure was located when in the On position, even if the FFGS was in the Off position. The expected values for the proportion of juvenile Chinook salmon passing the FFGS line according to a completely random process would all be equal to 0.125 (1.0/8 segments). Next, a goodness of fit test was conducted with the juvenile Chinook salmon that passed the FFGS line when the FFGS was On; expected values again were 0.125. Then, the proportions of juvenile Chinook salmon that passed through each segment when the FFGS was Off were used as expected values. The expected values were compared to observed values of juvenile Chinook salmon proportions passing through segments when the FFGS was On. Two types of goodness of fit tests were used. If the expected proportions in each segment were all > 0.05, then a chi-squared goodness of fit test was used. If some expected proportions were < 0.05, then Fisher's Exact Test was used (McDonald 2014). For all goodness of fit tests, the Relative Deviation for each segment was calculated:

Relative Deviation = (Observed Proportion – Hypothesized Proportion)/Hypothesized Proportion.

The Relative Deviation is calculated differently if tallied counts are all positive compared to when a tallied count has a value of zero. In the first case (all tallies are non-zero) the observed proportions are calculated simply: Tallied Count for a Segment/Sum of All Segment's Tallied Counts. However, when there are tallied counts with a

value of zero, one (1) unit must be added to the tallied count of all segments or the Relative Deviation for the zero count segment is undefined. However, adding one (1) unit to all segments maintains the Relative Deviation of segment's to each other in the Relative Deviation calculation. In the latter case (one or more tallies are zero) the raw tallied counts are reported for accuracy.

The Relative Deviation represents the difference between the observed and hypothesized (expected) proportion normalized by the magnitude of the hypothesized (expected) proportion. The sign of Relative Deviation indicates if a segment was crossed less often than expected (negative [-] sign) or more often than expected (positive [+] sign). In addition, the Relative Deviation provides a measure of the difference from the expected proportion and observed proportion (relative to each other) with the largest values representing those segments that were most extreme in the difference from expected to observed. The graphical presentation of Relative Deviation, provided

for all goodness of fit tests, provides a visual representation of each segments deviation from expected relative to other segments and the direction of that deviation.

Ten Segments

After the 8-segment analysis was completed, two study segments were added beyond the end of the FFGS structure and in alignment with Segment 8; these were numbered Segments 9 and 10 (**Figure 3.1-7**). Juvenile Chinook salmon that were deemed to have been eaten by a predator upstream of the FFGS were removed from the analysis. The number of juvenile Chinook salmon that passed under or through each segment, Segments 1-10, were tallied.

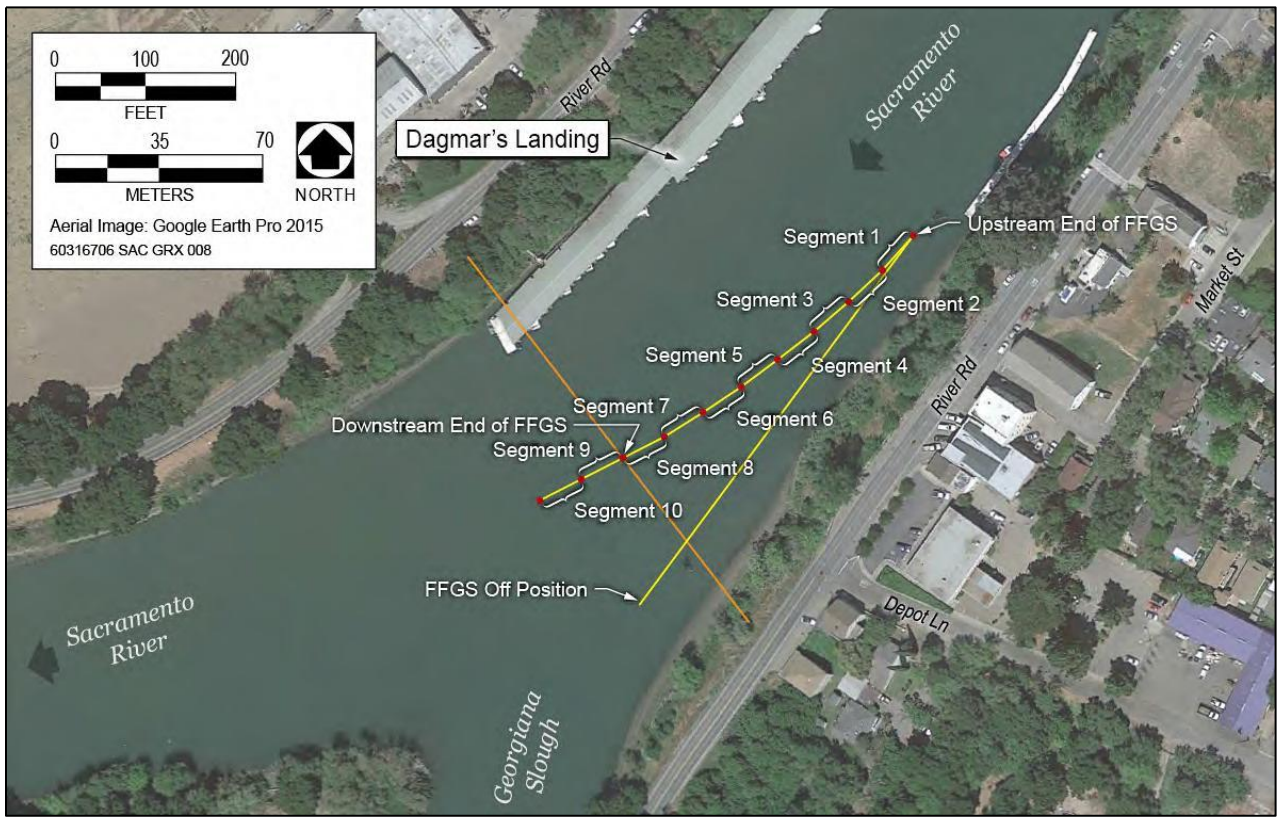

Note: Segments 9 and 10 were each 15 m (49 ft) in length, the same length as Segments 1 through 8, but they were past the distal end of the FFGS infrastructure.

Figure 3.1-7 Floating Fish Guidance Structure Divided into Eight Segments with Two Additional Segments

After tallying was completed, a goodness of fit test was conducted with the juvenile Chinook salmon that passed the FFGS line when the FFGS was Off; expected values were all equal to 0.1 (1.0/10 segments). Next, a goodness of fit test was conducted with the juvenile Chinook salmon that passed the FFGS line when the FFGS was On; expected values again were 0.1. Then, the proportions of juvenile Chinook salmon that passed through each segment when the FFGS was Off were used as expected values. The expected values were compared to observed values of juvenile Chinook salmon proportions passing through segments when the FFGS was On. Again, two types of goodness of fit tests were used. If the expected proportions in each segment were all greater than 0.05, then a chi-squared goodness of fit test was used. If some expected proportions were less than 0.05, then Fisher's Exact Test was used (McDonald 2014). For all goodness of fit tests, the Relative Deviation for each segment was calculated (see definition in 3.1.1 Methods, "Eight Segments") and presented graphically.

A total of four goodness of fit tests were conducted for each sample: 1) Eight segments—Equivalent Proportions as Expected; 2) Eight segments—FFGS Off as Expected and FFGS On as Observed; 3) Ten segments—Equivalent Proportions as Expected; and 4) Ten segments—FFGS Off as Expected and FFGS On as Observed. Thus, a Bonferroni method adjustment (Sokal and Rohlf 1995) to the critical alpha was required to maintain the experiment-wise error rate at the accepted level of 0.05. Four tests were conducted with each sample, and thus 0.0125 (0.05/4) was the critical alpha value for these comparisons. The P-value of a test had to be equal to or smaller than this value to reject the null hypothesis.

Failure Scenarios (Hypothesis H21)

The failures of the FFGS were defined as those tags that passed within 10 m (33 ft) of the FFGS and exited via Georgiana Slough. From these tags that exited the array in Georgiana Slough, a "Failure Scenario" was defined. Failure Group 1 included juvenile Chinook salmon that were determined to have not been eaten and passed under the FFGS. Failure Group 2 included juvenile Chinook salmon that were eaten upstream from the FFGS and then exited via Georgiana Slough in a predatory fish. Failure Group 3 included juvenile Chinook salmon that were determined to have not been eaten, passing to the right of the FFGS but then entrained into Georgiana Slough (**Figure 3.1-8**). After the failure scenario was assigned, all juvenile Chinook salmon from each of the three groups were tallied.

After tallying was completed, a goodness of fit test was conducted for the periods when the FFGS Off; expected values were all equal to 0.333 (1.0/3 failure groups), to test the hypothesis that the scenarios of failure occurred in equal proportion. Next, a goodness of fit test was conducted with the tags that passed through the array when the FFGS was On; expected values again were 0.333. Then, the proportions of tags found in each of the three failure groups that passed through the array when the FFGS was Off were used as expected values. The expected values were compared to observed values of proportions in each failure group when the FFGS was On. All expected proportions in each segment were greater than 0.05, and a chi-squared goodness of fit test was used.

Note: Two juvenile Chinook salmon tags 3079.423 (turquoise spheres) and 3877.593 (yellow spheres) passing the end of the FFGS when it was On and then turning left and exiting the array via Georgiana Slough.

Figure 3.1-8 Failure Group 3 Examples

Eaten Juvenile Chinook Salmon Removed

Failure Group 2 represented the behavior of predatory fishes: those tagged juvenile Chinook salmon that were eaten upstream from the FFGS line and subsequently exited via Georgiana Slough. Thus, Failure Group 2 was removed from consideration and Failure Groups 1 and 3 were compared. A goodness of fit test was conducted for periods when the FFGS was Off; expected values were all equal to 0.50 (1.0/2 failure groups). Next, a goodness of fit test was conducted with the tags from Failure Groups 1 and 3 that passed through the array when the FFGS was On; expected values again were 0.50. Then, the proportions of tags in Failure Groups 1 and 3 that passed through the array when the FFGS was Off were used as expected values. The expected values were compared to observed values of proportions in the two failure groups when the FFGS was On. An exact test of goodness of fit was used in all comparisons (McDonald 2014).

Two goodness of fit tests were conducted for the Failure Group 2 data sample: 1) Equivalent Proportions as Expected; and 2) FFGS Off as Expected and FFGS On as Observed. Thus, a Bonferroni method adjustment (Sokal and Rohlf 1995) to the critical alpha was required to maintain the experiment-wise error rate at the accepted level of 0.05. Two tests were conducted with each data sample, and thus 0.025 (0.05/4) is the critical alpha value for those comparisons involving Failure Group 2. The P-value of a test had to be equal to or smaller than this value to reject the null hypothesis.

Four goodness of fit tests were conducted that included the Failure Group 1 and 3 data samples: 1) Three failure groups (1, 2, and 3)—Equivalent Proportions as expected; 2) Three failure groups (1, 2, and 3)—FFGS Off as expected and FFGS On as observed; 3) Two failure groups (1 and 3)—Equivalent Proportions as expected; and 4) Two failure groups (1 and 3)—FFGS Off as expected and FFGS On as observed. Thus, a Bonferroni method

adjustment (Sokal and Rohlf 1995) to the critical alpha was required to maintain the experiment-wise error rate at the accepted level of 0.05. Four tests were conducted with each data sample, and thus 0.0125 (0.05/4) was the critical alpha value for comparisons involving Failure Groups 1 and 3. The critical alpha for Failure Group 2 comparisons, 0.025, was larger than that for Failure Groups 1 and 3 comparisons. Thus, when a comparison involved Failure Group 2 and Failure Groups 1 or 3, then 0.125 was used as the critical alpha because it was conservative. The P-value of a test must be equal to or smaller than this value to reject the null hypothesis.

Guidance Time

Expert opinion was used to determine whether deterrence or guidance had occurred in the vicinity of the FFGS. Deterrence was determined using the method described in Section "Testing Hypothesis 16: Deterrence Efficiency." Then the 2D track was evaluated for guidance behavior (**Figure 3.1-9**).

A juvenile Chinook salmon that changed direction within 10 m (33 ft) of the FFGS line and proceeded approximately parallel to the FFGS was deemed "guided" (**Figure 3.1-9**). The turning angle had to be greater than zero degrees; that is, a change in the fish's course had to have occurred, and the fish then had to proceed approximately parallel to the FFGS line.

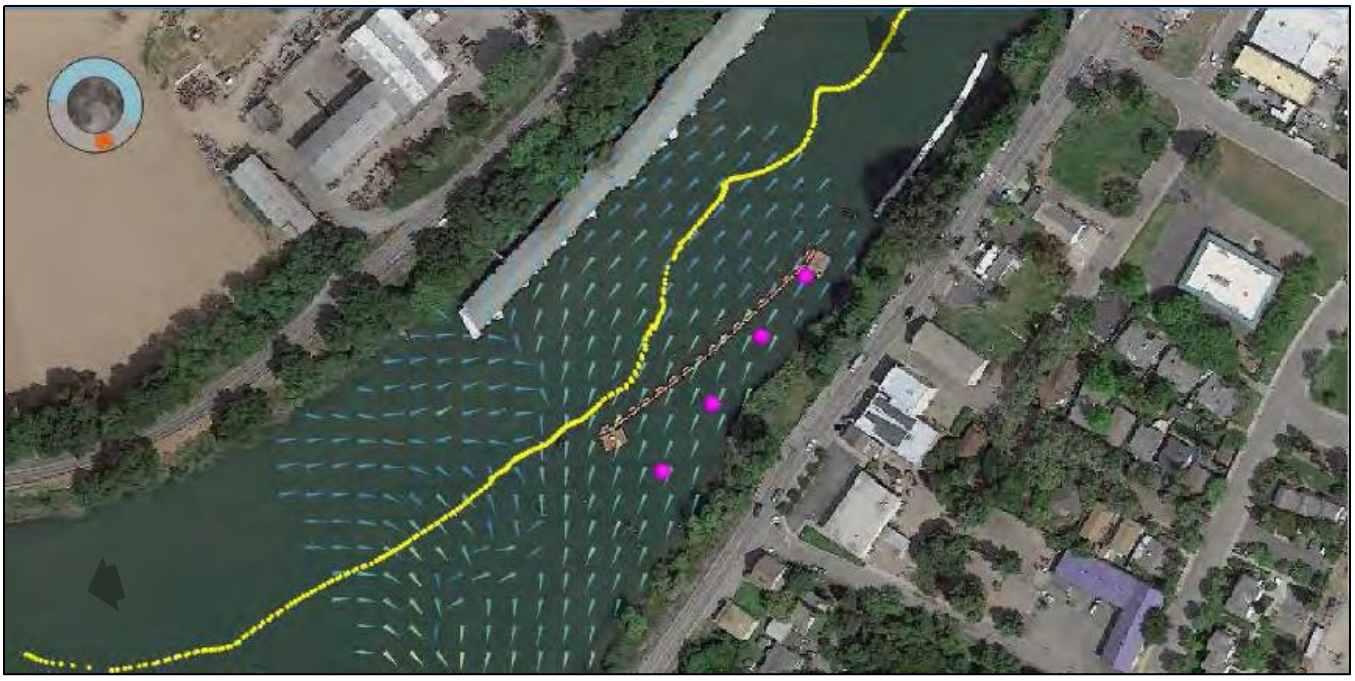

Note: This tagged juvenile Chinook salmon (4073.311) was determined to have not been eaten by a predator and appeared "guided" from 1252:53 hours until 1253:54 hours, and thus had an elapsed guidance time of 61 seconds. The pink spheres indicate the actual (Off) position of the FFGS.

Figure 3.1-9 Tagged Juvenile Chinook Salmon Passing the FFGS in the On Position on March 17, 2014

A "guided" juvenile Chinook salmon's guidance time was defined by expert opinion as the elapsed time beginning from the moment when the initial course change occurred to the end point: 1) a juvenile Chinook salmon moving past the FFGS line and changing course; 2) continuing along the guided line but moving past a line that was 10 m (33 ft) from the FFGS line; or 3) the point at which the juvenile Chinook salmon passed under

the FFGS. A "deterred" juvenile Chinook salmon was assigned a guidance time of 1 second because the amount of time the tag moved perpendicular to the barrier was less than the tag transmission interval.

Using these definitions, a juvenile Chinook salmon that passed under the FFGS could have been guided. A juvenile Chinook salmon that encountered the FFGS line, was guided some distance along the FFGS, and then went under, would have an elapsed guidance time. That juvenile Chinook salmon also would appear in Failure Group 1 (see "Failure Scenarios") for testing of Hypothesis H21: assess the scenarios of FFGS failure to determine whether one or more scenarios are significantly greater than other scenarios.

The elapsed guidance times for juvenile Chinook salmon were placed in samples in the same manner described in Section 3.1.1, "Methods". If only one fish in a sample was guided, then the elapsed guidance time of that fish represented the elapsed guidance time for that sample. If more than one fish occurred in a sample, the elapsed guidance time mean for all juvenile Chinook salmon in the sample was used.

The elapsed guidance time samples were compared with the FFGS On versus FFGS Off. The null Hypothesis H24 tested was:

$H24_0$ = The guidance time was the same when the FFGS was in the On and Off positions.

Then, the same steps were followed as described previously for the Hypothesis H16 tests. The hypothesis test for guidance time followed these four steps:

1. The data were tested to determine whether they met the assumptions of ANOVA: independence of observations, homogeneity of variance, and normality;

2. If the data met these three criteria, One-Way ANOVA was conducted for all light and velocity conditions combined;

3. Then, One-Way ANOVAs were conducted for each of the unique combinations of light and velocity outlined previously; and

4. If the data did not meet the assumptions of ANOVA, a nonparametric technique was used (e.g., Wilcoxon Two Sample test).

The first hypothesis tested was that of guidance time for all light and velocity levels combined. If the two-sided P-value obtained was less than or equal to the critical alpha, then the null hypothesis was rejected. A two-sided P-value was used because results of interest were that the FFGS significantly increased or decreased guidance time. Then, the guidance time data were partitioned by light level, using a threshold value of 5.4 lux. At each light level, the null hypothesis was tested—this was the second test using the guidance time data. Then, the guidance time data were partitioned by approach velocity level, using a threshold value of 0.25 m/s (0.82 ft/s). At each velocity level, the null hypothesis was tested—this was the third and final test using the guidance time data.

Three tests were conducted using the guidance time data samples. Thus, a Bonferroni method adjustment (Sokal and Rohlf 1995) to the critical alpha was required to maintain the experiment-wise error rate at the accepted level of 0.05. Three tests were conducted with the data sample, and thus 0.0167 (0.05/3) was the critical alpha value used for these comparisons. The P-value of a test had to be equal to or smaller than this value to reject the null hypothesis.

3.1.2 RESULTS

The total number of juvenile Chinook salmon that received a 2D track assessment was 979; these assessments allowed the determination of deterrence and predation through expert opinion. An additional 768 tagged fish did not come within 10 m (33 ft) of the FFGS but did pass through the study area. These 768 tagged fish were included in the overall efficiency, $E_{O,}$ analyses. To be clear, these tags arrived at the FFGS hydrophone array did not pass within 10 m (33 ft) of the FFGS, and they also arrived at the Sacramento River or Georgiana Slough downstream nodes. Thus, a total of 1,765 juvenile Chinook salmon were included in the analyses of overall efficiency. The number of samples obtained from tagged fish varied among barrier performance metrics (**Table 3.1-2**). Deterrence and protection efficiency sample sizes were similar and ranged from 50 to 61 for various states of the FFGS. Overall efficiency sample size was larger than that for E_D or E_P due to the 768 additional tags. The number of fish in these E_D, E_P, and E_O samples ranged from 2 to 25.

Table 3.1-2 Sample Size of Tags Encountering the FFGS during On and Off Operations for Three Evaluation Metrics

Barrier Efficiency Metric	Sample Size for FFGS On (N)	Sample Size for FFGS Off (N)
Deterrence Efficiency	61	54
Protection Efficiency	56	50
Overall Efficiency	83	79

Note: The number of tags (n) in each sample ranged from two to 25.

There was 9.5 percentage point greater deterrence on average with FFGS On compared to when the FFGS was Off (**Table 3.1-3**). The P-value for this statistical comparison was greater than the critical value for alpha, 0.0167 (see page 3.1-10). However, the P-value was less than 0.1 suggesting that there may be a true difference that could be determined through further testing. This 9.5 percentage point improvement contributed to a significant improvement in protection efficiency when the FFGS was On compared to when it was Off. There was an 18.2 percentage point greater protection efficiency on average when the FFGS was On compared to when it was Off. Protection efficiency does not include those tagged fish that were eaten before arriving at the FFGS. This result was possible because juvenile Chinook salmon could execute a turn >21°, not be deemed deterred, and continue downstream in the Sacramento River; thus, deterrence could be only 9.5 percentage point improved while protection efficiency showed a 18.2 percentage point improvement from FFGS Off to FFGS On. This result deviated from Chapter 3.2, "GLM Modeling" results and suggests that there was a difference in what tags were removed from analysis by the two methods. In this Chapter, 3.1, all tags that were deemed eaten by expert opinion were removed from the E_P calculation. In Chapter 3.2, a threshold value (0.66) from the Mixture Model was selected and all tags that had a predation probability above that threshold were removed from analysis.

When those juvenile Chinook salmon that were determined to have been eaten were not removed it had an effect; overall efficiency was not statistically different between FFGS On and Off. The result for overall efficiency was nearer significance (P = 0.0516) than deterrence efficiency (P = 0.0842), and this is most likely attributable to the higher sample size obtained for E_O than for E_D (**Table 3.1-3**). However, the P-values for both E_O and E_D were less than 0.1, and this suggests that further testing could show statistical differences in deterrence and overall efficiency for the FFGS On compared to FFGS Off.

Table 3.1-3 Comparison of FFGS On and Off Operations for Three Juvenile Chinook Salmon Response Metrics: Deterrence Efficiency, Protection Efficiency, and Overall Efficiency					
Comparison Metrics	**FFGS On Mean**	**FFGS Off Mean**	**Percentage Point Change in Efficiency**	**Wilcoxon Statistic**	**One-sided P-value**
Deterrence efficiency	0.470	0.375	9.5	3375.0	0.0842
Protection efficiency	0.728	0.546	18.2	3041.0	0.0085
Overall efficiency	0.777	0.738	3.9	6920.5	0.0516

The number of samples derived from juvenile Chinook salmon that passed the FFGS ranged from 53 to 66 for combinations of FFGS operation and light level (**Table 3.1-4**). The total number of samples with the FFGS Off was 119, and 118 samples occurred with the FFGS On. The number of fish in individual samples ranged from 2 to 25.

Table 3.1-4 Summary of Juvenile Chinook Salmon Samples Encountering the FFGS during On and Off Operations at Low (< 5.4 Lux) and High (≥ 5.4 Lux) Light Levels		
Comparison Metrics and Light Level	**FFGS On (N)**	**FFGS Off (N)**
Deterrence efficiency—low light	21	25
Deterrence efficiency—high light	23	29
Protection efficiency—low light	19	21
Protection efficiency—high light	23	25
Overall efficiency—low light	20	26
Overall efficiency—high light	27	28

For both low and high light conditions, juvenile Chinook salmon deterrence efficiency, E_D, was not statistically different between the FFGS in the On and Off positions (**Table 3.1-5**). Juvenile Chinook salmon's protection efficiency, E_P, was 18.2 percentage points higher on average with the FFGS On compared to Off under low light conditions (**Table 3.1-5**). This was not statistically significant because the P-value, 0.0221, was slightly larger than the Bonferroni-adjusted critical alpha level, 0.0167 (see subsection "Hypotheses H16, 22a, and 23a Testing"). A very similar result was obtained under high light conditions: E_P was 17.4 percentage points higher with the FFGS in the On position compared to Off. These results were not statistically significant, but both exhibited a P-value less than 0.1. Thus, there may be improvement in protection efficiency under all light conditions. This result warrants further research with a greater sample size to discern if the FFGS improves protection efficiency in a statistically significant manner. It is easy to see the mechanism through which juvenile Chinook salmon E_P would improve during high light conditions: juvenile Chinook salmon have large eyes compared to many other fish and vision is one of the primary anti-predator senses (Gregory 1993; Guthre and Muntz 1993). Under low light conditions, it seems possible juvenile Chinook salmon may have detected and avoided the FFGS with reduced visual cues to assist them. During these low light conditions, juvenile Chinook salmon possibly could have a stronger response to the turbulence created by the FFGS. Salmonids have demonstrated a variety of behavioral responses to varying rheotactic conditions (e.g., Hoar 1951; Taylor 1988; Thorpe and Moore 1997).

For low light conditions, overall efficiency was higher on average when the FFGS was On compared to when it was Off. The P-value, 0.0535, for this test was not smaller than the critical alpha for this test, 0.0167 (see page 3.1-7); however the P-value was less than 0.1 and thus further testing could show that in low light conditions there is a real

improvement in overall efficiency with FFGS On compared to the Off position. For high light conditions, there was no significant improvement in overall efficiency when the FFGS was On compared to when it was Off.

Table 3.1-5 Comparisons of Deterrence, Protection, and Overall Efficiencies for Juvenile Chinook Salmon during FFGS On and Off Operations under Low (< 5.4 Lux) and High (≥ 5.4 Lux) Light Levels

Comparison Metrics	FFGS On Mean	FFGS Off Mean	Percentage Point Change in Efficiency	Wilcoxon Statistic	One sided P-value
Deterrence efficiency—low light	0.407	0.383	2.4	835.0	0.3763
Deterrence efficiency—high light	0.552	0.367	15.5	827.0	0.1001
Protection efficiency—low light	0.772	0.590	18.2	755.0	0.0221
Protection efficiency—high light	0.683	0.509	17.4	779.5	0.0828
Overall efficiency—low light	0.779	0.721	5.8	1404.5	0.0535
Overall efficiency—high light	0.776	0.750	2.6	2125.0	0.2069

The distribution of samples was different between light (**Table 3.1-5**) and velocity combinations (**Table 3.1-6**). For example, the range of sample sizes observed for velocity was greater, 41 to 78, than for light. This occurred because more high velocity samples were obtained than low velocity samples. At least two possible mechanisms could explain this result: 1) the FFGS-2014 location tends to have higher approach velocities because the cross-sectional area of the river is smaller there than at the location of the BAFF in 2011 and 2012 (**Figure 1-2**); and 2) juvenile Chinook salmon were more likely to migrate under tidal conditions that exhibited high downstream velocities, perhaps to reduce predation risk. Juvenile Chinook salmon that passed the FFGS while experiencing negative approach velocities were removed from the analyses (Section 2.5.3) because the FFGS was not intended to function under those conditions. Of course, a combination of these two factors or other factors also may have influenced the sample sizes obtained.

Table 3.1-6 Summary of Juvenile Chinook Salmon Samples Encountering the FFGS during On and Off Operations at Low (< 0.25 m/s) and High (≥ 0.25 m/s) Approach Velocities

Comparison Metrics and Approach Velocity Level	FFGS On (N)	FFGS Off (N)
Deterrence efficiency—low velocity	7	8
Deterrence efficiency—high velocity	35	46
Protection efficiency—low velocity	7	6
Protection efficiency—high velocity	35	40
Overall efficiency—low velocity	9	9
Overall efficiency—high velocity	38	45

The significant improvement in juvenile Chinook salmon protection efficiency was driven by the significant 23.6 percentage point increase that occurred, for FFGS On compared to Off, under high velocity conditions (**Table 3.1-7**). Also, a significant 6.2 percentage point increase in overall efficiency occurred for FFGS On compared to Off under high velocity conditions. These results suggest that juvenile Chinook salmon may have detected and avoided the FFGS at higher approach velocities while also experiencing shorter barrier approach times. At least two possible explanations might explain these results: 1) under high velocity conditions, juvenile Chinook salmon are reluctant to, or have insufficient time to, sound under the FFGS; and/or 2) at higher water

velocities, the water deceleration upstream from the FFGS, caused by the FFGS structure, may be detectable at a greater distance from the barrier compared to lower velocities.

Table 3.1-7 Comparisons of Deterrence, Protection, and Overall Efficiencies for Juvenile Chinook Salmon during FFGS On and Off Operations under Low (< 0.25 m/s) and High (≥ 0.25 m/s) Approach Velocities

Comparison Metrics	FFGS On Mean	FFGS Off Mean	Percentage Point Change in Efficiency	Wilcoxon Statistic	One-sided P-value
Deterrence efficiency—low velocity	0.491	0.300	19.1	98.5	0.2340
Deterrence efficiency—high velocity	0.471	0.389	8.2	2314.5	0.1632
Protection efficiency—low velocity	0.444	0.500	-5.6	74.0	0.4379
Protection efficiency—high velocity	0.790	0.554	23.6	2203.5	0.0013
Overall efficiency—low velocity	0.560	0.619	-5.9	354.5	0.3475
Overall efficiency—high velocity	0.842	0.780	6.2	3335.0	0.0163

Segment Intersection (Hypothesis H17)

Eight Segments

All juvenile Chinook salmon that were determined to have been eaten were removed from consideration for the evaluation of where tags crossed the FFGS line. When the FFGS was in the Off position juvenile Chinook salmon did not pass the FFGS segments in a random fashion (**Table 3.1-8**; chi-squared = 23.98, P = 0.0011). Many more juvenile Chinook salmon passed through Segments 5 to 8 than would have been expected at random (**Figure 3.1-10**), and the most commonly passed was Segment 8 at the downstream end of the FFGS. This result is consistent with the hypothesis that juvenile Chinook salmon migrate in high velocity portions of the river's cross-section and avoid river margins where predators may be more common. It was concluded that the probability a juvenile Chinook salmon would pass the FFGS line is not uniform along the length of the FFGS line.

When the FFGS was On, juvenile Chinook salmon did not pass under the FFGS in a randomly distributed manner (**Table 3.1-8**; chi-squared = 24.96, P = 0.0008). Many more juvenile Chinook salmon passed through Segments 5 through 8 than would be expected at random (**Figure 3.1-11**), and the most commonly passed segment was Segment 8. Thus, $H17_0$ was rejected and it was concluded that the probability a fish would pass under the FFGS is not uniform along the length of the FFGS.

Table 3.1-8 Expected Frequency and Observed Number and Observed Frequency of Juvenile Chinook Salmon Crossing the FFGS Barrier Divided into Eight Segments of Equal Length

	Segment							
	1	2	3	4	5	6	7	8
Expected Proportion	0.125	0.125	0.125	0.125	0.125	0.125	0.125	0.125
FFGS-Off Count	3	1	2	1	7	8	12	13
Observed Proportion	0.0638	0.0213	0.0426	0.0213	0.1489	0.1702	0.2553	0.2766
FFGS-On Count	4	0	1	1	8	6	7	14
Observed Proportion	0.0976	0.0000	0.0244	0.0244	0.1951	0.1463	0.1707	0.3415

Note: Expected frequency is 1/8 Segments, or 0.125, the proportion of Chinook juveniles expected to pass through a barrier segment if the process was completely random.

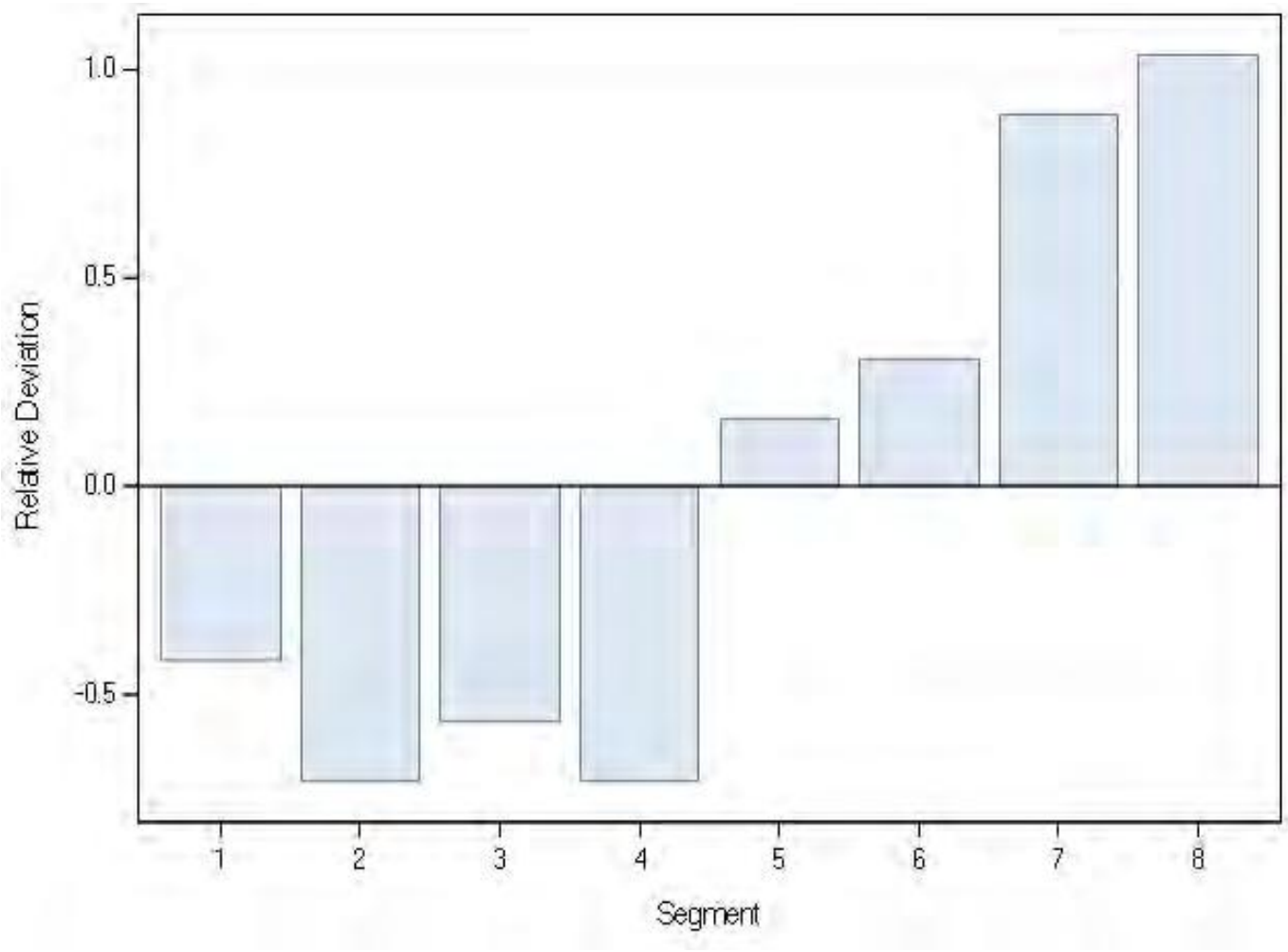

Note: Relative Deviation is the deviation in a segment, from the expected proportion, relative to the other segments. A negative Relative Deviation signifies fewer juvenile Chinook salmon passing through a segment than would have been expected through a random process. A positive Relative Deviation signifies more juvenile Chinook salmon passing through a segment than would have been expected through a random process. All segments had equal expected proportion of 0.125.

Figure 3.1-10 Relative Deviation of Juvenile Chinook Salmon Passing through Eight Segments with the FFGS Off

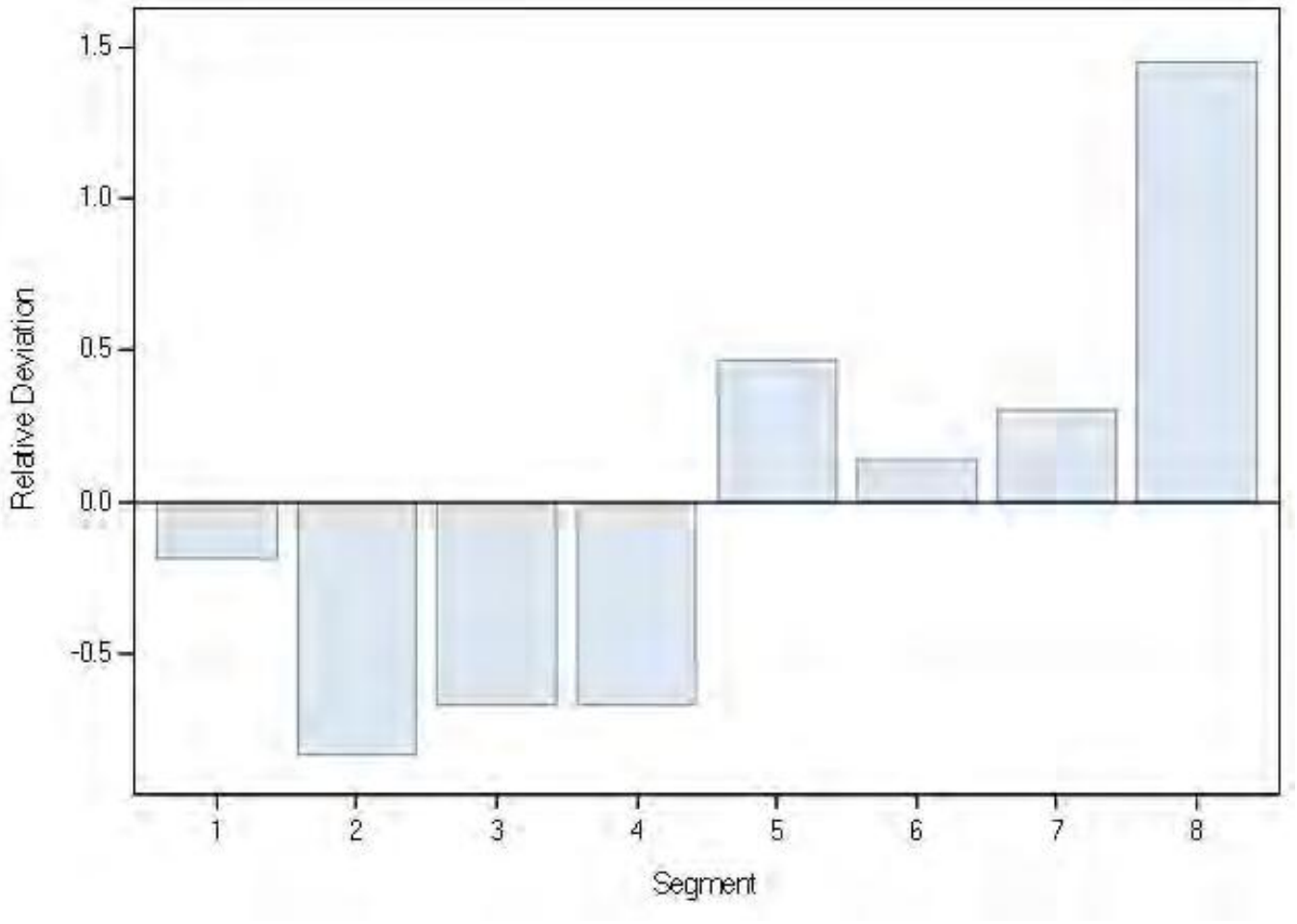

Note: Relative Deviation is the deviation in a segment, from the expected proportion, relative to the other segments. A negative Relative Deviation signifies fewer juvenile Chinook salmon passing through a segment than would have been expected through a random process. A positive Relative Deviation signifies more juvenile Chinook salmon passing through a segment than would have been expected through a random process. All segments had equal expected proportion of 0.125.

Figure 3.1-11 Relative Deviation of Juvenile Chinook Salmon Passing through Eight Segments with the FFGS On

Then, the observed proportions of juvenile Chinook salmon that passed through each segment when the FFGS was Off were used as expected values; **Table 3.1-9** summarizes these expected values (see FFGS-Off Observed Proportion). These "expected" values were compared to the observed proportions of juvenile Chinook salmon passing through the eight segments when the FFGS was in the On position. No difference occurred in the distribution of juvenile Chinook salmon passing through the area with the FFGS Off compared to the On position (Fisher's Exact Test, P = 0.9710). In addition, no pattern appeared for the observed (FFGS On) proportions that differed from the expected (FFGS Off) in any systematic way (**Figure 3.1-12**). It was concluded that the presence of the FFGS in the On position did not influence where a juvenile Chinook salmon passed the FFGS line.

Table 3.1-9 Counts and Proportions of Juvenile Chinook Salmon Passing the FFGS Line* through Segments 1-8 with the FFGS Off and On				
FFGS Line Segment	**FFGS Off, Number Crossing**	**FFGS Off, Proportion Crossing**	**FFGS On, Number Crossing**	**FFGS On, Proportion Crossing**
1	8	0.0625	9	0.1154
2	9	0.0703	5	0.0641
3	7	0.0547	5	0.0641
4	6	0.0469	2	0.0256
5	16	0.125	12	0.1538
6	23	0.1797	12	0.1538
7	25	0.1953	12	0.1538
8	34	0.2656	21	0.2692

Note: The "FFGS Line" was the footprint of the FFGS infrastructure when the FFGS was in the On position regardless of whether the FFGS was in the On position or the Off position.

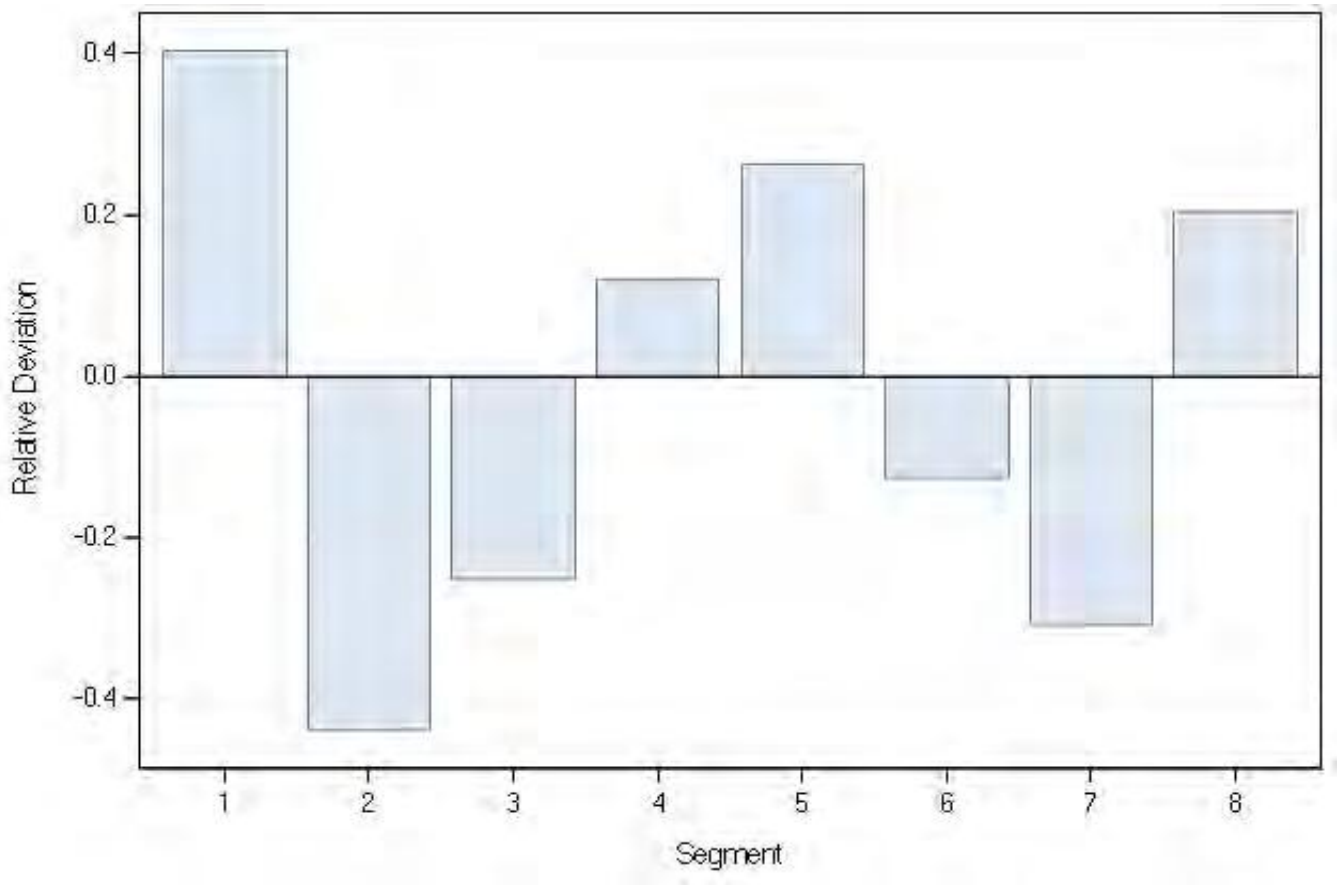

Note: Relative deviation of juvenile Chinook salmon passing through eight segments with the FFGS Off compared to the FFGS On. A negative relative deviation signifies fewer juvenile Chinook salmon passing through a segment with the FFGS On than would have been expected from FFGS Off proportion passing through.

Figure 3.1-12 Relative Deviation of Juvenile Chinook Salmon Passing through Eight Segments with the FFGS Off

Ten Segments

When the FFGS was Off, juvenile Chinook salmon did not pass the FFGS segments in a random fashion (**Table 3.1-10**; chi-squared = 85.50, P < 0.0001). Many more juvenile Chinook salmon passed through Segments 7 to 10 than would have been expected at random (**Figure 3.1-13**), and the most commonly passed was Segment 9 and Segment 10. It was concluded that, in the absence of the FFGS in the On position, the probability a juvenile Chinook salmon would pass the FFGS line is not uniform along the ten segments tested.

Table 3.1-10 Expected Frequency and Observed Number of Frequency Crossing FFGS Barrier Segments with Ten Segments

	Segment									
	1	**2**	**3**	**4**	**5**	**6**	**7**	**8**	**9**	**10**
Expected Frequency	0.1	0.1	0.1	0.1	0.1	0.1	0.1	0.1	0.1	0.1
FFGS-Off Count	3	1	2	1	7	8	12	13	31	25
Observed Proportion	0.0291	0.0097	0.0194	0.0097	0.0680	0.0777	0.1165	0.1262	0.3010	0.2427
FFGS-On Count	4	0	1	1	8	6	7	14	26	18
Observed Proportion	0.0471	0.0000	0.0118	0.0118	0.0941	0.0706	0.0824	0.1647	0.3059	0.2118

Note: Expected frequency is 1/10 Segments, or 0.1, the proportion of Chinook juveniles expected to pass through a barrier segment if the process was completely random.

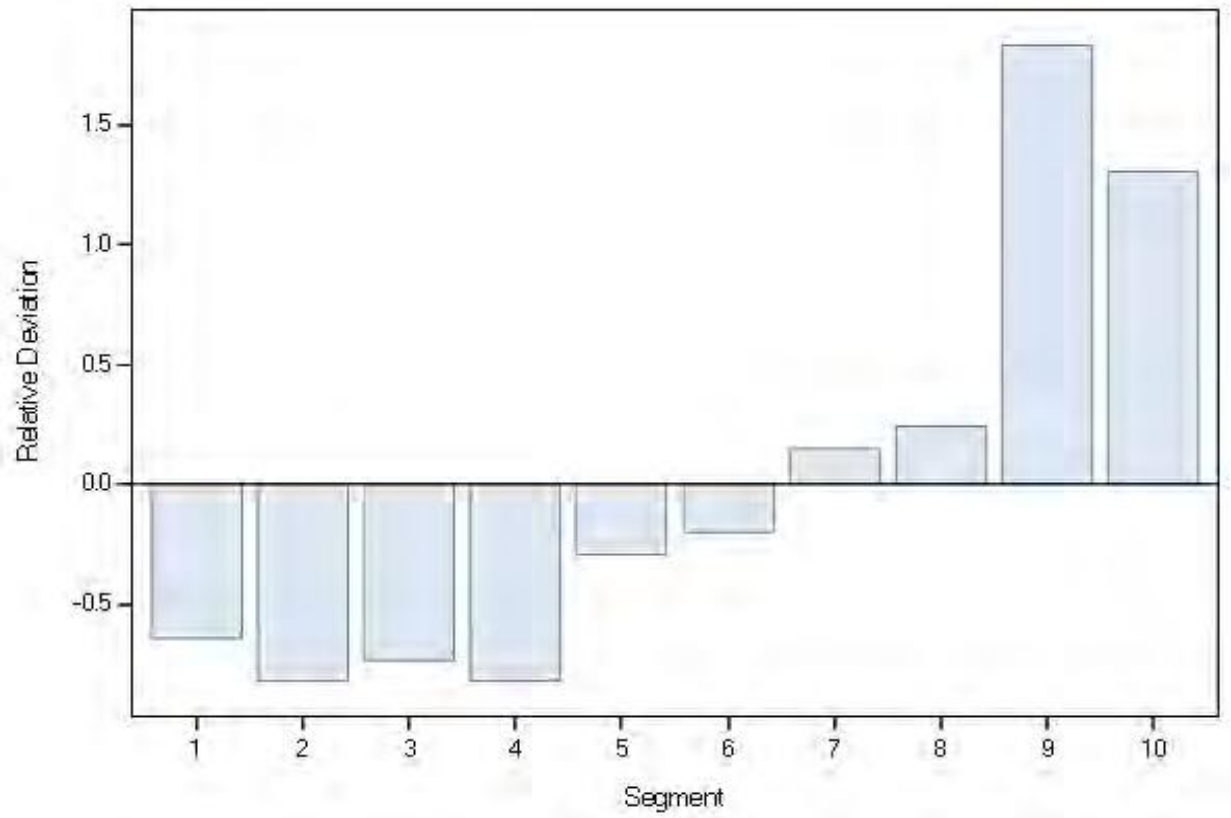

Note: Relative Deviation is the deviation in a segment, from the expected proportion, relative to the other segments. A negative Relative Deviation signifies fewer juvenile Chinook salmon passing through a segment than would have been expected through a random process. A positive Relative Deviation signifies more juvenile Chinook salmon passing through a segment than would have been expected through a random process. All segments had equal expected proportion of 0.125.

Figure 3.1-13 Relative Deviation of Juvenile Chinook Salmon Passing through Ten Segments with the FFGS Off

When the FFGS was On, juvenile Chinook salmon did not pass under or through the ten segments in a randomly distributed manner (**Table 3.1-10**; chi-squared = 54.222, P < 0.0001). Many more juvenile Chinook salmon passed through Segments 8 to 10 than would have been expected at random (**Figure 3.1-14**), and the most commonly passed was Segment 9. It was concluded that the probability a juvenile Chinook salmon would pass the FFGS line is not uniform among the ten segments tested. This result was consistent with the findings in Section 3.3, **Figure 3.3-26(d)** – for 79 percent of the 2014 experimental period the critical streakline lay to the right of the downstream end of the FFGS. Thus, when a neutrally buoyant particle had passed the physical structure of the FFGS, 79 percent of the time that particle would have been entrained into Georgiana Slough. So, it was not surprising that juvenile Chinook salmon should pass by the FFGS line most commonly in Segment 9.

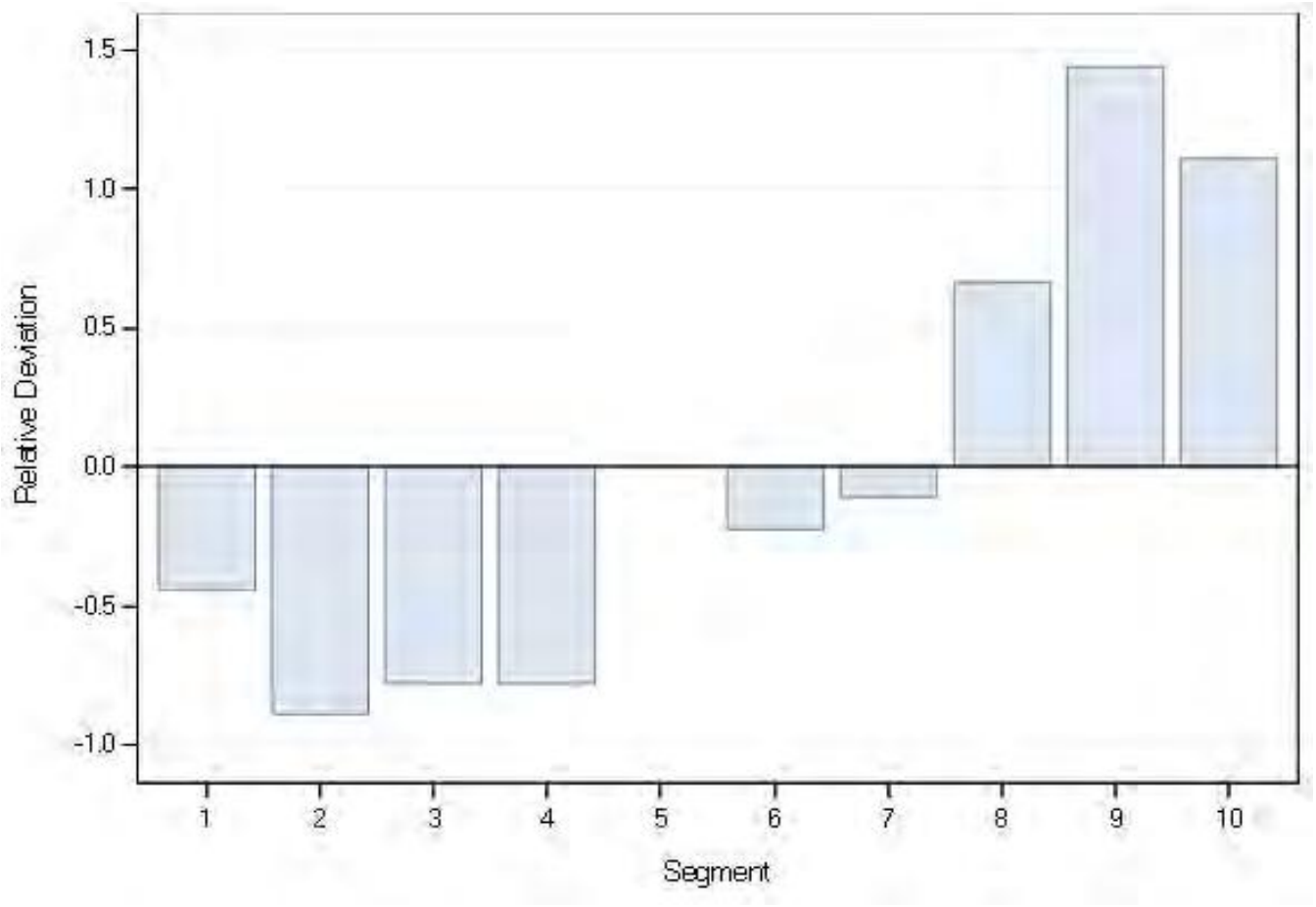

Note: Segments 1-8 are the FFGS proper. Segments 9 and 10 are immediately past the FFGS infrastructure but in the same alignment. All segments had equal expected proportion of 0.1. A negative relative deviation signifies fewer juvenile Chinook salmon passing through a segment than would have been expected through a random process.

Figure 3.1-14 Relative Deviation of Juvenile Chinook Salmon Passing through Ten Segments with the FFGS On

Then, the proportions of juvenile Chinook salmon that passed through each segment when the FFGS was Off were used as expected values. **Table 3.1-10** summarizes these expected values and the actual number of juvenile Chinook salmon that passed through each of Segments 1-10. The expected values were compared to the observed values of juvenile Chinook salmon proportions passing through segments when the FFGS was in the On position. No difference was noted in the distribution of juvenile Chinook salmon passing through the area with the FFGS Off compared to the On position (Fisher's Exact Test P = 0.9797). This result suggests that for those juvenile

Chinook salmon that passed the FFGS line, the FFGS did not influence the proportion of juvenile Chinook salmon that passed in any particular segment (**Figure 3.1-15**).

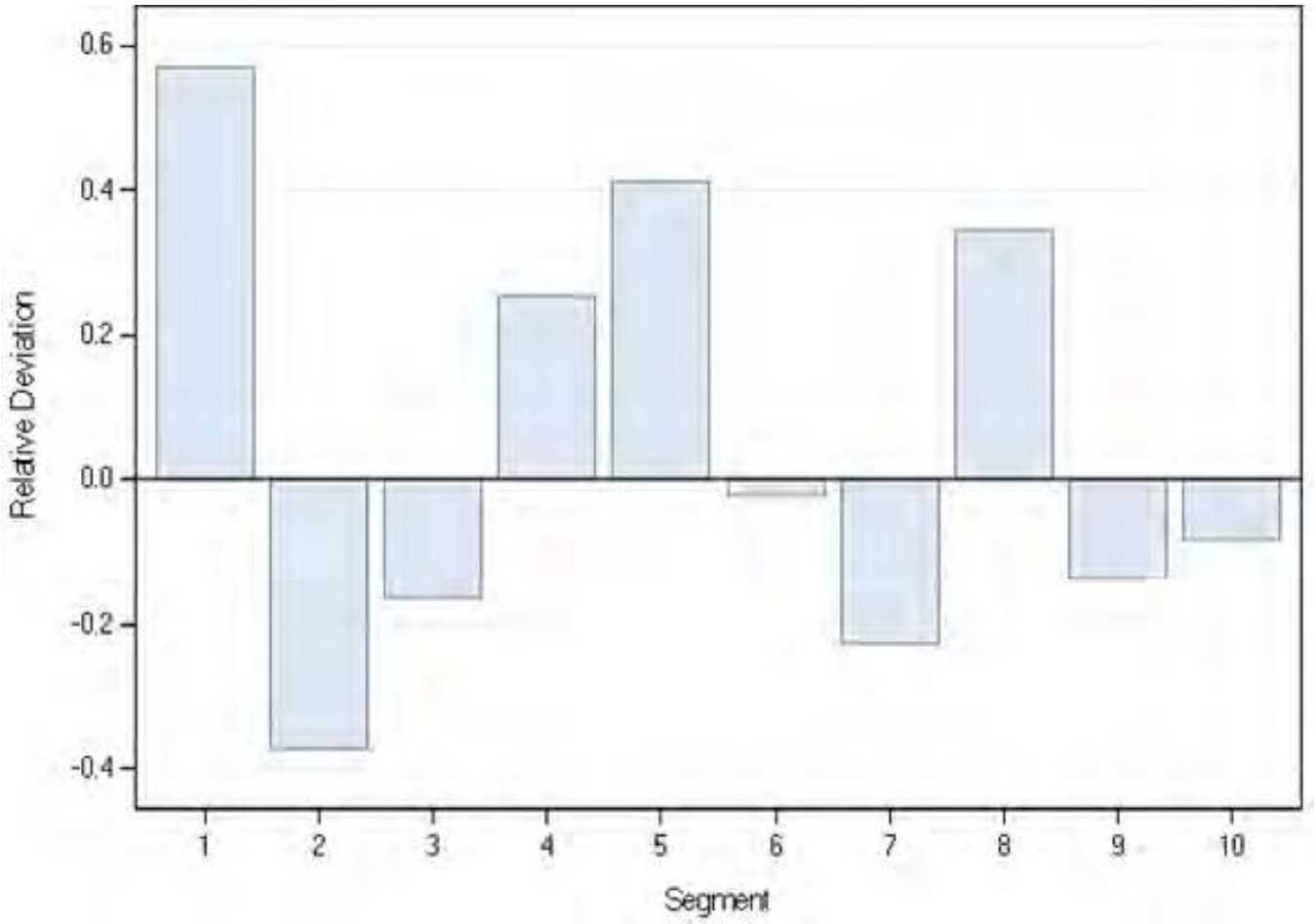

Note: Segments 1-8 are the FFGS proper. Segments 9 and 10 are immediately past the FFGS infrastructure but in the same alignment. A negative relative deviation signifies fewer juvenile Chinook salmon passing through a segment with the FFGS On than would have been expected from FFGS Off proportion passing through.

Figure 3.1-15 Relative Deviation of Juvenile Chinook Salmon Passing through Ten Segments with the FFGS Off compared to the FFGS On

Guidance Time

No difference was noted in the guidance time when the FFGS was Off compared to the On position (**Table 3.1-9**). This suggests that guidance time was not affected by the presence of the FFGS. Juvenile Chinook salmon took, on average, about 85 seconds to travel the length of the FFGS line, whether the FFGS was On or Off.

When the guidance time data were partitioned by approach velocity, very interesting patterns emerged. At low approach velocities, the FFGS in the On position produced significantly longer guidance time than did the FFGS in the Off position (**Table 3.1-11**). However, this result should be viewed with caution because of the small sample size for FFGS Off (N = 5). However, at high velocities, the inverse was true; the FFGS in the On position produced significantly shorter guidance time than did the FFGS in the Off position. This result was consistent with those results described in **Table 3.1-6** and the hypothesis that under high velocity conditions, juvenile Chinook salmon have less time to avoid the FFGS.

Table 3.1-11 Comparisons of Guidance Time (seconds) for Juvenile Chinook Salmon during FFGS On and Off Operations: Combined, under Low (< 5.4 Lux) and High (≥ 5.4 Lux) Light Levels, and under Low (< 0.25 m/s) and High (≥ 0.25 m/s) Approach Velocities

Comparison Metrics	FFGS On Mean(N)	FFGS Off Mean(N)	Change in Mean Guidance Time(s)	Wilcoxon Statistic	Two-sided P-value
Guidance Time	87.5(91)	83.0(82)	4.5	7,454.0	0.3313
Guidance time—low light	75.6(50)	85.4(39)	-9.8	1,866.5	0.3582
Guidance time—high light	101.9(41)	80.8(43)	21.1	1,733.0	0.9358
Guidance time—low velocity	136.3(16)	25.0(5)	111.3	21.0	0.0054
Guidance time—high velocity	77.1(75)	86.8(77)	-9.7	5,040	0.0102

Failure Scenarios (Hypothesis H21)

As described previously, failure scenario groups were defined as follows: Failure Group 1 included juvenile Chinook salmon determined to have not been eaten that passed under the FFGS. Failure Group 2 included juvenile Chinook salmon that were eaten upstream from the FFGS and then exited via Georgiana Slough in a predatory fish. Failure Group 3 included juvenile Chinook salmon determined to have not been eaten that passed to the right of the FFGS but then were entrained into Georgiana Slough.

When the FFGS was Off, tags that originally were inserted into juvenile Chinook salmon did not fail in a randomly distributed fashion (Goodness of Fit Exact P = 0.0045) (**Table 3.1-12**). Fewer juvenile Chinook salmon failed by passing the FFGS line (Failure Group 1) than expected. More juvenile Chinook salmon were eaten or passed to the right of the FFGS line than expected in a random process (**Figure 3.1-16**. It was concluded that with the FFGS in the Off position, the probability a tag would fail was not equivalent among the failure scenarios.

Table 3.1-12 Expected Frequency and Observed Number of Proportion of Tags in Three Failure Groups			
	Failure Group		
	1	2	3
Expected Frequency	0.33	0.33	0.33
FFGS-Off Count	29	59	53
Observed Proportion	0.2057	0.4184	0.3759
FFGS-On Count	24	53	45
Observed Proportion	0.1967	0.4344	0.3689

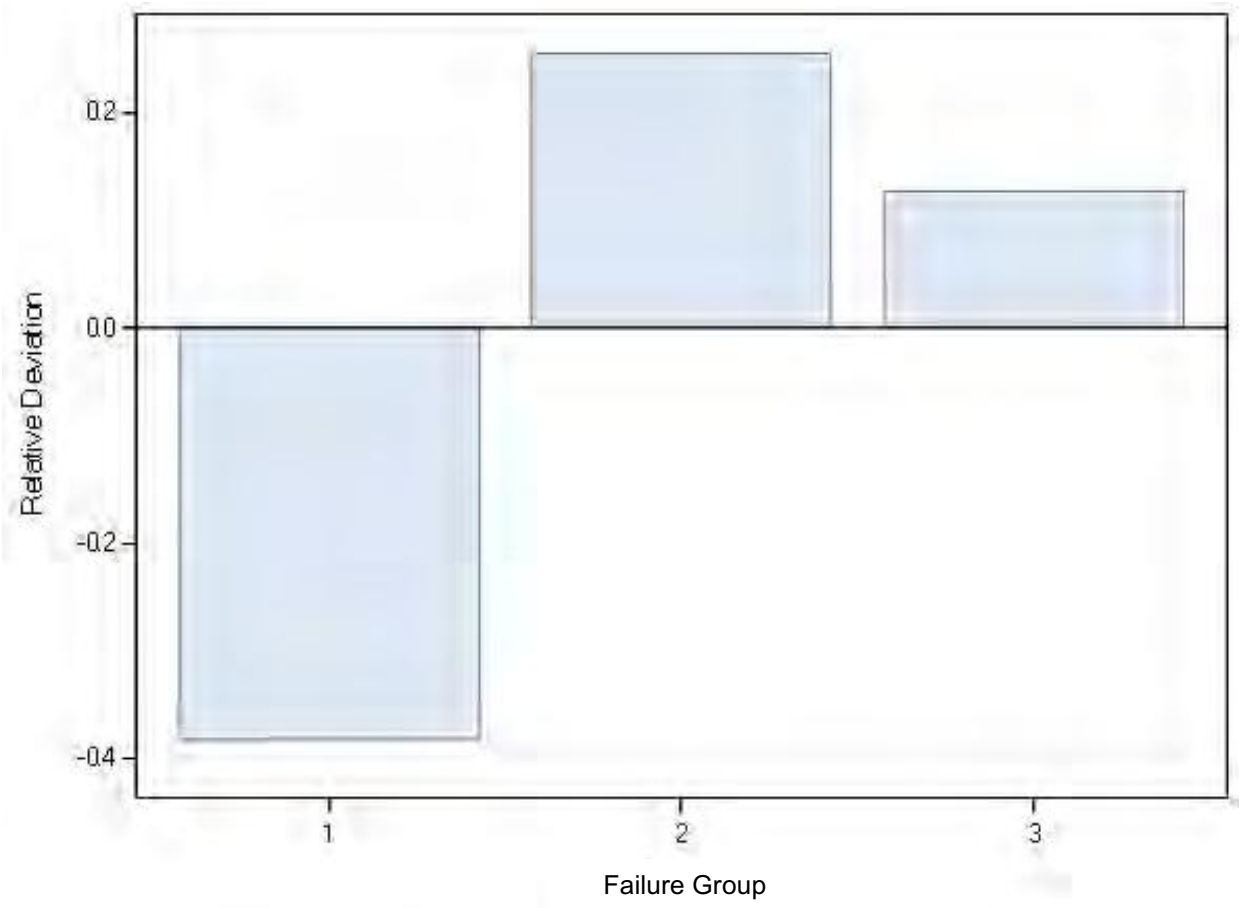

Note: A negative relative deviation signifies fewer juvenile Chinook salmon failing through a particular scenario than would be expected by a random process. Failure Group 1—juvenile Chinook salmon that passed under the FFGS or through the FFGS line. Failure Group 2—juvenile Chinook salmon that were eaten upstream from the FFGS and then exited via Georgiana Slough. Failure Group 3—juvenile Chinook salmon that passed to the right of the FFGS line but then were entrained into Georgiana Slough.

Figure 3.1-16 Relative Deviation of Tags with the FFGS Off

When the FFGS was On, tags did not fail in a randomly distributed way (Goodness of Fit Exact P = 0.0045). Fewer juvenile Chinook salmon failed by passing under the FFGS than expected. More juvenile Chinook salmon were eaten or passed to the right of the FFGS than expected to occur in a random process (**Figure 3.1-17**). Hypothesis $H21_0$ was rejected, and it was concluded that the proportion of juvenile Chinook salmon that enter Georgiana Slough is unequal for the barrier failure scenarios: 1) under the barrier structure; 2) eaten upstream

from the FFGS; or 3) passed to the right of the FFGS but entrained into Georgiana Slough. No other failure scenarios over (e.g., wave action), through (damage to the structure), or impinged were observed.

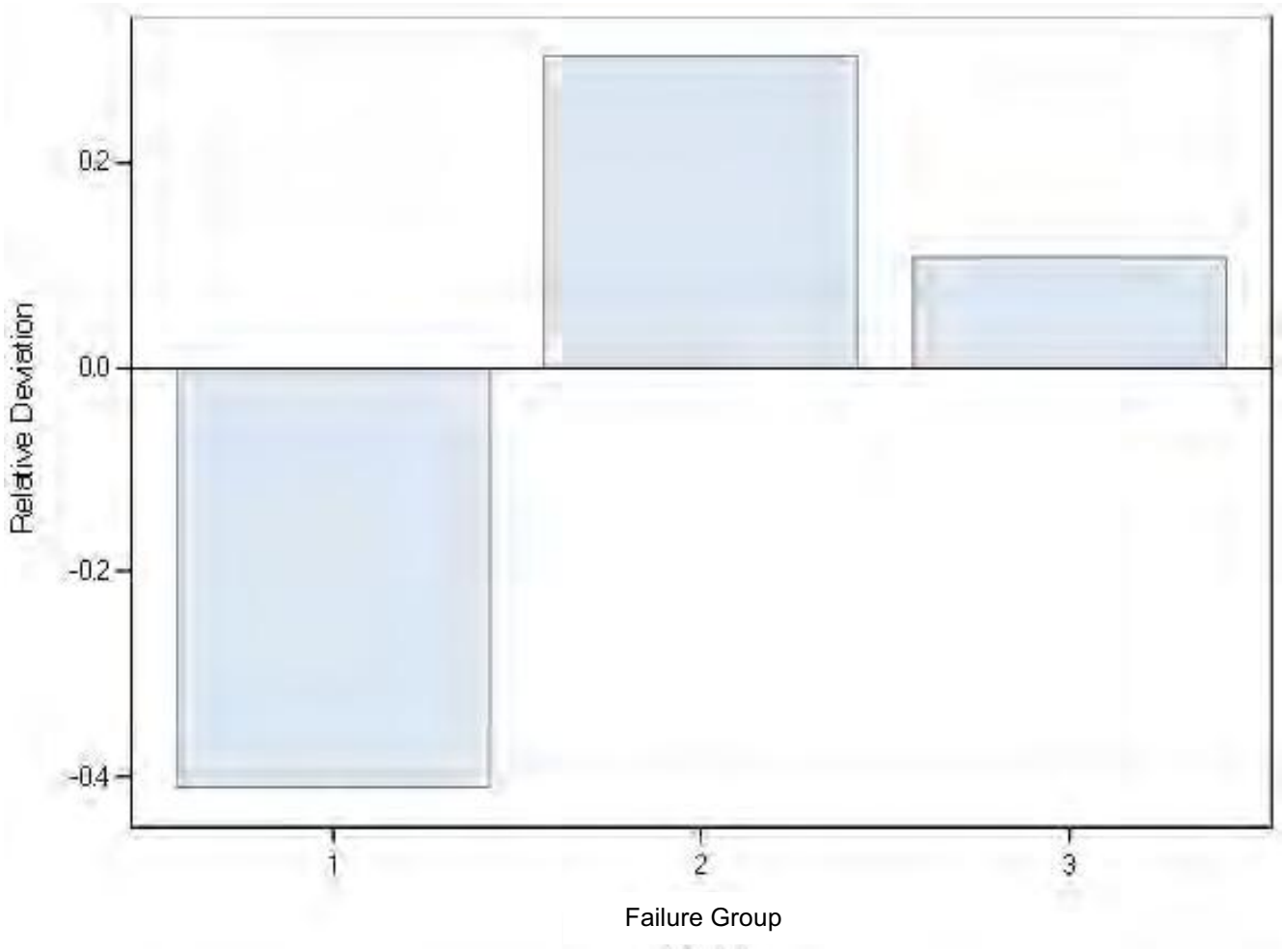

Note: A negative relative deviation signifies fewer juvenile Chinook salmon failing through a particular scenario than would be expected by a random process. Failure Group 1—juvenile Chinook salmon that passed under the FFGS or through the FFGS line. Failure Group 2—juvenile Chinook salmon that were eaten upstream from the FFGS and then exited via Georgiana Slough. Failure Group 3—juvenile Chinook salmon that passed to the right of the FFGS line but then were entrained into Georgiana Slough.

Figure 3.1-17 Relative Deviation of Tags with the FFGS On

The proportions of juvenile Chinook salmon that passed through each segment when the FFGS was Off were used as expected values; this 1 by 3-vector of expected values was 0.2057, 0.4184, and 0.3759. The expected values were compared to observed values of tags' failure scenarios when the FFGS was in the On position. No difference was observed in the distribution of failure scenarios with the FFGS Off compared to the On position (Goodness of Fit Exact P = 0.9439). This result suggested that the FFGS did not influence the probability of failure scenario.

The most common method for a tagged juvenile Chinook salmon to depart the array via Georgiana Slough was in a predatory fish (**Figure 3.1-18**). Thus, to evaluate failure scenarios of juvenile Chinook salmon only, tagged juvenile Chinook salmon that had been eaten were removed from the analysis.

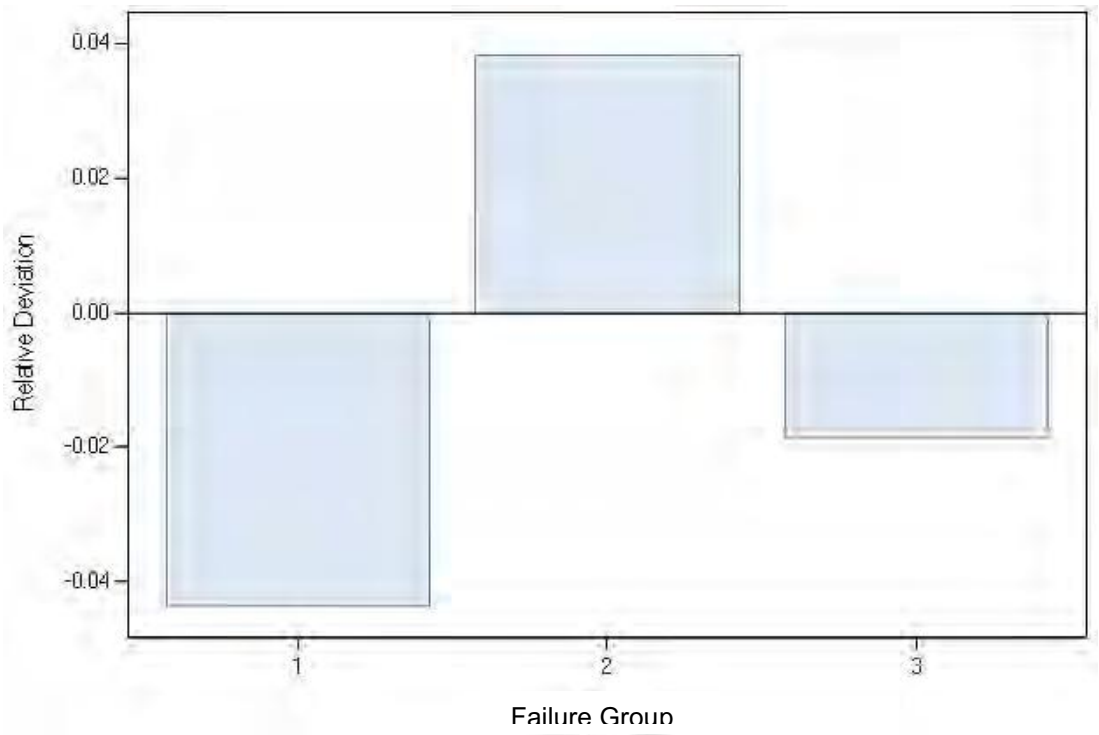

Note: A negative relative deviation signifies fewer juvenile Chinook salmon failing through a particular scenario than would be expected by a random process. Failure Group 1—juvenile Chinook salmon that passed under the FFGS or through the FFGS line. Failure Group 2—juvenile Chinook salmon that were eaten upstream from the FFGS and then exited via Georgiana Slough. Failure Group 3—juvenile Chinook salmon that passed to the right of the FFGS line but then were entrained into Georgiana Slough.

Figure 3.1-18 Relative Deviation of Tags with the FFGS On

Eaten Juvenile Chinook Salmon Removed

Failure Group 2 included tagged juvenile Chinook salmon that were eaten upstream from the FFGS line and the tag then exited via Georgiana Slough. In the vicinity of the FFGS, Failure Group 2 represented the behavior of predatory fishes. Therefore, Failure Group 2 was removed from consideration, and Failure Groups 1 and 3 were compared to allow an investigation of the failure scenario of tags in Chinook juveniles only.

When the FFGS was Off, Failure Groups 1 and 3 could not be differentiated statistically from a random process (Goodness of Fit Exact P = 0.0530) (**Table 3.1-12**). However, the P-value was small. This suggests that further research could address whether the pattern observed may be significant. The pattern observed was that a higher number of juvenile Chinook salmon than expected passed to the right of the FFGS line and then subsequently exited via Georgiana Slough (**Figure 3.1-19**).

Table 3.1-13 Expected Frequency and Observed Number of Proportion of Tags in Two Failure Groups		
	Failure Group	
	1	3
Expected Frequency	0.5	0.5
FFGS-Off Count	29	53
Observed Proportion	0.3537	0.6463
FFGS-On Count	24	45
Observed Proportion	0.3478	0.6522

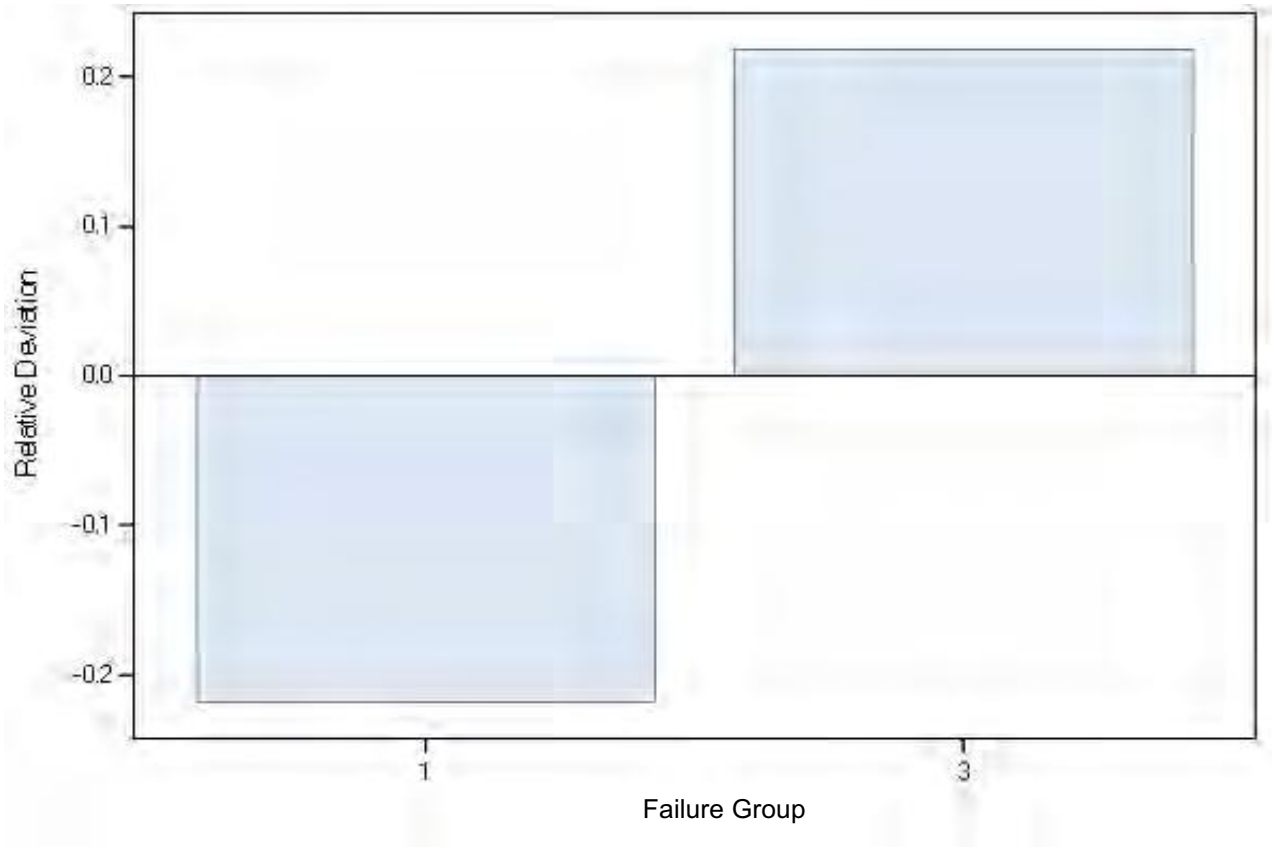

Note: A negative relative deviation signifies fewer juvenile Chinook salmon failing through a particular scenario than would be expected by a random process. Failure Group 1—juvenile Chinook salmon that passed under the FFGS or through the FFGS line. Failure Group 3—juvenile Chinook salmon that passed to the right of the FFGS line but then were entrained into Georgiana Slough.

Figure 3.1-19 Relative Deviation of Juvenile Chinook Salmon with the FFGS Off

When the FFGS was On, Failure Groups 1 and 3 could not be differentiated statistically from a random process (Goodness of Fit Exact P = 0.0319); the Bonferroni-adjusted critical α for this test was 0.0125 (see Section 3.1.1, "Methods"). However, the P-value was very small. This suggests that further research could address whether the pattern observed may be significant. The pattern observed was that a higher number of juvenile Chinook salmon than expected passed to the right of the FFGS line and then subsequently exited via Georgiana Slough (**Figure 3.1-20**).

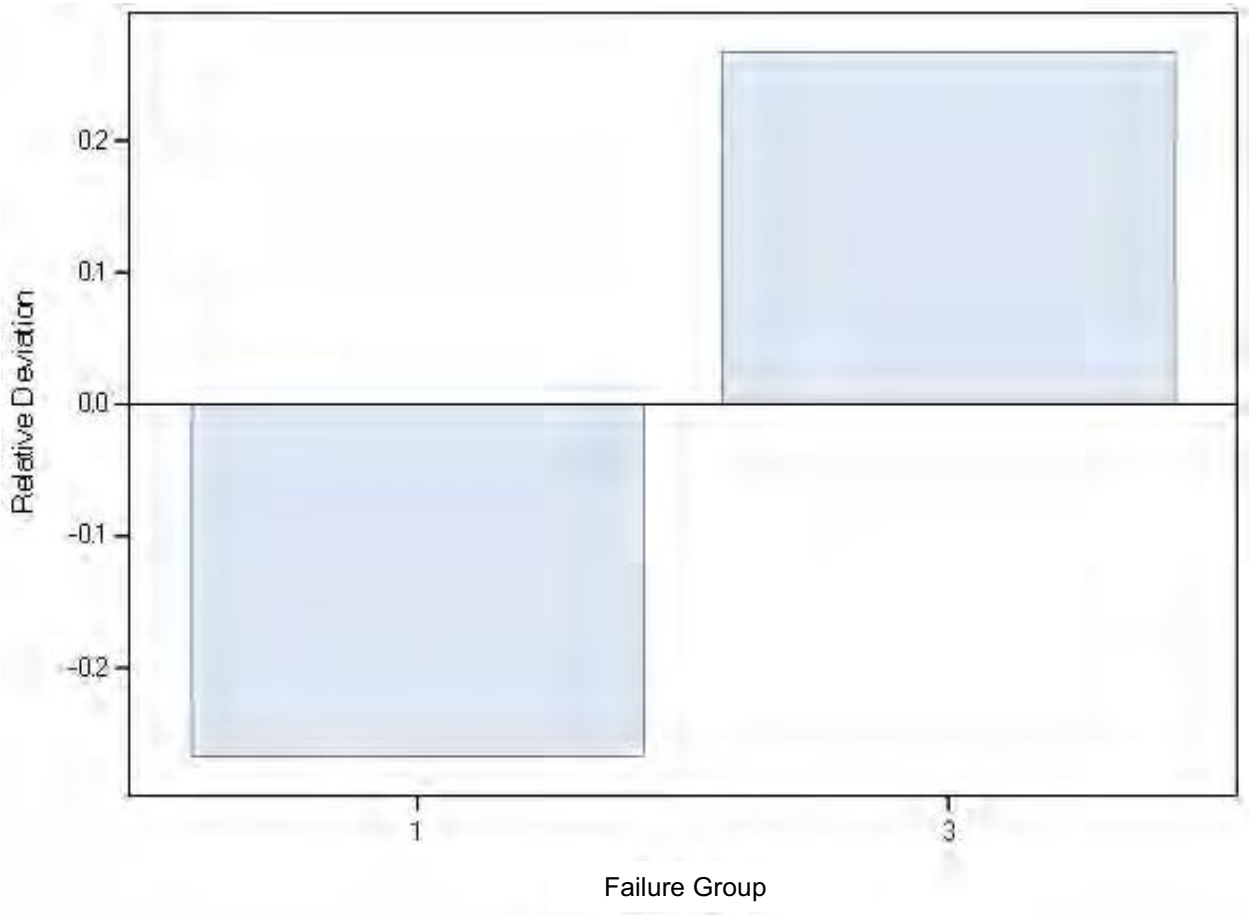

Note: A negative relative deviation signifies fewer juvenile Chinook salmon failing through a particular scenario than would be expected by a random process. Failure Group 1—juvenile Chinook salmon that passed under the FFGS or through the FFGS line. Failure Group 3—juvenile Chinook salmon that passed to the right of the FFGS line but then were entrained into Georgiana Slough.

Figure 3.1-20 Relative Deviation of Juvenile Chinook Salmon with the FFGS On

The proportions of juvenile Chinook salmon that passed through each segment when the FFGS was Off were used as expected values; this 1 by 2-vector of expected values was 0.3537 and 0.6463. The expected values were compared to observed values of tags' failure scenarios when the FFGS was in the On position. No difference occurred in the distribution of failure scenarios with the FFGS Off compared to the On position (Goodness of Fit Exact P = 0.7165) (**Figure 3.1-21**). This result suggested that the FFGS did not influence the probability of failing by any particular scenario for juvenile Chinook salmon determined to have not been eaten. Thus, other variables may have influenced how juvenile Chinook salmon failed to be deterred from entering Georgiana Slough.

Comparing BAFF (2011 and 2012 Grouped) and FFGS 2014 Performance

The BAFF performance samples for 2011 and 2012 were combined to improve statistical power, the probability that a test will correctly reject a false null hypothesis (Sokal and Rohlf 1995). The grouped BAFF On-2011 and BAFF On-2012 samples then were compared to FFGS On-2014 samples, to directly compare BAFF and FFGS performance. The sample sizes for these tests may be obtained by review of **Table 3.1-17**; for the grouped BAFF sample sizes: sum the 2011 and 2012 sample sizes.

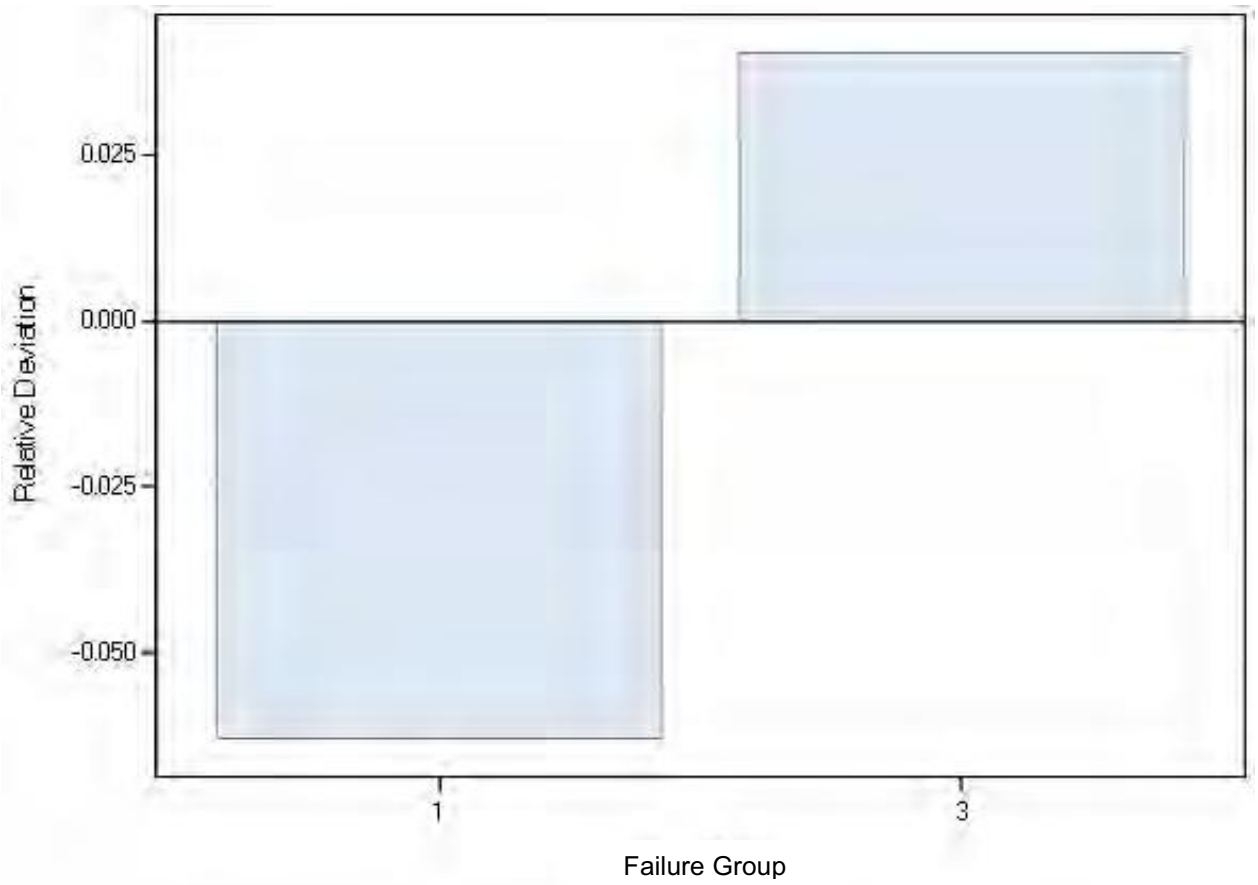

Note: A negative relative deviation signifies fewer juvenile Chinook salmon failing through a particular scenario than would be expected by a random process. Failure Group 1—juvenile Chinook salmon that passed under the FFGS or through the FFGS line. Failure Group 3—juvenile Chinook salmon that passed to the right of the FFGS line but then were entrained into Georgiana Slough.

Figure 3.1-21 Relative Deviation of Tags with the FFGS On

No significant difference was noted in deterrence between the BAFF and the FFGS (**Table 3.1-14**). However, the BAFF showed significantly higher protection and overall efficiency than did the FFGS. Two hypotheses could explain these results: 1) the BAFF spanned the entire entrance to Georgiana Slough and was therefore more effective; and 2) juvenile Chinook salmon that were guided by the FFGS encountered turbulence after they passed the FFGS's trailing edge, but those fish guided by the BAFF encountered less turbulence immediately downstream from the BAFF's infrastructure. In any large river, there is turbulent flow occurring (McQuivey 1973). But at the trailing edge of a fixed wall (e.g., the FFGS) set at an angle to the current, flow separation around such a large object would cause further turbulence to which salmonids respond (Smith et al. 2005).

Table 3.1-14 Comparisons of Deterrence, Protection, and Overall Efficiencies for Juvenile Chinook Salmon During Barrier On Operations for BAFF and FFGS

Comparison Metrics	BAFF On Mean	FFGS On Mean	Mean Difference in Efficiency	Wilcoxon Statistic	Two-sided P-value
Deterrence efficiency—Barrier On	0.531	0.474	5.7	5425.5	0.2473
Protection efficiency—Barrier On	0.892	0.728	16.4	4246.5	0.0017
Overall efficiency—Barrier On	0.894	0.777	11.7	7403.5	<0.0001

Note: FFGS-2014 analysed as one group while BAFF-2011 and BAFF-2012 were pooled and analysed as the second group. Sample size is reported in **Table 3.1-17**.

In both low and high light conditions, deterrence efficiency was not significantly different between the BAFF and the FFGS (**Table 3.1-15**). In low light conditions, no significant protection efficiency difference was noted between the BAFF and the FFGS. It is possible that this result could have been caused, in part, by the 18.2 percentage point improvement in protection efficiency the FFGS-On exhibited under low light conditions compared to the FFGS-Off (**Table 3.1-4**). Protection efficiency of the BAFF was significantly higher than the FFGS under high light conditions. In addition, under both low and high light conditions, the BAFF exhibited significantly higher overall efficiency compared to the FFGS.

Table 3.1-15 Comparisons of Deterrence, Protection, and Overall Efficiencies for Juvenile Chinook Salmon During Barrier On Operations for BAFF Grouped BAFF-2011 and BAFF-2012, and FFGS-2014 Barrier Types Under Low (< 5.4 Lux) and High (≥ 5.4 Lux) Light Levels

Comparison Metrics	BAFF On Mean	FFGS On Mean	Percentage Point Difference in Efficiency	Wilcoxon Statistic	Two-sided P-value
Deterrence—Barrier On – Low Light	0.470	0.407	6.3	1489.5	0.2825
Deterrence—Barrier On – High Light	0.596	0.552	4.4	1249.5	0.6265
Protection—Barrier On – Low Light	0.881	0.772	10.9	1213.0	0.2192
Protection—Barrier On – High Light	0.904	0.683	22.1	943.0	0.0015
Overall—Barrier On – Low Light	0.873	0.779	9.4	1665.0	0.0072
Overall—Barrier On – High Light	0.917	0.776	14.1	2068.0	<0.0001

Note: Sample size is reported in **Table 3.1-17**.

For both low and high approach velocities, deterrence efficiency was not significantly different between the FFGS and the BAFF (**Table 3.1-16**). In high velocity conditions, no significant protection efficiency difference occurred, but the FFGS provided a 7.9 percentage points improvement over the BAFF's E_P. The result was consistent with the good performance of the FFGS under high velocity conditions (**Table 3.1-7**). Protection efficiency of the BAFF was significantly higher than the FFGS when approach velocities were low. Overall efficiency exhibited the same pattern as protection efficiency, namely: 1) no statistically significant difference occurred, but the FFGS produced a higher E_O than the BAFF (12.3 percentage point improvement) under high velocity conditions; and 2) the BAFF showed significantly higher E_O than the FFGS under low velocity conditions.

Table 3.1-16 Comparisons of Deterrence, Protection, and Overall Efficiencies for Juvenile Chinook Salmon During Barrier On Operations for FFGS-2014 and BAFF Grouped BAFF-2011 and BAFF-2012 Barrier Types Under Low (< 0.25 m/s) and High (≥ 0.25 m/s) Approach Velocities

Comparison Metrics	BAFF On Mean	FFGS On Mean	Percentage Point Difference in Efficiency	Wilcoxon Statistic	Two-sided P-value
Deterrence—Barrier On – Low Velocity	0.554	0.491	6.3	565.0	0.8250
Deterrence—Barrier On – High Velocity	0.466	0.471	-0.5	1845.0	0.9829
Protection—Barrier On – Low Velocity	0.955	0.444	51.1	261.5	0.0001
Protection—Barrier On – High Velocity	0.711	0.790	-7.9	1609.5	0.3636
Overall—Barrier On – Low Velocity	0.955	0.560	39.5	565.0	<0.0001
Overall—Barrier On – High Velocity	0.719	0.842	-12.3	2067.0	0.4144

Note: Sample size is reported in **Table 3.1-17**.

It seems possible that a FFGS and a BAFF could work synergistically to improve overall efficiency for juvenile Chinook salmon. The FFGS worked best when high approach velocities occurred, with an 84.2 percent overall efficiency (**Table 3.1-16**). The grouped BAFF results showed a significantly higher overall efficiency (95.5%) than the FFGS (56.0%) when the approach velocities were low. If the FFGS was deployed upstream from the BAFF with the FFGS terminus approximately 50 m (164 ft) west of the origin of the BAFF's 2012 alignment, the FFGS could provide high protection at high velocities, the BAFF could provide high protection at low velocities, and each juvenile Chinook salmon entering the eastern third of the river channel would have two barriers to cross before entering Georgiana Slough.

Comparing BAFF 2011, BAFF 2012, and FFGS 2014 Performance

The sample sizes for Hypothesis 23a tests varied from 10 to 75 for BAFF-on and from 9 to 44 for FFGS-On (**Table 3.1-17**). No significant difference occurred in deterrence efficiency between any years or technologies (**Table 3.1-18**). However, the BAFF in 2011 and 2012 exhibited a significantly higher protection efficiency and overall efficiency than the FFGS. One possible explanation for this was the high number of juvenile Chinook salmon in Failure Group 3 in 2014 (**Figure 3.1-8**); juvenile Chinook salmon that moved past the end of the FFGS then were entrained into Georgiana Slough. The juvenile Chinook salmon in Failure Group 3 may have experienced a critical streakline that was right of the FFGS' downstream end or they could have possibly experienced turbulence or eddying flows just past the downstream terminus of the FFGS that may have steered them toward Georgiana Slough (see examples in **Figure 3.1-8**).

Table 3.1-17 Sample Size (N) of Barrier Evaluations During Barrier On Operations

Comparison Metrics	BAFF 2011	BAFF 2012	FFGS 2014
Deterrence efficiency—Barrier on	**77**	**86**	**54**
Deterrence efficiency—Barrier On—Low Light	42	42	29
Deterrence efficiency—Barrier On—High Light	35	44	25
Deterrence efficiency—Barrier On—Low Velocity	46	75	9
Deterrence efficiency—Barrier On—High Velocity	31	11	45
Protection efficiency—Barrier on	**77**	**82**	**50**
Protection efficiency—Barrier On—Low Light	42	41	25
Protection efficiency—Barrier On—High Light	35	41	25
Protection efficiency—Barrier On—Low Velocity	46	72	9
Protection efficiency—Barrier On—High Velocity	31	10	41
Overall efficiency—Barrier on	**77**	**86**	**79**
Overall efficiency—Barrier On—Low Light	42	42	35
Overall efficiency—Barrier On—High Light	35	44	44
Overall efficiency—Barrier On—Low Velocity	46	75	18
Overall efficiency—Barrier On—High Velocity	31	11	61

Table 3.1-18 Comparisons of Deterrence, Protection, and Overall Efficiencies for Juvenile Chinook Salmon During Barrier On Operations for All Study Years					
Comparison Metrics	**BAFF on 2011**	**BAFF on 2012**	**FFGS on 2014**	**Kruskal-Wallis X^2**	**P-value**
Deterrence efficiency—Barrier On	0.498	0.561	0.474	2.9556	0.2281
Protection efficiency—Barrier On	0.887	0.897	0.728	10.3251	0.0057
Overall efficiency—Barrier On	0.891	0.897	0.777	23.6511	<0.0001
Note: Sample size is reported in **Table 3.1-17**.					

No significant difference occurred in deterrence efficiency between any technology or year at high and low light levels (**Table 3.1-19**). Furthermore, in low light conditions, no difference was noted in protection efficiency between any technology or year. However, in high light conditions, significantly higher protection efficiency was exhibited by the BAFF in 2011 and 2012 compared to the FFGS in 2014. The E_O results suggest that under any light conditions, the BAFF in 2011 and 2012 produced a higher efficiency than the FFGS in 2014.

Table 3.1-19 Comparisons of Deterrence, Protection, and Overall Efficiencies for Juvenile Chinook Salmon During Barrier On Operations for All Study Years Under Low (< 5.4 Lux) and High (≥ 5.4 Lux) Light Levels					
Comparison Metrics	**BAFF 2011**	**BAFF 2012**	**FFGS 2014**	**Kruskal-Wallis X^2**	**P-value**
Deterrence efficiency—Barrier On—Low Light	0.449	0.492	0.407	1.8086	0.4048
Deterrence efficiency—Barrier On—High Light	0.556	0.628	0.552	0.9075	0.6352
Protection efficiency—Barrier On—Low Light	0.900	0.862	0.772	1.6930	0.4289
Protection efficiency—Barrier On—High Light	0.871	0.932	0.683	11.5464	0.0031
Overall efficiency—Barrier On—Low Light	0.903	0.842	0.779	8.2660	0.0160
Overall efficiency—Barrier On—High Light	0.877	0.950	0.776	19.0933	<0.0001
Note: Sample size is reported in **Table 3.1-17**.					

No deterrence efficiency difference was noted between treatments or years at any level of approach velocity (**Table 3.1-20**). However, the results for low velocity conditions were similar to those for the combined BAFF data (**Table 3.1-17**): the BAFF exhibited significantly higher protection efficiency than did the FFGS (**Table 3.1-20**). In high approach velocity conditions, the 2014 FFGS produced higher but not statistically significant protection and overall efficiency than the BAFF in 2011 or 2012.

Table 3.1-20 Comparisons of Deterrence, Protection, and Overall Efficiencies for Juvenile Chinook Salmon During Barrier On and Off Operations for All Study Years Under Low (< 0.25 m/s) and High (≥ 0.25 m/s) Approach Velocities					
Comparison Metrics	**2011**	**2012**	**2014**	**Kruskal-Wallis X^2**	**Two-sided P-value**
Deterrence efficiency—Barrier On—Low Velocity	0.523	0.573	0.491	1.0363	0.5956
Deterrence efficiency—Barrier On—High Velocity	0.459	0.485	0.471	0.0010	0.9995
Protection efficiency—Barrier On—Low Velocity	0.974	0.943	0.444	16.1787	0.0003
Protection efficiency—Barrier On—High Velocity	0.758	0.567	0.790	2.2283	0.3282
Overall efficiency—Barrier On—Low Velocity	0.977	0.942	0.560	31.4437	<0.0001
Overall efficiency—Barrier On—High Velocity	0.765	0.591	0.842	0.8412	0.6566
Note: Sample size is reported in **Table 3.1-17**.					

3.1.3 KEY FINDINGS AND CONCLUSIONS

The following summary presents the key findings and conclusions related to FFGS efficiencies.

- Null Hypothesis 16 was rejected for protection efficiency: the FFGS produced significantly higher protection efficiency (P = 0.0085) in the On position (Mean = 72.8%) compared to the Off position (Mean = 54.6%).
- The proportion of tagged juvenile Chinook salmon that entered Georgiana Slough did not pass the FFGS in a uniform manner along the length of the FFGS.
- The eight segments evaluation showed that tags passed in greater proportion in the second half (downstream) of the FFGS and the highest proportion passed in the final (most downstream) segment, Segment 8.
- The ten segments evaluation showed that tags passed in greater proportion in the two segments immediately downstream of the FFGS structure. The highest proportion passed the FFGS line in Segment 9, the segment closest to but immediately past the FFGS structure.
    - In Chapter 3.3, Figure 3.3-26d (Caption: "Histogram Plots Showing the Critical Streakline for (a) High, (b) Mid, (c) Low and (d) all River Discharges") showing that the FFGS crossed the critical streakline for just 21 percent of the study period.
    - It is possible the FFGS structure did not extend sufficiently far into the river channel, as a function of the 2014 flow regime, to move a larger proportion of juvenile Chinook salmon to the right of the critical streakline.
- For the eight and ten segment evaluations no statistically significant difference was found, in the distribution of where tags passed the FFGS, between FFGS Off and FFGS On. Thus, for tags that continued into Georgiana Slough, the FFGS did not influence where fish passed the FFGS line.
- Null Hypothesis 21 was rejected: the tags that passed the FFGS line did not fail in a randomly distributed fashion.

- The highest proportion of tagged juvenile Chinook salmon that crossed the FFGS line were eaten before they passed the FFGS line (0.4184) compared to an expected proportion of 0.33. Thus, these tags passed the FFGS line in a predatory fish.

- Hypothesis 22a was rejected for protection efficiency: the BAFF, when 2011 and 2012 were combined, showed significantly higher protection efficiency (Mean 89.2%) than did the FFGS (Mean = 72.8%).

- Hypothesis 22a was rejected for overall efficiency: the BAFF, when 2011 and 2012 were combined, showed significantly higher overall efficiency (Mean 89.4%) than did the FFGS (Mean = 77.7%).

- It is suggested that the BAFF and FFGS might work well in concert.

- The BAFF performed best under low approach velocity (< 0.25 m/s [< 0.82 ft/s]) conditions with overall efficiency (Mean = 95.5%) significantly higher than the FFGS (Mean = 56.0%).

- The FFGS performed best under high approach velocity (≥ 0.25 m/s [≥ 0.82 ft/s]) conditions with overall efficiency (Mean = 84.2%) higher than the BAFF (Mean = 71.9%). This difference was not significant.

3.2 SURVIVAL MODEL

The ultimate goal of the 2014 FFGS is to increase overall survival of juvenile Chinook salmon past Georgiana Slough and through the Delta by reducing entrainment into Georgiana Slough and increasing the proportion of fish remaining in the Sacramento River. This goal is expressed as Hypothesis H1 in **Table 2-1**. Previous work has suggested that survival is higher for fish that remain in the Sacramento River as opposed to those that enter the interior Delta via Georgiana Slough (Perry et al. 2010). To evaluate the effect of the FFGS on routing and survival of juvenile Chinook salmon, a multi-state mark-recapture model[10] was developed following the framework described in Perry et al. (2010).

A paired release approach[11] was implemented, using two different tag types developed by separate manufacturers, HTI and VEMCO. Because HTI's tag was a new model that had not yet undergone extensive field testing, a paired release design was implemented to avoid the possibility of premature tag failure. For example, if a tag's battery life expired before fish exited the greater study area at Chipps Island, survival estimates would have been negatively biased (Holbrook et al. 2013). Tag failure can be accounted for in the survival analysis if an unbiased estimate of the travel time distribution is available (Townsend et al. 2006); however, in the presence of tag failure, the travel time distribution also is negatively biased because fish with long travel times are under-represented in the travel time distribution. To overcome this issue, a subset of the fish was tagged with VEMCO tags, which were expected to have a longer battery life and minimal tag failure.

Two different tag types were used, operating under the assumption that if one tag type expired prematurely, the unbiased travel time distribution from the other tag type could be used to appropriately account for tag failure. Premature failure of both tag types was not expected. Both HTI and VEMCO tags experienced premature failure

[10] Once juvenile Chinook salmon are 'marked' by surgically inserting acoustic tags before release, they are not physically recaptured, but rather the 'recapture' is the 'hydroacoustic detection' of marked fish by hydrophones located at specific monitoring nodes sited throughout the Delta.

[11] 'Paired release' means fish tagged with either the HTI or VEMCO tags, but not both, were released simultaneously from the same release point, i.e., 'paired.' No fish were double tagged nor were fish tagged with Predator Detection Acoustic Tags (PDAT) used in the analysis.

caused by battery life issues (HTI) and tag programming errors (VEMCO). Consequently, previously established methods could not be used to account for tag failure. Therefore, new statistical methods using a Bayesian framework that are able to appropriately account for tag failure and allow for unbiased estimation of survival in the presence of tag failure were developed.

3.2.1 METHODS

DATA PROCESSING AND FALSE POSITIVE SCREENING

The two different tag models required different data processing protocols and false-positive filtering because of the manner in which the acoustic signals were recorded by receivers and pre-processed before statistical analysis. VEMCO detection data consisted of individual tag pulses, whereas HTI detection data were made up of tag detection events that summarized multiple tag pulses within each hourly data file. Therefore, screening for false-positive detections was conducted separately for each type of tag. In addition, data collected from HTI tags prior to May 6, 2014 were processed by USGS, and thereafter collected data were processed by HTI. These subsets of the data set were treated differently before survival analysis.

VEMCO data were screened for false-positive detections by defining a detection event as a minimum of two detected pulses from an individual tag at a specific location within 30 minutes of each other. Any tag pulses detected at VEMCO arrays that did not meet these criteria were considered potential false-positives and were removed from further analysis.

Two types of HTI tags were released: 1) the 900LD Micro Acoustic Tag, which was programmed to transmit an acoustic signal at a rate of one pulse every 2 to 4 seconds; and 2) a prototype Predator Detection Acoustic Tag (PDAT) that had the capability of sending an additional tag code if consumed by a predatory fish. Because the PDAT was a prototype, data from PDAT tags were not included in this analysis. Data obtained for 900LD model tags after the start of PDAT releases (May 6, 2014) were processed by HTI. Because the proprietary data processing algorithm used by HTI removes false positive detections, no further false-positive screening was performed for these data. Data from the 900LD model tags collected prior to May 6, 2014 initially were filtered for false-positives using FishCount software, developed by USGS. For a detailed description of FishCount software see Romine et al. (2013).

Detection events identified by FishCount underwent a second round of filtering for false-positives using two approaches. First, to estimate the false-positive rate of detection events a randomly chosen subset of 1,000 detection events was subjected to manual review for potential false-positives. Second, detection events were screened by using several criteria to identify detection events that had characteristics consistent with false-positive detections. This process began by forming a temporally ordered detection history for each HTI tag. Any detection event in a different location than the previous detection event was considered to have transitioned between locations. The latter detection event of a transition was then flagged as a potential false-positive detection based on several criteria. The criteria included spatial proximity, speed of transition (i.e., time between events/distance between locations), time since the previous detection event, and duration of the last transition in a tag's detection history. This screening procedure, described in more detail to follow, resulted in the manual review of an additional 2,330 detections.

To determine which detections should be flagged for manual review based on spatial proximity any transition whose tag would have gone undetected at an intermediate location to arrive at the second location, and which was not subsequently detected at that location more than once before being detected elsewhere, was flagged as a possible false-positive detection. In addition, all transitions were flagged if the tag would have had to travel at an average straight-line velocity greater than 0.6 m/s (2.0 ft/s) or which occurred more than seven days after the

previous detection. Furthermore, any transition occurring alone or with only one other detection in that location at the end of a tag's detection history also was flagged.

Each flagged detection event was manually reviewed by inspecting the individual tag pulses making up the detection event to determine if it was a valid detection event; flagged detections determined to be false positives were removed from further analysis. After removal of detections determined to be false-positives, detection histories for each tag were reassembled and the same flagging procedures were applied iteratively until no additional detections were flagged that had not been manually reviewed already.

As a result of random selection of 1,000 detection events, one detection event was identified as a false-positive and removed from the dataset. Thus, a false-positive rate was generated by FishCount processing of 0.10 percent, with a 95 percent confidence interval of 0-0.64 percent (adjusted Wald interval; Agresti and Coull 1998). An additional 26 detections were removed after manual review of unlikely detections. Overall, the 27 detections removed from the 55,071-detection dataset represent a false-positive rate of 0.049 percent.

PREDATOR FILTER

Tags that may have been consumed by predatory fishes were identified and removed from the data set by adapting the methods of Gibson et al. (2015). This process consisted of several steps. First, four metrics were selected to distinguish live juvenile Chinook salmon from consumed juvenile Chinook salmon based on known behavioral patterns of striped bass, smallmouth bass, and spotted bass. Next, these metrics were estimated from each tag's detection history and hierarchical cluster analysis was used to group the detection histories of each tag by the multivariate characteristics of the selected metrics. After identifying detection histories that had evidence of predatory fish-like movement characteristics, the metrics were examined manually to identify when the tag transitioned from juvenile Chinook salmon-like to predatory fish-like behavior. The detection history then was truncated at this point in the detection history. This process was conducted separately for fish released at Georgiana Slough and Sacramento River release sites. Both juvenile Chinook salmon tags and predator tags were included within the cluster analyses, which allowed examination of how movements of known predatory fishes could be grouped with putative predators of tagged juvenile Chinook salmon.

The metrics selected for use in the hierarchical cluster analysis were as follows:

1. Average rate of downstream movement in m/s (VDown);

2. Number of consecutive detection events occurring at the same location (NSame);

3. Total distance travelled divided by the total number of days spent in the array (path-days); and

4. Number of transitions that were deemed to be only possible by predatory fishes (i.e., movement upstream against the flow) (NPred).

The average rate of downstream movement (V_{Down}) was calculated as the average of the shortest channel distance between two successive detection events divided by the travel time between the sites for the entire detection history. Only consecutive detection events that indicated downstream travel were used. If a juvenile Chinook salmon remained at a detection site between detection events, the distance traveled was zero. All calculated distances between successive detections were estimated using the g-distance package in R and a digital elevation model developed in Environmental Systems Research Institute's, Inc. (ESRI) ArcMap 10.1. Measurements were constrained to the network of rivers and channels that make up the Delta. N_{Same} was calculated as the total number of detection events that occurred at the same site consecutively. For example, if a fish was detected at 15:35 at

Freeport, and then was detected at 16:35 at Freeport, a value of 1 was given to $N_{Same,i}$. All values of $N_{Same,i}$ were then summed over the *i*th detection history of a tag. Path-days was estimated by summing the total distance travelled within the array and dividing the distance by the total time the fish was in the array (release time to last detection time). N_{Pred} was calculated by summing the number of predatory fish-like transitions that occurred in a detection history. A summary of predatory fish-like transitions is provided in **Appendix F**. All metrics were standardized to have a mean of zero and a standard deviation of one.

The h-clust package in R was used to create a dendrogram of all the tags from the results of hierarchical clustering, based on Ward's minimum variance method (Ward 1963; Gibson et al. 2015). Using the dendrogram, the tags were divided into three groups, and then the group with the majority of the known predator tags was selected for further scrutiny. Any juvenile Chinook salmon tag that was assigned to this group was considered to exhibit behavioral patterns consistent with that of predatory fishes. Although this approach identified putative predators, it did not identify the point in the detection history at which the juvenile Chinook salmon was consumed. Therefore, as described previously, all detection histories of juvenile Chinook salmon tags that were grouped with predatory fishes were manually examined to identify the point in the detection history where the tag transitioned from juvenile Chinook salmon- to predatory fish-like behavior. Questionable detection histories where the truncation point was unclear were reviewed by the authors. One tag was removed altogether from analysis because its movement patterns appeared as if it was made up of two individual tags programmed to have the same code.

TAG LIFE STUDIES

Standard tag life studies were initiated for each type of acoustic tag used (HTI and VEMCO) to test the assumption that tagged fish exited the study area before tag failure occurred. However, because of unforeseen modes of failure in both tag types, each tag life study had to be repeated and standard methods had to be modified to accommodate the unforeseen modes of failure.

HTI

Several weeks after initiation of the standard tag life study, failure times were discovered to be strongly correlated to periodic handling of the tags with forceps to check whether the tags remained operational. This standard tag life study consisted of randomly selecting tags from those to be used in the study, placing them in a tank containing river water that mimicked Sacramento River temperatures, and then monitoring when tags failed. Without further knowledge of the exact mode of mechanical failure, the following two primary concerns existed: 1) that using forceps to implant tags into study fish might increase tag failure; and 2) that the tagged fish themselves might trigger mechanical failure as they migrated through the Delta. To address these concerns, a new tag life study was designed to emulate, as closely as possible, the tagging and field conditions that tags experienced in the larger study. The goal was to obtain, as closely as possible, a distribution of tag failure times that was representative of tagged fish in the field.

Following the procedures outlined in Section 2.4.3 "Fish and Fish Tagging," 100 juvenile Chinook salmon were surgically implanted with HTI acoustic tags. Because the mechanical failure mode might have involved handling of tags with forceps, and because approximately 17 percent of tagged study fish were implanted using forceps, 17 of the 100 tags were implanted using forceps. The tagged fish were immediately moved to a temperature-controlled tank following surgery. Water temperature was controlled over the next 90 days to mimic the mean daily temperature in the Sacramento River over the course of the study. Tags were continuously monitored, and fish were held until all tags had failed. The last time of detection of each tag was used to generate an empirical cumulative tag survival distribution (the proportion of tags remaining alive over time). These empirical failure times were fit to a four-parameter Vitality distribution via maximum likelihood estimation (Li and Anderson 2009), and these parameter estimates were used in subsequent analyses.

VEMCO

Near the end of the field study, field crews began to notice that VEMCO acoustic tags began to fail during the 24-hour holding period before release. Subsequent investigation by VEMCO staff revealed that all tags used in the study were subject to premature failure via what was termed the "kill switch bug." VEMCO tags come equipped with a timer (hereafter referred to as the kill switch timer) that shuts off a tag after a prescribed period of time, so that degrading battery life does not lead to sporadic or intermittent tag pulses. For the tag model used in this study, the kill switch timers should have been set to turn tags off 75 days after tag activation. However, for all tags used in this study, the kill switch timer was started inadvertently on the date of tag shipment. In addition, during the period before tag activation, the timers advanced at a variable rate that was faster than the speed of a properly functioning timer in an operational tag. Thus the VEMCO tag failure times depended not only on the time of activation but also on how much time had elapsed between tag shipment and tag activation.

A preliminary study that was conducted by VEMCO staff indicated that the rate at which the timer advanced before tag activation was assumed to be normally distributed, with 95 percent of tag kill switch timers advancing at a rate of 1.1 to 1.5 times the normal rate. This multiplier was termed the "shelf time factor." It also was projected that because of the range in times between tag shipment and tag activation for the tags in the study, the kill switch could be expected to shut off all tags well before they failed because of battery failure. Under this model for tag failure mode, a tag was expected to fail 75 days after activation, less the number of days between shipment and activation multiplied by the (normally distributed) rate at which the timer was advancing during the period before tag activation:

$$f_i = A_i + 75 - \left(A_i - M_i\right)\left(\mu_f + \varepsilon_i\right)$$

where f_i was the failure time of the ith tag, A_i is tag activation time, M_i is tag shipment time, μ_f is the mean shelf time factor, and $\varepsilon_i \sim \text{Normal}\left(0, \sigma_f^2\right)$, where σ_f^2 is the variance in the shelf time factors.

Because of the kill switch bug, this tag life study had the following three objectives: 1) to determine whether modes of failure were possible other than the proposed kill switch bug (e.g., random early failures); 2) to replicate the distribution of times between tag shipment and tag activation observed in the larger study; and 3) to independently estimate μ_f and σ_f^2. These parameter estimates then were used in subsequent analyses.

SURVIVAL MODEL DEVELOPMENT

Design of Mark-Recapture Model

A mark-recapture model was designed to estimate reach- and route-specific survival for primary outmigration routes through the Delta (**Figure 3.2-1** and **Figure 3.2-2**). Primary outmigration routes include the Sacramento River (Route A), Sutter and Steamboat sloughs (Route B), the DCC (Route C), and Georgiana Slough (Route D). Reaches within these routes were defined to separate the Delta broadly into the following three hydrodynamic zones:

1. Reaches dominated by river inputs and less influenced by tidal forcing. This region encompasses the Sacramento River from Sacramento to the junction of Steamboat and Sutter sloughs;

2. Reaches that transition from river- to tidal-dominated dynamics. This region begins downstream from the Sacramento River junction with Sutter and Steamboat sloughs and ends at telemetry stations $B_{1,2}$, $B_{2,2}$, A_5, and D_2 (**Figure 3.2-1**); and

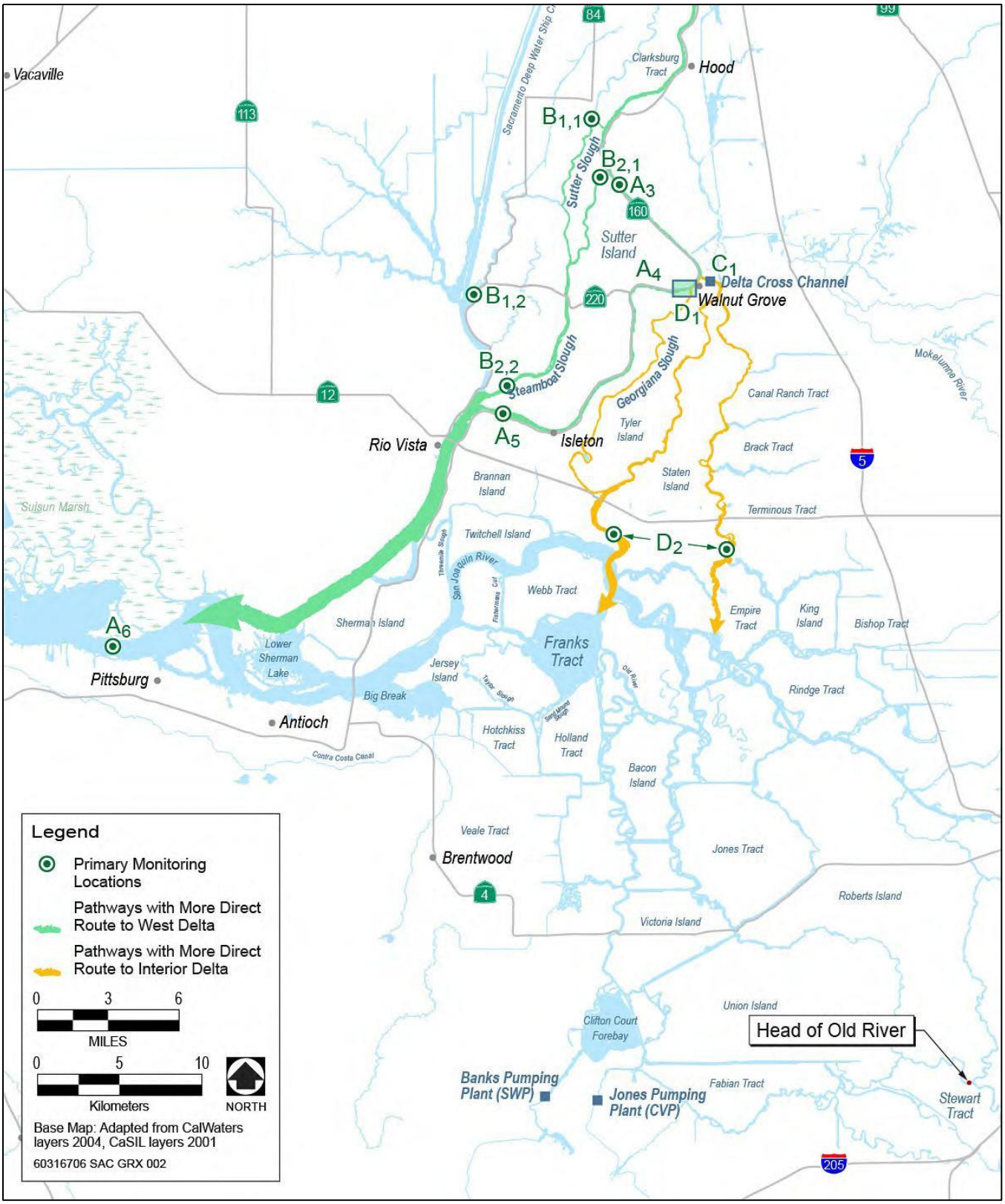

Note: Primary monitoring locations (green dots) are labeled according to sites used in the route-specific mark-recapture model (see **Figure 3.2-2**). Labels of primary stations (rj) correspond to the jth telemetry stations within the rth route (A = Sacramento River, B = Sutter and Steamboat sloughs, C = DCC, and D = Georgiana Slough/Interior Delta).

Figure 3.2-1 Location of Hydrophone Stations for Estimating Route-Specific and Delta-Wide Survival of Juvenile Chinook Salmon in 2014

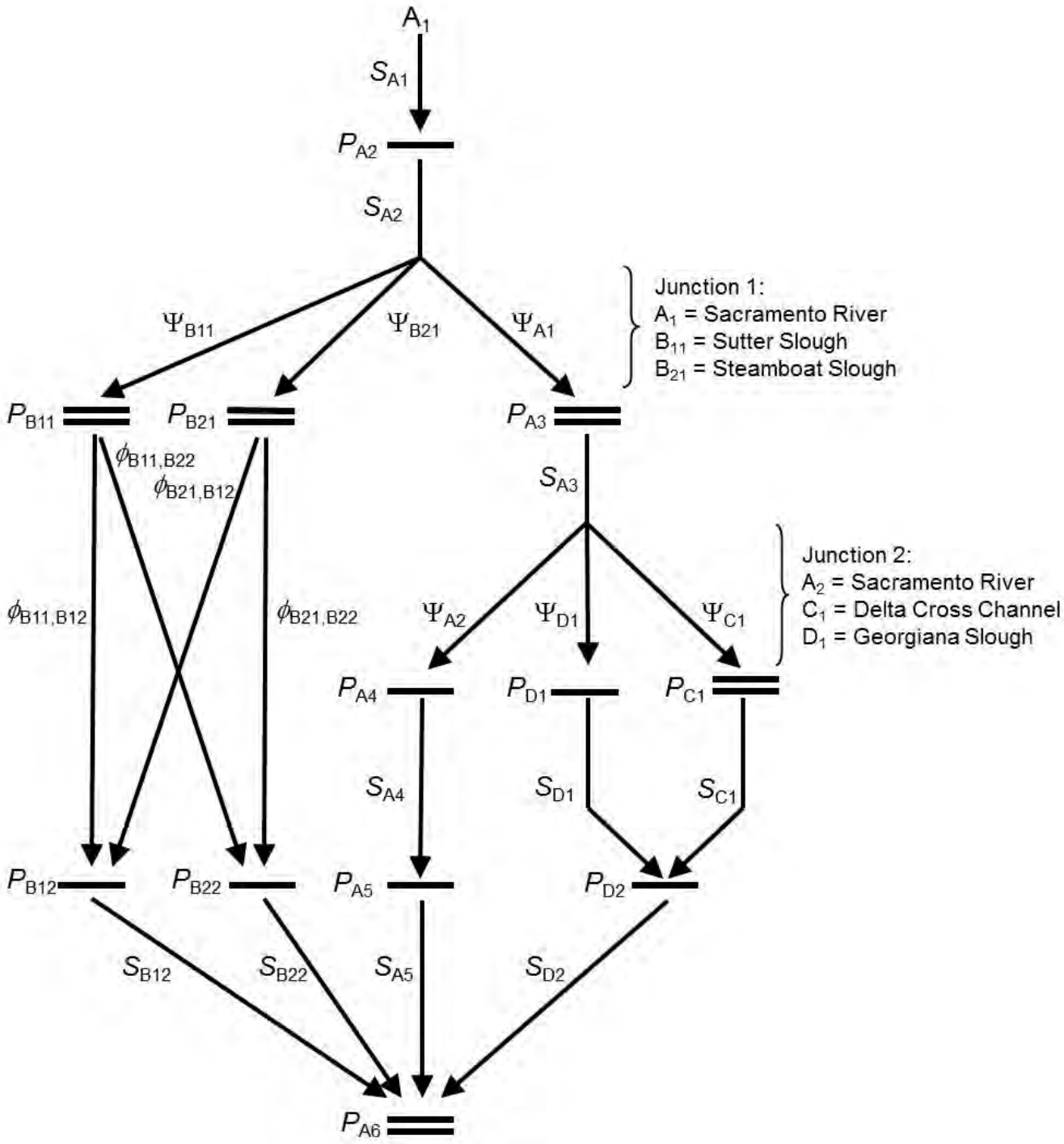

Note: Site A1 is the release site at Sacramento. Horizontal lines represent monitoring stations, shown in **Figure 3.2-1** with double lines representing dual detection arrays, and single lines representing a single acoustic telemetry monitoring station.

Figure 3.2-2 Schematic of the Route-Specific Mark-Recapture Model Used to Estimate Route-Specific and Delta-Wide Survival in 2014

3. Reaches dominated by tidal dynamics. This region begins at telemetry stations B1,2, B2,2, A5, and D2 and ends at Mallard Island[12] on the left bank of Carquinez Strait (typically and incorrectly referred to as Chipps Island which is on the right bank of Carquinez Strait) (**Figure 3.2-1**).

Hydrophone monitoring locations were identified that would be required to estimate survival within these four routes, and to separate survival among these three hydrodynamic regions (shown with green dots in **Figure 3.2-1**).

The mark-recapture model that is shown in **Figure 3.2-2** estimates the following four types of parameters from detections of tagged juvenile Chinook salmon:

S_{rj} = Survival Probability, defined as the probability of surviving from telemetry station j within route r to telemetry station j+1 (i.e., to the next downstream telemetry station);

Ψ_{rl} = Route Entrainment Probability, defined as the probability of entering route r at junction l, conditional on surviving to junction l;

$\phi_{rj,sk}$ = Joint Survival-Entrainment Probability, defined as the joint probability of surviving from site rj to sk and moving into route s; and

P_{rj} = Detection Probability, defined as the probability of detecting a tagged fish at telemetry station j within route r, conditional on fish and tags surviving to telemetry station rj.

To estimate these parameters, telemetry data first were summarized into alpha-numeric codes called a "capture history" that compactly represented each fish's movement history through the telemetry network by indicating detections at each telemetry station. Each capture history is viewed as one possible outcome from a multinomial distribution and has an associated probability of occurrence defined as a function of the model parameters. The most likely parameter values were then estimated, based on the observed frequencies of each capture history using the statistical methods described below.

Parameters were estimated separately for 10 groups of fish released over the study period. Tagged juvenile Chinook salmon were released approximately every 3 hours in groups of 12 to 14 fish near the City of Sacramento, and approximately every 6 hours in groups of 3 to 4 fish in Georgiana Slough. For analysis purposes, these smaller release groups were aggregated into larger groups over 5-day intervals (**Table 3.2-1**). Release groups were formed to examine temporal variation in FFGS effectiveness, migration routing, and survival over the course of the study period.

[12] Mallard Island is the location of the USGS gage and the downstream telemetry array. The Sacramento River ends upstream at its confluence with the San Joaquin River. Mallard Island is located in the Carquinez Strait, not the Sacramento River.

Table 3.2-1 Date Ranges of Release Groups for Tagged Juvenile Chinook Salmon, 2014			
Release Group	Dates	Number Released	
		City of Sacramento	Georgiana Slough
1	March 1-5	536	52
2	March 6-10	516	52
3	March 10-14	429	86
4	March 15-19	431	85
5	March 19-23	441	92
6	March 24-28	422	86
7	March 28-April 1	428	84
8	April 2-6	433	88
9	April 6-10	443	84
10	April 11-15	449	98
Note: Fish were released at one of two locations: into the Sacramento River at the City of Sacramento or into Georgiana Slough.			

Complete Data Likelihood

Estimation of migration route and survival parameters for multistate mark-recapture models commonly is achieved with Maximum Likelihood Estimation (MLE), using the Observed Data Likelihood (ODL). The ODL is constructed from the observed capture history for each marked fish and is very complex for most multistate models. Nevertheless, numerical methods and computer software are able to estimate parameters of complex multistate models (Perry et al. 2010). However, significant tag failure in the study area could present particular challenges for this method of analysis. It has been shown that when travel time estimates are negatively biased, the methods of Townsend et al. (2006) lead to negatively biased survival estimates, even after correction (Holbrook et al. 2013). The subset of fish released with VEMCO tags was intended to provide an unbiased estimate of travel times. However, with the expectation of both HTI and VEMCO tags failing in the study area, any travel time estimate obtained through MLE methods likely would have been negatively biased. The problem is essentially one of missing data, as missing travel times for undetected fish because of tag failure are what lead to bias in travel time estimates. In addition, it becomes increasingly difficult to determine whether undetected individuals escaped detection, died, or carried failed tags as observations at later detection occasions become sparser.

For these reasons, survival, detection, and routing parameters were estimated using the Complete Data Likelihood (CDL) of the multistate model, shown in **Figure 3.2-2** within a Bayesian framework. By viewing the likelihood as the product of the ODL with an auxiliary likelihood for unobserved data, the missing data may be treated as additional model parameters to be estimated (King et al. 2010; Link and Barker 2010). This approach allowed the likelihood of survival, migration route, travel time, detection, and tag failure to be specified within a single framework. By assuming an appropriate model for the travel time distribution of juvenile salmon, the travel time of an individual could be imputed for the unobserved data. Assuming the model for travel times is appropriate for juvenile salmon, the resulting estimates of travel time, tag failure probabilities, survival, and migration routing are unbiased. This CDL model was specified in the Markov Chain Monte Carlo (MCMC) software package JAGS (Just Another Gibbs Sampler) (available online at http://mcmc-jags.sourceforge.net/) as called from R, which allowed all model parameters to be simultaneously estimated and missing data imputed.

To clarify, because the CDL contains features such as imputed data that are not normally seen in an ODL framework, first the variable $z_{i,j}$ is introduced, which represents the state *r* of individual *i* at detection occasion *j* = 1, …, 6, where the state *r* = 1, …, 5 indexes the five unique migration routes through the Delta. Thus, the value of $z_{i,j}$ is an integer ranging from 1 to 5, corresponding to the *r*th migration route. When fish are detected at a particular telemetry station, the value of *z* is known. However, when fish are not detected either because of imperfect detection, death of the fish, or failure of the tag, a value of *z* is imputed. Thus, let:

$h_{i,j}$ = the state of individual *i* as detected at occasion *j*; $h_{i,j}$ = 0 if individual *i* is not detected at occasion *j*,

$d_{i,j}$ = the latent state of unobserved individual *i* at detection occasion *j*, and

$$z_{i,j} = \begin{cases} h_{i,j} & \text{if } h_{i,j} \neq 0 \\ d_{i,j} & \text{if } h_{i,j} = 0 \end{cases}.$$

Modifying the notation of King et al. (2010), the CDL for the data from this study is written as follows:

$$L\left[P,S,\Psi,\mu_\tau,\sigma_\tau^2,f\middle|z,T,\theta_{tag}\right] = L\left[P,S,\Psi\middle|f,z,T\right]\times L\left[\mu_\tau,\sigma_\tau^2\middle|z,T\right]\times L\left[f\middle|T,\theta_{tag}\right]$$

where the overall likelihood (left-hand side) is the product of three separate, factorable likelihoods, namely:

1. the likelihood for probabilities of survival, route migration, and detection, based on an individual's state and tag status;
2. the likelihood for the travel time distribution, based on an individual's state and travel time; and
3. the likelihood for tag status (functioning or non-functioning), based on an individual's travel time and the parameters of the tag failure distribution for each tag type.

The first likelihood is:

$$L\left[P,S,\Psi\middle|f,z,T\right] \propto \prod_{i=1}^{N}\prod_{j}^{J-1}\prod_{F_i\neq}\prod_{K_j}\left[P_{r,j+1}{}^{u_{i,j+1,r}}\left(1-P_{r,j+1}\right)^{v_{i,j+1,r}}\right]\left[S_{r,j,R_i}{}^{w_{i,j,r,\cdot}}\left(1-S_{r,j,R_i}\right)^{w_{i,j,r,\dagger}}\right]$$
$$\times\prod_{s\in K_{j+1}}\Psi_{r,s,j,FFGS_i,R_i}{}^{w_{i,j,r,s}}$$

where:

$P_{r,j+1}$ is the probability of detection in state *r* at occasion *j*+1, conditional on individual *i* and its tag having survived to state *r*, occasion *j*+1;

S_{r,j,R_i} is the survival probability for an individual in state *r* from occasion *j* to *j*+1 for release group *R*;

$\Psi_{r,s,j,FFGS_i,R_i}$ is the route entrainment probability from state *r* at occasion *j* to state *s* at occasion *j*+1, for release *R* and FFGS status (On, Off) at the arrival time for individual *I*;

$u_{i,j,r} = I\left(h_{i,j} \quad r\right)$; $u_{i,j,r}$ is one if individual *i* is observed in state *r* at detection occasion *j* and zero otherwise;

$I(\cdot)$ is the indicator function, which resolves to one if the argument inside the parentheses is true and zero otherwise;

$v_{i,j,r} = I\left(d_{i,j} \times r\right) \; I\left(f_i \quad \sum_{l=F_i}^{j-1} T_{i,l+1,r}\right)$; $v_{i,j,r}$ is one if individual *i* is imputed to be in state *r* at detection occasion *j*, and if the imputed tag failure time for that individual is greater than its total travel time from release until detection occasion *j*; zero otherwise;

$w_{i,j,r,s} = I\left(z_{i,j} \quad r\right) I\left(z_{i,j+1} \quad s\right)$; $w_{i,j,r,s}$ is one if individual *i* is in state *r* at detection occasion *j* and in state *s* at detection occasion *j*+1, zero otherwise;

$w_{i,j,r,\cdot} = \sum_{s \in K} w_{i,j,r,s}$ and $w_{i,j,r,\dagger} = 1 \quad \sum_{s \in K} w_{i,j,r,s}$. The dot represents any state except the death state, and the cross represents the death state. These resolve to 1 if an individual survives or does not survive from detection occasion *j* to *j*+1, respectively, and zero otherwise;

F_i is the occasion of release for individual *I*; and

K_j is the set of states available to an individual in state *r* at occasion *j*.

Under the form of this likelihood, detection of individual *i* in state *r* at occasion *j*+1 is seen as a draw from a Bernoulli distribution with probability $P_{r,j+1}$. Thus, the first term in brackets is the likelihood contribution for a Bernoulli distribution with probability $P_{r,j+1}$. Similarly, survival of individual *i* in state *r* from detection occasion *j* to *j*+1 follows a Bernoulli (S_{r,j,R_i}) distribution, with the second term in brackets representing its contribution to the likelihood. Furthermore, the state *s* of individual *i* in state *r* at detection occasion *j* follows a multivariate Bernoulli distribution (i.e., a multinomial distribution with a sample size of one) whose probability vector is { $\Psi_{r,s=1,j,FFGS_i,R_i}$, …, $\Psi_{r,s=5,j,FFGS_i,R_i}$ }. The third term above represents the contribution of this multivariate Bernoulli distribution to the overall likelihood. As the parameter subscripting indicates, separate survival and route entrainment probabilities were estimated for each release group, but assumed detection probabilities at a given telemetry station do not vary among release groups.

The likelihood for the travel time parameters is:

$$L\left[\mu_\tau, \sigma_\tau^2 \middle| z, T\right] \propto \prod_{i=1}^{N} \prod_{j}^{J-1} \prod_{F_i \neq \; K_j \; \in} \frac{e^{-\left(\ln\left(T_{i,j+1,r}\right) - \mu_{\tau,j,r,R}\right)^2 / 2\sigma^2_{\tau,j,r,R}}}{\left(\sigma_{\tau,j,r,R} T_{i,j+1,r}\right)}$$

where:

$T_{i,j+1,r}$ is the (observed or imputed) travel time for individual *i* in state *r* between detection occasion *j* and *j*+1;

$\mu_{\tau,j,r,R}$ is the mean of the logarithm of travel times from state *r* at occasion *j* to *j*+1 for release group *R*; and

$\sigma^2_{\tau,j,r,R}$ is the variance of the logarithm of travel times from state *r* at occasion *j* to *j*+1 for release group *R*.

The travel times with a lognormal distribution were modeled (i.e., the natural logarithms of the travel times were distributed normally). The lognormal distribution commonly is chosen to model travel times because travel times frequently are right-skewed, and the lognormal provides a good fit to this type of data (Muthukumarana et al. 2008). The means and standard deviations of the travel time distributions were estimated separately for each reach and release group.

Furthermore, the likelihood for tag failure is:

$$L\left[f \middle| T, \theta_{tag} \right] \propto \prod_{i=1}^{N} \Pr\left[f_i > \sum_{j=F_i}^{\max_j(h_{i,j}>0)} T_{i,j,r} \middle| \theta_{tag_i} \right]$$

where:

θ_{tag_i} is the vector of parameters governing the tag failure process for the tag type of individual *i* (estimated from each tag life study); and

f_i is the imputed tag failure time of tag *i*.

In essence, the likelihood contribution for individual *i* is the probability that the tag failed at some point in time after it was last known to be operational. For HTI tags, tag failure time was imputed from the best-fit four-parameter Vitality distribution (Li and Anderson 2009); for VEMCO tags failure time was imputed from the best-fit normal distribution. Both sets of parameters were estimated separately from the tag life study data, as noted previously, and both sets of parameters, after being estimated, were assumed to be known without error.

The locations and recapture occasions follow the schematic shown in **Figure 3.2-2**. For $j \in \{1, 2, 6\}$ only Route A (the Sacramento River, state $r = 1$) is available. Route A, B_1, and B_2 (B_1 = Sutter and B_2 = Steamboat Slough, states $r = 2$ and $r = 3$, respectively) become available at $j = 3$, and all Routes (A, B_1, B_2, plus D = Georgiana Slough, state $r = 4$) are available for $j \in \{4, 5\}$. Although the DCC was monitored, the DCC gate remained closed during the entire course of the study, preventing entrance to this route. The route entrainment probability $\Psi_{r,s,j,FFGS_i,R_i}$ is constrained by the channel network and equals zero for many of the *j*, *r*, and *s* combinations available under the model shown in **Figure 3.2-2** (e.g., where no river junction exists, fish remain in the same route (i.e., state) with probability one.). This situation occurred for all locations except Junction 1 and Junction 2, shown in **Figure 3.2-2**. At Junction 1, parameters Ψ_{A1}, Ψ_{B11}, and Ψ_{B21} in **Figure 3.2-2** related to likelihood

parameter $\Psi_{r,s,j,FFGS_i,R_i}$ where $j = 2$, $r = 1$, and $s \in \{1, 2, 3\}$. At Junction 2, parameters Ψ_{A2}, Ψ_{C1}, and Ψ_{D1} (shown in **Figure 3.2-2**) relate to likelihood parameter $\Psi_{r,s,j,FFGS_i,R_i}$ where $j = 3$, $r = 1$, and $s \in \{1, 4, 5\}$.

The above likelihood framework allowed for estimates of fundamental parameters within the model, such as reach-specific survival between adjacent telemetry stations. Although these parameters were of interest, a number of parameters derived from the fundamental parameters described above were also estimated. Because these derived parameters generally are those that hold the most direct interest for investigators, they are defined here:

$\Psi_{D1,FFGS,R} = \Psi_{D1,On,R} - \Psi_{D1,Off,R}$ is the difference in the probabilities of entering Georgiana Slough when the FFGS is On and when it is Off for release group *R*,

$\Psi_{Route,R}$ is the probability of migrating from Freeport to Chipps (Mallard) Island via a given *Route* in the set {A, B_1, B_2, C, D}, as described in the preceding paragraph. For Sutter and Steamboat sloughs (Routes B_1 and B_2) this probability is equivalent to the probability of entrainment into Sutter and Steamboat sloughs, respectively, as follows:

$\Psi_{B1,R} = \Psi_{B11,R}$; and

$\Psi_{B2,R} = \Psi_{B21,R}$.

Fish travelling the Sacramento River (Route A) and Georgiana Slough (Route D) must traverse two junctions, and so those probabilities are the product of the individual entrainment probabilities at each junction, as follows:

$\Psi_{A,R} = \Psi_{A1,R} \Psi_{A2,R}$;

$\Psi_{D,R} = \Psi_{A1,R} \Psi_{D1,R}$; and

where $\Psi_{A2,R}$ and $\Psi_{D1,R}$ represent the overall route entrainment probabilities at Junction 2, shown in **Figure 3.2-2**, and they are calculated as the sum of those entrainment probabilities when the FFGS is On and Off, weighted by the proportion of fish entrained into a route when the FFGS is On and Off, respectively, out of all fish entrained into that route, as follows:

$$\Psi_{D1,R} = \Psi_{D1,On,R}\left(\frac{\sum_{FFGS_i=On} w_{i,j=3,r=1,s=4}}{\sum_i w_{i,j=3,r=1,s=4}}\right) + \Psi_{D1,Off,R}\left(\frac{\sum_{FFGS_i=Off} w_{i,j=3,r=1,s=4}}{\sum_i w_{i,j=3,r=1,s=4}}\right); \text{ and}$$

$$\Psi_{A2,R} = \Psi_{A2,On,R}\left(\frac{\sum_{FFGS_i=On} w_{i,j=3,r=1,s=1}}{\sum_i w_{i,j=3,r=1,s=1}}\right) + \Psi_{A2,Off,R}\left(\frac{\sum_{FFGS_i=Off} w_{i,j=3,r=1,s=1}}{\sum_i w_{i,j=3,r=1,s=1}}\right).$$

$S_{Route,R}$ is the probability of survival for release group *R* from Freeport to Chipps (Mallard) Island for fish travelling a given route estimated as the product of reach-specific survival probabilities that trace a given migration route through the Delta. Here *Route* is as above, and $S_{Route,R}$ is explicitly defined as follows:

$S_{A,R} = S_{A2,R}S_{A3,R}S_{A4,R}S_{A5,R}$;

$S_{B1,R} = S_{A2,R}\left(\phi_{B11,B12,R}S_{B12,R} \quad \phi_{B11,B22,R}S_{B22,R}\right)$;

$S_{B1,R} = S_{A2,R}\left(\phi_{B21,B12,R}S_{B12,R} \quad \phi_{B21,B22,R}S_{B22,R}\right)$; and

$S_{D,R} = S_{A2,R}S_{A3,R}S_{D1,R}S_{D2,R}$.

$S_{Delta,R} = \sum_{Route \in \{A,B1,B2,D\}} S_{Route,R}\Psi_{Route,R}$ then is the overall survival probability from Freeport to Chipps (Mallard) Island, regardless of route, and is calculated by summing each route-specific survival, weighted by the proportion of fish travelling via that route.

$\mu_{\tau,Route,R}$ is the mean of the logarithm of travel times from Freeport to Chipps (Mallard) Island for fish in release group *R*, travelling a given route as defined above; and

$\sigma^2_{\tau,Route,R}$ is the variance of the logarithm of travel times from Freeport to Chipps (Mallard) Island for fish in release group *R*, travelling a given route as defined above.

Bayesian Estimation via Markov Chain Monte Carlo

Parameters were estimated and missing data was imputed simultaneously, using MCMC methods. Data input into the MCMC were the observed capture histories and times of detection for each tagged fish (**Appendix C** "Fish Tagging Effects Study"), the activation time of each tag and the manufacture date of each VEMCO tag, the location and time of release for each fish, and the estimated parameters of the tag failure distribution from both tag life studies. Prior distributions for survival and detection probabilities were assumed to be Beta(1,1), and a Dirichlet(α($s \in K_j(r)$)) prior distribution was placed on route migration probabilities, where α($s \in K_j(r)$) was a binary vector of possible state transitions out of state *r* at occasion *j*. A diffuse normal prior was placed on μ_τ (mean = 0; variance = $1x10^{-6}$) and a Gamma (α = 0.01, β = 0.01) prior on σ_τ.

The JAGS software package uses Gibbs sampling and Metropolis-Hastings methods to sequentially update each parameter value, conditional on the latest value for all other parameters. Four separate MCMC chains were run in JAGS for 12,000 iterations each, treating the first 9,000 iterations as a "burn-in" period and discarding them. The four chains were checked for convergence, and autocorrelation within chains was reduced by thinning the values to one in six. The resulting 2,000 values for each parameter formed a draw from the posterior distribution for that parameter, from which the medians and 95 percent credible intervals were reported as point estimates and uncertainty estimates, respectively.

The model was fit, and parameter values were estimated, separately for each release group. In addition, detection probabilities at each site were estimated separately for the two tag types used, while parameters governing survival, migration routing, and travel time distributions were assumed to be common to both tag types. Survival in the

interior Delta (from the Mokelumne River to Chipps [Mallard] Island) was assumed to be common among fish that were released in the Sacramento River and those released into Georgiana Slough.

3.2.2 RESULTS

PREDATOR FILTER

The movement metrics varied widely between juvenile Chinook salmon and predator tags, which allowed the hierarchical clustering routine to clearly distinguish predator- from juvenile Chinook salmon-like behaviors. The average downstream velocity (V_{Down}) of juvenile Chinook salmon tags released at Sacramento was 0.17 m/s (0.56 ft/s) (Standard Deviation [SD] = 0.11 m/s [0.36 ft/s]; **Figure 3.2-3A**). Downstream velocity of the predator tags was much slower and had less variance than juvenile Chinook salmon tags. Smallmouth bass had a downstream velocity of 0.04 m/s (0.13 ft/s) (SD = 0.06 m/s [0.20 ft/s]). Spotted bass and striped bass downstream velocities were similar to that of smallmouth bass, 0.05 m/s (0.16 ft/s) (SD = 0.09 m/s [0.30 ft/s]) and 0.04 m/s (0.13 ft/s) (SD = 0.06 m/s [0.20 ft/s]), respectively. The number of times spotted bass and smallmouth bass were detected consecutively at the same site (N_{Same}) averaged 184 (SD = 262) and 173 events (SD = 284), respectively (**Figure 3.2-3B**). Juvenile Chinook salmon tags and striped bass tags were not detected at the same site over consecutive detection events as often as spotted and smallmouth bass. N_{Same} for juvenile Chinook salmon tags averaged 14 events (SD = 65), and striped bass tags averaged 28 events (SD = 46). On average, the juvenile Chinook salmon tags had a much greater movement rate through the array. For juvenile Chinook salmon tags, the path-day metric averaged 17.2 km/d (SD= 10.5), 0.25 km/d (SD= 0.65) for smallmouth bass, 0.17 km/d (0.11 mi/d) (SD = 0.48 km/d [0.30 mi/d]) for spotted bass, and 3.2 km/d (2.0 mi/d) (SD = 4.4 km/d [2.7 mi/d]) for striped bass. On average, the basses had a greater number of predator transitions than the juvenile Chinook salmon tags. Juvenile Chinook salmon tags averaged 0.16 (SD = 0.65) predator transitions, smallmouth bass averaged 1.2 (SD = 1.1) predator transitions, spotted bass averaged 1.0 (SD = 0.99) predator transitions, and striped bass averaged 2.0 (SD = 2.3) predator transitions.

The dendrogram for the Sacramento and Georgiana Slough released juvenile Chinook salmon was divided into the top three hierarchical clusters, and juvenile Chinook salmon tags in Group I were considered to have predatory fish-like movement characteristics (**Figure 3.2-4**). Group I consisted of 705 juvenile Chinook salmon tags released from the Sacramento release site (17%), 57 tags from the Georgiana Slough release site (10%), and the majority of the predator tags (**Table 3.2-2**). In general, Group I was characterized by moderate downstream velocity, a high number of repeated detections at a site, a slower rate of travel, and at least one upstream movement per tag (**Table 3.2-3**). Group II was characterized by slow downstream velocity, a moderate number of repeated detections at the same site, a greater rate of travel throughout the array, and zero predator transitions. Group III was characterized by the fastest downstream average velocity, the fewest number of repeated detections at a site, the highest movement rate within the array, and no predator transitions with the exception of two tags.

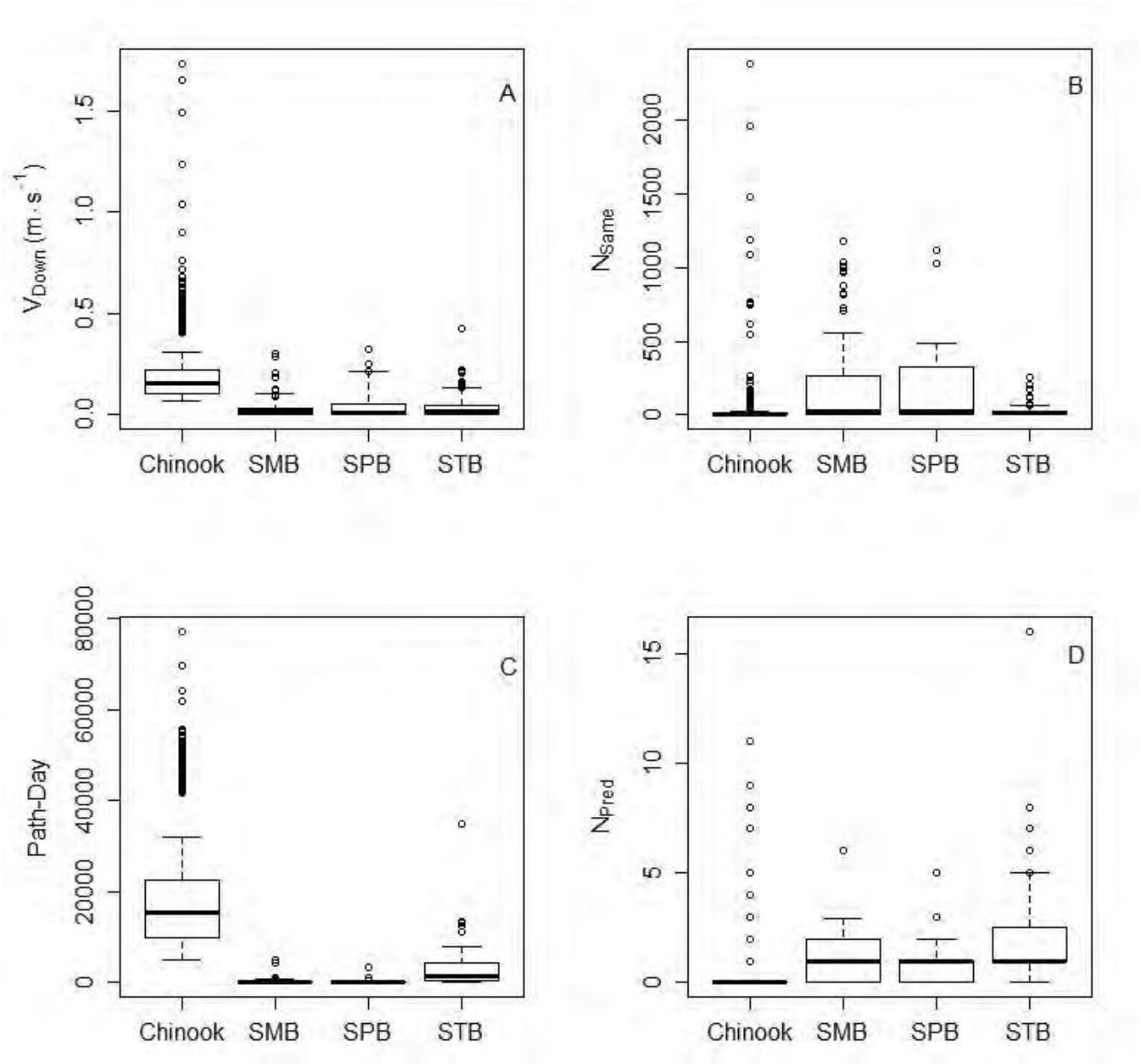

Note: Boxes indicate the 25th, 50th and 75th quantiles, and the whiskers indicate the 10th and 90th quantiles. (SMB=Smallmouth Bass, SPB=Spotted Bass, STB=Striped Bass)

Figure 3.2-3 Boxplots of the Four Metrics Used in the Hierarchical Cluster Analysis to Identify Juvenile Chinook Salmon Tags Released at Sacramento that May Have Been Consumed by Predatory Fishes

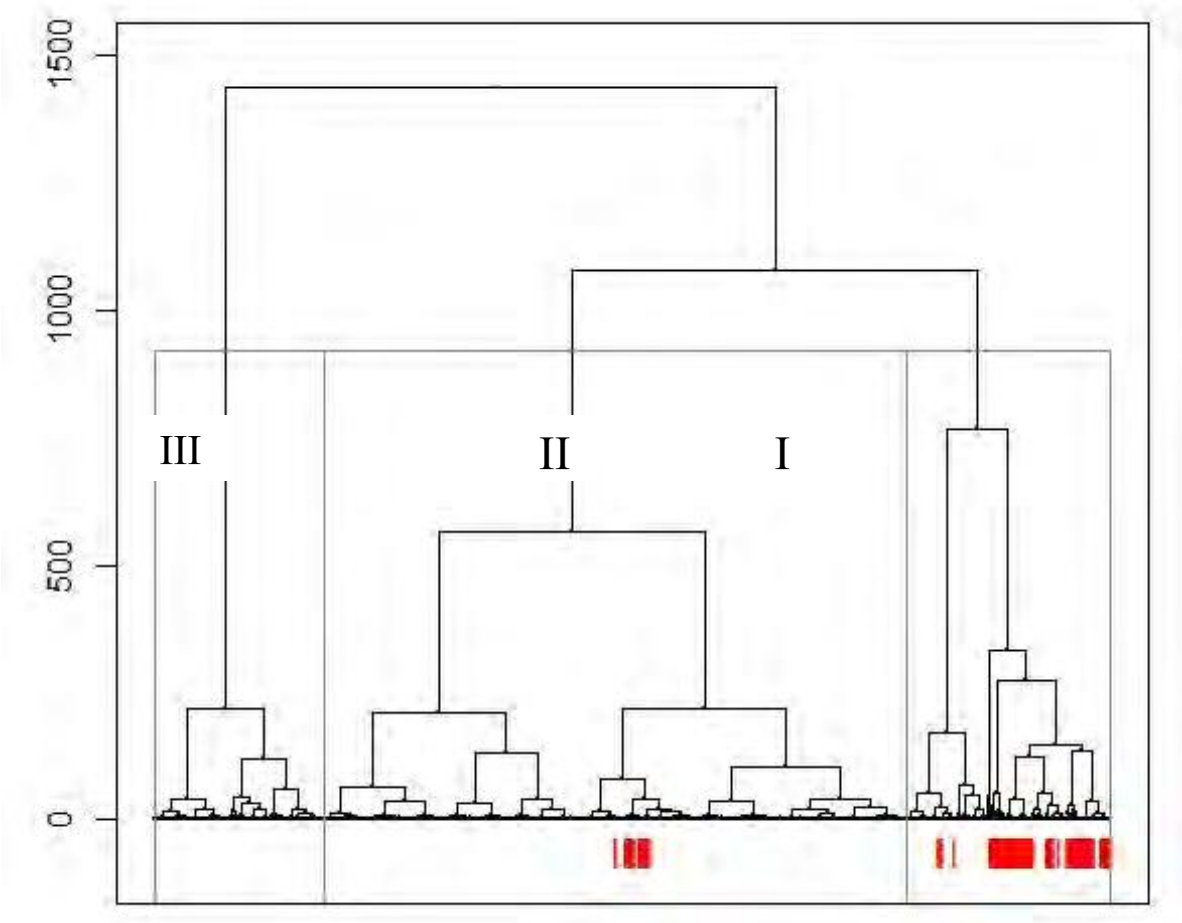

Note: The dendrogram was split into three clusters, as indicated by the grey boxes labeled Groups I, II, and III. The red marks at the bottom of the dendrogram indicate where each predator (red) occurred within the groupings, relative to tagged juvenile Chinook salmon. The y-axis measures dissimilarity between groups (Gibson et al. 2015).

Figure 3.2-4 Dendrogram of Tag Groupings Based on the Four Movement Metrics for Sacramento- and Georgiana Slough-Released juvenile Chinook Salmon and Predators Released at the Georgiana Slough Junction

Table 3.2-2 Grouping Results from the Hierarchical Cluster Analysis for Juvenile Chinook Salmon and Predator Tags

Chinook Release Location	Group	Chinook	Smallmouth Bass	Spotted Bass	Striped Bass
Sacramento	1	705	91	43	99
	2	2108	21	7	20
	3	1304	0	0	0
Georgiana Slough	1	57	56	28	41
	2	152	0	0	11
	3	337	56	22	67

Note: Tags that fell into Group I were manually evaluated to determine the point at which the detection history should be truncated. All predators were used in both the cluster analyses for Sacramento and Georgiana Slough released fish.

Table 3.2-3 Mean Metrics Used in the Hierarchical Cluster Analysis by Cluster Group					
Chinook Release Location	Group	V_{Down} (m\s) Mean (SD)	N_{Same} Mean (SD)	Path-day (km\d) Mean (SD)	N_{Pred} Mean (SD)
Sacramento	1	0.21 (0.18)	56 (185)	6.1 (6.5)	1.10 (1.50)
	2	0.11 (0.05)	14 (14)	12.8 (5.1)	0.00 (0.00)
	3	0.23 (0.08)	6 (5)	29.0 (8.6)	0.02 (0.12)
Georgiana Slough	1	0.039 (0.06)	207 (292)	2216 (2622)	2.64 (2.23)
	2	0.134 (0.07)	7 (9)	12574 (4065)	0.50 (0.92)
	3	0.081 (0.08)	11 (17)	3324 (2945)	0.30 (0.47)
Note: SD = Standard Deviation.					

Table 3.2-4 Parameter Estimates of Vitality Distribution Fitted to HTI Tag Life Study, Tag Failure Times				
	Parameter			
	R	S	K	U
Estimate	0.019	0.057	0.0084	0.14
Note: Parameters were estimated based on maximum likelihood.				

The juvenile Chinook salmon tags in Group I were manually examined to determine the point at which to truncate the detection history. Many of the reviewed tags did not require truncation because the tag ceased to move and remained at a detection site for the duration of the tag's life. In total, 383 of the 762 reviewed detection histories were truncated at some point in the detection history. Typically, detection histories that were truncated were truncated prior to transitions that were considered to be only possible by a predatory fish. However, some detection histories were truncated prior to transitions that were indicative of a predatory fish, if other evidence such as movement rate supported truncation.

TAG LIFE STUDIES

HTI

Failure times from the 100 HTI tags in the tag life study ranged from 0.15 to 103 days after tag activation (**Figure 3.2-5**). The failure times of the 17 tags handled with forceps were distributed throughout this period and showed little evidence of a higher failure rate compared to tags that were not handled with forceps (**Figure 3.2-5**). The Vitality distribution (Li and Anderson 2009) fit the empirical tag failure curve very well (**Table 3.2-4**).

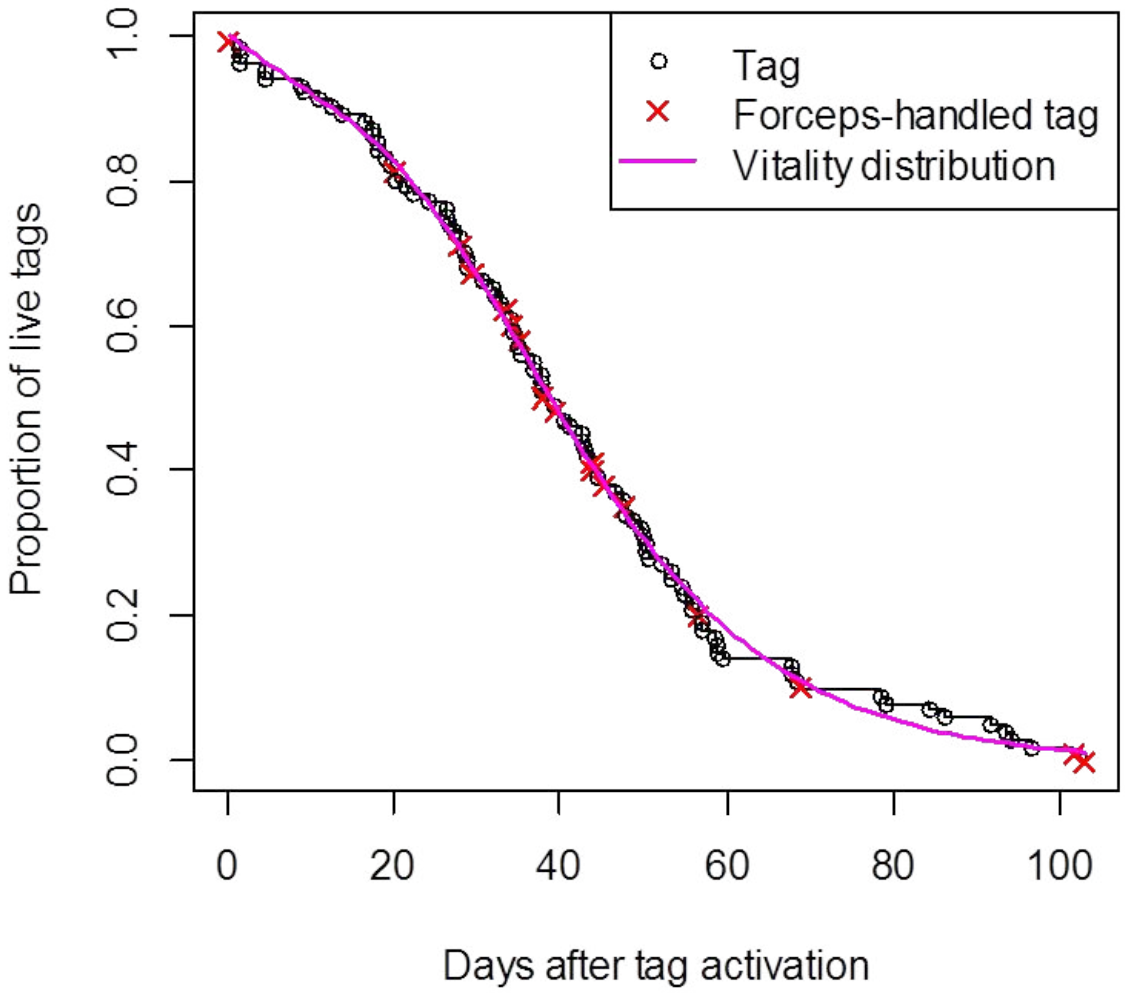

Figure 3.2-5 Survival Function of Four-Parameter Vitality Distribution Fitted to HTI Tag Life Study Tag Failure Times

VEMCO

Failure times of the 100 VEMCO tags used in the tag life study ranged from 13.3 to 54.0 days after tag activation (**Figure 3.2-6**), and from 52.3 to 72.1 days after tag shipment (**Figure 3.2-7**). The shelf time factor quantifying how quickly the kill switch timer advanced between manufacture and activation times ranged from 1.12 to 1.58 (**Figure 3.2-8**). A normal distribution fitted to these data (**Figure 3.2-8**) estimated a mean of $\hat{\mu}_f = 1.30$ and standard deviation $\hat{\sigma}_f^2 = 0.0956$.

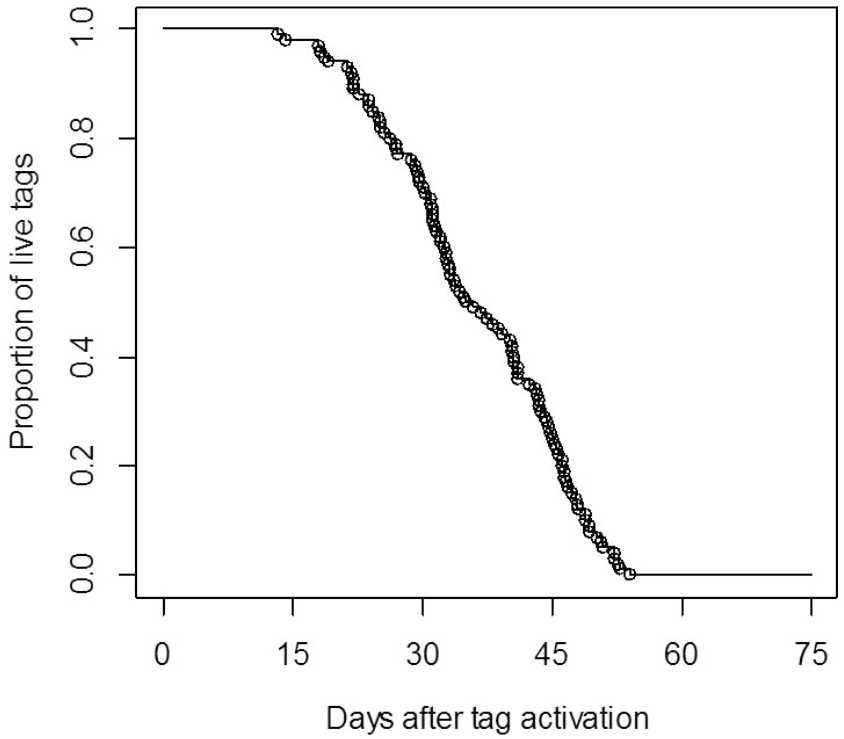

Figure 3.2-6 **VEMCO Tag Life Study Tag Failure Times and Empirical Tag Survival Curve, in Days from Individual Tag Activation**

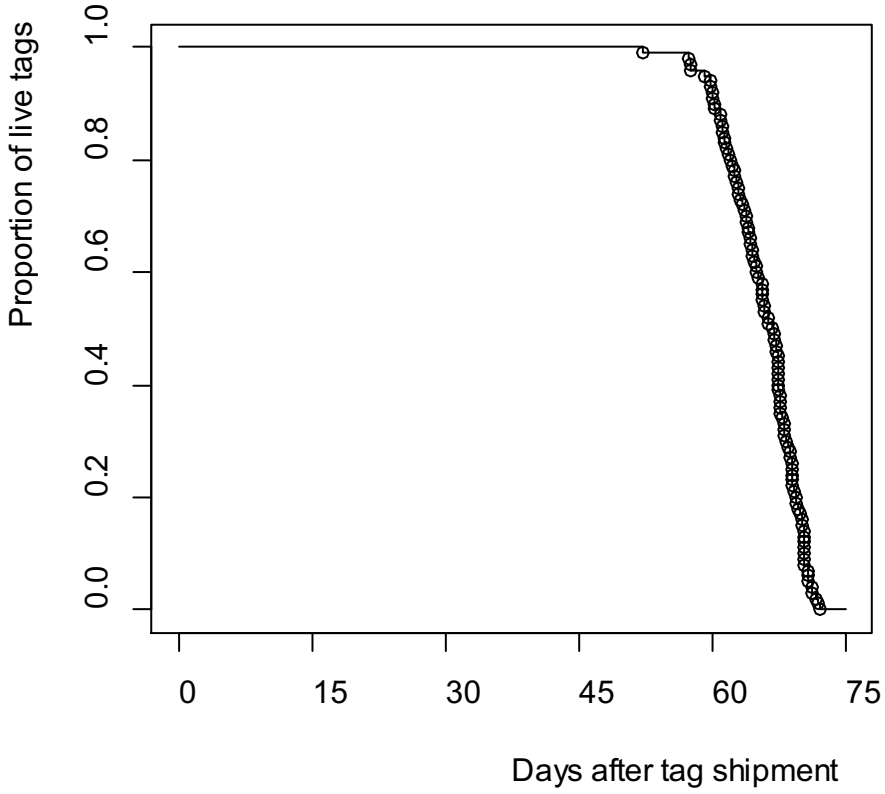

Figure 3.2-7 **VEMCO Tag Life Study Tag Failure Times and Empirical Tag Survival Curve, in Days from Individual Tag Shipment**

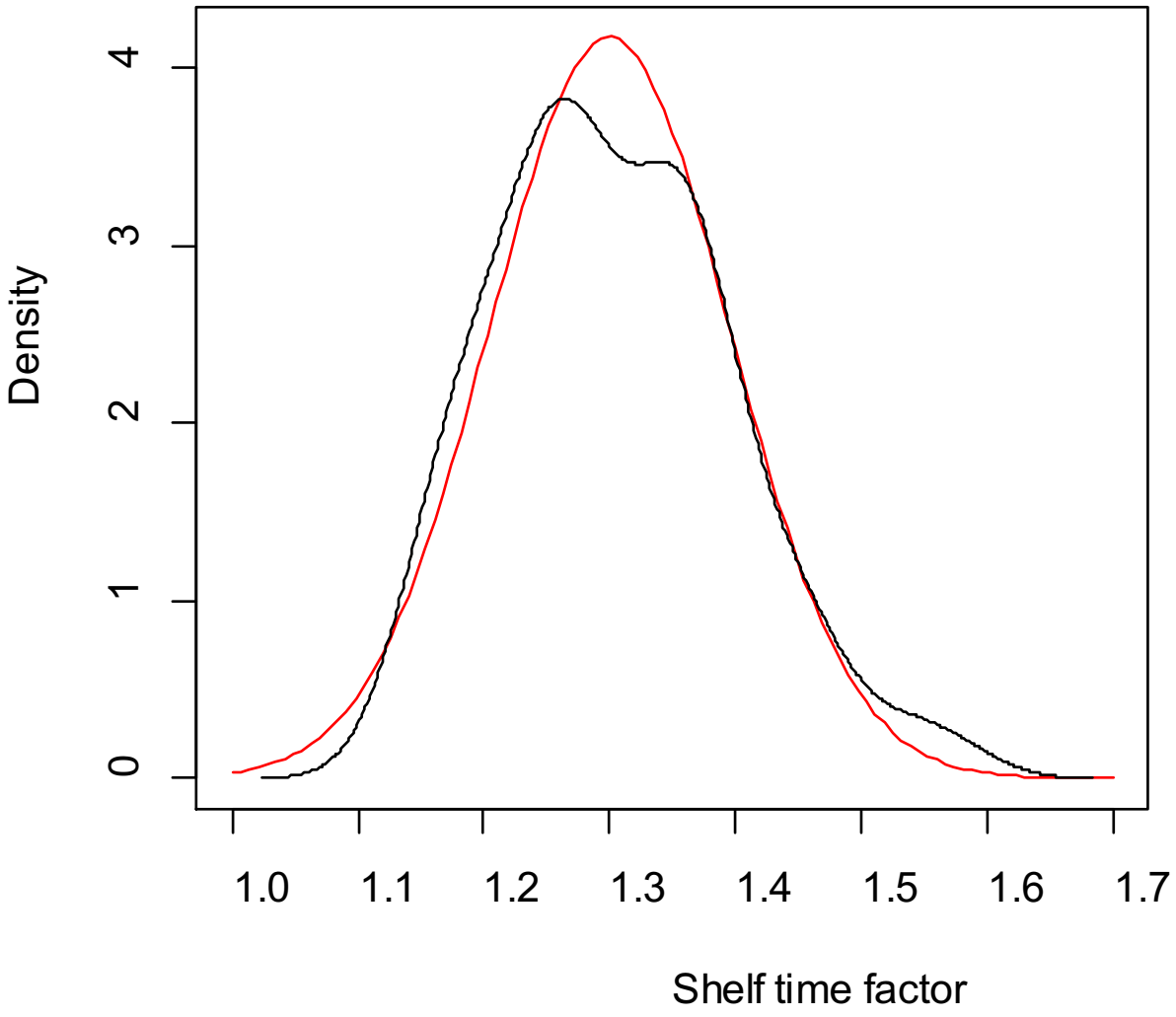

Figure 3.2-8 **Normal Density (Red) Fitted to Empirical "Shelf Time Factor" Kernel Density (black), as Calculated from VEMCO's Tag Life Study Tag Failure Times**

MIGRATION ROUTING

Little difference was found in entrainment into Georgiana Slough between FFGS On and FFGS Off (**Table 3.2-5**). Estimates of entrainment into Georgiana Slough when the FFGS was Off ($\Psi_{D1,Off}$) ranged from 0.215 to 0.359. For FFGS On, estimates of entrainment into Georgiana Slough ($\Psi_{D1,On}$) ranged from 0.200 to 0.342. Posterior distributions of the difference in entrainment into Georgiana Slough between FFGS On and Off indicated little evidence of a significant FFGS effect (**Figure 3.2-9**). For release 1, a 98.0 percent probability existed that entrainment into Georgiana Slough during the FFGS-On period was lower than for the FFGS-Off period. However, for all other release groups, little evidence was found that the difference in entrainment between FFGS On and Off was different from zero.

Table 3.2-5 Median Entrainment Probability Estimates for Tagged Juvenile Chinook Released at the City of Sacramento into the Sacramento River and Georgiana Slough between March 1 and April 15, 2014

Release Group	ΨA, Route A, FFGS On	ΨA, Route A, FFGS Off	ΨD, Route D, FFGS On	ΨD, Route D, FFGS Off
1	0.800 (0.679, 0.885)	0.674 (0.614, 0.728)	0.200 (0.115, 0.321)	0.326 (0.272, 0.386)
2	0.748 (0.683, 0.803)	0.785 (0.710, 0.853)	0.252 (0.197, 0.317)	0.215 (0.147, 0.290)
3	0.731 (0.655, 0.798)	0.748 (0.667, 0.814)	0.269 (0.202, 0.345)	0.252 (0.186, 0.333)
4	0.715 (0.635, 0.784)	0.658 (0.577, 0.733)	0.285 (0.216, 0.365)	0.342 (0.267, 0.423)
5	0.665 (0.572, 0.745)	0.680 (0.586, 0.759)	0.335 (0.255, 0.428)	0.320 (0.241, 0.414)
6	0.728 (0.635, 0.810)	0.641 (0.528, 0.747)	0.272 (0.190, 0.365)	0.359 (0.253, 0.472)
7	0.676 (0.589, 0.750)	0.709 (0.624, 0.783)	0.324 (0.250, 0.411)	0.291 (0.217, 0.376)
8	0.658 (0.584, 0.735)	0.741 (0.666, 0.804)	0.342 (0.265, 0.416)	0.259 (0.196, 0.334)
9	0.682 (0.596, 0.762)	0.664 (0.577, 0.735)	0.318 (0.238, 0.404)	0.336 (0.265, 0.423)
10	0.764 (0.676, 0.835)	0.714 (0.616, 0.799)	0.236 (0.165, 0.324)	0.286 (0.201, 0.384)

Note: Entrainment probability estimates are listed by route of entrainment (A=Sacramento River, D=Georgiana Slough), FFGS status, and release group (dates listed in **Table 3.2-1**). Values in parentheses are the 95 percent credible intervals (CI) which represent the 2.5th and 97.5th quantiles of the posterior distribution.

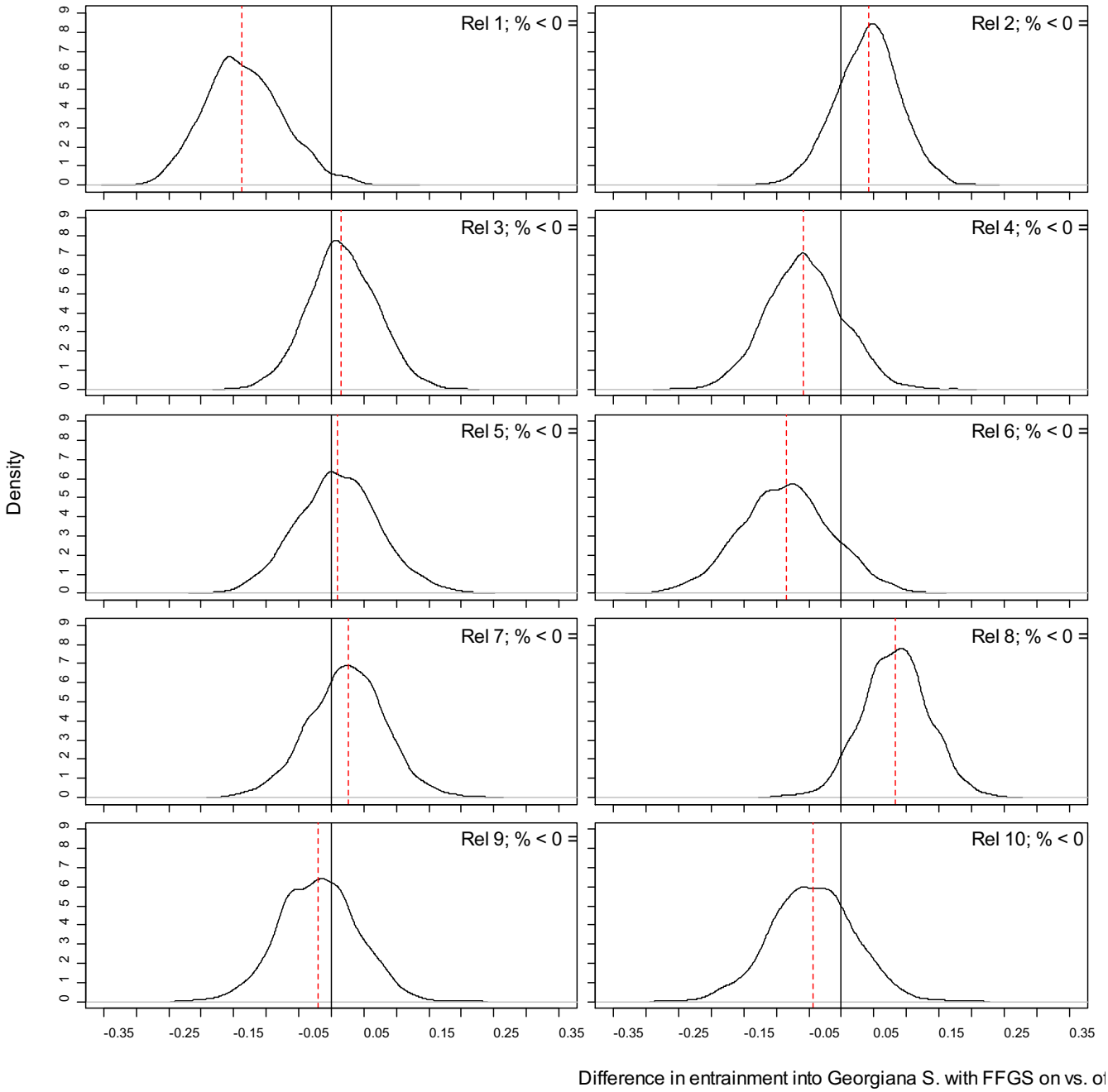

Note: Density is the posterior distribution of the difference in entrainment into Georgiana Slough with FFGS On versus Off positions (i.e., positive values indicate higher entrainment into Georgiana Slough with FFGS On). Red dashed lines indicate medians of the posterior distributions. Percentages in the upper right of each plot indicate portion of the posterior which is less than zero; a statistically significant negative effect of FFGS On position on Georgiana Slough entrainment is indicated by percentages greater than 95.

Figure 3.2-9 Effect of FFGS Position on Entrainment Probability into Georgiana Slough by Release Group

Estimates of route entrainment probabilities at the junction of Sutter Slough, Steamboat Slough, and the Sacramento River varied little across release groups (**Table 3.2-6**). The probability of remaining in the Sacramento River downstream of the junctions with Sutter and Steamboat sloughs (Ψ_{A1}) was remarkably consistent among release groups, ranging from 0.698 to 0.784. Likewise, entrainment probabilities into Sutter

Slough (Ψ_{B1}) and Steamboat Slough (Ψ_{B2}) varied little over release groups, with estimates of Ψ_{B1} ranging from 0.097 to 0.163, and Ψ_{B2} ranging from 0.083 to 0.149.

Table 3.2-6 Entrainment Probabilities Estimates (medians) for Tagged Juvenile Chinook Released at the City of Sacramento into the Sacramento River, Sutter Slough, and Steamboat Slough between March 1 and April 15, 2014

Release Group	Ψ_{A1} Route A	Ψ_{B1} Route B_1	Ψ_{B2} Route B_2
1	0.704 (0.663, 0.744)	0.148 (0.117, 0.181)	0.148 (0.119, 0.182)
2	0.706 (0.664, 0.747)	0.149 (0.119, 0.184)	0.143 (0.114, 0.178)
3	0.716 (0.669, 0.760)	0.151 (0.118, 0.190)	0.131 (0.100, 0.165)
4	0.774 (0.730, 0.814)	0.142 (0.109, 0.182)	0.083 (0.058, 0.114)
5	0.784 (0.739, 0.827)	0.106 (0.074, 0.141)	0.109 (0.079, 0.146)
6	0.741 (0.690, 0.792)	0.135 (0.097, 0.180)	0.123 (0.087, 0.163)
7	0.698 (0.650, 0.744)	0.163 (0.128, 0.202)	0.138 (0.105, 0.177)
8	0.720 (0.677, 0.760)	0.130 (0.101, 0.165)	0.149 (0.116, 0.186)
9	0.778 (0.734, 0.819)	0.097 (0.070, 0.131)	0.123 (0.092, 0.159)
10	0.778 (0.729, 0.823)	0.117 (0.081, 0.157)	0.105 (0.073, 0.145)

Note: Entrainment probability estimates are listed by route of entrainment (A=Sacramento River, B1=Sutter Slough, B2=Steamboat Slough) and release group (dates listed in **Table 3.2-1**). Ψ represents values in parentheses and these are the median and 95 percent credible intervals (CI) that represent the 2.5th and 97.5th quantiles of the posterior distribution.

Migration route probabilities (the probability of migrating through the entire migration route) showed little variation across release groups, regardless of route (**Figure 3.2-10**). The estimated probability of migrating via the Sacramento River ($\hat{\Psi}_A$) ranged from 0.48 to 0.57. Estimates of migration probabilities via Sutter and Steamboat sloughs remained consistent across release groups, with Sutter Slough entrainment ($\hat{\Psi}_{B1}$) ranging from 0.10 to 0.16, and Steamboat Slough entrainment ($\hat{\Psi}_{B2}$) ranging from 0.08 to 0.15. Migration via Georgiana Slough ($\hat{\Psi}_D$) was estimated to range from 0.17 to 0.26. The total contribution to Delta survival from each route was found by calculating the area of the box for that route, as shown in **Figure 3.2-11**.

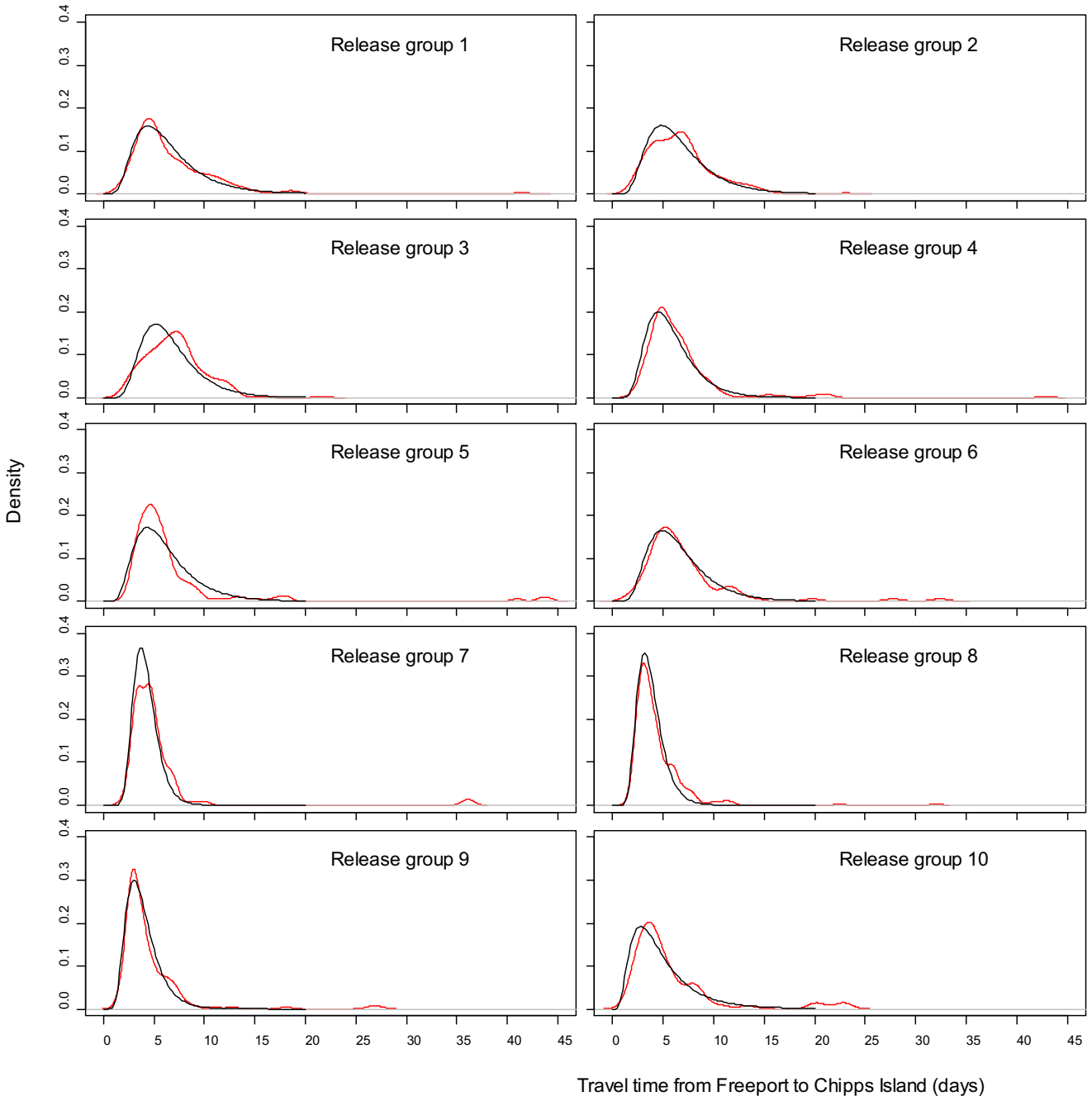

Note: The median posterior means and variances of CDL travel times were used to generate the lognormal distributions.

Figure 3.2-10 Empirical Densities for Observed Travel Times (Red) and Lognormal Densities for CDL Travel Times (Black), from Freeport to Chipps Island by Release Group for All Routes

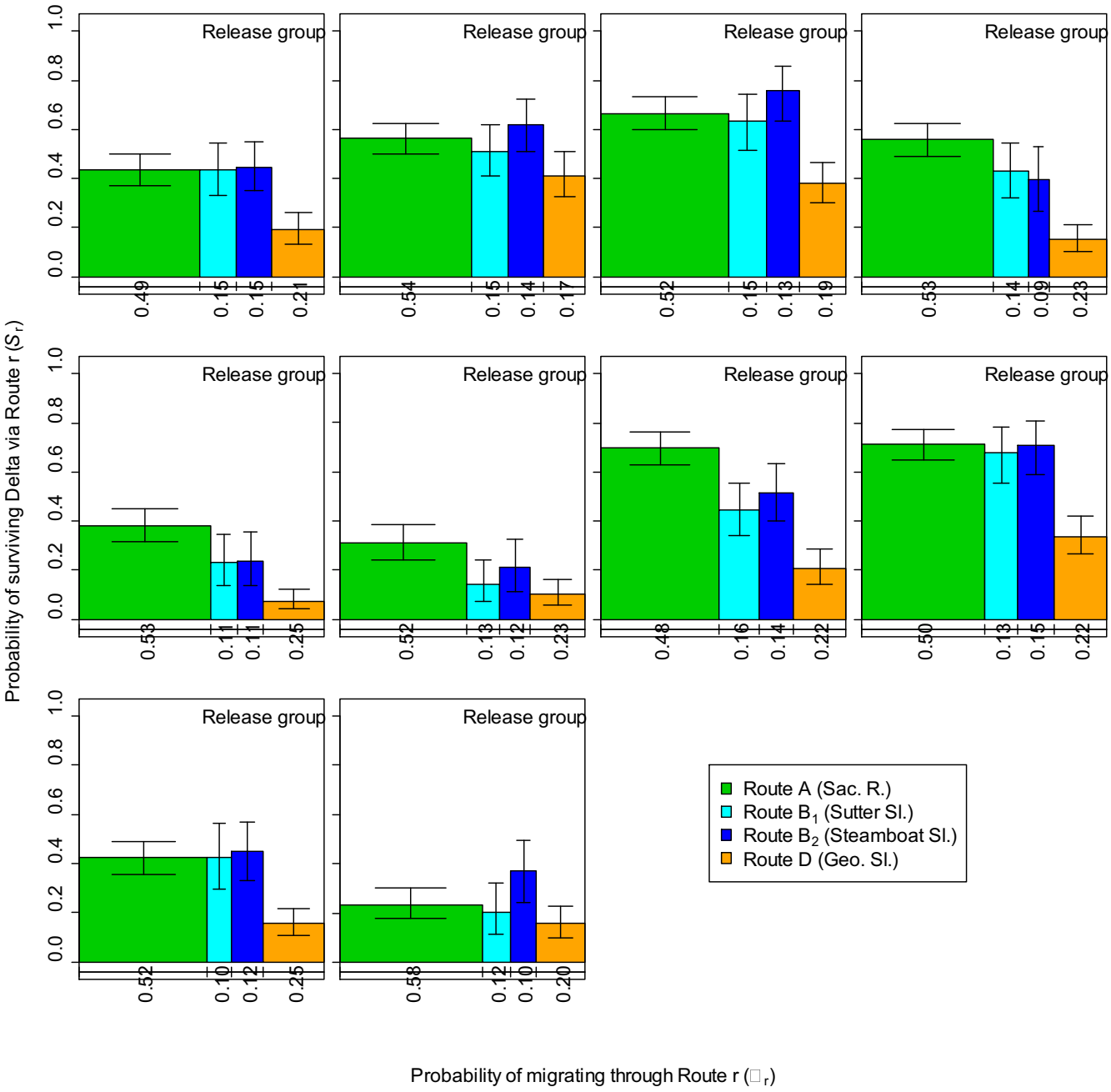

Note: Within each boxplot, bars from right to left represent the proportion of fish surviving through the Sacramento River, Sutter Slough, Steamboat Slough, and Georgiana Slough, respectively.

Figure 3.2-11 Two-Way Boxplots Showing Route-Specific Survival and Entrainment Probability by Release Group

TRAVEL TIME, TAG FAILURE, AND SURVIVAL

Compared to estimates of travel times through the Delta from other studies (Perry 2010; Perry et al. 2012), travel times from Freeport to Chipps Island in 2014 were remarkably short. Overall Delta-wide travel time from Freeport to Chipps Island, estimated by release group, displayed modes between 2.79 and 5.14 days (**Figure 3.2-12**). Travel times tended to vary by route, however, with travel times from Freeport to Chipps Island via the interior Delta generally taking longer than via any of the three other routes (**Figure 3.2-11**). Modes of release

group-specific travel time distributions via Georgiana Slough and the interior Delta ranged from 4.59 to 7.44 days. Travel times were similar for fish travelling via the Sacramento River, Sutter Slough, or Steamboat Slough. Modes for release group-specific travel time distributions for these three routes ranged from 2.33 to 5.56 days, and generally were within a day among the three routes for any given release group.

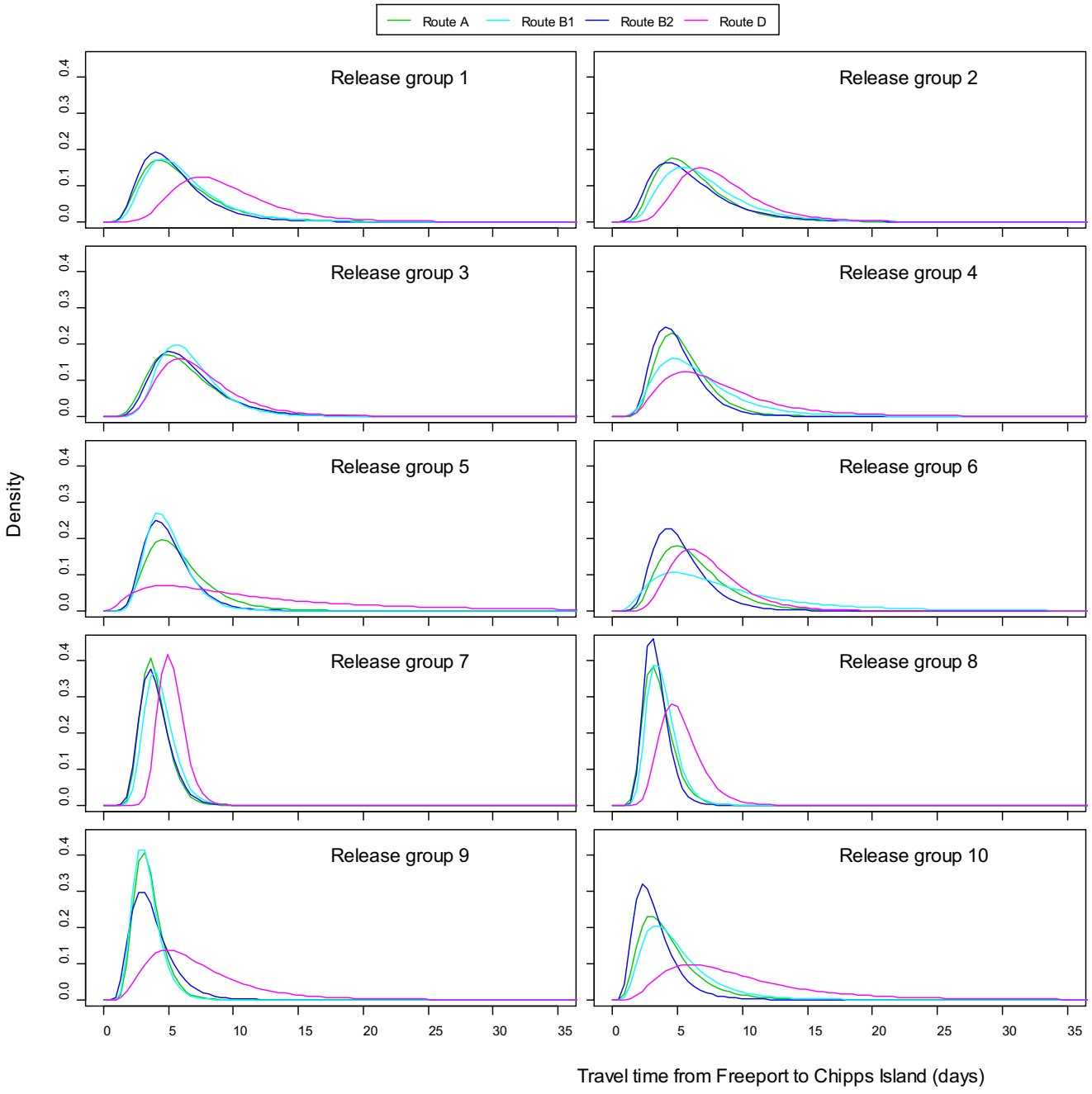

Note: Route A = Sacramento River, Route B1 = Sutter Slough, Route B2 = Steamboat Slough, Route D = Georgiana Slough. Parameters for lognormal densities are the median posterior means and variances of CDL travel times.

Figure 3.2-12 Lognormal Density of Travel Times from Freeport to Chipps Island by Release Group and Route

Despite unexpected premature tag failure for both tag types, short travel times of tagged juvenile Chinook salmon resulted in a high probability of these fish arriving at Chipps Island with operational tags (**Table 3.2-7**). For HTI tags, the estimated probability of a tag remaining operational in the study area ranged from 0.846 for Release 5 to 0.961 for Release 8. For all but one release group, VEMCO tags had a 100 percent chance of remaining operational while fish were in the study area. For Release 10, a 0.929 probability existed of a tag remaining operational in the study area.

Table 3.2-7 Estimates of the Median Proportion of HTI and VEMCO Tags Remaining Active (λ) in the Study Location

Release Group	λ_{HTI} HTI	λ_{Vemco} VEMCO
1	0.933 (0.892, 0.972)	1.000 (1.000, 1.000)
2	0.935 (0.901, 0.962)	1.000 (1.000, 1.000)
3	0.932 (0.901, 0.965)	1.000 (1.000, 1.000)
4	0.918 (0.880, 0.966)	1.000 (0.974, 1.000)
5	0.846 (0.779, 0.917)	1.000 (0.870, 1.000)
6	0.885 (0.812, 0.945)	1.000 (1.000, 1.000)
7	0.936 (0.903, 0.967)	1.000 (0.977, 1.000)
8	0.962 (0.934, 0.987)	1.000 (1.000, 1.000)
9	0.917 (0.871, 0.960)	1.000 (0.974, 1.000)
10	0.904 (0.843, 0.962)	0.929 (0.786, 1.000)

Notes: Values in parentheses are the 95 percent credible intervals (CI) which represent the 2.5th and 97.5th quantiles of the posterior distribution. Tags remaining active are estimated separately by release group.

Survival of tagged juvenile Chinook salmon from Freeport to Chipps Island in 2014 varied considerably among migration routes and release groups (**Table 3.2-8**). Among migration routes, survival was consistently lower for fish traveling through the interior Delta relative to other routes, with $\hat{S}_{\mathrm{D}}$ ranging from 0.05 to 0.36 lower than $\hat{S}_{B1}$ (Sutter Slough), 0.10 to 0.37 lower than $\hat{S}_{B2}$ (Steamboat Slough), and 0.05 to 0.50 lower than $\hat{S}_{A}$ (Sacramento River). Survival of fish for the interior Delta ranged from 0.076 to 0.42 among release groups, whereas survival of fish remaining in the Sacramento River ranged from 0.216 to 0.704. Among release groups, Delta-wide survival varied from 0.221 to 0.624. Survival probabilities tended to follow the pattern of discharge at Freeport, with higher survival associated with higher discharge periods and lower survival occurring during lower discharge periods (**Figure 3.2-13**).

Table 3.2-8 Estimates of Survival (median) from Freeport to Chipps Island for Tagged Juvenile Chinook Released at the City of Sacramento between March 1 and April 15, 2014

Release Group	Route A	Route B1	Route B2	Route D	Delta Wide
1	0.435 (0.374, 0.501)	0.423 (0.322,0.531)	0.450 (0.346, 0.553)	0.194 (0.136, 0.266)	0.384 (0.342, 0.428)
2	0.566 (0.500, 0.631)	0.496 (0.390,0.604)	0.616 (0.512, 0.719)	0.420 (0.325, 0.516)	0.537 (0.490, 0.584)
3	0.655 (0.596, 0.728)	0.638 (0.518, 0.753)	0.755 (0.643, 0.854)	0.385 (0.306, 0.472)	0.617 (0.569, 0.665)
4	0.563 (0.493, 0.625)	0.430 (0.319, 0.550)	0.386 (0.253, 0.520)	0.157 (0.109, 0.221)	0.428 (0.379, 0.479)
5	0.372 (0.307, 0.447)	0.209 (0.122, 0.322)	0.230 (0.137, 0.345)	0.076 (0.043, 0.124)	0.266 (0.225, 0.311)
6	0.295 (0.231, 0.364)	0.146 (0.074, 0.250)	0.197 (0.103, 0.309)	0.102 (0.059, 0.163)	0.221 (0.178, 0.266)
7	0.697 (0.627, 0.758)	0.449 (0.342, 0.566)	0.521 (0.402, 0.639)	0.195 (0.135, 0.263)	0.521 (0.473, 0.571)
8	0.704 (0.634, 0.765)	0.693 (0.569, 0.796)	0.698 (0.584, 0.793)	0.330 (0.262, 0.411)	0.624 (0.577, 0.669)
9	0.424 (0.357, 0.489)	0.420 (0.290, 0.553)	0.447 (0.329, 0.567)	0.152 (0.107, 0.208)	0.356 (0.310, 0.404)
10	0.216 (0.162, 0.275)	0.203 (0.109, 0.321)	0.365 (0.246, 0.495)	0.164 (0.103,0.233)	0.219 (0.179, 0.262)

Note: Survival estimates are listed by Route A (Sacramento River), Route B1 (Sutter Slough), Route B2 (Steamboat Slough), Route D (Georgiana Slough) and release group (dates listed in **Table 3.2-1**). Values in parentheses are the 95 percent credible intervals (CI) which represent the 2.5th and 97.5th quantiles of the posterior distribution.

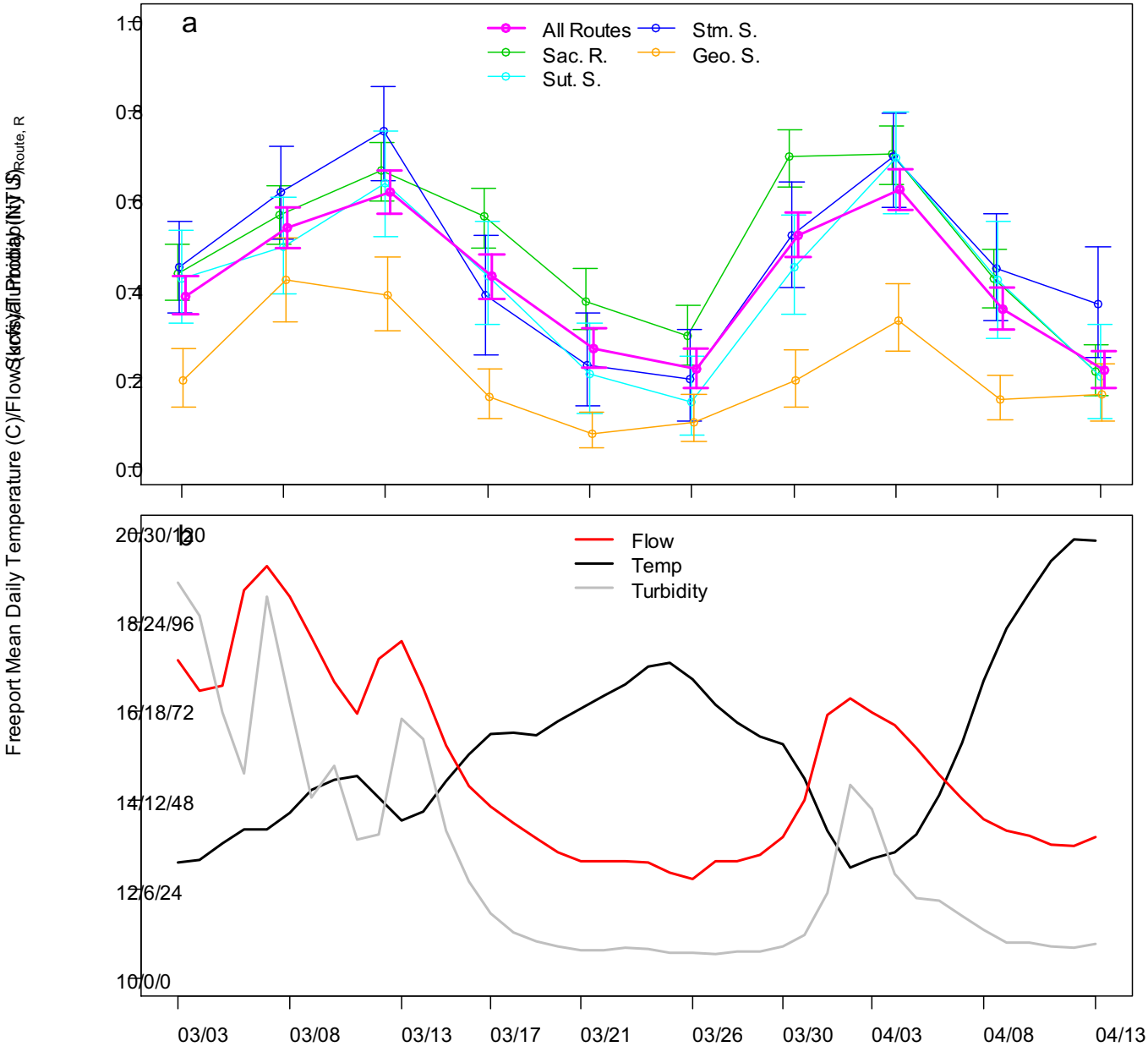

Note: Error bars represent 95 percent credible intervals for each estimate.

Figure 3.2-13 (a) Route-Specific and Delta-Wide Survival Estimates (medians) from Freeport to Chipps Island by Release Group, with (b) Mean Daily Temperature, Flow, and Turbidity at Freeport

3.2.3 DISCUSSION

The overarching goal of the FFGS and other guidance technologies is to increase Delta-wide survival by decreasing the proportion of the population entering the interior and southern Delta, where survival is lower than in the Sacramento River. Although the primary purpose of the survival study was to estimate the magnitude of

change in Delta-wide survival in response to reducing entrainment into Georgiana Slough, this analysis indicates entrainment into Georgiana Slough was similar between FFGS On and Off. Because the FFGS likely did not alter reach-specific survival and did not appear to reduce overall entrainment consistently over the entire study, Delta-wide survival was unaffected by operation of the FFGS. Although little effect of the FFGS was observed based on the 2014 study, the route-specific survival analysis provides information about the change in Delta-wide survival that likely would have been realized had the FFGS altered entrainment into Georgiana Slough. Any reduction in entrainment into Georgiana Slough results in an increase in the probability of remaining in the lower portion of the Sacramento River, where survival was higher (Perry et al. 2013). The relationship between entrainment and Delta-wide survival can be seen by varying entrainment probability into Georgiana Slough while holding other parameters fixed and calculating Delta-wide survival at each point (**Figure 3.2-14** and **Figure 3.2-15**). Based on the route-specific survival estimates from the 2014 study and other route entrainment probabilities, reduction of entrainment into Georgiana Slough to zero would have resulted in an increase in Delta-wide survival, ranging by release group from 2 to 11 percentage points (**Figure 3.2-14**). Likewise, halving entrainment into Georgiana Slough could have resulted in a 1 to 6 percentage point increase in survival.

Although the effect of the FFGS on Delta-wide survival could not be fully evaluated, this survival study made a number of important discoveries, contributing to new insights about migration and survival of juvenile Chinook salmon in the Delta. First, unexpected tag failure led to the development of new statistical models that were able to provide unbiased estimates of survival in the event of tag failure. This new modeling framework should prove useful to all future survival studies in the Delta. Second, this survival study represents the largest and most expansive season-wide evaluation of Delta-wide survival relative to date. Third, by measuring survival continuously across a migration season, route-specific survival varied considerably over time, as river discharge varied. Discussion of each of these topics is expanded on next.

The CDL formulation within a Bayesian estimation framework allowed:

1. An appropriate account of missing travel times resulting from tag failure;

2. An estimate of model tag failure probabilities associated with expected travel times; and

3. A joint estimate of survival while accounting for tag failure.

Unexpected tag failure has plagued telemetry studies in the Delta and elsewhere (Holbrook et al. 2013; Romine et al. 2013), and available statistical methods do not completely eliminate negative bias in survival estimates that is induced by tag failure. The original approach in this study was to use available methods (Townsend et al. 2006) along with an independent estimate of the travel time distribution, obtained from the VEMCO tags. Unexpected tag failure in both tag models precluded this approach and forced a new statistical model to be developed that did not rely on an independent estimate of travel times. By providing an estimate of a transmitter's survival distribution function, obtained from a controlled tag life study, survival estimates that accounted for tag failure without releasing a separate subset of tags for estimating travel times (VEMCO tags in this study) were possible. Now that these methods have been developed they can be applied to future studies as well as to previous studies, such as Holbrook et al. (2013) and Romine et al. (2013).

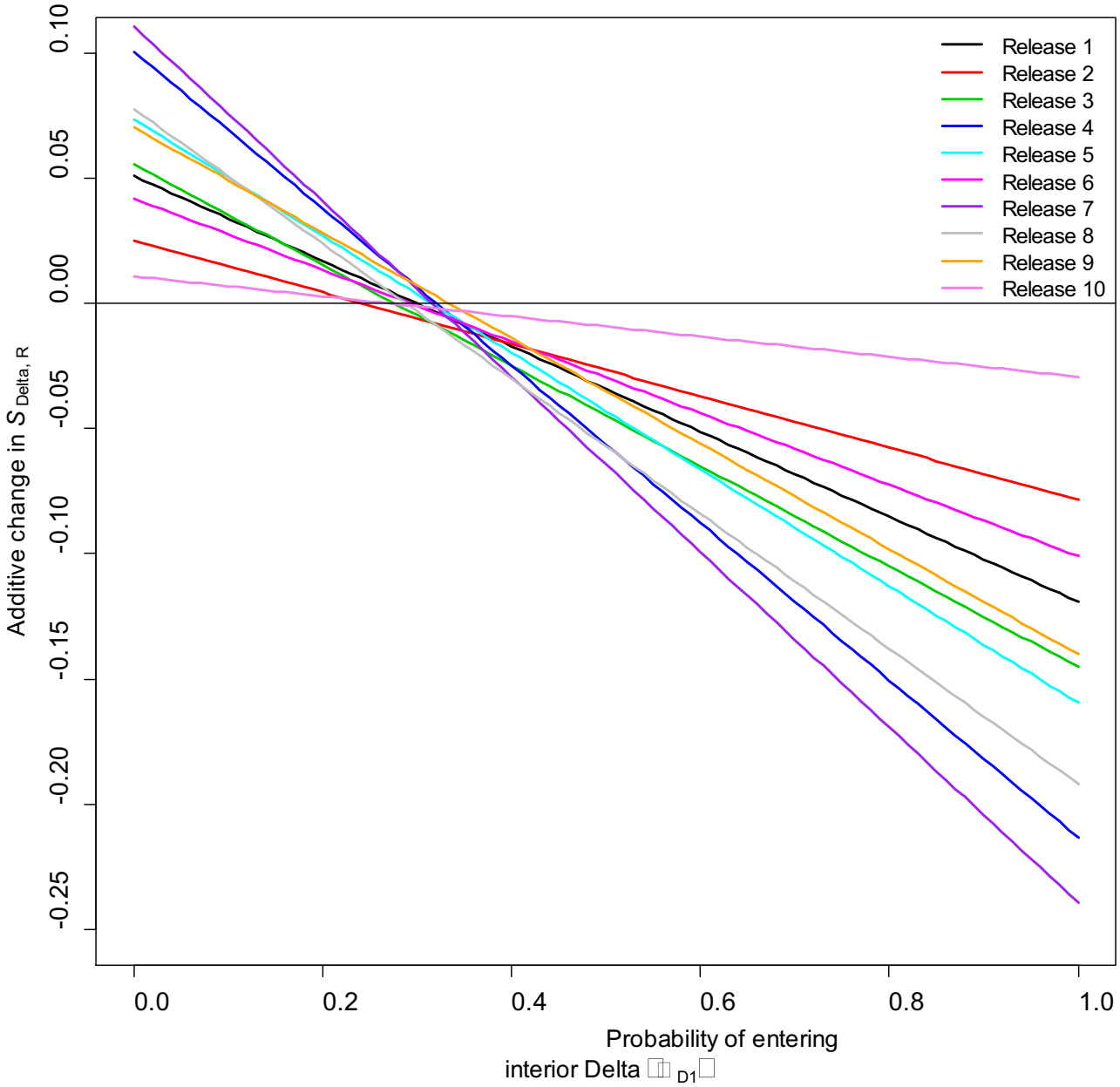

Figure 3.2-14 **Theoretical Additive Change in Delta-Wide Survival Calculated over the Possible Range of Entrainment Probabilities into Georgiana Slough, based on Median Route-Specific Survival Estimates and Other Route Entrainment Probabilities for each Release Group**

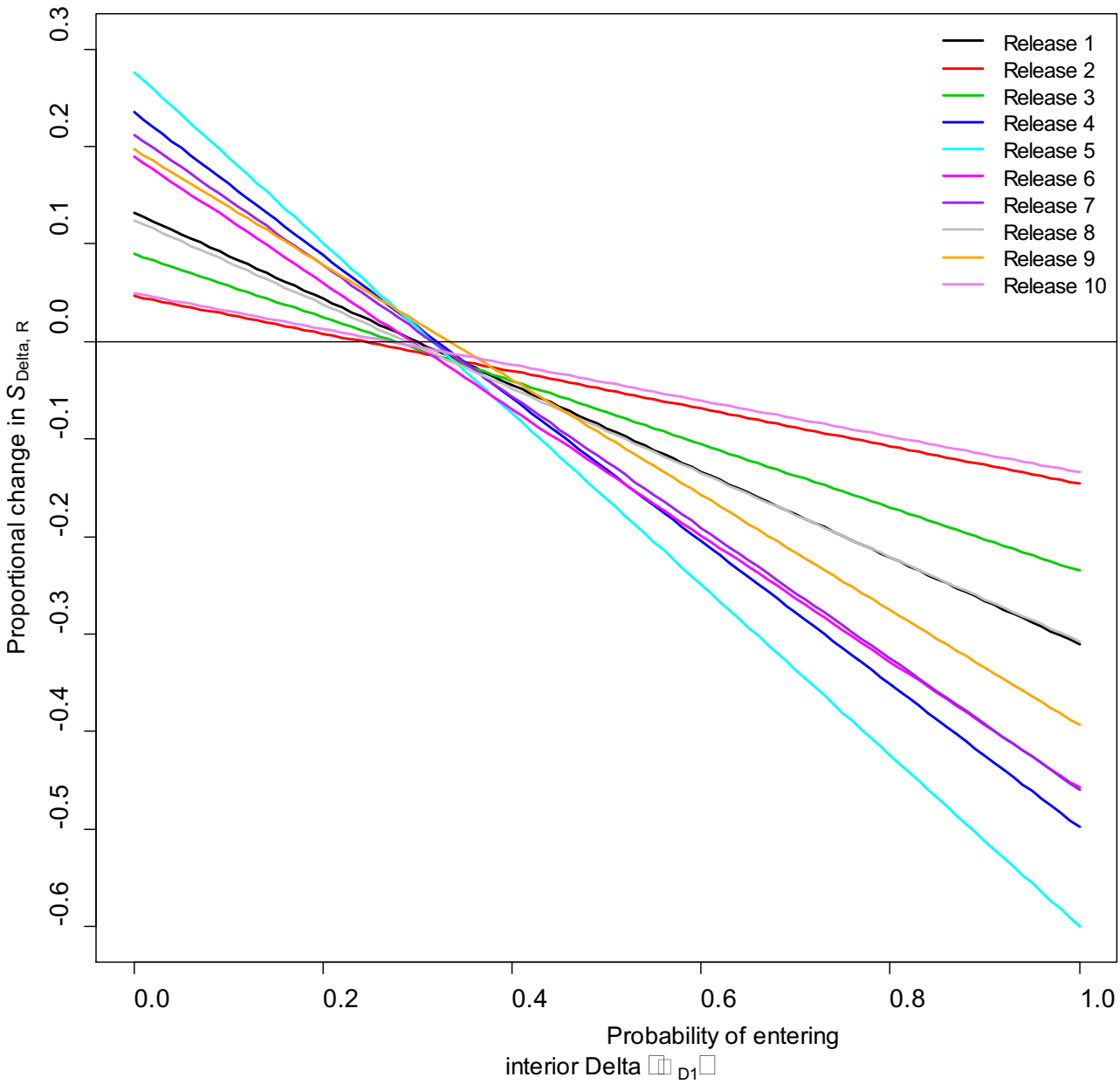

Figure 3.2-15 **Theoretical Proportional Change in Delta-Wide Survival Calculated over the Possible Range of Entrainment Probabilities into Georgiana Slough, based on Median Route-Specific Survival Estimates and Other Route Entrainment Probabilities for Each Release Group**

Relative to the extent of premature tag failure identified in both tag models, most release groups had high probabilities of tags remaining operational when fish passed Chipps Island, the terminus of the study area. These "tag survival" probabilities were high, owing to much shorter travel times than expected relative to river flow and observations from previous studies. The modes of the travel time distributions were 5 days or less, and most fish passed Chipps Island in well under 15 days (**Figure 3.2-10**). In a previous study during similar river discharge, Perry et al. (2012) estimated a median travel time to Chipps Island of 29 days, with a 90th percentile of 55 days for fish released in December 2010. Median observed travel times of tagged late fall Chinook outmigrating through the mainstem Sacramento River or interior Delta in December 2006 to January 2007 ranged from 11 to 18 days (Perry 2010). The primary difference between this study and previous studies is release timing. Most

other studies released salmon in December, January, and early February, whereas this study released fish in March and April. Because late-fall Chinook salmon typically are released from Coleman National Fish Hatchery from December through January, it is possible that fish in this study were in an advanced stage of juvenile Chinook smoltification that led to fast migration rates through the study area. Although fish migrated quickly and tag survival probabilities were relatively high, failure to account for tag failure still would have caused a negative bias on the order of 5 percentage points. If the study had been conducted earlier in the late-fall Chinook salmon migration season, travel times possibly would have been longer and the potential for negative bias could have been more extreme. It seems plausible that results of an FFGS evaluation conducted in the December-February period might produce qualitatively different results than were found in this study. This is because if a juvenile Chinook salmon is in an advanced state of smoltification it may be more strongly motivated to reach the ocean quickly and might have a very different response to a FFGS for this reason. It is suggested that an evaluation of an FFGS in the winter months is a potentially profitable area of future research.

Estimates of route-specific survival generally were comparable to those from previous studies (Perry et al. 2010; Perry et al. 2013). Estimates of survival from Freeport to Chipps Island among fish entering Georgiana Slough were consistently lower than for all other routes, with no overlap in 95 percent credible intervals between survival in that route and survival in any other route for 7 of the 10 release groups (**Figure 3.2-13a**). Release group-specific median survival estimates for fish entering Georgiana Slough were 20 percent to 76 percent of the median estimates of survival for fish remaining in the Sacramento River, and 33 percent to 85 percent of the median estimates of survival for fish entering Steamboat and Sutter sloughs. Median release group-specific survival estimates from Freeport to Chipps Island were fairly similar among fish remaining in the Sacramento River and fish entering Sutter and Steamboat sloughs (**Figure 3.2-13a**). Survival appeared to track closely with mean daily flow at Freeport, but also followed positively with the trend of turbidity and inversely with water temperature (**Figure 3.2-13b**).

Little evidence was found that the configuration of the FFGS evaluated in this analysis significantly altered migration routing on the release group scale, measured by the parameter estimates. It is important to note, however, that while the overall range of entrainment into Georgiana Slough is comparable with the entrainment rates estimated elsewhere in this report (see Section 3.4, "Generalized Linear Modeling of Fish Fates"), the level of detail and finer scale of the generalized linear modeling analysis allows conclusions to be drawn about entrainment at different flow levels and diel periods that were not apparent in the coarser, Delta-wide scale of this analysis. Posterior distribution medians for the difference in entrainment into Georgiana Slough with the FFGS On and Off for each of 10 release groups were grouped fairly closely around zero, with 5 release group level estimates below and 5 above zero (**Figure 3.2-9**). Credible intervals overlapped zero for each of these estimates, indicating that the level of uncertainty in the parameter estimates was greater than any small differences in median entrainment between FFGS On and Off.

3.3 HYDRODYNAMICS AND CRITICAL STREAKLINE

3.3.1 INTRODUCTION, BACKGROUND, AND CONTEXT

This subchapter addresses the hydrodynamic aspects of juvenile salmon entrainment at the Georgiana Slough/Sacramento River riverine junction (i.e., the divergence of Georgiana Slough from the Sacramento River). These hydrodynamic processes create the physical environment in which juvenile salmon are distributed among the various migration routes in the Delta (**Figure 3.3-1**). Understanding the mechanics of entrainment rates in

riverine junctions is critical to understanding overall Delta survival because juvenile fish survival differs among the various outmigration routes (Perry et al. 2010, 2013).

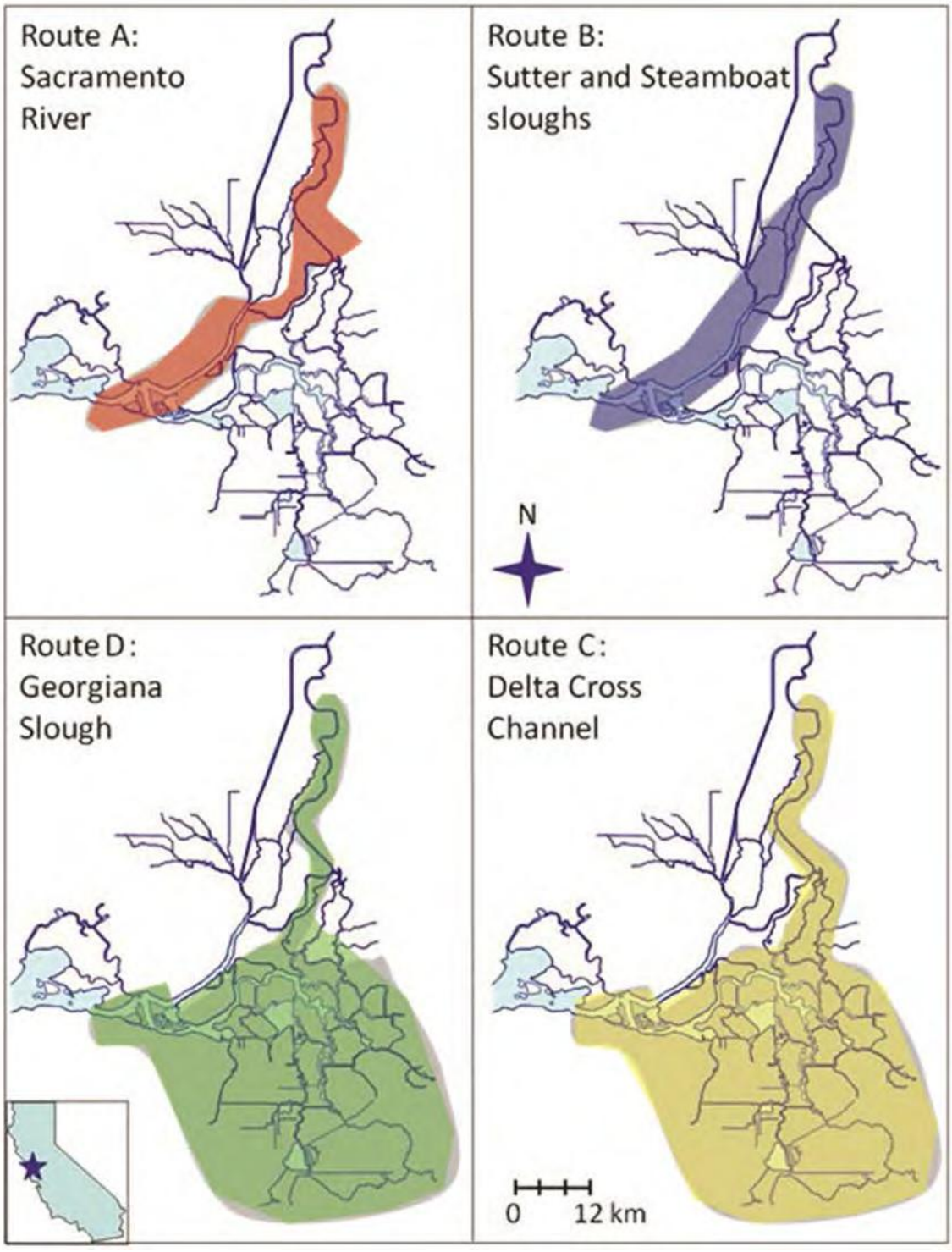

Note: Possible routes as determined by junction entrainment rates. Route A: the Sacramento River (no-entrainment) route; Route B: The Sutter and Steamboat slough route as determined by the entrainment rates of the Sacramento River into these channels, The Georgiana Slough route as determined by the entrainment rates of the Sacramento River into Georgiana Slough and Route C; the DCC route as determined by the entrainment rates of the Sacramento River into the DCC with fish also traveling through the Mokelumne system.

Source: Perry et al. 2010

Figure 3.3-1 Possible Routes of Juvenile Salmon in the Delta

The design of the FFGS was intended to elicit a behavioral response that reduced the entrainment rate of juvenile salmon into Georgiana Slough while minimally affecting the bulk distribution of water at this junction with the Sacramento River. The objective of the FFGS was to maintain the flow rates into Georgiana Slough, maintain salinity standards in the western Delta (http://www.swrcb.ca.gov/waterrights/water_issues/programs/bay_delta/decision_1641/index.shtml), and export rates at state and federal water projects, while reducing entrainment of juvenile salmon into Georgiana Slough. The goal of this study was to assess the efficacy of the FFGS while acquiring a process-level understanding of the interactions between the FFGS, the structure's hydrodynamic characteristics, and behavioral responses of salmon to the FFGS.

A process-level understanding the FFGS' hydrodynamic characteristics and behavioral responses of salmon is necessary to inform future barrier designs (e.g., length, depth, angle with river, position relative to the junction) that would maximize the effect on entrainment rates on this and other barrier technologies at Georgiana Slough and other junctions in the Delta. A process-level understanding is particularly relevant in this application because this study represents the first time this technology was applied in a river system that is capable of conveying water associated with large uncontrolled flow events where reversing tidal flows also occur.

The effect on fish behavioral response from a particular FFGS configuration (length, depth, angle with river, position relative to the junction) in this circumstance was virtually unknown prior to this study (see Section 3.2 on barrier design). The data from this study will dramatically reduce the guesswork in future applications of this technology, including applications in other junctions in the Delta.

Understanding entrainment rates at junctions located in the upstream periphery of the Delta (i.e., Sutter Slough, Steamboat Slough, DCC, and Georgiana Slough on the Sacramento River; Old River, Turner Cut and Columbia Cut on the San Joaquin River) is critically important because population-level survival through the Delta depends on the number of fish that take a particular path multiplied by survival within that path and summed over all the paths.

There are three basic ways through-delta survival can be increased:

1. Improve the survival within a particular path;

2. Increase entrainment into higher-survival paths; and

3. Decrease entrainment into lower-survival paths.

Because survival varies between paths, changing entrainment rates can influence through-Delta survival (**Figure 3.3-2**). If a substantial percentage of the population can be routed through a targeted pathway by altering the entrainment rate at an upstream junction, then restoration efforts can be strategically focused on: 1) a limited number of pathways that are amenable to restoration; and 2) pathways which are also downstream of junctions that are a good match for fish guidance technologies.

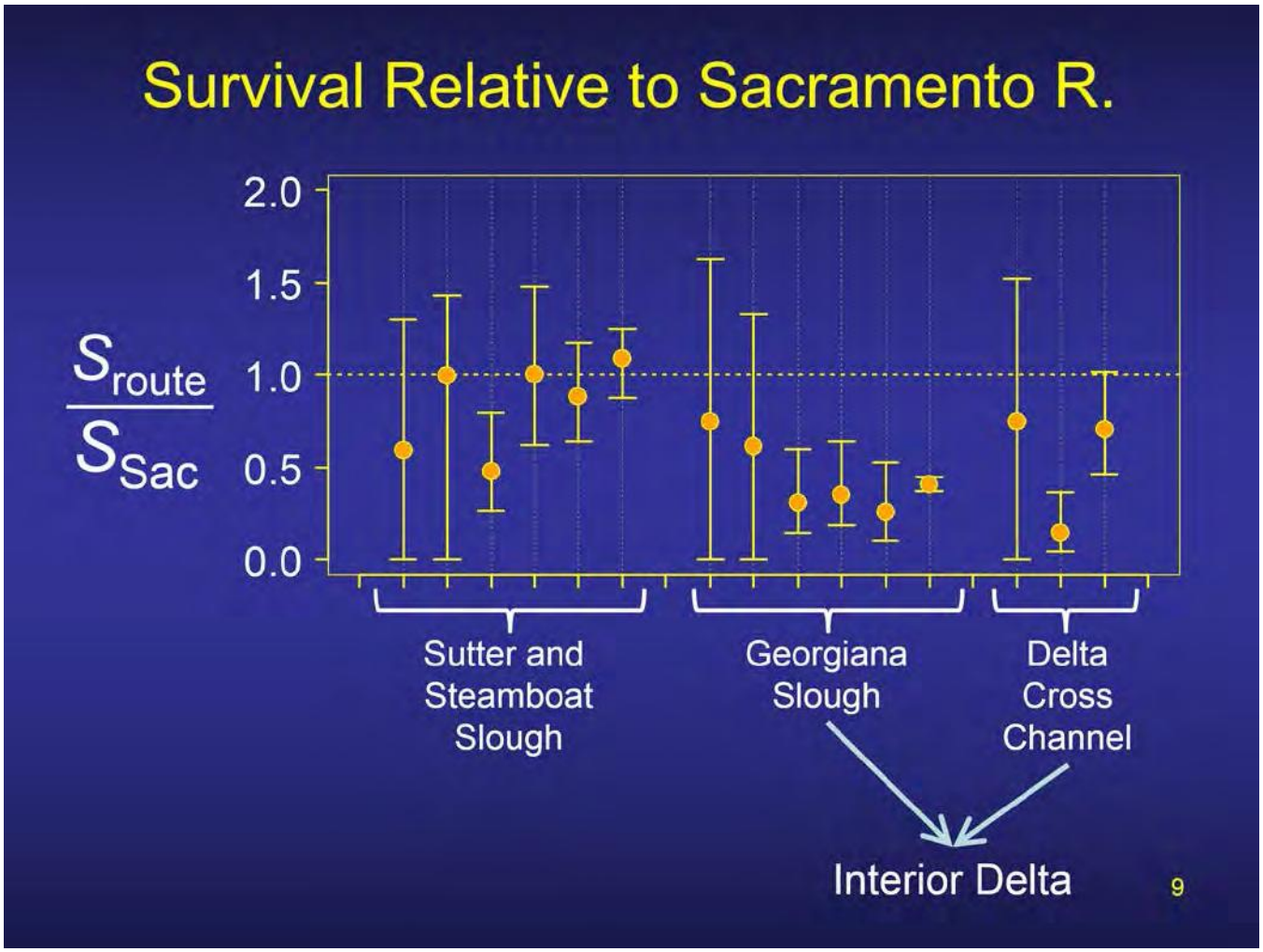

Source: Perry et al. 2010

Figure 3.3-2 Survival in the North Delta by Route Normalized by the Sacramento Route based on Acoustic Telemetry Data

ENTRAINMENT ZONE/CRITICAL STREAKLINE CONCEPTUAL MODEL

In order to change juvenile salmon routing through the Delta while maintaining bulk flow conveyance, an understanding of how water is apportioned at river junctions is required. This is combined with an understanding of juvenile salmon spatial distributions to develop fish guidance structures that can change entrainment rates independent of the hydrodynamics.

This section describes the theoretical foundation for the entrainment zone and critical streakline conceptual model. These concepts provide: 1) a way of representing the complexity of tidally forced hydrodynamics that occur in junctions in the Delta; 2) a framework for understanding fish movements in tidal junctions; and 3) a framework for understanding the effects of barriers on juvenile salmon as they transit junctions.

The model is based on the idea that water entering a junction can be divided into two hydraulic entrainment zones: a side channel and main channel (**Figure 3.3-3**). The extent of each hydraulic entrainment zone is determined by the location of the critical streakline, which is the spatial divide between water that enters the side channel or remains in the main channel**.**

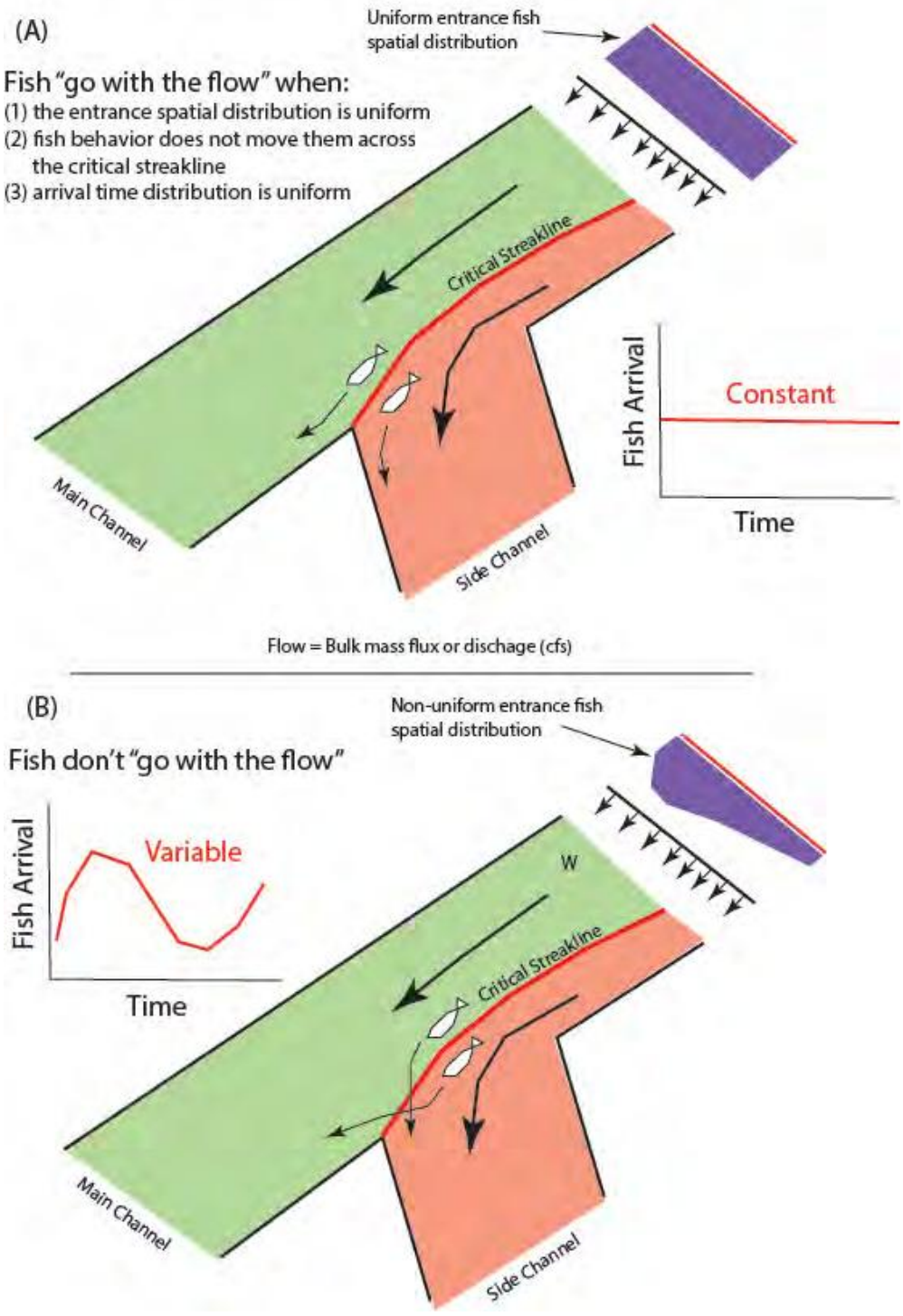

Note: Red regions denote the entrainment zone for the side channel, whereas the green regions show the region where fish continue along the main channel. The red line between these regions is the critical streakline. The top panel shows the required conditions for fish to "go with the flow"—in this case, the bulk as measured discharge in each channel. These conditions include the uniform entrance, fish spatial distribution that is shown and behaviors that do not result in fish crossing the critical streakline. The bottom panel shows those conditions that create conditions where fish are not distributed in proportion to the flows in each channel. These conditions include a non-uniform entrance fish distribution and behaviors that cause fish to transit the critical streakline.

Figure 3.3-3 Conceptual Diagram of Entrainment in a Junction

The position of the critical streakline is a physical metric (e.g., a basic fluid mechanic property). Entrainment rates can be predicted by understanding how the combination of critical streakline position and distribution of fish is affected by environmental variables such as tidal forces. The upstream extent of the fish entrainment zone is determined by the balance between the species' sustained swimming performance and the water velocities within the hydraulic entrainment zone. Thus, species behavior enters into entrainment rate calculations when the streakline position is combined with the fish spatial distribution when influenced by variables such as tidal current phase, river flows, day/night period, and turbidity.

Behavior is expressed in the fish spatial distributions in three ways:

1. A fish species swimming performance and rheotaxis behavior will determine the extent of overlap between a junction's hydraulic entrainment zone and that fish species' entrainment zone;

2. A fish species' outmigration behavior combined with upstream hydrodynamics will determine the spatial distribution of fish at the upstream margins of the species' entrainment zone; and

3. A fish species' outmigration behavior combined with a variety of environmental signals will determine the arrival time distribution of any group of fish transiting the junction.

The findings of this model consist of:

1. There is a single streakline that marks the dividing line between water that enter one channel over the other; and

2. The streakline also marks the dividing line between regions where fish enter one channel over the other.

Do Fish Go with the Flow?

The critical streakline concept is identical to the discharge ratio for *water apportionment* in riverine junctions, however, the critical streakline accounts for non-uniform velocity distributions and geometry and provides a better geo-referenced estimate of the separate hydraulic entrainment zones (**Figure 3.3-4**). In order for the discharge ratio to accurately predict fish apportionment in junctions, biologic entrainment must be identical to hydraulic entrainment in the junction. The condition under which fish enter river channels in direct proportion to flow is when their cross-sectional distribution is uniform and constant in time (**Figure 3.3-3**). Fish entrainment rates that follow the proportion of flow entering each channel in a junction (e.g., "go with the flow") under conditions of non-uniform spatial and arrival time distributions violates the basic math behind fluxes and entrainment rates (**Appendix A**).

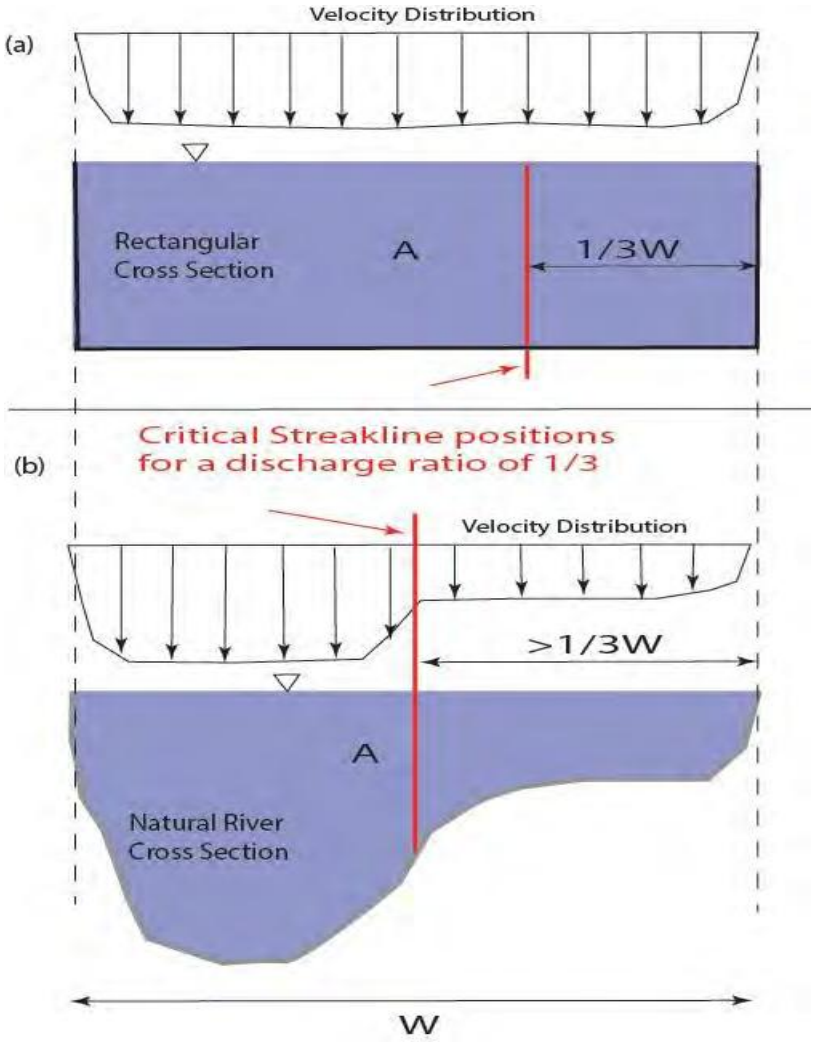

Note: Two example river cross-sections: (a) a rectangular cross-section and (b) a natural river channel. A rectangular, or trapezoidal channel is often a reasonable approximation of the channels in the Delta because the channels in the Delta are highly engineered, essentially canals. W is the cross-sectional width, A the cross-sectional area of the river, which are identical, the salient difference is the bottom topography. In (A) one can predict the critical streakline based on the discharge ratio: 1/3 of the channel width. However, in (B) with variable bathymetry both the cross-sectional area and velocity vary across the section, so a discharge ratio of 1/3 will place the streakline position greater than 1/3W across the channel. The location of the critical streakline can be found by integrating velocity vectors over the channel cross-section until the accumulated discharge just equals the discharge entering the side channel (**Appendix A**).

Figure 3.3-4 Comparison of Streakline Position for Different Cross-sectional Geometries for an Identical Discharge Ratio of 1/3

Migrating and rearing juvenile salmon are seldom uniformly distributed within a river channel (Horn and Blake 2004; Perry et al. 2014), leading to entrainment rates that deviate from the proportion of flow entering each channel (Perry et al. 2015). The fish arrival time distribution becomes particularly important when the proportion of the net (or tidally averaged) flow is correlated with or used to predict entrainment rates (**Appendix A**). However, entrainment rates can be predicted by understanding how the combination of critical streakline position and cross-sectional position of fish vary as a function of environmental variables (such as tidal forcing, turbidity, day/night, etc.) no matter the type of behavior fish are exhibiting (Section 3.5), because the point at which the streakline bisects the fish's spatial distribution at the upstream extent of the fish's entrainment zone determines the entrainment probability.

In summary, the critical streakline conceptual model illustrates why we should not expect juvenile salmon to distribute among channels in junctions in direct proportion to discharge. Nevertheless, when averaged over a tidal time period the fish spatial distributions may be approximately uniform, in which case fish entrainment rates may follow the tidal timescale discharge ratio. Additionally, there may be junctions where the fish spatial distributions entering the junction are consistent over a broad range of hydrodynamic conditions. In these cases, predictive relations to apportion fish based on the distribution of the flows in the junction may become available. In fact, developing relationships between hydrodynamic conditions and fish spatial distributions should be a primary goal because it would simplify the analysis and allow for simple predictive fish passage models based on flow splits (Cavallo et al. 2013; Cavallo et al. 2015).

Collapsing Flow Field Complexity

The velocity distributions in riverine junctions within tidally-forced regions of the Delta are complex in both space and time. Ocean tides propagating into the Delta influence water levels, discharges, and velocity structures well into the upland fringes of the Delta (**Figure 3.3-5**). The tidal currents reverse in all river junctions during low river discharges; although flow reversals rarely occur in Georgiana Slough and the DCC, making them an anomaly.

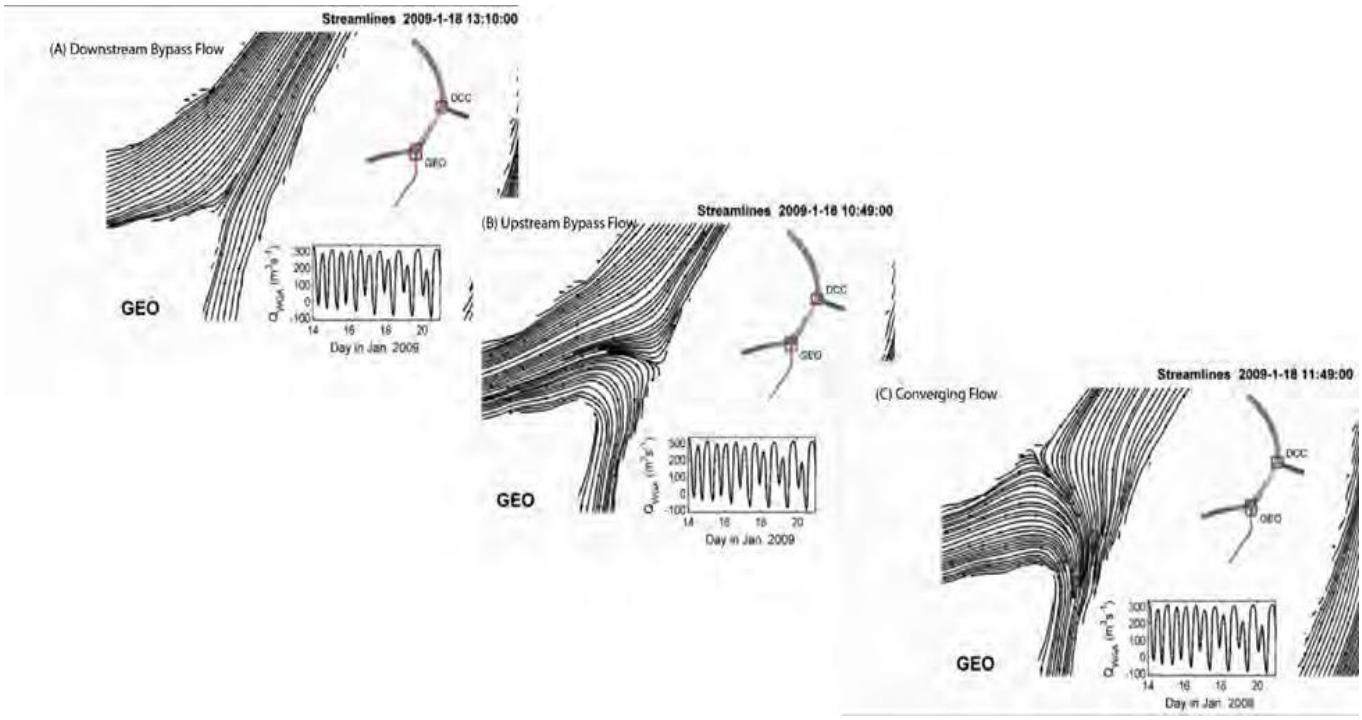

Note: From a 3D model simulation 50 minutes apart: (A) downstream bypass flow, (B) upstream bypass flow, and (C) converging flow.
Source: Cintia Casanas, University of Granada, Granada, (post-doctoral research fellow, USGS)

Figure 3.3-5 Sequence of Surface Velocity Streamlines of Georgiana Slough, 2009, and Movement of the Critical Streakline during a "Slack Water" Period.

The critical streakline concept is therefore a method of simplifying of the tidally forced flow fields within junctions (**Figure 3.3-6**) to their general features. For example, instead of having to compute the entire velocity field within the entire junction, only the critical streakline can be used to predict the location where fish will split between channels. The critical streakline position can be estimated based on flow station data corrected for local bathymetric variations.

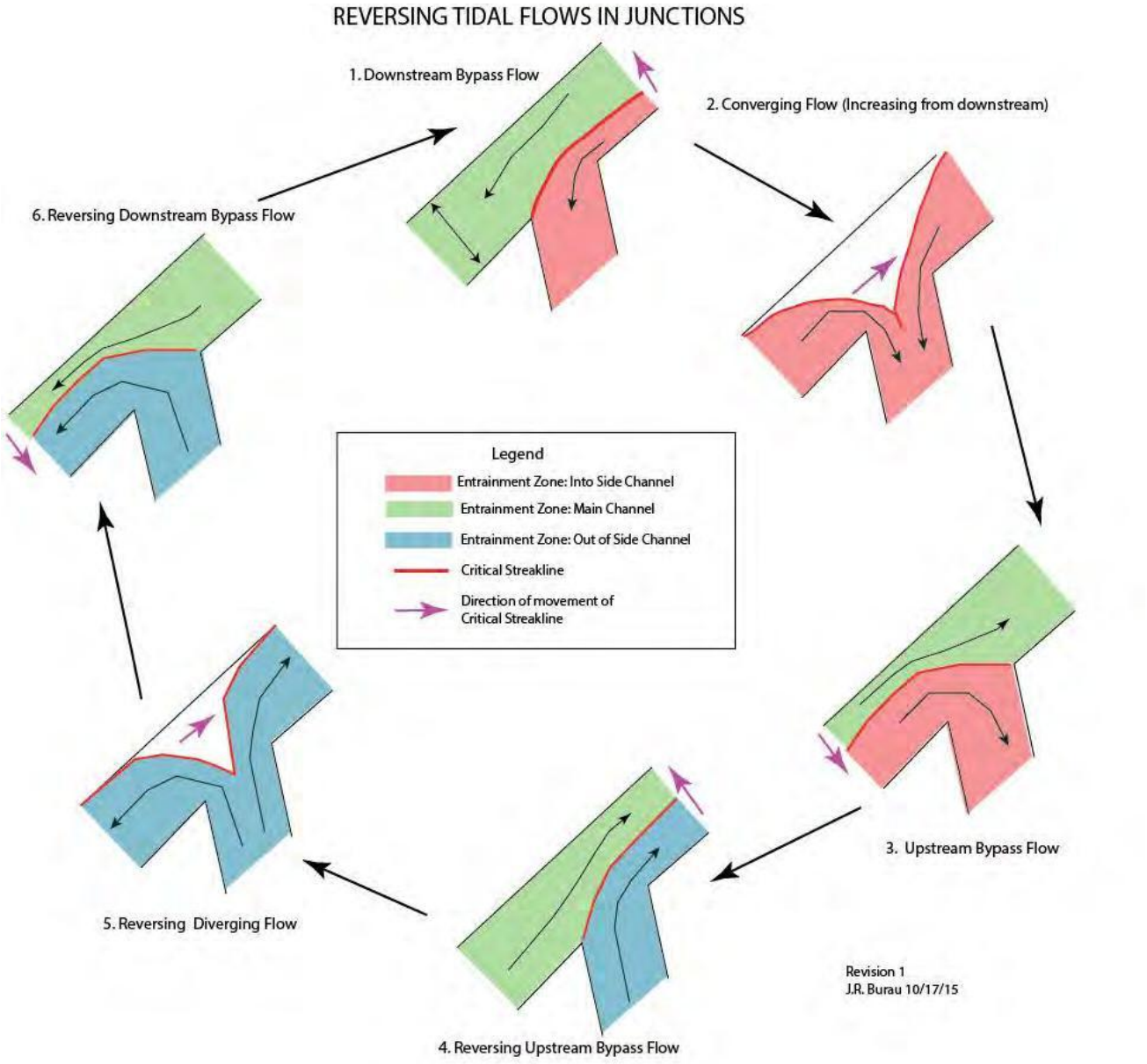

Note: Almost all channel junctions in the Delta exhibit this sequence of changing flow patterns during periods of low river inflow. The exceptions are junctions at the DCC and Georgiana Slough: in these junctions, reversing flows rarely occur and when they do it is weak and short lived. Finally, this sequence, including the direction of movement of the streakline can be reversed depending on the phase relation between the main and side channels. The white (unshaded) regions represent "slack water" or negligible velocity regions.

Figure 3.3-6 Critical Streakline Dynamics at a Typical River Junction in the Delta as the Tide Changes from Flood to Ebb Twice a Day Vertical Variation in the Critical Streakline Position

The critical streakline propagates vertically through the water column to the bed. In the north Delta the river water column with respect to salinity and in temperature is typically well mixed (i.e., vertical stratification is virtually non-existent); the hydrodynamics are purely barotropic. The Sacramento River/Georgiana Slough junction is well upstream of the salinity intrusion from the San Francisco Bay, and the river currents are too energetic for temperature stratification to occur. Thus, no vertical variation in the streakline position based on shear and buoyancy interactions is expected.

However, the hydrodynamics of the critical streakline can be more complicated than the simple surface expression described previously because there is an exchange of along channel momentum into cross-channel momentum at the critical streakline. This momentum exchange can create two secondary circulation cells when there is a sharp bend in the critical streakline. These twin cells create a surface flow toward the critical streakline and down-welling at the critical streakline (Lane et al. 2000; Lane and Ferguson 2005). This circulation pattern was modeled by Bever and MacWilliams (2014) downstream of the DCC as flow reversed at the DCC and was positive on the Sacramento River.

The extent to which juvenile salmon outmigrating at the surface are physically influenced by the twin secondary circulation cells at the streakline interface depends on the strength of the twin secondary circulation cells relative to the magnitude of the downstream advection, because advection controls how long fish are exposed to the twin secondary circulation cells.

Surface velocities are biased toward the critical streakline in junctions from both sides of the critical streakline, which would expose salmon in this area to localized down-welling and large scale horizontal turbulence that might move them across the critical streakline. While exchange across the critical streakline strictly due to horizontal turbulence should average out over time, these processes might make it difficult to predict the fate of an individual fish near the critical streakline. At distances greater than the channel depth from the critical streakline (approximate scale of the largest surface "boils"), temporal variability in entrainment of fish associated with large-scale turbulence near the critical streakline is reduced.

Understanding Barrier Efficacy

The goal of a barrier like the BAFF or FFGS is to "move" fish away from a channel that has the lower survival rate into channels with higher survival. The critical streakline conceptual model tells us two things:

1. Except for horizontal turbulence created stochasticity about the streakline position, physical processes do not move fish across the streakline; and

2. Behaviors that do not ultimately move fish across critical streakline will not change entrainment.

Thus, the critical streakline conceptual model clearly identifies the mechanistic goal of a barrier: Move as many fish across the critical streakline as possible so they remain in the higher survival entrainment zone (**Figure 3.3-7**).

Thus, the assumption that fish follow streakline or any other behavior is not required for the critical streakline conceptual model to be useful. The critical streakline quantifies where and how far fish need to be relocated, individually or on average, to avoid entrainment. Additionally, the critical streakline identifies behaviors that have no impact on entrainment rates; fish responses to a barrier that move them within entrainment zones have no impact on changing entrainment rates, and fish responses that temporarily alter their location relative to the critical streakline will not impact entrainment rates if they do not enter a different entrainment zone before leaving the junction.

For example, fish that are "moved" away from the lower survival channel by a barrier but stay within the green region or red region of the river (**Figure 3.3-7**) have no impact on entrainment rates.

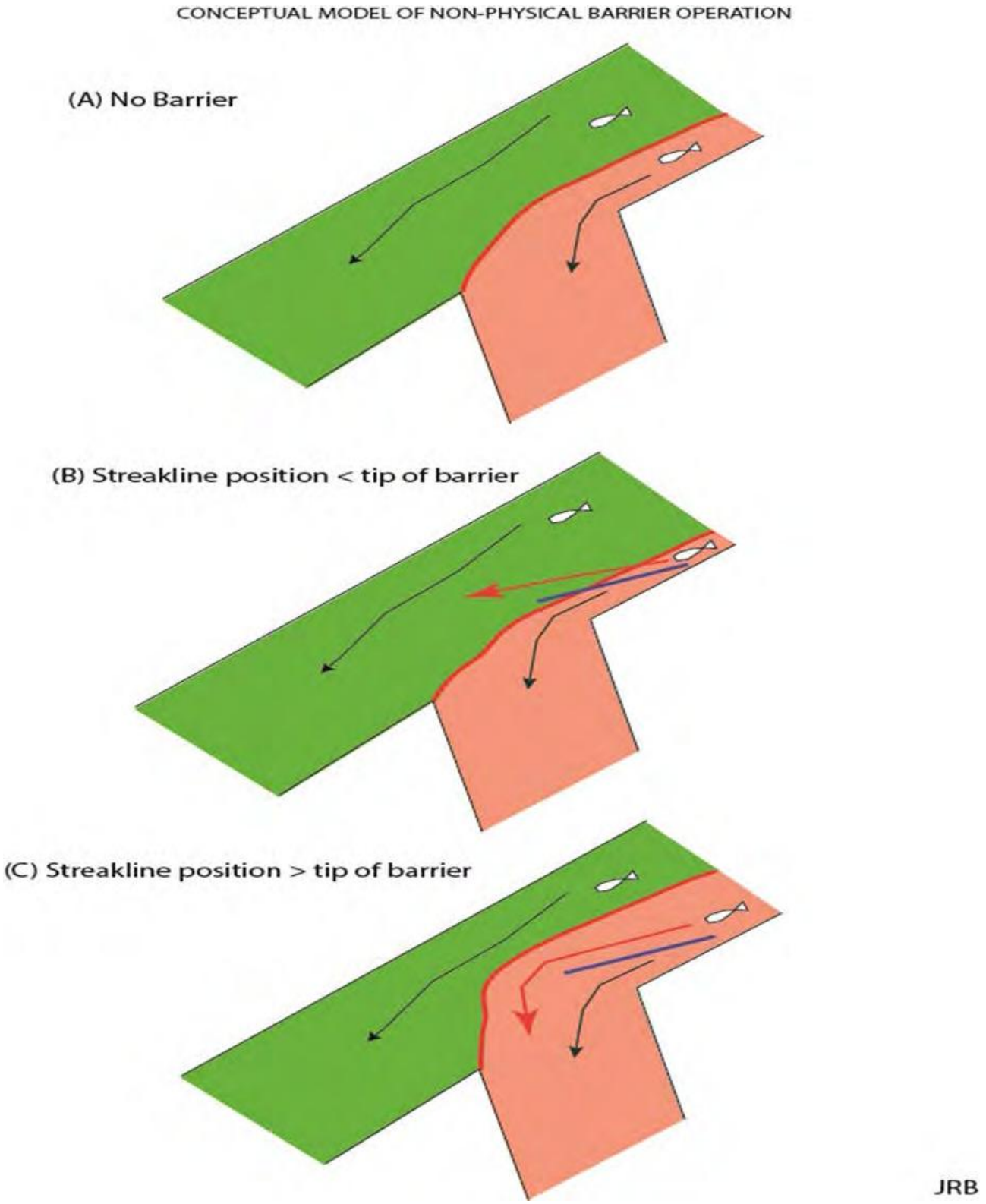

Note: Panel A shows where juvenile salmon that reside in the main channel (colored green) and side channel (colored red) entrainment zone are expected to stay in those zones, except during periods near slack water and flood tides. Panel B shows a barrier whose downstream tip is farther out in the channel than the critical streakline, the (red) boundary between entrainment zones. Barriers are expected to move fish across the critical streakline and effectively alter entrainment rates if the barriers downstream tip is farther out in the river than the critical streakline, as is shown in Panel B. Panel C shows the condition where the critical streakline is farther out in the channel than the downstream tip of the barrier, a condition under which a barrier is not expected to change entrainment rates.

Figure 3.3-7 Conceptual Model of Barrier Operation

Accurately computing the critical streakline and fish positions is important because the variability in these distributions control the entrainment rate in junctions and provides a mechanistic explanation on how and why entrainment rates are changed by barriers. For example, it is clear that the decrease in entrainment during the 2011 and 2012 BAFF experiments (DWR 2012, 2015b) involved a behavioral response that shifted the leading edge of the fish distribution near the right bank a relatively short distance of 5-10 m (16-33 ft). The shift in the portion of the distribution within the Sacramento River entrainment zone contributed nothing to the reduction in the entrainment rate, only the shift in the portion of the fish distribution within the Georgiana Slough entrainment zone across the streakline into the Sacramento River entrainment zone accounted for the observed reduction in entrainment. Thus, a combination of the knowledge of the location of the fish distribution relative to the critical streakline allows us to understand the mechanics of entrainment.

In the following discussion, a variety of ways of computing the critical streakline are discussed. Additional discussion addresses verifying the accuracy of the estimates by comparisons to drifter data, because minimal locational variation can make substantial difference in results, as described previously.

In Section 3.5 the observed spatial distribution of juvenile salmon is combined with the estimated critical streakline location to understand how barrier operation effected the distribution of juvenile Chinook salmon relative to the critical streakline with the ultimate objective of understanding mechanistically how these effects alter entrainment into Georgiana Slough.

3.3.2 METHODS

The critical streakline can be estimated using three different methods described in this section. These methods are compared to determine the most accurate approach for predicting entrainment of water into Georgiana Slough, because the position of the critical streakline relative to the fish spatial distribution and barrier placement are important design considerations.

The SL-ADCP data were used to estimate the location of the critical streakline and to generate a time series of 2D velocity fields at 15-minute intervals for the duration of the study. Then, entrainment into Georgiana Slough at multiple timescales and river discharges is discussed, and furthermore, the influence of the FFGS operational the SL-ADCP measurements immediately downstream of the FFGS are examined.

Previous studies have shown that juvenile salmon outmigrants typically inhabit the upper portion of the water column while emigrating from the Delta (Horn and Blake 2004). The study's design and hydrodynamic analysis is focused on documenting and understanding temporal patterns in surface currents in Georgiana Slough. The motivation for using the streakline for some parts of the analysis instead of the ratio of the discharges is because the streakline explicitly incorporates the combination of longitudinal changes in the cross-section area and the concomitant change in lateral variability in the surface currents.

Although measurements of the mean surface currents were obtained quite carefully for this study, simplified bulk metrics were also sought: the discharge ratio and critical streakline (as outlined in **Figure 3.3-4**). These metrics are intended to be used outside the context of detailed experiments which are often expensive and thus require a level of effort that cannot be sustained for extended periods. For that reason they may be generally more useful for gaining a mechanistic understanding of entrainment rates because they make use of ongoing (and less expensive) monitoring program data.

These simplified metrics could be used to quantify and predict entrainment of juvenile salmon under a wide range of conditions, and could be used in simplified models such the Delta Simulation Model II (DSM2) as applied by Cavallo et al. (2015). To summarize, the discharge ratio is the metric of choice for correlative analysis and for comparisons between junctions when detailed deployments of SL-ADCP data are not available as part of a large-scale experiment because in the prismatic channels typical of the Delta temporal variability in the streakline can be approximated by the discharge ratio in some cases – the absolute value of the streakline position is another matter.

HYDROLOGIC FORCING

The Sacramento River inflows to the Delta were at near-historic lows during the study period, based on peak flow frequency at Sacramento at Freeport. Historically, the yearly peak flow observed at Freeport (from 1949-2014 can exceed 60,000 cf. (**Figure 3.3-8a**). However, the range of river discharges during this study was not abnormal (**Figure 3.3-8b**). During the wet season (November-May) daily flow at Freeport can be frequently below 30,000 cfs (~ 65 % of the time). When flows at Freeport are below ~20,000 cfs (historically 50% occurrence) then tidal conditions can be dominant at the Georgiana Slough junction. When Freeport discharge is below 15,000 cfs (historically 35% occurrence) reversing flows are observed on a daily basis at the Georgiana Slough junction (**Figure 3.3-8c**).

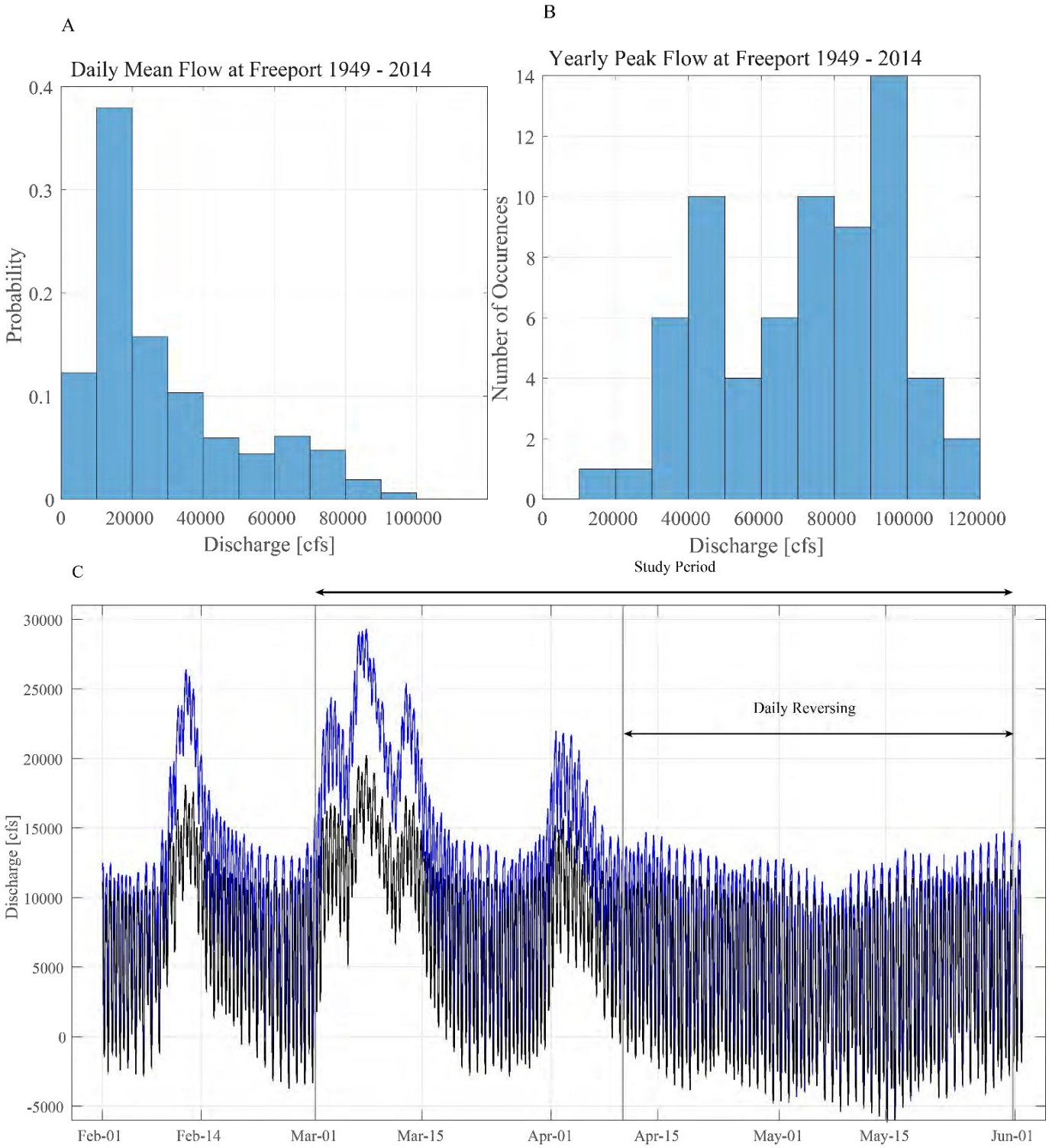

Note: Panel A shows the frequency of peak flow at Freeport. Panel B shows the frequency of mean daily flow at Freeport during the wet season (Nov – May). Panel C shows the hydrograph for the study period where the blue line is flow at Freeport and the black line is flow Walnut Grove at the study area.

Figure 3.3-8 Discharge Measured in the Sacramento River at Freeport during the Study Period

ADCP DATA COLLECTION

Six SL-ADCPs were mounted on floats, attached to stationary steel pilings within the Sacramento River and Georgiana Slough junction (see **Figure 3.3-9**), so that the vertical position of the SL-ADCP would remain stationary relative to the water surface by rising and falling with the tides, and by following increases in stage associated with high Sacramento River inflows that can occur in response to precipitation from wintertime storms. The SL-ADCPs were placed to measure surface currents and were positioned as near to the surface as possible by being pitched them down about 1°, so the acoustic signal "skimmed" just below the water surface, which had a secondary benefit of extending the range of the velocity profile. The SL-ADCPs were deployed between March 1 and May 22, 2014. Five of the SL-ADCPs deployed were Teledyne RDI 1200 kHz Horizontal Workhorse ADCP, and one was a Teledyne RDI 1200 kHz Horizontal ChannelMaster ADCP. The raw velocity data were averaged over 15 minutes.

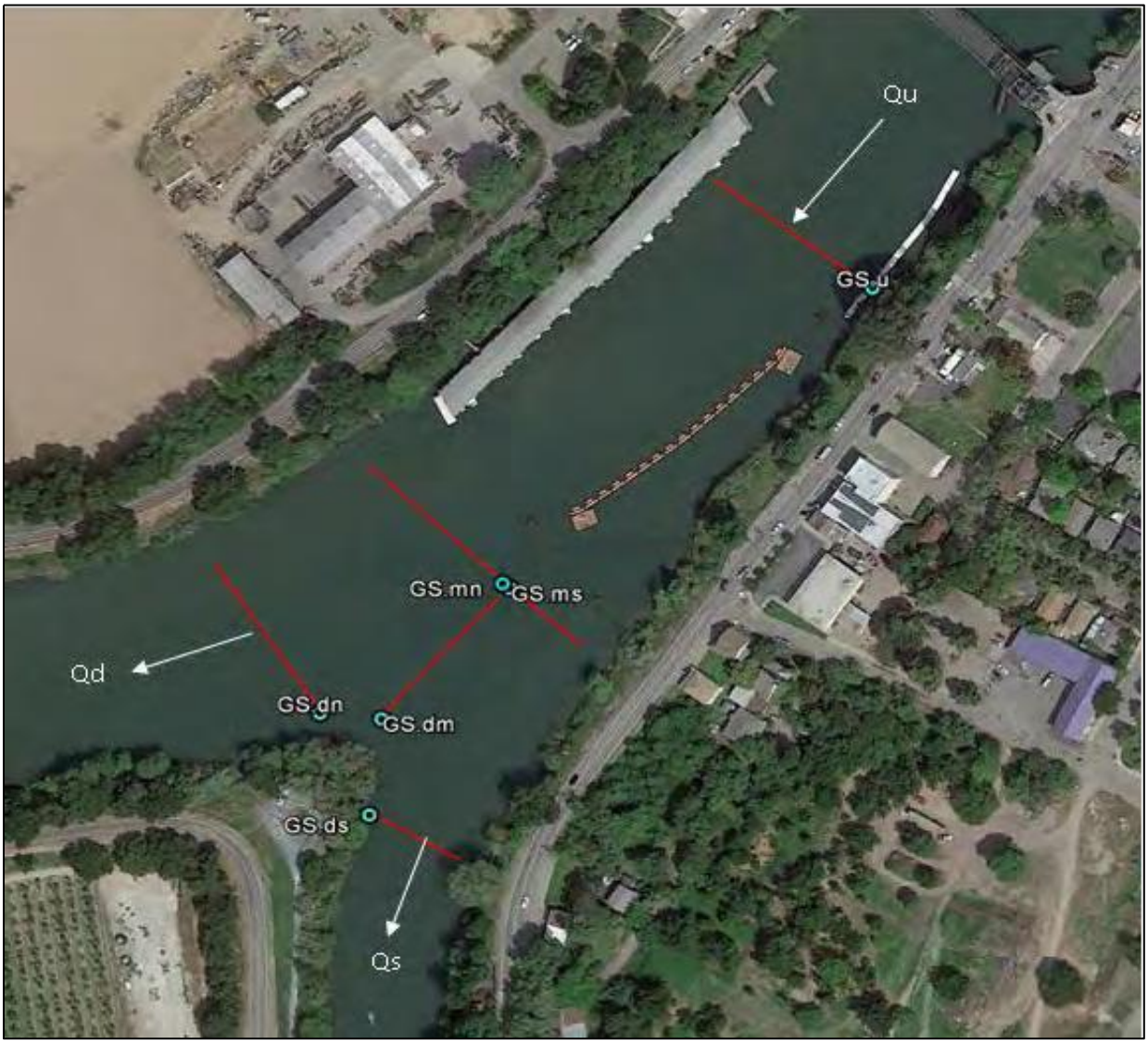

Note: The red lines represent the approximate location, orientation, and extent of the measurement profiles. The critical streakline parameters Qu, Qd, and Qs are shown as well as the positive flow directions with white arrows. The FFGS in the On position is shown (in orange) between the GS.u and GS.mn measurement locations.

Figure 3.3-9 Aerial View of the Six Side-Looking Acoustic Doppler Current Profilers located at the Study Location

Several sampling schemes were tested to reduce acoustic interference with hydrophones deployed as part of the acoustic telemetry array which was deployed in the same region. The final sampling scheme used nine water pings every 1.1 seconds, with a 30-second sampling frequency. This resulted in 270 water pings, averaged over a 15-minute period using a bin size of 1 m (**Table 3.3-1**). Because of the telemetry array in the region, the bin size was reduced and the number of pings per averaging period was increased to reduce the impact of electronic noise from the instrument and turbulence on the standard deviation of the 15-minute average measured velocities. Based on this sampling scheme the theoretical standard deviation of the measurements was 0.34 cm/s (0.01 ft/s).

Table 3.3-1 Summary of SL-ADCP Deployments

Profile Name	GS.u	GS.mn	GS.ms	GS.dn	GS.dm	GS.dm2	GS.ds
Easting	629914	629781	629784	629711	629735	629735	629711
Northing	4233606	4233490	4233488	4233435	4233435	4233435	4233393
Instrument Heading	294	300	115	320	24	204	95
Bin Size (meters)	1	1	1	1	1	0.6	1
Number of Bins	70	75	35	75	75	27	41

SL-ADCP Data Processing

The SL-ADCP data were processed to geo-reference the velocity profiles in the junction, filter out bad data along each profile, extrapolate velocity profiles in the horizontal and vertical, and merge all of the data onto a common time base. Prior to March 14, 2014, the SL-ADCP parameters were adjusted several times, in collaboration with HTI staff, to reduce the amount of acoustic noise generated by the initial higher frequency SL-ADCP sampling strategy. Two SL-ADCPs were not functional for a portion of this period. The upstream SL-ADCP (GS.u) was not functional for over a week (March 3 to March 14, 2014). This SL-ADCP is important for generating the interpolated velocity fields in the region surrounding the FFGS. Because of these complications, the data were not processed prior to March 14. Instead, the interpolated velocity fields were estimated using multi-linear regression from velocity data at nearby gaging stations. The SL-ADCP located downstream on the Sacramento River (GS.dn) was not functional from April 19 to April 21, 2014. The interpolation algorithm could not run during this period because this SL-ADCP was a domain boundary; therefore, interpolated data for this period also was estimated using the same multi-linear regression approach.

Lagrangian GPS Drifters

Drifters outfitted with GPS receivers were deployed as an independent velocity field measure for comparison with the interpolated fields, based on the SL-ADCP data. On three days (March 14, 17, and May 19, 2014), DWR staff released GPS drifters over the course of half-tidal cycles (10 to 12 hours). The GPS drifters have a neutrally buoyant subsurface drogue that extended about 1 m (3.3 ft) below the water surface.

The Tristar drogue type (Niiler et al. 1995) has been shown to accurately measure surface velocity within 1 to 2 cm/s (0.03-0.06 ft/s) during periods of light winds (Ohlmann et al. 2005). A Garmin eTrex® GPS was placed in a small water-tight canister with a stated absolute horizontal accuracy of 15 m (49 ft); however, the relative accuracy between successive measurements (every 7 seconds) is much better, but is unknown. The GPS units were programmed to record data every 7 seconds.

On each day of releases, 12 drifters were released about 100 meters upstream from the FFGS and travelled through the study domain until they passed the Sacramento River and Georgiana Slough junction, constituting a single drifter set. The drifters then were picked up and were released back at the original upstream location. This process was repeated for the entire 10 to 12-hour study period.

The drifter data is summarized in **Table 3.3-2**. The drifter data files for each drifter were compiled into a single file, and the start and end of all tracks were trimmed in accordance with the stop and end times identified in the field notes. The processed drifter tracks then were exported to Google Earth .kml (Keyhole Markup Language) and .csv (Comma-Separated Value) files.

Table 3.3-2 Summary of GPS Drifter Releases

Release Date	Time Range	Barrier State	Number of Sets	Flow Range[1] (cfs)
March 14	0509–1632	Off	19	7.,590 – 15,110–428
March 17	0738–1507	On	15	4,410 – 12,110
May 19	0649–1720	On	17	-3,640 – 11,190

Note: [1] cfs = cubic feet per second. Flow as measured at the Sacramento River upstream of Walnut Grove.

The drifter data were processed to calculate velocity and remove other spurious data points. The drifter velocity *($u(t_i)$)* was calculated using the central difference method $u(t_i) = \frac{d(t_{i+1}) - d(t_{i-1})}{2dt}$, where the *d* is the distance traveled along a path calculated from the x,y position, and *dt* is the time difference between record values (7 seconds).

The drifter velocities then were then compared to the 2D interpolated velocity fields. The interpolated velocity fields at a point represents a time averaged value (15 minutes), whereas the velocity from the drifter is more of an instantaneous value (computed over 14 seconds). Because of this sampling interval disparity, a 10-sample moving average was applied to the computed drifter velocity so that the data represent a more comparable time average, without introducing too much spatial averaging. In addition, velocities within a drifter set were calculated before the moving average as a noise reduction strategy and computed velocities greater than three standard deviations from the mean were removed.

CRITICAL STREAKLINE ESTIMATION

The metric used to characterize the critical streakline is the position of the flow split at a fixed distance upstream of a junction. In this case, the streakline is a spatial metric that quantifies the distribution of water between the Sacramento River and Georgiana Slough.

Three methods were used to estimate the critical streakline that involve various levels of complexity (see DWR 2015b Chapter 3.4 for more detail). Two of these methods required two ADCPs placed upstream and downstream of the junction to estimate discharge using the cross-channel velocity profile.

The first method evaluated was the integral method, which theoretically yields a more accurate estimate because it accounts for bathymetry and velocity variability across the measurement cross-section. However, this approach

requires several ADCP be deployed within the junction, a strategy that is cost prohibitive for long-term monitoring of discharge.

The critical streakline is estimated from a fully discretized discharge profile using the velocity profile method (VPM). At the upstream (Q_u) and the downstream (Q_d) cross-sections, the critical streakline is estimated using both the discharge ratio and integral method (DWR 2015b, Chapter 3.4). Both of these methods are validated using drifter tracks over a range of river discharges.

The second method, the discharge ratio method, uses discharge calculated from the index velocity method (IVM) to determine the distance along a cross-section, where the flow split is based on Q_d/Q_u, and has the advantage of using data from existing long-term flow stations. In the end, both methods may be sufficiently accurate if used as a covariate in the analysis of acoustic telemetry data, particularly if the cross-section being analyzed is relatively prismatic (i.e., is approximately trapezoidal).

The third method extracts streaklines generated from the interpolated velocity field, and then used in the spatial analysis of fish tracks (see Sections 3.4 and 3.5). These streaklines required a suite of ADCPs to generate an interpolated velocity field which is resource intensive. Because of the expense such data on detailed velocity fields usually are limited to relatively short-duration experiments.

The purpose of comparing various methods for calculating the streakline was to determine the least expensive and most robust method for generating data of sufficient accuracy to be used in correlations with acoustic telemetry data and for barrier design. The discharge ratio method was the least expensive because it relied on ongoing data collection, the integral method was the next least expensive because it required two ADCP's deployed within the junction, and streaklines calculated from an interpolated velocity field were the most expensive because it required data from numerous ADCPs, in this case six.

TWO-DIMENSIONAL VELOCITY INTERPOLATION

The ADCP data interpolation uses a Lagrangian particle tracking (LPT) and inverse path-length weighted (IPLW) algorithms (see DWR 2015b, Chapter 3.4 for more details). With the LPT algorithm, an initial velocity field is generated from an inverse distance weighted function. Particles are then released and tracked upstream and downstream at every grid node. The number of particle paths that cross into each channel is then accounted for. The velocity field is then updated, using an IPLW interpolation along the generated particle paths. A mass conservation routine also is built in. The number of particles that enter each junction branch is tracked, and if the ratio of particles matches the flow ratio, then the LPT algorithm has converged; if not, then the updated velocity field is used to generate a new set of particle paths, and so on.

For this effort, the following parameters were chosen:

- The grid spacing was set to 10 meters (33 ft). This was chosen because a rich 2D velocity field is achieved without a large computational expense—increasing the grid size increases the computation time by the square of the increase in the resolution;
- The weighting parameter for the IPLW function was set to 2 for downstream river discharges and 4 for reverse river discharges. These values were chosen because the pathline ratios closely matched the flow ratios on a subset of data; and

- The algorithm was considered converged if the difference between the particle pathline ratio and the discharge ratio was less than 10 percent. The maximum number of iterations before a solution converged at each timestamp was set to 5 because in previous interpolations, the velocity field was found to show minimal change after this many iterations.

ESTIMATING DATA GAPS

Two data gaps occurred between March 1 and 14, and between April 19 and 21, 2014. The mean water velocity, measured at Georgiana Slough gage station (GEO.vel) and at the Sacramento River downstream of the Georgiana Slough gage station (WGB.vel), were used in the regression model to predict water velocity at each of the 320 grid nodes. Linear models with one variable were explored, but the following multi-linear model yielded more accurate results:

$$y = \beta_0 + \beta_1 * GEO.vel + \beta_2 * WGB.vel + \beta_3 * GEO.vel * WGB.vel$$

where y is the prediction value and β_i are the regression coefficients.

The mean R^2 for all grid nodes were 0.944 (SD = 0.07) and 0.950 (SD = 0.04) for the U and V components, respectively. The lowest R^2 values for U occurred near the point where the Sacramento River flows into Georgiana Slough (**Figure 3.3-10**). In this area, the V component of velocity was dominant, and thus errors in the U component prediction were likely to have minimal effect on the resultant velocity vector. The lowest R^2 values for the V component were somewhat randomly distributed, but a concentration existed near the right bank, about mid-domain (**Figure 3.3-10**). These R^2 were still 0.8 and greater.

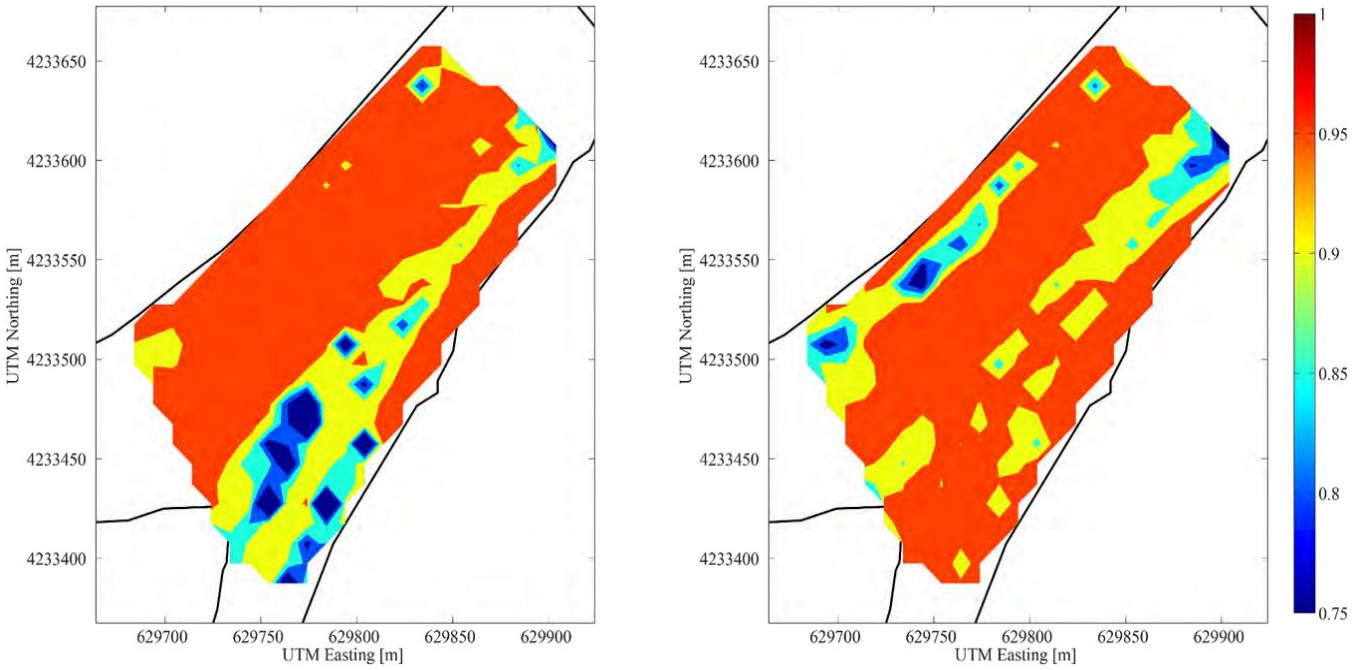

Note: For U (east-west) (to the left) and V (north-south) (to the right) components of velocity.

Figure 3.3-10 Color Contour Plots of the R^2 Values for the Multi-Linear Regression

Overall, the regression model appeared to do a good job of estimating U and V components of velocity throughout most of the domain.

3.3.3 RESULTS

The results of critical streakline estimates, 2D velocity interpolation, and a comparison of the critical streakline with velocities measured from the fixed ADCP's (Eulerian) measurements and drifter (Lagrangian) measurements, are discussed in this section. For the Georgiana Slough experiment, the critical streakline position is the distance from the left bank at the upstream ADCP location (GS.u, shown as a solid black line in **Figure 3.3-11**). A line from the tip of the FFGS that extended upstream was approximately 35 meters (115 ft) from the left bank A line extending downstream was located approximately at the Sacramento River and Georgiana Slough junction.

As shown in **Figure 3.3-11**, the distance from the left bank can vary substantially, depending on where in the junction it is calculated. Therefore, the channel location where it is calculated must be specified. The location of the streakline cross-section changes the streakline position by a constant amount; therefore, as long as the cross-section remains constant, the exact location would have no impact on correlative analysis of acoustic telemetry data. This is because the cross-section location does not change the time history of the streakline, only its absolute value. However, the location of the streakline cross-section has to be taken into account to georeference the streakline position (i.e., relative to fish positions, barriers).

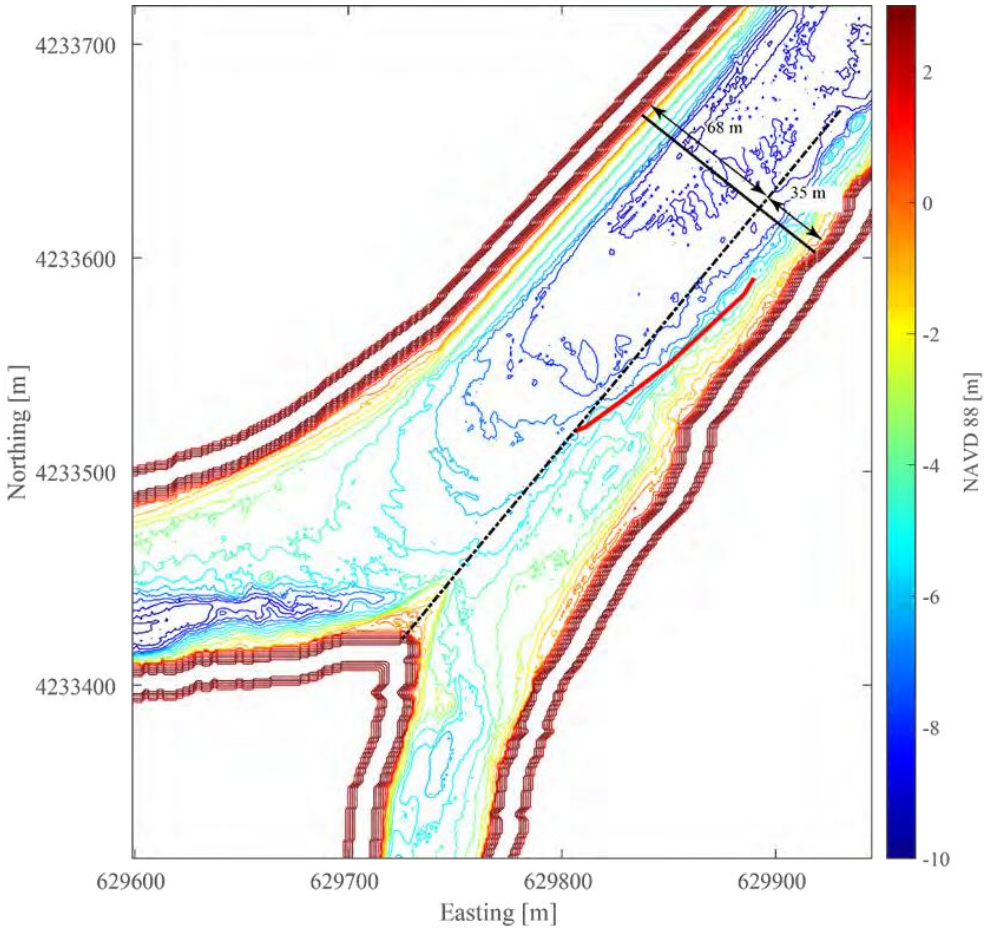

Note: The solid black line represents the upstream ADCP cross-section. The red line represents the placement with the FFGS On. The dashed black line represents the critical streakline position from a line extended upstream and downstream from the tip of the FFGS The downstream tip of the FFGS is located at 35 m (115 ft), as measured from the left bank, looking downstream. The range of 0-35 m is therefore the range we expect the FFGS to move fish and be effective.

Figure 3.3-11 Plan View of Critical Streakline Representation

CRITICAL STREAKLINE ESTIMATION USING DISCHARGE

Discharge estimated from the IVM is used to estimate the critical streakline with the discharge ratio method, and discharge estimated from the VPM is used in the integral method. The IVM is more widely accepted method to estimate a one-dimensional discharge (Simpson 2000) but a cross-sectional discretized two dimensional discharge is needed.

The first validation step for calculating the critical streakline is to compare the accuracy of the IVM and VPM methods with a least squares regression and verify the accuracy of the VPM (see **Figure 3.3-12**, **Figure 3.3-13**, and **Figure 3.3-14**). The regression plot confirms two things:

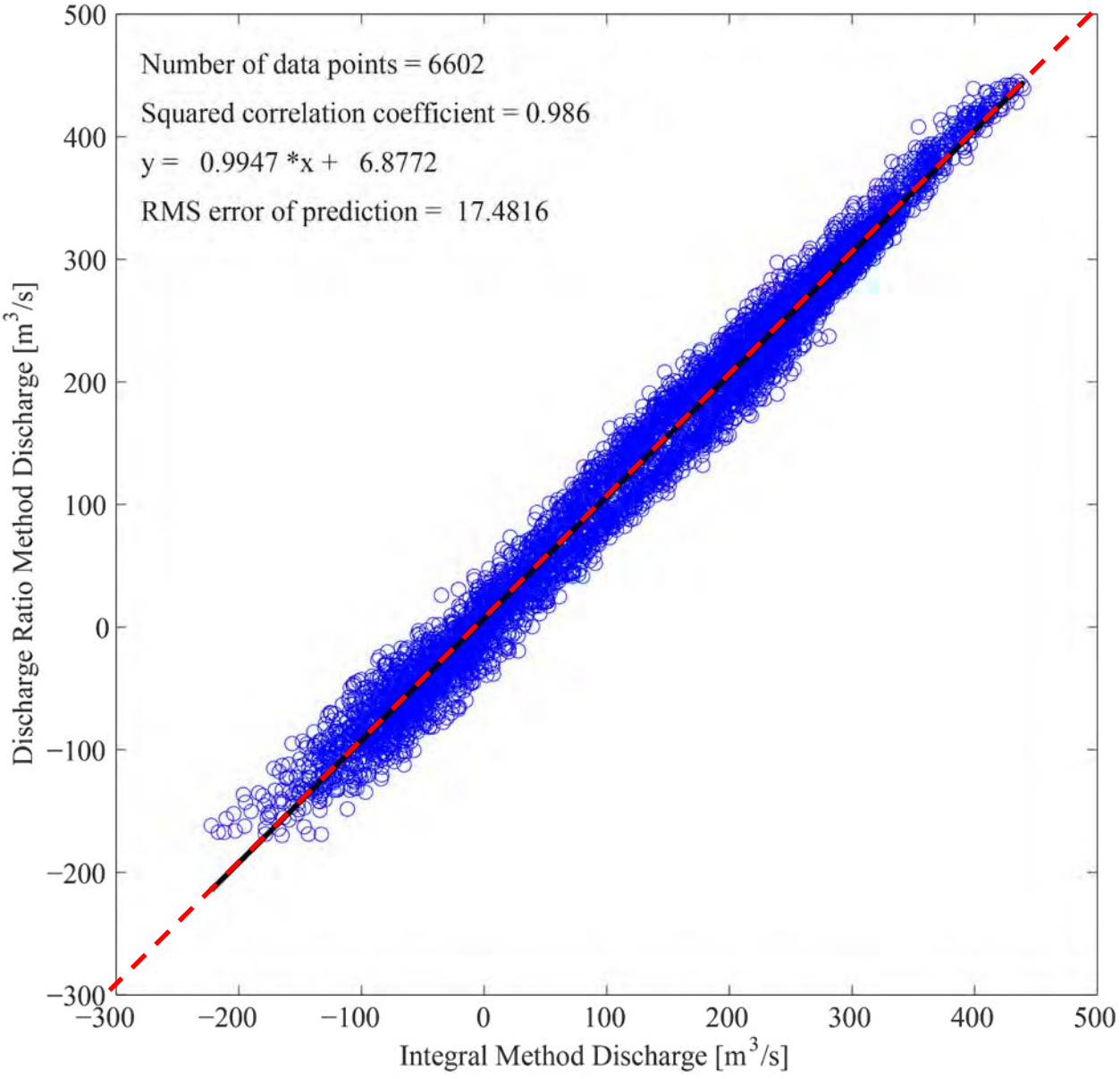

Note: The red dashed line represents the 1:1 ratio.

Figure 3.3-12 Linear Regression between Discharge, Calculated with Integral Method, and Discharge Ratio Method at Upstream Location Georgiana Slough Upstream

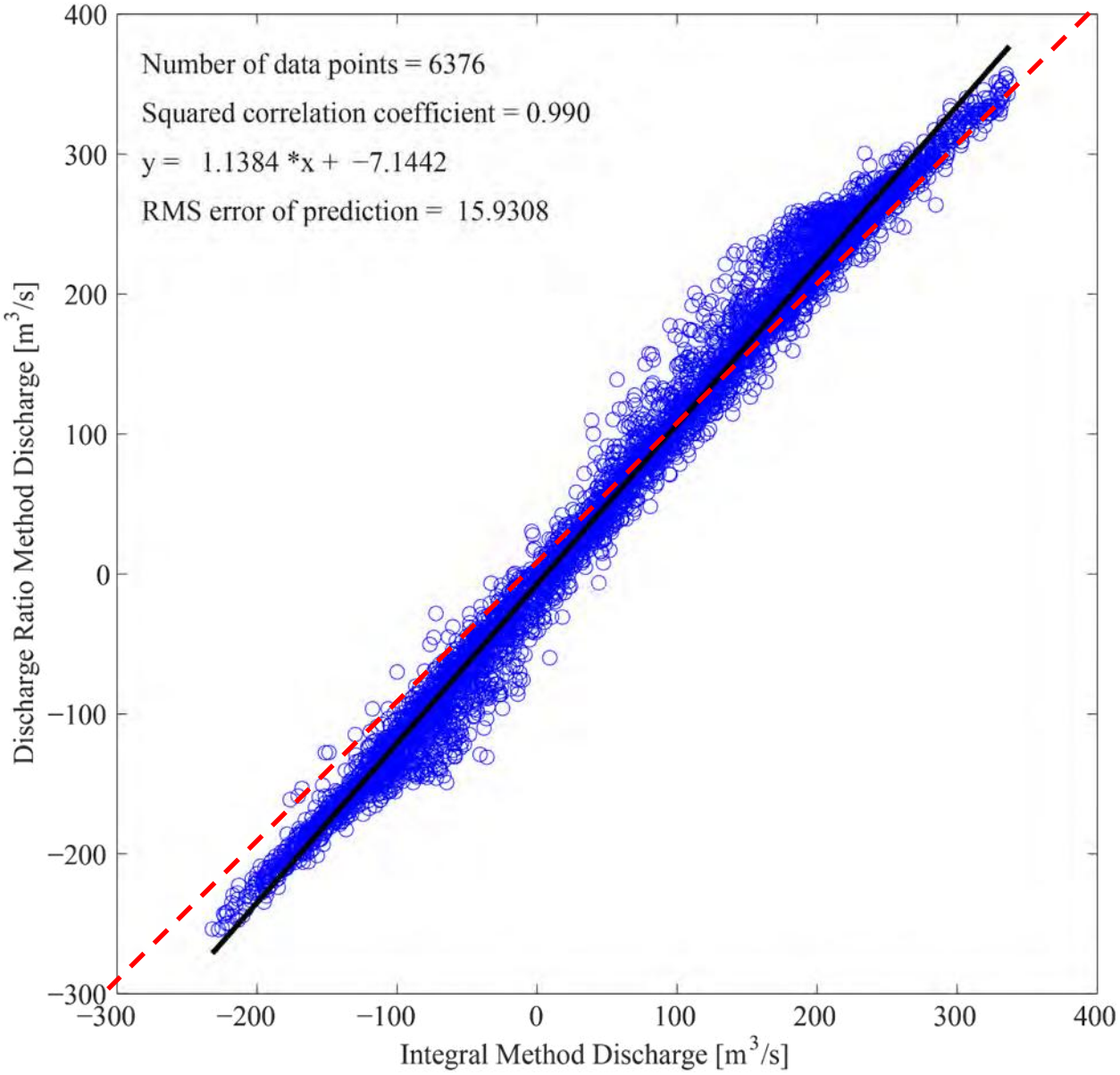

Note: The red dashed line represents the 1:1 ratio.

Figure 3.3-13 Linear Regression between Discharge, Calculated with Integral Method, and Discharge Ratio Method at Downstream Location Georgiana Slough Downstream

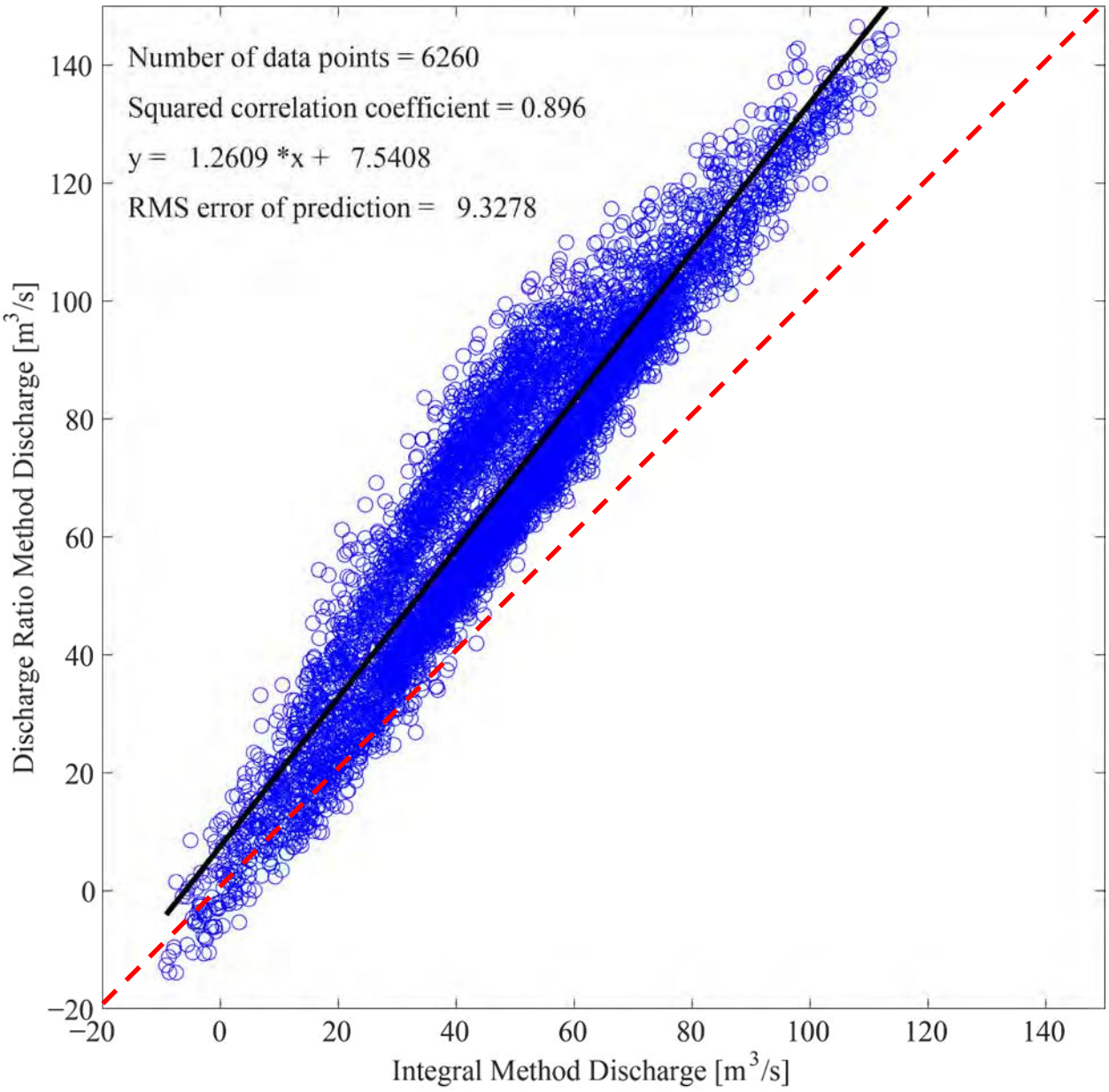

Note: The red dashed line represents the 1:1 ratio.

Figure 3.3-14 Linear Regression between Discharges, Calculated with Integral Method, and Discharge Ratio Method at Side Channel Location Georgiana Slough

1. How precisely the cross-sectionally averaged discharge using the VPM can predict the cross-sectionally averaged discharge using the IVM; and

2. How accurate the VPM method is relative to the IVM method using a 1:1 fit.

This IVM was not used because: 1) it was logistically difficult to collect cross-sectional velocity upstream or downstream of the ADCP measurement locations that would have been a representative of the velocity profile because of docks and marinas; and 2) acoustic noise generated by moving boats over a tidal cycle would have been potentially detrimental to fish tracking.

At sites Q_u and Q_d, the statistical correlation is excellent, $R^2 = 0.986$ and 0.990 respectively, with little scatter in the data and a nearly 1:1 correlation between the two discharge estimations. At site Q_s, the statistical correlation is good, $R^2 = 0.896$, but more scatter exists, and the VPM under predicts discharge at higher discharge values.

As a secondary measure of quantifying the accuracy of discharge estimates using each method, a mass balance at the junction ($Q_u = Q_d + Q_s$) is compared (**Table 3.3-3**). By this metric, the IVM is more accurate than the VPM. The VPM at site Q_s yielded higher estimates than the IVM, which is the primary reason the VPM mass balance is less accurate. Considering that sites Q_u and Q_d yield more accurate results, the ratio of flow between these two sites is used for the critical streakline estimate.

Table 3.3-3 Tidally Averaged Error Statistics for Mass Balance Calculations at the Georgiana Slough Junction

Method	Mean Square Error[1] (cubic meter per second)	Standard Deviation (cubic meter per second)	Mean Difference[1] (percent)	Standard Deviation (percent)
IVM	-2.61	3.40	-1.17	1.41
VPM	14.91	6.24	8.28	3.64

Note:
[1] Positive values indicate $Q_1 > Q_2$ and negative values indicate $Q_1 < Q_{2S}$. To convert cubic meters/ second to cubic feet/second multiply cubic meters/second by 35.3147.

The mean critical streakline calculated from the discharge ratio and integral methods is 36.7 m (120.4 ft) (SD = 28.1 m [92.2 ft]) and 49.3 m (161.7 ft) (SD = 23.6 m [87.3 ft]) at the upstream location, respectively. The discharge ratio method biases the value toward the left bank by an average of about 13 m (43 ft). At the upstream location, the bathymetry is close to prismatic with little asymmetry and a relatively less biased estimate from the discharge ratio method is expected.

The mean critical streakline is 67.4 m (221.1 ft) (SD = 30.6 m [100.4 ft]) and 65.4 m (214.6 ft) (SD = 28.5 m [93.5 ft]) at the downstream location, respectively.

There is a scour hole near the left bank at the downstream location that would bias the flow distribution towards the left bank. The non-linear relationships between the two critical streakline methods at the upstream and downstream locations are very good, with R^2 of 0.993 and 0.995, respectively (**Figure 3.3-15**). These relationships are non-linear because the bathymetry and concomitant velocity variability is not accounted in the discharge ratio method. Thus, if the bathymetry remains relatively stable at the cross-section used in the streakline calculation, the relationship generated could be used to calibrate the relatively inexpensive discharge ratio method.

TWO-DIMENSIONAL VELOCITY INTERPOLATION

The 2D velocity field was estimated separately for positive river discharges (approximately 67 percent of the data set) and negative river discharges. For the purposes of this study, the tidally averaged discharge ratio was defined as positive flow when the flow was greater than zero at the downstream location ($Q_d > 0$).

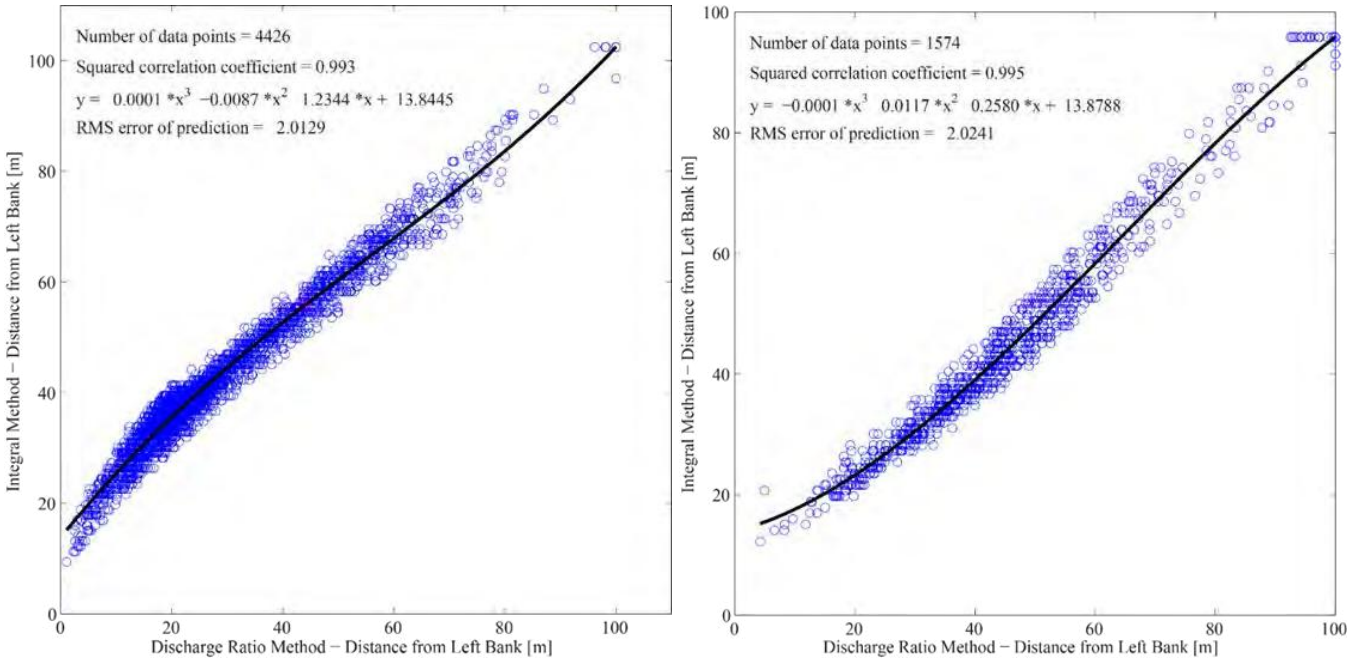

Note: Outliers that are three standard deviations from the residual distribution were removed. The graphic on the left is for positive river discharges only, and the graphic on the right is at GS/dn; for negative river discharges only.

Figure 3.3-15 Non-Linear Regression of the Critical Streakline from the Left Bank Estimated from the Discharge Ratio and Integral Methods

The key metric used to determine the performance of the algorithm was the difference between the flow ratio (Q_r) and particle pathline ratio (P_r). The difference between *Qr* and *Pr* was less than 10 percent for 96 percent of the positive river discharges and 80 percent for the negative river discharges. The histogram plots of these differences are shown in **Figure 3.3-16**. The negative river discharges are more complex because the flow patterns change from primarily entering Georgiana Slough to also bypassing it as the flood tide progresses. Thus, more spatial variability exists in the flow patterns during flood conditions (compare **Figure 3.3-17** and **Figure 3.3-18**, for example).

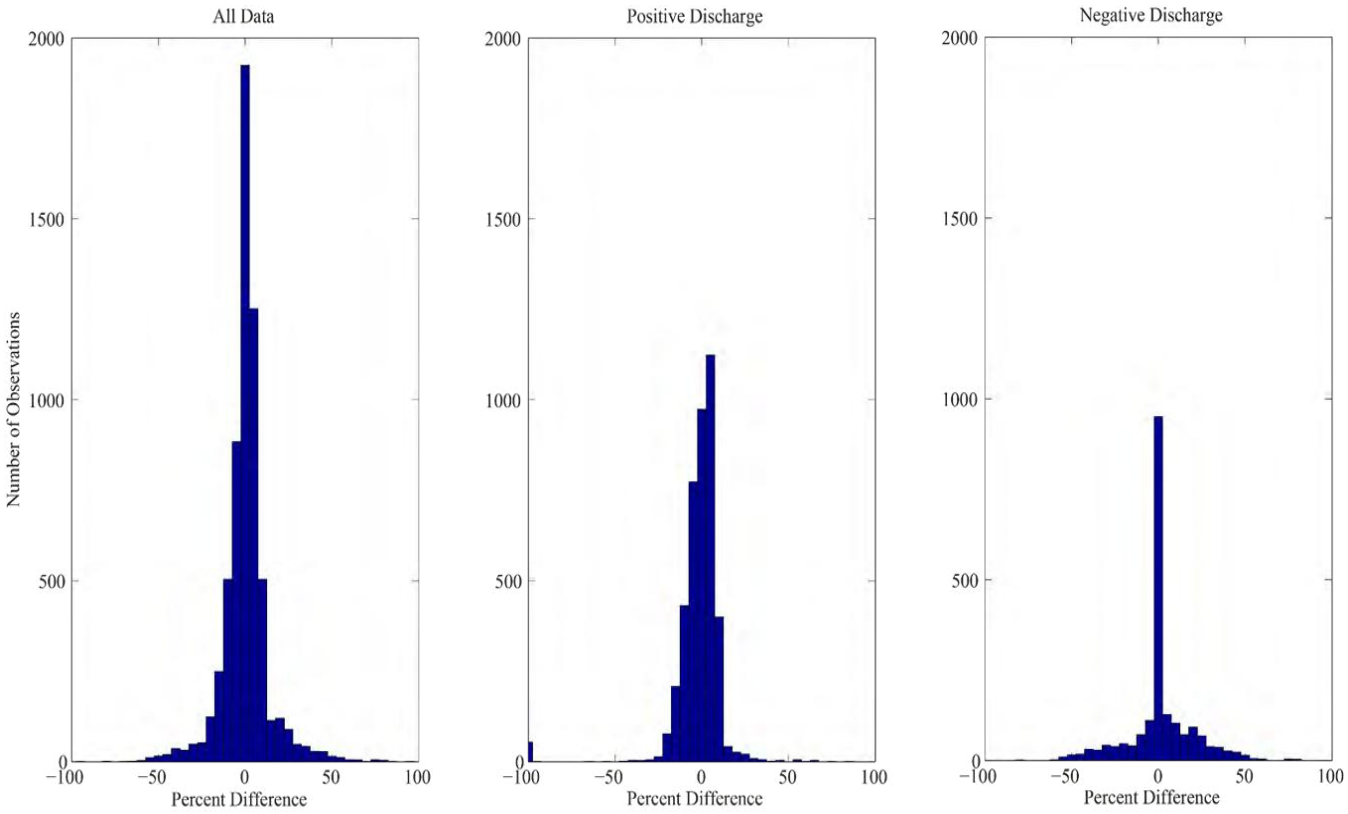

Figure 3.3-16 Histogram Plots of the Difference between the Flow Ratio and Particle Path Line Ratio for the LPT Algorithm after the Solution Converges

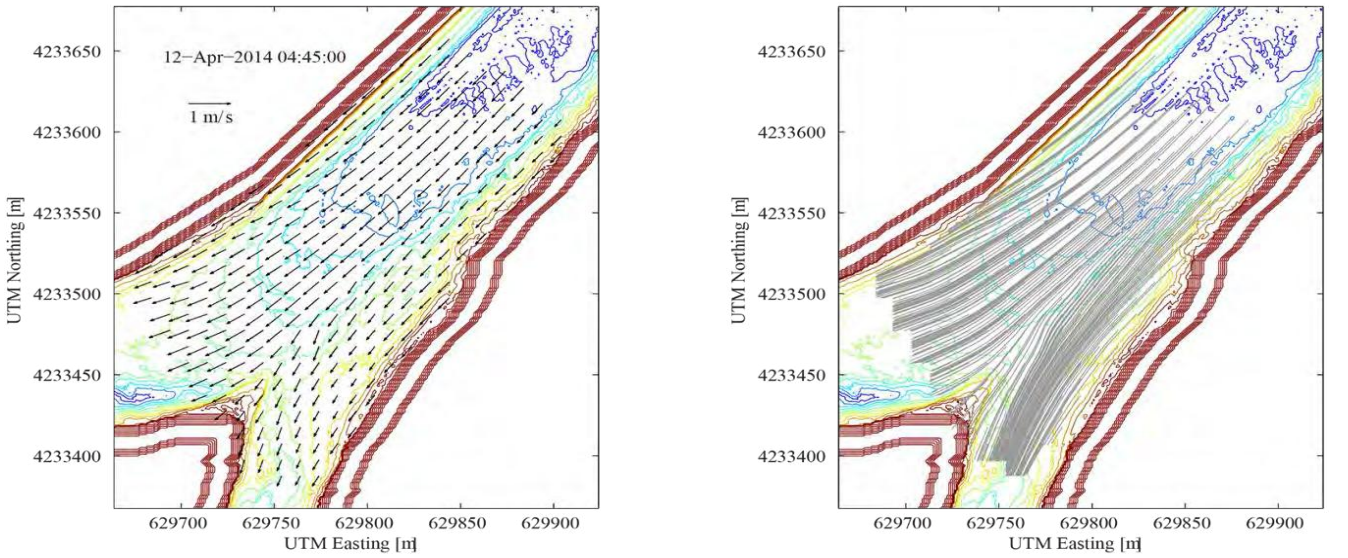

Figure 3.3-17 Plan View Plots during Typical Positive River Discharges—Velocity Vectors (on the left) and Particle Pathlines (on the right)—both Overlain on the Bathymetry Plot

Nevertheless, the results of this algorithm are quite good. A flag data file is included in the final results, in which a flag of 0 indicates the velocity field was interpolated with Qr - Pr < 10 percent and a flag of 1 indicates Qr - Pr > 10 percent confirming this finding. A flag of 2 indicates that the velocity field was estimated from the regression model.

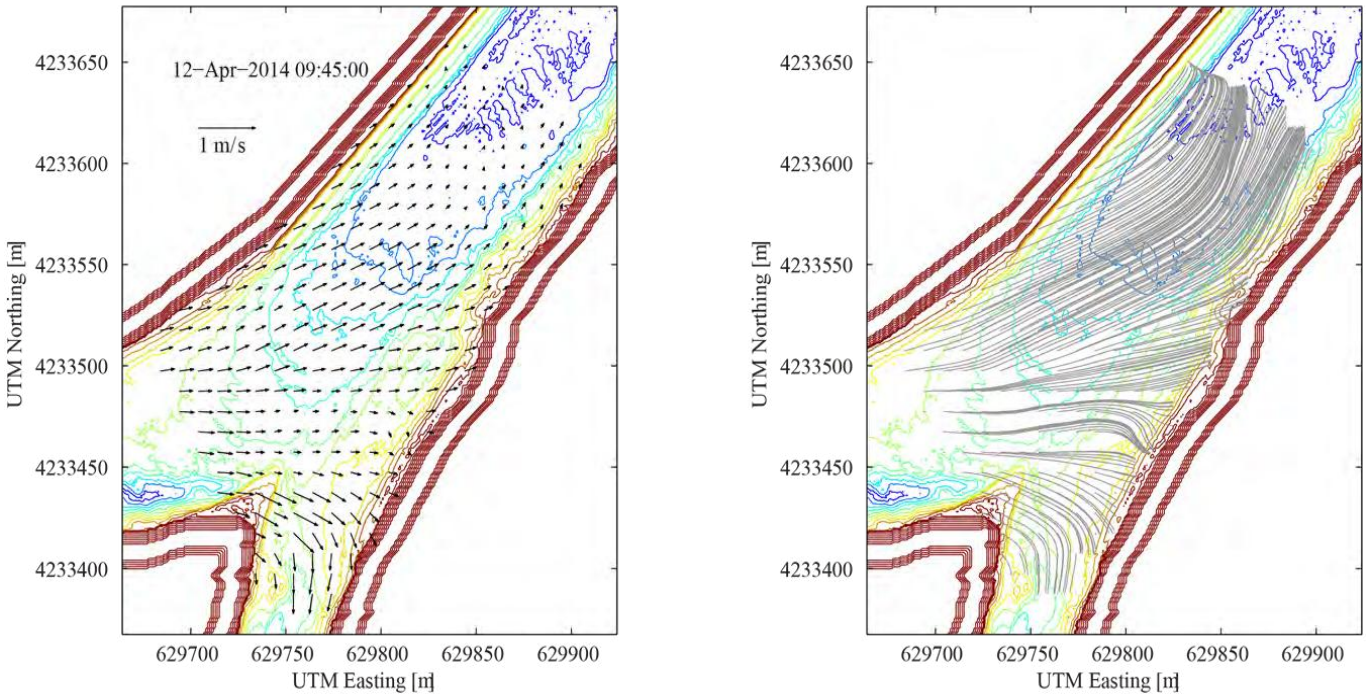

Figure 3.3-18 Plan View Plots during Typical Negative River Discharges—Velocity Vectors (on the left) and Particle Pathlines (on the right)—both Overlain on the Bathymetry Plot

COMPARISON OF CRITICAL STREAKLINE ESTIMATES TO DRIFTER TRACKS

The critical streakline was extracted from the drifter tracks by determining the point along the upstream cross-section (Q_u) where the drifters diverge. To do this, the location of the two drifters that are closest to the point where the Sacramento River and Georgiana Slough flows split was determined, then the distance along the cross-section of these two drifters was calculated and the positions of these drifters was averaged to calculate the streakline position.

Drifter sets that did not have drifters enter both the Sacramento River and Georgiana Slough were not included in the comparison because the drifter release sets were performed on March 17 and May 19 with the FFGS operational. For the majority of the drifter sets, the barrier physically diverted drifters (presumably bound for Georgiana Slough) into the Sacramento River; therefore, only drifter sets that included drifters that travelled into both the Sacramento River and Georgiana Slough were used for comparison (26 of 51).

A linear regression was performed between the critical streakline position from the drifter sets, the critical streakline position from the discharge ratio, and the critical streakline position from the integral method (**Figure 3.3-19**). The time series of critical streakline position (**Figure 3.3-20**) show that, for most instances, the integral method prediction is within the error bars of the drifter estimate, whereas most instances of the discharge ratio method under predicts the drifter estimate. For these two reasons, the integral method for estimating the critical streakline position is the better match with the drifter data. The integral method is slightly more statistically accurate in predicting the upstream point of flow divergence (R^2 = 0.90 and RMSE = 5.3 m [17.4 ft]), compared to the discharge ratio method (R^2 = 0.84, RMSE = 6.8 m [22.3 ft]).

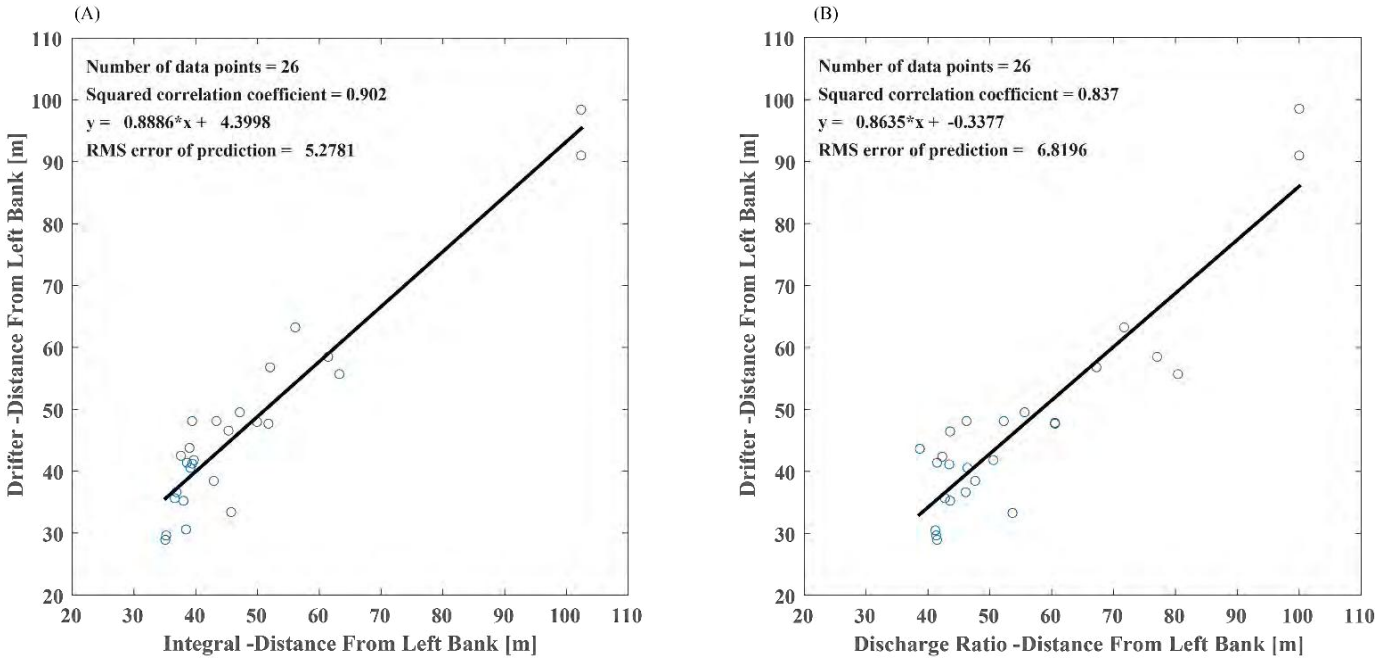

Note: (a) Linear regression between integral method and drifter sets; (b) Linear regression between discharge ratio method and drifter sets.

Figure 3.3-19 Linear Regressions of the Critical Streakline Extracted from Drifter Sets, Calculated by the Discharge Ratio and Integral Methods

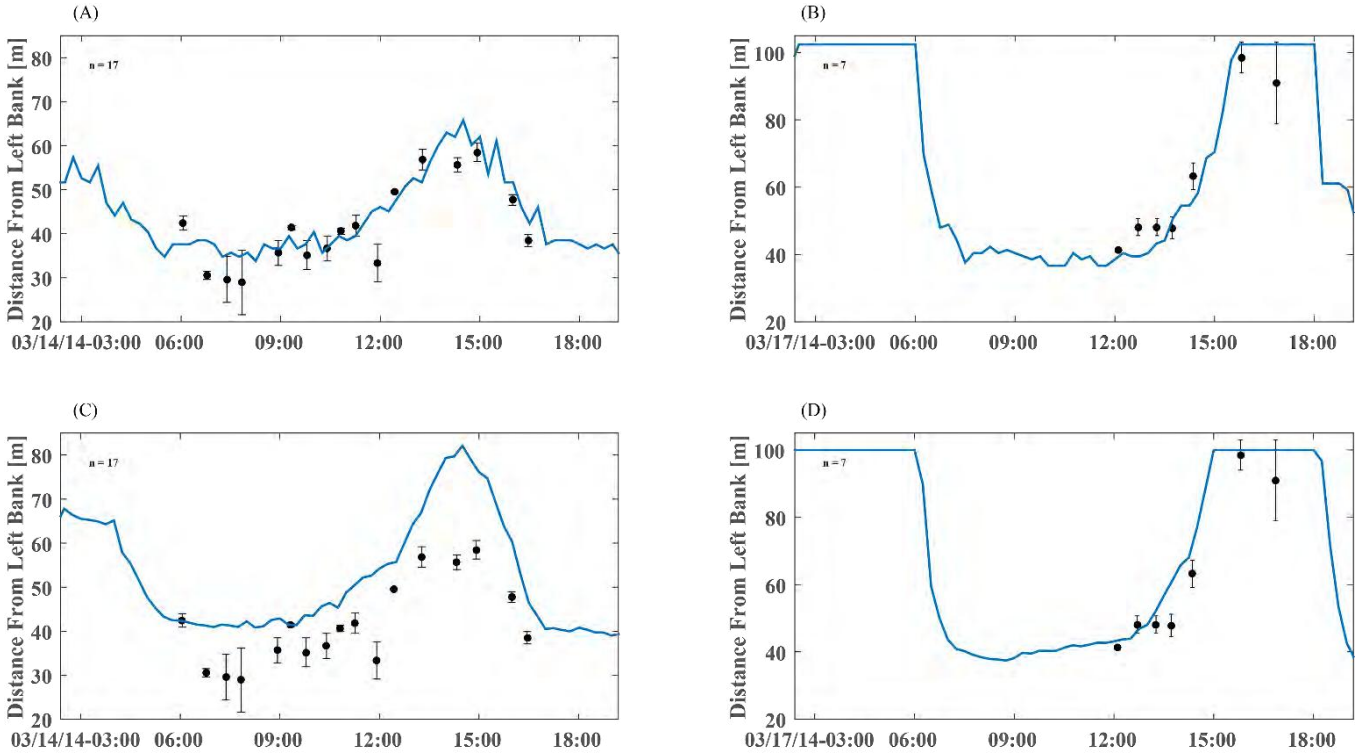

Note: Calculated by the discharge ratio and integral methods (a, b) Time series of integral method (blue line) and drifter sets (black dots) on March 14 and March 17; (c, d) Time series of integral method (blue line) and drifter sets (black dots) on March 14 and March 17. Error bars on the drifter data represent the distance between the two drifters used in the average position of the streakline.

Figure 3.3-20 Time Series Comparisons of the Critical Streakline Extracted from Drifter Sets

A few observations can be noted about critical streakline calculations based on drifter data:

1. During the steady state conditions from 0600 to 1200 on March 14, the drifter critical streakline shows considerable variance (approximately 15 m [49 ft]) (**Figure 3.3-20**). In addition, there were several instances where a drifter closer to the Sacramento River bank went into Georgiana Slough, and a drifter closer to the Georgiana Slough bank went into the Sacramento River;

2. These observations highlight: 1) the stochastic nature of the critical streakline (large scale turbulence can substantially affect the final fate of a single drifter path); and 2) the critical streakline is not an infinitesimally narrow line but probably fairly wide, on the order of 10 m (33 ft) wide because of the effects of turbulent motions on streakline positions (e.g. large scale turbulence scales with the depth ~10 m [~33 ft]); and

3. The "width" of the critical streakline narrows as the drifters (and fish) approach the Sacramento River and Georgiana Slough junction because turbulence has less time to influence drifter (and fish) motion. Juvenile Chinook salmon experience the same level of stochasticity as the drifters do, so a larger sample size is important when looking at spatial distributions relative to the streakline, especially when analyzing mid-stream structures such as the FFGS.

COMPARISON OF CRITICAL STREAKLINE ESTIMATES TO VELOCITY FIELD STREAMLINES

The critical streakline was extracted from the interpolated velocity field by determining the last streamline to enter Georgiana Slough closest to the Sacramento River junction. An example is shown in **Figure 3.3-21**. This was done for all time periods where discharge was non-reversing ($Q_d > 0$).

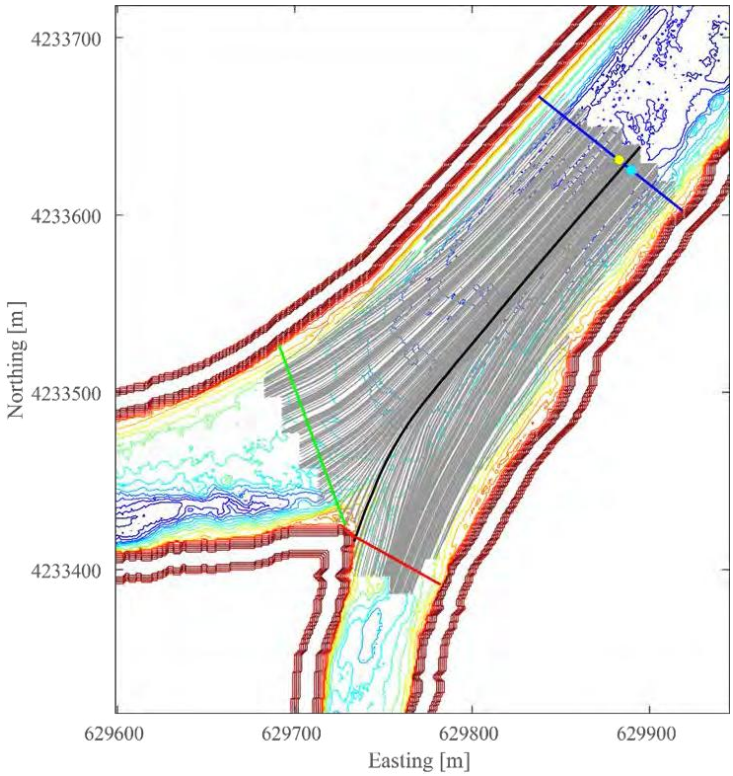

Note: The closest streamline to junction entering Georgiana Slough is considered the critical streakline. For comparison, the critical streakline is shown along the upstream ADCP cross-section (blue line), for the integral method (yellow dot), and for the discharge ratio method (cyan dot).

Figure 3.3-21 Example of Critical Streakline (black line) Extracted from Streamlines (gray lines) from the Interpolated Velocity Field

For the entire time period, the critical streakline from the velocity field (CSL_v) is compared to the discharge ratio (CSL_d) and integral (CSL_i) methods. These differences are shown in **Figure 3.3-22**. As shown, the CSL_v is over-predicting the streakline position compared to CSL_d on average by 5.2 m (17.1 ft) (SD = 9.1 m [29.8 ft]) and is under-predicting compared to CSL_i on average by -8.6 m (-28.2 ft) (SD = 10.9 m [35.8 ft]).

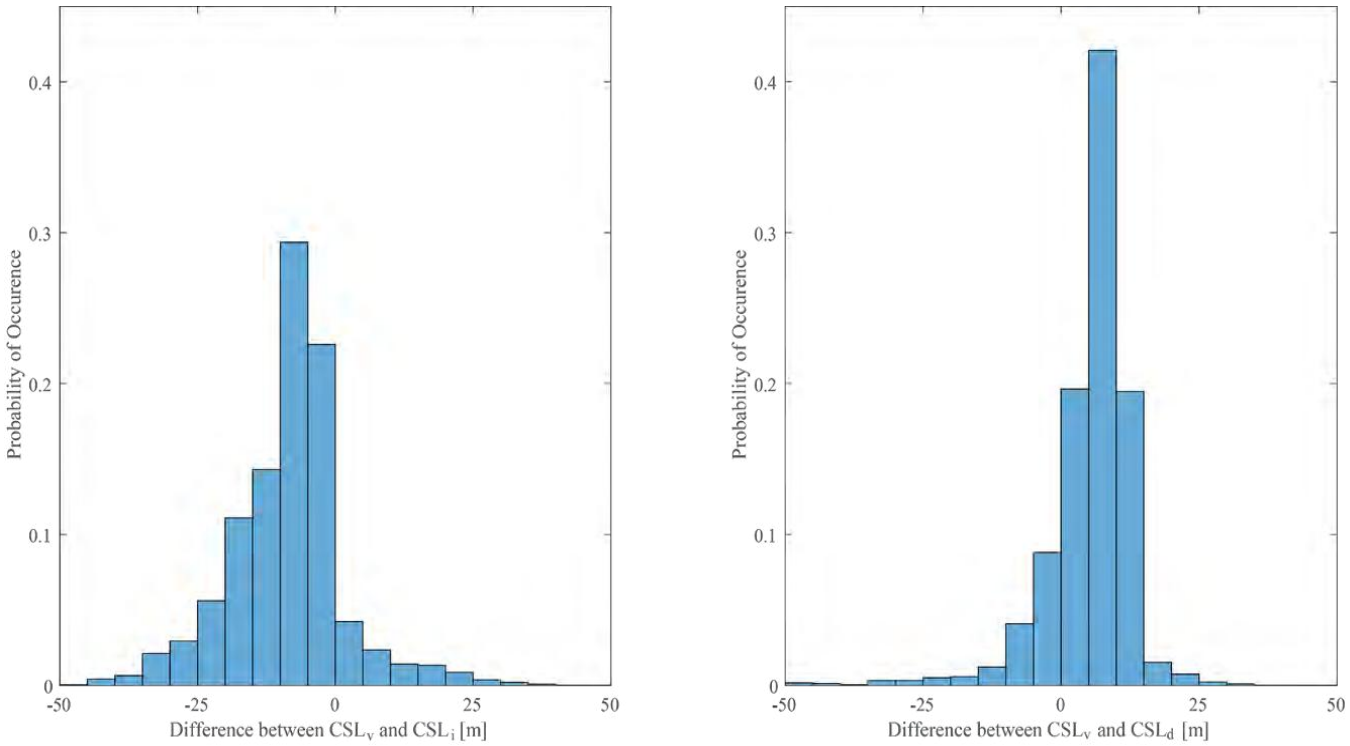

Figure 3.3-22 Histogram Plots of Differences in Critical Streakline: Difference between CSLv and CSLi; and Difference between CSLv and CSLd

The results presented in Section 3.3.3 showed that CSL_i was a better predictor of the critical streakline location, based on drifter data compared to CSL_d. The critical streakline also was observed to vary considerably during steady state conditions.

If a reasonable level of accuracy for these calculations is a critical streakline within +/- 10 m (+/- 33 ft), then all CSL_v that are within this range would be considered accurate. In this data set 60 percent of the CSL_v are within +/- 10 m (+/- 33 ft) of CSL_i. Because the CSL_v is a Lagrangian estimate of the critical streakline based on a fixed (Eulerian) set of measurements, errors in the interpolation of the Eulerian estimates contributes to some of the above errors. Furthermore, if the turbulence is isotropic relative to the streakline, then drifter and fish tracks do not bias the mean position of the streakline but merely create greater scatter about the mean.

COMPARISON OF INTERPOLATED VELOCITY TO DRIFTER TRACK VELOCITY

When addressing the 2D interpolated velocity as compared to the drifter track velocity data, the interpolated velocity values are between the two measurements reflect two different timescales consisting of instantaneous for the drifter data and an average for the interpolated velocity. A 1-minute moving average was applied to the drifter data to compensate for the timescale discrepancy, while minimizing the spatial averaging. For this comparison, only the drifter's tracks collected with the FFGS not operating (collected on March 14) were used because it was difficult to determine whether the drifters physically interacted with the FFGS when it was operational.

The U (east-west) and V (north-south) velocity components were compared separately, where U_i and V_i is the velocity from the interpolated velocity field and U_d and V_d is the velocity computed from drifter sets. At each grid node of the interpolated velocity field, the position of the drifter closest to that grid node was selected for comparison. If a grid node was greater than 10 m (33 ft) away from a drifter point, then that node was not included.

Figure 3.3-23 shows the probability histograms of the differences between $U_i - U_d$ and $V_i - V_{d.}$ 75 percent of U_i velocities and 65 percent of V_i velocities were within +/- 5 cm/s (+/- 0.16 ft/s) of U_d and V_d, respectively. The mean difference in the U component was 1.2 cm/s ().04 ft/s) (SD = 6.1 cm/s [0.20 ft/s]), and the mean difference in the V component was 4.0 cm/s ().13 ft/s) (SD = 7.1 cm/s [0.23 ft/s]).

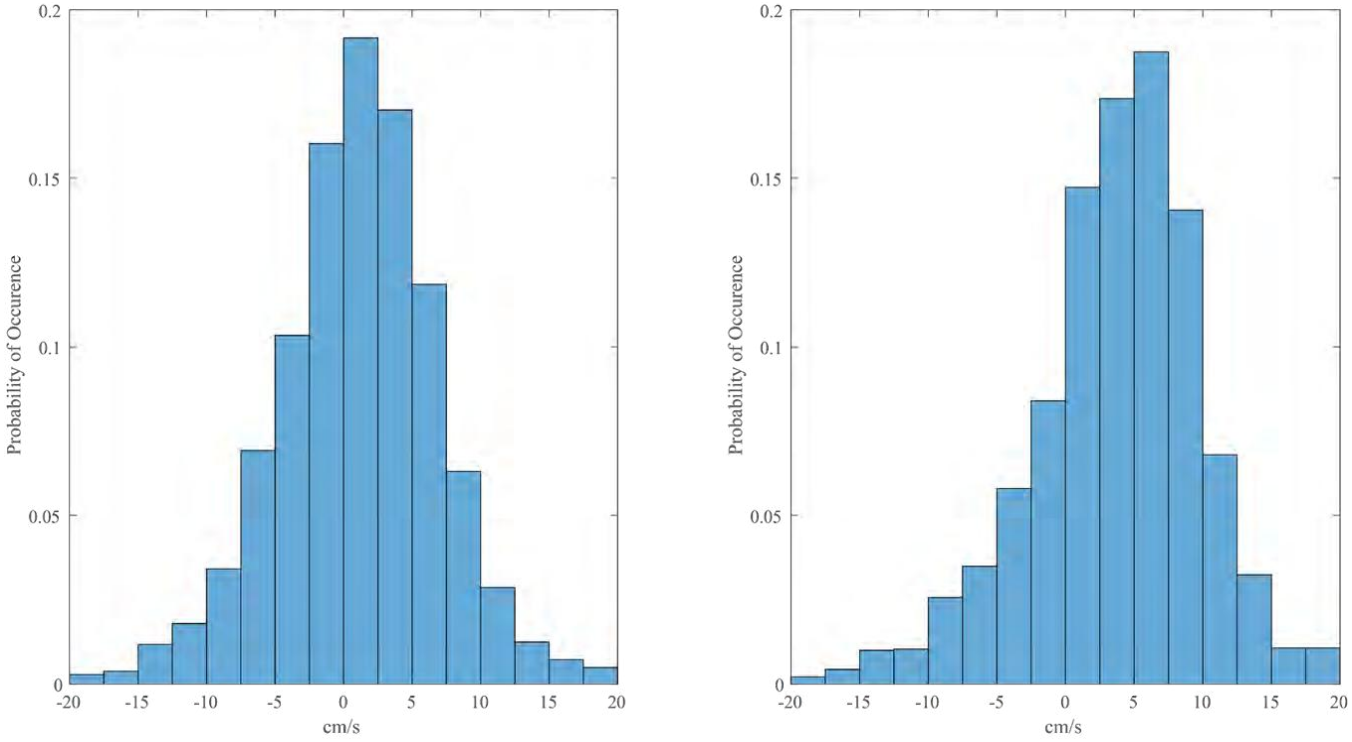

Note: Calculated for U component (shown on left) and V component (shown on right). Positive values are interpolated velocity higher than drifter velocity.

Figure 3.3-23 Histogram Plots Showing Difference in Interpolated Velocity and Velocity Calculated from Drifter Tracks

The mean difference for each grid node velocity component is shown in **Figure 3.3-24**. The U component shows greater differences closer to the left bank and near the Sacramento River and Georgiana Slough junction. The V component shows greater differences closer to the right bank and near the Sacramento River and Georgiana Slough junction. The differences in the U and V components near the Sacramento River and Georgiana Slough junction indicate that this location was the most poorly resolved in the entire domain.

Drifter tracks indicate flow divergence near the Sacramento River and Georgiana Slough junction, yet measuring this with a fixed ADCP is difficult because the algorithm to compute velocity from the ADCP assumes homogeneous flow across the acoustic beams. Nevertheless, the interpolated velocity represented the surface velocity field derived from the drifter data field reasonably well, despite the time scale discrepancies inherent in each of these approaches.

In summary, the integral method appears to be the most accurate for quantifying the critical streakline at the Georgiana Slough junction over the range of river discharges observed at the study location (-6000 to 20,200 cfs).

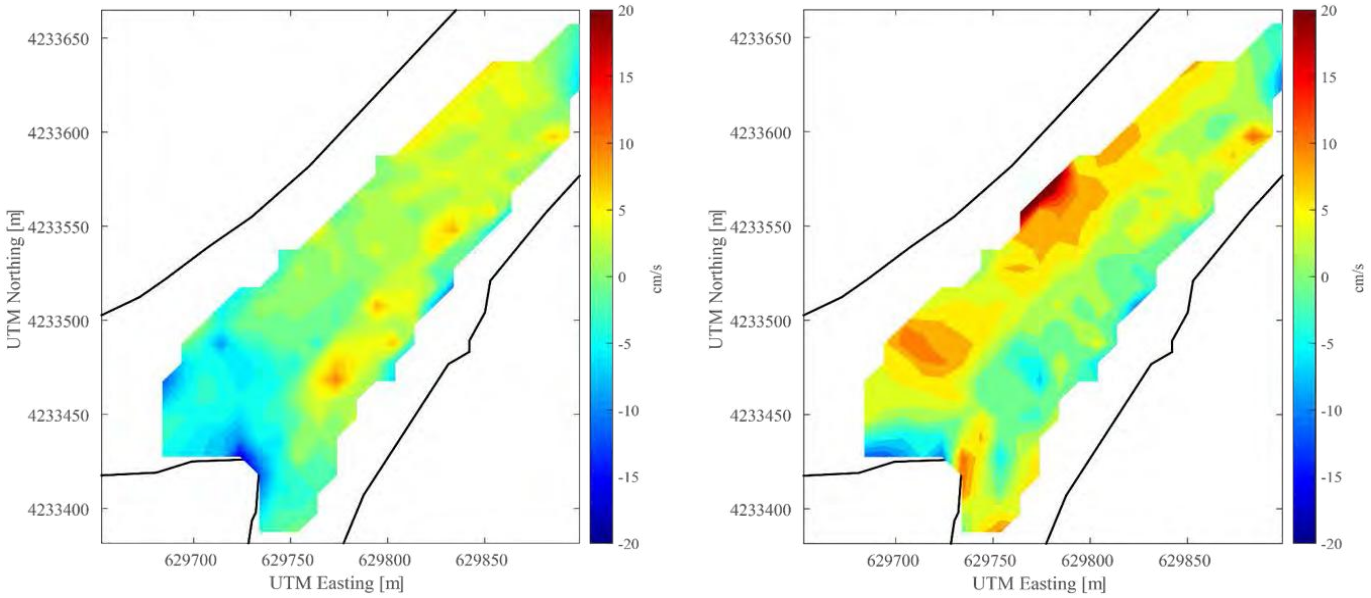

Note: Positive values are interpolated velocity higher than drifter velocity. The graphics show where a drifter track traveled for U velocity component (on the left) and V velocity component (on the right).

Figure 3.3-24 Contour Plots of the Average Velocity Differences at Each Interpolated Velocity Grid Node

INFLUENCE OF FFGS ON THE VELOCITY FIELD

Two ADCPs (sites GS.mn and GS.ms) were deployed downstream from the FFGS to characterize the influence of the FFGS on the mean and turbulent velocity field. The sampling scheme of the ADCP was not adequate to be used in a direct quantitative analysis of large scale turbulence generated by the barrier. However, the error velocity measured by ADCPs can be used to qualitatively determine the degree of turbulence in the ADCP's sampling volume.

The error velocity is a measure of the homogeneity in the velocity vectors between the two acoustic beams. Higher values in error velocity could be indicative of non-homogeneous velocities over the sampling interval, which can be interpreted as the passage of larger coherent turbulent structures past the instrument locations. This approach is somewhat limited because the ADCPs beams diverge, so that samples that are taken further from the instrument may have higher error velocities caused by increasing inhomogeneity in the water volume sampled across the two beams.

The velocity profile data from sites GS.mn and GS.ms were grouped according to having the FFGS either operational or nonoperational, and then further subdivided into three different flow regime as described in the previous analysis for consistency. The data used for this period were from March 14 to April 25. The data prior to March 14 was recorded using different ADCP programming; the switch in programming to reduce acoustic noise resulted in an increase in error velocity because less temporal and spatial averaging occurred in the revised scheme. After April 27, the barrier was left operational. Including data after this date could bias the number of samples towards periods when the FFGS was operational. Therefore, only data from March 14 to April 25 was

used, which resulted in a low number of samples for the high flow regime because the majority of high river flow occurred from March 1 to March 15.

A summary of the analysis is shown in **Table 3.3-4**. For the low flow regime, the U and V velocity components were similar between sites for both the FFGS On and Off. For the mid and high flow regime, the U velocity component was higher at site GS.mn, with no difference between FFGS operational or nonoperational. For all flow regimes, the mean error velocity was a little higher at site GS.mn, but no difference was noted between the FFGS being operational or nonoperational at either site. In addition, at each site the error velocity remained relatively constant throughout a range of flows. This may mean that the error velocity simply was not a good qualitative measure of turbulence, or the degree of turbulence did not substantially increase over the range of flows measured.

Table 3.3-4 Summary of the Average Velocity Magnitude and Error Velocity for Three Flow Regimes and Barrier States

Site	Flow Regime	Barrier State	N	Bin-Averaged U component (cm/s)	Bin-Averaged V component (cm/s)	Bin-Averaged Error Velocity (cm/s)
GS.mn	Low	On	1368	-8.61 (0.99)	-10.82 (3.12)	2.33 (0.92)
		Off	1418	-8.94 (0.83)	-11.11 (2.95)	2.27 (0.90)
	Mid	On	507	-37.62 (4.04)	-31.51 (5.37)	2.21 (1.43)
		Off	501	-37.35 (3.14)	-31.82 (4.88)	2.11 (1.40)
	High	On	118	-44.88 (4.60)	-38.37 (6.20)	1.95 (1.33)
		Off	127	-45.70 (3.82)	-39.52 (5.80)	2.03 (1.43)
GS.ms	Low	On	1365	-4.43 (0.18)	-14.48 (0.32)	1.59 (0.23)
		Off	1418	-4.43 (0.29)	-14.15 (1.13)	1.66 (0.32)
	Mid	On	502	-17.25 (3.35)	-27.73 (3.71)	1.41 (0.15)
		Off	501	-17.16 (3.63)	-25.68 (5.70)	1.52 (0.23)
	High	On	117	-21.72 (4.13)	-35.48 (4.22)	1.47 (0.17)
		Off	127	-21.83 (4.41)	-33.70 (6.98)	1.67 (0.32)

Based on this analysis, the state of the FFGS was concluded to have had no observable effect on the mean velocity or the ADCPs error velocity over a range of flow rates at the points of observation. However, the thermal camera data collected during this study should be analyzed to further address this issue.

3.3.4 DISCUSSION

ENTRAINMENT INTO GEORGIANA SLOUGH

This section discusses the hydrodynamic entrainment into Georgiana Slough on tidal and tidally averaged timescales. From a hydrodynamic perspective, two very distinct hydrodynamic regimes occurred during the experiment:

1. Unidirectional flows past Georgiana Slough that occurred at higher Sacramento River flows; and
2. Reversing flows into Georgiana Slough that corresponded to low Sacramento River inflows (**Figure 3.3-25**).

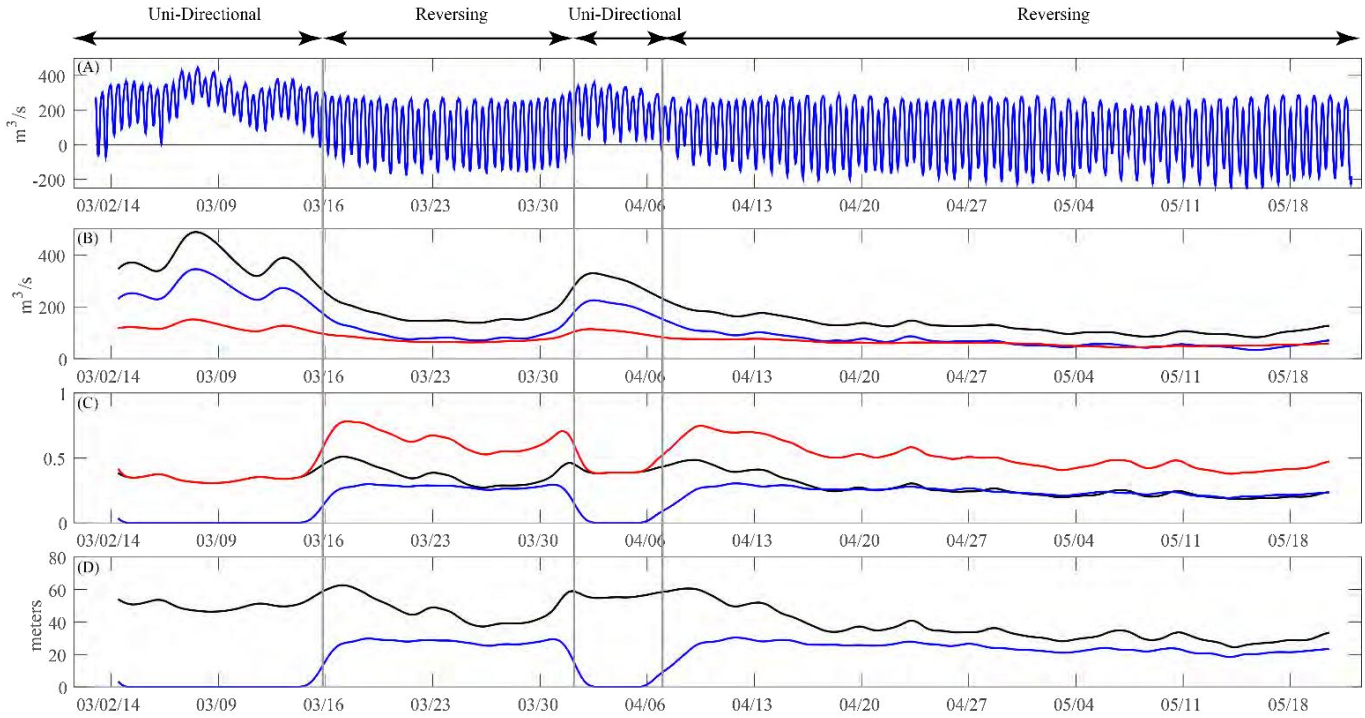

Note: a) the as-measured discharge in the Sacramento River downstream from Georgiana Slough; (b) tidally filtered discharge upstream (black), downstream (blue), and side channel (red), (c) tidally filtered discharge ratio at upstream (black), downstream (blue), and total (red); and (d) tidally filtered critical streakline in distance from upstream left bank (black) and downstream left bank (blue).

Figure 3.3-25 Time Series Data Estimated Using the Index Velocity Method for Discharge Calculation and Discharge Ratio Method for Critical Streakline Calculation at Georgiana Slough Junction

Unidirectional flow regimes were further grouped into three separate sub-regimes to maintain consistency with analysis of acoustic telemetry data. These flow sub-regimes were determined by grouping the discharge data into three flow quantiles, as determined by time periods when fish arrived in the study area. These flow regimes were 0 - 10,170 cfs (0 to 288 cms) for low flow, 10,170 – 12,850 cfs (288 to 364 cms) for mid flow, and greater than 12,850 cfs (364 cms) and greater for high flow.

The total discharge ratio represents the ratio of discharge from the Sacramento River into Georgiana Slough. The tidal average of the upstream discharge ratio is <Ru> = <Qs/Qu> not <Qs>/<Qu>, where < > represents the tidal average. The order of operation is important, where the latter ratio is incorrect and represents the ratio of the net flows which does not include the tidal timescale effects encapsulated in the <Qs/Qu> calculation.

During the study period, several key points were noted based on review of the tidally filtered discharge ratio (**Figure 3.3-25**). First, during flood tides, flow entered Georgiana Slough simultaneously from the Sacramento River from upstream and downstream of the junction (see "Convergence" panel shown in **Figure 3.3-7**). Thus, flows originating from the Sacramento River downstream of Georgiana Slough contributed to a significant portion of the total discharge ratio or hydrodynamic entrainment into the junction. Secondly, the total ratio was routinely above 0.5, which means that over half of the Sacramento River water was entrained into Georgiana Slough during flood tides. Furthermore, the total ratio was lowest during the highest and lowest river discharges (**Figure 3.3-25c**). The tidally filtered critical streakline exhibited similar patterns to the discharge ratio (**Figure 3.3-25d**), where the peaks in the upstream critical streakline position occurred during the rising and falling limbs

of the peaks in discharge. Outside these time periods, the tidally averaged critical streakline position was more stable.

A closer examination of the critical streakline during a tidal period (periods less than 25 hours) is needed to understand the dynamics on a tidal timescale (**Figure 3.3-26**). The time period shown in **Figure 3.3-26** was chosen because it is a representative of reversing river discharges. The minimum upstream discharge ratio and critical streakline position occurred during the rising limb of peak positive discharge and as the discharge remained steady. The discharge ratio and critical streakline rose during the falling limb of positive discharge and reached a maximum just before slack tide. This was because of a phase difference of -3.5 hours between peak discharge in the Sacramento River and Georgiana Slough. For the time period selected, the critical streakline was rarely lower than 35 m (115 ft) (**Figure 3.3-26c**) during the positive discharge period; 35 m (115 ft) corresponds to the cross-stream location of the downstream tip of the FFGS, and is the greatest critical streakline position value at which the FFGS was expected to be effective.

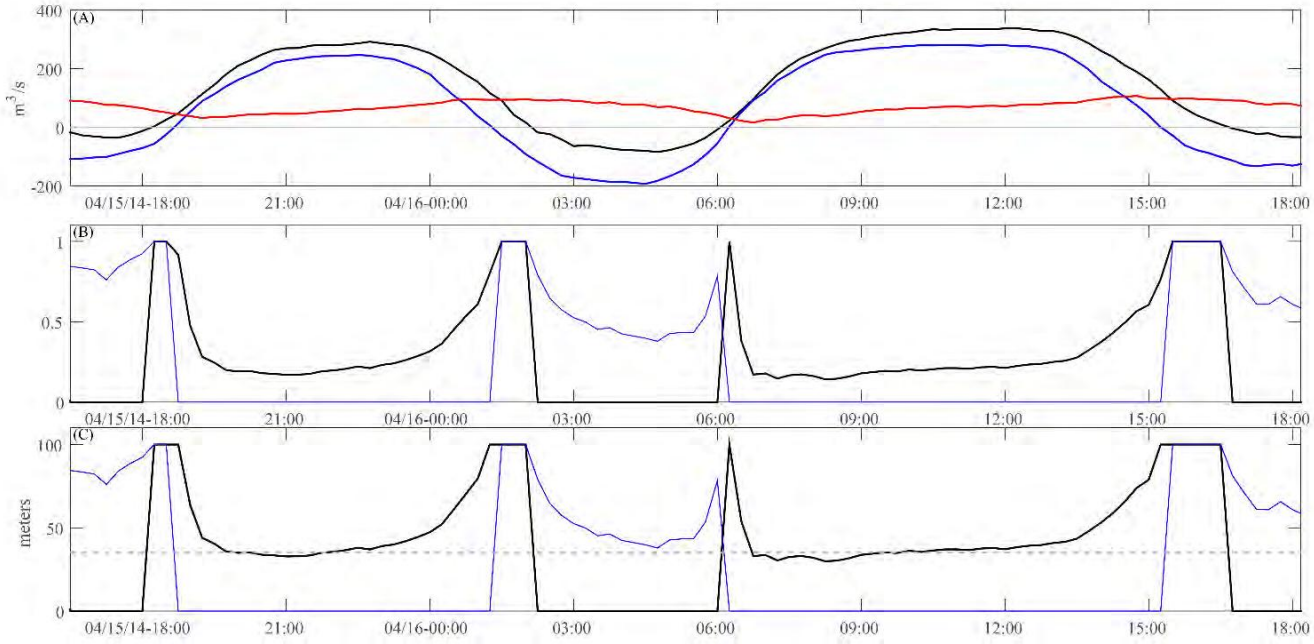

Note: (a) 15-minute averaged discharge upstream (black), downstream (blue), and side channel (red); (b) 15-minute averaged discharge ratio at upstream (black) and downstream (blue); and (c) 15-minute averaged critical streakline in distance from upstream left bank (black) and downstream left bank (blue). The dashed gray line represents the 35 m (115 ft) with the FFGS On.

Figure 3.3-26 Time Series Data Estimated Using the Velocity Profile Method for Discharge Calculation and Integral Method for Discharge Ratio and Critical Streakline Calculation at Georgiana Slough Junction

These observations suggest that the critical streakline position and water entrainment into Georgiana Slough vary as a function of discharge. These observations were further examined by grouping the discharge data into three flow quartiles, as determined by periods when fish arrived in the study area. In **Figure 3.3-27**, the critical streakline distributions are plotted for each flow regime.

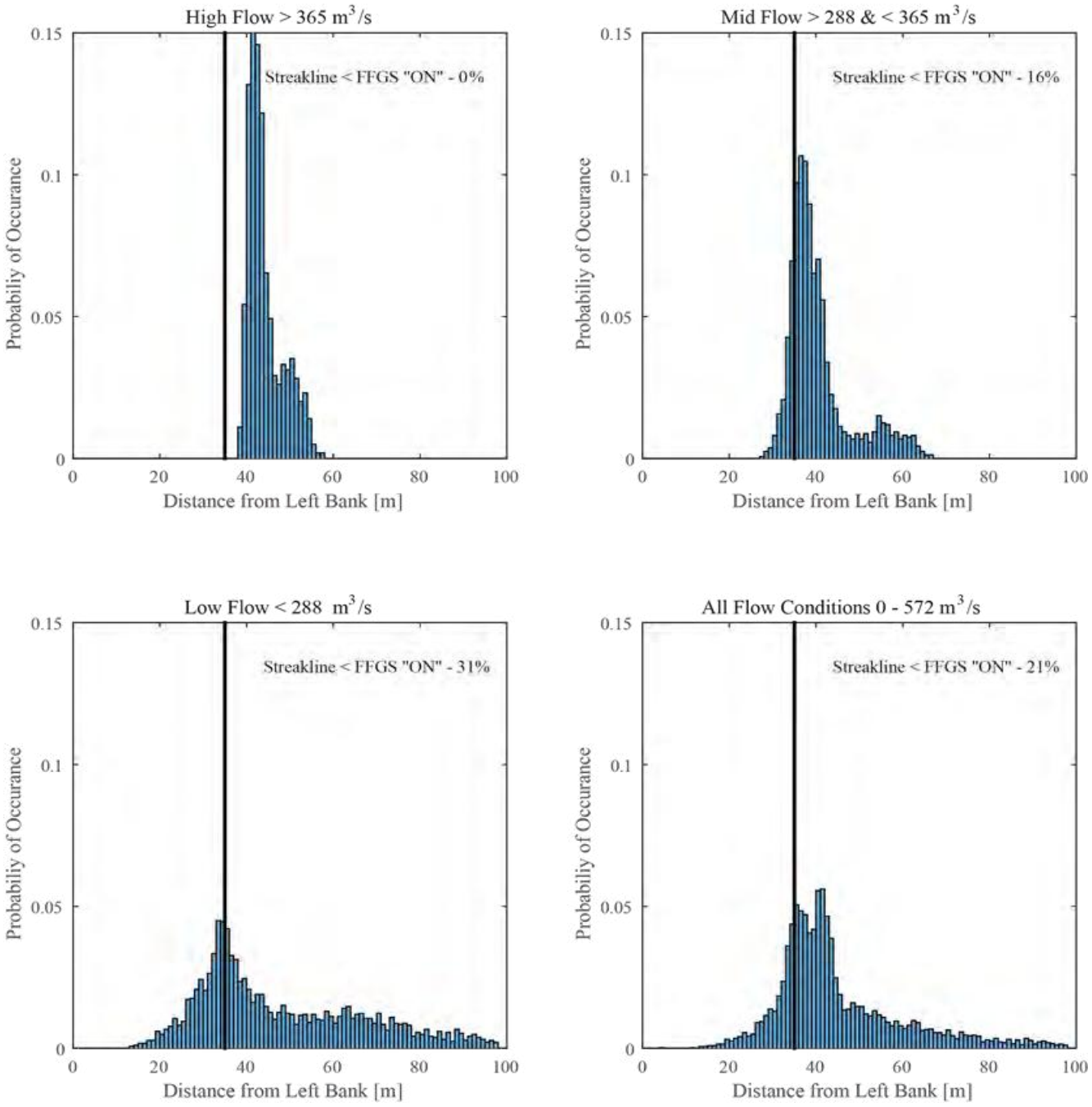

Note: The vertical black line in all plots shows the 35 meters with the FFGS On.

Figure 3.3-27 Histogram Plots Showing the Critical Streakline for High, Mid, Low, and All River Discharges

For high flow, the peak in critical streakline occurred at approximately 42 m (138 ft), and no occurrences of the critical streakline were less than the position of the FFGS operational, of 35 m (115 ft). For mid flow, the peak was approximately 38 m (125 ft), and only 16 percent of the critical streakline positions were less than the FFGS operational. For low river discharges, the peak was approximately 35 m (115 ft), and 31 percent of the critical streakline positions were less 35 m (115 ft) with the FFGS operational. The percentage of time that the critical streakline was less than the position of the FFGS operational represents the hydrodynamic potential for the FFGS to be effective for that particular river discharge.

For high and mid river discharges, the critical streakline position was farther away from the left bank than the downstream tip of the FFGS for most of the observations (**Figure 3.3-27 a** and **b**). Because the role of the FFGS is to move fish to the right of the critical streakline and to keep them to the right, the FFGS would only be effective in doing so if the critical streakline were positioned to the left of the barrier tip (see **Figure 3.3-7b**). Even during low river discharges, the critical streakline peak is right at the position with the FFGS operational, and thus the FFGS is expected to be effective less than 31 percent of the time that it was operational.

In summary, two important points can be made based on the hydrodynamics at tidal and residual timescales over three different flow regimes:

1. First, the timing of fish passage matters. For example, if fish move through the domain during the rising or falling limbs of the higher river discharge, then entrainment into Georgiana Slough can increase on a residual timescale. If juvenile salmon move at night (Chapman et al. 2013; Plumb et al. 2015) and during the falling discharge limb, then entrainment will change on tidal timescales because the diurnal and tidal cycles change relative to each other by roughly an hour every day. Because the phase between the diurnal and tidal cycles change by about an hour every day, this procession will change the net or tidally averaged entrainment rate in the absence of a real actual change in the net entrainment rate. For example, fish that arrive at night only will experience a slightly different tidal phase each night (e.g., changing about 1 hour in a 12 hour period ~ 8 percent); and

2. Secondly, based on analysis of three different river discharges, the position of the FFGS may not have been ideal to reduce entrainment in Georgiana Slough because the barrier was positioned too close to the left bank shore for the river discharges measured. Placement of the FFGS further into the river and further downstream may have increased barrier effectiveness under the low river discharges that occurred during the study.

3.3.5 RECOMMENDATIONS AND CONCLUSIONS

Because entrainment rates in riverine junctions could have a substantial influence on through-Delta survival, the NMFS has used the RPA process to promulgate the testing of management actions designed to “move” juvenile salmon into pathways with higher overall survival potential, or to deter them from pathways with lower survival potential (as was the case in this study). In response to this RPA, DWR funded two studies to evaluate a bio-acoustic fish fence (BAFF) in Georgiana Slough (conducted in 2011 and 2012) and this study to evaluate the efficacy of an FFGS. Ultimately, this experiment was aimed at examining the efficacy of the FFGS, a relatively inexpensive technology, as compared to the BAFF, in terms of the upfront capital, installation, and maintenance costs. If the FFGS were determined to change entrainment in junctions, it could be used as a relatively inexpensive approach to “move” juvenile salmon into pathways with greater survival potential.

As part of this investigation, three different approaches were evaluated for calculating the critical streakline with the aim of increasing the accuracy of critical streakline position estimates. The position of the critical streakline relative to fish spatial distributions is critical in understanding entrainment in junctions. In the case of Georgiana Slough, several meters of imprecision in the critical streakline position relative to the fish spatial distribution matter was found to be substantial.

Among these methods, the integral method was determined to be more accurate for use in the Sacramento River and Georgiana Slough junction. Based on an analysis of the ADCP data, this study found that the state of the FFGS had no observable effect on the mean or turbulent velocity fields over the range of flows studied.

However, the drought conditions that prevailed during the study were largely outside the conditions for which the barrier was designed. The barrier was not expected to work during reversed river discharges or to perform well when streakline positions extended farther into the channel than the location of the downstream tip of the barrier. These were precisely the conditions that occurred during most of this study.

The potential for hydrodynamic entrainment into Georgiana Slough was investigated, and assuming that fish distributions are aligned spatially and temporally with the flow distribution the timing of fish passage was determined to effect entrainment. For example, if fish moved through the domain during the rising or falling limbs of the higher river discharge (Q_u > 364 cms [12,855 cfs]), then entrainment into Georgiana Slough would potentially be altered because of the barrier. If juvenile salmon moved at night (Chapman et al. 2013; Plumb et.al. 2015) and during the falling discharge limb, then entrainment could change at sub-tidal timescales, which, when averaged over time could affect the tidally averaged entrainment rates (see **Appendix A**).

Based on the analysis at three different river discharges, the FFGS was not fully effective during the study because its design placement assumed critical streakline conditions that were essentially not present. Placement of a longer FFGS further into the river and further downstream to deter fish with the observed Type 2 behavior in Section 3.5 could potentially increase barrier effectiveness based on hydrodynamic entrainment alone.

A barrier would also need to be longer to minimize the angle to the flow and the velocity normal to the barrier. A longer barrier may have been more effective for two reasons. First, the stochasticity seen in the drifter data suggests that fish distributions would have less time to relax. Second, the channel widens closer to the junction, therefore the barrier could be placed further out into the channel and the tip of the barrier would be positioned greater than 35 m (115 ft) (in the streakline coordinate system) and still provide enough clearance for navigation.

JUNCTION SUITABILITY FOR NON-PHYSICAL BARRIERS AND ALTERNATIVE JUNCTIONS

Streakline Position

A junction's suitability for installation of a non-physical barrier can be evaluated based on streakline position and its temporal variability. For example, a junction with an expected critical streakline location that would require a barrier that could not be feasibly installed and operated (e.g., a barrier that would restrict navigation or be exposed to excessive debris or hydraulic forces), would be a poor choice for a guidance structure. Similarly, a junction with a highly variable critical streakline location would be a poor choice because the barrier would only be effective for a fraction of the time. Conversely, a junction may be well suited for a non-physical barrier if the critical streakline is near shore (so barrier placement would not interfere with navigation) and flow is stable over a broad range of hydrodynamic conditions (so the barrier is effective most of the time).

Based on these criteria, Sacramento River junctions with Sutter and Steamboat sloughs are good candidates for non-physical barriers. For Sutter and Steamboat sloughs, the same methods to calculate the critical streakline during the same time period that data were collected for the FFGS evaluation study. The results show the critical streakline in these junctions is located closer to the bank and is more stable over a range of river discharges than in the Georgiana Slough junction (**Figure 3.3-28**). Moreover, the peak in the normalized discharge is near the entrance to Sutter and Steamboat sloughs because these channels are situated on a river bend; whereas, the peak in the normalized discharge in Georgiana Slough is near mid-channel away from the entrance to Georgiana Slough.

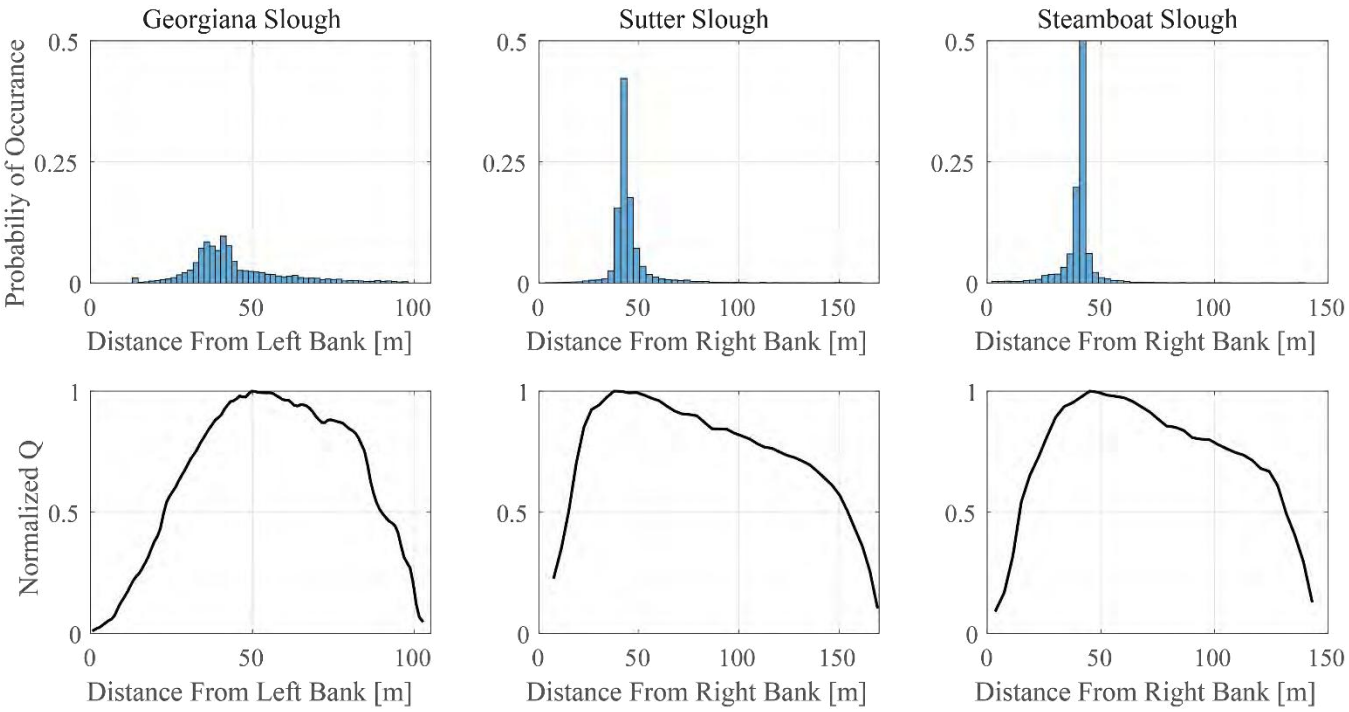

Figure 3.3-28 Critical Streakline Frequency Distribution (top row), and the Averaged Flow Distribution across the Sacramento River Upstream of each Junction (bottom row) with Zero Distance Referenced to the Left Bank for Georgiana and Right Bank for Sutter and Steamboat Sloughs

Juvenile salmon have been shown to have increased densities on the outside of bends because of secondary circulation. Therefore, it can be expected that the fish distribution would be skewed towards the side channel with the maximum in the distribution near the critical streakline. These conditions increase the likelihood of a non-physical barrier to change entrainment rates in such junctions.

Fish Spatial Distributions

Figure 3.3-29 and **Figure 3.3-30** show the distribution of the entrainment rate and spatial distribution of fish that pass Sutter Slough during night and day periods, respectively. The area of high entrainment rate corresponds almost identically with the streakline position in **Figure 3.3-28**. A barrier extending roughly 1/2 of the width of the Sacramento River upstream of Sutter Slough could significantly increase entrainment rates into Sutter Slough, because this is where the concentration peak is for fish that pass Sutter Slough.

Unlike Georgiana Slough, salmon outmigrants entering the north Delta interacts with the Sutter Slough junction, so a guidance structure positioned in this junction would interact with about 35 percent more outmigrants than a barrier placed in Georgiana Slough. Because the survival is appreciably higher in the Sutter Slough route over the Georgiana Slough route (see **Figure 3.3-2**) a barrier that increases entrainment in Sutter Slough could achieve the same (or greater) population effect as a barrier that decreases entrainment in Georgiana Slough.

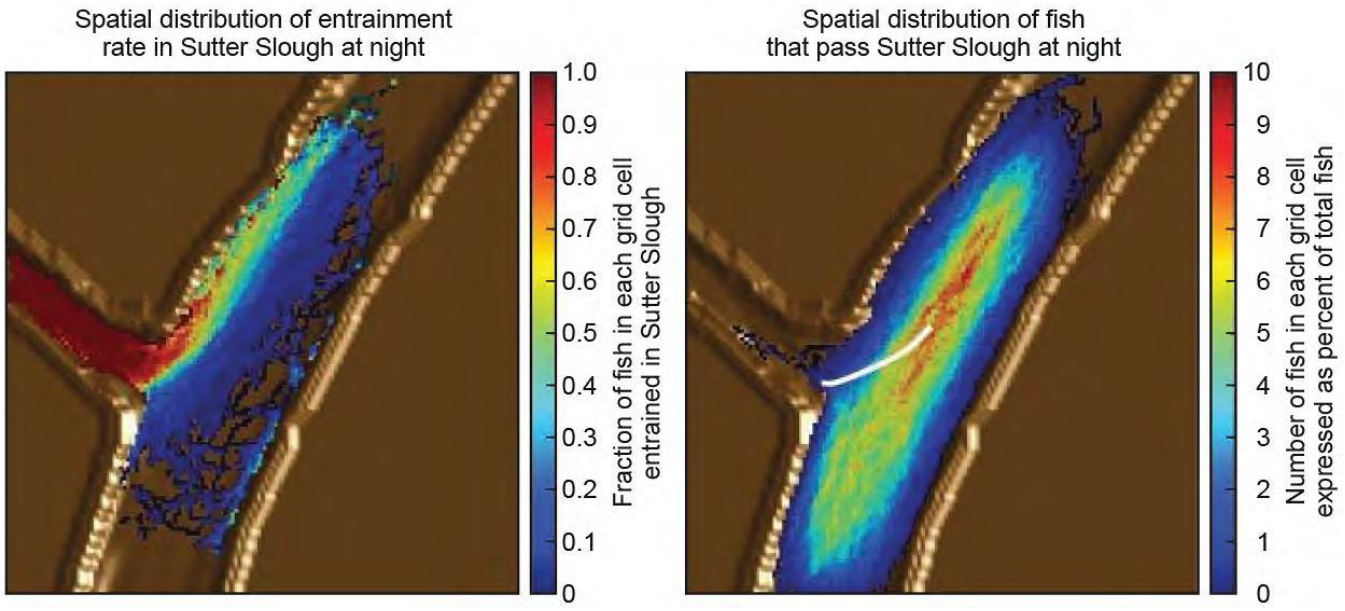

Figure 3.3-29 Fish Spatial Distribution of Entrainment Rate in Sutter Slough (left) and Spatial Distribution of Fish that Pass Sutter Slough at Night

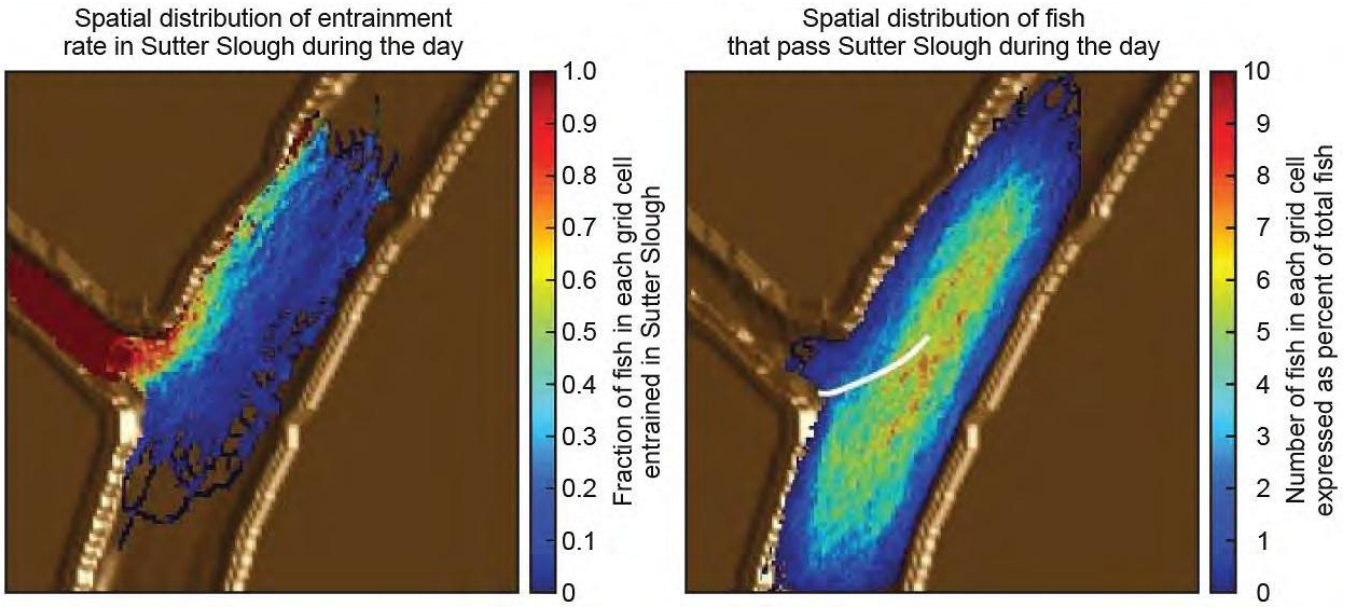

Figure 3.3-30 Fish Spatial Distribution of Entrainment Rate in Sutter Slough (left) and Spatial Distribution of Fish that Pass Sutter Slough during the Day

Comparing the Potential for Engineering Solutions to Change through Delta Survival in Junctions

How can the effectiveness of alternative solutions for improving through Delta survival singly or in combination be prioritized? One approach is to use the non-dimensional management number to compare the effectiveness of proposed solutions:

- Nm = (size of change in the environment that can be created) / (size of change needed to create desired outcome);

- Nm ~ 1 means solutions can achieve desired outcome. Conversely Nm << 1 suggests the solution under consideration simply will not work. In the case of the efficacy of increasing survival through the Delta with non-physical barriers, it is only necessary to compare the numerator in the management numbers;
- Size of change in the environment solutions can create = (percent of population transiting the junction)*(difference in survival between routes)*(change in entrainment rate due to barrier);
- Potential increase in survival due to barrier in Georgiana Slough = (0.65)*(0.2)*(change in entrainment);
- Potential increase in survival due to barrier in Georgiana Slough = 0.13*(change in entrainment);
- Potential increase in survival due to barrier in Sutter Slough = (1.0)*0.2)*(change in entrainment); and
- Potential increase in survival due to barrier in Sutter Slough = 0.2*(change in entrainment).

Thus, even without habitat improvements in the Sutter Slough route to increase survival, the management number for the barrier in Sutter Slough shows greater promise assuming the difference in survival among routes and the change in entrainment is identical in both junctions. However, given the stability of the streakline in the Sutter Slough junction and the fish distribution relative to the mean streakline position in the junction, it is likely that a greater change in entrainment with a barrier at Sutter Slough can be achieved. The potential increase in survival is ultimately most sensitive to survival in the Sutter Slough route, because if survival into Sutter Slough is significantly higher than the Sacramento River, then routing a large number of fish into Sutter Slough could actually increase through-Delta survival significantly.

In the final analysis, the combination of behavior and physics that controls the apportionment of juvenile salmon in tidally forced junctions needs to be understood. The critical streakline concept when combined with fish spatial distribution data has been used to good effect in both understanding why fish "go where they go" at riverine junctions and in evaluating the suitability, design and optimization of non-physical barriers.

Overall, using critical streakline analysis to prioritize the deployment of fish guidance structures in the Delta is recommended, and that critical streakline analysis be used to inform and optimize the design of these structures. Combining the growing understanding of the processes that control juvenile salmon route selection with targeted restoration efforts that improve route specific survival will provide the opportunity to develop cost effective strategies for increasing juvenile chinook survival through the Delta.

3.4 GENERALIZED LINEAR MODELING OF FISH FATES[13]

3.4.1 INTRODUCTION

In the spring of 2011 and 2012 a BAFF consisting of a bubble curtain, strobe lights, and low frequency pulsing sound was installed across the divergence of Georgiana Slough from the Sacramento River to reduce entrainment of juvenile salmonids into Georgiana Slough (see Perry et al. 2014 for project description). The BAFF successfully reduced entrainment by 14.7 percentage points in 2011 and 12.7 percentage points in 2012. The success of the BAFF was due to its ability to shift fishes towards the Sacramento River side of the junction when

[13] The material included in this section forms the basis for a recent peer-reviewed publication (Romine et al. 2016).

turned On. Although the BAFF system was found successful; the cost, deployment logistics, and in season maintenance were considerable. Thus, alternative methods to reduce entrainment to Georgiana Slough were sought. In 2014 an FFGS was placed at the junction to reduce entrainment to Georgiana Slough.

During both years of the evaluation of the BAFF deployments, a statistically robust approach was used to model entrainment to Georgiana Slough as a function of covariates using a GLM with the log link function (logistic regression). Results from the models were used to evaluate the efficacy of the BAFF during observed conditions during the study periods and to predict entrainment under different levels of the covariates. Here this report takes a similar approach to model entrainment of tagged juvenile Chinook salmon at the Georgiana Slough divergence as a function of the state of the FFGS and environmental covariates when tagged fish entered the study area. This is accomplished by using the 2D tracks of tagged juvenile Chinook salmon as they transited the Sacramento River and Georgiana Slough junction during March and April of 2014. This subchapter addresses Hypothesis 3 in **Table 2-1**: The FFGS reduces the probability of juvenile Chinook salmon entering Georgiana Slough.

3.4.2 METHODS

A logistic regression was used to model route selection of juvenile Chinook salmon at the Georgiana Slough divergence as a function of covariates. Fish entering Georgiana Slough were given a value of R = 1, and fish that remained in the Sacramento River were assigned a value of R = 0. The probability of being entrained into Georgiana Slough was modeled using GLMs with the logit link function in R (R Core Team 2014). Covariates were selected that were consistent with the findings of Perry et al. (2014): FFGS state (B; On = 1, Off = 0), time of day (D; day = 1, night = 0), discharge entering the junction (Q_U in cfs, USGS streamflow gauge 11447890), cross-stream position (X), and location of the critical streakline (S) in the channel cross-section. Discharge was reduced by three orders of magnitude for standardization (divided by 1,000); all other values used in the model were the observed values. Turbidity is another factor that could affect guidance of fish along the FFGS; however in this system turbidity is positively correlated with discharge thus the study allowed discharge to serve as a proxy for turbidity (USGS, unpublished data). Prior to analysis, data were filtered following the methods of Romine et al. (2014) to remove presumed predatory fishes that may have consumed tagged juvenile Chinook salmon.

The FFGS was in the On position (B = 1) when the structure was pivoted out into the Sacramento River upstream of the junction (**Figure 3.4-1**) and was in the Off position (B = 0) when the structure was parallel to the southern shore (left bank) of the Sacramento River upstream of the junction. Cross-stream position (X) was defined as the distance from the divergence origin along an axis that was perpendicular to the thalweg of the Sacramento River when passing the upstream end of the FFGS in relation to a Cartesian coordinate system. The origin of the Cartesian coordinate system was aligned with the thalweg of the Sacramento River and intersected the endpoint of the FFGS when in the on position (B=1), so that fish with positive cross-stream positions were on the Sacramento River side of the end of the FFGS and fish with negative values were to the Georgiana Slough side of the end point of the FFGS channel.

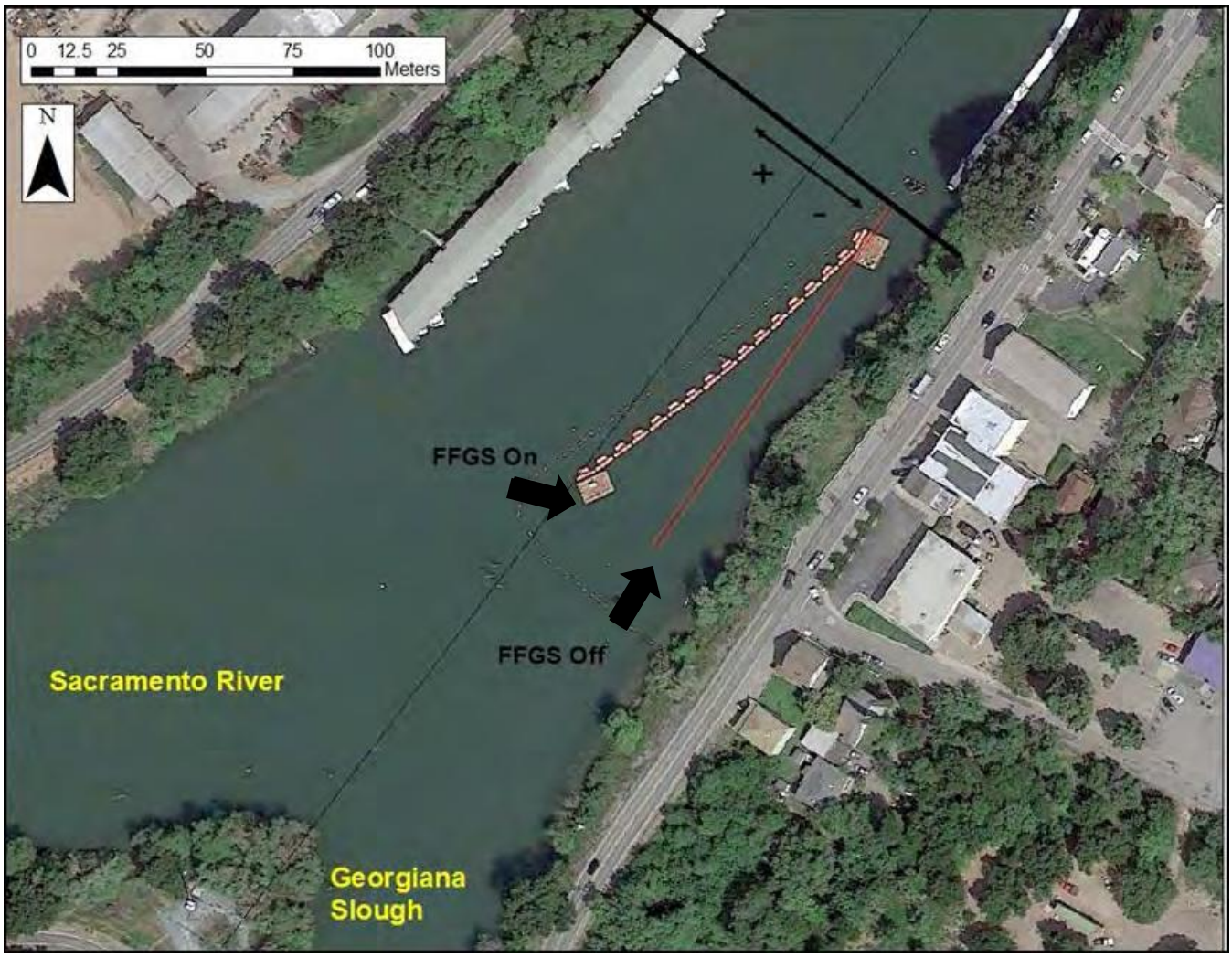

Note: Fish north of the dashed line were given a positive value, and fish south of the dashed line were given a negative value. The FFGS is in the On position. The orange line running parallel to the shore line indicates the position of the FFGS in the Off position. Cross-stream position (X) was measured as the distance along the solid black line from the dashed line bisecting the Sacramento River.

Figure 3.4-1 Coordinate System Used to Estimate the Cross-Stream Position Covariate (X)

Critical Streakline (S) was calculated as:

$$(0.1) \qquad S = W\left(\frac{Q_G}{Q_S + Q_G}\right) \quad 47,$$

where W is the width of the Sacramento River, Q_G (USGS stream flow gauge 11447903) is the discharge of Georgiana Slough and Q_S (USGS stream flow gauge 11447905) is the discharge of the Sacramento River downstream of the junction. The critical streakline was offset by 47 m (154 ft) to align with the coordinate system described previously and was measured from the left bank of the Sacramento River at the upstream end of the FFGS. When flow was reversing downstream of the junction, but not at *Qu*, the critical streakline was located at the right bank or north side of the Sacramento River. This indicates that all discharge was entering Georgiana Slough. When discharge was reversing at *Qwgb* and *Qu* the streakline was located on the left bank. Under this scenario fish should not be arriving as all discharge was in the upstream direction.

Based on previous modeling of fish behavior within the study area (Perry et al. 2014), a suite of *a priori* candidate models were selected for evaluation. The candidate models contained combinations of these covariates in addition to the FFGS state (B). All models included B regardless of the comparison between On and Off states. Interaction terms that were biologically or physically sensible also were evaluated (**Table 3.4-1**). For example, as Q_U increased, the location of S shifted towards the Georgiana Slough side of the river. Therefore, the interaction of Q_U and S was evaluated. In addition to the main effects and interaction terms, quadratic effects also were included because of the complex hydrodynamics at the Georgiana Slough divergence. For example, under negative flows (upstream flow), the barrier was not be expected to perform similarly as during positive river discharges. Conversely, at the highest flows, the FFGS could generate turbulence that could alter the performance of the FFGS (Scruton et al. 2003). To address these hypotheses, a model that interacted quadratic effects of flow with FFGS state allowed the effect of the FFGS to vary with flow.

Interaction	Hypothesis
S x Q_U	Discharge influences the critical streakline which influences entrainment
X x Q_U	Discharge influences cross-stream position which influences entrainment
B x Q_U	Discharge influences the efficacy of the FFGS which influences entrainment
B x Q_U^2	Discharge influences the efficacy of the FFGS which influences entrainment non-linearly

Model selection was based on Akaike Information Criterion (AIC) (Akaike 1973; Burnham & Anderson 2002). The candidate model yielding the lowest AIC value was selected as the final model. Model goodness of fit was evaluated using the Hosmer–Lemeshow goodness of fit test (Hosmer and Lemeshow 2000). In addition, the area under the receiver operator characteristic (ROC) curve was estimated to determine the predictive accuracy of the selected model (Hosmer and Lemeshow 2000). Variance inflation factors of parameters were estimated and only those with values of less than five were included within the models.

3.4.3 RESULTS

RIVER CONDITIONS

During the study period from March 3 to May 2, 2014, flows entering the junction ranged from -4,350 cfs to 21,090 cfs (**Figure 3.4-2**). The majority of juvenile Chinook salmon (61%) arrived at the junction when flows were between 7,063 and 14,125 cfs. The highest flows occurred during the first 3 weeks of the study and during the first week of April. Aside from these time periods, the flow remained below 7,063 cfs. At this level of discharge, flows typically reverse twice daily on flood tides (**Figure 3.4-2**).

Table 3.4-1 Entrainment into Georgiana Slough Binned by Low, Intermediate, and High Discharge Levels

Discharge Level	Time of Day	FFGS	QU (cfs)*1000	S (m)	X (m)	N	Number Entrained	Fraction Entrained	Predicted Probability of Entrainment
Low	Night	Off	4.69 (2.07)	16.40 (25.75)	17.99 (17.34)	36	23	0.639 (0.080)	0.495 (0.032)
		On	4.44 (2.26)	18.81 (29.13)	10.09 (19.10)	40	23	0.575 (0.078)	0.510 (0.032)
	Day	Off	4.21 (1.91)	21.18 (25.58)	17.23 (18.87)	55	20	0.364 (0.065)	0.478 (0.025)
		On	4.52 (1.73)	15.57 (26.95)	15.57 (21.55)	47	15	0.319 (0.068)	0.446 (0.029)
Middle	Night	Off	10.78 (1.72)	-15.76 (11.41)	15.15 (13.93)	344	82	0.238 (0.023)	0.262 (0.009)
		On	10.84 (1.77)	-18.65 (9.82)	14.72 (14.61)	279	57	0.204 (0.024)	0.216 (0.009)
	Day	Off	10.91 (1.65)	-19.66 (8.80)	15.39 (16.46)	199	48	0.241 (0.030)	0.185 (0.010)
		On	11.09 (1.64)	-21.50 (7.80)	14.34 (15.57)	191	33	0.173 (0.027)	0.157 (0.008)
High	Night	Off	16.23 (1.38)	-19.39 (3.85)	14.42 (14.60)	130	16	0.123 (0.029)	0.113 (0.008)
		On	16.76 (1.90)	-19.65 (3.48)	12.98 (15.35)	137	28	0.204 (0.034)	0.187 (0.011)
	Day	Off	15.60 (1.35)	-21.30 (3.02)	13.53 (15.00)	95	6	0.063 (0.025)	0.096 (0.008)
		On	16.09 (1.19)	-21.33 (3.13)	12.73 (16.88)	60	10	0.167 (0.048)	0.147 (0.015)

Notes: Values represent the mean and standard deviation (SD) when fish were in the study area for Q_U, S and X. N is the total number of fish observed in each bin. The values in parentheses for fraction entrained and the predicted probability of entrainment are standard errors (SE). Levels are defined by the 33rd and 66th quantiles (Low flow= < 7,062 cfs; Intermediate = 7,062 to 14,125cfs; High = >14,125 cfs)

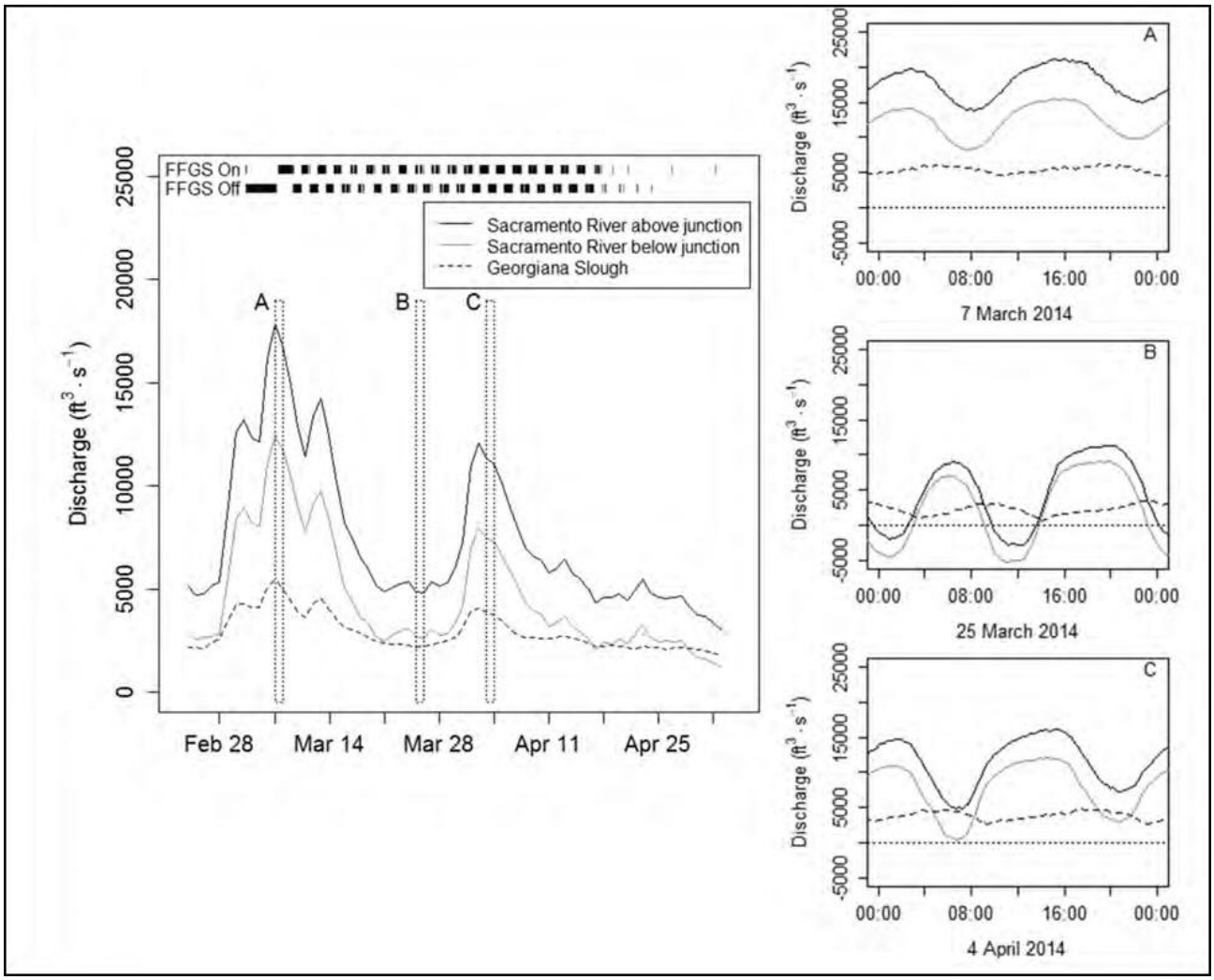

Note: The solid black line represents the total amount of discharge entering the junction. The grey and dashed lines represent the amount of flow entering each divergence at the junction. Discharge values are daily average discharge. The vertical dashes indicate when fish arrived in the study area and the state of the FFGS. Panels A, B, and C correspond to measured flow over 24 hours based on 15-minute-averaged data, indicated in the main panel. The dotted horizontal line originates at zero. In panel B during low river discharges, flows are negative at both locations in the Sacramento River during the ebb tides.

Figure 3.4-2 Discharge (daily average cfs) and Juvenile Chinook Salmon Arrivals when the FFGS was in the On and Off Positions

ENTRAINMENT SUMMARY

A total of 3,303 tagged juvenile late fall–run Chinook salmon were released between March 1 and April 15, 2014. Of these, 1,613 arrived at the study area and were deemed to be live juvenile Chinook salmon. They were used to model the probability of entrainment into Georgiana Slough. When the FFGS was in the On position, 754 fish transited the array. Of these, 166 fish (22.0%) entered Georgiana Slough. When the FFGS was in the Off position, 859 fish transited the array. Of these, 195 fish (22.7%) entered Georgiana Slough. Of the 754 fish that transited the array when the FFGS was in the On position, 313 fish passed within or 5 m (16 ft) from the buoy line surrounding the FFGS and associated structures.

Entrainment into Georgiana Slough was highest during low flows (less than 7,062 cfs, see Section 3.3.4) at night when the FFGS was in the Off position (63.9%) and was lowest during high flows (14,125 cfs) during the day when the FFGS was in the Off position (6.3%, **Table 3.4-1**). Overall entrainment at low flows was approximately

twice the entrainment rate at intermediate and high flows. Entrainment was lower when the FFGS was On during daytime low river discharges (low flow, day, On = 31.9%; low flow, day Off = 36.4%). At night during low flows, entrainment was approximately the same between On and Off states. Under intermediate flows, entrainment was lower when the FFGS was On, for both day and night periods. At night, entrainment was lower by 3 percentage points, and during the day, entrainment was lower by 6.8 percentage points. Under high river discharges (greater than 14,125 cfs) entrainment was higher when the FFGS was On, by approximately 8 percentage points at night (**Table 3.4-1**).

MODEL SELECTION

A total of 14 alternative models were fit to the data, representing different structures for the effects of covariates on entrainment in Georgiana Slough. All models provided a better fit to the data than the null model, which estimated a constant mean entrainment probability. The top five models were all within ten AIC units of the lowest AIC model, and the top three models were within two AIC units (**Table 3.4-2**). The second and third-ranked models differed from the top model by exclusion of a diel effect (*D*) and exclusion of quadratic effects of flow, respectively. Because there was an observed change in the effect of the FFGS over the range of flows (**Table 3.4-3**), a model was selected that included quadratic effects and the lowest overall AIC as the final model. An empirical LOESS fit of the binary entrainment data in relation to flow also supported this model structure (**Figure 3.4-3**). The best fit model included all covariates plus interactions of FFGS state with quadratic effects of flow (**Table 3.4-3**). The final model provided a good fit to the data and had good predictive power. The Hosmer-Lemeshow goodness of fit test was not significant ($X^2 = 8.39$, $df = 17$, $P = 0.958$), and the area under the ROC curve was 0.78, indicating the model's good predictive power (**Figure 3.4-4** and **Figure 3.4-5**).

Table 3.4-2 Model Selection Statistics for Alternative Models Used to Describe the Probability of Entrainment to Georgiana Slough

Model	Rank AIC	No. of Parameters	NLL	Deviance	AIC	ΔAIC
$\sim 1 + B + S + X + D + Qu + S{\cdot}Qu + X{\cdot}Q + B{\cdot}Qu + B{\cdot}Qu^2 + Qu^2$	1	11	719	1438	1459.76	0
$\sim 1 + B + S + X + S{\cdot}Qu + X{\cdot}Qu + Qu + B{\cdot}Qu + B{\cdot}Qu^2 + Qu^2$	2	10	720	1440	1460.03	0.27
$\sim 1 + B + X + S + Qu + D + X{\cdot}Qu + S{\cdot}Qu$	3	8	722	1444	1460.14	0.37
$\sim 1 + B + X + S + Qu + X{\cdot}Q + S{\cdot}Q$	4	7	723	1447	1460.73	0.97
$\sim 1 + B + X + S + Qu + D + D{\cdot}B + S{\cdot}Q + X{\cdot}Qu + B{\cdot}Qu + B{\cdot}Qu^2 + Qu^2$	5	12	719	1438	1461.53	1.77
$\sim 1 + B + X + S + Qu + S{\cdot}Q$	6	6	727	1454	1465.90	6.14
$\sim 1 + B + S + X + Qu + B{\cdot}Q + B{\cdot}Qu^2 + Qu^2$	7	8	731	1463	1478.94	19.18
$\sim 1 + B + X + S + Qu + D$	8	6	744	1487	1499.14	39.38
$\sim 1 + B + X + S + Qu + X{\cdot}Qu$	9	6	744	1488	1500.02	40.25
$\sim 1 + B + X + S + Qu$	10	5	746	1493	1502.82	43.06
$\sim 1 + B + S + Qu + B{\cdot}Qu + B{\cdot}Qu^2 + Qu^2$	11	7	765	1530	1543.58	83.82
$\sim 1 + B + X + Qu + X{\cdot}Qu + B{\cdot}Qu + B{\cdot}Qu^2 + Qu^2$	12	8	771	1543	1558.88	99.12
$\sim 1 + B + X + Qu + B{\cdot}Qu + B.x{\cdot}Qu^2 + Qu^2$	13	7	776	1553	1566.95	107.19
$\sim 1 + B + Qu + B{\cdot}Qu + B.x{\cdot}Qu^2 + Qu^2$	14	6	807	1615	1626.89	167.12
Null model	15	1	858	1715	1717.21	257.45

Note: Models are listed by AIC rank. (AIC= Akaike Information Criterion; NLL= negative log-likelihood)

Table 3.4-3 Model Parameter Estimates for the Final Model with Standard Errors and 95% Confidence Intervals

Variable	Parameter Estimate	SE	Lower CI	Upper CI
Intercept(FFGS Off, Night)	-0.777	0.341	-1.468	-0.123
B	0.470	0.413	-0.332	1.297
S	0.010	0.005	0.001	0.019
X	-0.012	0.008	-0.028	0.003
D	-0.247	0.138	-0.519	0.022
Q_U	0.214	0.023	0.090	0.347
Q_U^2	-0.009	0.0004	-0.002	-0.0003
$S^* Q_U$	0.006	0.0003	0.001	0.003
$X^* Q_U$	-0.002	0.0003	-0.001	-0.0003
$B^* Q_U$	-0.169	0.030	-0.119	-0.002
$B^* Q_U^2$	0.011	0.0006	0.0003	0.002

Note: SE= standard error; CI =confidence interval

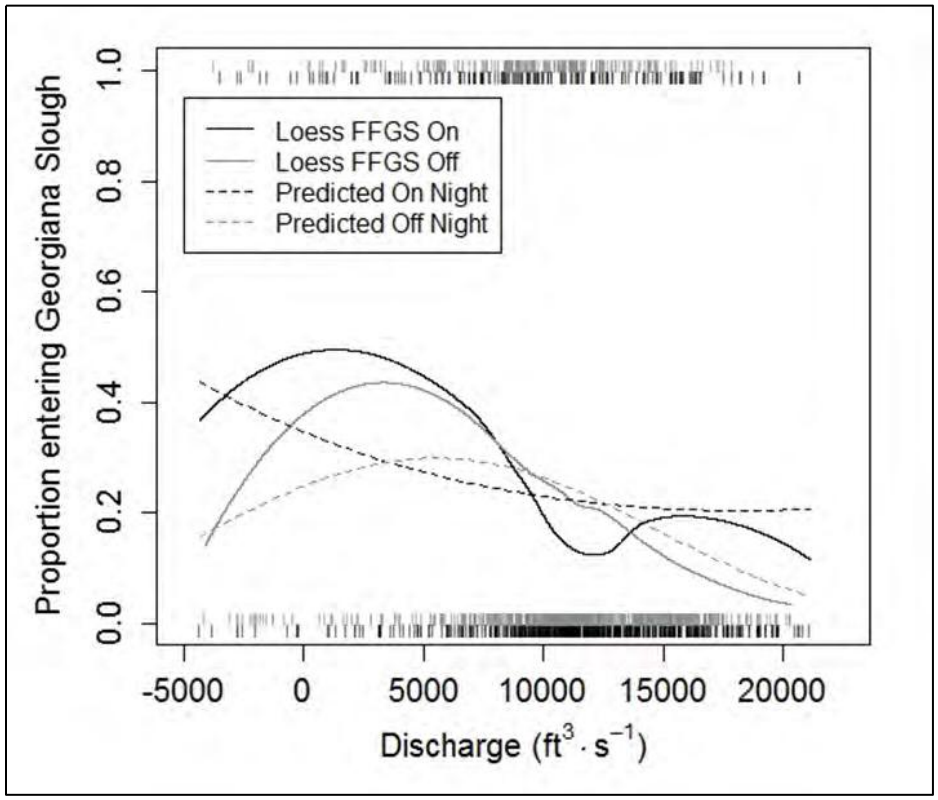

Note: The grey and black points indicate the fate of the fish when the FFGS was On (black points and line) and FFGS Off (grey points and line). The dashed lines indicate model predicted entrainment at night for mean cross-stream position and mean critical streakline location.

Figure 3.4-3 LOESS Fitted Splines for FFGS On and FFGS Off Across Flows during March and April 2014

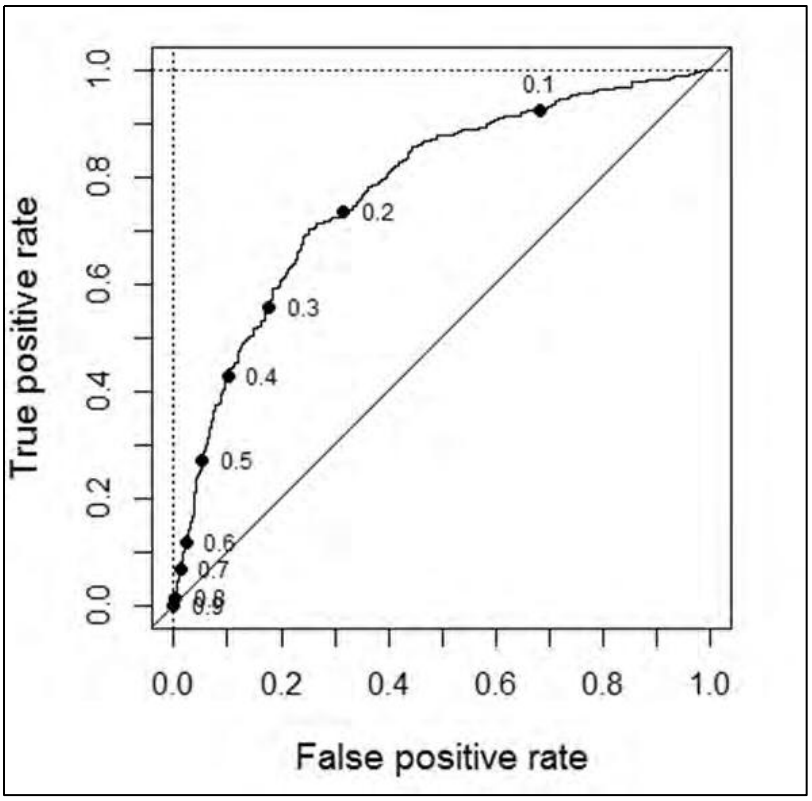

Note: The area under the curve was 0.77, indicating the model's good predictive power.

Figure 3.4-4 The Receiver Operating Characteristic Curve of the Final Model

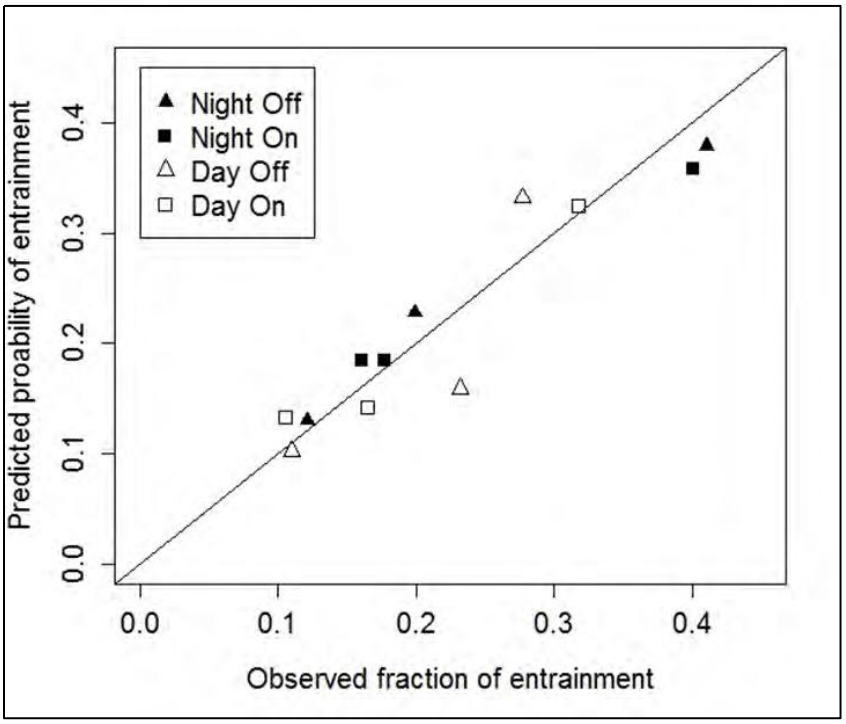

Note: The diagonal line has a slope of one. Values that are intersected by the line indicate full agreement between observed and predicted values.

Figure 3.4-5 Comparison of Observed and Predicted Georgiana Slough Entrainment Values for Night, Day, and Flow Categories

The interaction between B and Q_U^2 was significantly different from zero at an alpha level of 0.10 (z = 1.77, P = 0.078), suggesting the effect of the FFGS varied across flow (**Table 3.4-1**). These effects in the model revealed that the FFGS reduced entrainment at an intermediate range of flows, but not at higher or lower flows (**Figure 3.4-3**). As with previous studies (Perry et al. 2014), the interaction between S and Q_U was substantially different from zero (z = 3.943, P <0.001). As flow increased, the critical streakline became more negative (closer to the Georgiana Slough side of the junction), and the probability of entrainment decreased. However, the rate of decrease was greater when the FFGS was Off at high flows, rather than when the FFGS was On.

3.4.4 DISCUSSION

Overall, a similar proportion of fish entrained into Georgiana Slough were observed with the FFGS On and Off. At first glance, these findings seem to indicate that the FFGS was unsuccessful at reducing entrainment into Georgiana Slough. However, by carefully considering how an individual's probability of entrainment into Georgiana Slough changed with flow and FFGS operation, intermediate river discharges under which the FFGS reduced entrainment probability were identified. Entrainment was 3.4 to 6.8 percentage points lower when the FFGS was on at intermediate flows (7,062 to 14,125 cfs), but had the opposite effect during higher and lower flows. Entrainment was increased by 8.1 to 10.4 percentage points during high flows, when the FFGS was On. The fraction entrained during low flows at night was approximately equal between FFGS positions, but during the day, entrainment was 4 percentage points higher when the FFGS was Off. Because the study was conducted in a hydrodynamically complex location, the analysis highlights how the performance of a guidance structure can vary with environmental conditions. Considering factors such as fish distribution in the cross-section, behavioral responses that vary over the diel cycle, and the influence of flow variation can help to shed light on how guidance structures can be optimized to perform over a range of conditions.

In general, entrainment into Georgiana Slough increased as flow decreased, until the point at which flow reversed. At the lowest positive flows, the average location of the critical streakline (S) was located 15 to 20 m (33-66 ft) closer to the Sacramento side of the river or right bank (**Table 3.4-1**). This translated to higher entrainment rates and is in agreement with Perry et al (2014). As the critical streakline moved closer to the right bank, a greater percentage of fish were on the Georgiana Slough side of the critical streakline, leading to a higher probability of entrainment into Georgiana Slough and suggesting that the FFGS was unable to shift fish to the Sacramento side of the critical streakline as intended. For example, the mean location of the critical streakline during low flows intersected the FFGS in the on position. If fish were guided by the FFGS during these conditions, their cross-stream location at the end of the FFGS would have been on the Sacramento River side of the critical streakline, resulting in a lower entrainment probability. However, a small number of fish encountered the FFGS under these conditions.

The final model suggested that entrainment probabilities differed between day and night under low river discharges. However over all river discharges, entrainment into Georgiana Slough was greater at night than during the day, but only by approximately 3 percentage points. Entrainment during both FFGS states was similar during the day (day, On = 19.4 percent; day, Off = 21.2 percent). The same was true during the night (night, On = 23.68 percent; night, Off = 23.73 percent). On average, cross-stream position (X) and critical streakline (S) were similar between day and night, suggesting the cross-sectional distribution of fish as they arrived in the study area was similar. Other studies at this river junction observed no difference in entrainment probabilities between day and night (Perry et al. 2014; Perry et al. 2016). Interestingly, the interaction between B and D was not significant in the model in which it was included suggesting that the FFGS did not account for the differences in entrainment

between night and day (**Table 3.4-2**). Two possible mechanisms were identified that may have caused a difference in entrainment probabilities between day and night. First, the difference in entrainment between night and day may have been due to behavioral stimulus. The FFGS was surrounded by a stationary buoy line that was put in place to prevent boats from interacting with the FFGS. The buoy line did not move throughout the study period and may have guided fish during the day when it was more visible. A second potential reason for the observed difference in entrainment between night and day may have been differences in discharge. Although mean discharge when fish arrived in the study area was similar between night and day, nighttime flood tides tended to be of larger magnitude than daytime flood tides (**Figure 3.4-6**). In addition, there can be considerable variability in the entrainment, especially during low discharge conditions. This variability is shown in the standard deviation of the critical streakline position (**Table 3.4-1**), where the variance in the critical streakline position is high at lower discharge and low at higher discharge. This resulted in somewhat less variance in the fraction entrained between day/night and FFGS states, as the discharge increased. Although discharge was included in the model, this covariate may not have captured the variability of the hydrodynamics that affected entrainment probability differentially between day and night.

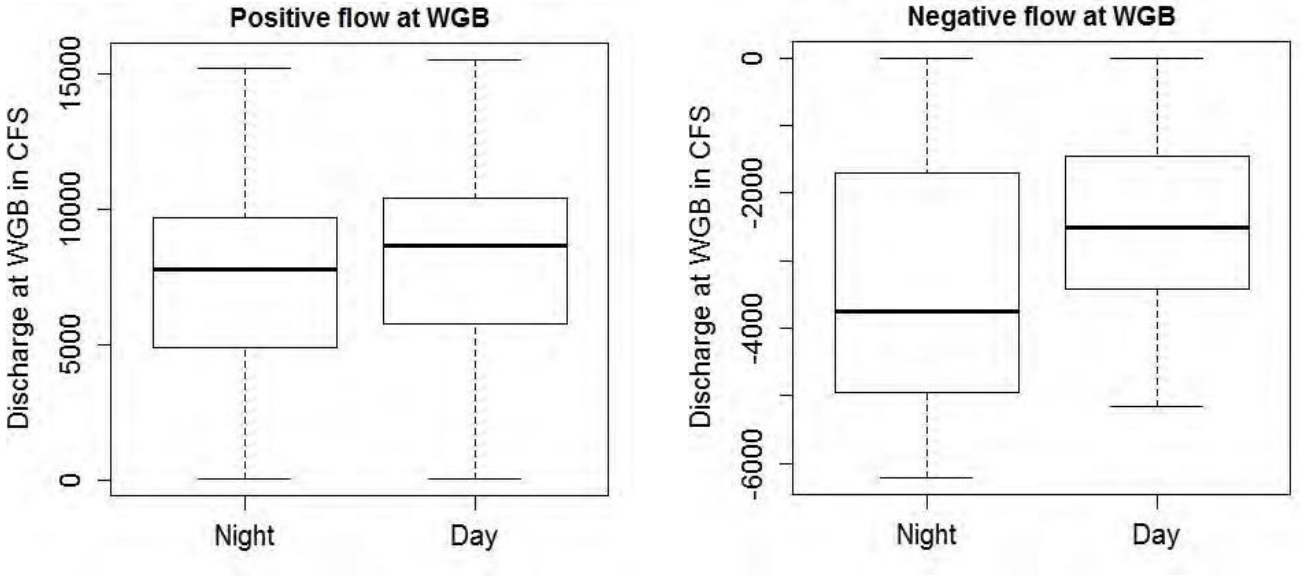

Figure 3.4-6 Comparison of Flows Observed during Night and Day during the Study Period at USGS Streamflow Gauge 11447905

Scruton et al. (2003) found that the angle of the guidance structure was extremely important and observed different guidance efficiencies at differing angles of the guidance structure. Failure of the structure to guide fish was attributed to hydraulic turbulence and irregularities in the guidance velocities along the structure. For example, when water velocity varied widely along the guidance structure and in the vertical direction, guidance efficiency was low (24.3%). Alteration of the guidance structure angle increased the efficiency by 30 to 49 percentage points (Scruton et al. 2003). Given the changing effectiveness of the FFGS across different discharges, it is plausible that the FFGS as deployed in this study may have increased turbulent conditions, such as eddy size around the FFGS that could have reduced the efficiency of the FFGS. In addition, high discharge may have been sufficient to increase the velocity of water moving under the FFGS, thereby reducing the functional depth of the FFGS (Mulligan 2014).

From previous studies (Dauble et al. 1999; Faber et al. 2010; Kock et al. 2012), FFGSs clearly are successful at guiding fishes in unidirectional rivers where velocity is low. For example, Faber et al. (2010) reported a fish guidance structure that reduced entrainment and was successful at guiding fishes to a desired location in the forebay of the second powerhouse at Bonneville Dam. Water velocities were approximately 0.2 m/s (0.6 ft/s). In contrast, water velocity at the USGS streamflow gauge 11447890 (Qu) during the 2014 FFGS study averaged 0.28 m/s (0.941 ft/s) (SD = 0.20 m/s [0.66 ft/s]) and average water velocity during ebb tides estimated from ADCP data collected within the study area was 0.29 m/s (0.946 ft/s) (SD = 0.16 m/s [0.53 ft/s]). Because of the hydrodynamic complexity of the river junction, a slight alteration in length or angle in relation to flow may have yielded different results (Scruton et al. 2003).

In conclusion, the effect of the FFGS on entrainment into Georgiana Slough varied across flows. At intermediate flows (7,062 to 14,125 cfs) the FFGS was partly successful and entrainment into Georgiana Slough was appreciably lower when the FFGS was On (during the day), but at the lowest (<7,062 cfs) and highest (>14,125 cfs) flows, the FFGS was not as effective and actually may have slightly increased entrainment into Georgiana Slough during high flows (**Table 3.4-1**). These results, coupled with the complex hydrodynamics, suggest that dynamic deployment of the FFGS should be considered. To maintain statistically robust sample sizes, the FFGS was operated in only two positions, On and Off. Intermediate positions or angles may have yielded different results. For example, under high flows, the FFGS appeared to have increased entrainment. In such instances, it may be advisable to move the FFGS to a shallower angle or even to the Off position to reduce potential turbulence created by the FFGS that may have caused entrainment into Georgiana Slough to increase. Under reversing flows, placing the FFGS in the Off position may reduce some entrainment, but because of the hydrodynamics, little could be done to prevent fish from entering Georgiana Slough because all flow entered the slough under these conditions. Future research should focus on developing an understanding of the hydrodynamics and fish response to the FFGS over a wide range of flows, and on deployment designs to increase encounter rates with the FFGS and reduce entrainment.

3.5 SPATIAL ANALYSIS OF FISH DISTRIBUTION AND BEHAVIOR

3.5.1 INTRODUCTION

As discussed in Section 3.3, the critical streakline/entrainment zone conceptual model provided a starting point for the FFGS evaluation process. The central hypothesis that the FFGS would reduce entrainment in Georgiana Slough only if it was effective at moving juvenile Chinook salmon across the critical streakline into the entrainment zone for the Sacramento River was assessed using this model. Based on this conceptual model, it is expected that the magnitude of the change in entrainment would be a product of four factors:

1. The amount of time the critical streakline was left (toward the shore) of the downstream tip of the barrier;

2. The number of juvenile salmon that encounter the barrier during periods when the critical streakline is left of the downstream tip of the barrier. This number is controlled by the arrival time and spatial distribution of juveniles at the upstream end of the barrier;

3. The barrier's ability to consistently move fish from the Georgiana Slough entrainment zone across the critical streakline into the Sacramento River entrainment zone; and

4. The rate at which fish moved between hydraulic entrainment zones after passing downstream of the barrier.

The statistical analysis in Section 3.3 showed that the barrier did not reduce overall entrainment in Georgiana Slough, but this analysis also showed that there was a discharge range where the entrainment was reduced when the barrier was On. The spatial analysis in the section described how various factors controlling barrier efficacy combined to produce these results, and to refine the conceptual model of juvenile salmon entrainment at tidal junctions.

3.5.2 METHODS

DATA SOURCES AND RELEASE GROUPS

In this section spatial aggregation is used to increase the overall sample size to allow for statistically meaningful sub-sampling of the entire data set based on various covariates, such as hydrodynamic conditions, day vs. night, and so on using the covariate aggregation approach described in the 2012 GSNPB report (DWR 2015b). To do this, tracks from multiple studies and release groups were combined to improve the spatial resolution and statistical power of the 2D statistics that are calculated for each group. Because spatial analyses are conducted on groups of fish aggregated based on covariate values, rather than on temporal continuity, fish tracks from multiple release groups and different studies can be integrated as long as all of the covariates needed for this integration were measured in a similar manner across all studies. Aggregating data from multiple release groups and studies helps to expand the range of conditions that fish in a covariate group experience, which can make comparisons between covariate groups more robust to factors that were not explicitly measured or addressed in any analyses.

For this analysis, tracks of acoustically tagged juvenile Chinook salmon that were released during the 2008 North Delta Study (Romine et al. 2013) were used to provide information on fish distributions during low flow periods when no barrier was present. The 2008 study data were chosen as a measure of baseline conditions for several reasons:

1. Fish were released over a similar range of Sacramento River flows in both 2008 and 2014;

2. Fish were released into the Sacramento River at the same location in 2008 and 2014; and

3. Fish experienced similar trucking, tagging, and handling conditions in 2008 and 2014.

It is important to note that during the 2014 study, fish were released later in the year than the 2008 study fish. Because of this later release, fish were larger in 2014 and were subjected to higher water temperatures than the 2008 study fish, so comparisons between these study years may be affected by these differences. Fish tracks collected during periods when the BAFF was not operating in 2011 and 2012 were not used for barrier-Off baseline conditions because this study was conducted during substantially higher river discharges. In addition, during the 2011 and 2012 study, fish were released much closer to the Georgiana Slough junction. Finally, even though the BAFF was not operating, considerable infrastructure associated with the BAFF was in place during 2011 and 2012, so the 2008 data are the only truly non-barrier data set.

TRACK PROCESSING

Fish tracks for the 2014 and 2008 studies were generated using the FishCount and GeneticFish software packages previously described (see Section 2.5.2)[14]. Before the spatial analysis pre-processing steps were conducted, the 2008 data was processed through an outlier removal program that removed data points that increased the overall track length by 5 m (16 ft), and removed any two points that jointly increased the overall track length by 10 m (33 ft) (excepting the start and end points). This effort greatly reduced the number of outliers caused by multipath echoes.

The 2014 tracking data were run through a genetic smoothing algorithm that moved each data point location within a predicted uncertainty radius while seeking to reduce the track's overall tortuosity and sum of squared acceleration. The resulting smoothed tracks were then processed through the same outlier removal program as the 2008 tracks.

These smoothing processes were aimed at improving the spatial resolution of fish density distributions to better detect changes in fish density in the 5-meter (16-ft) gap between the stand-off buoys and the face of the FFGS. As a result, these processes were not applied to the tracks prior to other analyses discussed in this report. The smoothing of the post-processed 2014 data removed low-amplitude, high-frequency noise. These tracks showed less high frequency motion than the 2008 tracks, but the two data sets remain comparable over time scales greater than 10-20 seconds.

TRACK SEGMENTATION

During the 2008 and 2014 studies Sacramento River inflow was low enough that the flows on the Sacramento River below Georgiana Slough reversed on flood tides and entered the junction from the downstream direction. As a result, it was possible for an tagged juvenile salmon to pass through the junction multiple times.

In order to separate each fish's exposure to the junction into individual "treatments", each fish's track was divided into individual segments based on temporal gaps in the track. This applied to fish which moved outside the array for some period of time then re-entered the array. Each separate segment was then treated as an independent observation. The track segmentation process was carried out using the same methods developed for the 2012 GSNPB spatial analysis (DWR 2015b), with several additional steps added to reduce the influence of predatory fishes. This filtering identified movement patterns that could only be the result of fish with greater sustainable swimming performance than juvenile Chinook salmon. After the tracks were segmented, the following rules were used to discard such track segments:

1. Any segment that started and ended upstream of the junction area were discarded, as these fish did not interact with the FFGS or the junction area. Subsequent segments for each tag code were still considered potentially valid;

2. Any segment that originated in Georgiana Slough and moved upstream into the junction were considered to be predatory fishes because Georgiana Slough never reversed during the study period. All subsequent tracks for these tag codes were removed from further analysis;

[14] Note that the 2008 study data were processed as part of the 2012 GSNPB study (DWR 2015b).

3. Any segment that originated in the Sacramento River downstream of the junction and moved upstream into the junction during ebb tides were considered to be predator fishes. All subsequent tracks for these tag codes were removed from further analysis; and

4. Any segment that remained in the junction for more than 24 hours or moved upstream into the junction from the Sacramento River more than 24 hours after first exiting the junction were considered to be predatory fishes and all subsequent tracks for those tag codes were discarded.

Estimating the Location of the Critical Streakline (Downstream Tip of Barrier)

The maps of streamline locations and critical streakline locations (see Section 3.3, "Hydrodynamics and Critical Streakline") showed that the critical streakline maintained curvature over the range of hydrodynamic conditions observed during the 2014 study. For this reason, the location of the critical streakline at the upstream start of the barrier could not be used to reliably predict the location of the critical streakline at the downstream tip of the barrier.

Because it is anticipated that the location of the critical streakline at the downstream tip of the barrier would be a key variable in predicting the barrier's efficacy, the cross-stream location of the critical streakline at the downstream tip of the barrier at the time that each 2014 fish passed the downstream tip of the barrier was directly estimated using 15-minute streamline maps produced as part of the hydrodynamic analysis described in Section 3.3.

Two-dimensional water velocity maps for the 2008 study period were not available, so the location of the critical streakline relative to the location of the downstream tip of the barrier for 2008 study fish tracks was estimated by developing a relationship to link the location of the critical streakline relative to the downstream tip of the barrier to the location of the critical streakline at the upstream start of the barrier calculated using the flow ratio method (Section 3.3). In order to develop this relationship, 2014 streamline maps were used to create a set of data points relating the location of the critical streakline calculated using the flow ratio method to the observed cross-stream location of the critical streakline relative to the downstream tip of the barrier for every 15-minute streamline map. A polynomial regression was used to predict the cross-stream location of the critical streakline relative to the tip of the 2014 barrier for each 2008 track segment based on the flow ratio calculated for each 2008 track segment.

Calculating Track Cross-Stream Movement Relative to the Critical Streakline

In order to compare the cross-stream motion of each fish to the cross-stream path of the critical streakline, every track was transformed into a coordinate system defined by the shape of the critical streakline at the time that the fish track passed the downstream tip of the barrier. For every fish track in the 2014 FFGS data, the x, y, coordinates of the critical streakline were extracted from the nearest 15-minute streamline map. These values were used to define the along-stream axis of a curvilinear coordinate system.

The cross-stream axis was defined as being instantaneously perpendicular to the along-stream axis with positive values increasing towards the right bank of the Sacramento River (away from the barrier and Georgiana Slough). This coordinate system was then used to calculate the cross-stream location of each 2014 fish track when it passed the upstream start of the barrier and when it passed the downstream tip of the barrier. The difference between these two values was reported as the change in cross-stream location relative to the critical streakline, with positive values indicating that the fish moved away from the barrier in the cross-stream direction. This process

was repeated for the 2008 data using a lookup table based on flow ratio to pick a 15-minute streamline map for each 2008 study fish track.

Calculation of Continuous Entrainment Curves

Continuous entrainment rate curves were calculated to show entrainment into Georgiana Slough as a function of various covariates. The method used to compute these curves is conceptually similar to LOESS smoothing methods. A vector of binary entrainment values (0 for Georgiana Slough, 1 for Sacramento River) describing the fate of each fish track was sorted by the independent variable of interest. A rolling window function was used to calculate the average entrainment rate for the fish in the window, and the average covariate value of the fish within the window was logged as the independent value associated with the observed window entrainment rate. This window function was then repeated over the entire record without wrapping. A window size of 100 fish was used to calculate the entrainment rate curves referenced in this section.

Turning Point Analysis and Type Classification

Several different categories of motions were observed in the individual fish tracks. In order to classify fish tracks into type categories based on the differences in the observed motions, software was developed to identify "turning points" where fish tracks initiated sustained cross-stream excursions. This software mapped each fish track into an along-stream and cross-stream coordinate system with the along-stream axis defined by an approximation of the location of the thalweg in the Sacramento River, and the cross-stream axis defined as being instantaneously perpendicular to this axis, increasing in the positive towards the right bank.

Once tracks were transformed into this coordinate system, time series of cross-stream velocity and acceleration were calculated using standard numeric methods, and spectral analysis was used to quantify the strength of the periodicity in these cross-channel movement metrics. Turing points were extracted by using a standard LabVIEW view peak detection algorithm to find peaks in a low-pass filtered signal relating cross-stream position to along-track position. This information was combined with measures of tortuosity, net cross-stream displacement, and estimated along stream water velocities to classify the tracks as belonging to one of four types which we define and discuss in greater detail in the results section.

3.5.3 Results

FFGS's Expected and Observed Effect on Entrainment in Georgiana Slough

As discussed in Section 3.3.1, "Introduction, Background, and Context", the FFGS was initially evaluated within the framework of the critical streakline conceptual model. Based on this framework, the FFGS was expected to reduce entrainment in Georgiana Slough for fish that encountered the FFGS when the critical streakline was to the left of the downstream tip of the barrier during tides (see **Figure 3.3-6** in Section 3.3, "Hydrodynamics and Critical Streakline"). While hydraulic conditions were not optimal for this FFGS, the hydrodynamic analysis did show that the critical streakline was in a position where the barrier could have been effective about 30 percent of the time the barrier was operational (Section 3.3). However, knowing the amount of time the critical streakline was in a location where the barrier was expected to be effective does not reveal the percentage of study fish that may be influenced by the barrier. The number of fish that encountered the barrier during these times must be known because this value the product of the overall fish arrival time distribution and the tidal timescale spatial distribution of fish arriving at the barrier.

Additionally, the possibility that fish might respond to the hydrodynamic effects of the barrier or the stand-off buoys along the face of the barrier without directly encountering the barrier was considered likely during the barrier design process. If the barrier or the stand-off buoys increased the barrier's effective cross-stream signature this would expand the range of critical streakline positions associated with barrier efficacy and would increase the number of fish that we would expect the barrier to influence.

In order to understand how many fish interacted with the barrier when the critical streakline position was optimal, and to understand how increasing the barrier's effective zone of influence could change the number of fish protected by the FFGS, two dimensional frequency distributions were computed for fish transiting the junction during tides.

These frequency distributions show the number of study fish that shared a pair of covariate values; in this case the functions show how many study fish experienced a particular critical streakline condition as a function the fish's cross-stream location at the start of the barrier. By plotting the distribution of study fish in this manner the number of fish interacting with the barrier when the critical streakline was within an optimal range can be estimated along with the number of fish that might have been guided if the barrier's cross-stream signature was expanded (see **Figures 3.5-1**, **3.5-2**, and **3.5-3**).

The region containing fish corresponding to values that were expected to be predictive of FFGS efficacy are indicated by the dashed lines on **Figures 3.5-1** through **3.5-3**, while the dotted lines show the range of values corresponding to fish that could have been potentially protected if the buoy line (located +5 m [16 ft] in the cross-stream direction from the barrier) moved fish across the critical streakline into the Sacramento River entrainment zone. The number of fish contained in each region for the FFGS On, FFGS Off, and no barrier (2008 data) conditions are shown in **Table 3.5-1**.

Table 3.5-1 Number of Fish With the Covariate Values Associated FFGS and Buoy Line Efficacy

	Number of Fish that Arrived Under Conditions where it was Expected the FFGS to be Effective	Number of Fish that Arrived Under River Discharges where the Buoy Line could have Influenced Fish Behavior	Number of Fish Entrained in Georgiana Slough with the Values for Expected Efficacy (% Entrained)
2014 FFGS Operational	17	66	6 (35%)
2014 FFGS Non-Operational	26	46	4 (8%)
2008	12	78	3 (25%)

The probability distributions shown in **Figures 3.5-1** and **3.5-2** for FFGS non-operating and operating conditions are very similar, and show that most fish were concentrated in the river cross-section between +10 m (+33 ft) and +50 m (+164 ft) (+ sign = right of the barrier tip). These distributions also show that the majority of fish passed the barrier when the critical streakline was between +2.5 m (+8.2) and + 12.5 m (+41.0 ft) to the right of the barrier's tip. Thus, very few fish had the combination of cross-stream location and critical streakline position values expected for the FFGS to be effective for (17 barrier operational, 26 barrier non-operational).

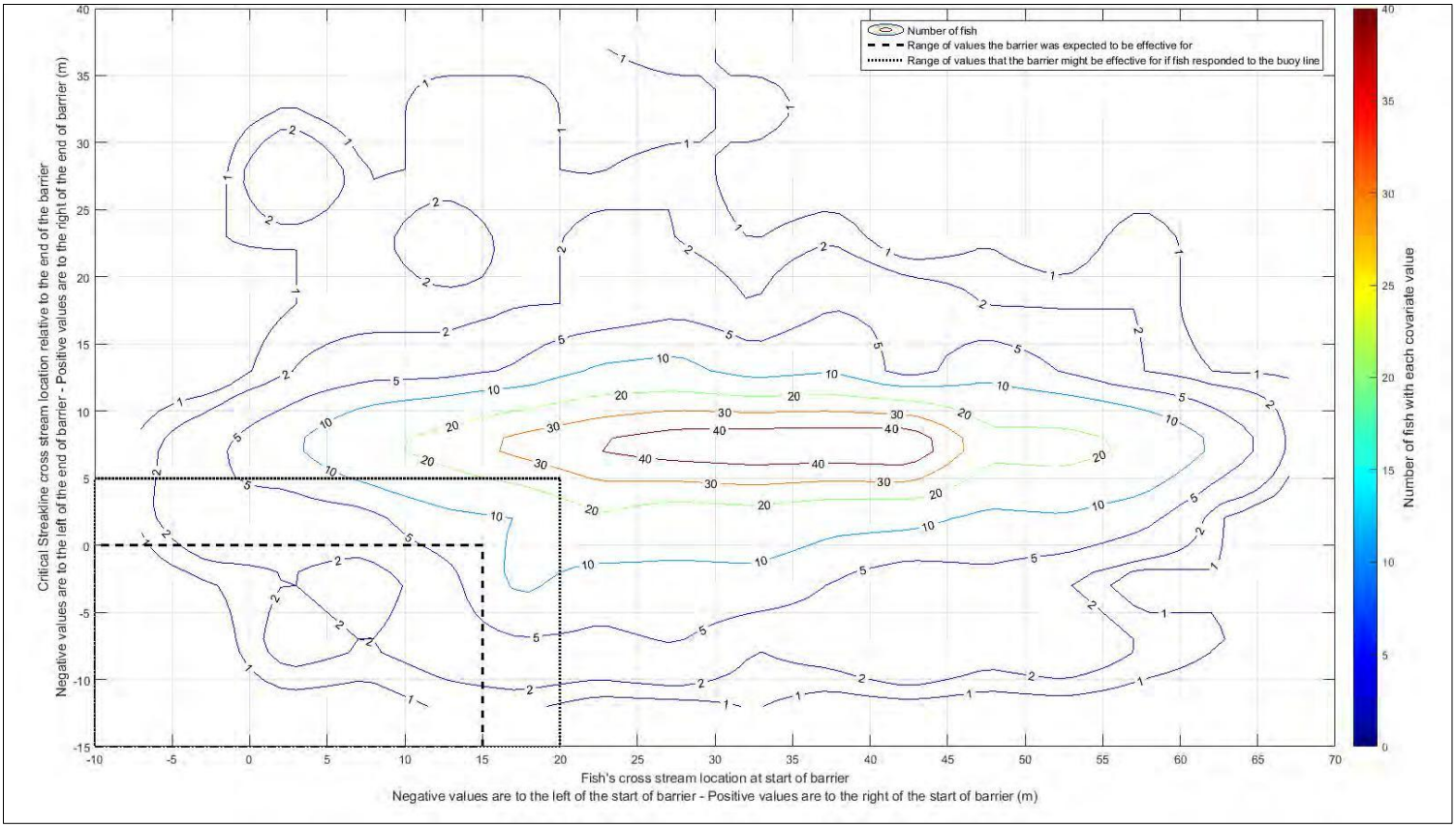

Figure 3.5-1 Contour Plot Showing Distribution of Cross-Stream Location and Critical Streakline Location for Study Fish Passing by the FFGS on Ebb Tides (FFGS On)

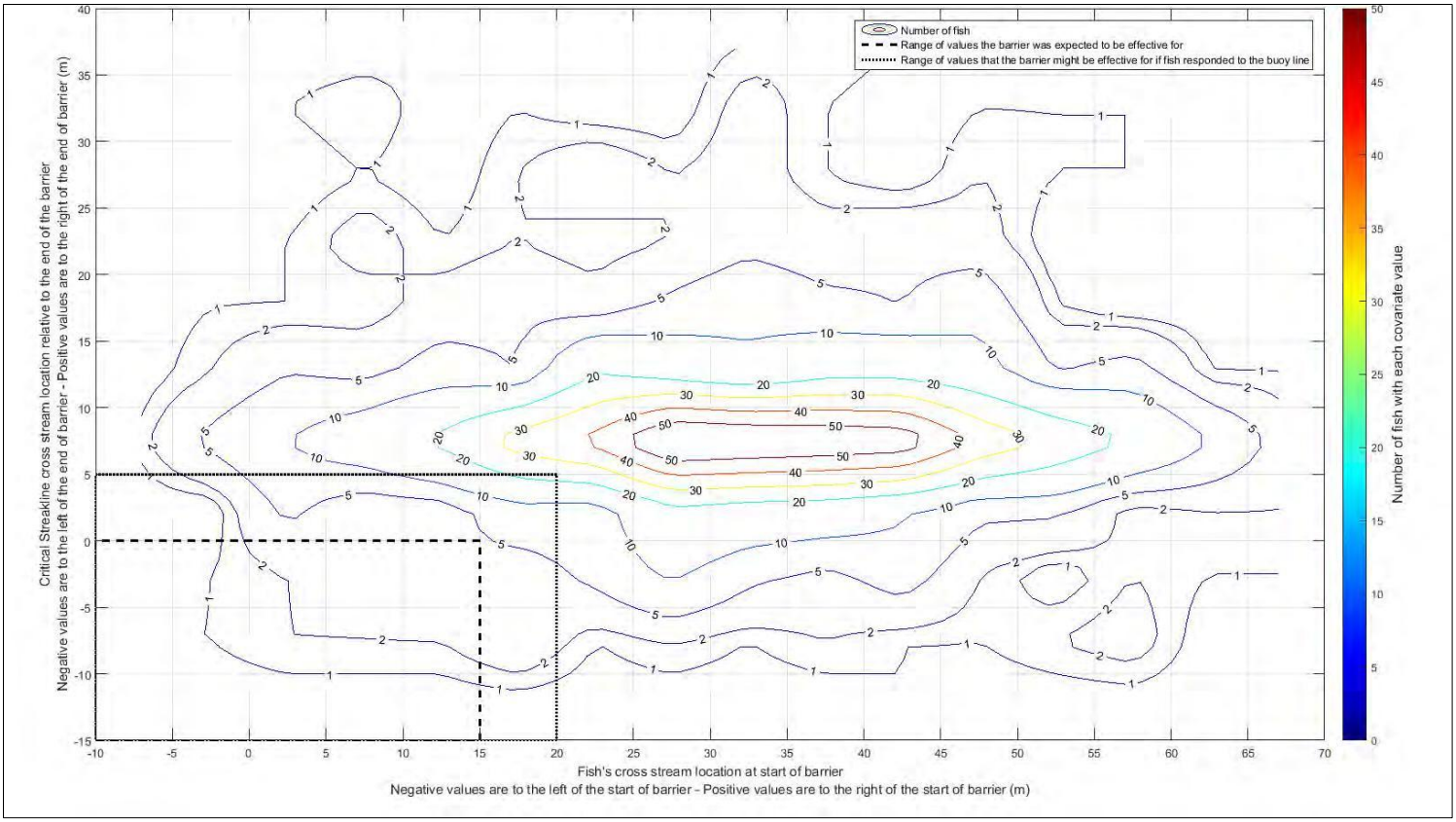

Figure 3.5-2 Contour Plot Showing Distribution of Cross-Stream Location and Critical Streakline Location for Study Fish Passing by the FFGS on Ebb Tides (FFGS Off)

Because of the high gradient in the cross-stream distribution of fish and the narrow range of critical streakline values these fish experienced, a behavioral response occurring at the buoy line could have influenced the fate of 4 times as many fish (66 barrier On, 46 barrier Off). Although these numbers still represent a small portion of the overall ebb tide samples (818 ebb fish barrier On, 919 ebb fish barrier Off), a significant reduction in the entrainment rate for 50-70 fish distributed across such a narrow range of covariate values would result in an observable reduction in entrainment.

The frequency distribution for 2008 ebb tide fish in **Figure 3.5-3** shows that that the bulk of the 2008 fish encountered a slightly narrower range of critical streakline values, but that these fish were more broadly distributed in the river cross-section. This resulted in similar numbers of fish in the expected and possible zones of barrier efficacy (12 and 78, respectively). These observations suggest that the 2008 data should be a good "baseline" data set for comparing entrainment rates during ebb tide periods, but, differences between the cross-stream distributions of fish at the upstream start of the barrier is likely to make direct comparisons of spatial data difficult.

Continuous entrainment rate curves were calculated to see if there was a lower entrainment rate for fish that passed the barrier when the critical streakline was near the tip of the barrier. Differences in the entrainment of ebb tide fish between FFGS operational and non-operational, 2008 conditions as a function of critical streakline location (**Figure 3.5-4**, solid lines), and cumulative distribution curves were calculated to illustrate the proportion of ebb tide fish that experienced each critical streakline condition (**Figure 3.5-4**, dashed lines). These curves show that for critical streakline values ranging from -5 meters (-16 ft) to +2.5 m (+8.2 ft), there was a slight reduction in the entrainment of fish transiting the junction during tides with the barrier On versus barrier Off.

For this range of critical streakline values both barrier operational and non-operational, fish experienced lower entrainment than 2008 study fish. Additionally, the 2014 fish study demonstrated lower entrainment with the barrier operating for all ebb tide critical streakline values greater than +6 m (+20 ft), even though the 2008 study fish study showed lower entrainment than the barrier operational fish for ebb tide critical streakline values greater than + 10 m (+33 ft).

While barrier operational entrainment was lower than barrier non-operational entrainment for a broad range of ebb tide critical streakline values, the barrier appeared to either increase entrainment or produce very little change in entrainment over the narrow range of critical streakline values experienced by the majority of the study fish (as shown by the dashed lines on **Figure 3.5-4**). The combination of the two effects results in a minimal difference in overall entrainment rates between all FFGS operational and FFGS non-operational fish tracks.

The LOESS-smoothed entrainment curves shown in **Figure 3.4-3** in Section 3.4, "Generalized Linear Modeling of Fish Fates" indicate that the barrier reduces entrainment in Georgiana Slough over a range of Sacramento River flows. However, these reductions were offset by periods when entrainment was higher with the FFGS operational over the study period.

This page intentionally left blank.

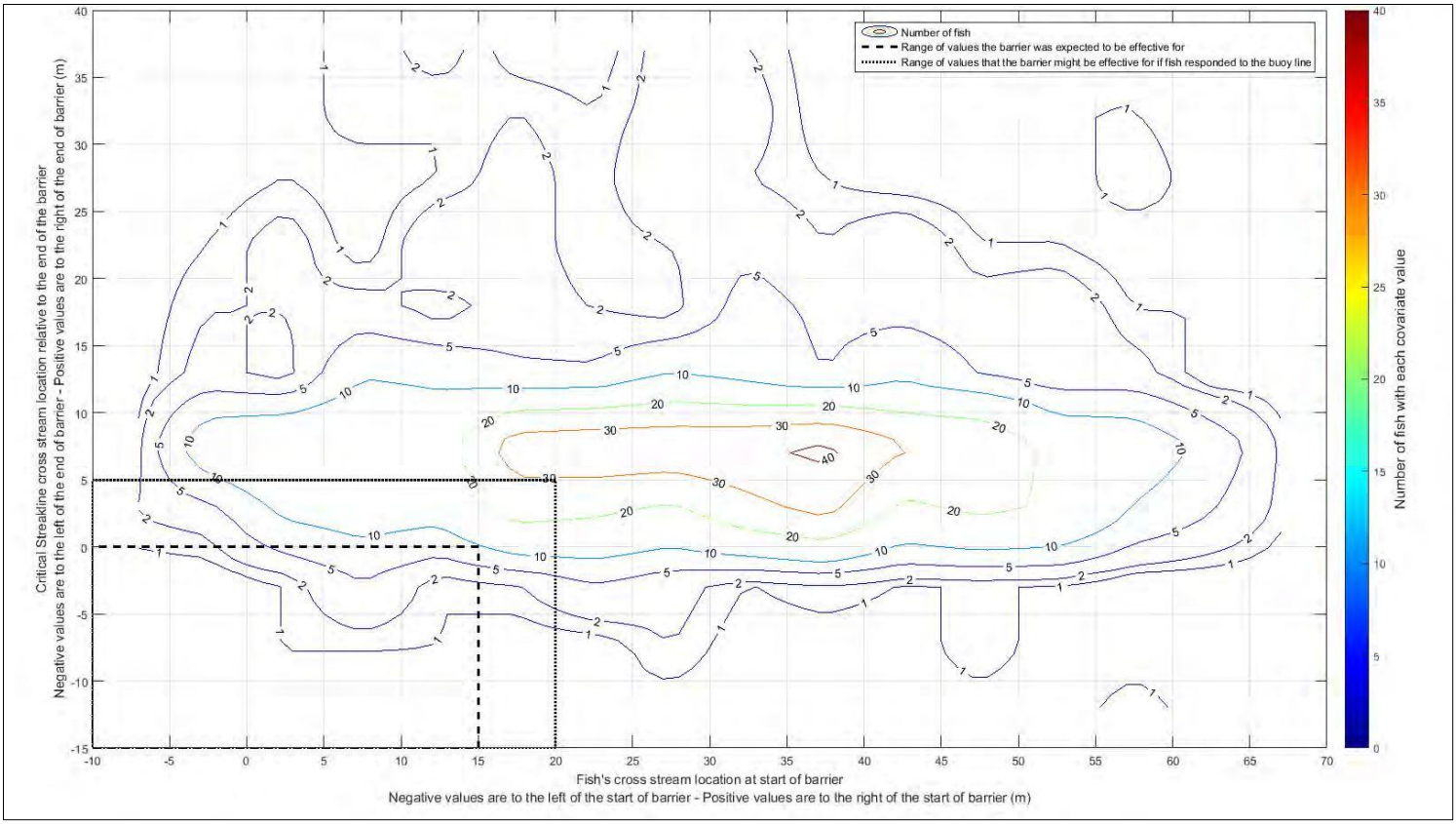

Figure 3.5-3 Contour Plot Showing Distribution of Cross-Stream Location and Critical Streakline Location for Study Fish Passing by the FFGS On Ebb Tides (2008 Study Data)

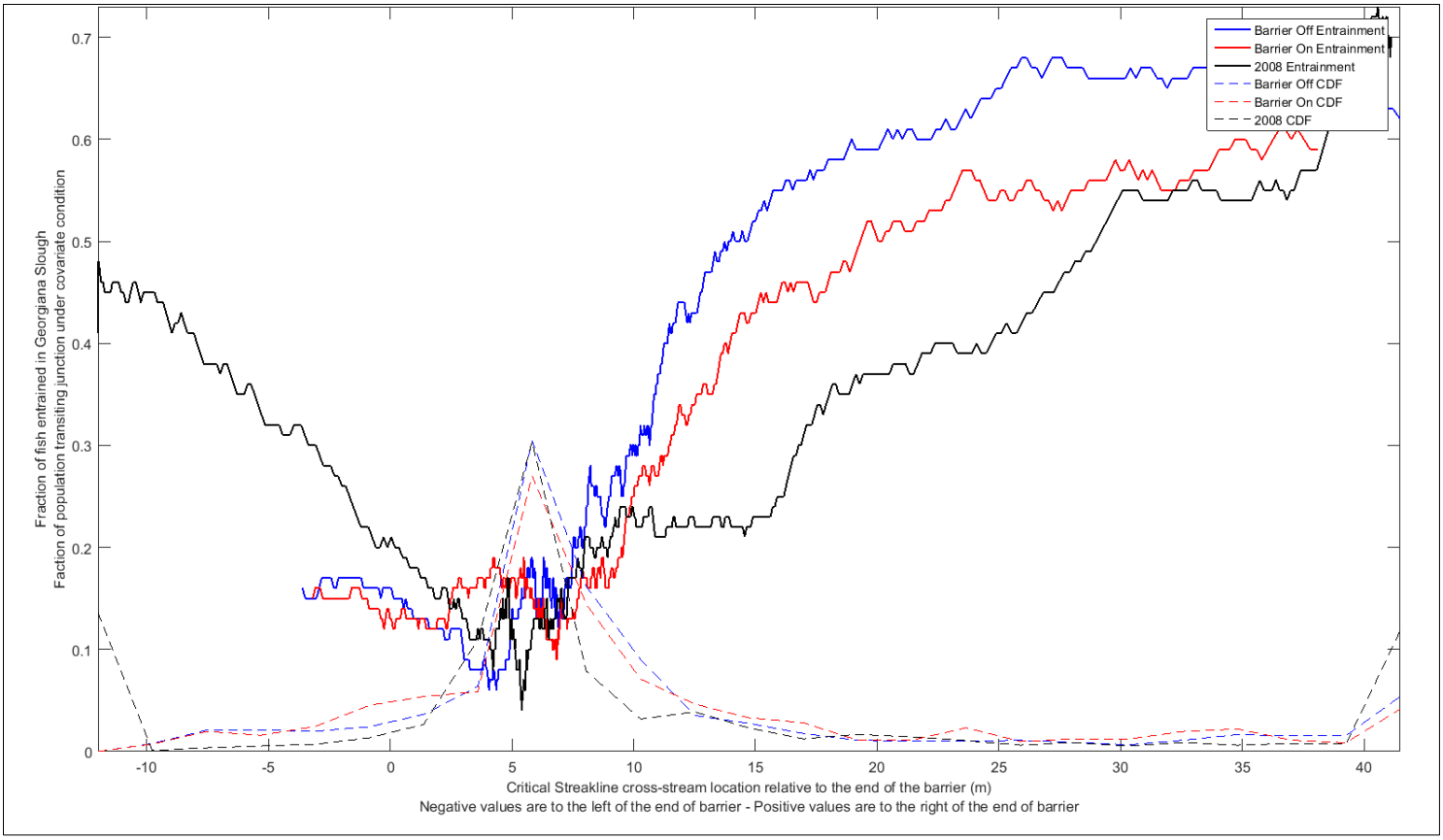

Figure 3.5-4 **Continuous Entrainment Rate in Georgiana Slough as a Function of Critical Streakline Location**

In order to investigate whether this trend was because of an underlying relationship between flow and the location of the critical streakline: 1) continuous entrainment rate curves were calculated as a function of instantaneous flow in the Sacramento River upstream of Walnut Grove (**Figure 3.5-5** solid lines); 2) cumulative distributions that show the proportion of ebb tide fish that transited the junction at each flow value (**Figure 3.5-5** dashed lines); and [33]) a plot of each fish's critical streakline location as a function of the corresponding instantaneous flow for 2014 tracks (**Figure 3.5-6**).

The method used for calculating continuous entrainment rates is similar to the LOESS method used in Section 3.4 and the curve in **Figure 3.5-5** shows the same trends but with more high-frequency variance. The relationship between Sacramento River flow and critical streakline location appears to explain several trends in the flow versus entrainment curves for low to medium flow values:

1. The strong negative relationship between flow and critical streakline location when flows are less than 10,600 cfs likely explains the negative relationship between Sacramento River flow (as measured at station WGA);

2. Entrainment in this same flow range; and

3. The increased share of critical streakline values near the barrier tip for Sacramento River flow values between 3,600 cfs (100 cms) and 12,400 cfs (350 cms) may explain why the barrier reduced entrainment at intermediate flow values.

However, the slope of the relationship between flow and critical streakline location is near zero when flows exceed 12,400 cfs (350 cms) (**Figure 3.5-6**), suggesting that there is only a very weak relationship between critical streakline location and Sacramento River flow during higher flows. Therefore, trends in entrainment at higher flow values are unlikely to be driven by a relationship between flow and critical streakline location.

In order to identify whether the reduction in entrainment produced by the FFGS at low critical streakline values was because of a change in fate for the fish that were expected to be protected by the FFGS, two dimensional frequency distributions were computed showing the change in the number of fish entrained in Georgiana Slough as a function of critical streakline location relative to the downstream tip of the barrier and the fish's cross-stream position at the upstream start of the barrier (**Figure 3.5-7**). This figure is similar to the distributions in **Figures 3.5-1** through **3.5-3**, except that instead of showing the number of fish that transited the junction under each condition, it shows how changes in entrainment in Georgiana Slough were distributed across the two covariate ranges.

Georgiana Slough entrainment distributions for each condition were normalized to fish per 1000 samples before calculating the difference to account for the different sample sizes between FFGS operational and non-operational conditions. Surprisingly, this plot shows that reductions in entrainment when the FFGS was operational were not associated with the combination of covariate values predicted by our critical streakline conceptual model. Most of the reduction in entrainment at low critical streakline values (less than +2.5 m [+8.2 ft]) was because fish that entered the junction in the center of the river cross-section where streamlines did not come into contact with the FFGS or the buoy line.

At the same time, there was a relative increase in entrainment when the FFGS was operational for fish the FFGS was expected to protect. The most significant reduction in entrainment when the FFGS was operational occurred for fish with median cross-stream starting positions and critical streakline values.

None of these findings are consistent with the hypothesis that the FFGS will reduce entrainment for fish that are advected toward the FFGS at times when the critical streakline is at or near the tip of the FFGS. Instead, **Figure 3.5-7** suggests that the observed trends in entrainment for FFGS operational vs. FFGS non-operational conditions are because a mechanism that is not explained by fish that fundamentally follow flow streamlines (e.g., a purely advective model of fish movement).

SPATIAL ANALYSIS OF FISH TRACKS FROM EBB TIDE

A spatial analysis of the 2014 data was performed using an approach similar to that described in the 2012 GSNPB Report (DWR 2015b); during this analysis the distribution of fish tracks, distributions of entrainment rates, and distributions of overall entrainment in the junction area were mapped. These distributions were compared between entrainment groups based on light, critical streakline location, starting cross-stream location, and water velocity magnitude in the study area. This analysis did not suggest any clear relationship in the distribution of these parameters as a function of the observed covariates, but comparisons between the summary distributions for the FFGS On, FFGS Off, and 2008 data sets are informative.

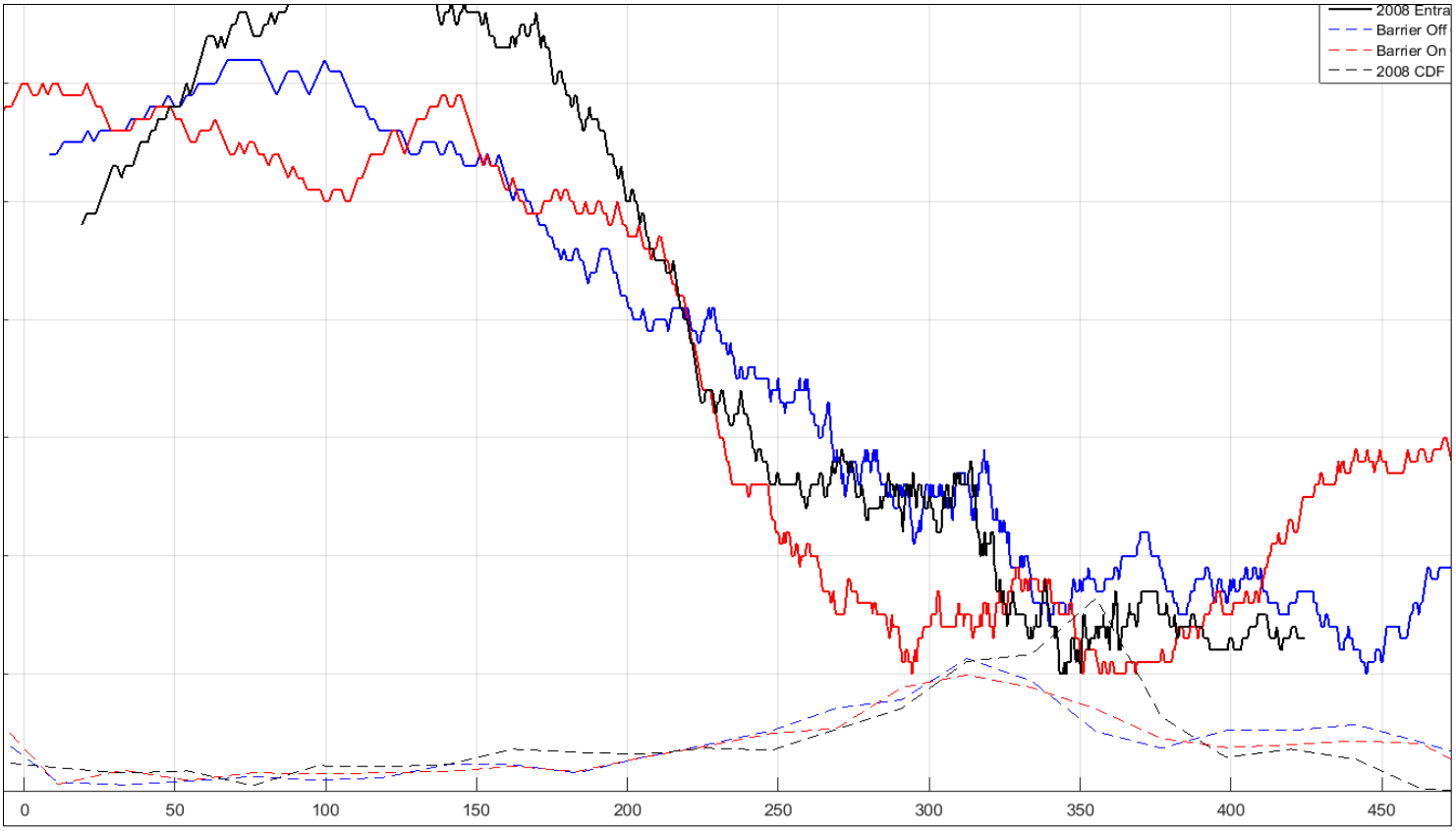

Figure 3.5-5 Continuous Entrainment Rate in Georgiana Slough as a Function of Sacramento River Sacramento River Flow

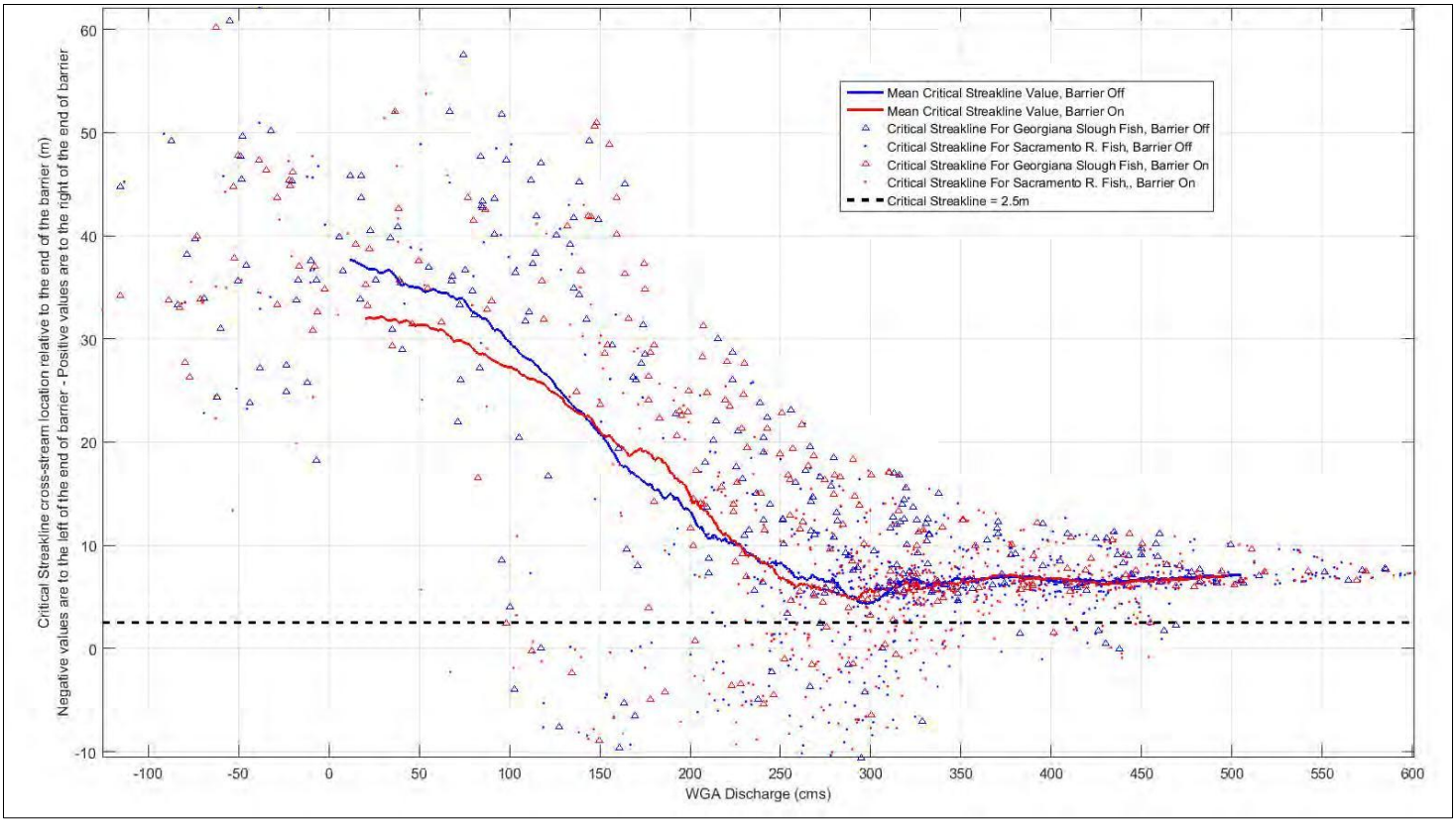

Figure 3.5-6 **Plot Showing the Relationship of Sacramento River Flow and the Critical Streakline Location when Study Fish Passed the FFGS**

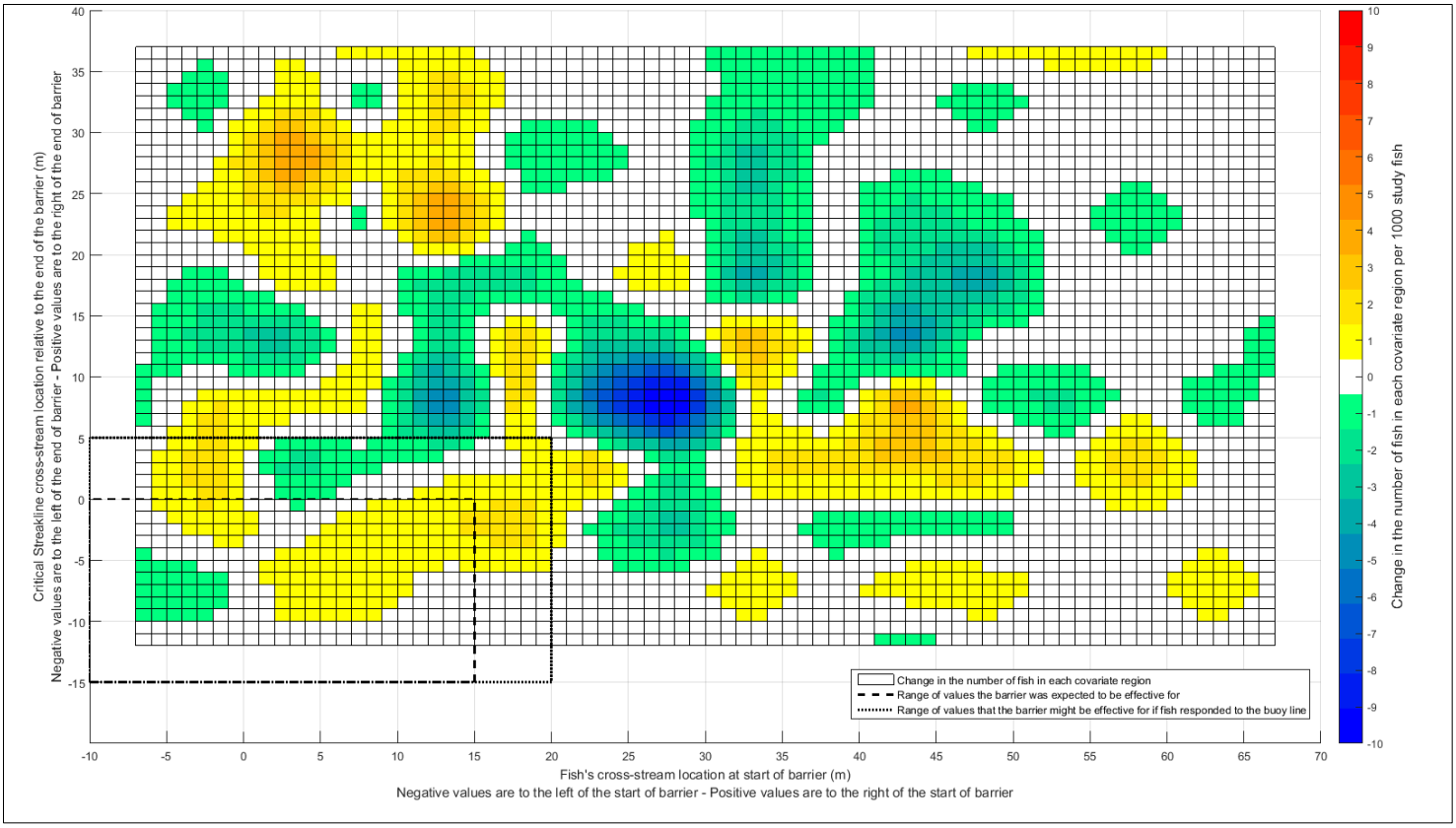

Figure 3.5-7 Flood Plot Showing the Change in the Number of Fish Entrained in Georgiana Slough for Cross-Stream and Critical Streakline Location (FFGS On and FFGS Off)

The spatial distribution of all ebb tide fish for FFGS Off and FFGS On conditions are shown in **Figure 3.5-8** and **Figure 3.5-9**, and the difference between these distributions is shown in **Figure 3.5-10**. For comparison, the spatial distribution of all ebb tide fish from 2008 is shown in **Figure 3.5-11**, and the difference between the barrier operational distribution and the 2008 distribution is shown in **Figure 3.5-12**.

As with **Figure 3.5-7**, all distributions shown were normalized to a sample size of 1000 fish to account for differences in sample sizes.

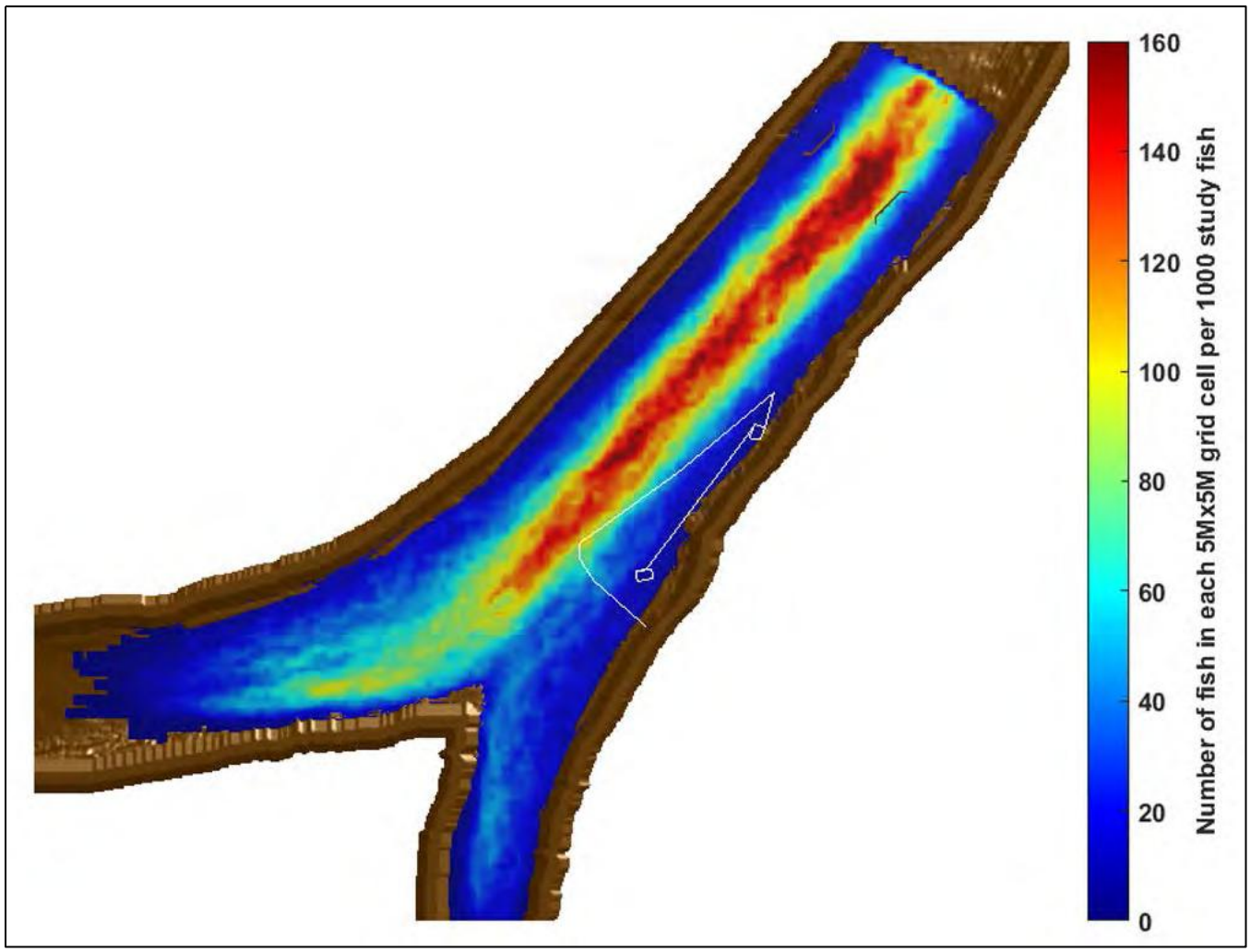

Note: The location of the standoff buoys and FFGS structures in the non-operational position are drawn in white. The measured fish densities are artificially low at the edges of the domain due to variance in tracking performance between fish tracks at the peripheries of the hydrophone array. Note the shift the high-density zone drawn in red when the edge of this zone contacts the stand-off buoys.

Figure 3.5-8 Spatial Distribution of Fish Tracks Passing Through the Junction During Ebb Tide (FFGS Off; N=909)

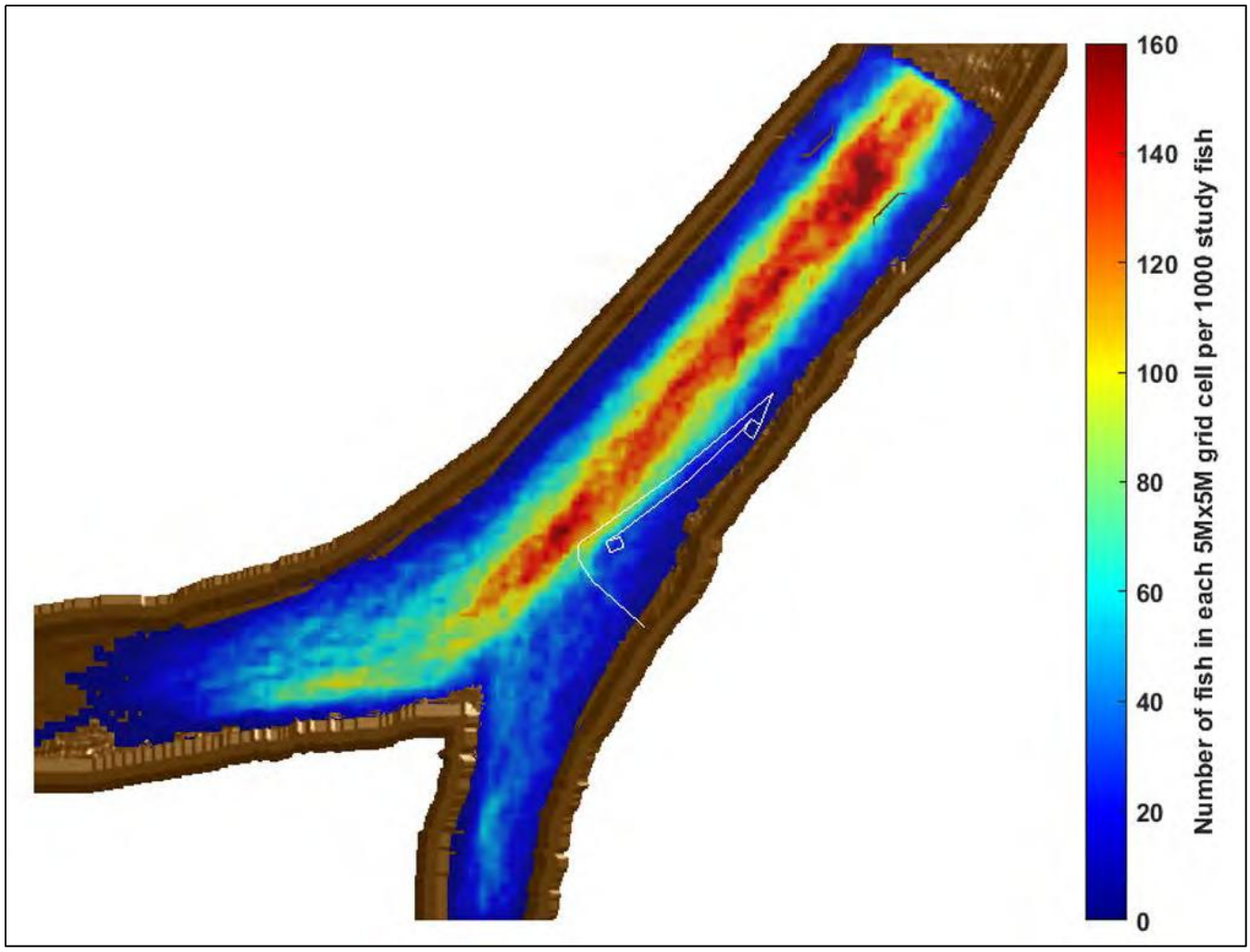

Note: The location of the standoff buoys and FFGS structures in the operational position are drawn in white. The measured fish densities are artificially low at the edges of the domain due to variance in tracking performance between fish tracks at the peripheries of the hydrophone array. The front between the moderate density zone (green) and the low density zone (blue) follows the face of the barrier. Also note that the slight shift the high-density zone drawn in red when the edge of this zone contacts the stand-off buoys is still apparent.

Figure 3.5-9 Spatial Distribution of Fish Tracks Passing Through the Junction During Ebb Tide (FFGS On; N=818)

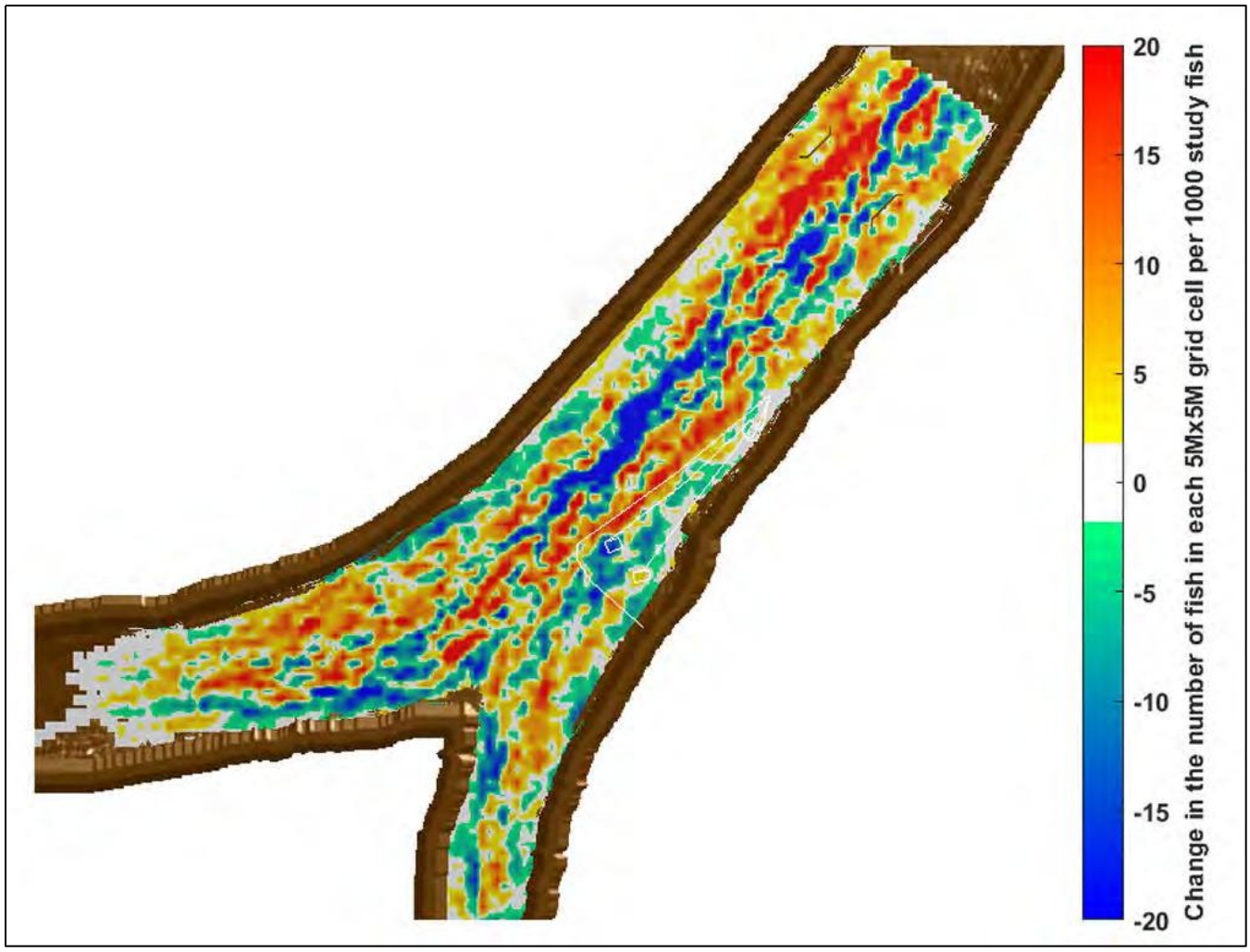

Note: The location of the stand-off buoys and FFGS structures in the operational and non-operational position are drawn in white. The measured fish densities are artificially low at the edges of the domain due to variance in tracking performance between fish tracks at the peripheries of the hydrophone array. Fish densities were consistently higher in the area immediately in front of the barrier-on location when the barrier was operational versus when the barrier was non-operational (Illustrated by the red and orange zones along the front of the barrier operational position). Correspondingly, fish densities were consistently lower in the area immediately behind the barrier-On location when the barrier was operational versus when the barrier was non-operational (Illustrated by the blue and green zone behind the barrier-On position). There is no clear pattern in the rest of the domain, especially in the area downstream of the barrier's downstream tip. This indicates that the effects of the barrier operational fish density distributions do not propagate downstream along streamlines.

Figure 3.5-10 Change in the Spatial Distribution of Study Fish (FFGS On – FFGS Off)

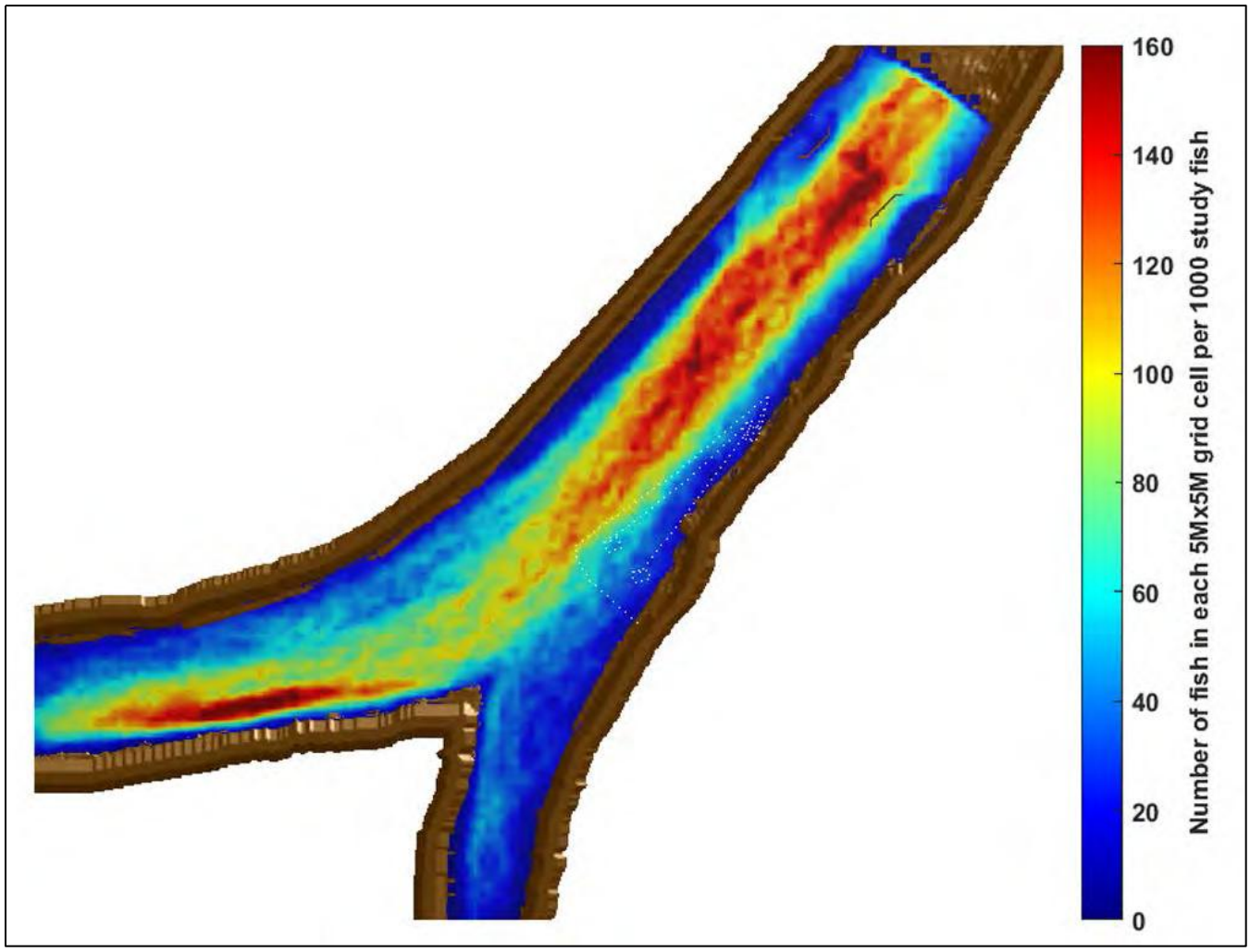

Note: The location of the stand-off buoys and FFGS structures in the operational and non-operational position are drawn in dotted white for reference, these structures were not deployed in 2008. The measured fish densities are artificially low at the edges of the domain due to variance in tracking performance between fish tracks at the peripheries of the hydrophone array.

Figure 3.5-11 Spatial Distribution of Fish Tracks Passing Through the Junction during Ebb Tide (2008 Study Data; N=836)

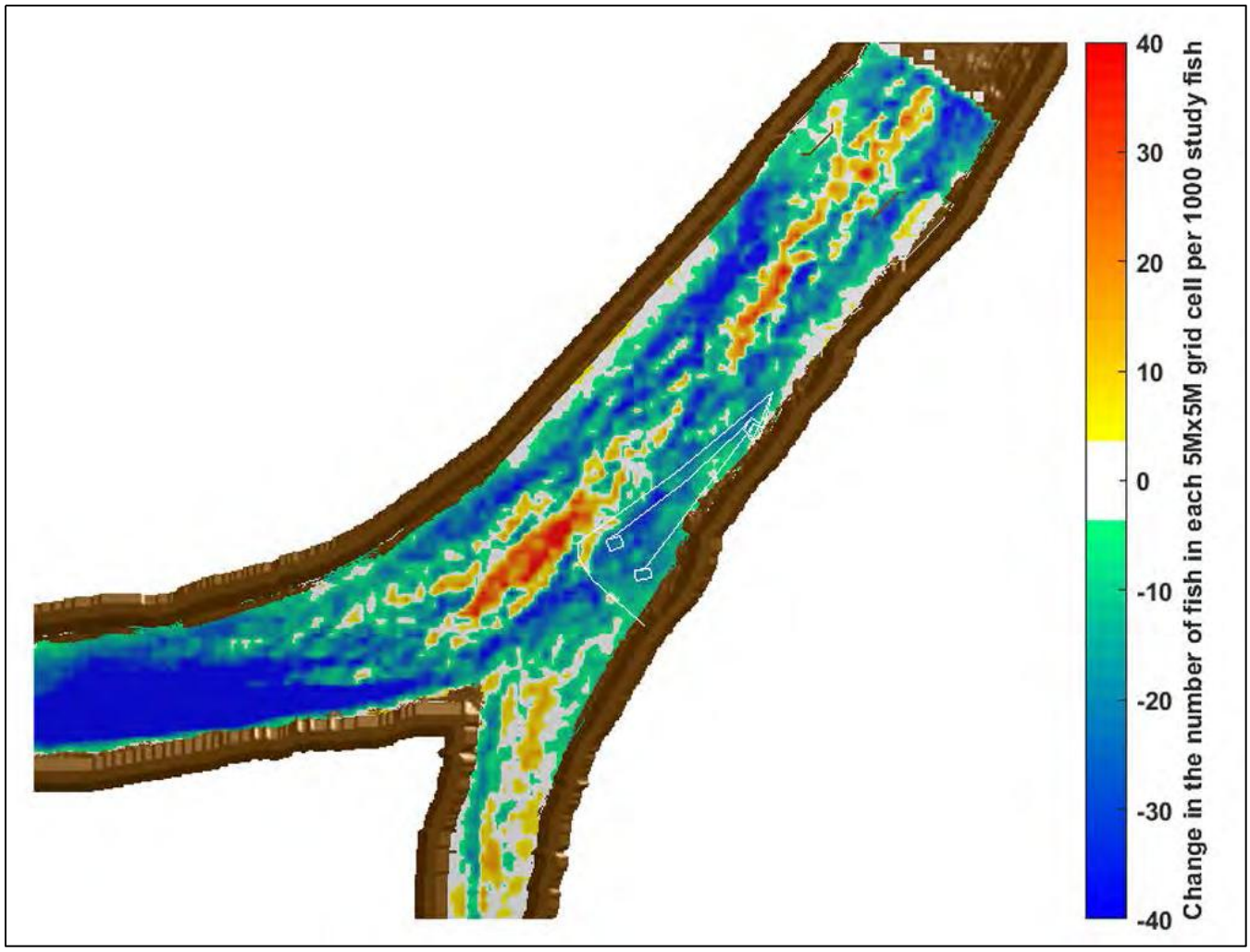

Note: The location of the stand-off buoys and FFGS structures in the operational and non-operational position are drawn in dotted white for reference, these structures were not deployed in 2008. The observed changes in fish density on the periphery of the array were erroneous due to different tracking array performance between the 2008 study and the 2014 FFGS study. Fish densities were higher in the area immediately in front of the barrier-On downstream tip when the barrier was operational versus 2008 (Illustrated by the red and orange zones in front of the barrier's downstream tip). Correspondingly, fish densities were lower in the area immediately behind the barrier-On location when the barrier was operational versus 2008 (Illustrated by the blue and green zone behind the barrier-On position). In the rest of the domain there is a clear pattern of decreased fish densities near the banks (blue and green), and increased fish densities in the center of the river (red and orange) when the barrier was operational versus the 2008 data. This pattern shows that fish density was more concentrated in the cross-channel direction in 2014 versus 2008. This is likely due to differences in environmental conditions or fish condition between the two studies. The overall tendency of the 2014 fish to be more centralized in the river cross-section makes it difficult to detect any underlying shift in fish density due to the barrier's operation.

Figure 3.5-12 Change in the Spatial Distribution of Study Fish (FFGS On - 2008 Study Data; No Barrier)

The spatial distribution plots show that operating the barrier decreased the number of fish in the junction between the river-left bank of the Sacramento river and the barrier, operating the barrier increased the number of fish along the buoy line and along the face of the lower portion of the barrier, and operating the barrier increased the number of fish in the junction immediately downstream of the barrier. Analysis of the 2011 and 2012 study data showed similar changes in overall fish densities in the immediate vicinity of the BAFF during BAFF operations, but, changes in fish density during BAFF operations appeared to propagate further downstream along streamlines, while the concentration of fish along the face of the FFGS decays rapidly downstream of the junction.

Additionally, there are patterns in the overall change in fish density shown in **Figure 3.5-10** that are hard to explain with a purely advective model of fish movement. These patterns include the decrease in the number of fish in the center of the channel along the face of the barrier, the decrease in the number of fish along the outside of the bend immediately downstream of the junction, and the increase in the number of fish downstream of Dagmar's Landing. The spatial distribution of ebb fish from the 2008 data was similar to that of the FFGS barrier non-operational fish, but the 2008 fish were more broadly distributed in the river cross section throughout the study area.

In addition to the overall distributions, spatial distributions of the number of fish entrained into Georgiana Slough during tides for barrier Off and barrier On conditions were computed (**Figure 3.5-13** and **Figure 3.5-14**), and the difference in the distribution of fish entrained in Georgiana Slough was calculated for barrier operational versus barrier non-operational and barrier operational versus 2008 data (**Figure 3.5-15** and **Figure 3.5-16**). These distributions show that operating the barrier reduced the number of fish entrained in Georgiana Slough between the left bank of the Sacramento River and the barrier, and reduced the number of fish entrained in Georgiana Slough in the center of the channel between +10 m (+33 ft) from the face of the barrier and +20 m (+66 ft) from the face of the barrier.

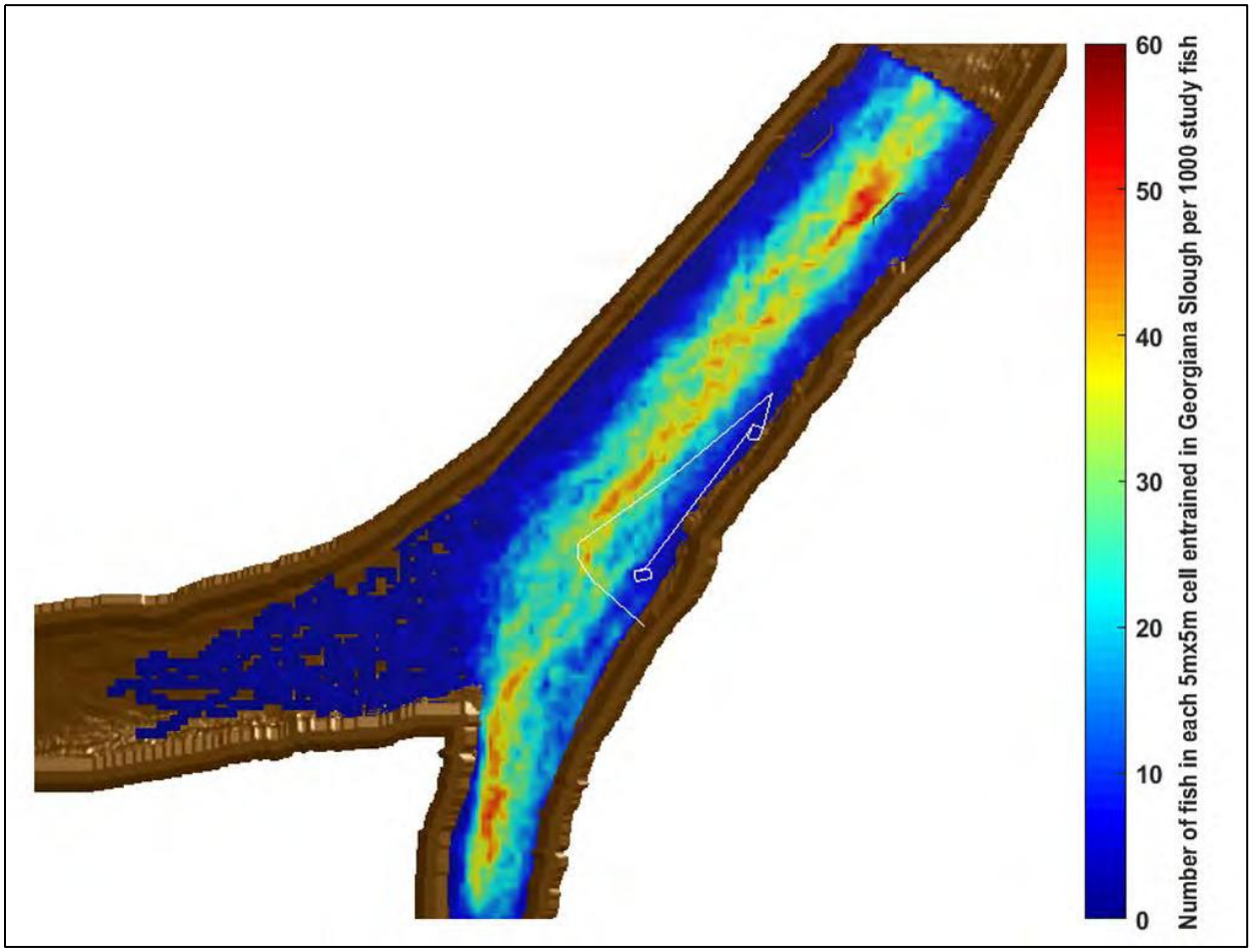

Note: The location of the stand-off buoys and FFGS structures in the non-operational position are drawn in white. The measured fish densities are artificially low at the edges of the domain due to variance in tracking performance between fish tracks at the peripheries of the hydrophone array. Note that this series of plots show the spatial distributions of the fish that were entrained in Georgiana Slough only.

Figure 3.5-13 Spatial Distribution of Study Fish Entrained in Georgiana Slough during Ebb Tide (FFGS Off; Total Entrained = 230 out of 909 [25%])

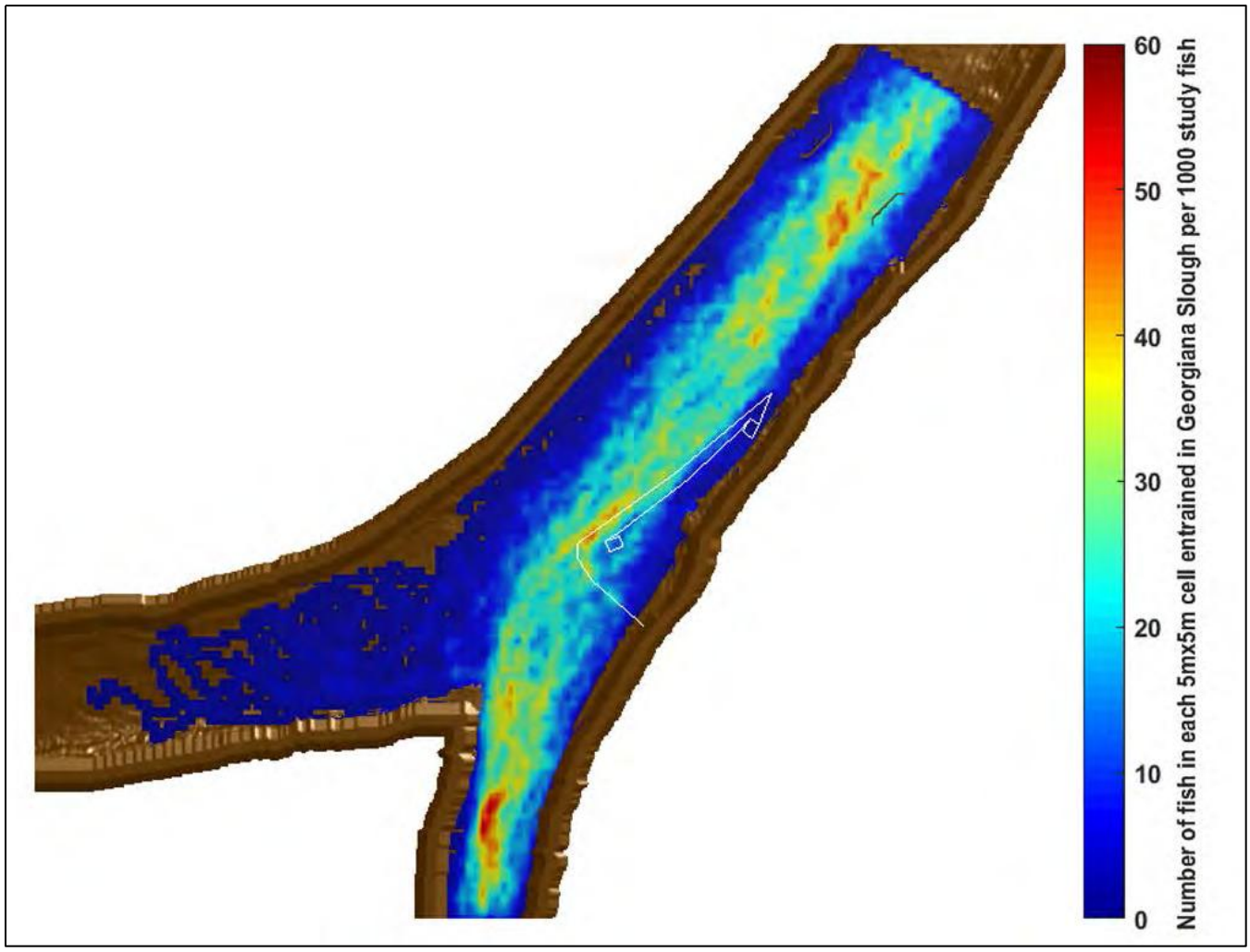

Note: The location of the stand-off buoys and FFGS structures in the operational position are drawn in white. The measured fish densities are artificially low at the edges of the domain due to variance in tracking performance between fish tracks at the peripheries of the hydrophone array. Note the concentration of fish density at the buoy line at the downstream tip of the barrier. Also, the density of fish entering Georgiana Slough is lower in the area immediately behind the barrier than when the barrier was Off, with the exception of a plume of higher fish density passing through the lower 1/3 of the barrier. This could indicate location where fish were passing under or through the barrier.

Figure 3.5-14 Spatial Distribution of Study Fish Entrained in Georgiana Slough during Ebb Tide (FFGS On; Total Entrained = 186 out of 818 [23%])

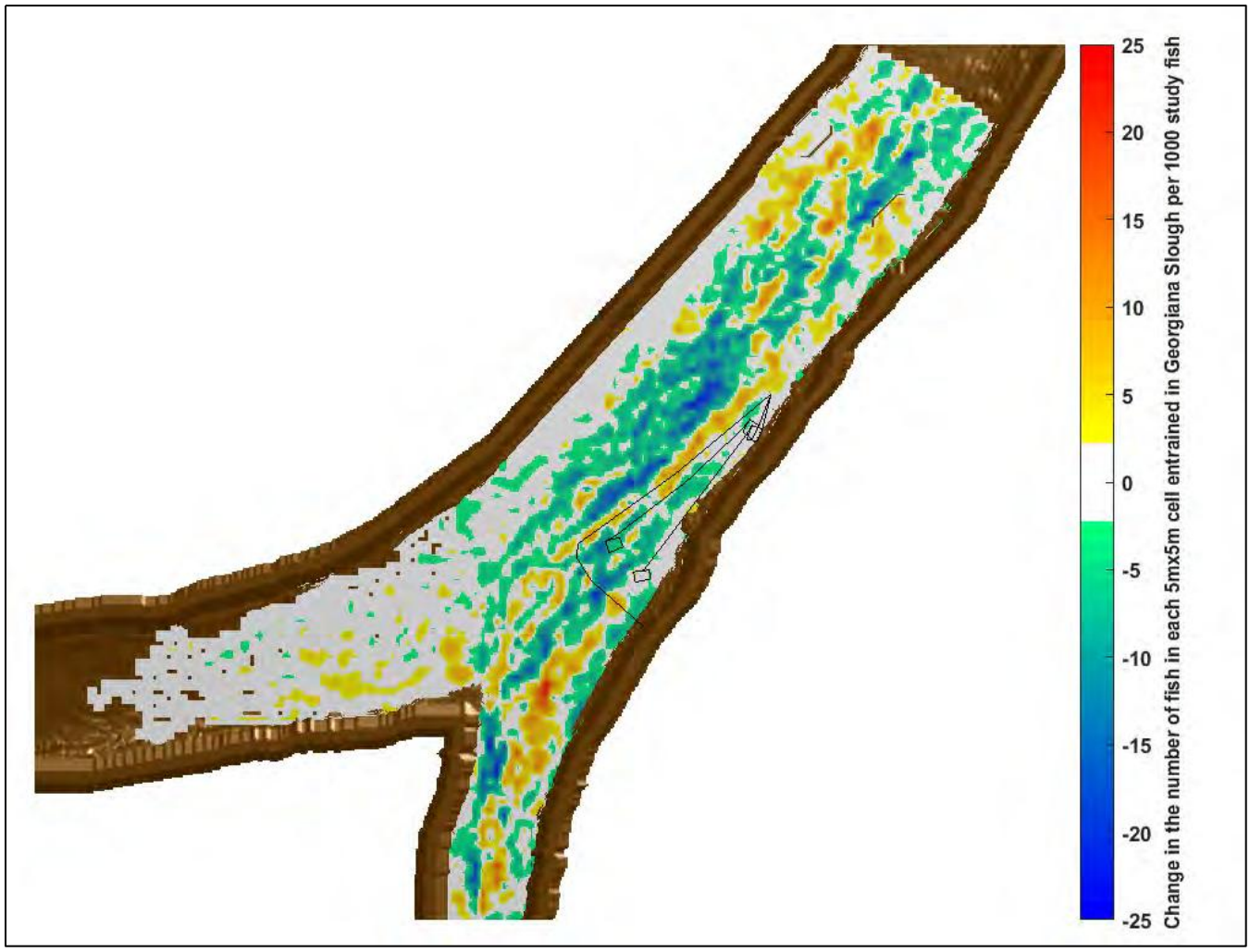

Note: The location of the stand-off buoys and FFGS structures in the operational and non-operational positions are drawn in black. The measured fish densities are artificially low at the edges of the domain due to variance in tracking performance between fish tracks at the peripheries of the hydrophone array. Note the concentration of fish density at the buoy line (orange zone along bouy line). Also, the density of fish entering Georgiana Slough is lower in the area immediately behind the barrier than when the barrier was non-operational (blue and green zone), with the exception of a plume of higher fish density passing through the lower 1/3 of the barrier (yellow streak passing through the barrier operational location). This could indicate location where fish were passing under or through the barrier. This figure also shows a decrease in the number of fish entering Georgian Slough in the river cross-section between the bouy line and Dagmar's landing, indicating that there is a complex response to the barrier.

Figure 3.5-15 Spatial Distribution of the Change in the Number of Study Fish Entrained into Georgiana Slough during Tide (FFGS On – FFGS Off)

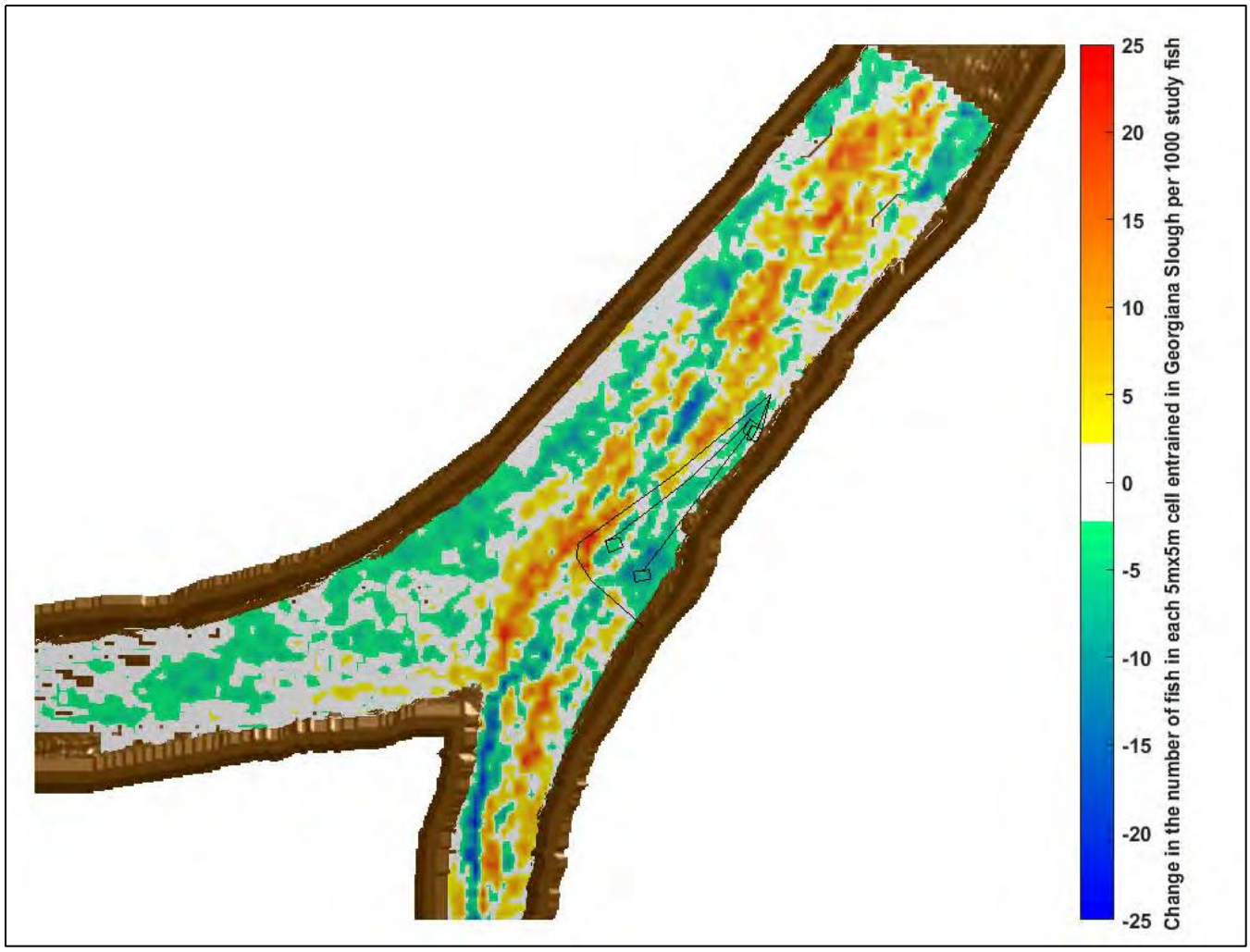

Note: The location of the stand-off buoys and FFGS structures in the operational and non-operational positions are drawn in black. The measured fish densities are artificially low at the edges of the domain due to variance in tracking performance between fish tracks at the peripheries of the hydrophone array. Note the concentration of fish density at the bouy line (orange zone along bouy line). Also, the density of fish entering Georgiana Slough is lower in the area immediately behind the barrier than when the barrier was non-operational (blue and green zone).

Figure 3.5-16 Spatial Distribution of the Change in the Number of Study Fish Entrained into Georgiana Slough during Ebb Tide (FFGS On - 2008 Study Data)

Analysis of Fish Motion Relative to the Critical Streakline

The critical streakline conceptual model of barrier efficacy predicts that a barrier will reduce entrainment if it causes fish to move in the cross-stream direction across the critical streakline and into streamlines entering a different branch of the junction. For this reason, the test was set up to determine whether the FFGS was successful at moving fish relative to the critical streakline even if it did not cause the fish to cross the critical streakline.

To test the FFGS net effect on each fish's cross-stream location relative to the critical streakline two dimensional frequency distributions were compared that show distribution of each fish's net cross-stream movement relative to the critical streakline as a function of the fish's cross-stream position at the upstream start of the barrier. These distributions are shown for barrier Off and barrier On conditions in **Figure 3.5-17** and **Figure 3.5-18**, the difference between the barrier operational and non-operational distributions are shown in **Figure 3.5-19**, and the distribution of estimated 2008 values is shown in **Figure 3.5-20**.

This page intentionally left blank.

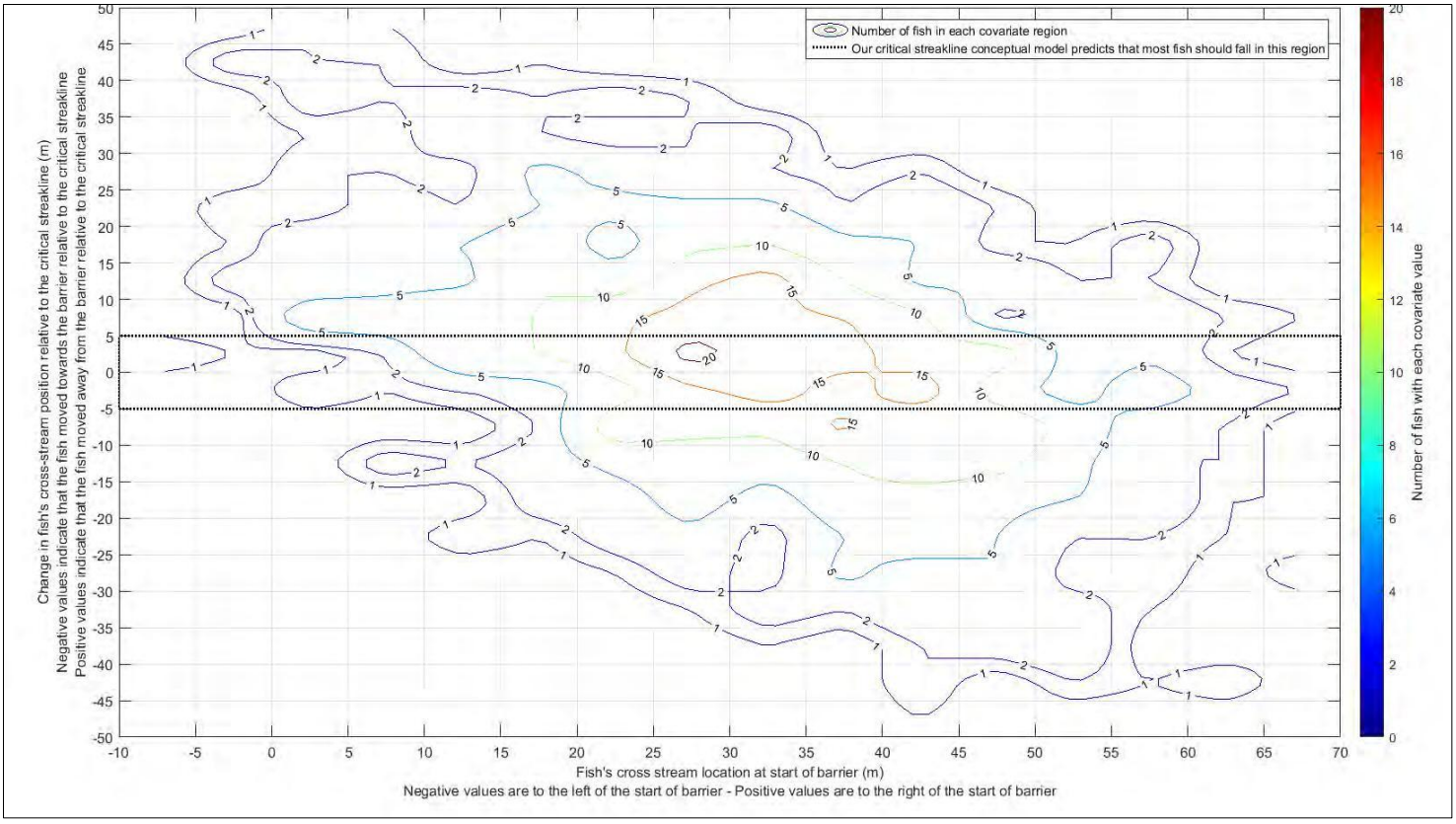

Figure 3.5-17 Contour Plot Showing Distribution of the Change in Study Fish Cross-Stream Location Relative to the Critical Streakline Location in the Area of the FFGS (FFGS Off)

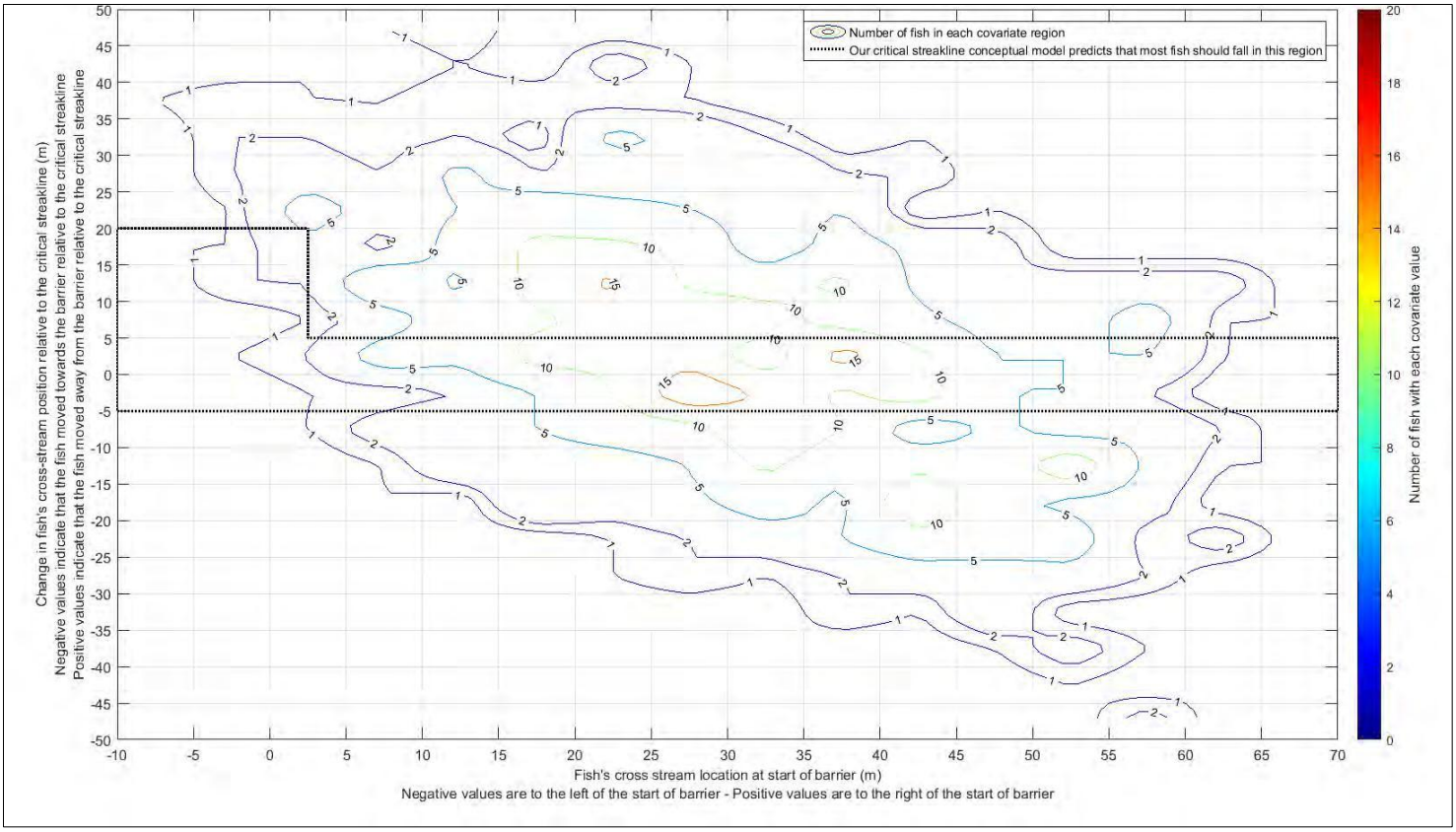

Figure 3.5-18 Contour Plot Showing Distribution of the Change in Study Fish Cross-Stream Location Relative to the Critical Streakline Location in the Area of the FFGS (FFGS On)

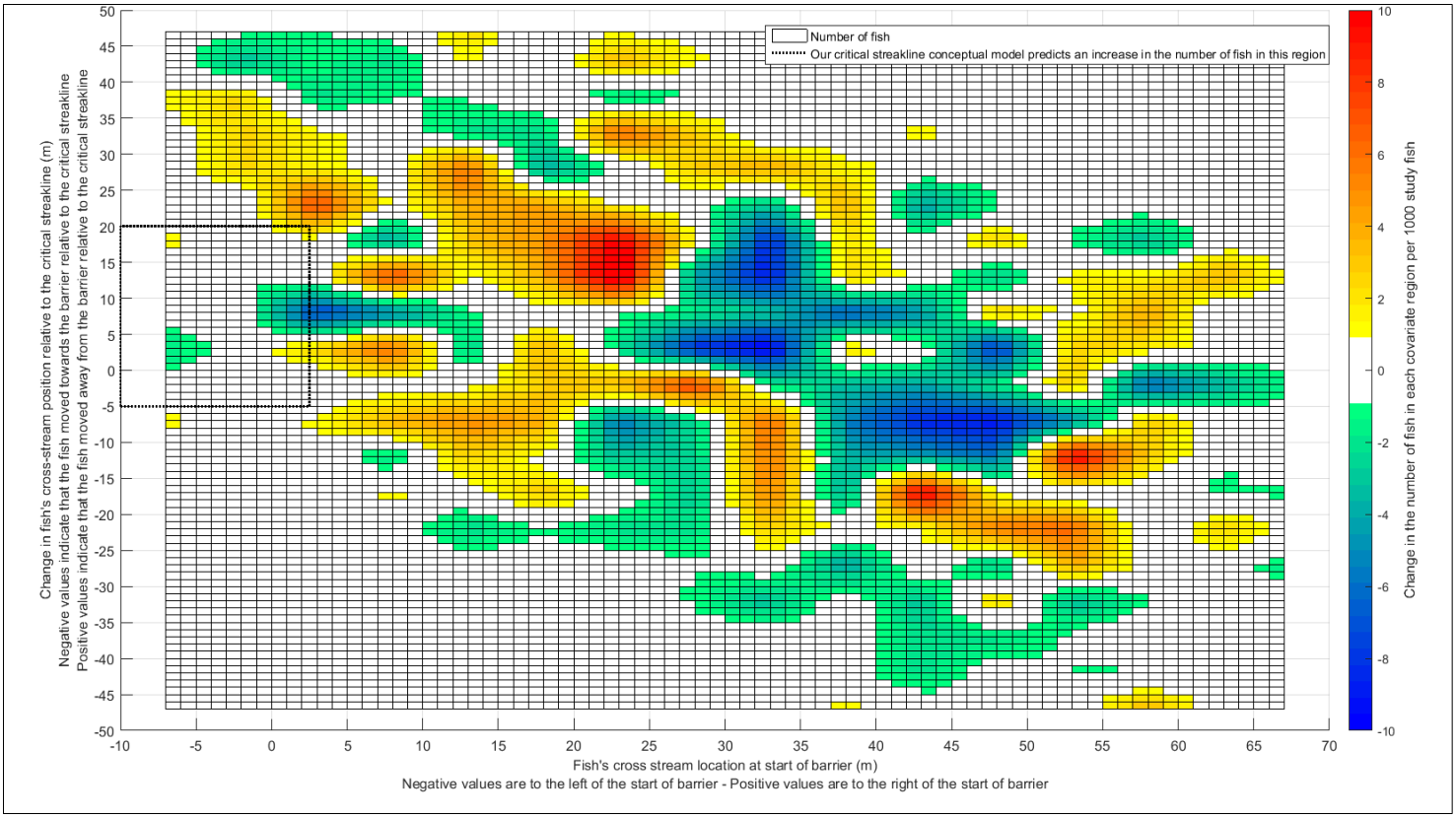

Figure 3.5-19 Flood Plot Showing the Distribution of the Change in Study Fish Cross-Stream Location Relative to the Critical Streakline Location in the Area of the FFGS (FFGS On – FFGS Off)

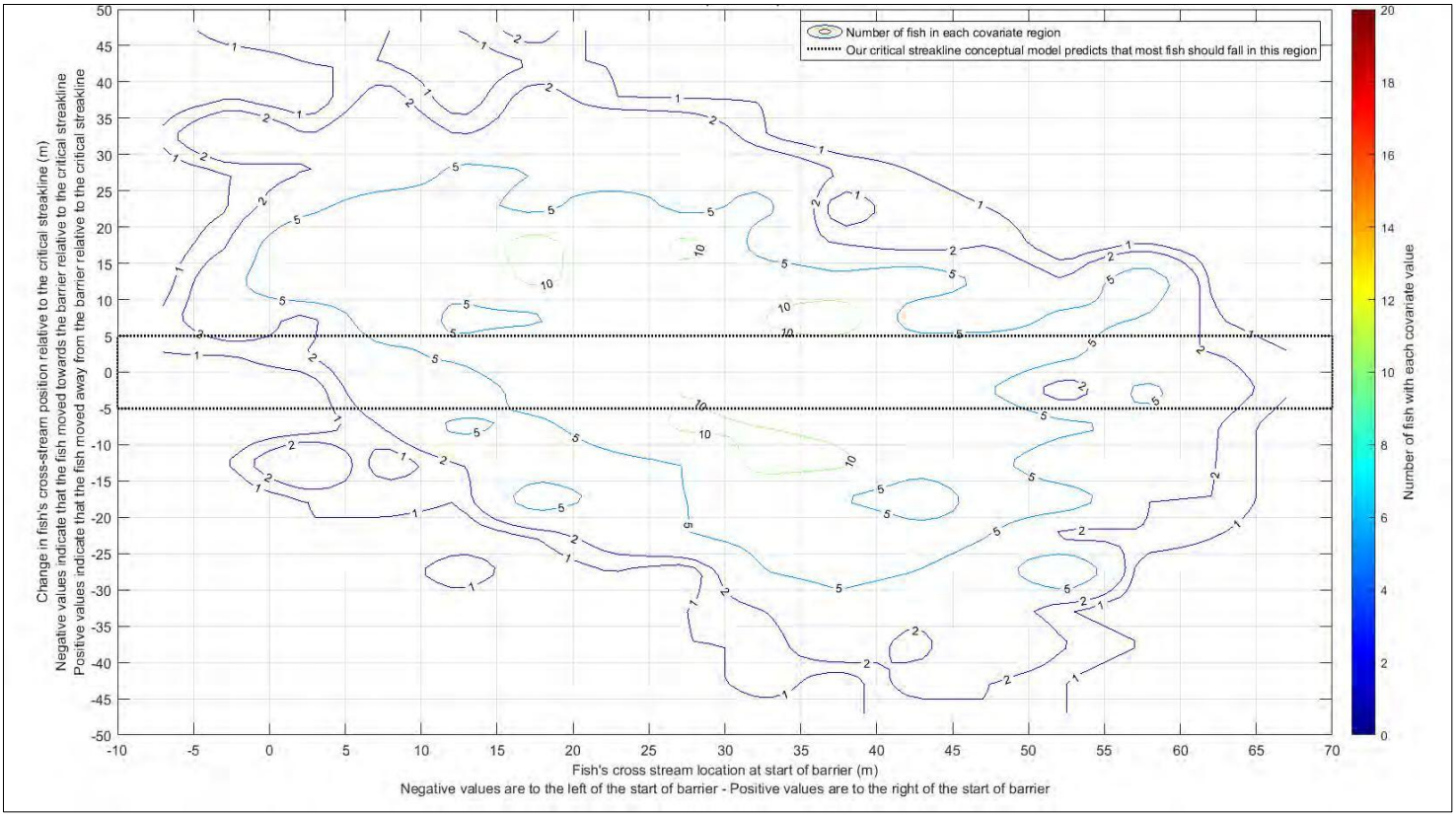

Figure 3.5-20 Contour Plot Showing Distribution of the Change in Study Fish Cross-Stream Location Relative to the Critical Streakline Location in the Area of the FFGS (2008 Study Data; No Barrier)

The distributions in **Figure 3.5-17** and **Figure 3.5-18** show that the majority of barrier non-operational and barrier operational fish exhibited very large net movements in the cross-stream direction both to the right and to the left of the critical streakline, and, the distribution in the change in these values between the barrier operational and barrier non-operational conditions shown in **Figure 3.5-19** shows that the barrier caused fish to change their motion relative to the critical streakline in both the positive and negative directions throughout the river cross-section.

The distribution of values for the 2008 data is similar to the 2014 barrier operational and barrier non-operational conditions, and indicates that the majority of 2008 fish exhibited significant cross-stream movements relative to the critical streakline in the barrier area in the absence of a barrier. These findings show that many fish engaged in a swimming behavior that caused them to move laterally in the river relative to the critical streakline with the FFGS On and Off, and the 2008 data shows that fish engaged in this behavior in the absence of the FFGS. The magnitude of many fish's cross-stream change in position relative to the critical streakline was greater than the cross-stream extent of the FFGS, which suggests that the FFGS did not reduce entrainment because the fish's swimming behavior overwhelmed any change in cross-stream position produced by the FFGS.

Qualitative Observation of Fish Tracks and Type Classification

A large number of 2014 and 2008 tracks were qualitatively analyzed to develop hypotheses that would better explain the observed patterns of fish movement and entrainment. While most quantitative analyses of fish movement during the 2011, 2012 and 2014 studies were limited to track segments in the immediate vicinity of the Georgiana Slough junction, longer length tracks were used for the quantitative assessment, which provided information on the position history of fish from upstream of the DCC to downstream of the Georgiana Slough junction. The use of the turning point analysis of longer tracks coupled with periods of slower currents in the 2008 and 2014 data sets uncovered four categories of movement:

1. Type 1 tracks: Tracks from fish that appeared to advect downstream along streamlines in a manner that indicated minimal cross-stream swimming behavior;

2. Type 2 tracks: Tracks from fish that exhibited periodic cross-stream movements greater than 8 m (26 ft) in magnitude that were strongly periodic in nature;

3. Type 3 tracks: Tracks from fish that appeared to be milling, holding near structures, or not moving downstream in a directed manner; and

4. Type 4 tracks: Tracks from fish that approached the junction from downstream during flood tides. These tracks were quantified but not used for further analyses since the FFGS was only designed to be effective during ebb tide periods.

Software was developed to analyze the motion of each fish as they moved from the Walnut Grove Bridge downstream to the center of the junction, and classify each track as either Type 1, Type 2, Type 3, or Type 4 based on multiple movement parameters. This software also identified and recorded locations where fish initiated sustained cross-stream excursions which are referred to as "turning points".

Figure 3.5-21 shows examples of the three types of fish tracks associated with downstream movement and the turning points identified in each track (turning points are shown as white dots). **Table 3.5-2** shows a similar proportion of Type 1, Type 2, and Type 3 tracks in the 2014 and 2008 studies, and show that Type 1 tracks make up a relatively small portion of each data set. As shown in **Figure 3.5-22** and **3.5-23**, many of the Type 2 fish tracks identified in the 2008 data appeared to interact with the barrier and/or the buoy line when plotted on top of images of the barrier from 2014. This corroborates the hypothesis that the barrier was built in an area where a

hydrodynamic or physical que was initiating a behavioral response when the barrier was in the non-operational position or not installed, which could partially explain the lack of a difference between FFGS Off vs. On.

Panel A – Example of a Type 1 fish track (Roughly advecting along streamlines)

Panel B – Example of a Type 2 fish track (Periodic Cross-Stream Motion)

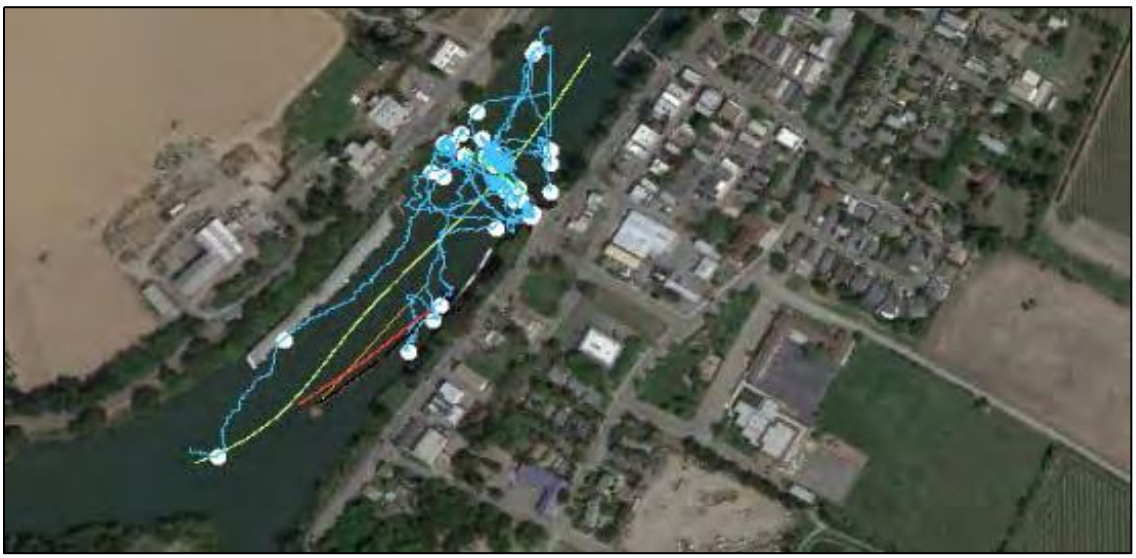

Panel C – Example of a Type 3 fish track (Milling)

Figure 3.5-21 Example 2014 Fish Tracks Illustrating the Three Types of Downstream Movement Patterns

Table 3.5-2 Fish Track Type Classification Results		
	2014GSB Study	2008 Study
Number of Type 1 Tracks	221 (11%)	117 (10%)
Number of Type 2 Tracks	1,417 (72%)	648 (57%)
Number of Type 3 Tracks	246 (12%)	237 (21%)
Number of Type 4 Tracks	94 (5%)	130 (11%)

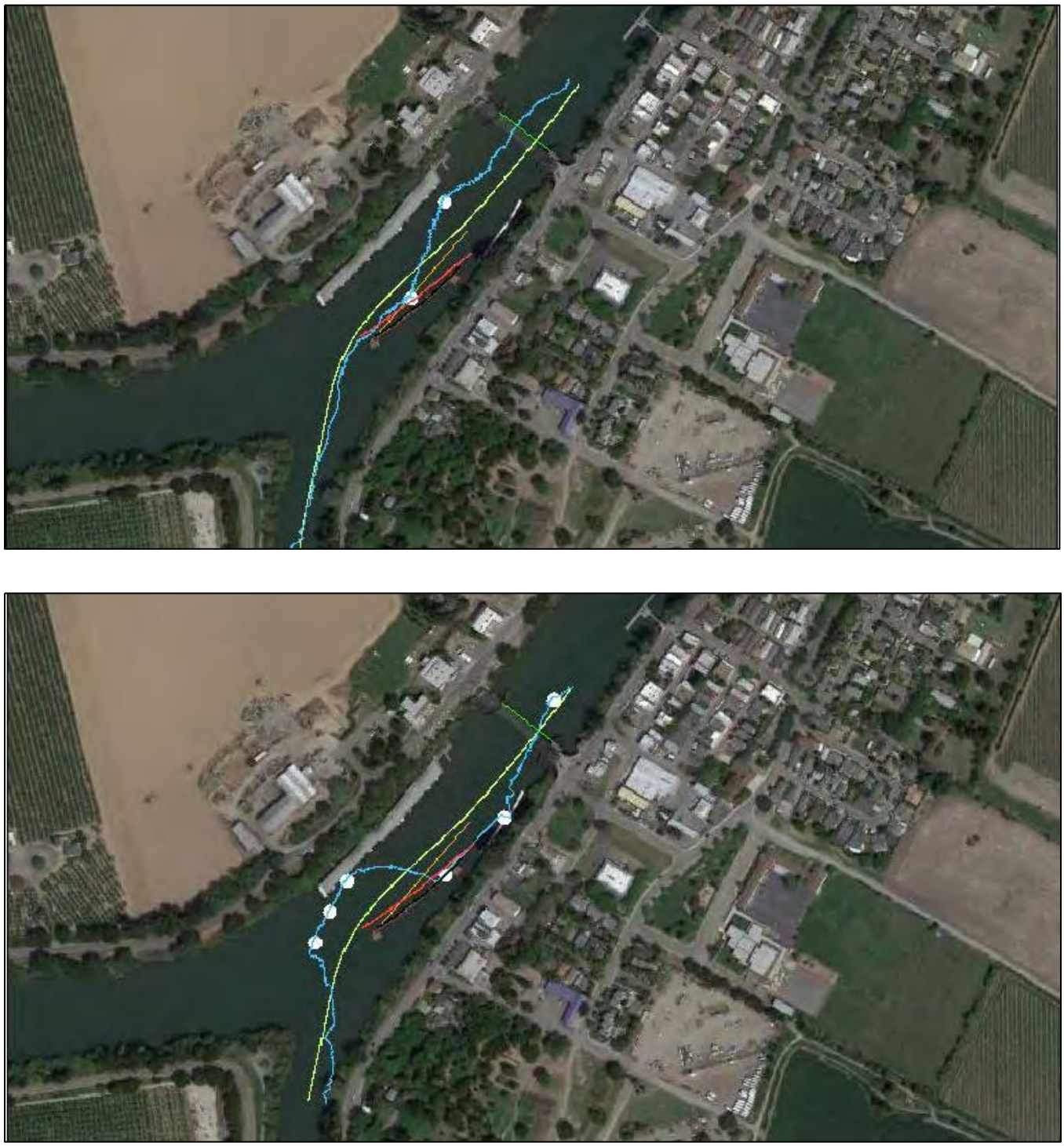

Figure 3.5-22 Example 2008 Fish Tracks Classified as Type 2

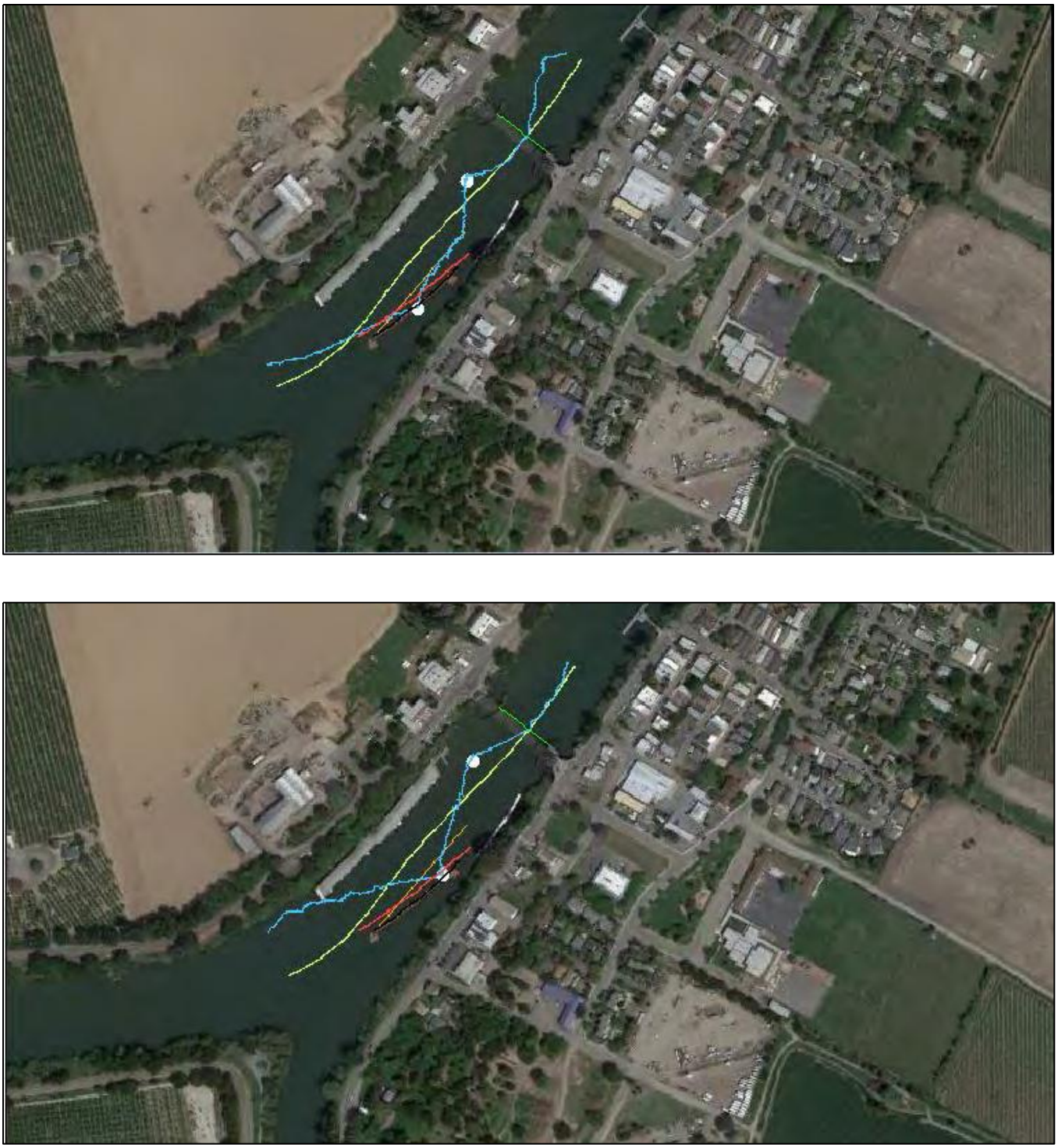

Figure 3.5-23 Example 2008 Fish Tracks Classified as Type 2

SPATIAL ANALYSIS OF TURNING POINTS EXTRACTED FROM TYPE CLASSIFICATION

In order to test whether the barrier caused Type 2 fish to initiate a change in the direction of cross-stream movement, the turning points identified in Type 1 and Type 2 tracks were spatially aggregated using the same techniques that were used to aggregate fish track data. Type 3 tracks were excluded from this analysis based on the observation that many Type 3 tracks entered the area behind the barrier from the downstream direction during periods of extremely low water velocity.

The spatial distribution of turning points for Type 1 and Type 2 fish were computed for ebb tide conditions when the barrier was Off, when the barrier was On, and for the 2008 data (**Figures 3.5-24** through **3.5-26**) and then the difference in the distributions between barrier operational and barrier non-operational conditions (**Figure 3.5-27**) and between barrier operational conditions and the 2008 data (**Figure 3.5-28**) were calculated. These distributions show a large number of turning points in the vicinity of the barrier and the buoy line for barrier non-operational and 2008 tracks, but, moving the barrier to the operational position increased the density of turning points along the face of the barrier and decreased the number of turning points behind the barrier.

This can be seen in the shift in turning point density from the area behind the barrier-On position in **Figure 3.5-24** to the area directly in front of the barrier operational position in **Figure 3.5-25**. The shift in turning point density caused by moving the barrier from the non-operational position to the operational position can also be seen in **Figure 3.5-27**; in this figure the area behind the barrier-operational position is blue and green, illustrating a decrease in turning point density on the order of -5 to -10 turning points per cell per 1,000 fish (out of a maximum value of 20), while the area along the face of the barrier operational location is orange and red illustrating an increase in turning point density on the order of +5 to + 10 turning points per cell per 1,000 fish (out of a maximum value of 20).

This shift in turning point density strongly suggests that the majority of Type 1 and Type 2 fish that encounter the barrier initiate a cross-stream excursion away from the barrier rather than passing underneath the barrier. The difference in the distribution between barrier On turning points and 2008 turning points shown in **Figure 3.5-28** shows a similar pattern to that seen in **Figure 3.5-27** which indicates that the barrier and associated structures caused fish to change the direction of their cross-stream movement earlier than they would have without the structures in place.

The fact that the barrier appeared to initiate sustained changes in cross-stream movement for Type 2 fish is significant, because the cross-stream excursions of Type 2 fish were often much greater than the cross-stream extent of the barrier itself (**Figure 3.5-29**), with many fish exhibiting cross-stream excursions on the order of 15 to 30 m (49-98 ft) after encountering the barrier. The magnitude of Type 2 cross-stream excursions also explains the distributions seen in **Figures 3.5-17**, **3.5-18**, and **3.5-20**; fish on the left side of the river are likely to turn and move back towards the right bank resulting in a net positive shift relative to the critical streakline, fish on the right bank are likely to turn and move back towards the left bank resulting in a net positive shift relative to the critical streakline, and in the middle of the river fish are equally likely to be moving in either direction so the net shift is zero, but the variance is high.

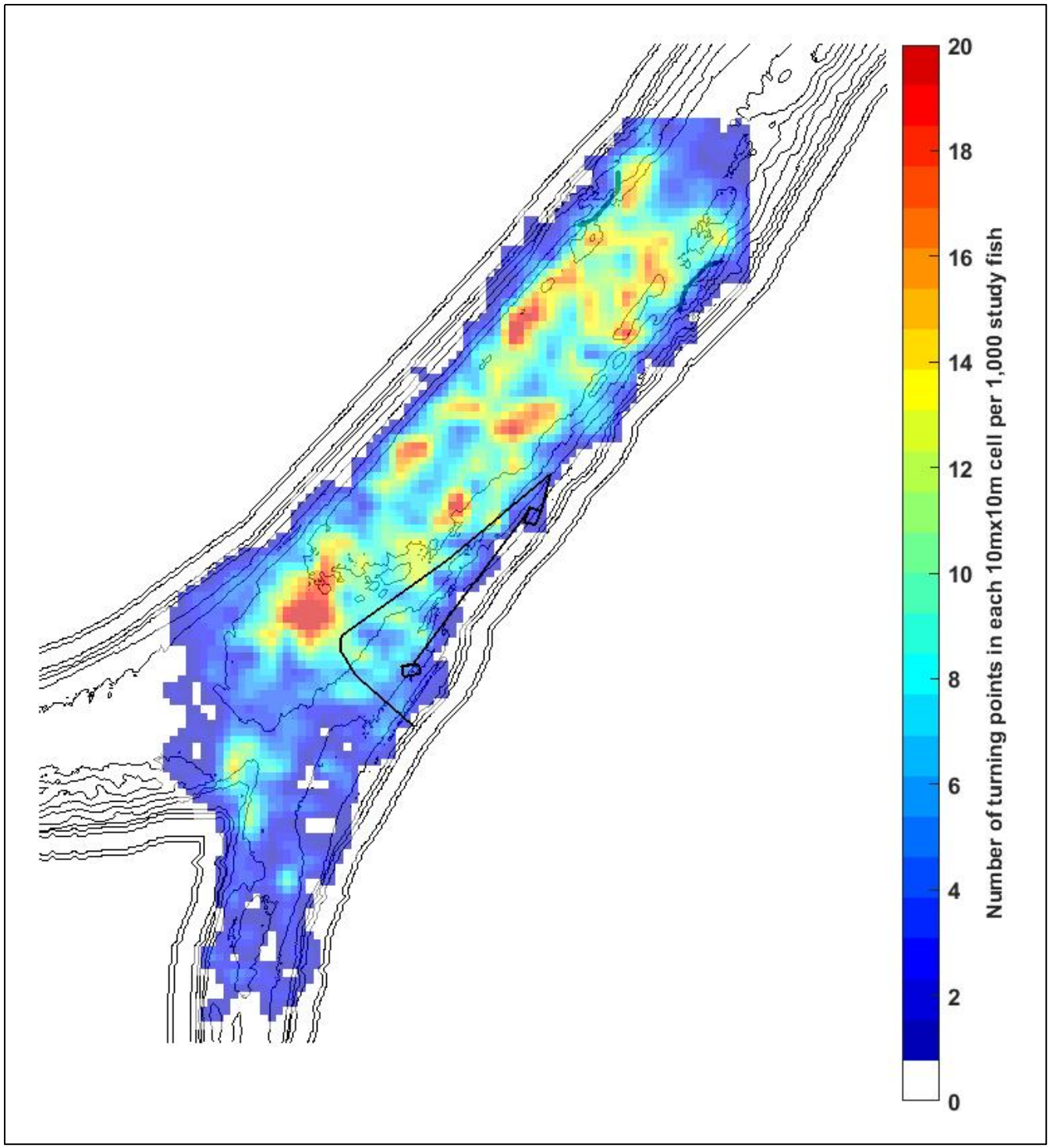

Note: The location of the stand-off buoys and FFGS structures in the non-operational positions are drawn in black. Turning point densities in front of the barrier-Off position are moderate, and occur at a similar density as in other areas along the bathymetric gradient on the river-left bank and indicate that many fish are changing their cross-channel swimming direction at the edge of the channel. The area between the guidance buoys and front of the barrier-Off location shows a continuous, moderate density of turning points, indicating variance in the location of turning point initiation.

Figure 3.5-24 Spatial Distribution of Turning Points from Type 1 and Type 2 Fish Tracks (FFGS Off)

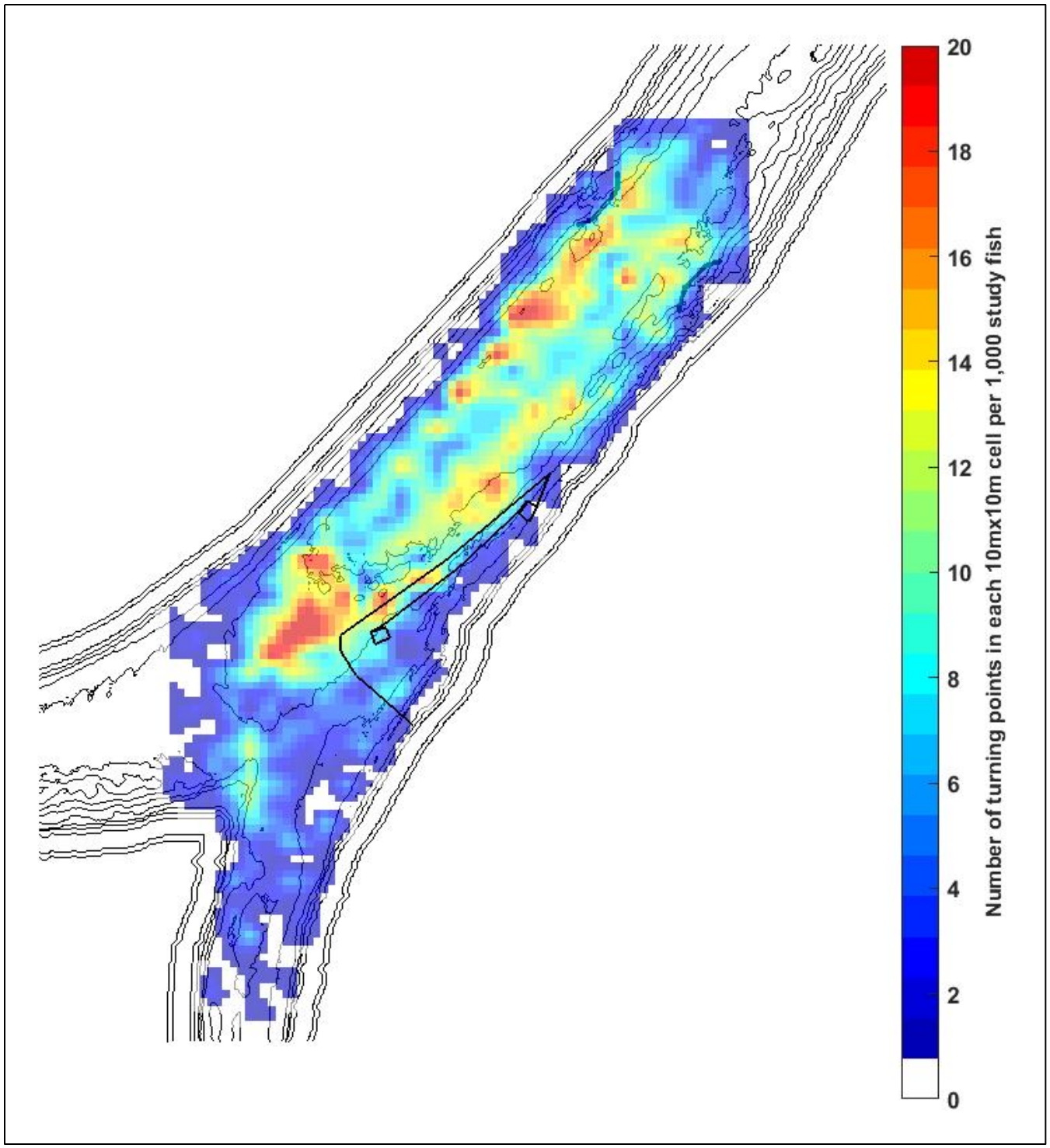

Note: The location of the stand-off buoys and FFGS structures in the On positions are drawn in black. The turning point density is much higher along the face of the barrier and much lower behind the barrier when compared to the barrier non-operational condition. This indicates that the barrier prompting fish to initiate cross-stream excursions, and that the spatial distribution of this behavior effect is more concentrated than the fish's response to the edge of the channel.

Figure 3.5-25 Spatial Distribution of Turning Points from Type 1 and Type 2 Fish Tracks (FFGS On)

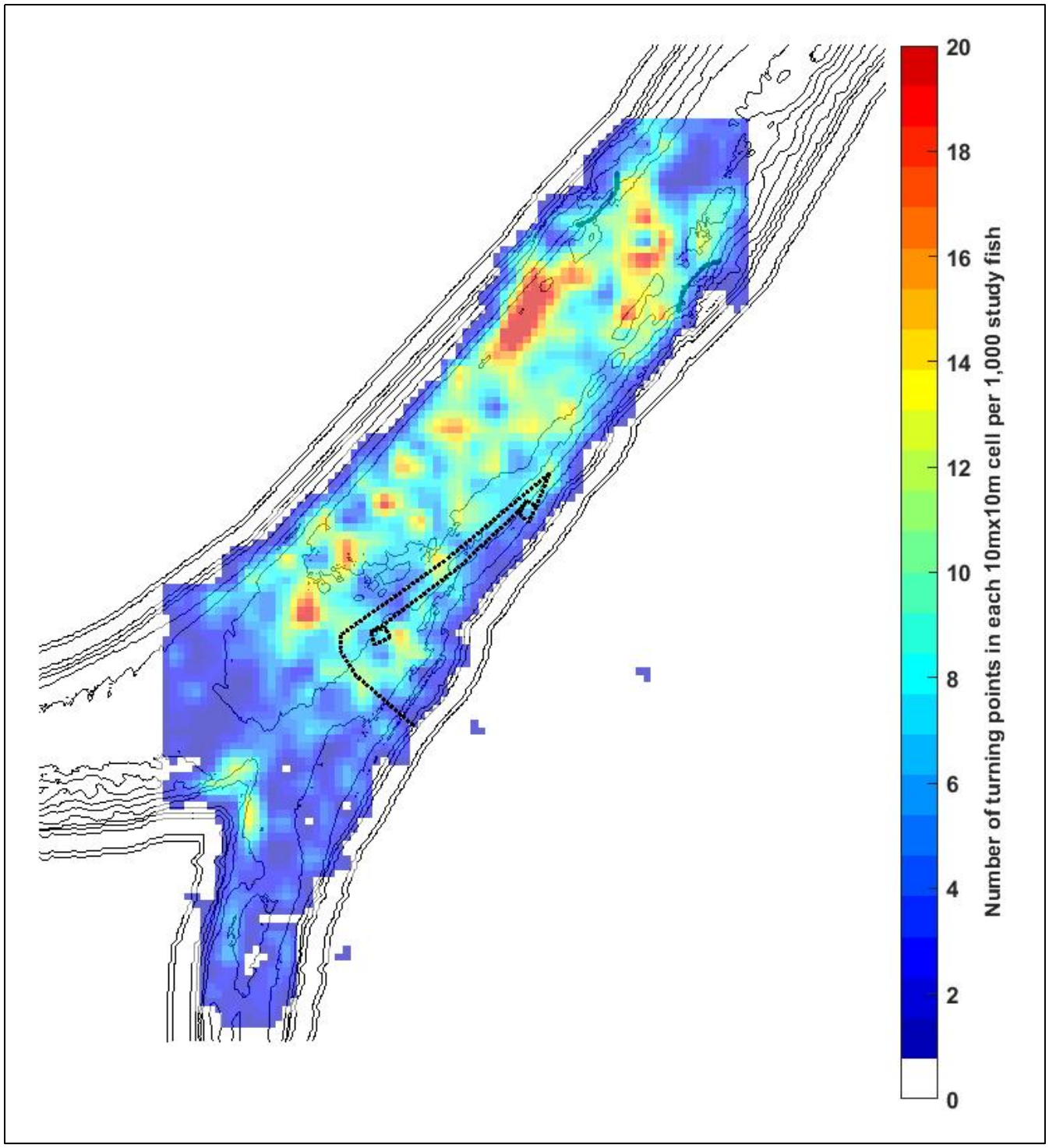

Note: The location of the standoff buoys and FFGS structures in the On position are drawn in black dotted lines for reference (These structures were not deployed in 2008). Turning point densities in front of the barrier-Off position are moderate, and occur at a similar density as in the other areas along the bathymetric gradient on the river-left bank and indicate that many fish are changing their cross-channel swimming direction at the edge of the channel.

Figure 3.5-26 Spatial Distribution of Turning Points from Type 1 and Type 2 Fish Tracks (2008 Study)

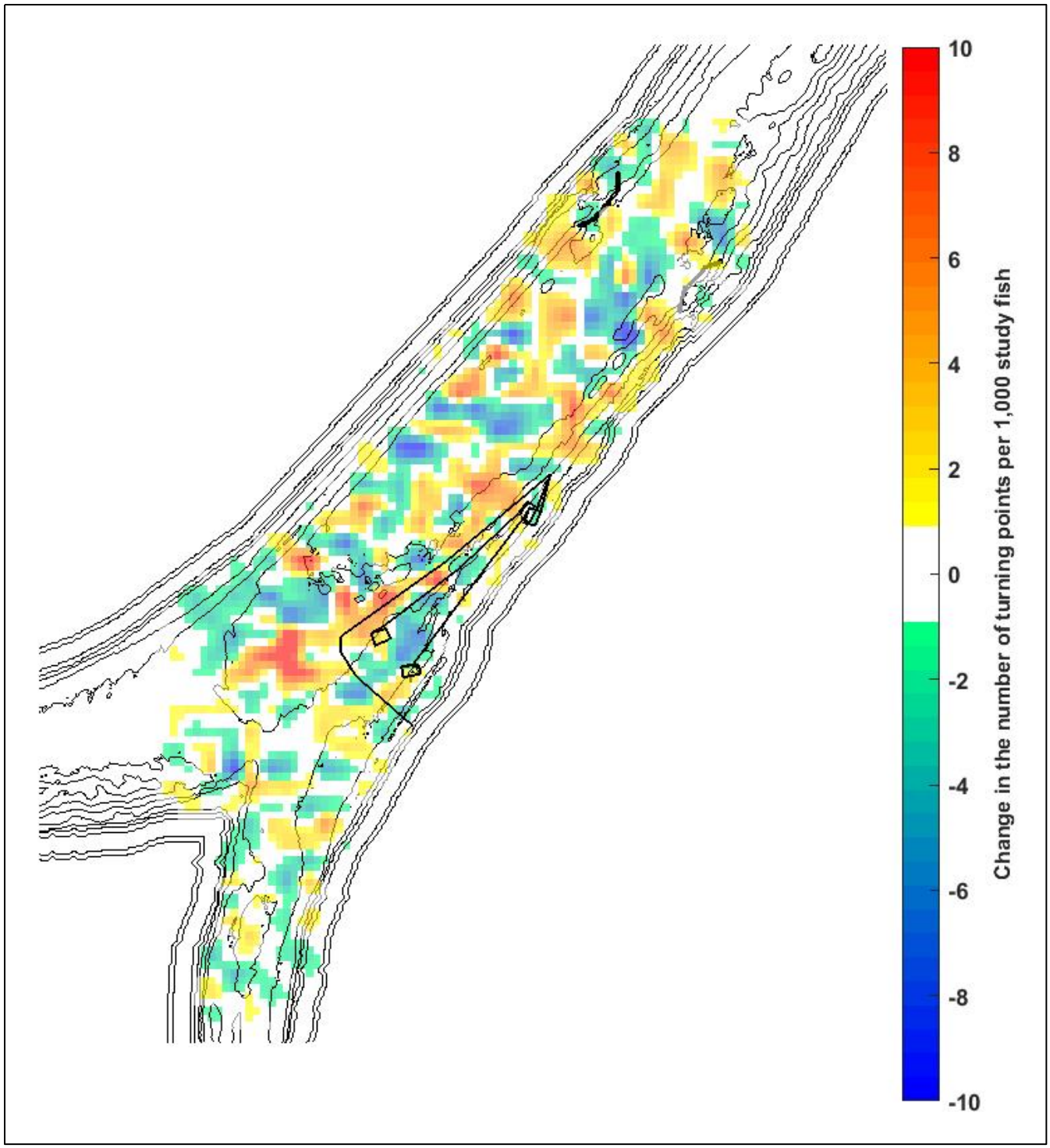

Note: The location of the standoff buoys and FFGS structures in the On and non-operational positions are drawn in black. The turning point density increased along the face of the barrier decreased behind the barrier when barrier was On versus when the barrier was Off. This indicates that the barrier prompting fish to initiate cross-stream excursions, and that the spatial distribution of this behavior effect is more concentrated than the fish's response to the edge of the channel.

Figure 3.5-27 Difference in Turning Point Distributions (FFGS On – FFGS Off)

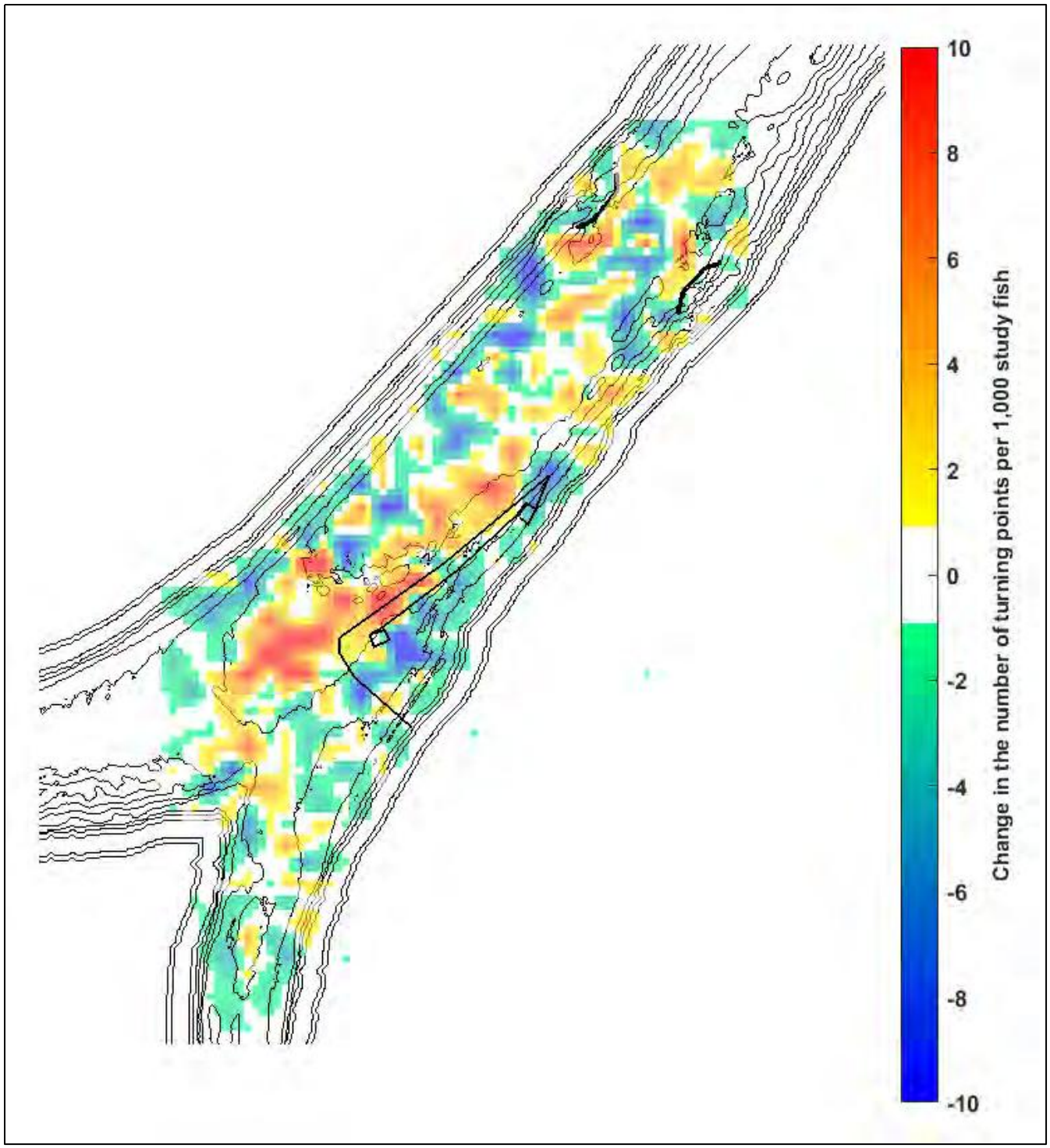

Note: The location of the stand-off buoys and FFGS structures in the On position are drawn in black. The turning point density increased along the face of the barrier decreased behind the barrier when barrier was On versus the 2008 data. This indicates that the barrier prompting fish to initiate cross-stream excursions, and that the spatial distribution of this behavior effect is more concentrated than the fish's response to the edge of the channel.

Figure 3.5-28 Difference in Turning Point Distributions (FFGS On – 2008 Study [No Barrier])

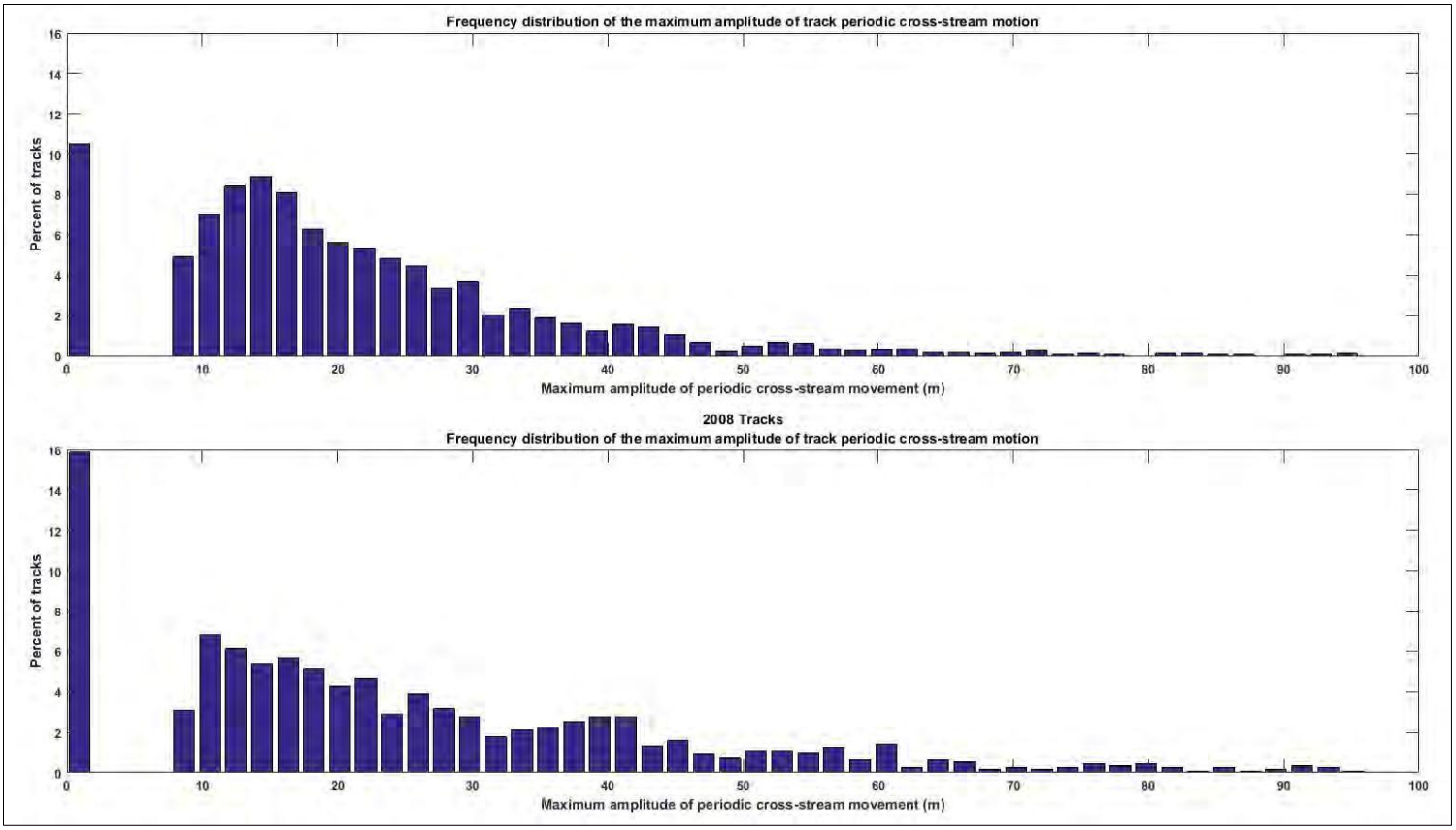

Figure 3.5-29 Frequency Distribution of the Maximum Amplitude of Track Periodic Cross-Stream Motion (2014 and 2008 Study Data)

3.5.4 DISCUSSION

The limited range of critical streakline positions that occurred during the 2014 study significantly reduced the percentage of time that the barrier was expected to be effective; however, all of the analyses performed in this section suggest that the minimal effect of the FFGS to overall salmon entrainment reduction over the course of the 2014 study was due to a more complicated combination of effects that resulted from unexpected fish behavior in the vicinity of the barrier. Specifically, automated track classification suggests that the majority of the fish transiting the junction during tides in 2014 and 2008 engaged in sustained, periodic cross-stream movements in the study area, instead of moving through the junction along streamlines, as was the case for the majority of fish tracks analyzed during the 2011 and 2012 BAFF studies.

Additionally, spatial analysis of fish track data and turning point data indicate that many fish responded to physical or hydrodynamic cues in the area near the barrier, which produced a behavioral response in Type 2 fish when there was no barrier (2008) or the barrier was non-operational that was similar to the response produced by the barrier, reducing the net effect of barrier operations on entrainment.

Finally, it appears that a small number of fish did not initiate a cross-stream excursion at the barrier but instead guided along the buoy line and became entrained in Georgiana Slough. While only a small percentage of study fish exhibited this behavior, any behavioral response that increased entrainment would partially minimize the apparent protection effects of the barrier and make the real protection effects harder to detect and measure.

The large ratio of Type 2 to Type 1 fish identified in the 2014 and 2008 data sets, combined with evidence of Type 2 behavior in the 2006 Clarksburg Bend data set (Blake and Burau 2015), strongly suggests the need to revise our conceptual model of juvenile salmon entrainment to account for fish that move downstream via a series of periodic cross-stream excursions. When the entrainment zone – critical streakline conceptual model was applied to the FFGS design it was assumed that study fish would exhibit nearly perfectly negative rheotaxis after encountering the barrier, so that their rheotaxis swimming behavior would have no mean effect on the cross-stream evolution of fish tracks downstream of the FFGS. This assumption was based on the observed 2011 and 2012 BAFF study tracks; the majority of these tracks are nearly parallel to streamlines in the vicinity of the BAFF (Type 1 tracks), and many of the fish that encountered the BAFF moved downstream of the barrier parallel to streamlines after leaving the immediate vicinity of the BAFF. If the 2014 fish had behaved in a similar manner then the FFGS would have reduced entrainment risk for the limited number of fish that encountered the FFGS when the critical streakline was to the left of the downstream tip of the barrier.

After analyzing the 2014 and 2008 study tracks for the FFGS analysis it appears that the apparent difference between the rheotaxis behavior observed in 2011 and 2012 and the rheotaxis behavior observed in 2014 and 2008 was due to a combination of the following factors:

1. The downstream water velocities were much higher during the 2011 study than velocities that occurred during the 2014 study. (**Figure 3.5-30** and **Figure 3.5-31**);

2. A greater percentage of the fish tracks from the 2012 study classified as predatory fishes (which may not have been) moved through the junction at lower velocities than the fish classified as juvenile salmonids (**Figure 3.5-32**). This removed many of the low-velocity tracks from the analysis pool, possibly biasing our understanding of juvenile salmon behavior during the GSFFGS Study towards fish transiting the junction under high water velocities;

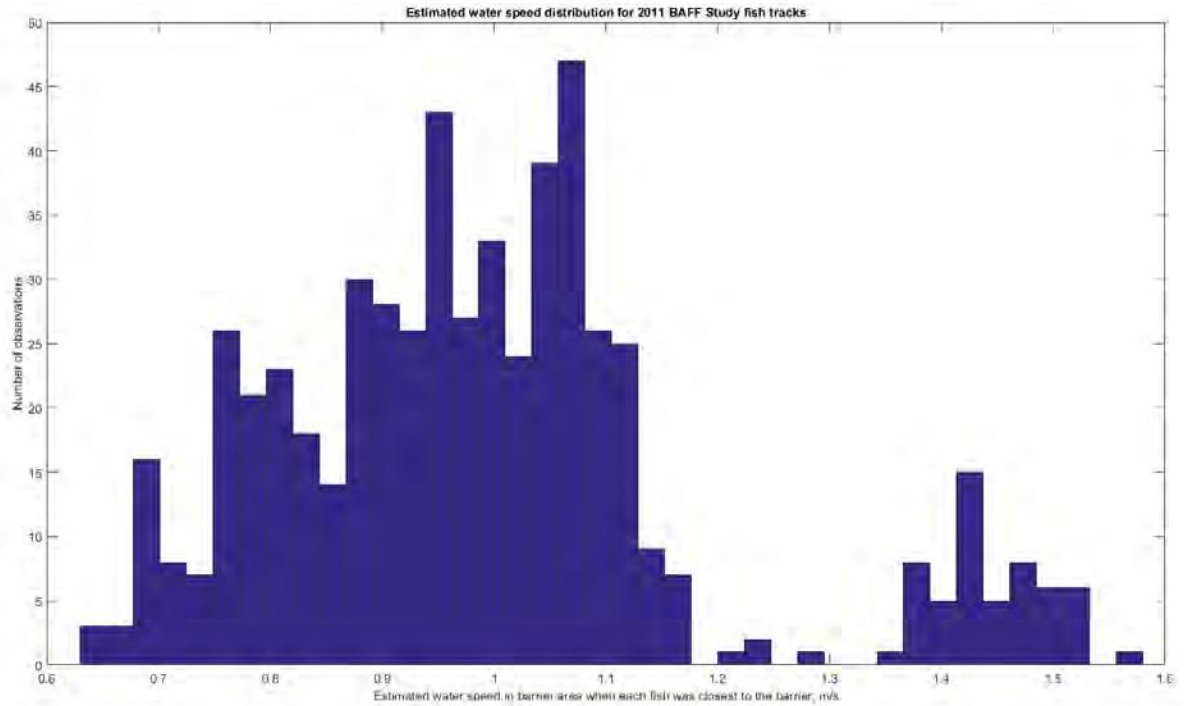

Note: Frequency distribution showing the estimated water speed at the time each 2011 track was closest to the BAFF.

Figure 3.5-30 Estimated Water Speed Distribution for 2011 BAFF Study Fish

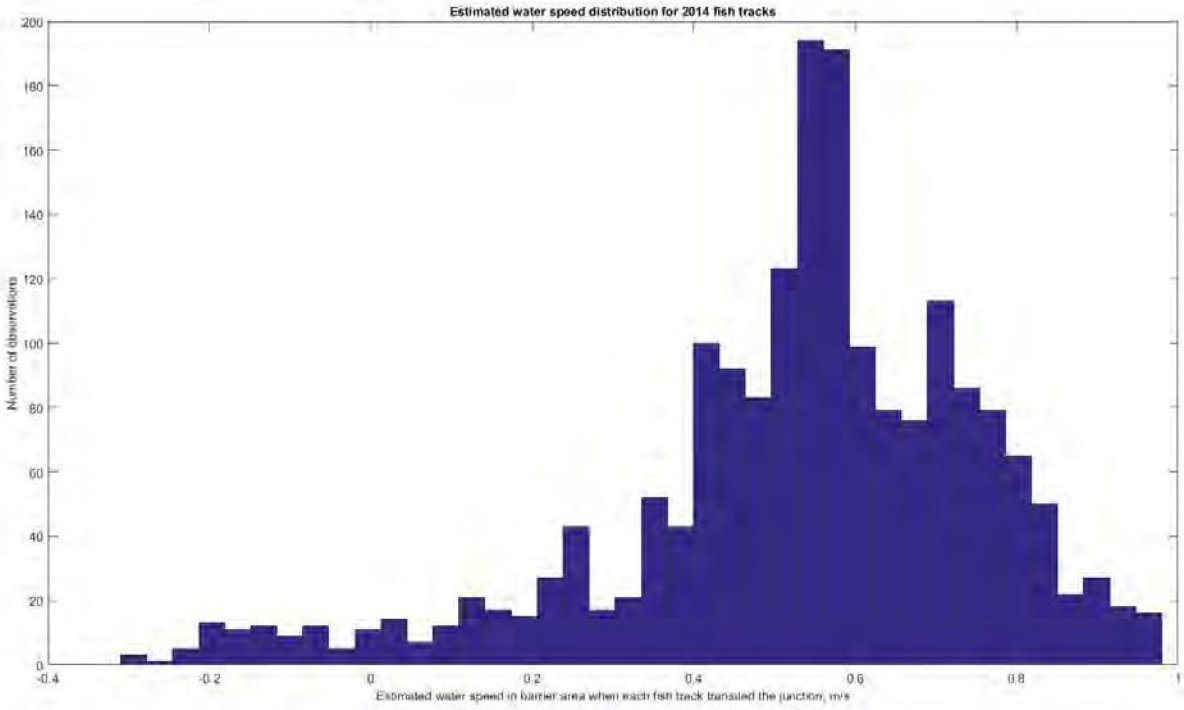

Note: Frequency distribution showing the estimated water speed at the time each 2014 was in the center of the junction.

Figure 3.5-31 Estimated Water Speed Distribution for 2014 Study Fish

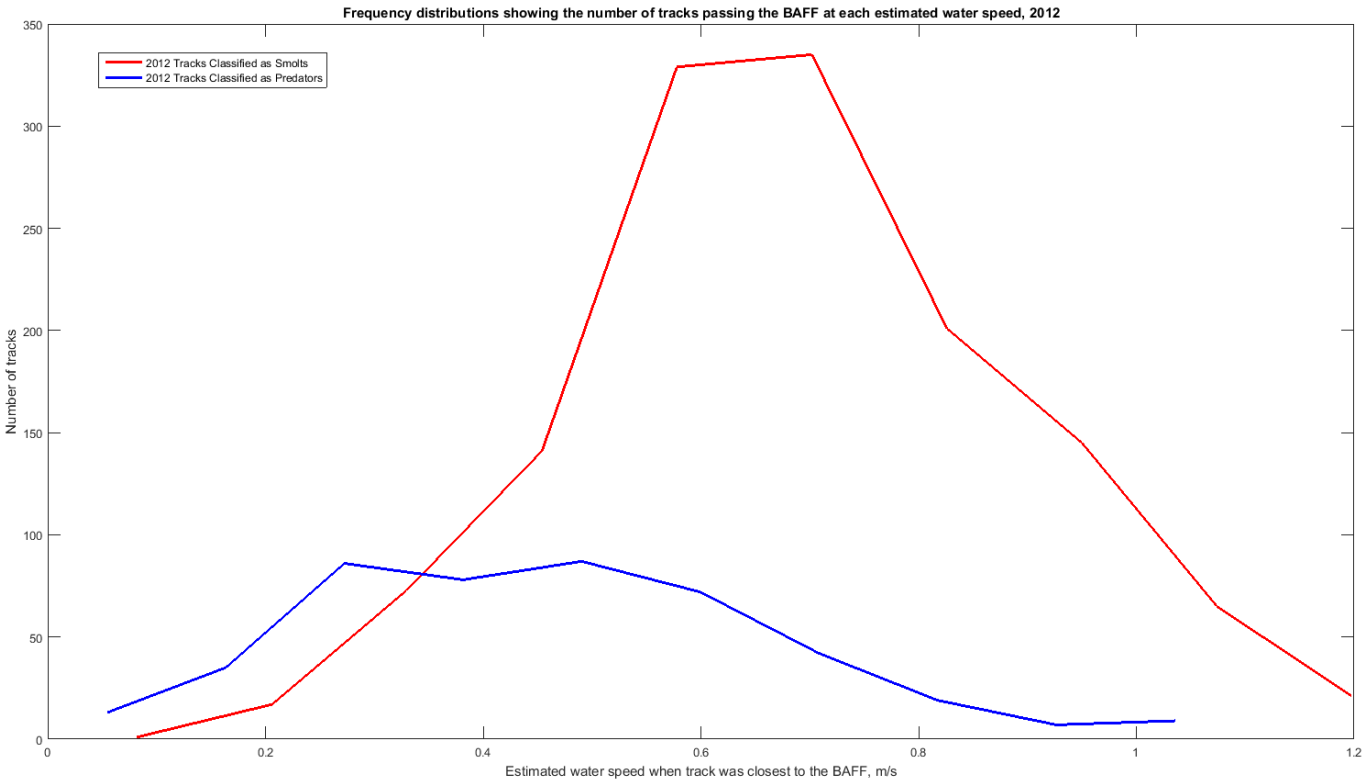

Note: Frequency distributions showing the estimated water speed at the time each 2012 track was nearest to the BAFF. The distribution for fish classified as juveniles and used for analysis is shown in red. The distribution of fish classified as predatory fishes and removed from the analysis is shown in blue. Note that the "predator" distribution is biased towards fish that transited the junction at lower water velocities.

Figure 3.5-32 Estimated Water Speed Distribution by Predator Classification, 2012 BAFF Study

3. The 2011 and 2012 BAFF tracking arrays only extended several hundred meters upstream of the junction, so these tracks provided limited information on the upstream behavior of these fish. In contrast, the 2014 and 2008 arrays extended upstream for nearly a kilometer, which allowed observations of the periodic nature of Type 2 tracks upstream of the junction area; and

4. The 2011 and 2012 study fish were released about 3 km (5 mi) upstream of the study area, while the 2008 and 2014 study fish were released in the City of Sacramento, approximately 50 km (31 mi) upstream. As a result, the 2008 and 2014 study fish may have adopted different rheotaxis behavior due to their increased acclimation time.

As a result of a combination of these factors the pool of 2011 and 2012 tracks selected for analysis were consistent with the hypothesis that study fish were drifting downstream through the junction while maintaining rheotaxis by swimming roughly parallel with streamlines. In retrospect, it is unclear whether these fish were engaging in sustained cross-stream swimming behavior that was not detected because of the high advection speeds within the limited tracking array, or f these fish were exhibiting a different range of rheotaxis behaviors encountered during the 2014 and 2008 studies. However, it is clear that understanding of juvenile salmon movement in general and in junctions specifically needs to be modified to explicitly consider the ratio of advective speeds to cross-stream rheotaxis swimming speeds.

Although the movements of juvenile salmon within junctions involve both advection by the local velocity fields and behavioral responses to a broad range of biotic and abiotic stimuli, the degree to which either plays a role, varies by the ratio of the magnitude of advection relative to swimming performance. Accordingly, the relative importance of behavior and hydrodynamics on governing the observed movements of juvenile salmon in junctions (e.g., fish tracks) can be characterized using the non-dimensional swim number (Horn and Blake 2004),

S = (fish swimming speed)/(current speed) = 1(BL/s)/U

where S is the swim number, U is the water velocity and the sustained swimming performance for juvenile salmon is typically on the order of 2 BL/s.

However, it is likely that juvenile salmon maintain rheotaxis during outmigration with a swim speed below their maximum sustainable swimming performance, so a lower swim speed for scaling outmigration behavior is used. Assuming a rheotaxis swimming speed of around 1.0 BL/s, then for fry (fork length < 75mm [3 in]), the high end of their rheotaxis swimming performance is on the order of 0.08 m/s (0.25 ft/s); for smolts on the order of 150 mm (6 in), 0.15 m/s (0.5 ft/s).

Current speeds at peak Sacramento River flows (85,000 cfs) downstream of Georgiana Slough and during the peak ebb tidal flows can be greater than 1.2 m/s (4 ft/s). Advection is expected to dominate the shape of the fish tracks over behavior when the velocity magnitude is much greater than the rheotaxis swimming speed during high flow events and the peak ebb tides (for fry [red] and juveniles [blue] in **Figure 3.5-33** and **Figure 3.5-34)**.

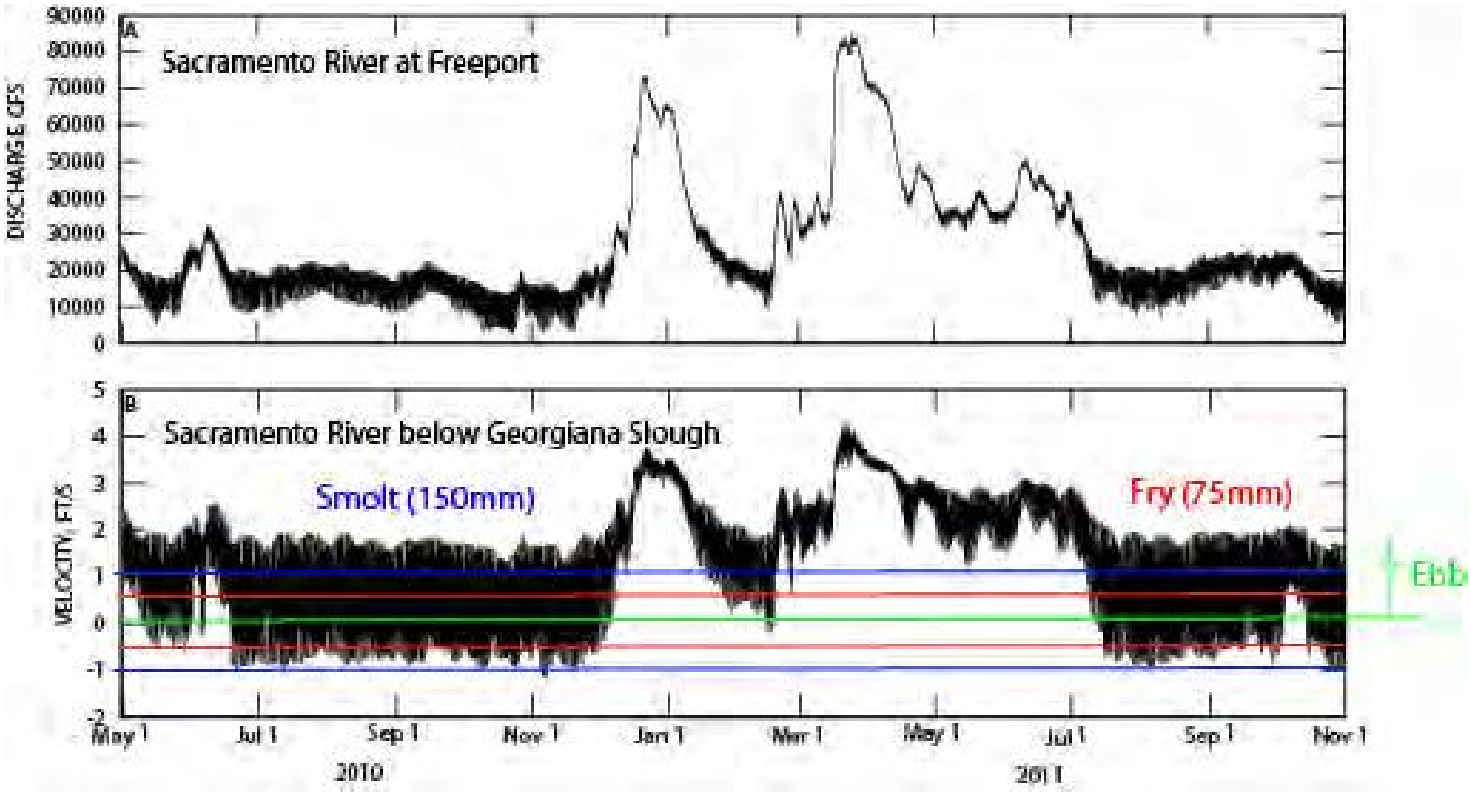

Note: Time series plot of (A) discharge (cfs) at the Sacramento River at Freeport, and (B) velocity in the Sacramento River downstream of Georgiana Slough (black) and an estimate of the smolt (blue) and fry reotaxis swimming speeds. Positive velocities (above the green zero line) represent ebb tides, negative, flood tides.

Figure 3.5-33 Time Series of Discharge at Freeport and Velocity in the Sacramento River

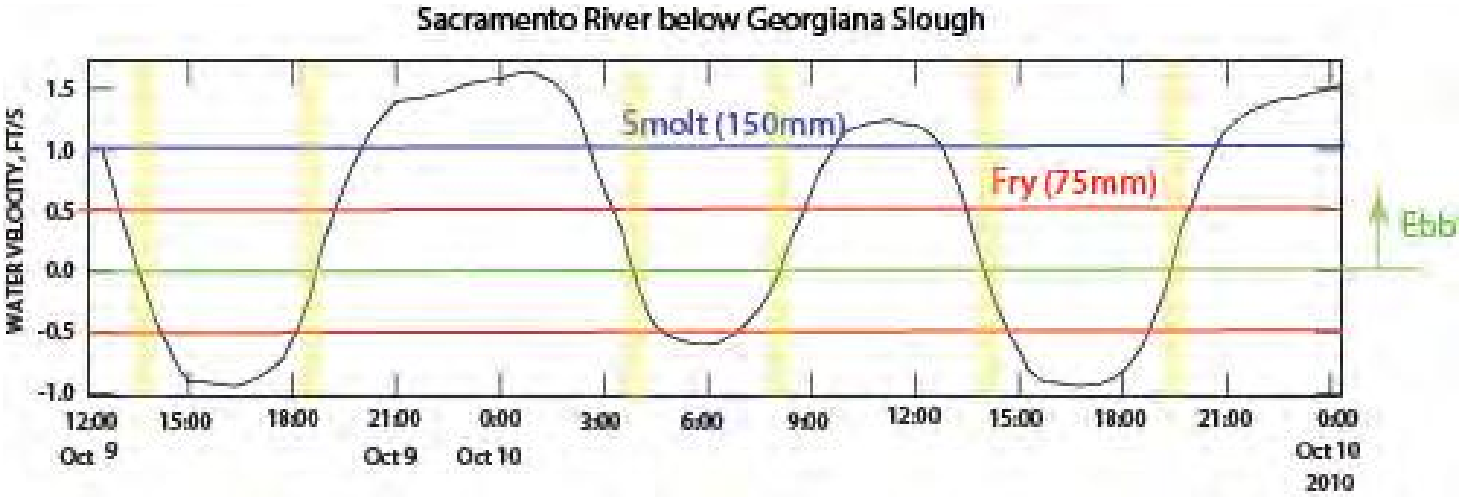

Note: Time series plot of in the Sacramento River downstream of Georgiana Slough (black) and an estimate of the smolt (blue) and fry reotaxis swimming speeds. The yellow vertical bars indicate slack water periods.

Figure 3.5-34 Tidal Time-Scale Time Series of Velocity in the Sacramento River

As is the case throughout much of the north Delta, outmigrants have more control (including resting and holding behaviors) over where they go during flood tides when the Sacramento River flows are low because the velocities are weaker on flood tides. This may explain why fewer fish are observed to move upstream into Georgiana Slough on flood tides (see Section 3.5).

There is very little velocity refugia in the steep sided, rocked, narrow, high velocity canals that make up the majority of the habitat in the Delta. This observation also naturally leads to downriver selective tidal stream transport (Levey and Candenhead 1995) (e.g., tidal surfing) – easier to hold on flood tides, which push fish back upstream. Finally, during the relatively short low-velocity periods (~1-2 hours), when the current speeds are weak, behavior is expected to contribute significantly to the shape of the fish tracks (**Figure 3.5-34**). Although low-velocity periods are relatively short, they can contribute significantly to entrainment because converging river discharges into Georgiana Slough occur when velocities are weak.

Thus, the shape of fish tracks made by juvenile salmon exhibiting identical rheotaxis behavior can vary widely depending on the velocity magnitude and the tidal phase of the ambient velocity fields. When S<<1, tracks will approximate neutrally buoyant non-behaving particles because advection dominates over behavior, but when S >>1 tracks can appear to exhibit milling or seeking behavior because ambient velocities are low and behavior dominates over advection. When S ~ 1 then both advection and rheotaxis behavior play and important role and tracks can show periodic cross-stream motion combined with directed downstream movement. The shape of the along-channel distance of the zig-zag behavior can be estimated based on the rheotaxis wavenumber:

$$\lambda_{rheo} = \frac{2WU_x}{U_y}$$

where W is the width of the channel, U_x is downstream advection and U_y is the reotaxis speed (see **Figure 3.5-39**).

When the swim number scaling concept is applied to the 2014 tracks collected during ebb tides, the results are consistent with the hypothesis that the majority of the 2014 ebb tide tracks were made by fish exhibiting similar

rheotaxis behavior. However, differences in the ratio between rheotaxis swim speed and water velocity resulted in a wide variety of 2D track shapes. For example, during periods of very strong currents the rheotaxis wave number was significantly longer than the domain of the telemetry network so the zig-zag behavior resulting from similar rheotaxis behavior was not able to be detected.

To perform this analysis, each track's integral averaged cross-stream velocity was used as an estimate of effective rheotaxis swim speed and scaled by the estimated water velocity when each track was closest to the barrier; resulting in a swim number estimate for each fish track transiting the junction during tides.

The resulting distributions of individual fish swim numbers by track type show that the majority of Type 1 fish tracks were made by fish with the lowest swim numbers, the majority of Type 3 fish tracks were made by fish with very high swim numbers, and the majority of Type 2 tracks were made by fish with intermediate swim numbers between 0.2 and 0.6 (**Figure3.5-35**).

When the data used for the swim number scaling into distributions for cross-channel velocity and downstream advection velocity are separated for each track type (**Figure 3.5-36**, and **Figure 3.5-37**), the combined variance in the water velocity and cross-channel velocity distributions accounted for the observed swim numbers, rather than changes in water velocity or cross-channel velocity. One can see that fish that made Type 1 tracks tended to transit the junction at higher water velocities than fish that made Type 3 or Type 2 tracks, but the water speed distributions for all three types overlap for moderate water velocities (**Figure 3.5-36**). Similarly, the cross-channel velocity distributions that were used as estimates of rheotaxis velocity show fish with Type 1 tracks tended to have lower cross-channel swim speeds, fish with Type 3 tracks tended to have higher cross-channel swim speeds, and fish with Type 2 tracks tended to have median swim speeds, but again the distributions all overlap (**Figure 3.5-37**).

By putting all of these observations together the conceptual model of juvenile movement in junctions can be updated as follows:

1. Any population of juveniles will have a distribution of rheotaxis swim speeds that will have a significant cross-stream velocity component. The mean and variance of the population's cross-stream rheotaxis swim speed distribution will be driven by the population's physiology; based on the 2008 and 2014 data the mean of this distribution can be estimated to be around 0.2 m/s (0.65 ft/s) (**Figure 3.5-38**);

2. The balance between freshwater outflows and tidal forcing in the junction of interest will determine the range of velocity conditions that juvenile salmonids encounter. For example, low outflows tidal forcing might result in a observed velocity distribution with a low mean and high variance, such as was observed in 2014 (**Figure 3.5-31**), or during high outflows the velocity distribution might have a very high mean (**Figure 3.5-30**);

3. The population's cross- stream rheotaxis swim speed distribution combined with the populations observed advection velocity distribution will determine the mix of track types within a junction (or channel); if there are a significant number of fish with swim numbers greater than 0.1 a mix of Type 1 and Type 2 tracks can be expected, if water velocities are low enough for swim numbers to reach and exceed 1.0 then a significant proportion of Type 3 tracks is expected;

4. The anticipated balance between advection velocity and cross-stream rheotaxis velocity can be used to predict the overlap between a junction's hydraulic entrainment zones and fish entrainment zones. As swim numbers decrease (higher velocities), the fish's entrainment zones will increasingly overlap with the hydraulic entrainment zones; and

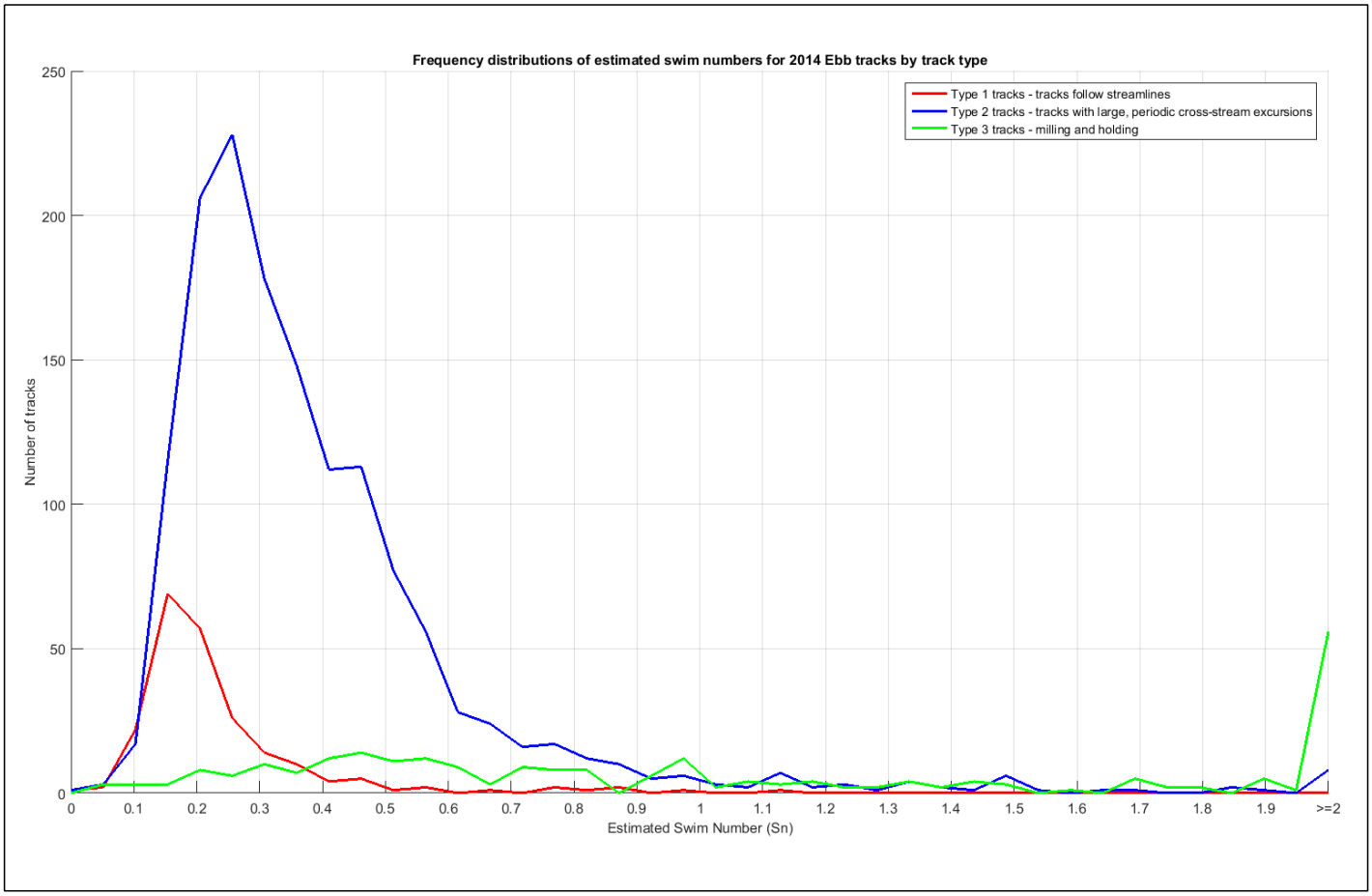

Note: Frequency distributions showing the distribution of swim numbers for each track type classification for the 2014 study tracks. Note that the Type 1 fish had the lowest swim numbers (red line), the Type 3 fish had the highest swim numbers (green line), and the Type 2 fish had intermediate swim numbers less than 1.0 (blue line).

Figure 3.5-35 Estimated Swim Number Distributions for 2014 Tracks by Track Type

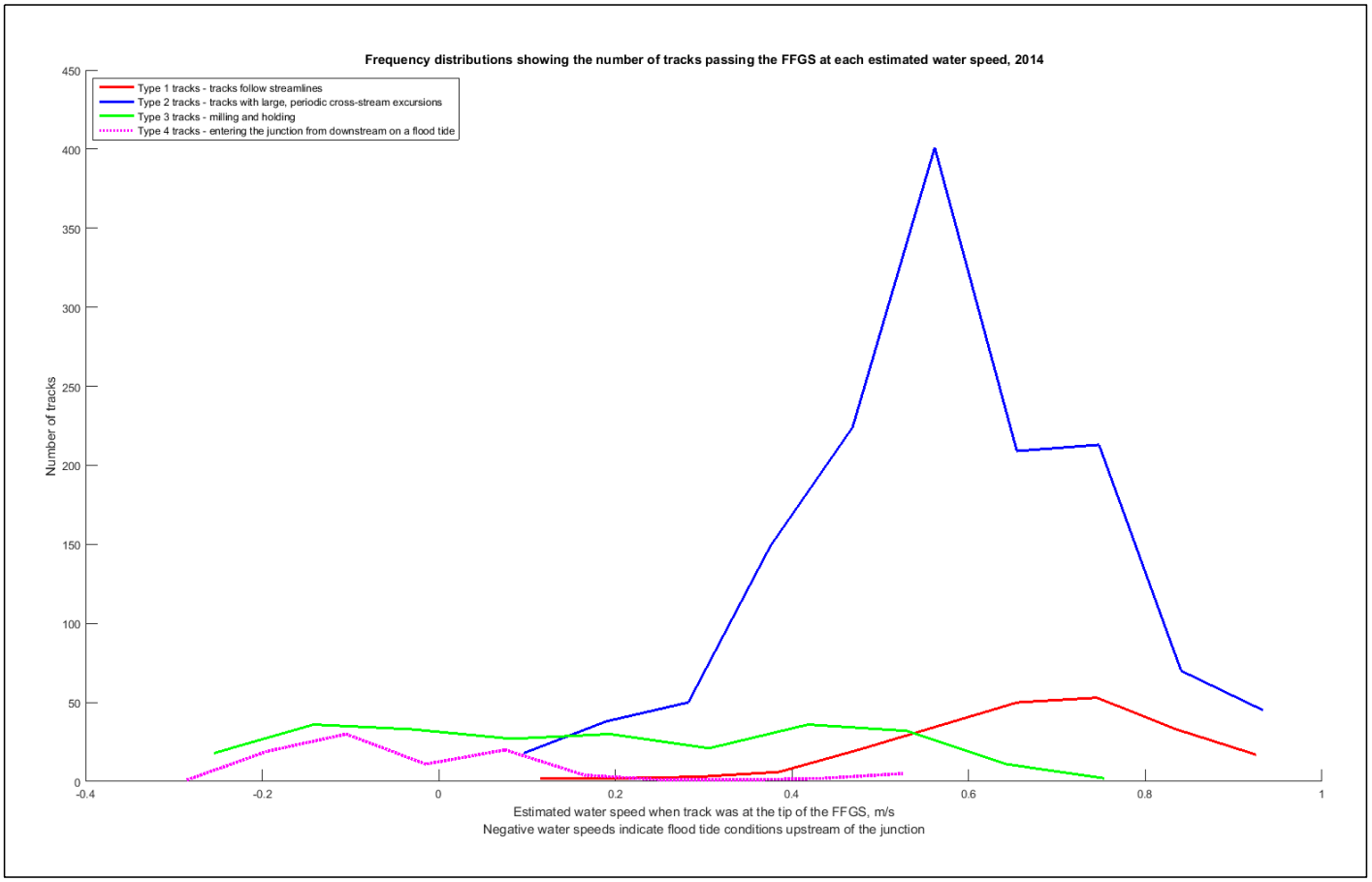

Note: Frequency distributions showing the distribution of advection velocity (water velocity) for each track type classification for the 2014 study tracks. Note that the Type 1 tracks occurred at higher velocities (red line), the Type 3 tracks did not occur at the highest observed velocities (green line), and the Type 2 tracks mostly occurred between 0.3 m/s and 0.6 m/s (1-2 ft/s) (blue line).

Figure 3.5-36 Estimated Advection Velocity Distributions for 2014 Tracks by Track Type

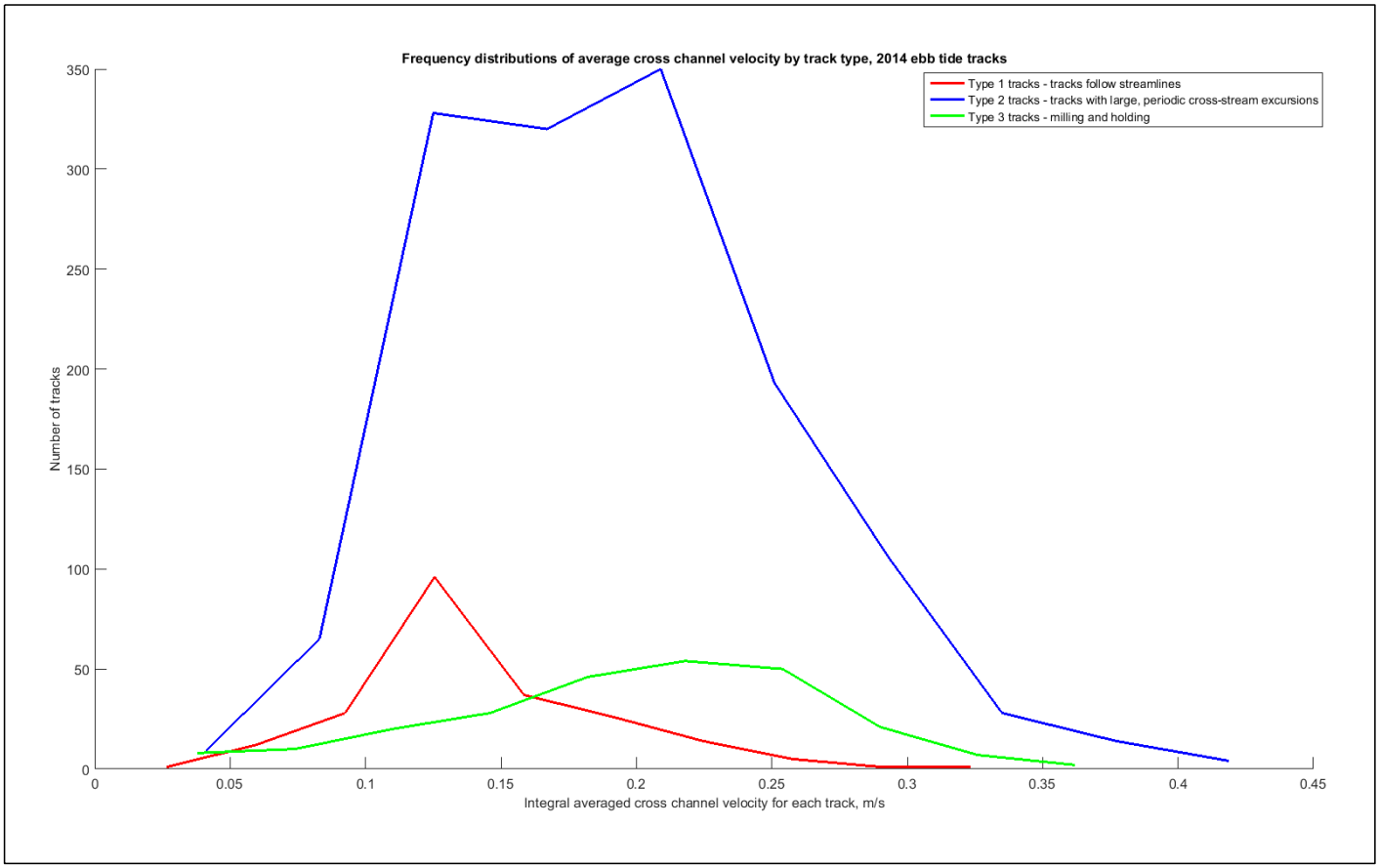

Note: Frequency distributions showing the distribution of cross-stream velocity (estimated rheotaxis velocity) for each track type classification for the 2014 study tracks. Note that the three distributions overlap significantly. The Type 1 tracks had lower cross-stream velocities (red line), fish with Type 3 tracks tended to come from the upper half of the velocity distribution (green line), and Type 2 tracks mostly belonged to fish from the center of the velocity distribution (blue line).

Figure 3.5-37 Integral Averaged Cross-Stream Velocity Distributions for 2014 Tracks by Track Type

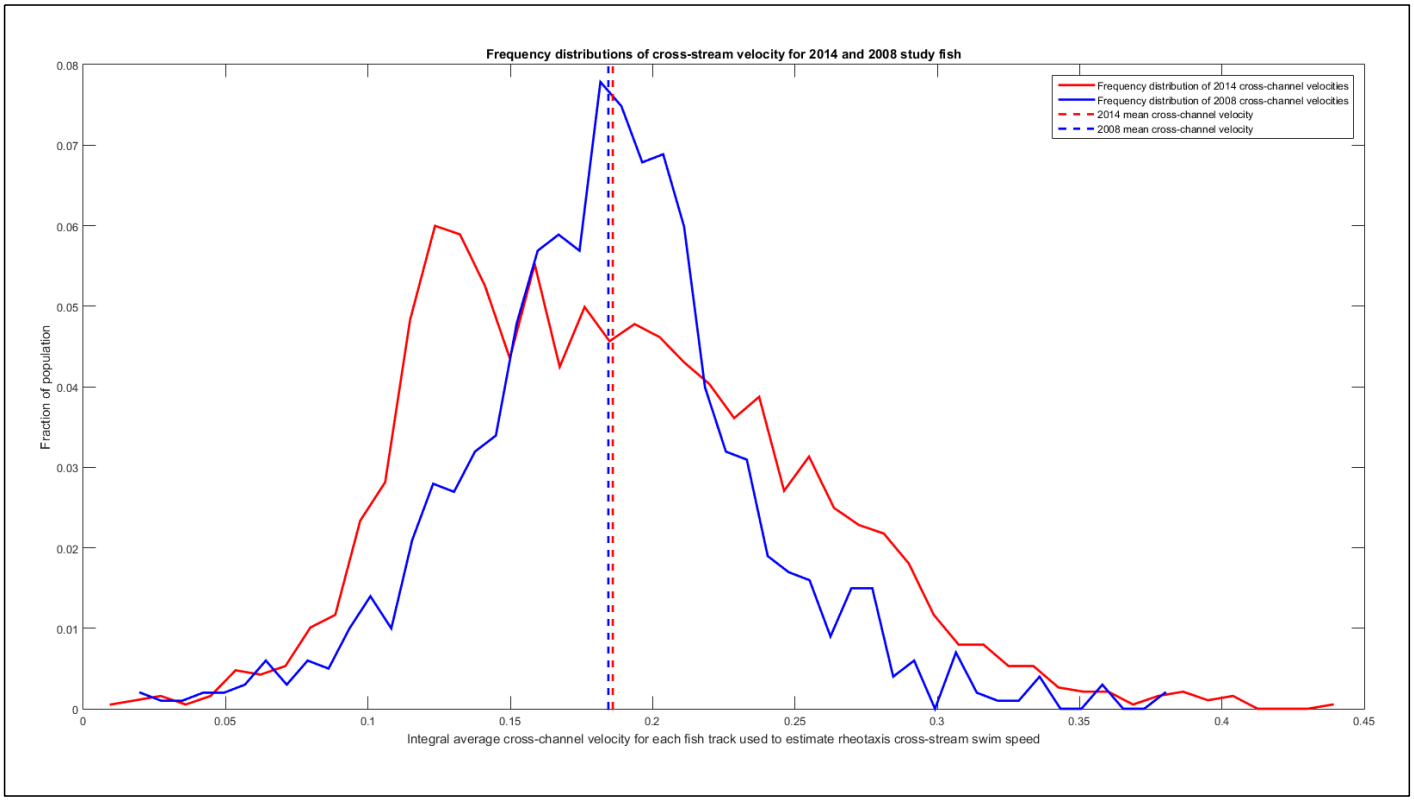

Note: Frequency distributions showing the distribution of integral average cross-channel velocity for each 2014 and 2008 fish track. The integral average cross-channel velocity is an estimate of the cross-channel rheotaxis swim speed. The 2014 distribution is shown in red and the 2008 distribution is shown in blue, with the means of each distribution represented by the dashed lines. Note that while the 2014 distribution had greater variance, but the means are almost identical, at approximately 0.18 m/s (0.59 ft/s).

Figure 3.5-38 Overall Estimated Cross-Channel Velocity Distributions from 2014 and 2008 Study Fish

5. Similarly, the anticipated distance downstream where the FFGS is expected to be effective under worst-case conditions based on the balance between advection velocities and rheotaxis velocities, and the anticipated location of the critical streakline relative to the downstream tip of the barrier (**Figure 3.5-39** and **Figure 3.5-40**) can be described by:

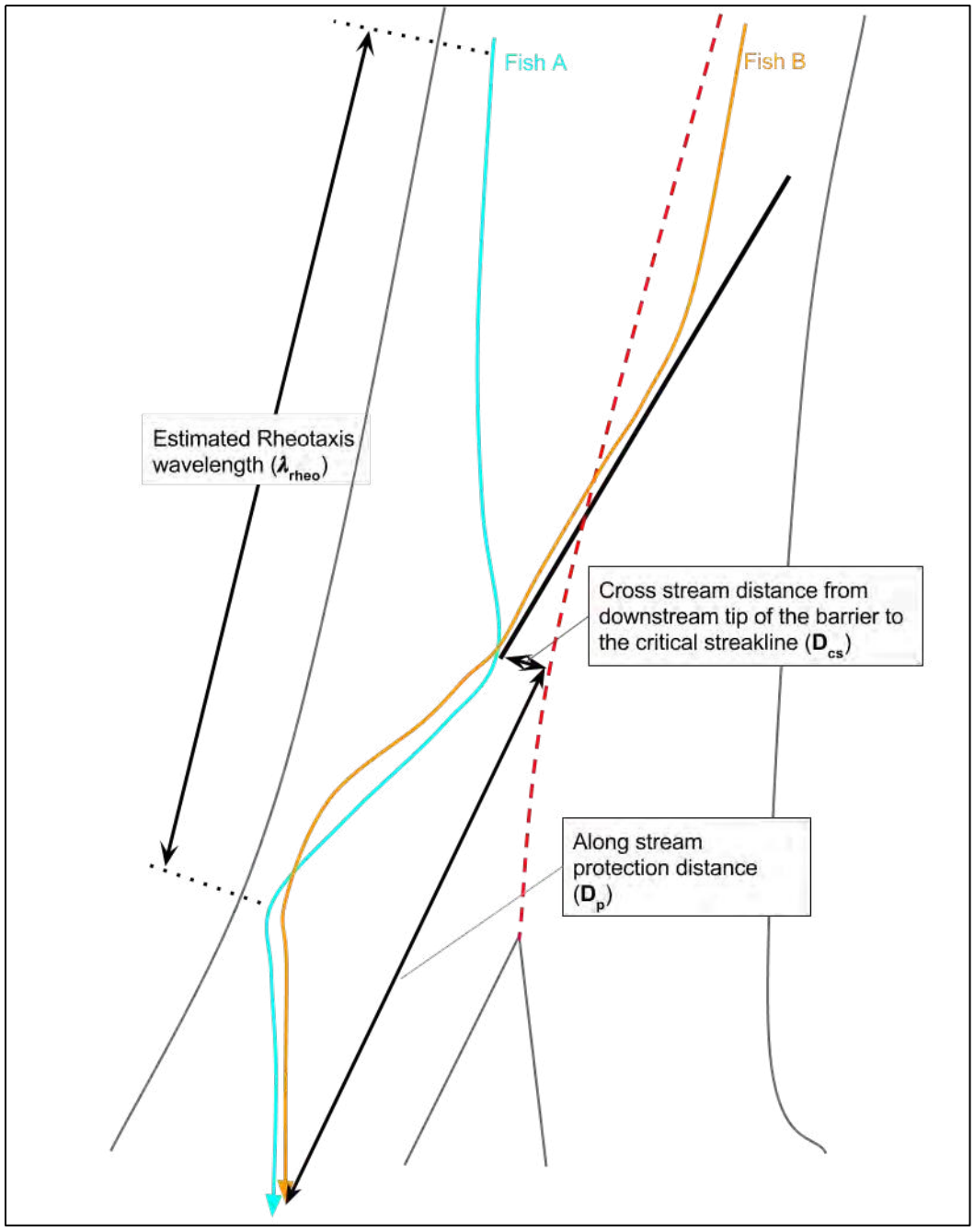

Note: Conceptual illustration of the "best case" interaction of FFGS barrier with two different Type 2 fish. The banks of the junction are drawn in light grey, the hypothetical FFGS is the solid black line, the location of the critical streakline in this scenario is shown by the red dashed line, and the hypothetical fish tracks are drawn in orange and light blue. Fish A encounters the downstream tip of the FFGS and swaps its cross-stream rheotaxis swim direction resulting in sustained cross-stream swimming towards the Sacramento River side of the junction. Fish B encounters the barrier, changes its rheotaxis to move downstream parallel to the barrier, then resumes cross-stream rheotaxis swimming downstream of the tip of the barrier towards the Sacramento River side of the junction. Either of the scenarios will result in the greatest downstream protection distance (black arrow in along-stream direction) for Type 2 fish with this combination of barrier alignment and critical streakline location.

Figure 3.5-39 Conceptual Diagram of the Best Case Interaction between a FFGS Barrier and Type 2 Fish

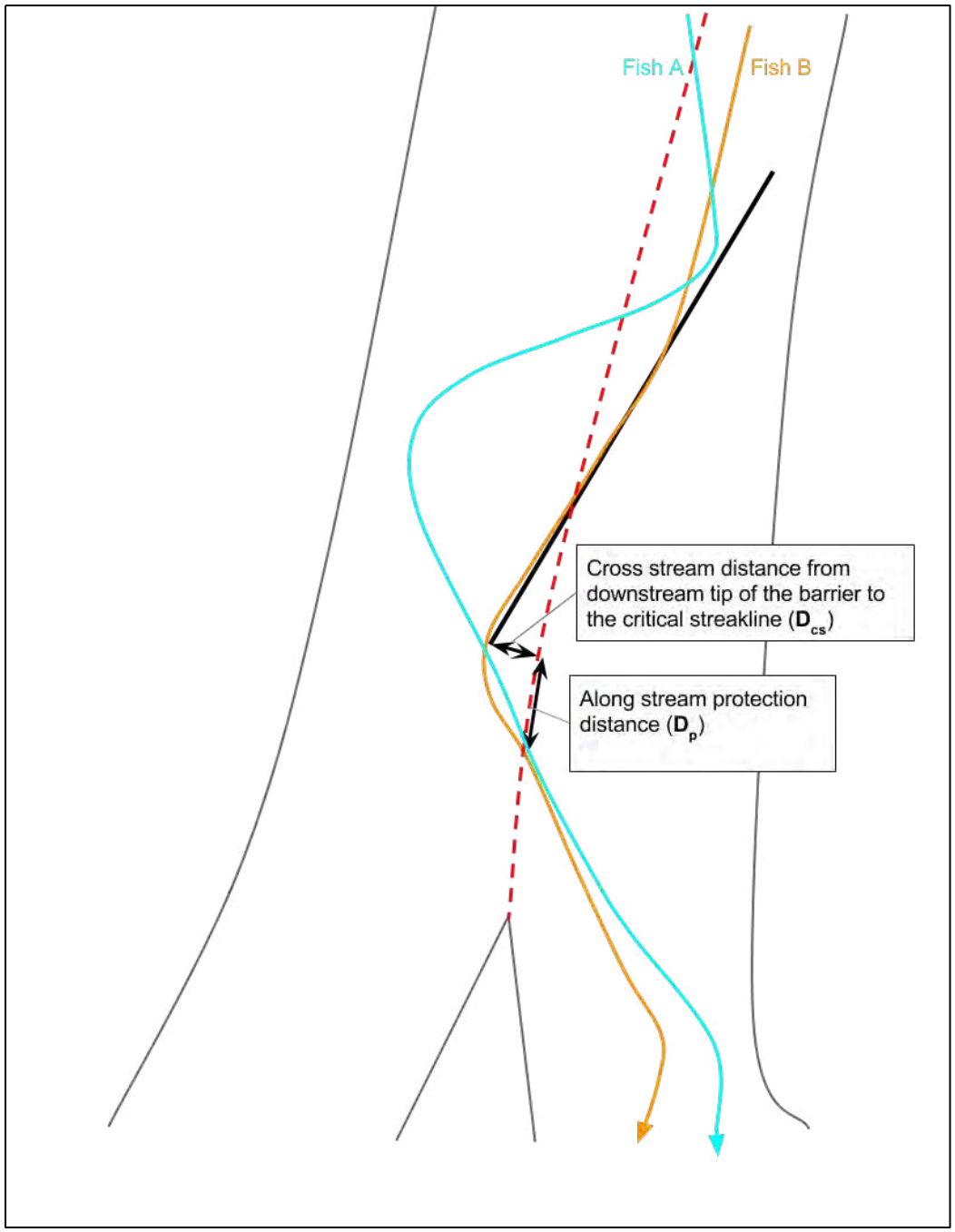

Note: Conceptual illustration of the "worst case" interaction of a FFGS barrier with two different Type 2 fish. The banks of the hypothetical junction are drawn in light grey, the hypothetical FFGS is the solid black line, the location of the critical streakline in this scenario is shown by the red dashed line, and the hypothetical fish tracks are drawn in orange and light blue. Fish A encounters the FFGS and swaps its cross-stream rheotaxis swim direction resulting in sustained cross-stream swimming towards the desired outcome, but this fish changes its cross-stream swimming direction again upon encountering the opposite bank, initiating another excursion towards Georgiana Slough, passing just downstream of the tip of the barrier and into Georgiana Slough. Fish B again encounters the barrier, changes its rheotaxis to move downstream parallel to the barrier, and again resumes cross-stream rheotaxis swimming downstream of the tip of the barrier, but this time the rheotaxis swimming is towards Georgiana Slough. Either of the scenarios will result in the shortest downstream protection distance (black arrow in along-stream direction) for Type 2 fish with this combination of barrier alignment and critical streakline location.

Figure 3.5-40 Conceptual Diagram of the Worst Case Interaction between a FFGS Barrier and Type 2 Fish

*Downstream Protection Distance = (Cross-stream distance from downstream tip of barrier to critical streakline/ Rheotaxis speed) * Advection Speed*

$$D_P = \frac{D_{CS}}{U_x} * U_y$$

Based on this revised fish entrainment conceptual model, it can be understood why the 2014 FFGS was not effective for the few fish that passed the barrier when the critical streakline was to the left of the barrier tip: if the critical streakline was 5 m (16 ft) to the left of the downstream tip of the 2014 FFGS, the mean downstream advection velocity was 0.57 m/s (1.87 ft/s), and the mean cross-stream rheotaxis swim speed was 0.186 m/s (0.61 ft/s), then the worst case downstream protection distance can be estimated as follows:

*Downstream Protection Distance = (Distance to Critical Streakline/Rheotaxis speed) * Advection Speed*

= (5m / 0.186m/s)*0.57m/s

=15 m (50 ft).

Given that the downstream tip of the barrier was about 110 meters (363 ft) upstream from the shoal separating the Sacramento River from Georgiana slough, it can be seen that the low water velocities observed provided more than enough time for a fish's cross-stream rheotaxis velocity to move it back cross the critical streakline to the Georgiana Slough side of the junction even if the barrier performed as expected.

However, if the 2014 FFGS had been deployed during high out-river discharges, such as those that occurred in 2011, the foregoing calculation would have yielded an estimated worst case protection distance of about 100 meters (330 ft). It is expected that the FFGS barrier would have been much more effective under the 2011 conditions.

While barrier operations did not result in a large decrease in overall entrainment, the reduction in the number of fish between the barrier operational and non-operational position observed when the barrier was operational during ebb tides indicates that few fish passed under or through the barrier during this time. Turning point analyses show that moving the barrier to the operational position shifted the density of turning points from behind the barrier-operational position when the barrier was non-operational, to the area immediately in front of the barrier when it was operational.

These observations support the hypothesis that the barrier or its hydrodynamic signature is triggering a sustained change in the cross-stream movement of Type 1 and Type 2 fish away from the barrier. If this is the case, then a structure similar to the FFGS that extended further downstream could be used to successfully deter fish away from Georgiana Slough, or a similar structure could be installed in other junctions to move fish towards low-risk migration corridors. Moreover, a barrier placed farther out into the channel would likely have been more effective, given the majority of fish were concentrated in the center of the channel adjacent to the barrier with most of the fish well river right of the barrier (**Figure 3.5-11**) with relatively few fish interacting with the barrier under the conditions during which it was expected to work. However, accommodation for navigation limited how far into the channel the barrier could be placed.

Finally, it should be emphasized that although the FFGS structure did not reduce entrainment, it appears to have consistently initiated sustained cross-stream motion away from Georgiana Slough for Type 2 fish tracks, which indicates that a revised FFGS design could be effective at changing entrainment rates in junctions if the structure

was optimally positioned. Nevertheless, given that fish appear to be guiding off some structure in this general region, it is difficult to assess how the FFGS technology would work in other junctions given that the response to the non-operational position in this junction is was affected by fish responding to other phenomenon in the barrier-Off location.

In the future, it is recommended that using the enhanced understanding of the effects of cross-stream rheotaxis swimming to design barriers by scaling anticipated advection velocities against anticipated rheotaxis velocities to estimate the best along-stream location for the FFGS, and then using the critical streakline analysis techniques laid out in Section 3.3, determine the best cross-stream location of the FFGS (**Figure 3.5-39**).

3.6 ANALYSIS OF PREDATORS AND PREDATION

As an engineering option being considered to further reduce entrainment of emigrating juvenile salmonids into the interior and south Delta, a FFGS was constructed and evaluated in the Sacramento River at the divergence of Georgiana Slough in 2014. In-channel water structures can often create important habitat locations for predatory fishes, and therefore they could provide an elevated risk of predation on juvenile salmonids and other native fishes (Vogel 2011). For example, Sabal et al. (2016) found that striped bass were associated more with anthropogenic habitats than with natural habitats in the lower Mokelumne River, and that decreasing their density below a major in-channel structure (Woodbridge Irrigation District Dam) increased juvenile salmon survival. Therefore, it is of management importance to assess the potential for the FFGS to provide predatory fish habitat and how the structure may affect rates of predation on juvenile salmonids passing the FFGS. As described in this section, the study employed several different methods to address the primary objective of assessing predator behavior and predation in the FFGS vicinity.

In-channel structures pose a concern because of the potential for increased predation on juvenile Chinook salmon and other species. The predation risk to juvenile Chinook salmon from predatory fishes associated with in-channel structures such as the FFGS has received some study in the Delta. A very low rate of predation on acoustically tagged juvenile Chinook salmon in the FFGS study area (3.7%) was found during the 2011 BAFF study (DWR 2012). Nearly 60 percent of predation events occurred upstream from the BAFF section of the study area (analogous to upstream from the FFGS section in the present study; see below), with the remainder occurring downstream from the BAFF section. Most predation evaluated within the BAFF study area occurred more than 5 m (16 ft) away from the BAFF, with a fairly even split in the number of predation events 5 to 80 m (16-262 ft) from the BAFF and greater than 80 m (262 ft) from the BAFF. Over half (65%) of the predation events occurred with the BAFF Off. Predation frequency was positively correlated with water temperature. The 2012 BAFF study (DWR 2015b) found a higher rate of predation (23%) on acoustically tagged juvenile Chinook salmon than in 2011, possibly because of lower flows leading to greater juvenile Chinook salmon transit time and greater predator habitat suitability, and therefore a greater chance of encountering predators in 2012 than 2011. Most predation (76% of events) occurred upstream from the BAFF section of the study area. Similar patterns were observed for juvenile steelhead, although the overall rate of predation was higher (33%) than for juvenile Chinook salmon. The majority of predation events occurred more than 80 m (262 ft) from the BAFF (74% for Chinook salmon; 81% for steelhead), whereas very little predation occurred less than 5 m (16 ft) from the BAFF (9% for Chinook salmon; 2% for steelhead). For Chinook salmon, a greater percentage of predation events occurred with the BAFF Off (62%) than with the BAFF On (38%), whereas for steelhead the opposite was true (BAFF On: 57%; BAFF Off: 43%).

3.6.1 PREDATION (HYPOTHESES H5 AND H6)

MAIN FINDINGS

The main findings of the predation analyses were:

- The probability of predation of Chinook salmon juveniles in the study area with FFGS On and FFGS Off was not significantly different;
- The probability of predation was negatively related to turbidity;
- The probability of predation was lowest less than 5 m and 5 to 10 m (16 ft and 16-33 ft) from the FFGS buoy line and highest more than 10 m (33 ft) from the FFGS buoy line;
- The spatial distribution of predation events did not differ between FFGS On and FFGS Off; and
- A relatively high proportion of predation events occurred near the Walnut Grove Bridge and the Offshore Downstream Dolphin to which the FFGS was attached.

OBJECTIVES

In the present study, predation data, based on classifications from the Fish Fates Conference (see Section 2.6.3, "Fish Fates Classification and Assignment"), were used to assess whether the FFGS affected the predation risk of acoustically tagged juvenile Chinook salmon in the study area. The objectives of this component of the study were to assess whether predation risk increased with FFGS On and whether proximity to the FFGS affects predation risk (i.e., because of the FFGS harboring predatory fishes or increasing their predation effectiveness). Specifically, this study component tested Hypothesis H5: The probability of juvenile Chinook salmon being eaten within the Georgiana Slough hydrophone array is greater with the FFGS On than with the FFGS Off; and Hypothesis H6: The probability of juvenile Chinook salmon being eaten at the Georgiana Slough divergence increases with decreasing distance from the FFGS. In addition, other potentially important environmental variables affecting the probability of predation were explored.

METHODS

Data Analysis

Hypotheses H5 and H6 (Resampling Analysis)

The analysis of predation to test Hypotheses H5 and H6 used the classifications of juvenile Chinook salmon fates from the fates conference and follow-up work (see Section 2.6.3, "Fish Fates Classification and Assignment"). Note that the analysis of predation is biased toward tags that approached within 10 m (33 ft) of the buoy line at some point during their occurrence in the study area (as detected by the hydrophone array); this criterion was used to subset the overall number of tags to those that were more likely to have interacted with the FFGS, in order to assess barrier effectiveness. The fates data were reduced based on the following filtering steps of data in the master data set:

- Included only fish for which tracks had not been corrected (TRK_CORR 1 = 0);

- Included only fish for which the responses to the FFGS were not guided by the FFGS, were guided by the FFGS, or never experienced the FFGS (RESPONSE 1a (within 10 m [33 ft]) = 0, 1, or 2; RESPONSE 1b (within 5 m [16 ft]) = 0, 1, or 2);

- Included only fish for which the classification of predation upstream and downstream from the FFGS was not eaten, eaten more than 10 m (33 ft) from the FFGS, eaten 5 to 10 m (16-33 ft) from the FFGS, or eaten less than 5 m (16 ft) from the FFGS (PREDATION 1 = 0, 1, 2, or 3; PREDATION 2 = 0, 1, 2, or 3); and

- Included only fish for which the classifications were made with the FFGS Off or FFGS On (FFGS = 0 or 1).

As described in Section 2.6.3, "Fish Fates Classification and Assignment," predation was classified as being upstream or downstream from the FFGS. Upstream predation events occurred upstream from an imaginary line drawn perpendicular to the channel thalweg at the downstream tip of the FFGS, and were classified according to one of the three distances described previously for the PREDATION 1 variable. Downstream from FFGS predation events (PREDATION 2 variable) occurred downstream from the imaginary line drawn perpendicular to the channel thalweg at the downstream tip of the FFGS, with these events classified as being in the Sacramento River if they were on the Sacramento River side of an imaginary line drawn from the FFGS tip to the middle of the point of land separating the Sacramento River from Georgiana Slough; predation events occurring on the other side of this line were classified as Georgiana Slough. For the purposes of testing of Hypotheses H5 and H6, predation events upstream and downstream from the FFGS were combined and classified according to the distances discussed previously.

The analysis of Hypotheses H5 and H6 included only the first period of occurrence of acoustically tagged juvenile Chinook salmon in the study area; fish that were either advected back upstream or for which the tags were classified as having returned within predatory fishes were excluded from the analyses. To test Hypothesis H5, a resampling method ("bootstrapping") (Brown et al. 2012) was used to produce statistical summaries of the data. The fate of each juvenile Chinook salmon was classified as eaten (numeric value = 1) or not eaten (numeric value = 0). The fates for each FFGS treatment (On or Off) were resampled with replacement until each resample contained the same number of observations (i.e., number of fish) as the original sample. The resampling procedure was repeated 10,000 times, and the arithmetic mean fate was calculated for each of the 10,000 resamples, which resulted in 10,000 resampled means of the proportion of juvenile Chinook salmon eaten. The 10,000 resamples then were used to generate statistical summaries for the proportion eaten by the FFGS treatment (On or Off). The quantities estimated included the mean (50th percentile of the 10,000 resampled means), interquartile range (25th and 75th percentiles of the 10,000 resampled means), and 95 percent confidence interval (2.5 and 97.5 percentiles of the 10,000 resampled means). Hypothesis H5 was accepted if the mean proportion eaten with the FFGS On was greater than with the FFGS Off, and if the 95 percent confidence intervals for the treatments did not overlap.

To test Hypothesis H6, juvenile Chinook salmon were divided into three categories, based on their closest upstream approach to the FFGS buoy line: less than 5 m (16 ft), 5 to 10 m (16-33 ft), and greater than 10 m (33 ft). These classifications were based on the RESPONSE 1a variable described previously. Because predation on fish greater than10 m (33 ft) upstream from the FFGS was appreciable (particularly in the vicinity of the Walnut Grove Bridge; see following "Results"), only fish successfully reaching the FFGS were included in the analysis for the greater than 10 m (33 ft) approach distance category. For each of the approach distance categories, the fates (eaten = 1, not eaten = 0) were classified according to FFGS treatment (On/Off). Similar to the analysis of

Hypothesis H5, resampling (bootstrapping) was used to test Hypothesis H6, with random samples drawn with replacement for each combination of approach distance and FFGS treatment. Hypothesis H6 was accepted if the mean proportion of juvenile Chinook salmon eaten less than 5 m (16) from the FFGS buoy line was greater than the mean proportion eaten further from the FFGS buoy line (i.e., 5 to 10 meters [16-33 ft], and greater than 10 m [33 ft]) and the 95 percent confidence intervals did not overlap.

Generalized Linear Modeling

In addition to the resampling methods described above to test Hypotheses H5 and H6, generalized linear modeling (GLM) was conducted to provide additional insight and a broader perspective into potential factors affecting the probability of predation for tagged juvenile Chinook in the study area. The predictors used to test the probability of entrainment into Georgiana Slough and FFGS performance (i.e., flow [discharge], FFGS On/Off, juvenile Chinook salmon cross-stream position in the study area, critical streakline location, and day/night; see Section 3.4, "Generalized Linear Modeling of Fish Fates") also were included in the GLM assessing the probability of predation. Additional variables included in the GLM were water temperature, turbidity, river stage, and density of predatory fish. *A priori* hypotheses and additional information related to the predictors, included in the GLM, are as follows:

- **FFGS On/Off**: As with the testing of Hypothesis H5, it was hypothesized that the probability of predation would be significantly greater with FFGS On than with FFGS Off, reflecting the FFGS's position in the channel providing greater predator habitat;

- **Flow**: Flow is highly correlated with velocity, and was chosen for inclusion in GLM rather than velocity because it is the more commonly used variable for planning and operations purposes. Flow has been positively associated with salmonid survival probability in the Delta in several studies[15] (Cavallo et al. 2013; Newman 2003; Perry 2010; but also see Zeug and Cavallo 2013), possibly because greater flow results in shorter travel time or more direct migration routing, and therefore, less exposure to predators (Anderson et al. 2005). It was hypothesized that this predictor would be negatively related to predation probability in the study area. The probability of predation GLM used 15-minute mean flow data from the Sacramento River downstream of Georgiana Slough (WGB; USGS site number 11447905), for consistency with the data from other predictors that were recorded at this location;

- **Water temperature**: Juvenile salmonid survival in the Delta has been demonstrated to be negatively associated with water temperature (Newman 2003; Zeug and Cavallo 2013), perhaps because predatory fishes energy requirements increase at higher temperatures, and thus food requirements are greater (Hanson et al. 1997). It was hypothesized that water temperature would be positively related to predation probability in the study area. This predictor was based on 15-minute mean WGB water temperature;

- **Turbidity**: Studies have found a positive relationship between turbidity and survival of Delta native fishes, both in the field (for Chinook salmon: Newman 2003; DWR 2015a) and in the laboratory (for delta smelt: Ferrari et al. 2014), presumably because the visual range of predators is less under more turbid conditions (Aksnes and Giske 1993). It was hypothesized that predation probability would be negatively related to turbidity. This predictor was based on 15-minute median WGB turbidity;

[15] Note that other variables that are often correlated with flow (e.g., turbidity) have not necessarily been examined in such studies, which could mean that associations of flow with survival are aliasing the effects of these variables.

- **Stage (water level)**: River stage could influence the potential for predatory fishes to prey on juvenile Chinook salmon (e.g., the probability of predatory fishes encountering their prey may decrease with greater stage if a greater extent of shallow-water habitat becomes accessible on the river margins, or if the volume of the river channel increases). It was hypothesized that predation probability would be negatively related to stage. This predictor was based on 15-minute mean WGB stage;

- **Ambient light**: Similar to turbidity, ambient light level affects the visual range of predators (Aksnes and Giske 1993), and some predatory species, such as largemouth bass, predominantly feed during the day (Moyle 2002). Ambient light was significantly positively related to predation probability of juvenile Chinook salmon at the Head of Old River, as assessed by GLM (DWR 2015a). Accordingly, it was hypothesized that predation probability in the study area would be positively related to light level. This predictor was based on 1-hour CIMIS data (California Irrigation Management Information System 2014) measured at Twitchell Island Station located near Rio Vista approximately 19 km (12 mi) southwest of Walnut Grove; and

- **Predatory fish density**: Predatory fish density in the study area was hypothesized to be positively related to predation probability because evidence indicates that predator abundance is negatively related to juvenile Chinook salmon survival in the Delta (Cavallo et al. 2013). This predictor was based on split-beam transducer hydroacoustic data[16], collected to evaluate predatory fish density near the FFGS at two locations: one at Dagmar's Landing, opposite the FFGS; and one just downstream from the FFGS on the east side (left bank) of the Sacramento River (see Section 3.6.6, "Active Hydroacoustics [Hypotheses H7 and H10]"). It was assumed that the density of fish targets 30 to 100 cm (12-39 in) in length was representative of predatory fish density[17].

The acoustic tag detections for each juvenile Chinook salmon entering the study area were merged with the data for the continuous predictors above, with means of these predictors calculated for the time period that each juvenile Chinook salmon was in the study area; for fish classified as having been eaten, the means were based only on data up to and including the estimated time of predation. Because ambient light and predatory fish density data were not available for all juvenile Chinook salmon, GLM was undertaken twice: once with all predictors except ambient light and predatory fish density (n = 431 juvenile Chinook salmon); and once with all predictors including ambient light and predatory fish density, while omitting day/night because it represented the same mechanism as ambient light but in categorical form (n = 209 juvenile Chinook salmon)[18]. All continuous predictors were standardized (mean subtracted, then divided by standard deviation) before statistical analysis. No continuous predictors had a correlation coefficient greater than |0.66| with any other continuous predictor, so all were retained in the analysis per the |0.70| threshold used by Zeug and Cavallo (2013).

The probability of predation analyses were undertaken using a GLM within a model averaging/information theoretic framework (Burnham and Anderson 2002), based on the R software (Version 3.1.0; R Core Team 2014) package "glmulti" (Calcagno and de Mazancourt 2010). This modeling technique has been applied on a number

[16] As described in Section 3.6.6, electrical power failure resulted in the transducer on the Walnut Grove side of the river resulted in non-operational periods, principally in March.

[17] However, it acknowledged that hydroacoustic split-beam transducer surveys may underestimate the density of demersal species such as *Micropterus* spp. and catfishes.

[18] The range of environmental conditions represented in the two GLMs were similar but with some differences. For example, mean (± SD) flow for the GLM excluding ambient light and predatory fish density was 8,330 ± 3,495 cfs, compared to 7,324 ± 3,498 cfs for the GLM including these predictors.

of occasions for fish research in the San Francisco Bay–Delta and Central Valley (e.g., Beakes et al. 2012; Zeug and Cavallo 2013). In addition to the standard reference text (Burnham and Anderson 2002) for this modeling technique, a useful summary is provided by Mazerolle (2006).

The gmulti package was used to provide all possible first-order GLMs for probability of predation (eaten, response = 1) versus survival (not eaten, response = 0), with the response modeled with a binomial distribution and logit link function. The relative level of support for each possible model was estimated in glmulti with AIC, corrected for small sample sizes (AIC_c) (Mazerolle 2006). The difference in AIC_c, Δ_i, between each model and the best model (i.e., the model with the lowest AIC_c) was calculated, and Akaike weights (w_i) were calculated based on the Δ_i. Model averaging of the predictor coefficients was undertaken based on the Akaike weights for each model, and unconditional confidence intervals were calculated for each coefficient (Mazerolle 2006). The importance of each predictor was assessed by summing the w_i of all models in which the predictor appeared; following Calcagno and de Mazancourt (2010), importance of 0.8 or greater was used to infer support for a predictor's potential influence on predation probability, in addition to unconditional 95 percent confidence intervals for variable coefficients not overlapping zero (per Zeug and Cavallo 2013).

GLMs, including predictors, were assessed to provide a better fit to the data than intercept-only models if the AIC_c of the full model (with all predictors included) was three or more units greater than the AIC_c of the intercept-only model (Zeug and Cavallo 2013). Model fit to observed data was assessed using similar methods to those of Beakes et al. (2012) and Perry et al. (2014). Model-fit assessment was conducted with the PresenceAbsence package of the R software (Freeman and Moisen 2008). As described by Beakes et al. (2012), an optimized threshold based on Kappa was calculated for each GLM. The threshold value was set where Kappa was maximized for each GLM, and this threshold value was used to estimate Kappa and several additional threshold-dependent model performance statistics: Cohen's Kappa statistic, percent correctly classified (PCC), sensitivity, and specificity. Each statistic is a measure of the capacity to accurately discriminate the correct outcome of predation of tagged juvenile salmonids observed in the data, where probabilities that exceed the threshold were classified as predation (positive) and probabilities below the threshold were classified as survival (negative). Beakes et al. (2012) described these statistics as follows:

> The Kappa statistic is a measure of all possible outcomes of presence or absence that are predicted correctly, after accounting for chance predictions; it is generally accepted as a conservative and standardized metric for comparing the predictive accuracy of binary models regardless of their statistical algorithm (Manel et al. 2001). PCC compares the proportion of outcomes correctly classified. In this application, sensitivity represents the proportion of true positives correctly identified, and specificity is the proportion of true negatives correctly identified, where 1-specificity is the proportion of false positives.

In addition to the threshold-dependent model performance statistics, a threshold-independent measure of model performance also was used: the area under the ROC curve. This measure indicates the probability of detecting a true signal (sensitivity) versus a false signal (1–specificity) (Hosmer and Lemeshow 2000) (i.e., in this application, to discriminate fish that were preyed on from those that survived). The area under the ROC curve is interpreted based on the following general rule (Hosmer and Lemeshow 2000: 162):

- If area under ROC curve = 0.5, this suggests no discrimination (i.e., the net result is the same);
- If 0.7 ≤ area under ROC curve < 0.8, this is considered acceptable discrimination;

- If 0.8 ≤ area under ROC curve < 0.9, this is considered excellent discrimination; and
- If area under ROC curve ≥ 0.9, this is considered outstanding discrimination.

Hypothesis 5 (Univariate Nonparametric Statistical Analysis)

In addition to the resampling analysis and GLM analyses discussed above, a univariate nonparametric statistical analysis was conducted to investigate the influence of the FFGS on predation rate by determining the proportion of each sample eaten. Tagged juvenile Chinook salmon were assigned to samples based on the procedures outlined in Section 3.1.1 "Methods" for Floating Fish Guidance Structure Performance. For each sample, the predation event positions were then aggregated into two areas: 1) > 10 m (> 33 ft) from the FFGS; and 2) ≤ 10 m (≤ 33 ft) from the FFGS. Similar procedures for determining the appropriate statistical test were used as described in Section 3.1.1 "Methods" for Hypotheses H16, H22a, and H23a. These procedures showed that the data did not meet the assumptions of ANOVA and so nonparametric statistics (Wilcoxon two-sample tests) were used.

Hypothesis H5 was tested with a series of analyses to examine the potential influence of light and velocity on proportion eaten. The first analysis included all light and velocity levels combined. If the two-sided P-value obtained was less than or equal to the critical alpha the null hypothesis was rejected. A two-sided P-value was used because results of interest were that the FFGS significantly increased or decreased predation rate. Then, the proportion eaten data were partitioned by light level using a threshold value of 5.4 lux (see Section 3.1.1 "Methods"). Hypothesis H5 was tested at both light levels. Finally, the proportion eaten data were partitioned by approach velocity level using a threshold value of 0.25 m/s (0.82 ft/s) (see Section 3.1.1, "Methods"). Hypothesis H5 was then tested at both velocity levels.

A total of three tests were conducted with the proportion eaten data samples so a Bonferroni method adjustment (Sokal and Rohlf 1995: 240) to the critical alpha was used to maintain the experiment-wise error rate at the accepted level of 0.05. Three sets of analyses were conducted (i.e., all samples combined; samples partitioned by light level; and samples partitioned by velocity) so 0.0167 (0.05/3) was the critical alpha value used for these comparisons. Hypothesis H5 was rejected if the p-value of the test was greater than the critical alpha value.

Spatial Distribution of Predation Events

Two additional analyses were undertaken to examine the spatial distribution of predation events in the study area in relation to various in-channel structures, including the FFGS. The in-channel features included in the analysis were the FFGS (based on the average alignments for FFGS On and FFGS Off); Dagmar's Landing; the Walnut Grove Bridge; Boon Dox; the Upstream Dolphin[19] to which the FFGS was moored (also referred to as Dolphin D1 in **Figure 2-4**); the Offshore Downstream Dolphin to which the FFGS was moored and pulled near when in the On position (also referred to as Dolphin D3 in **Figure 2-4**); the Nearshore Downstream Dolphin to which the FFGS was moored and pulled near when in the Off position (also referred to as Dolphin D4 in **Figure 2-4**); and the Three Science Piles just downstream of the FFGS to which various monitoring instruments were attached (**Figure 3.6-1**). These structures were chosen because they represented potential habitat for predatory fishes, e.g., as velocity breaks and ambush habitat.

[19] A dolphin is a man-made structure consisting of a number of piles driven into the riverbed that are unconnected to shore, extend above the water level, and are connected to form a fixing point, to which structures (in this case the FFGS) can be moored.

In the first analysis, the distance to each predation event was calculated for each of the in-channel structures. There was assessed to be no significant difference between FFGS On and FFGS Off if the resampled 95 percent confidence intervals for each feature overlapped (see previous description of resampling in the methods for Hypotheses H6 and H6 [Resampling Analysis]). In the second analysis, the proportion of predation events within 5 m (16 ft) and within 10 m (33 ft) of each the structures was calculated. Resampling was again used to assess whether there were significant differences between FFGS On and FFGS Off.

RESULTS

Hypotheses H5 and H6 (Resampling Analysis)

A total of 431acoustically tagged juvenile Chinook salmon met the criteria for inclusion in the analysis of predation (see "Data Analysis" section of the Methods). Of these, 223 were present in the study area with the FFGS Off and 208 with the FFGS On (**Table 3.6-1**). Around 17 percent of juvenile Chinook salmon were eaten with the FFGS Off, compared to around 15 percent with the FFGS On. Just over 130 juvenile Chinook salmon passed within 5 m (16 ft) of the FFGS buoy line and 12 were eaten (9%), all downstream from the FFGS section of the study area and mostly more than 10 m (33 ft) from the FFGS buoy line. Nearly 260 juvenile Chinook salmon passed within 5 to 10 m (16-33 ft) of the FFGS buoy line and 19 were eaten (or 7%), all but one downstream from the FFGS section of the study area. Then, 42 juvenile Chinook salmon remained more than 10 m (33 ft) from the FFGS buoy line, and nearly all were eaten (or 93%), with most of the predation occurring

upstream from the FFGS section of the study area (**Table 3.6-1**) and, in particular near the Walnut Grove Bridge (**Figure 3.6-1**). Of the 38 predation events occurring more than 10 m (33 ft) from the FFGS buoy line, 29 were excluded from the bootstrapping analysis because they occurred well upstream from the FFGS. Overall, it was visually apparent that predation was relatively frequent in the vicinity of the Walnut Grove Bridge and near the Offshore Downstream Dolphin to which the FFGS was attached, and that predation in both of these areas occurred with the FFGS On and FFGS Off (**Figure 3.6-1**). Further examination of the spatial distribution of predation events is provided in the following section entitled "Spatial Distribution of Predation Events."

In addition to the 431 juvenile Chinook salmon included in this analysis, 25 of the tags returned to the study area, of which nearly all (24, or 96%) were classified as being within predatory fishes[20]; only one was classified as having left the study area when in a juvenile Chinook salmon.

Table 3.6-1 Number of Acoustically Tagged Juvenile Chinook Salmon Preyed On near the Floating Fish Guidance Structure

Closest Upstream Approach to FFGS Buoy Line:	Less than 5 Meters		5 to 10 Meters		More than 10 Meters		Total	
Predation Distance from FFGS Buoy Line	Off	On	Off	On	Off	On	Off	On
Less than 5 meters	0	2	1	2	0	0	1	4
5 to 10 meters	1	1	5 (1)	2	0	1	6 (1)	4
More than 10 meters	4	4	4 (1)	5	23 (20)	15 (14)	31 (21)	24 (14)
Not eaten	55	64	129	110	1	2	185	176
Total	**60**	**71**	**139**	**119**	**24**	**18**	**223**	**208**

Note: Numbers in parentheses indicate predation upstream from the FFGS section of the study area. Fish exiting the study area and subsequently being advected back into the study area or returning as predators are not included in this table.

[20] It is possible that other predatory taxa could have consumed the juvenile Chinook salmon, e.g., diving birds such as cormorants and mergansers, or otters. The analysis herein assumes predation was by predatory fishes.

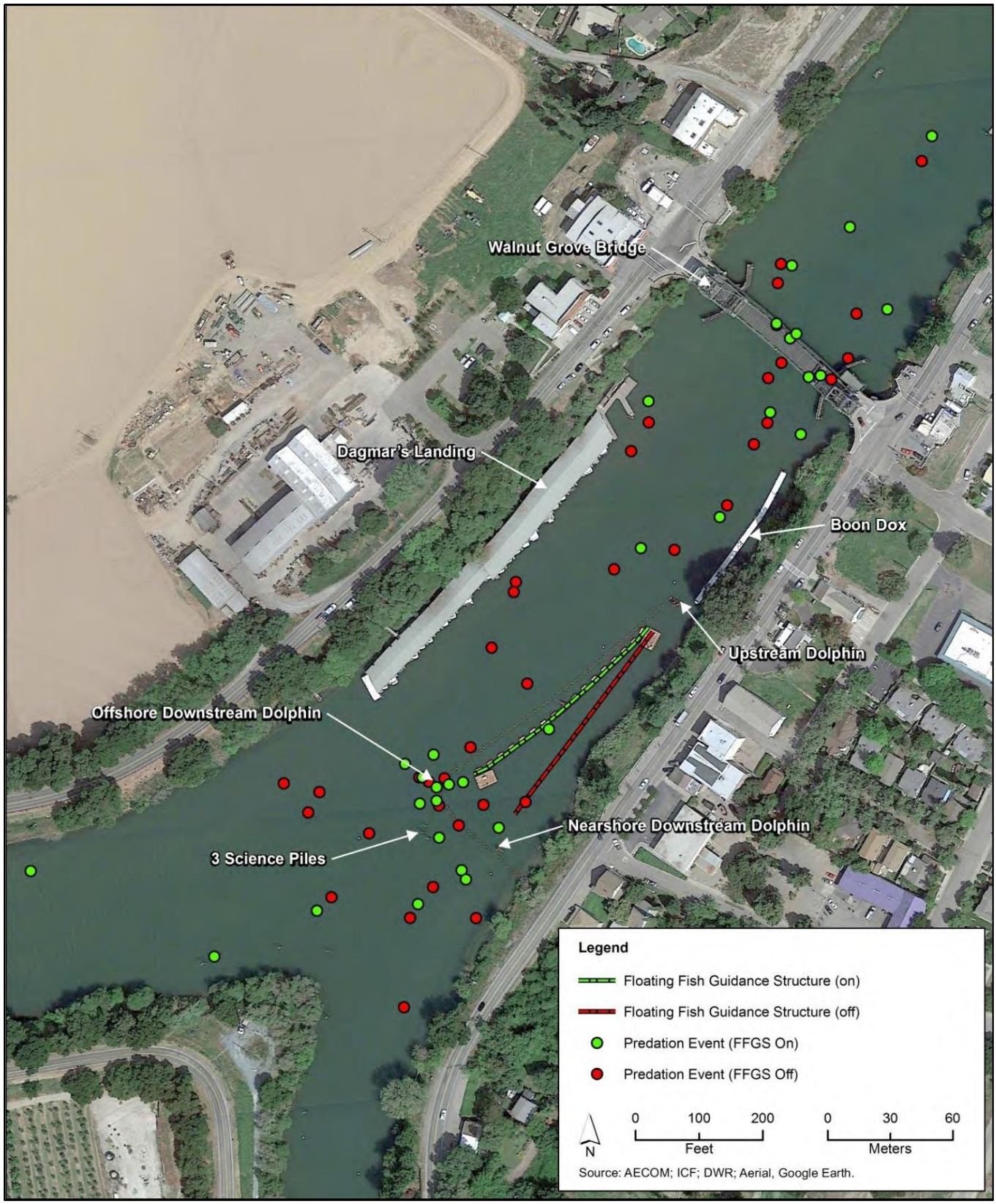

Note: Symbols indicate closest upstream approach distance to the FFGS buoy line.

Figure 3.6-1 Estimated Locations of Predation Events on Tagged Juvenile Chinook Salmon

There was no significant difference between the proportion of juvenile Chinook salmon eaten with the FFGS On (bootstrapped mean proportion = 0.15; 95 percent confidence interval 0.11 to 0.20) and the proportion eaten with the FFGS Off (bootstrapped mean proportion = 0.17; 95 percent confidence interval 0.12 to 0.22; **Figure 3.6-2**). Therefore, Hypothesis H5 was rejected. This overall pattern also was evident from the data divided by closest approach to the FFGS buoy line, which were used to test Hypothesis H6. Hypothesis H6 also was rejected, because the proportion of juvenile Chinook salmon eaten was either not significantly different between distances from the FFGS, or was greater further from the FFGS (for fish more than 10 m [33 ft] from the FFGS, with FFGS Off), contrary to the hypothesis that the probability of predation would be greater closer to the FFGS. A very high proportion of fish were eaten that approached more than 10 m (33 ft) from the FFGS buoy line (bootstrapped mean proportion with FFGS Off = 0.89 [95 percent confidence interval: 0.67 to 1.00]; bootstrapped mean proportion with FFGS On = 0.33 [95 percent confidence interval: 0.00 to 1.00]), although the confidence intervals were quite wide because there were relatively few fish included in the analysis for FFGS Off (n = 9) and FFGS On (n = 3). The proportion of fish that were eaten approaching less than 5 m (16 ft) from the FFGS buoy line (none eaten with FFGS Off; bootstrapped mean proportion with FFGS On = 0.03 [95 percent confidence interval: 0.02 to 0.08]) generally was similar in magnitude to the proportion eaten that approached 5 to 10 m (16-33 ft) from the FFGS buoy line (bootstrapped mean proportion with FFGS Off = 0.04 [95 percent confidence interval: 0.01 to 0.07]; bootstrapped mean proportion with FFGS On = 0.02 [95 percent confidence interval: 0.00 to 0.04]) (**Figure 3.6-2**).

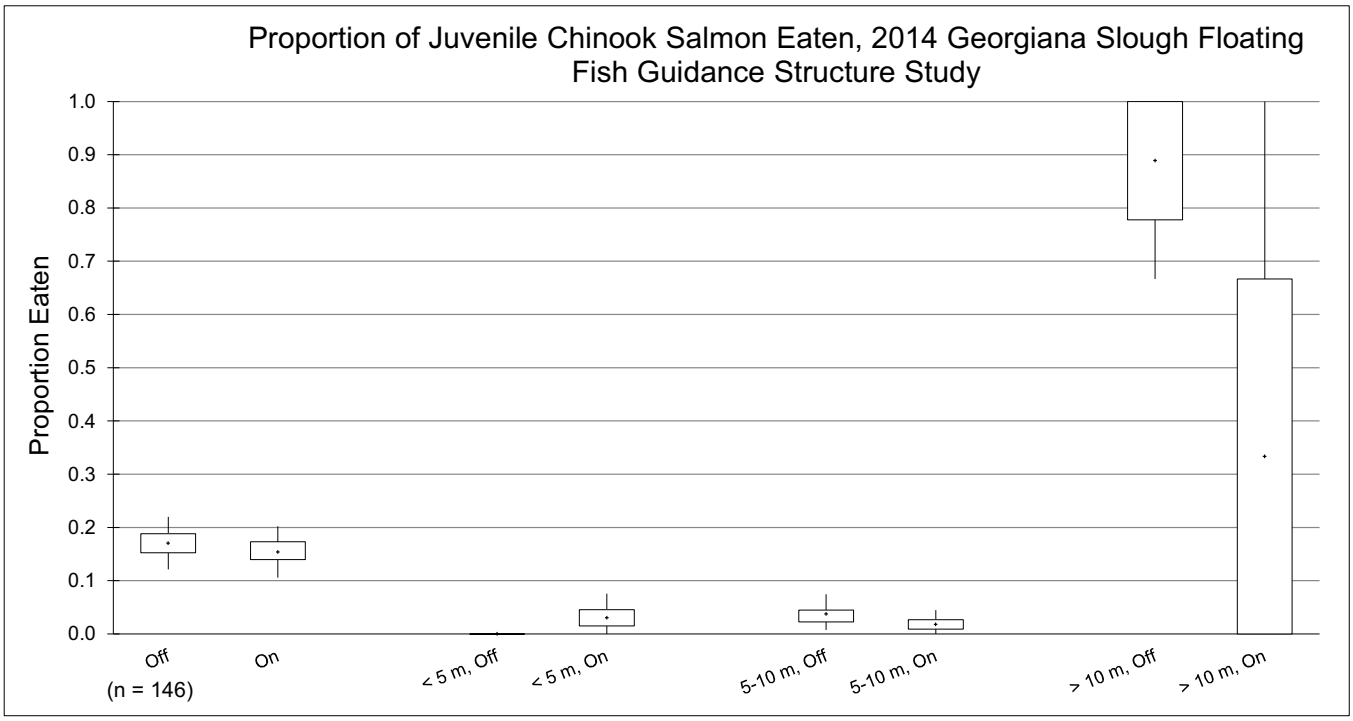

Note: Boxplots represent bootstrapped mean (+), interquartile range (box), and 95 percent confidence interval (whiskers).

Figure 3.6-2 Proportion of Acoustically Tagged Juvenile Chinook Salmon Classified as Being Eaten in the Study Area by FFGS Treatment (On/Off) and Closest Upstream Approach to FFGS Buoy Line

Generalized Linear Modeling

GLM with model averaging found good support only for the *a priori* hypothesis that probability of predation would be negatively related to turbidity, as indicated by turbidity coefficient 95 percent confidence intervals

excluding zero and importance greater than 0.8. This finding was consistent between the GLM including all 431 juvenile Chinook salmon (**Table 3.6-2**) and the GLM including the subset of 209 juvenile Chinook salmon that included the ambient light and predator density predictors (**Table 3.6-3**). For the larger dataset of 431 fish, mean ± standard deviation turbidity was 16.4 ± 13.8 nephelometric turbidity units (NTU) for fish that were preyed on and 42.6 ± 30.9 NTU for fish that survived through the study area. For the smaller dataset of 209 fish, turbidity was 13.6 ± 8.5 NTU for fish that were preyed on and 30.0 ± 18.9 NTU for fish that survived. No other predictors were well supported as being related to probability of predation, including FFGS On/Off; this latter observation was consistent with the resampling analysis conducted to test Hypothesis H5.

Table 3.6-2 Model-Averaged Coefficients, 95 Percent Confidence Limits, and Predictor Importance for Generalized Linear Modeling of Predation Probability of Tagged Juvenile Chinook Salmon (n = 431), 2014 Study

Variable	Coefficient	95 Percent Confidence Limits		Importance
		Lower	Upper	
Turbidity	-1.743	-2.466	-1.021	1.00
Night	-0.234	-0.821	0.353	0.53
FFGS On	-0.119	-0.525	0.286	0.39
Flow	-0.073	-0.337	0.191	0.38
Critical streakline location	0.046	-0.124	0.215	0.37
Stage	-0.043	-0.237	0.151	0.33
Temperature	-0.023	-0.155	0.109	0.29
Cross-stream location	-0.019	-0.127	0.090	0.29

Note: FFGS On and nighttime coefficients are in relation to baseline estimates with FFGS Off during daytime.

Table 3.6-3 Model-Averaged Coefficients, 95 Percent Confidence Limits, and Predictor Importance for Generalized Linear Modeling of Predation Probability of Tagged Juvenile Chinook Salmon (n = 209) Including Predator Density and Ambient Light, 2014 Study

Variable	Coefficient	95 Percent Confidence Limits		Importance
		Lower	Upper	
Turbidity	-1.432	-2.180	-0.684	1.00
Predator density (Walnut Grove Bridge)	-0.174	-0.770	0.421	0.41
Ambient light	-0.042	-0.220	0.136	0.32
Critical streakline location	0.045	-0.149	0.239	0.32
Temperature	-0.054	-0.299	0.190	0.31
FFGS On	-0.052	-0.344	0.240	0.28
Predator density (Dagmar's Landing)	-0.022	-0.151	0.107	0.28
Cross-stream location	0.022	-0.114	0.158	0.28
Stage	-0.017	-0.170	0.135	0.27
Flow	-0.006	-0.168	0.156	0.27

Note: FFGS On coefficient is in relation to baseline estimates with FFGS Off.

The GLMs with predictors included provided a better fit to the data than the intercept-only models. For the GLM with all 431 juvenile Chinook salmon, the full model with all predictors had AIC_c of 328.5, in comparison to AIC_c of 384.4 for the intercept-only model. For the GLM with the subset of 209 juvenile Chinook salmon, the full model with all predictors had AIC_c of 201.6, in comparison to AIC_c of 219.8 for the intercept-only model.

The optimum threshold for the model-averaged predictor coefficients was 0.28, based on the maximum Kappa method, for both the GLM with all juvenile Chinook salmon and the GLM with the subset of juvenile Chinook salmon that included ambient light and predator density as predictors. For the GLM including all juvenile Chinook salmon, the Kappa statistic indicated that approximately 38 percent of all possible predation and survival fates were correctly predicted by the model-averaged coefficients, adjusting for correct predictions by chance. A total of 78.4 percent of outcomes were correctly classified. The model-averaged coefficients correctly predicted 68.6 percent of true positives (i.e., juveniles that had been preyed on [sensitivity]) and 80.3 percent of true negatives (i.e., juveniles that had survived [specificity]), indicating a false-positive classification of 19.7 percent. The area under ROC curve was 0.80, indicating that the model-averaged coefficients were at the lower end of the "excellent discrimination" range (Hosmer and Lemeshow 2000:162) for discriminating fish that had been preyed on from those that had survived. For the GLM including the subset of 209 juvenile Chinook salmon, the Kappa statistic indicated that approximately 33 percent of all possible predation and survival fates were correctly predicted by the model-averaged coefficients, adjusting for correct predictions by chance. A total of 77.8 percent of outcomes were correctly classified. The model-averaged coefficients correctly predicted 69.3 percent of true positives and 67.1 percent of true negatives, indicating a false-positive classification of 33.9 percent. The area under ROC curve was 0.77, indicating "acceptable discrimination" (Hosmer and Lemeshow 2000:162) of fish that were preyed on from those that had survived.

Hypothesis H5 (Univariate Nonparametric Statistical Analysis)

The proportion eaten was not significantly different for tagged juvenile Chinook salmon consumed with the FFGS in the On or Off positions, both > 10 m (> 33 ft) and ≤ 10 (≤ 33 ft) from the FFGS (**Table 3.6-4**); Hypothesis 5 was rejected. These results confirmed the results of the resampling and GLM analyses in suggesting that the position of the FFGS did not have a statistically significant influence on the proportion of juvenile Chinook salmon eaten.

Table 3.6-4 Comparison of FFGS On and Off Operations for Two Areas – Proportion Eaten Greater than 10 m from the FFGS or Eaten Within 10 m of the FFGS

Comparison Metrics	FFGS On Mean	FFGS Off Mean	Percentage Point Difference in Consumption	Wilcoxon Statistic	Two-sided P-value
Proportion eaten >10 m from FFGS	0.149	0.137	1.2	4928.0	0.9748
Proportion eaten ≤ 10 m from FFGS	0.036	0.020	1.6	3676.5	0.6733

There was no difference between the proportion eaten for FFGS On compared to FFGS Off (**Table 3.6-5**) at low or high light levels. Similarly, there was no difference in proportion eaten at either level of approach velocity, for FFGS On compared to Off (**Table 3.6-6**). These results suggest that, under the range of conditions tested, operation of the FFGS did not increase predation rate at any light or velocity level.

Table 3.6-5 Comparison of FFGS On and Off Operations for those Fish Two Comparison Metrics – Eaten Greater than 10 m from the FFGS or Eaten Within 10 m or the FFGS -under Low (< 5.4 Lux) and High (≥ 5.4 Lux) Light Levels

Comparison Metrics	FFGS On Mean	FFGS Off Mean	Percentage Point Change in Efficiency	Wilcoxon Statistic	Two-sided P-value
Proportion eaten >10 m from FFGS—low light	0.060	0.149	-8.9	960.5	0.3056
Proportion eaten >10 m from FFGS—high light	0.220	0.126	9.4	1291.0	0.3705
Proportion eaten < 10 m from FFGS—low light	0.040	0.004	3.6	869.0	0.9862
Proportion eaten < 10 m from FFGS—high light	0.031	0.033	-1.5	952.5	0.6082

Table 3.6-6 Comparison of FFGS On and Off Operations for those Fish Two Comparison Metrics – Eaten Greater than 10 m from the FFGS or Eaten Within 10 m or the FFGS -under Low (< 0.25 m/s) and High (≥ 0.25 m/s) Approach Velocities

Comparison Metrics	FFGS On Mean	FFGS Off Mean	Percentage Point Change in Efficiency	Wilcoxon Statistic	Two-sided P-value
Proportion eaten >10 m from FFGS—low velocity	0.248	0.327	-7.9	348.0	0.3967
Proportion eaten >10 m from FFGS—high velocity	0.101	0.081	2.0	2451.5	0.6569
Proportion eaten < 10 m from FFGS—low velocity	0.049	0.030	1.9	156.5	0.8282
Proportion eaten < 10 m from FFGS—high velocity	0.030	0.018	1.2	2016.5	0.4909

Spatial Distribution of Predation Events

There were a total of 68 predation events within the study area for which point estimates of predation locations were available. The analysis of the spatial distribution of predation events suggested that there was little evidence of changes in the spatial distribution of predation events between FFGS On and FFGS Off. There was no significant difference in the distance to predation event between FFGS Off and FFGS On for any of the in-channel structures (**Figure 3.6-3**).

There were no significant differences between FFGS Off and FFGS On in the proportion of predation events occurring within 5 or 10 m (16 or 33 ft) of each structure. As noted in the analysis of Hypotheses H5 and H6, there was a relatively high proportion of predation events close to the Walnut Grove Bridge (**Figure 3.6-1**): 4 of 37 predation events occurred within 5 and 10 m (16 and 33 ft) of the bridge with FFGS Off (bootstrapped mean proportion = 0.11, 95 percent confidence interval = 0.03-0.22), whereas 5 of 31 predation events occurred within 5 and 10 m (16 and 33 ft) of the bridge with FFGS On (bootstrapped mean proportion = 0.16, 95 percent confidence interval = 0.03-0.29) (**Figure 3.6-4** and **Figure 3.6-5**). In addition, there was a relatively high proportion of predation events near the Offshore Downstream Dolphin, particularly within 10 m (33 ft) (3 of 37 predation events with FFGS Off: bootstrapped mean proportion = 0.08, 95 percent confidence interval = 0.00-

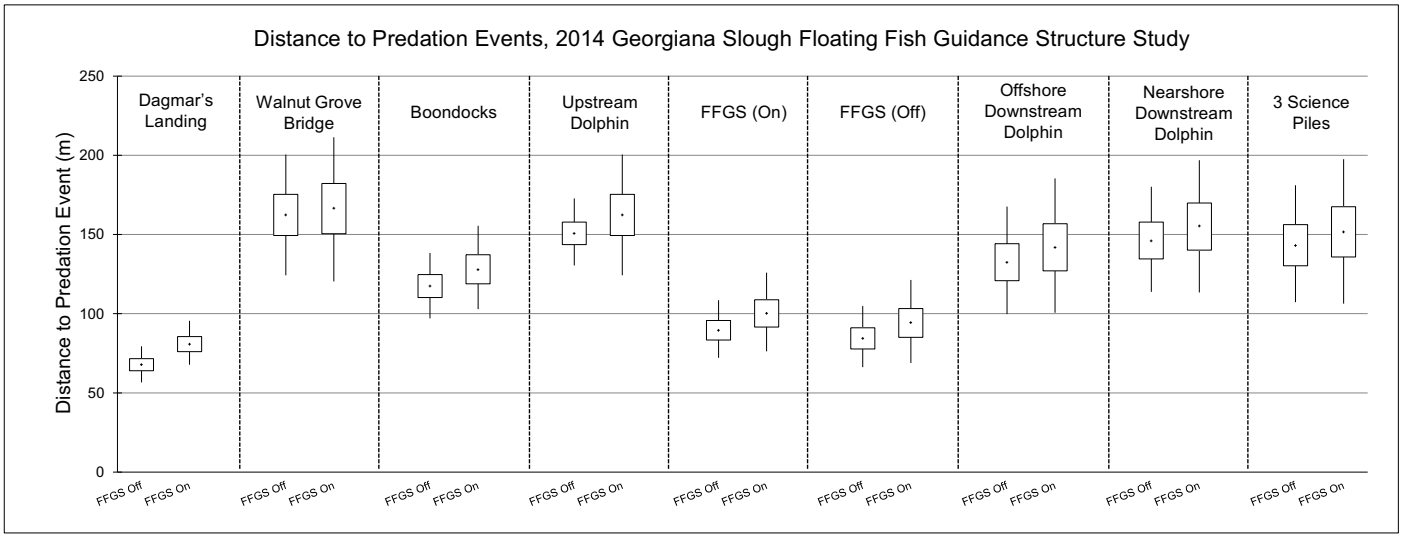

Note: Boxplots represent bootstrapped mean (+), interquartile range (box), and 95% confidence interval (whiskers). Both the FFGS (On) and FFGS (Off) alignments (in-channel positions) are included for the FFGS On and FFGS Off treatments. Thus, for example, FFGS (On) represents the actual location of the barrier with the FFGS On, whereas it represents a spatial area with the FFGS Off.

Figure 3.6-3 Distance to Predation Events of Various In-Channel Structures.

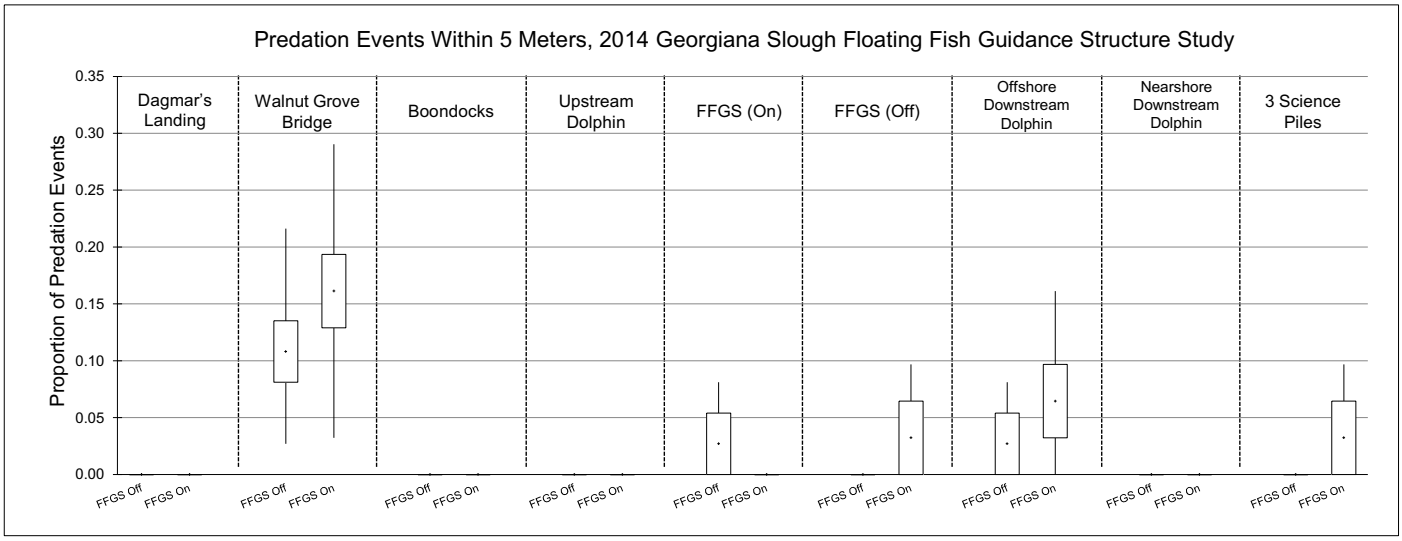

Note: Boxplots represent bootstrapped mean (+), interquartile range (box), and 95% confidence interval (whiskers). Both the FFGS (On) and FFGS (Off) alignments (in-channel positions) are included for the FFGS On and FFGS Off treatments. Thus, for example, FFGS (On) represents the actual location of the barrier with the FFGS On, whereas it represents a spatial area with the FFGS Off.

Figure 3.6-4 Proportion of Predation Events within 5 Meters of Various In-Channel Structures

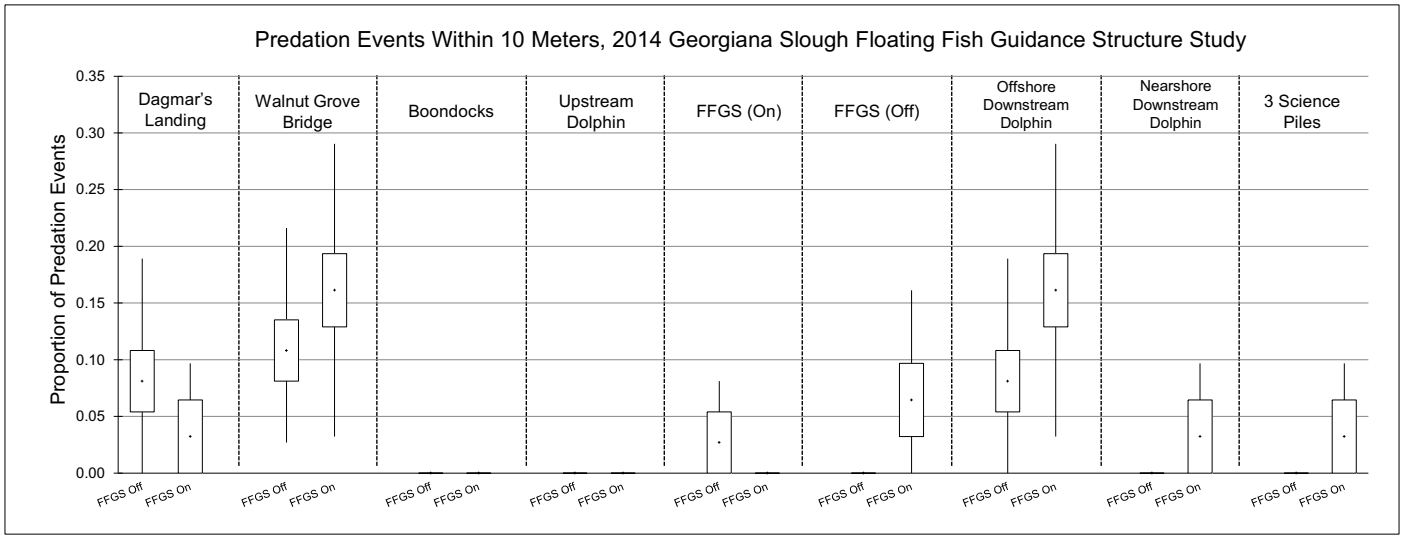

Notes: Boxplots represent bootstrapped mean (+), interquartile range (box), and 95% confidence interval (whiskers). Both the FFGS (On) and FFGS (Off) alignments (in-channel positions) are included for the FFGS On and FFGS Off treatments. Thus, for example, FFGS (On) represents the actual location of the barrier with the FFGS On, whereas it represents a spatial area with the FFGS Off.

Figure 3.6-5 Proportion of Predation Events within 10 Meters of Various In-Channel Structures

0.19; 5 of 31 predation events with FFGS On: bootstrapped mean proportion = 0.16, 95 percent confidence interval = 0.03-0.29). This non-significant difference was noteworthy in that the bootstrapped mean proportion of predation events was higher with the FFGS On, which might be expected if, for example, the FFGS guided a greater proportion of juvenile Chinook salmon toward the dolphin when in the On position. As with any statistical analyses, the power to detect significant differences is limited by the number of samples. Had the number of predation events been 8 times greater (n = 296 with FFGS Off, n = 248 with FFGS On) but with the same proportion of predation events within 10 m (33 ft) of all of the structures, the 95 percent confidence intervals for the Offshore Downstream Dolphin with FFGS Off (0.05-0.11) would have not overlapped those with FFGS On (0.12-0. 21).

3.6.2 ACOUSTIC TAGGING OF PREDATORY FISHES

The methods for capturing and tagging of predatory fishes were previously present in Section 2.4.4, "Study of Predatory Fishes and Tagging."

RESULTS

Predatory Fishes Catch Composition

A total of 523 predatory fishes were caught during the 2014 GSFFGS Study, and 195 of these fish were acoustically tagged (**Table 3.6-6**). Of the 523 fish, 343 were caught during roving angling (66%) and 180 were caught during standardized angling (34%). A total of 251 of the 523 predatory fishes were caught in the study area (48%), 192 were caught outside the study area but within a 1.6 km (1 mi) radius (37%), and 80 were caught outside the 1.6 km (1 mi) radius (15%). Boat angling crews caught 487 of the 523 fish (93%), of which 187 were tagged (96% of tagged fish). Crews restricted to the release dock caught 36 of the 523 fish (7%), of which 8 were tagged (4% of tagged fish). Roving angling catch locations are shown in **Figure 3.6-6**. Species caught included striped bass, smallmouth bass, spotted bass, redeye bass, largemouth bass, white catfish, and Sacramento pikeminnow. Target species accounted for 87 percent of all captures. Catch and tagging composition by sample day and species is shown in **Table 3.6-6**. Smallmouth bass were captured and tagged most frequently, and largemouth bass were captured least frequently. Largemouth bass, white catfish, and Sacramento pikeminnow were not tagged during the 2014 GSFFGS Study.

The total catch included 210 smallmouth bass[21] (40% of total catch), 141 striped bass (27%), 104 spotted bass (20%), 43 white catfish (8%), 9 Sacramento pikeminnow (2%), 9 redeye bass (2%), and 7 largemouth bass (1%) (**Table 3.6-7**). On average, largemouth bass was the shortest and lightest species caught (mean 225 mm [8.8 in]; 178 g [0.4 lb]) and striped bass was the longest and heaviest (mean 409 mm [16.1 in]; 1,091 g [2.4 lb]).

[21] As described subsequently, there was evidence of hybridization between *Micropterus* spp. (excluding largemouth bass), so the nominal catch by species reported here may not be completely accurate.

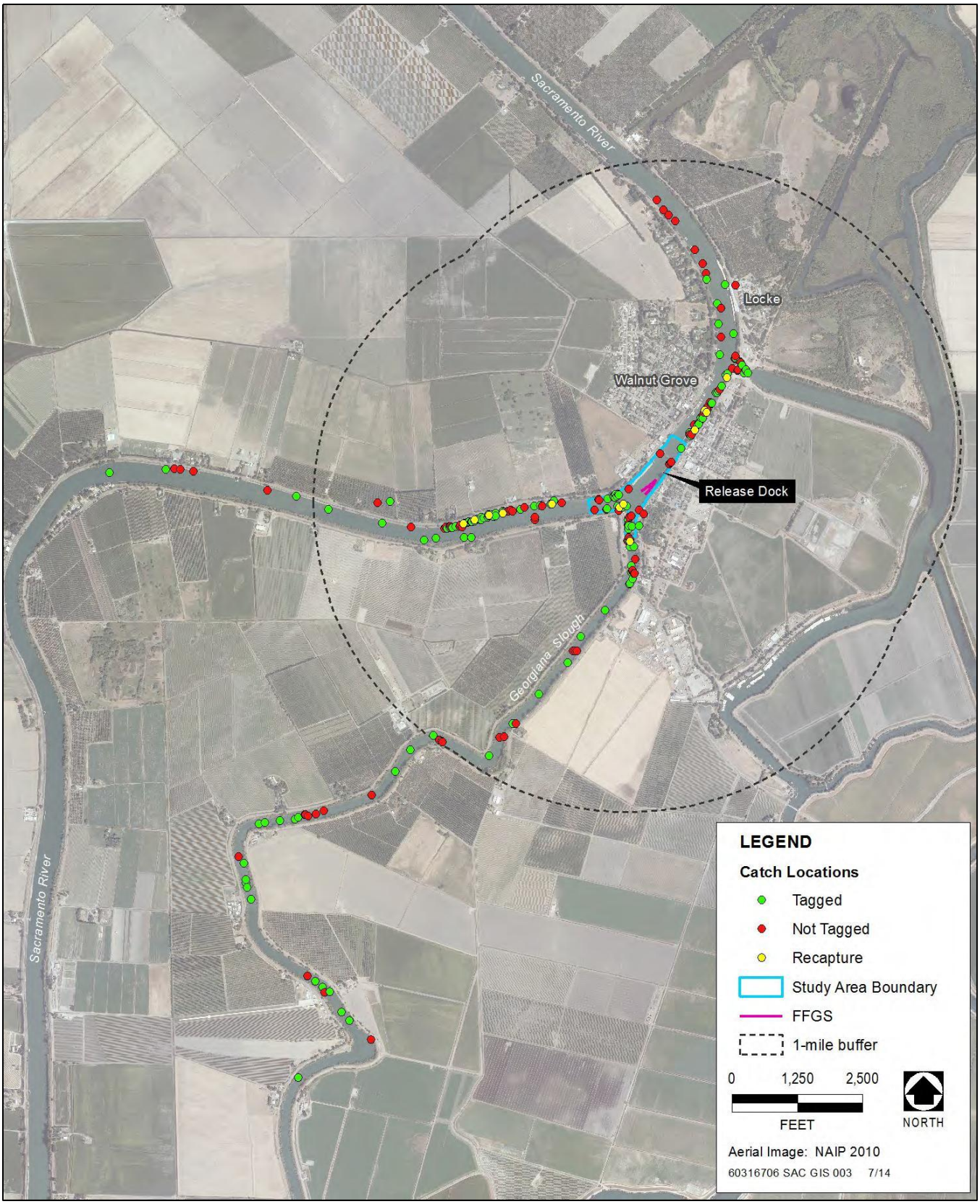

Figure 3.6-6 **Predatory Fish Catch Locations during Roving Angling for the 2014Floating Fish Guidance Structure Study**

Table 3.6-7 Predatory Fish Total Catch and Number Tagged by Sampling Date during the 2014 Study

Sample Date	Striped Bass		Smallmouth Bass		Spotted Bass		Largemouth Bass		White Catfish		Sac Pikeminnow		Redeye Bass		Totals	
	Total Catch	No. Tagged	Total Catch	No. Tagged	Total Catch	No. Tagged	Total Catch	No. Tagged	Total Catch	No. Tagged	Total Catch	No. Tagged	Total Catch	No. Tagged	Catch	Tagged
Feb-28	10	7	6	4	4	0	0	0	0	0	0	0	0	0	20	11
Mar-01	3	3	1	1	1	0	0	0	0	0	0	0	0	0	5	4
Mar-02	1	0	1	0	0	0	0	0	2	0	0	0	0	0	4	0
Mar-03	2	0	0	0	0	0	0	0	7	0	0	0	0	0	9	0
Mar-07	1	1	0	0	1	1	0	0	1	0	1	0	0	0	4	2
Mar-08	1	1	0	0	0	0	0	0	2	0	0	0	0	0	3	1
Mar-09	0	0	0	0	0	0	0	0	5	0	2	0	0	0	7	0
Mar-14	1	1	0	0	0	0	0	0	5	0	0	0	0	0	6	1
Mar-15	0	0	0	0	0	0	0	0	5	0	1	0	0	0	6	0
Mar-16	2	1	1	1	0	0	0	0	5	0	1	0	0	0	9	2
Mar-17	9	0	1	1	2	1	0	0	0	0	1	0	0	0	13	2
Mar-21	9	6	5	5	1	1	1	0	1	0	0	0	0	0	17	12
Mar-22	3	2	4	4	1	1	0	0	0	0	0	0	0	0	8	7
Mar-23	2	1	11	8	6	4	0	0	1	0	0	0	0	0	20	13
Mar-28	6	3	10	5	8	5	0	0	2	0	0	0	0	0	26	13
Mar-29	9	5	5	4	1	1	0	0	1	0	0	0	0	0	16	10
Mar-30	18	14	1	0	2	2	0	0	0	0	1	0	0	0	22	16
Mar-31	3	3	0	0	2	2	0	0	0	0	0	0	0	0	5	5
Apr-11	1	0	17	13	3	1	0	0	0	0	0	0	3	1	24	15
Apr-12	4	3	8	4	0	0	0	0	0	0	0	0	0	0	12	7
Apr-13	9	0	10	4	1	1	0	0	1	0	1	0	1	0	23	5
Apr-14	10	2	9	3	1	0	2	0	1	0	1	0	0	0	24	5
Apr-18	8	2	10	1	6	2	0	0	0	0	0	0	1	0	25	5
Apr-19	5	0	15	2	18	5	1	0	1	0	0	0	3	0	43	7
Apr-21	6	1	19	8	13	5	0	0	1	0	0	0	0	0	39	14
Apr-22	7	2	32	15	20	8	1	0	2	0	0	0	1	0	63	25
Apr-24	11	6	44	4	13	3	2	0	0	0	0	0	0	0	70	13
Totals	141	64	210	87	104	43	7	0	43	0	9	0	9	1	523	195

Table 3.6-8 Predatory Fishes Total Catch: Species Composition, Total Length, and Weight Summary Statistics for the 2014 Study								
Species	Catch (n)	Total (%)	Min Length (mm)	Max Length (mm)	Ave Length (mm)	Min Weight (g)	Max Weight (g)	Ave Weight (g)
Smallmouth Bass	210	40	140	441	312	45	1,179	452
Striped Bass	141	27	175	824	409	54	5,375	1,091
Spotted Bass	104	20	169	420	302	54	1,148	450
White Catfish	43	8	220	419	298	127	1,043	357
Sac Pikeminnow	9	2	290	660	407	249	2,268	672
Redeye Bass	9	2	210	351	295	136	612	355
Largemouth Bass	7	1	170	295	225	45	408	178
Total	523	100	140	824	336	45	5,375	614

Tagged Predatory Fishes Composition

A total of 195 predatory fishes were caught, tagged, and released in the study area during the 2014 GSFFGS Study. All predatory fishes were released at the release dock. A total of 153 of the predatory fishes were caught during roving angling (78%) and 42 were captured during standardized angling (22%); 68 of the tagged captures were caught in the study area (35%), 99 were caught outside the study area but within a 1.6 km (1 mi) radius (51%), and 28 were caught outside the 1.6 km (1 mi) radius (14%). The furthest distance from the study area that a fish was caught and subsequently tagged was a striped bass caught approximately 5.3 km (3.3 mi) downstream in Georgiana Slough. Species composition of tagged predatory fishes included striped bass, smallmouth bass, spotted bass, and redeye bass. Efforts were made to tag the target sample sizes for each species; however, sample sizes among species were adjusted over time, based on the observed proportions of different species caught by the sampling crews. Spotted bass was the most challenging species to target and catch, relative to target sample size. The tagged sample size for smallmouth bass exceeded the target sample size, and the tagged sample size for striped bass and spotted bass was slightly below target sample sizes (**Table 3.6-9**). However, as described herein, evidence of hybridization was shown between the black basses.

Table 3.6-9 Target and Tagged Sample Sizes (Number of Fish) during the 2014 Study					
	Striped Bass	Smallmouth Bass	Spotted Bass	Redeye Bass	Total
Target Sample Size (% total)	78 (40)	59 (30)	58 (30)	0 (0)	**195**
Tagged Proportion (%)	33	45	22	1	**100**
Tagged Sample Size (n)	64	87	43	1	**195**

A summary of tagged predatory fish species composition, total length (mm), and weight (g) is shown in **Table 3.6-10**. Tagged fish included 87 smallmouth bass (45%), 64 striped bass (33%), 43 spotted bass (22%), and 1 redeye bass (1%). The average length and weight was similar between the three *Micropterus* species (mean 342 to 348 mm [13.5-13.7 in]; 586 to 632 g[1.3-1.4 lb]), whereas striped bass on average were appreciably larger (mean 530 mm [20.9 in]; 1,814 g [4.0 lb]) than *Micropterus* (**Table 3.6-10**).

Table 3.6-10 Tagged Predatory Fishes Catch: Species Composition, Total Length, and Weight Summary Statistics for the 2014 Study								
Species	Tagged (n)	% of Total	Min Length (mm)	Max Length (mm)	Ave Length (mm)	Min Weight (g)	Max Weight (g)	Ave Weight (g)
Smallmouth Bass	87	45	302	416	348	281	1,075	586
Striped Bass	64	33	297	824	530	286	5,375	1,814
Spotted Bass	43	22	284	420	342	318	1,148	632
Redeye Bass	1	1	347	347	347	612	612	612
Total	195	100	284	824	406	281	5,375	997

Micropterus Hybridization

In contrast to other parts of the Delta, the study area regularly was found to have four common species of the genus *Micropterus*. Smallmouth and spotted bass are common throughout the north Delta, largemouth bass are found throughout the Delta, while redeye bass are localized to the north Delta, presumably from a source population in the Cosumnes River (Moyle 2002).

Micropterus species readily hybridize (West and Hester 1966; Childers 1971), and many caught during the study appeared to be hybrids based on external morphological characteristics. A percentage of caught smallmouth and spotted basses were noted on datasheets as appearing to be hybrids, but were recorded to species based on subjective interpretation of morphological characteristics. Smallmouth × spotted bass hybrids were the most commonly observed hybrid. Hybrids having largemouth bass morphological characteristics were not observed during the study. Redeye bass morphological characteristics were observed in some fish that were noted as appearing to be hybrids. Nine apparently pure strain redeye bass were caught during the study. The challenge of identifying captured *Micropterus* to species because of hybridization may have influenced the study's tagged predatory fish sample size. Reflecting the uncertainty in identification to species, subsequent data analyses generally grouped smallmouth bass, spotted bass, and redeye bass together as *Micropterus* species (*Micropterus* spp.)

3.6.3 Residence Time (Hypothesis H8)

Main Findings

The main finding of the residence time evaluation was:

- No difference existed in residence time between FFGS On and FFGS Off for striped bass or *Micropterus* spp.

Objectives

Predatory fishes have been found to occupy areas near in-channel physical structures in the Delta for long time periods, presumably reflecting suitability of the structures as habitat for ambushing prey and providing refuge from higher currents or larger predators. For example, Miranda et al. (2010) reported that acoustically tagged Sacramento pikeminnow were detected at the SWP/CVP export facilities salvage release sites up to approximately 80 percent of days over several months following tagging and release; in contrast, striped bass were detected on very few days (less than 2 percent) following release. Through its provision of in-channel physical structure, the FFGS has the potential to increase the residence time of predatory fishes in the area, potentially increasing

predation risk to juvenile Chinook salmon and other species of concern. The objective of this component of the 2014 FFGS Study was to assess whether the physical structure of the FFGS and its effect on study area hydrodynamics results in changes in the amount of time spent by individual predatory fish near the FFGS footprint (e.g., by providing more structure for ambushing prey or resting). Data for residence time of tagged predatory fishes in relation to FFGS treatment (On/Off) were used to test Hypothesis H8: Tagged predatory fish released in the vicinity of the FFGS footprint reside there longer when the FFGS is On than when the FFGS is Off.

METHODS

Field Methods

The data used to test Hypothesis H8 were obtained from acoustically tagged predatory fishes (see Section 3.6.2, "Acoustic Tagging of Predatory Fishes" for detailed description). As noted in Section 3.6.2, all tagged predatory fish (**Table 3.6-6**) were released from the release dock after the tag implantation surgery was performed.

Data Analysis

The analysis to test Hypothesis H8 used the same filtered, smoothed, and discretized acoustic tag detection data that were prepared following the methods of Romine et al. (2014) to identify presumed predators that may have consumed tagged juvenile Chinook salmon (see Section 3.4.1, "Methods", in Section 3.4, "Generalized Linear Modeling of Fish Fates"). Residence time of each predatory fish was taken to be the time between first and last detection in the first segment following release. Segments based on 60 or less original detections (approximately 2-minute duration) were omitted from the analyses. This resulted in the exclusion of one striped bass from the analyses.

The residence time of each predatory fish was calculated based on the first segment after release, which was matched with the FFGS treatment (i.e., On or Off) at the time of release. As with the analysis of predation for Hypotheses H5 and H6, a resampling method ("bootstrapping") (Brown et al. 2012) was used to produce statistical summaries of the data. For each species (i.e., striped bass or *Micropterus* spp.), the residence time for each FFGS treatment (On or Off) was resampled with replacement until each resample contained the same number of observations (i.e., number of fish) as the original sample. For striped bass, 45 were released with the FFGS Off and 15 were released with the FFGS On. For *Micropterus* spp., 58 were released with the FFGS Off and 68 were released with the FFGS On. The resampling procedure was repeated 10,000 times and the arithmetic mean was calculated for each of the 10,000 resamples. The 10,000 resamples then were used to generate statistical summaries for residence time by FFGS treatment (On or Off). The quantities estimated included the mean (50th percentile of the 10,000 resampled means), interquartile range (25th and 75th percentiles of the 10,000 resampled means), and 95 percent confidence interval (2.5th and 97.5th percentiles of the 10,000 resampled means). Hypothesis H8 was accepted if the mean residence time for the FFGS On was greater than for the FFGS Off and the 95 percent confidence intervals for the treatments did not overlap.

RESULTS

Residence time for striped bass ranged from 0.3 to 76.9 hours with the FFGS Off (n = 45 fish), and from 0.3 to 15.6 hours with the FFGS On (n = 15 fish). There was no significant difference in residence time between the FFGS Off (bootstrapped mean: 7.8 hours; 95 percent confidence interval: 3.6 to 13.4 hours) and the FFGS On (bootstrapped mean: 3.8 hours; 95 percent confidence interval: 1.5 to 6.5 hours) (**Figure 3.6-7**). Hypothesis H8 was rejected for striped bass.

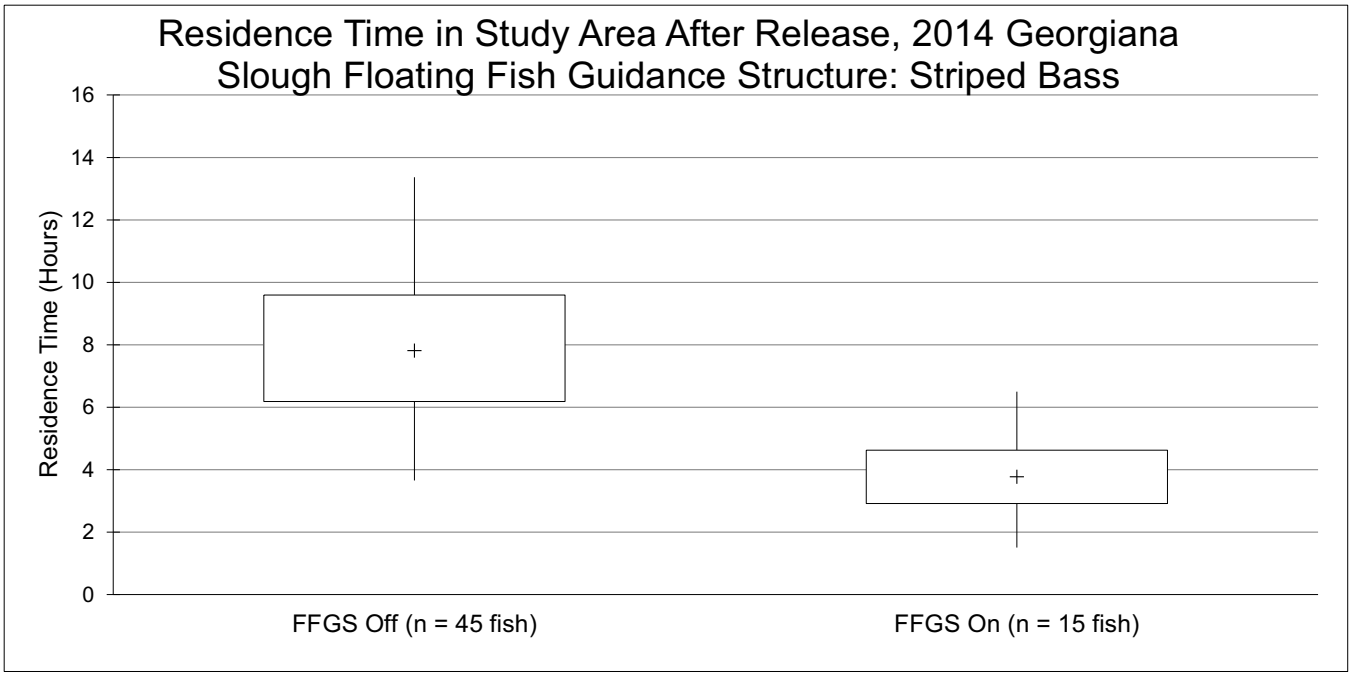

Note: Boxplots represent bootstrapped mean (+), interquartile range (box), and 95 percent confidence interval (whiskers).

Figure 3.6-7 Striped Bass: Residence Time Following Release with FFGS On/Off

Residence time for *Micropterus* spp. ranged from 0.1 to 416.9 hours with the FFGS Off (n = 58 fish), and from 0.05 to 589.4 hours with the FFGS On (n = 68 fish). There was no significant difference in residence time between the FFGS Off (bootstrapped mean: 44.7 hours; 95 percent confidence interval: 23.5 to 71.5 hours) and the FFGS On (bootstrapped mean: 30.8 hours; 95 percent confidence interval: 15.3 to 55.5 hours) (**Figure 3.6-8**). Hypothesis H8 was rejected for *Micropterus* spp.

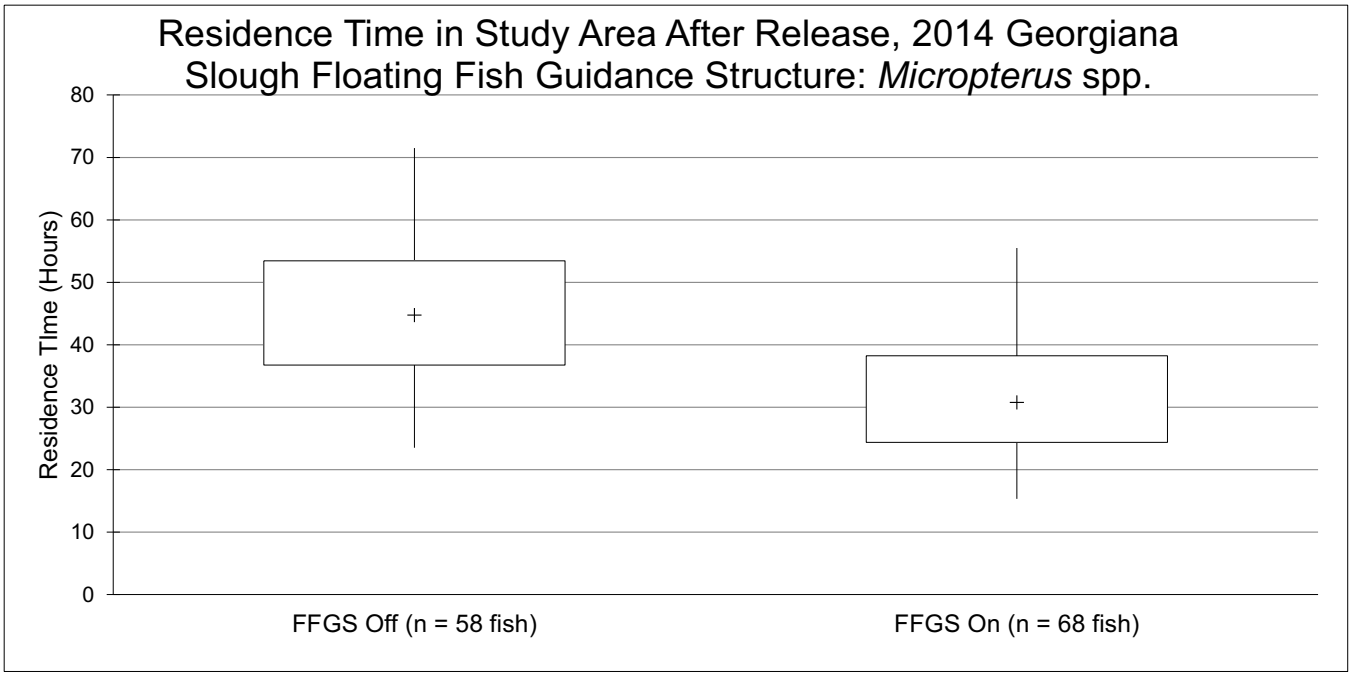

Note: Boxplots represent bootstrapped mean (+), interquartile range (box), and 95 percent confidence interval (whiskers).

Figure 3.6-8 *Micropterus* spp.: Residence Time Following Release with FFGS On/Off

MAIN FINDINGS

The difference in standardized angling catch rate between areas hypothesized to be affected by the FFGS and reference sites did not differ between FFGS On and FFGS Off for striped bass or *Micropterus* spp.

OBJECTIVES

The physical structure of the FFGS has the potential to harbor predatory fishes by providing velocity refuge and ambush habitat, as noted for other in-channel structures in the Delta (e.g., Vogel 2011), and may increase predation risk for juvenile Chinook salmon (Sabal et al. 2016). Standardized angling presumably provides an indication of predation risk through catch per unit effort (CPUE) of predatory fishes, which reflects factors such as predatory fish density and propensity to attack potential prey. Standardized angling for this study was conducted with the objective of comparing catch rates of predatory fishes in the vicinity of the FFGS between the FFGS On and the FFGS Off treatments. The study design accounted for temporal (seasonal) differences in catch rate, which is influenced by many factors such as changes in water temperature or predatory fishes' migrations, by sampling throughout the study time period. As noted in Section 3.6.2, standardized angling was undertaken during the day. Standardized angling formed the basis for testing of Hypothesis H9: The standardized angling catch rate of predatory fish in the vicinity of the FFGS footprint is greater when the FFGS is On compared to when the FFGS is Off.

3.6.4 STANDARDIZED ANGLING (HYPOTHESIS H9)

Field methods for standardized angling were previously presented in Section 2.5, "Standardized Angling."

Data Analysis

Hypothesis H9 was tested by assessing the difference in CPUE (i.e., catch per sampling session) of predatory fishes between the FFGS and the reference site SAA 2 for the FFGS On and FFGS Off treatments. Expressing the response as a difference between the "impact" site (i.e., the FFGS) and the reference site (SAA 2) aimed to account for the broad-scale temporal/seasonal differences in predatory fish density (e.g., the striped bass upstream spawning migration). Analyses were conducted separately for all predatory fishes, striped bass, and *Micropterus* spp. Predatory fish were classified as larger predators if they met minimum length criteria (i.e., 360-mm [14 in] TL for striped bass and Sacramento pikeminnow, 300-mm [12 in] TL for all other species) that aimed to account for the ability to consume medium-sized prey, such as juvenile Chinook salmon; analyses were conducted separately for all predatory fishes and for larger predators alone.

As with testing of Hypothesis H8, resampling (bootstrapping) was used to produce statistical summaries of the data. For each treatment (i.e., FFGS On/Off), the difference in CPUE was resampled with replacement until each resample contained the same number of observations (n = 10 standardized angling sessions) as the original sample. This procedure was repeated 10,000 times, and the arithmetic mean was calculated for each of the 10,000 resamples. The 10,000 resamples then were used to generate statistical summaries for the difference in CPUE within each treatment. The quantities estimated included the mean (50th percentile of the 10,000 resampled means), interquartile range (25th and 75th percentiles of the 10,000 resampled means), and 95 percent confidence interval (2.5th and 97.5th percentiles of the 10,000 resampled means). Hypothesis H9 was accepted if the mean CPUE difference for the FFGS On was greater than for the FFGS Off and the 95 percent confidence intervals for the treatments did not overlap. The analysis was repeated for the difference in CPUE between SAA 3 (impact site) and SAA 1 (reference site).

Further exploration of the potential influences on predatory fish CPUE within the FFGS SAA was undertaken with GLM, similar to the predation probability analyses described in Section 3.6.1. The analyses were conducted for all sizes of predatory fishes that were caught. The predictors analyzed, and the hypotheses as to their relationship with CPUE in the FFGS SAA, were as follows:

- **FFGS treatment:** Greater CPUE with the FFGS On because of the provision of greater in-channel habitat for predatory fishes (Vogel 2011; Sabal et al. 2016);
- **CPUE in SAA 2:** Greater CPUE with greater CPUE in SAA 2, reflecting broad scale changes in predatory fish abundance (e.g., because of seasonal spawning migrations or other factors triggering mass migration, such as seeking abundant prey);
- **Flow:** Greater CPUE with lower flow because of more suitable habitat for predatory fishes (DWR 2015b);
- **Water temperature:** Greater CPUE with greater temperature because of increased bioenergetic demands and seasonality (e.g., increased upstream migration of predatory fishes as water warms) (DWR 2015b); and
- **Turbidity:** Greater CPUE with lower turbidity because predatory fishes would be better able to see and capture prey (Ferrari et al. 2014).

Flow, temperature, and turbidity data were obtained from the USGS station WGB (Sacramento River downstream of Georgiana Slough, gauge 11447905) and were averaged for each sampling session, then standardized (mean subtracted, then divided by standard deviation) before statistical analysis.

The glmulti package in R was used to provide all possible first-order GLMs for CPUE in the FFGS as a function of predictor variables, with the response modeled with a negative binomial distribution and log link function. In addition to first-order models, the interaction of the FFGS On/Off treatment and CPUE in SAA2 also was included to account for the potential effect of the FFGS on CPUE in the FFGS SAA in relation to the CPUE in SAA 2; based on the principle of marginality (Calcagno and de Mazancourt 2010), the interaction term was included only in models including both main effects. The relative level of support for each possible model was estimated in glmulti with the quasi-likelihood equivalent of AIC corrected for small sample sizes ($QAIC_c$) (Mazerolle 2006). The variance inflation factor, $\hat{c}$, required to compute $QAIC_c$ was estimated by initially running a single GLM with all predictor variables included, and then providing $\hat{c}$ to the glmulti package for the automated model averaging procedure. The difference in $QAIC_c$, Δ_i, between each model and the best model (i.e., the model with the lowest $QAIC_c$) was calculated, and Akaike weights (w_i) were calculated based on the Δ_i. Model averaging of the predictor variable coefficients was undertaken based on the Akaike weights for each model, and unconditional confidence intervals were calculated for each coefficient (Mazerolle 2006). The importance of each predictor variable was assessed by summing the w_i of all models in which the variable appeared. Following Calcagno and de Mazancourt (2010), importance of 0.8 or greater was used to infer support for a variable's potential influence on FFGS CPUE, in addition to unconditional 95 percent confidence intervals for variable coefficients not overlapping zero (per Zeug and Cavallo 2013). GLMs including predictors were assessed to provide a better fit to the data than intercept-only models if the $QAIC_c$ of the full models (with all predictors included) was 3 or more units greater than the $QAIC_c$ of the intercept-only models (Zeug and Cavallo 2013).

RESULTS

Predatory Fish Catch Composition - Standardized Angling

A total of 180 predatory fish were captured during the 20 standardized angling sampling events (**Table 3.6-11**). The species caught included 60 smallmouth bass (33%), 57 striped bass (32%), 29 spotted bass (16%), 25 white catfish (14%), 3 largemouth bass (2%), 3 redeye bass (2%), and 3 Sacramento pikeminnow (2%). On average, largemouth bass was the shortest and lightest species caught, Sacramento pikeminnow was the longest, and spotted bass was the heaviest. Untagged fish were released at the capture site, and tagged fish were released from the release dock where tagging had occurred. Of the 180 predatory fish that were caught during standardized angling sampling, 42 were tagged (23%) and included 19 smallmouth bass (45%), 14 spotted bass (33%), 8 striped bass (19%), and 1 redeye bass (2%).

Table 3.6-11 Species Composition, Total Length, and Weight for Predatory Fish Caught by Standardized Angling during the 2014 Study

Species	Catch (n)	% of Total	Min Length (mm)	Max Length (mm)	Ave Length (mm)	Min Weight (g)	Max Weight (g)	Ave Weight (g)
Striped bass	57	32	175	513	290	54	1,247	283
Smallmouth bass	60	33	185	441	318	68	1,179	481
Spotted bass	29	16	220	376	317	141	998	514
Largemouth bass	3	2	170	221	202	45	136	91
White catfish	25	14	220	419	306	127	1,043	383
Sacramento pikeminnow	3	2	331	412	384	308	658	508
Redeye bass	3	2	315	350	337	318	612	491
Total	180	100	170	513	307	45	1,247	403

A total of 90 predatory fish were caught with the FFGS On (50%), and 90 were caught with the FFGS Off (50%). A total of 99 predatory fish were caught using artificial lures (55%) and 81 were caught using dead bait (45%). The highest number of fish was caught in the FFGS SAA and the least number was caught in SAA 3 (**Table 3.6-12**). The highest number of striped bass was caught in the FFGS SAA and the least number was caught in SAA 2. The highest number of smallmouth bass was caught in SAA 2 and the least in SAA 3. The highest number of spotted bass was caught in SAA 2 and the least in SAA 3.

Table 3.6-12 Predatory Fishes Species Composition by Standardized Angling Area during the 2014 Study

Species	FFGS	SAA 1	SAA 2	SAA 3
Striped bass	25	8	3	21
Smallmouth bass	16	12	28	4
Spotted bass	12	4	13	0
Largemouth bass	0	1	1	1
White catfish	9	5	11	0
Sacramento pikeminnow	0	2	0	1
Redeye bass	0	0	3	0
Total	62	32	59	27

Hypothesis H9

The bootstrapped mean CPUE for all predatory fishes ranged from 0.4 fish (larger predators in SAA 3 with the FFGS Off) to 3.2 fish (all predators in FFGS with the FFGS Off) (**Figure 3.6-10**). There was no evidence that the difference in CPUE between impact and reference sites was greater with the FFGS On than with the FFGS Off, for either larger predators or all predators. The differences in CPUE between impact and reference sites (i.e., CPUE in FFGS minus CPUE in SAA 2 and CPUE in SAA 3 minus CPUE in SAA 1) were not significantly different between the FFGS On and the FFGS Off, based on the overlap of the 95 percent confidence intervals (**Figure 3.6-11**). Therefore Hypothesis H9 was rejected for all predatory fish species combined.

The bootstrapped mean CPUE for striped bass ranged from zero (larger predators with the FFGS On in FFGS, SAA 1, and SAA 2; also for larger predators with the FFGS Off in SAA 2) to 1.3 fish (all predators in FFGS with the FFGS On, plus all predators in SAA 3 with the FFGS Off) (**Figure 3.6-12**). As with all predatory fish species combined, there was no evidence that the difference in CPUE differed between the FFGS On and the FFGS Off, for either larger striped bass or all sizes of striped bass. The differences in CPUE between impact and reference sites for the FFGS On and the FFGS Off were not significantly different, based on the overlap of the 95 percent confidence intervals (**Figure 3.6-13**). Therefore Hypothesis H9 also was rejected for striped bass.

The bootstrapped mean CPUE for *Micropterus* spp. ranged from 0.1 (larger predators with the FFGS On in SAA 3) to 2.2 fish (all predators in SAA 2 with the FFGS On/Off) (**Figure 3.6-14**). As with all predatory fish species combined and striped bass, there was no evidence that the difference in CPUE differed between the FFGS On and the FFGS Off, for either larger *Micropterus* spp. or all sizes of *Micropterus* spp. The differences in CPUE between impact and reference sites for the FFGS On and the FFGS Off were not significantly different, based on the overlap of the 95 percent confidence intervals (**Figure 3.6-15**). Therefore, as with all predatory fish species combined and striped bass, Hypothesis H9 was rejected for *Micropterus* spp.

Generalized Linear Modeling

GLM found low support for importance of any the hypothesized variables in influencing CPUE of all sizes of predatory fish in the FFGS SAA. For all species combined, the intercept-only model had the second most support (QAICc = 58.1, wi = 0.14) after the model that included water temperature and an intercept (QAICc = 57.2, wi = 0.21), which was well within a 3-unit QAICc difference, and therefore suggested little importance of the temperature variable. For striped bass, the intercept-only model had the most support, and therefore suggested that none of the hypothesized variables had much explanatory power for variation in CPUE. For *Micropterus* spp., the model with the lowest AICc included water temperature (and an intercept), and had QAICc = 59.1, wi = 0.20. This was nearly 5 QAICc units less than the intercept-only model (QAICc = 64.9, wi = 0.01), and was reflected in the importance value of temperature (0.87) exceeding the 0.8 threshold suggested by Calcagno and de Mazancourt (2010) as indicating potential importance of a variable; however, the unconditional 95 percent confidence interval for the temperature coefficient overlapped zero (0.78 ± 0.82), which means that water temperature was not well supported as an influence on *Micropterus* CPUE (per Zeug and Cavallo 2013); however, the relationship was as hypothesized (i.e., greater CPUE with greater temperature) and generally appeared to be supported when examining the raw data underlying the analysis (**Figure 3.6-16**).

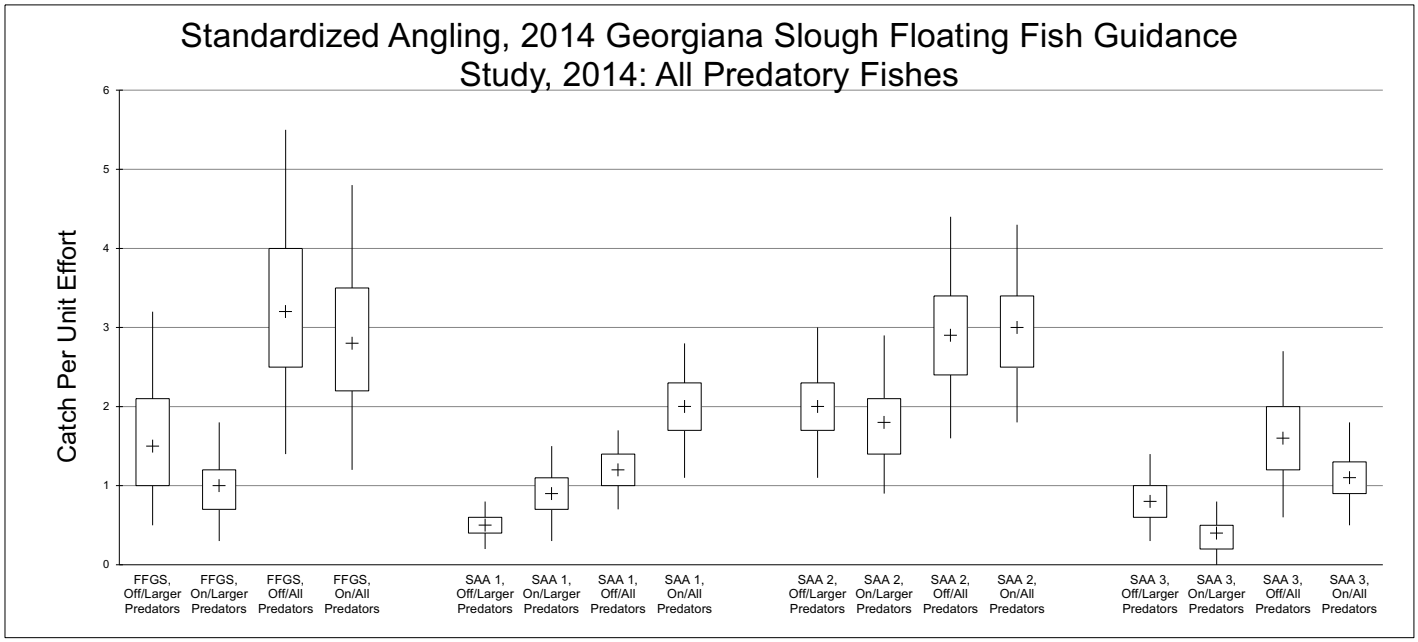

Note: Boxplots represent bootstrapped mean (+), interquartile range (box), and 95 percent confidence interval (whiskers). Larger predators are ≥ 360-mm TL (striped bass and Sacramento pikeminnow) and ≥ 300-mm TL (all other species). n = 10 samples in each category.

Figure 3.6-10 All Predatory Fishes: Catch per Unit Effort by Standardized Angling Area with FFGS On/Off

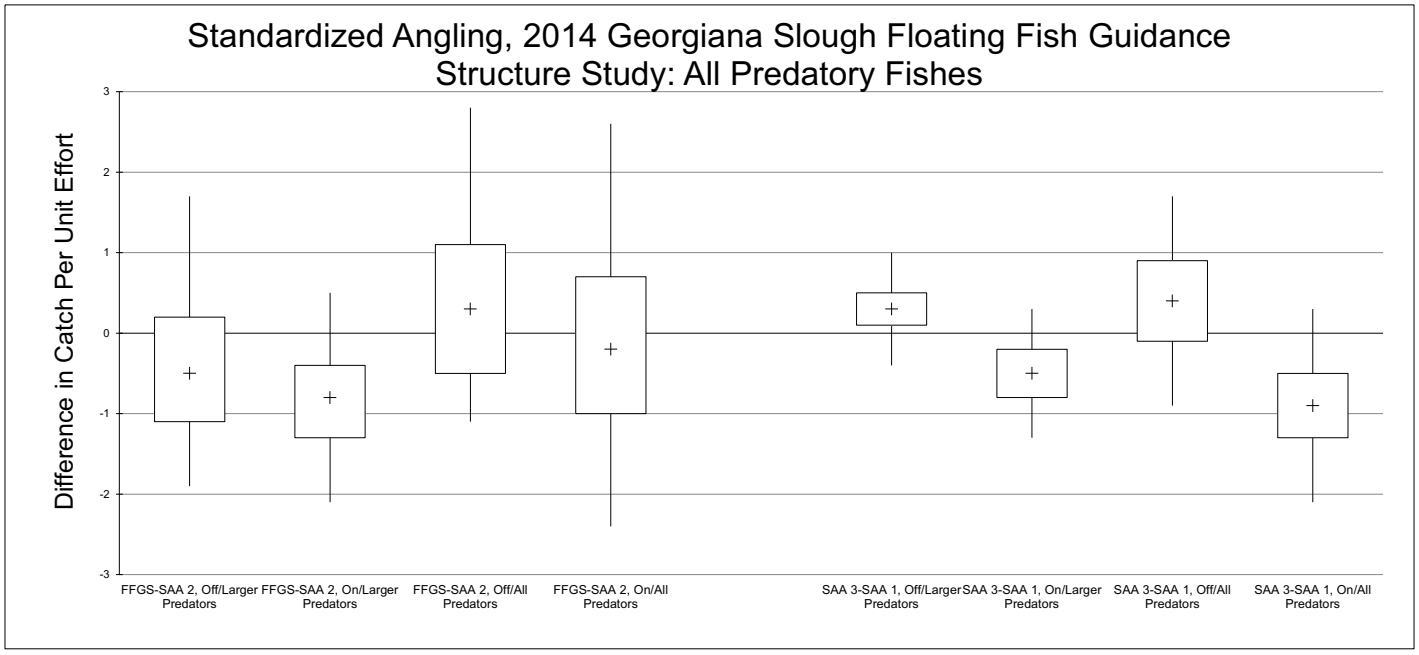

Note: Boxplots represent bootstrapped mean (+), interquartile range (box), and 95 percent confidence interval (whiskers). Larger predators are ≥ 360-mm TL (striped bass and Sacramento pikeminnow) and ≥ 300-mm TL (all other species). n = 10 paired samples in each category.

Figure 3.6-11 All Predatory Fishes: Difference in Catch per Unit Effort between Impact and Reference Standardized Angling Areas with FFGS On/Off

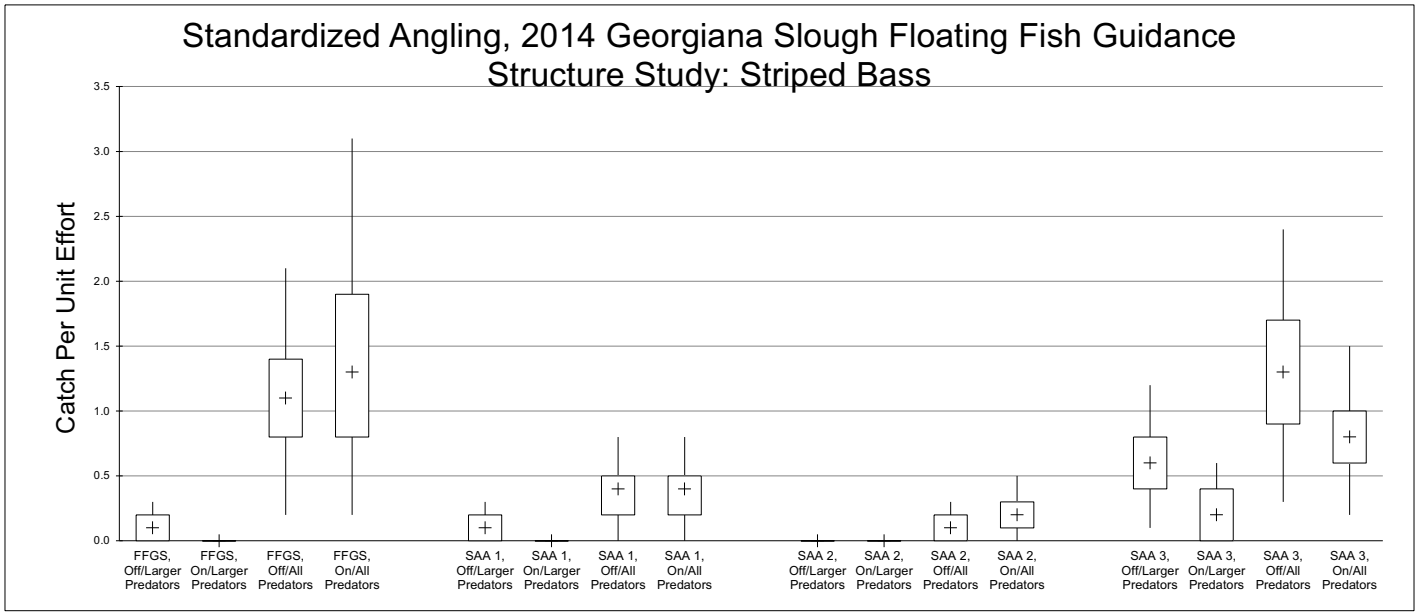

Note: Boxplots represent bootstrapped mean (+), interquartile range (box), and 95 percent confidence interval (whiskers). Larger predators are ≥ 360-mm TL. n = 10 samples in each category.

Figure 3.6-12 Striped Bass: Catch per Unit Effort by Standardized Angling Area with FFGS On/Off

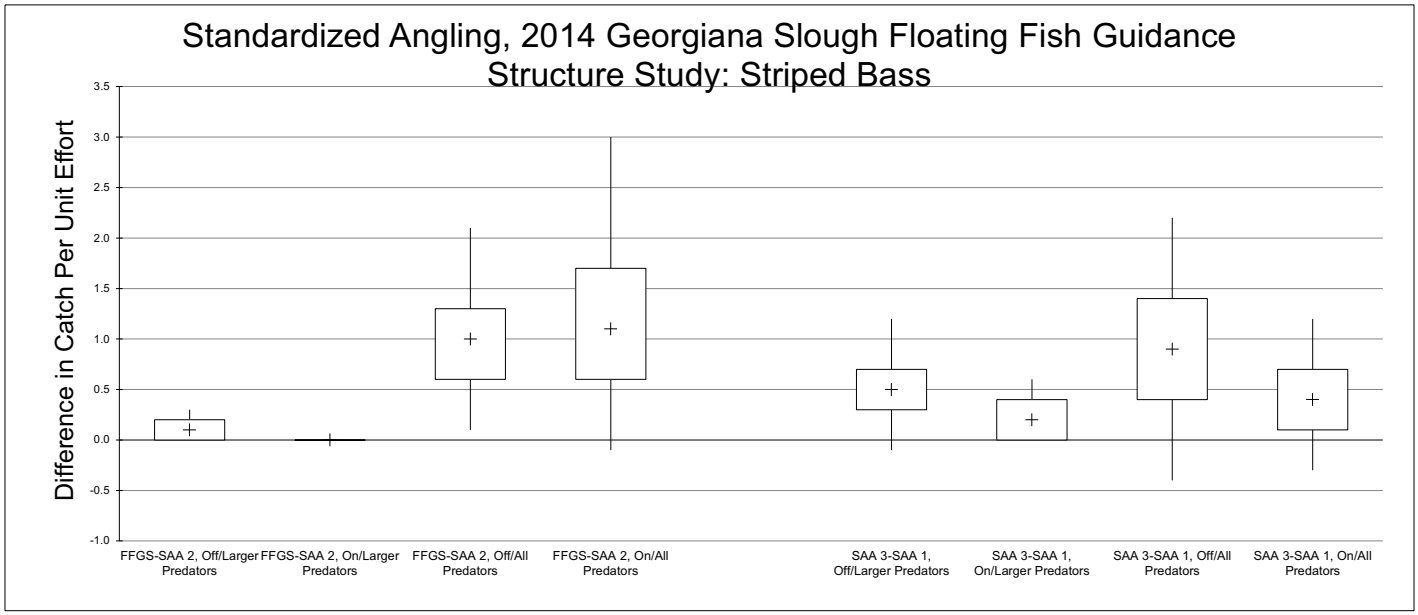

Note: Boxplots represent bootstrapped mean (+), interquartile range (box), and 95 percent confidence interval (whiskers). Larger predators are ≥ 360-mm TL. n = 10 paired samples in each category.

Figure 3.6-13 Striped Bass: Difference in Catch per Unit Effort between Impact and Reference Standardized Angling Areas with FFGS On/Off

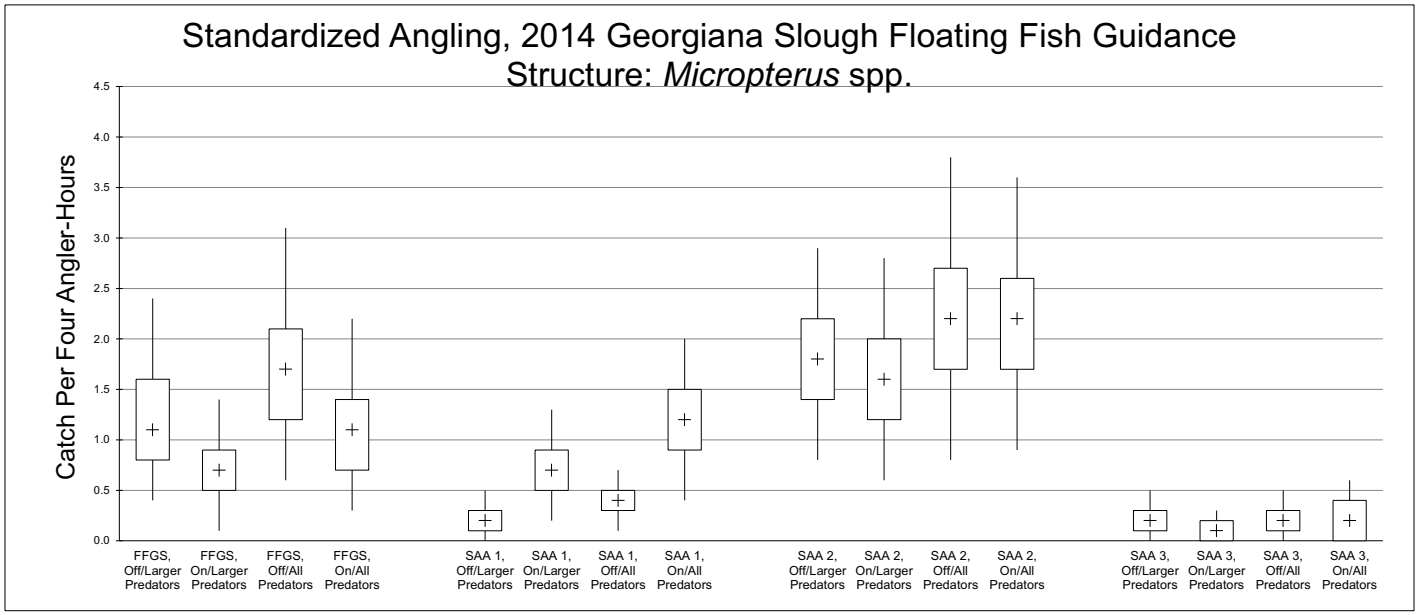

Note: Boxplots represent bootstrapped mean (+), interquartile range (box), and 95 percent confidence interval (whiskers). Larger predators are ≥ 300-mm TL. n = 10 samples in each category.

Figure 3.6-14 ***Micropterus*** **spp.: Catch per Unit Effort by Standardized Angling Area with FFGS On/Off**

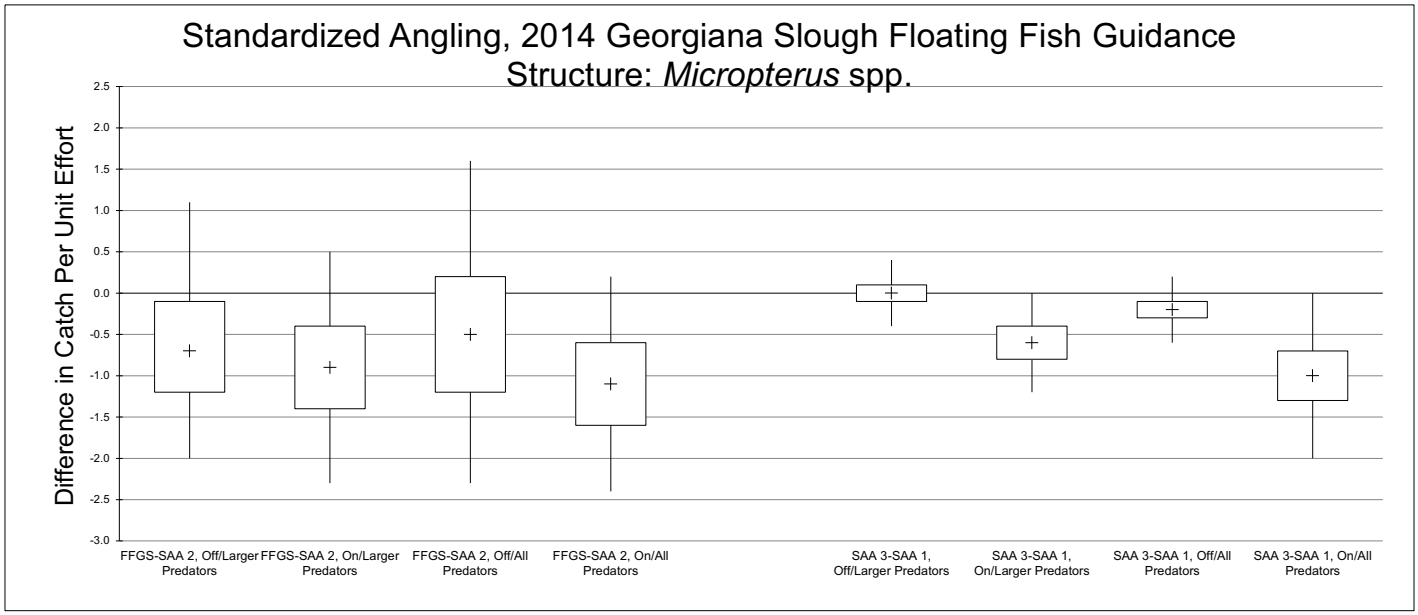

Note: Boxplots represent bootstrapped mean (+), interquartile range (box), and 95 percent confidence interval (whiskers). Larger predators are ≥ 300-mm TL. n = 10 paired samples in each category.

Figure 3.6-15 ***Micropterus*** **spp.: Difference in Catch per Unit Effort between Impact and Reference Standardized Angling Areas with FFGS On/Off**

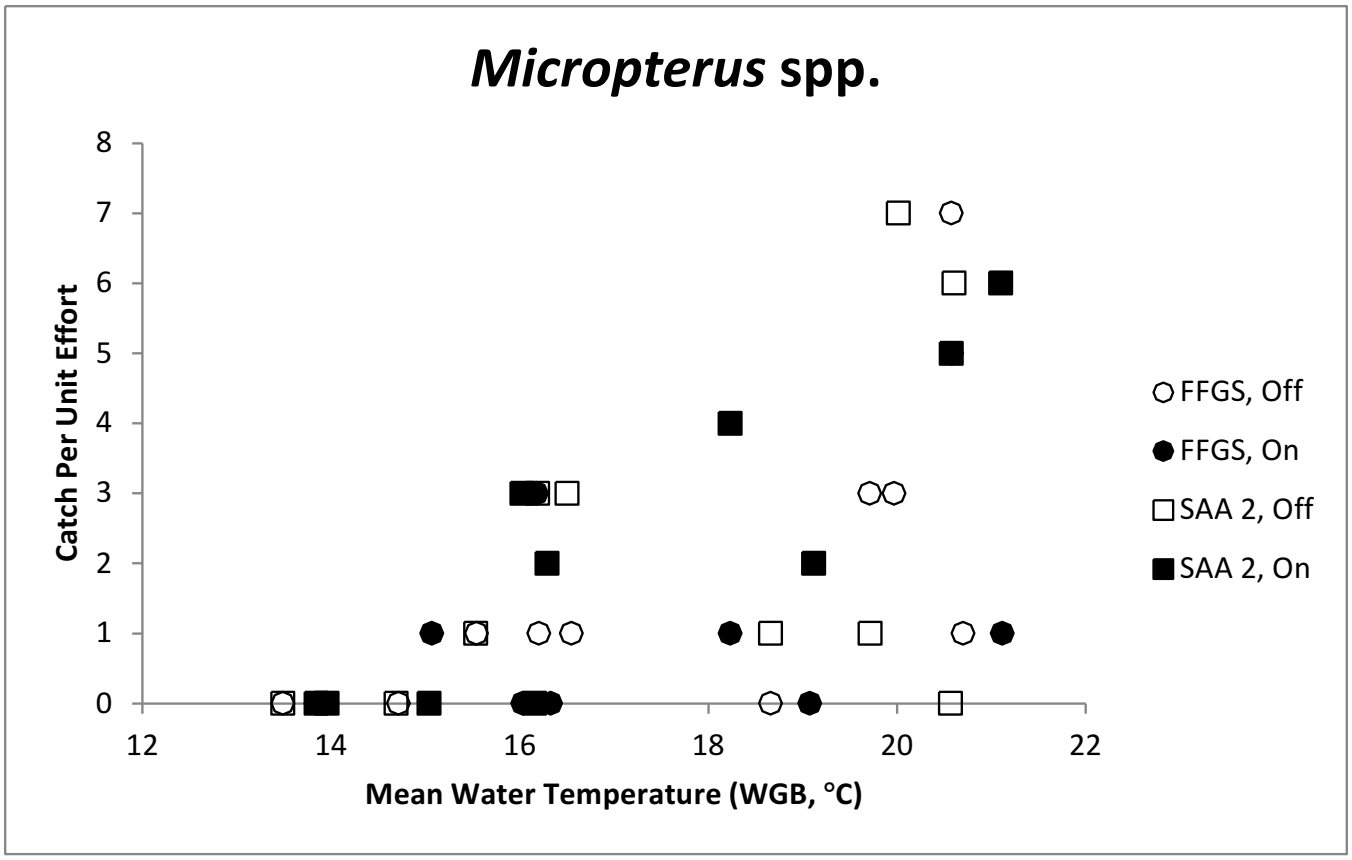

Figure 3.6-16 ***Micropterus*** **spp.: Standardized Angling Catch per Unit Effort in Relation to Mean Water Temperature at the WGB Station**

3.6.5 HABITAT USE (HYPOTHESES H11 AND H12)

MAIN FINDINGS

- Striped bass spent little time near the FFGS (generally significantly less than expected based on zone area) and occupied the Open Water habitat zone significantly more than any other habitat zone;
- *Micropterus* spp. often were found in the nearshore area near the FFGS, as well as other zones on the same bank (left bank) as the release dock (and occurred in these areas significantly more than expected based on the zones' area);
- *Micropterus* spp. behavior appeared partly related to homing to initial capture area;
- Striped bass were found in low velocity (0-0.05 m/s [0-0.16 ft/s]) significantly less than expected based on available velocity; and
- *Micropterus* spp. were found in high velocity (0.45 m/s [1.47 ft/s]) significantly less than expected based on available velocity.

OBJECTIVES

Habitat use by predatory fishes in the study area is of considerable importance because different habitats may be used to differing degrees by different species and at different life stages, as shown in the 2012 BAFF study (DWR 2015b) and other observations in the Delta (Vogel 2011; Sabal et al. 2016). It is of management importance to investigate the relative habitat value that the FFGS provides in the context of the available habitat mosaic of the study area. Data from acoustically tagged predatory fishes were used to achieve the objective of assessing different habitat use in the study area and specifically to test Hypothesis H11: The percentage of time that predatory fishes spend within different habitat types in the study area is not equal.

In addition to stationary elements of habitat such as riprap banks and docks, dynamic habitat also is of importance to predatory fishes, including water velocity (Edwards et al. 1983; McMahon et al. 1984). Studies of the BAFF found that acoustically tagged predatory fishes generally were closer to shore in 2011 than in 2012, presumably because of the higher water velocity associated with very high river discharge in 2011 (DWR 2012; DWR 2015b). At the Head of Old River, striped bass were found to occupy a wide range of velocities whereas largemouth bass and channel catfish occurred mostly at low velocity (Greenwood 2014; DWR 2015a). With respect to water velocity, the study had the objective of assessing the use of different water velocities by acoustically tagged predatory fishes in relation to those available, by testing Hypothesis H12: The percentage of time that predatory fishes spend in different water velocities in the study area is not equal.

METHODS

Field Methods

The data used to test Hypotheses H11 and H12 were derived from acoustically tagged predatory fishes (see Section 3.6.2 “Acoustic Tagging of Predatory Fishes” for detailed description). As noted in Section 3.6.2, all tagged predatory fish (**Table 3.6-9**) were released at the release dock after tag implantation surgery was performed.

The estimates of near-surface velocity used for testing Hypothesis H12 were based on hydrodynamic data collected using side-looking acoustic Doppler current profilers (SL-ADCP), deployed near the bank that profiled across the river at six locations in the study area, as described in section 3.3.2. The SL-ADCP measurements were made continuously at 15-minute intervals, from 8:15 a.m. on March 15 to 5:15 p.m. on May 25, 2014.

Data Analysis

Habitat Zones (Hypothesis H11)

The study area was divided into a number of predator habitat zones using GIS to examine habitat use in relation to various physical features, including the FFGS (**Figure 3.6-9**). The predatory fish habitat zones were adapted from those used in the DWR study of the 2012 BAFF (DWR 2015b). Nearshore habitats such as riprapped banks were demarcated from Open Water habitat by the 4.3-m (14-ft) depth contour. In-channel structures such as docks and bridge pilings included buffers of 5 m (16 ft) around them to represent potential near-field association of predatory fishes. The FFGS was represented by two zones, FFGS On and FFGS Off, which were based on hypothesized potential zones of influence on predatory fishes for the FFGS On/Off treatments (i.e., between the river bank and the FFGS and a distance of 5 m (16 ft) to the water side), again representing near-field association potential as for other in-channel structures.

The analysis to test Hypothesis H11 used the same filtered, smoothed, and discretized acoustic tag detection data that were prepared following the methods of Romine et al. (2014) to identify putative predators that may have consumed juvenile Chinook salmon (see Section 3.4.1, "Methods", in Section 3.4, "Generalized Linear Modeling of Fish Fates"). For each FFGS treatment (On/Off), the percentage of acoustic tag detections by habitat zone was calculated for each predatory fish. Predatory fish with at least 1,000 detections in each FFGS treatment (On/Off) were included in the analysis. As with testing of Hypotheses H8 and H9, resampling (bootstrapping) was used to produce statistical summaries of the data for striped bass and *Micropterus* spp. For each treatment (i.e., FFGS On/Off), the percentage of detections in each habitat zone was resampled with replacement until each resample contained the same number of observations (i.e., number of fish) as the original sample. Hypothesis H11 was accepted if the 95 percent confidence intervals for percentage of detections did not overlap across zones. The differences between FFGS treatments (On/Off) were also tested in this manner.

The resampled percentages of detections by habitat zones also were converted into habitat selection indices for each habitat zone by dividing by the percentage of the study area attributable to each zone (**Table 3.6-13**). A habitat selection index greater than 1 means a predatory fish occupied a particular habitat zone more frequently than expected based on its area, whereas a velocity selection index less than 1 means a predatory fish occupied a particular zone less frequently than expected based on its area; habitat selection equal to 1 means the habitat zone was occupied in equal proportion to its area. This analysis essentially is a refinement of the analysis conducted for the 2012 BAFF study (DWR 2015b) because it incorporates variability from individual fish as opposed to summing overall detections across all fish.

Table 3.6-13 Area of Predator Habitat Zones

Zone	Area (Hectares)	Area (Acres)	Percentage of Study Area
Open Water	5.21	12.87	60.7
Dock 2	0.55	1.37	6.5
Rip Rap 1	0.48	1.19	5.6
FFGS (Off)	0.32	0.79	3.7
Mud Flat 4	0.28	0.69	3.3
Mud Flat 2	0.23	0.57	2.7
Mud Bank 2	0.20	0.50	2.4
Dock 3	0.20	0.49	2.3
FFGS (on)	0.18	0.45	2.1
Rip Rap 4	0.18	0.44	2.1
Mud Bank 3	0.13	0.33	1.6
Mud Bank 4	0.11	0.26	1.2
Bridge Right	0.10	0.25	1.2
Bridge Left	0.09	0.23	1.1
Rip Rap 2	0.08	0.19	0.9
Mud Flat 3	0.07	0.17	0.8
Mud Flat 1	0.05	0.12	0.6
Dock 4	0.05	0.11	0.5
Dock 1	0.02	0.06	0.3
Rip Rap 3	0.02	0.05	0.3
Mud Bank 5	0.02	0.04	0.2
Mud Bank 1	0.02	0.04	0.2
Total	8.58	21.21	100

Velocity (Hypothesis H12)

To provide estimates of velocity to test Hypothesis H12, the SL-ADCP velocity data were interpolated to generate a near-surface 2D velocity field (see Section 3.3.2, subsection "Two-Dimensional Velocity Interpolation"). The 2D interpolated velocity fields were generated for a 10-m by 10-m (33-ft by 33-ft) set of grid points (**Figure 3.6-17**) every 15 minutes.

The analysis to test Hypothesis H12 used the same filtered, smoothed, and discretized acoustic tag detection data that were prepared following the methods of Romine et al. (2014) to identify putative predators that may have consumed telemetered juvenile Chinook salmon (see Section 3.4.1, "Methods", in Section 3.4, "Generalized Linear Modeling of Fish Fates"). Each acoustic tag detection was matched to the closest velocity grid point (**Figure 3.6-17**); detections further than 10 m (33 feet) from any grid point were excluded from the analysis. Predatory fish with at least 1,000 detections[22] in each FFGS treatment (On/Off) were included in the analysis. Each velocity estimate was rounded to the nearest 0.05-m/s (0.16 ft/s) increment, and the percentage of all detections in each increment by FFGS treatment was calculated for each predatory fish retained in the analysis. All available velocities (i.e., at all 320 velocity grid points) at the time of each acoustic tag detection also were retained, and the percentage of these observations in each velocity increment was calculated for each fish. A velocity selection

index was calculated for each velocity increment, as the percentage of detections occurring in that increment divided by the percentage of all modeled velocity estimates occurring in the same increment. As with Hypothesis H11, a velocity selection index greater than 1 means a predatory fish occupied a particular velocity increment more frequently than expected based on its availability in the study area, whereas a velocity selection index less than 1 means a predatory fish occupied a particular velocity increment less frequently than expected based on its availability in the study area; velocity selection equal to 1 means the velocity increment was occupied in equal proportion to its availability in the study area.

As with testing of Hypotheses H8, H9, and H11, resampling (bootstrapping) was used to produce statistical summaries of the data for striped bass and *Micropterus* spp. For each treatment (i.e., FFGS On/Off), the velocity selection index in each 0.05-m/s (0.16 ft/s) velocity increment was resampled with replacement until each resample contained the same number of observations (i.e., number of fish) as the original sample. Hypothesis H12 was accepted if the 95 percent confidence intervals for velocity selection differed across velocity increments with respect to neutral selection (i.e., a velocity selection index of 1). This analysis focused only on the velocity selection indices rather than the actual velocity because of the dynamic nature of the velocity field, which was frequently changing based on river flow, tidal stage, and other factors.

[22] For perspective, the actual time represented by 1,000 detections is around 8,000 seconds (133 minutes) for the 8-second discretized data; these were not necessarily consecutive detections.

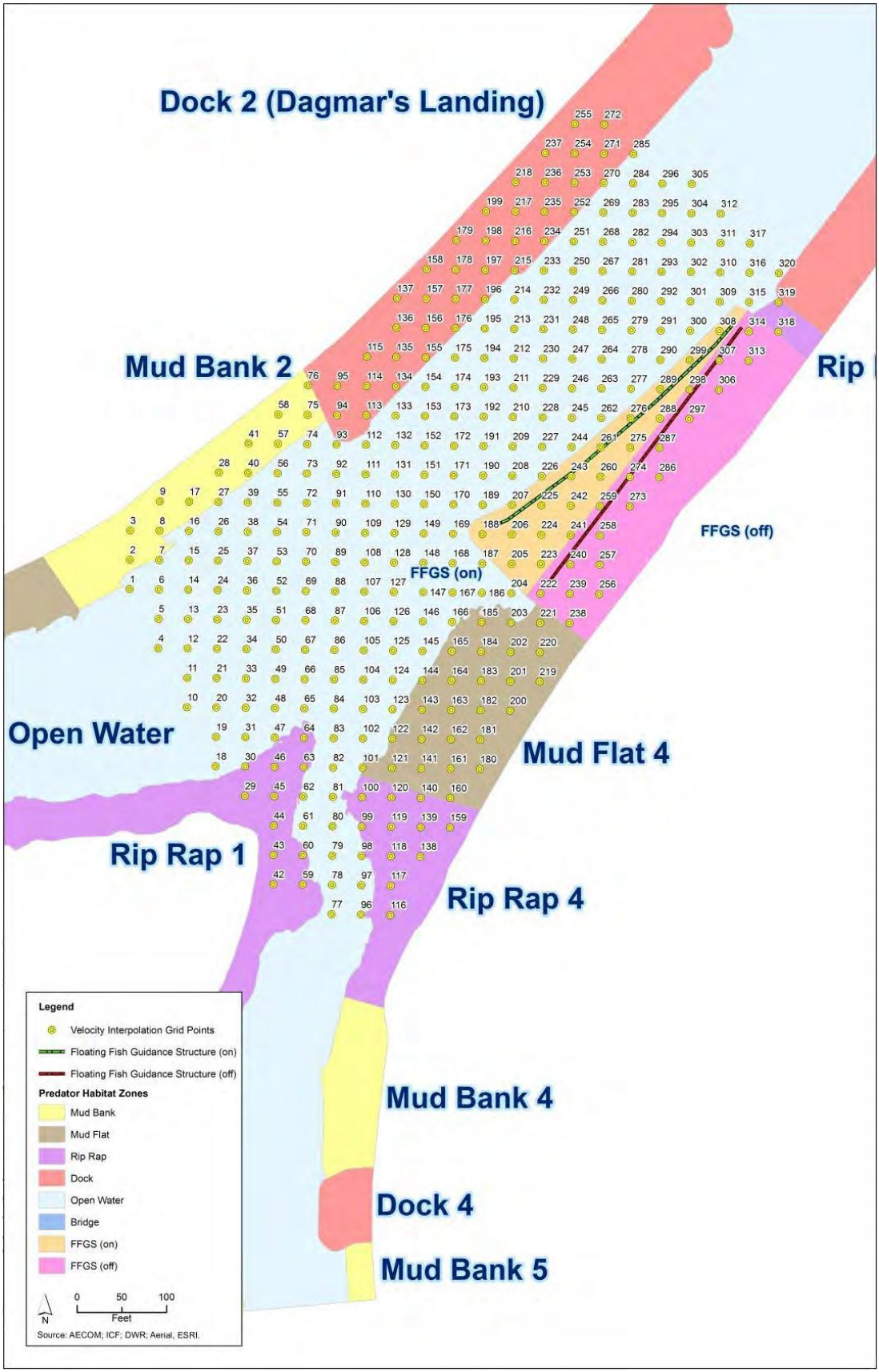

Figure 3.6-17 Interpolated Velocity Grid Points from SL-ADCP Measurements

Homing and Recapture (Micropterus spp.)

During the analysis of habitat zones in relation to Hypothesis H11 (see foregoing), it became apparent that further investigation of homing of *Micropterus* spp. was warranted because of the relatively frequent use of the FFGS (Off) habitat zone. The frequent use of this zone may be attributable to the importance of the FFGS, or it simply may be because *Micropterus* spp. originally were caught in this area, tagged, and then returned to the area after release. Data for *Micropterus* spp. captured in the four standardized angling areas (SAA) were summarized for the percentage of detections after release that each fish spent in three different locations during FFGS On/Off treatments (see **Figure 3.6-10**):

- Near the capture site
  - FFGS (i.e., in habitat zones FFGS Off and FFGS On)
  - SAA 1 (i.e., in habitat zones Mud Bank 3 and Bridge Right)
  - SAA 2 (i.e., in habitat zones Rip Rap 2, Bridge Left, and Mud Flat 3)
  - SAA 3 (i.e., in habitat zones Mud Flat 2 and Mud Bank 2);
- Near the release site (i.e., in habitat zone Dock 3 [Boon Dox]); and
- Near the FFGS (i.e., in habitat zones FFGS Off and FFGS On).

Bootstrapped means and confidence intervals were calculated for the percentage of detections spent at these locations for fish released from each of the four SAAs, using the resampling methods described above for the analyses related to Hypotheses H11 and H12. Evidence for homing was considered to have been provided when the percentage of detections near the capture site (i.e., following return to the area after release) was greater than the percentage of detections near the release site. Evidence for the importance of the FFGS was provided if the percentage of detections near the FFGS was greater than the percentage of detections near the capture site or the release site.

In addition to the investigation for evidence of homing, a general examination of recaptures of *Micropterus* spp. was undertaken. This examination focused on predatory fishes released in the study area, in particular those released at the surgery dock (Dock 3), for which the transition from one area to another could be discerned based on patterns in the track data.

RESULTS

Habitat Zones (Hypothesis H11)

Striped bass occupied the Open Water habitat zone significantly more than any other habitat zone: for the 15 striped bass included in the analysis, the bootstrapped mean percentage of detections for the FFGS Off (66.2%) and the FFGS On (69.2%) were similar and an order of magnitude greater than the percentage of detections in any of the other zones (**Figure 3.6-18**). Therefore, Hypothesis H11 was accepted for striped bass. No significant difference occurred in the percentage of detections between the FFGS On/Off treatments in either the FFGS Off or FFGS On habitat zones, and relatively few detections were made in these zones: the bootstrapped means for the FFGS Off zone were 0.7 percent (95 percent confidence interval: 0.2 to 1.4 percent) for the FFGS Off and 0.6 percent (95 percent confidence interval: 0.2 to 1.3 percent) for the FFGS On; the bootstrapped means for the FFGS On zone were 1.1 percent (95 percent confidence interval: 0.2 to 2.9 percent) for the FFGS Off and 0.6 percent (95 percent confidence interval: 0.1 to 1.4 percent) for the FFGS on. Striped bass were not detected within several small zones in Georgiana Slough (i.e., Dock 4, Mud Bank 5, and Mud Bank 1) (**Figure 3.6-18**).

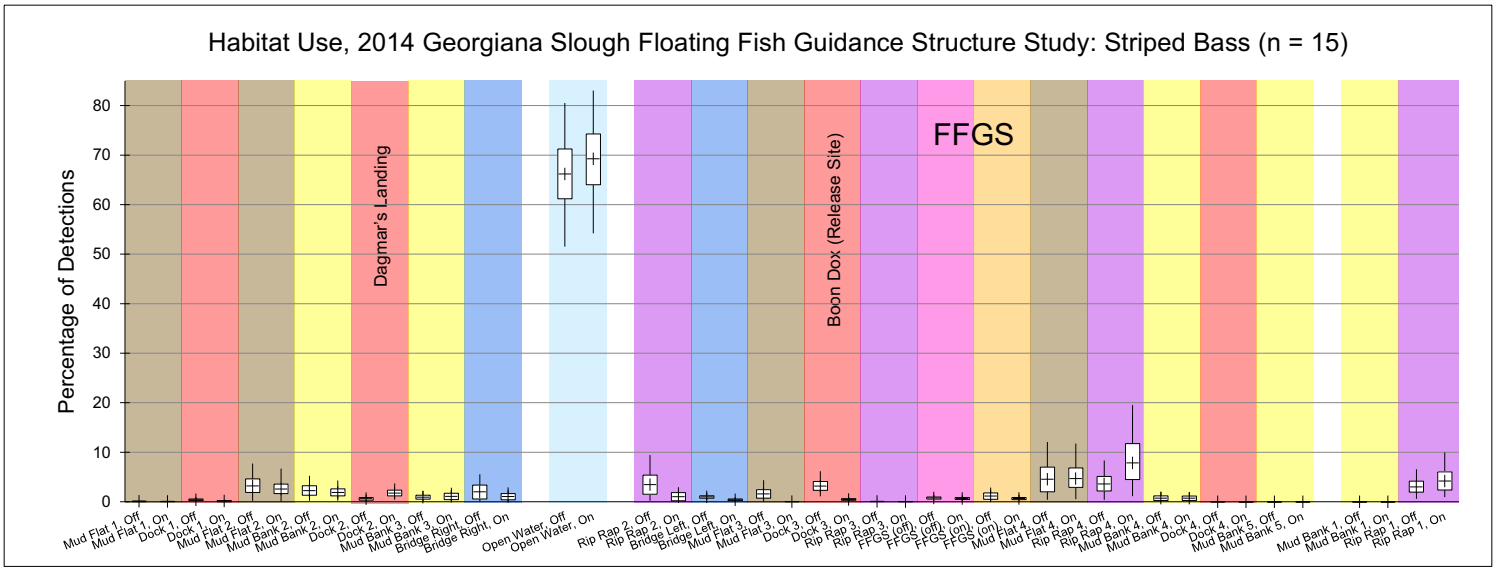

Note: Boxplots represent bootstrapped mean (+), interquartile range (box), and 95 percent confidence interval (whiskers). Habitat zones are color-coded as in **Figure 3.6-10** and are arranged in sequential clockwise order corresponding to **Figure 3.6-10**. n = 15 samples (fish) in each category.

Figure 3.6-18 Striped Bass: Percentage of Detections by Habitat Zone with FFGS On/Off

Striped bass did not select any of the habitat zones significantly more than expected based on zone area (i.e., habitat selection index greater than 1), although the Open Water habitat zone was the closest to meeting the criteria for statistical significance (95 percent confidence intervals of 0.8 to 1.3 for the FFGS Off and 0.9 to 1.4 for the FFGS On) (**Figure 3.6-19**). Most habitat zones had habitat selection 95 percent confidence intervals overlapping 1 (i.e., neutral selection as expected, based on a zone's area), but a number were selected significantly less frequently than expected, based on area (i.e., 95 percent confidence intervals below 1). Among these were the FFGS Off and FFGS On zones (**Figure 3.6-19**).

In contrast to striped bass, the 71 *Micropterus* spp. meeting the criteria for inclusion in the analysis spent less time in the Open Water habitat zone (bootstrapped mean: 12 to 13 percent) than in some nearshore habitat zones, particularly in the vicinity of the release site (Dock 3, or Boon Dox, with bootstrapped mean 15 to 18 percent) and the FFGS Off zone, for which the bootstrapped means were 15 to 20 percent (**Figure 3.6-19**). The percentage of detections was significantly greater in these habitat zones than most other zones, thus Hypothesis H11 also was accepted for *Micropterus* spp. A significantly greater percentage of detections occurred in the FFGS Off habitat zone (bootstrapped mean: 15 to 20 percent) than in the FFGS On habitat zone (bootstrapped mean: 0.7 to 1.6 percent), but no significant difference occurred in percentage of detections between the FFGS Off and the FFGS On treatments in either of the FFGS habitat zones. A very low or zero percentage of detections was observed in a number of zones, particularly at the downstream edge of the study area (e.g., zones Mud Flat 1 and Dock 1 in Sacramento River; and zones Dock 4, Mud Bank 5, and Mud Bank 1 in Georgiana Slough) (**Figure 3.6-20**).

Micropterus spp. generally selected[23] nearshore habitat zones on the same bank as the release site significantly more often than expected, based on zone area (i.e., habitat selection index 95 percent confidence interval greater than 1), ranging from Rip Rap 2 downstream to the FFGS Off zone (**Figure 3.6-21**). There was also significant selection occurred for the Rip Rap 1 zone, a relatively large zone with an appreciable percentage of detections (**Figure 3.6-21**). Selection of the offshore FFGS On habitat zone was significantly less than expected, based on its area during the FFGS on treatment, whereas this zone's selection during the FFGS Off treatment was not significantly different from neutral (habitat selection index equal to 1). The Open Water habitat zone was selected significantly less often than expected, based on its large area (i.e., habitat selection index 95 percent confidence interval less than 1), which also was true for the aforementioned zones at the downstream edge of the study area, as well as various other zones including Mud Bank 2 and Mud Flat 4 (**Figure 3.6-21**).

Velocity (Hypothesis H12)

A total of 7 striped bass and 30 *Micropterus* spp. met the criteria for inclusion in the analysis of velocity. The range of velocity increments examined in the analysis was limited to 0 to 0.45 m/s (1.48 ft/s) because relatively few velocity estimates were higher than this range. The median velocity of detection for striped bass ranged from 0.16 to 0.43 m/s (0.52-1.41 ft/s), which was slightly higher than the range of available median velocity (0.14 to 0.36 m/s [0.46-1.18 ft/s]).

[23] "Selection" reflects initial release following tagging (i.e., at Dock 3) and, for some *Micropterus* spp., recapture and re-release (often at Dock 3, but not always), as discussed in the "Homing and Recapture (*Micropterus* spp.)" section that follows.

This page intentionally left blank.

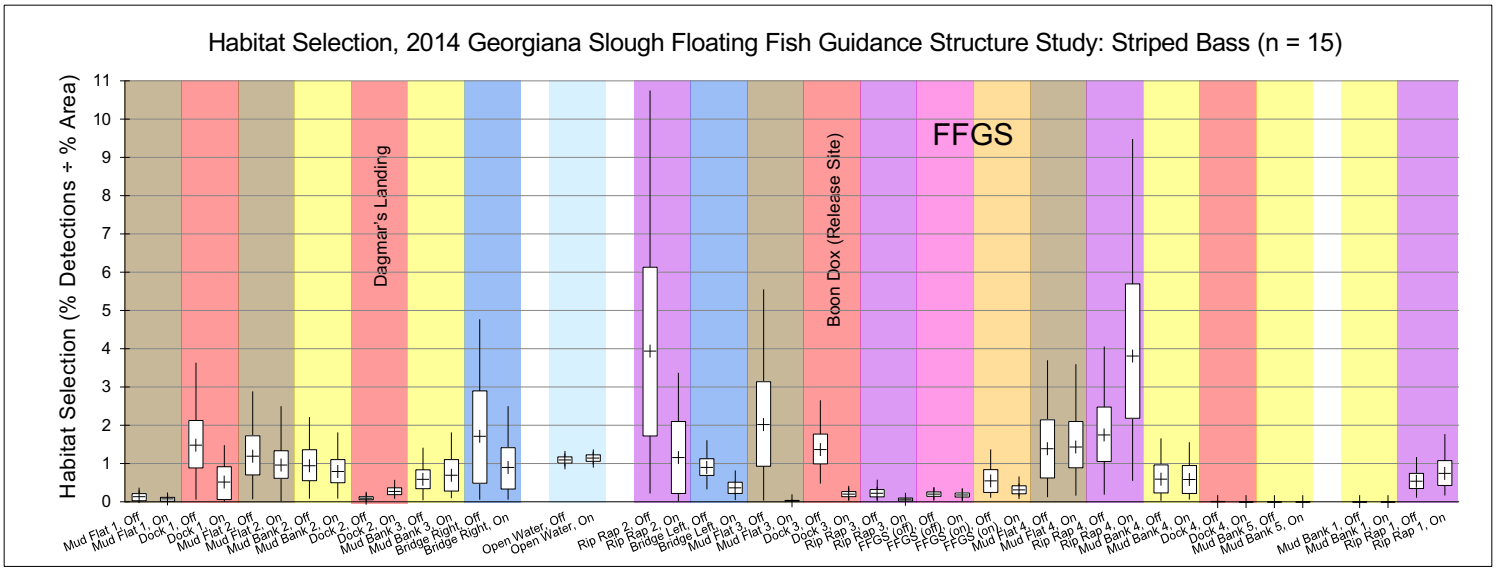

Note: Boxplots represent bootstrapped mean (+), interquartile range (box), and 95 percent confidence interval (whiskers). Habitat zones are color-coded as in **Figure 3.6-10** and are arranged in sequential clockwise order corresponding to **Figure 3.6-10**. n = 15 samples (fish) in each category.

Figure 3.6-19 Striped Bass: Habitat Selection with FFGS On/Off

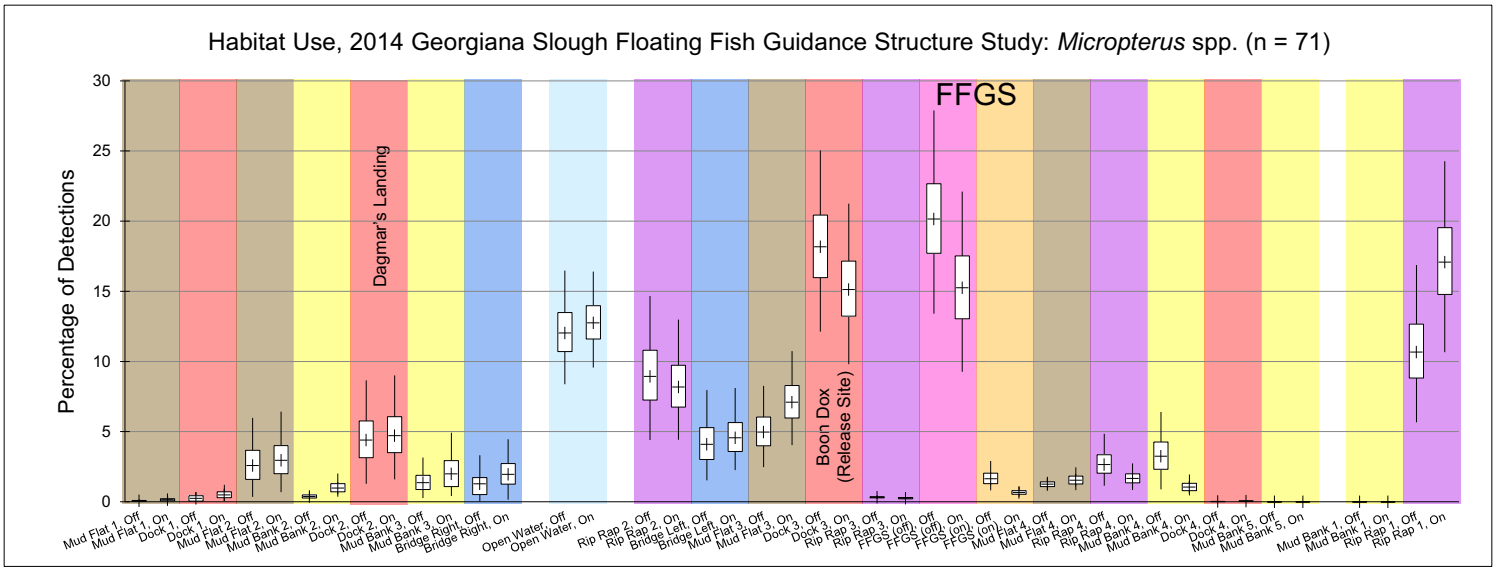

Note: Boxplots represent bootstrapped mean (+), interquartile range (box), and 95 percent confidence interval (whiskers). Habitat zones are color-coded as in **Figure 3.6-10** and are arranged in sequential clockwise order corresponding to **Figure 3.6-10**. n = 71 samples (fish) in each category.

Figure 3.6-20 ***Micropterus*** **spp.: Percentage of Detections by Habitat Zone with FFGS On/Off**

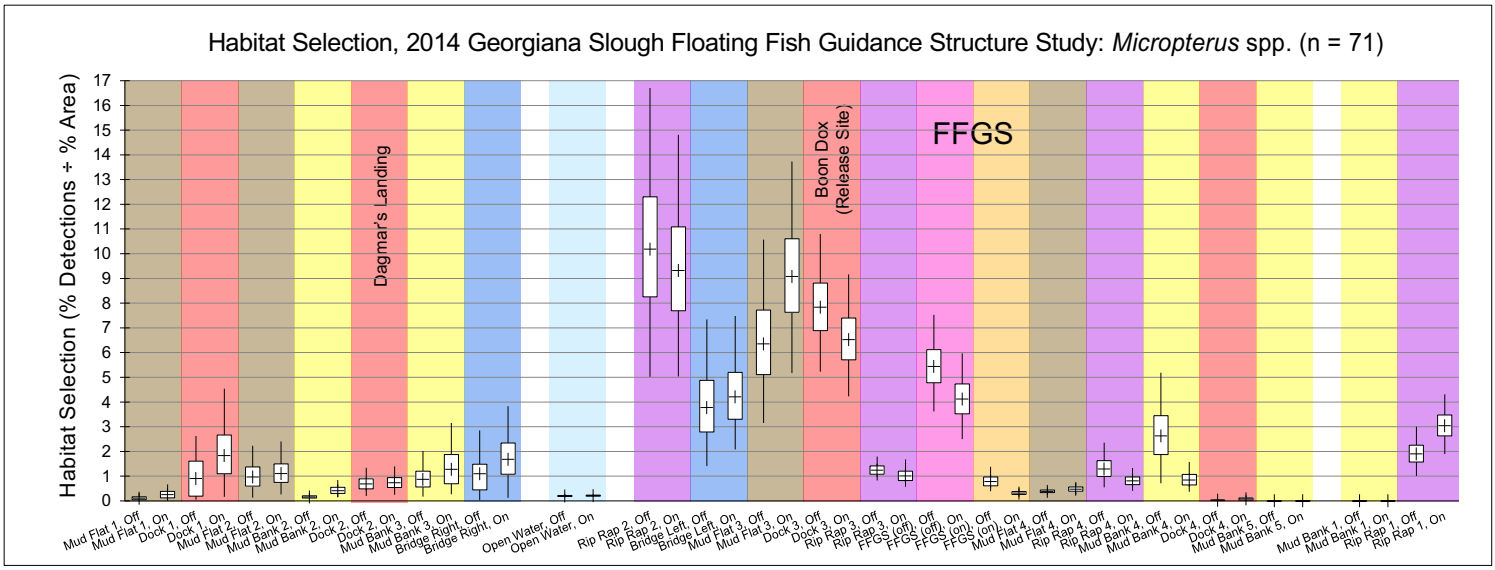

Note: Boxplots represent bootstrapped mean (+), interquartile range (box), and 95 percent confidence interval (whiskers). Habitat zones are color-coded as in **Figure 3.6-10** and are arranged in sequential clockwise order corresponding to **Figure 3.6-10**. n = 71 samples (fish) in each category.

Figure 3.6-21 ***Micropterus*** **spp.: Habitat Selection with FFGS On/Off**

Striped bass generally had significantly lower selection of the 0 to 0.05 m/s (0-0.16 ft/s) velocity increments than expected, based on the availability of these velocity increments (i.e., velocity selection index 95 percent confidence intervals less than 1; the 0.05 m/s (0.16 ft/s) increment with FFGS Off had an upper 95 percent confidence limit equal to 1.008) (**Figure 3.6-22**). The 0.4 m/s (1.31 ft/s) and 0.45 m/s (1.48 ft/s) velocity increments each had one of the FFGS treatments with velocity selection less than 1, but these treatments differed (i.e., FFGS Off for 0.4 m/s [1.31 ft/s], FFGS On for 0.45 m/s [1.48 ft/s]). No velocity increments were selected significantly more than expected, based on their availability (i.e., none had velocity selection index 95 percent confidence intervals greater than 1), and most increments were selected as expected based on their availability (i.e., velocity selection index 95 percent confidence intervals overlapping 1). Hypothesis H12 was accepted for striped bass.

The median velocity of detection for *Micropterus* spp. ranged from 0.07 to 0.38 m/s (0.23-1.25 ft/s), which was comparable to the range of available median velocity (0.08 to 0.39 m/s [0.26-1.28 ft/s]). The only velocity increment for which velocity selection in both the FFGS Off and FFGS On treatments was significantly different than expected based on availability was 0.45 m/s (1.48 ft/s), the greatest velocity increment in the range examined, which *Micropterus* spp. selected less than expected (**Figure 3.6-23**). The 0.35 m/s (1.15 ft/s) velocity increment was selected more than expected based on its availability, but only for the FFGS Off treatment. The remaining velocity increments were selected as expected based on their availability (i.e., velocity selection index 95 percent confidence intervals overlapping 1). Hypothesis H12 also was accepted for *Micropterus* spp.

Homing and Recapture (*Micropterus* spp.)

There was evidence that *Micropterus* spp. homed to the sites where they initially were captured: the bootstrapped mean percentage of detections at the capture site was greater than the percentage of detections at the release site or near the FFGS for all four capture areas[24] (**Figure 3.6-24**). The percentage of detections in each site was consistent between FFGS On and FFGS Off. Fish caught in the FFGS SAA homed at the greatest rate (bootstrapped mean percentage of detections in capture area: 60 to 65 percent), followed by fish captured in SAA 2 (42 to 43 percent), and fish captured in SAA 1 (25 to 27 percent). Only three fish were captured in SAA 3 that were included in this analysis, so more variability existed in these data; of these three fish, one returned to spend a substantial portion (83 to 90 percent) of its time near SAA 3, whereas the others spent relatively little time (0 to 3 percent) near SAA 3. Tag codes were identified for 12 of 39 *Micropterus* spp. for which recapture data were examined (**Table 3.6-14**). Of these fish, only one (tag code # 4199) was recaptured twice. This fish initially was captured at the surgery dock on March 16 at 12:14 p.m. Pacific Standard Time (PST) (8:24 p.m. Coordinated Universal Time [UTC]). It subsequently was recaptured for the first time in SAA 2 on April 18 at 12:55 p.m. PST (8:55 p.m. UTC), followed by a second recapture on April 24 at 1:41 p.m. PST (9:41 p.m. UTC) (**Table 3.6-14** and **Figure 3.6-25**). This fish had over 90 percent of its detections in Mud Flat 3 and Open Water. It remained in the study area until May 6.

[24] For fish captured in the FFGS SAA, the percentage of detections near the capture area was the same as the percentage of detections near the FFGS because the capture area was the same as the FFGS SAA (i.e., habitat zones FFGS On and FFGS Off).

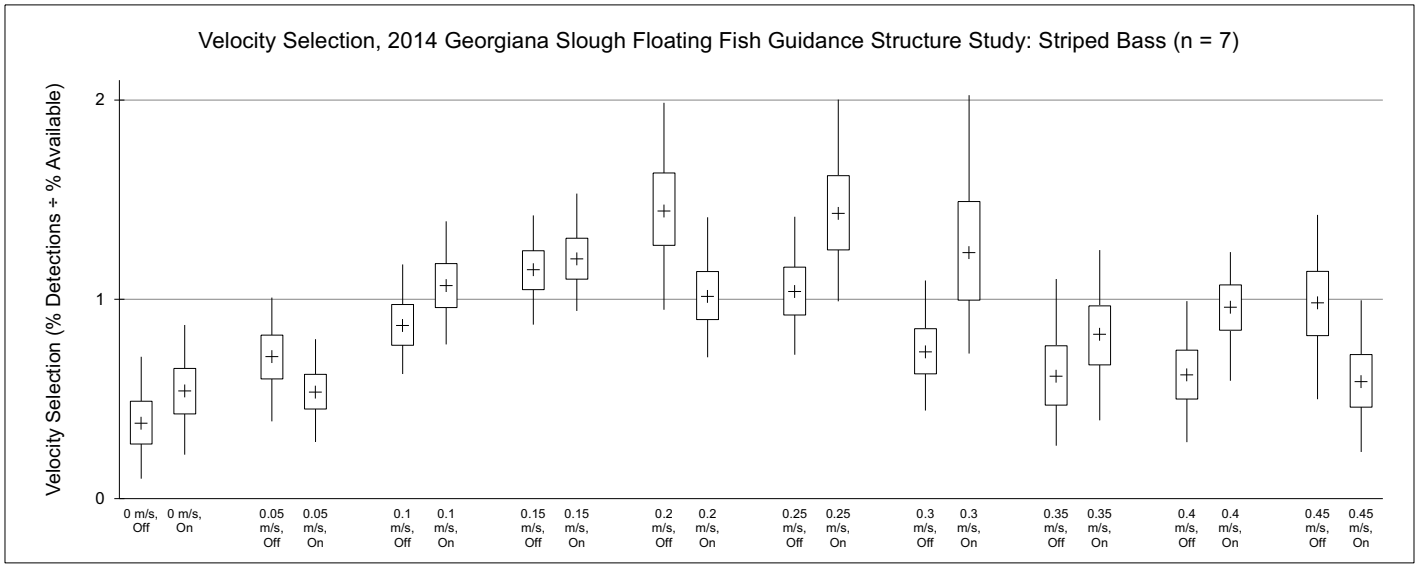

Note: Boxplots represent bootstrapped mean (+), interquartile range (box), and 95 percent confidence interval (whiskers). n = 7 samples (fish) in each category.

Figure 3.6-22 Striped Bass: Velocity Selection with FFGS On/Off

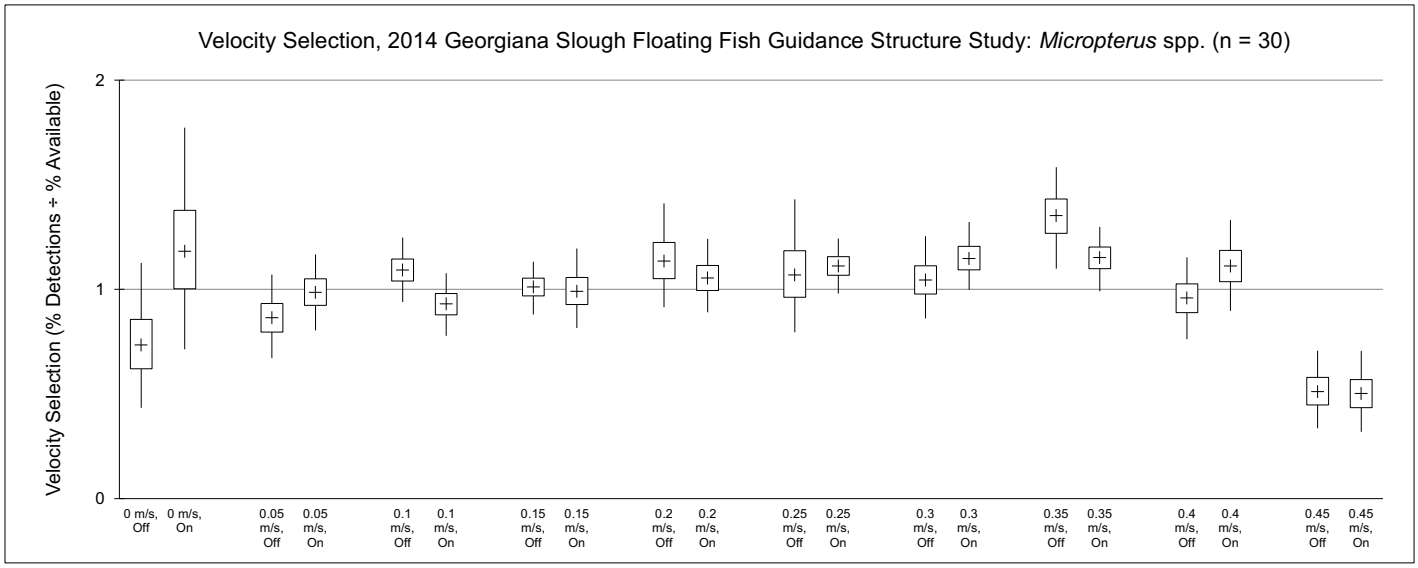

Note: Boxplots represent bootstrapped mean (+), interquartile range (box), and 95 percent confidence interval (whiskers). n = 30 samples (fish) in each category.

Figure 3.6-23 ***Micropterus*** **spp.: Velocity Selection with FFGS On/Off**

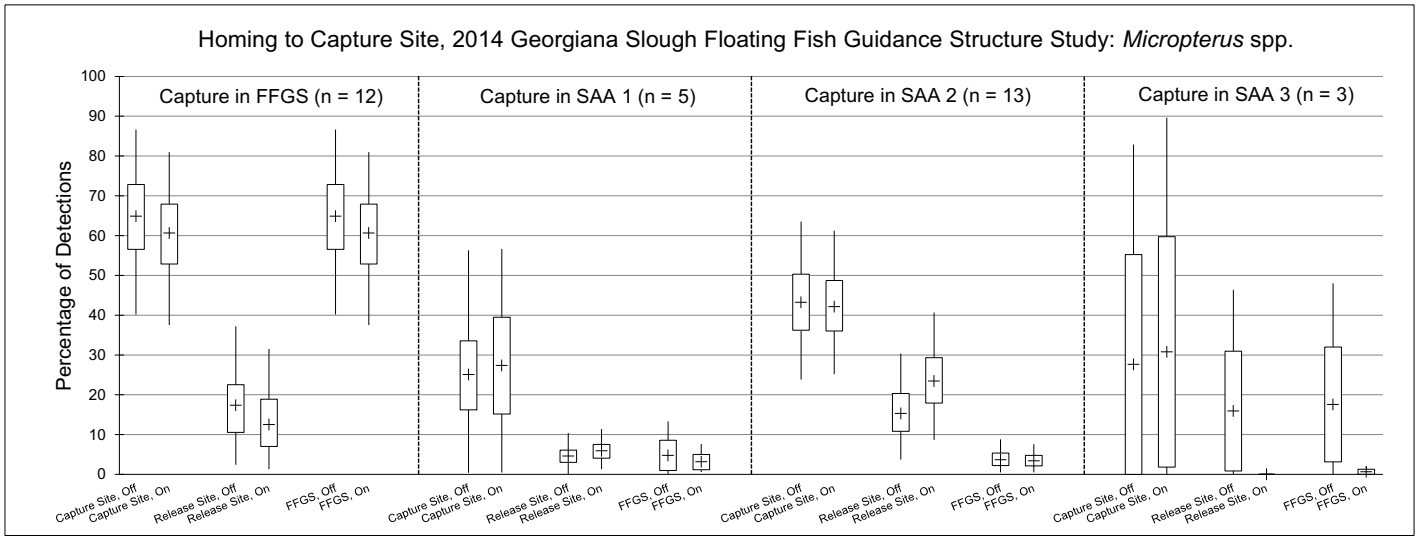

Note: Boxplots represent bootstrapped mean (+), interquartile range (box), and 95 percent confidence interval (whiskers). The number of samples (fish) in each category is indicated in subheaders.

Figure 3.6-24 *Micropterus* spp.: Percentage of Detections near Capture Site, Release Site, and FFGS with FFGS On/Off

Table 3.6-14 *Micropterus* spp.: Summary of Recaptures Assessed for Tag Codes									
Recapture Date/Time (PST/UTC)	Recapture Location	Release Date/Time (PST/UTC)	Release Location	Tag Code	Recapture Date/Time (PST/UTC)	Recapture Location	Release Date/Time (PST/UTC)	Release Location	Tag Code
4/11/14 06:14/14:14	SAA 2	4/11/14 06:59/14:59	Boon Dox	ND	4/21/14 10:11/18:11	Unknown	4/21/14 10:13/18:13	Boon Dox	ND
4/11/14 10:03/18:03	SAA 3	4/11/14 10:29/18:29	SAA 3	ND	4/21/14 12:26/20:26	SAA 2	4/21/14 12:53/20:53	Boon Dox	ND
4/11/14 13:27/21:27	Sac Downstream	4/11/14 13:56/21:56	Boon Dox	4675	4/21/14 11:58/19:58	SAA 2	4/21/14 12:54/20:54	Boon Dox	ND
4/12/14 08:22/16:22	SAA 1	4/12/14 08:30/16:30	SAA 1	2113	4/21/14 12:31/20:31	SAA 2	4/21/14 12:54/20:54	Boon Dox	ND
4/12/14 09:29/17:29	SAA 2	4/12/14 09:45/17:45	Boon Dox	ND	4/21/14 12:16/20:16	SAA 2	4/21/14 12:55/20:55	Boon Dox	ND
4/12/14 12:01/20:01	Sac Downstream	4/12/14 14:00/22:00	Boon Dox	4465	4/22/14 05:22/13:22	Unknown	4/22/14 07:23/15:23	Boon Dox	ND
4/13/14 10:09/18:09	SAA 2	4/13/14 10:37/18:37	Boon Dox	ND	4/22/14 06:51/14:51	Geo. Sl.	4/22/14 08:04/16:04	Boon Dox	4297
4/14/14 11:07/19:07	SAA 2	4/14/14 11:08/19:08	SAA 2	ND	4/22/14 09:55/17:55	Open Water	4/22/14 11:11/19:11	Boon Dox	3947
4/14/14 11:12/19:12	FFGS	4/14/14 11:44/19:44	FFGS	ND	4/22/14 10:00/18:00	Rip Rap 1	4/22/14 11:14/19:14	Boon Dox	4339
4/18/14 10:45/18:45	SAA 2	4/18/14 12:55/20:55	Boon Dox	4199	4/22/14 13:37/21:37	FFGS	4/22/14 13:44/21:44	Boon Dox	ND
4/18/14 11:36/19:36	SAA 2	4/18/14 12:57/20:57	Boon Dox	ND	4/22/14 12:55/20:55	FFGS	4/22/14 13:50/21:50	Boon Dox	3667
4/18/14 11:19/19:19	SAA 2	4/18/14 13:00/21:00	Boon Dox	4885	4/22/14 14:13/22:13	Unknown	4/22/14 15:00/23:00	Boon Dox	ND
4/18/14 11:01/19:01	SAA 2	4/18/14 13:02/21:02	Boon Dox	ND	4/24/14 10:48/18:48	Unknown	4/24/14 13:17/21:17	Boon Dox	3653
4/19/14 07:17/15:17	SAA 2	4/19/14 07:19/15:19	SAA 2	ND	4/24/14 10:33/18:33	Unknown	4/24/14 13:18/21:18	Boon Dox	ND
4/19/14 07:07/15:07	SAA 2	4/19/14 09:18/17:18	Boon Dox	2323	4/24/14 13:45/21:45	FFGS	4/24/14 13:46/21:46	FFGS	ND
4/19/14 07:10/15:10	SAA 2	4/19/14 09:20/17:20	Boon Dox	ND	4/24/14 13:49/21:49	FFGS	4/24/14 13:49/21:49	FFGS	ND
4/19/14 06:01/14:01	Unknown	4/19/14 09:21/17:21	Boon Dox	ND	4/24/14 13:41/21:41	SAA 2	4/24/14 14:47/22:47	Boon Dox	4199
4/19/14 12:20/20:20	Sac. Downstream	4/19/14 12:21/20:21	Unknown	ND	4/24/14 13:57/21:57	SAA 2	4/24/14 14:47/22:47	Boon Dox	ND
4/19/14 12:06/20:06	Sac. Upstream	4/19/14 13:37/21:37	Boon Dox	ND	4/24/14 14:02/22:02	SAA 2	4/24/14 14:47/22:47	Boon Dox	ND
4/21/14 06:00/14:00	Unknown	4/21/14 06:39/14:39	Boon Dox	ND					

Note: Sac. Downstream/Upstream = Sacramento River downstream or upstream from the study area; Geo. Sl. = Georgiana Slough; ND = not determined

Micropterus spp. tag code # 3947 was noteworthy in demonstrating strong and rapid homing behavior to the same location in Rip Rap 1. Following initial capture in Rip Rap 1 on April 21, the fish was tagged and released from Dock 3 (i.e., Boon Dox) at 10:29 a.m. PST (6:29 p.m. UTC); the fish had returned to Rip Rap 1 and an apparent territory that it generally occupied by around 11:03 a.m. PST (7:03 p.m. UTC) the same day, during its first liberty period (**Figure 3.6-26**). The fish was recaptured in Rip Rap 1 the following day, April 22, at 9:55 a.m. PST (5:55 p.m. UTC). It was released from Dock 3 (Boon Dox) at 11:11 a.m. PST (7:11 p.m. UTC) the same day. Similar to the first release, it rapidly returned to its apparent territory in Rip Rap 1 by around 11:44 p.m. PST (7:44 p.m. UTC) of its second liberty period, and it remained in the study area until May 6. On both occasions, the fish took around 30 minutes to return to its apparent territory. The straight line distance between release location and apparent territory was ~300 m (~1,000 ft).

3.6.6 ACTIVE HYDROACOUSTICS (HYPOTHESES H7 AND H10)

MAIN FINDINGS

The main findings for active hydroacoustics and predatory fishes are:

- The density of predatory fishes in the FFGS footprint at the middle of the FFGS and just downstream of the FFGS was not significantly different between FFGS On and FFGS Off;
- In contrast, the density of predatory fishes in the FFGS footprint at the downstream end of the FFGS was significantly greater with FFGS On than FFGS Off;
- The density of predatory fishes was significantly greater nearer the FFGS than farther away; and
- The proportion of predatory fishes in the FFGS footprint did not differ between FFGS On and FFGS Off.

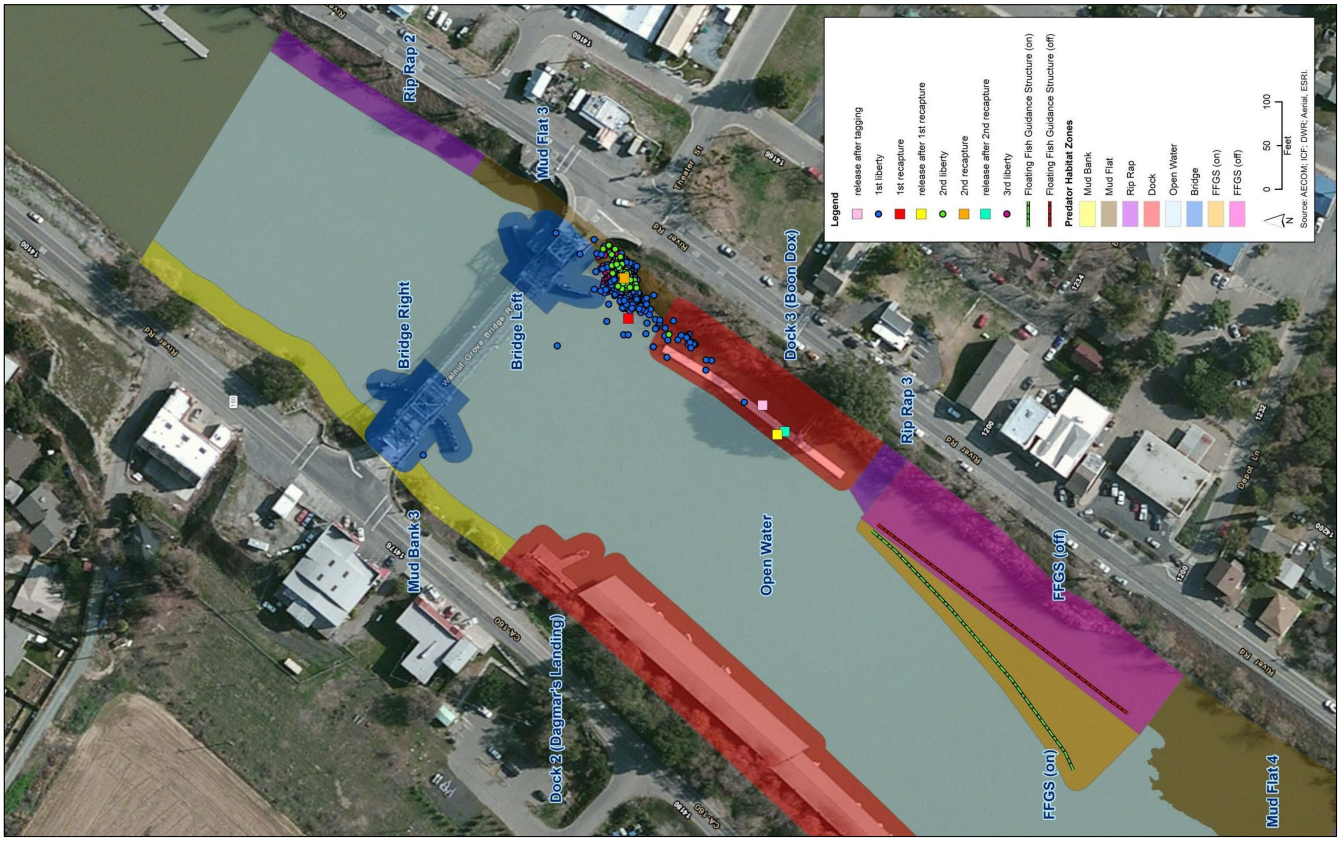

Note: The fish originally was caught from Dock 3 (Boon Dox). Points show detections every 2 hours during each liberty period, in addition to capture and release locations.

Figure 3.6-25 Detections of *Micropterus* spp. Tag # 4199

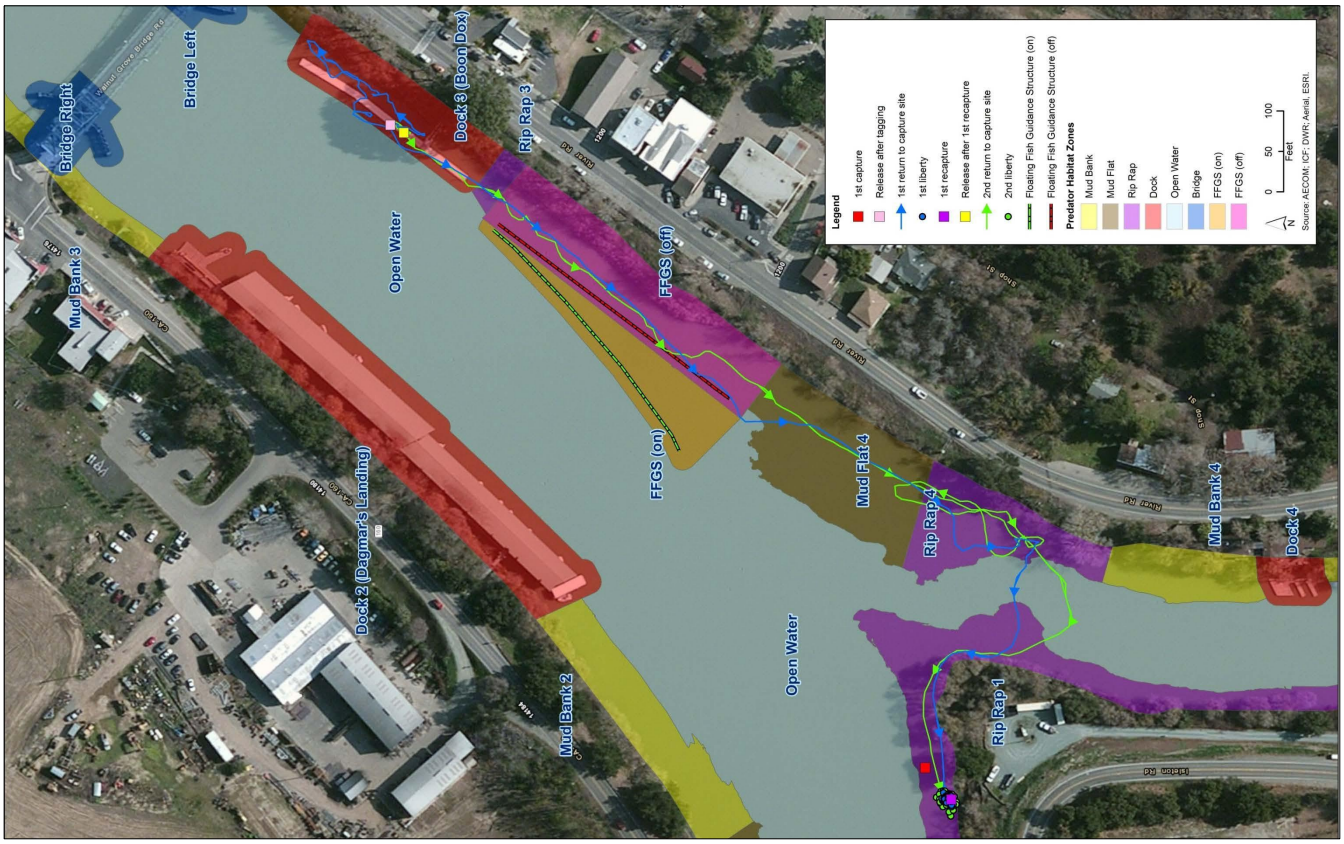

Note: Lines and arrows show return tracks to an apparent territory after release. Points show detections every 2 hours in the apparent territory.

Figure 3.6-26 Detections of *Micropterus* spp. Tag # 3947

OBJECTIVES

Acoustic tagging, as used for testing Hypotheses H8, H11, and H12, is extremely useful in describing fish movement patterns around the FFGS, but the results are limited by: 1) the number of fish that were tagged; 2) fish leaving the study area (or at least the study area near the FFGS); and 3) the fact that tagging does not generate an estimate of potential predator density. Active hydroacoustics overcomes these issues, although this method generally does not allow individual fish to be identified; in addition, this approach assumes that most sufficiently large targets detected by the equipment are predatory fishes, although it is likely that large non- predatory fishes such as common carp (*Cyprinus carpio*) and American shad (*Alosa sapidissima*) occur in the study area. Active hydroacoustics provided a complementary approach to acoustic tagging and standardized angling, which aimed to provide useful information on predatory fish distribution in relation to the FFGS. The two active hydroacoustics methods used in the 2014 FFGS Study were split-beam transducers and Dual-Frequency Identification Sonar (DIDSON).

The objective of the active hydroacoustics component of the 2014 FFGS Study was to assess whether the physical structure of the FFGS and its effect on study area hydrodynamics results in changes in predatory fish density and the proportion of predatory fish density near the FFGS (e.g., by providing structure for ambushing prey or resting near the structure, or by changing the hydrodynamics of the study area so that changes in predator behavior are evident further from the FFGS). Specifically, the active hydroacoustics study provided the data to test Hypothesis H7 (i.e., the density of predatory fish in the vicinity of the FFGS footprint is greater with the FFGS On than with the FFGS Off) and Hypothesis H10 (i.e., the proportion of predatory fish in the study area that is in the vicinity of the FFGS footprint is greater with the FFGS On than with FFGS Off).

METHODS

Field Methods and Data Processing

Split-Beam Transducers

All split-beam acoustic data were collected using two fixed Biosonics® DT-X Digital Scientific Portable Echosounders operating at either 200 or 420 kHz, depending on the location. One transducer was just downstream from the FFGS on the left bank (Walnut Grove side) of the Sacramento River and is hereafter referred to as the Walnut transducer (**Figure 3.6-27**). The other transducer was approximately midway down Dagmar's Landing on the right bank of the Sacramento River across from the FFGS ad is hereafter referred to as the Dagmar's transducer (**Figure 3.6-27**). The transducers were angled generally to be perpendicular to typical river flow, with the Walnut transducer pointed towards the opposite bank, perpendicular to the shore, and the Dagmar's transducer pointed slightly upstream. The Dagmar's transducer was suspended on a metal pipe hanger about 1.5 m (5 ft) below the surface and was pitched down at 1.5 to 2.5°, depending on river discharges. The transducer beam was 7° and had a maximum effective range of 55 m (180 ft) (**Figure 3.6-27**), beyond which the rising river bank on the far shore, and buoy and guy lines associated with the FFGS interfered with the beam. The Walnut transducer was fixed to a metal tripod, set on the river bottom in about 3 m (10 ft) of water. The transducer itself was about 0.3 m (1 ft) off the bottom and was pitched at varying angles upward or downward, depending on river depth. The transducer beam angle was 6.5° and had a maximum effective range of 30 m (98 ft) (**Figure 3.6-27)** before barrier anchors and pilings interfered with the beam.

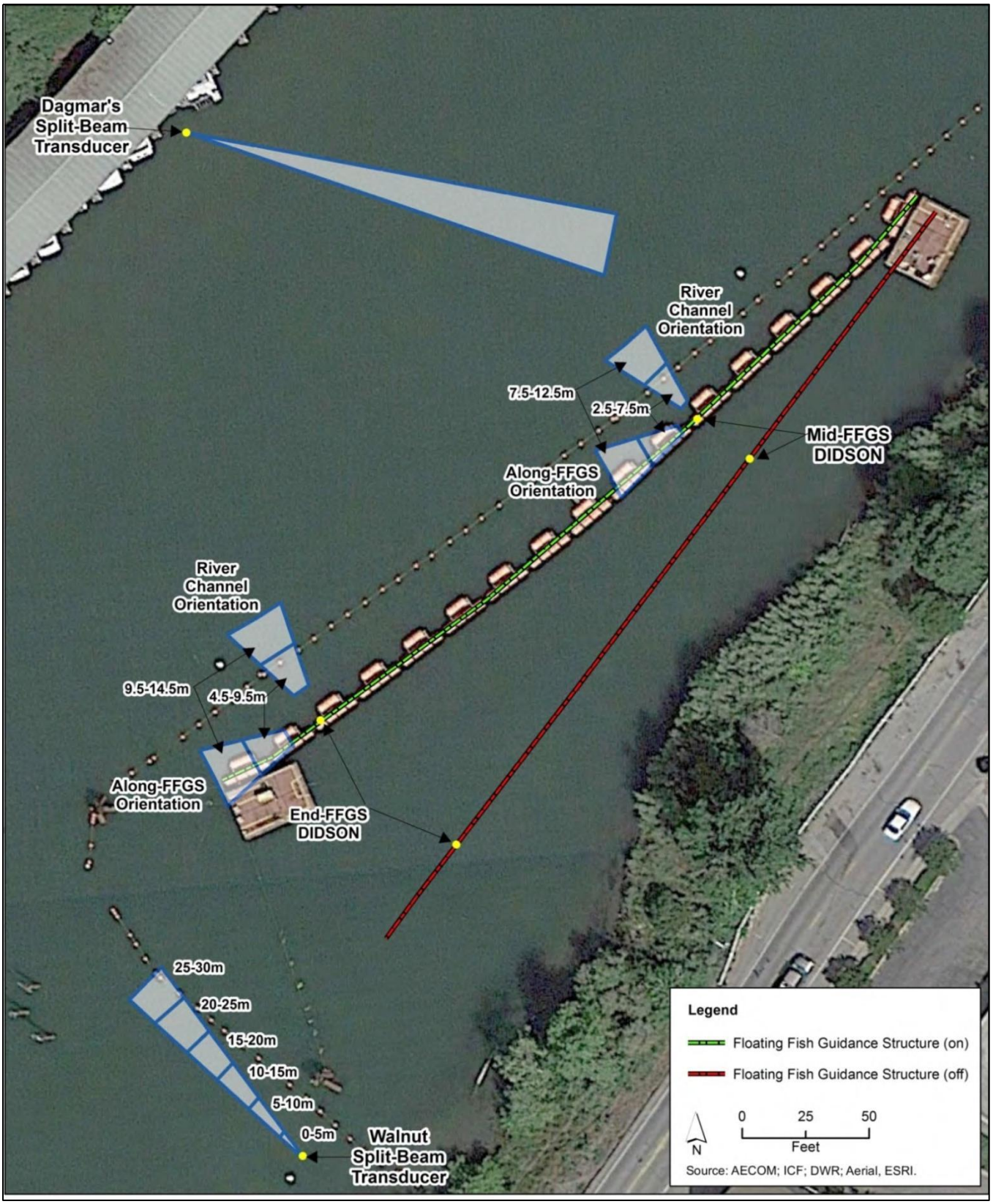

Note: Split-beam transducer sampling coverage is georeferenced, whereas DIDSON sampling coverage is approximate. Sampling ranges are indicated for the Walnut transducer and the DIDSON units.

Figure 3.6-27 Location of Active Hydroacoustics Units

The Walnut transducer was operated from March 11 to April 24, whereas operation of the Dagmar's transducer started on March 10 and stopped on April 16. All data were collected using BioSonics Visual Acquisition Software, version 6 (BioSonics, Inc., Seattle, WA). Electrical power failures associated with the Walnut transducer resulted in periods of non-operation, principally in March. Data were recorded as a new file every 30 minutes, to minimize potential for data loss during a system failure; collection thresholds were set at -75 decibels (dB), 5 pings per second (pps), and a 0.4-millisecond (ms) pulse width. Data were downloaded at least once a week. Further details of the steps employed in processing the split-beam transducer data are provided in **Appendix A**.

DIDSON

DIDSON data were collected and analyzed using similar techniques to the split-beam transducer, with some differences related to the type of data collected. Unlike the split-beam transducers, the DIDSON sonar is a multibeam unit employing up to 96 beams (when run in high-frequency mode, as in the present study), with each beam having an angle of 0.3° in the horizontal and 14° in the vertical, producing an overall 29° by 14° beam. Although the DIDSON sonar does have a vertical component to the beam, the data obtained with the vertical component are not available for multibeam analysis. For this reason, all data output is 2D (range and left-right positioning in the beam). It is possible, however, to account for the volume sampled within different ranges from the DIDSON unit (Johnson et al. 2013; see "Data Analysis" section).

Two DIDSON units were used in the study, one mounted approximately 37 m (121 ft) from the upstream end of the FFGS (hereafter referred to as the mid-FFGS DIDSON) and the other mounted approximately 14 m (46 ft) from the downstream end of the DIDSON (hereafter referred to as the end-FFGS DIDSON) (**Figure 3.6-27**). Both DIDSON units were mounted approximately 1.8 to 2.2 m (5.9-7.2 ft) below the water surface and were attached to the crossbars linking the smaller boatbusters (flotation devices). The DIDSON units were operated in high-resolution mode and were set to provide data outputs every 30 minutes. The mid-FFGS DIDSON sampled 2.5 to 12.5 m (8.2-41.0 ft) from the unit, whereas the end-FFGS DIDSON sampled 4.5 to 14.5 m (14.8-47.6 ft) from the unit. Different sampling ranges were used for each unit because of differences in how each unit operated. The mid-FFGS DIDSON is a first generation unit and had trouble maintaining a consistent data stream when the range was extended. After the study, an internal electrical problem was noted with the unit, which may have produced this result.

The mid-FFGS DIDSON was operated from March 12 to April 22, and was oriented either perpendicular to the FFGS (i.e., pointing into the river channel) or along the FFGS in a downstream direction, to examine predatory fish density along, near, and further from the FFGS (**Table 3.6-15**; see also **Figure 3.6-27**). The mid-FFGS DIDSON was tilted so that it sampled different portions of the water column. Initially, it sampled primarily in the upper water column (termed "upper") and was tilted down sufficiently to avoid water surface reflections (**Figure 3.6-28**), with the underside of the FFGS visible toward the end of the sampled range when oriented along the FFGS (**Figure 3.6-29**). Between March 24 and 31, the unit was angled further downward (termed "middle") so that the river bed was visible with the FFGS Off (**Figure 3.6-30**) but not with the FFGS On. From March 31 to April 3, the unit was angled downward further (termed "lower") so that the river bed was visible with the FFGS On (**Figure 3.6-31**), although this meant that with the FFGS Off, no usable data could be collected because the DIDSON was viewing the rocky substrate from close up and the images were unclear. For the remainder of the deployment, from April 3 to 22, the mid-FFGS DIDSON again was set in the upper position. The tilt and orientation of both DIDSON units could be described only qualitatively because neither unit nor their attached

rotators were equipped with heading, pitch, and roll sensors to allow tilt and orientation to be measured accurately.

Table 3.6-15 Summary of Positions of Mid-FFGS DIDSON during the 2014 Study

Start (PST/UTC)	End (PST/UTC)	Orientation	Horizontal Tilt	Notes
3/12/14 15:43/23:43	3/22/14 08:52/16:52	River channel	Upper	Perpendicular to FFGS, viewing open water (**Figure 3.6-29**).
3/22/14 08:52/16:52	3/24/14 09:25/17:25	Along FFGS	Upper	Bottom of FFGS visible (**Figure 3.6-30**).
3/24/14 09:25/17:25	3/31/14 16:10 / 4/1/14 00:10	Along FFGS	Middle	River bed visible with FFGS Off (**Figure 3.6-31**).
3/31/14 16:10 / 4/1/14 00:10	4/3/14 09:14/17:14	Along FFGS	Lower	River bed visible with FFGS On (**Figure 3.6-32**).
4/3/14 09:14/17:14	4/8/14 08:44/16:44	River channel	Upper	Similar to 3/12-3/22 and 4/10-4/22 (**Figure 3.6-29**).
4/8/14 08:44/16:44	4/10/2014 17:22 / 4/11/2015 01:22	Along FFGS	Upper	Similar to 3/22-3/24 (**Figure 3.6-30**).
4/10/2014 17:22 / 4/11/2015 01:22	4/22/2014 08:00/16:00	River channel	Upper	Similar to 3/12-3/22 and 4/3-4/8 (**Figure 3.6-31**).

The end-FFGS DIDSON was operated from March 12 to April 25; however, a data processing malfunction meant that reliable data collection ended on April 15 (**Table 3.6-16**). The end-FFGS DIDSON generally was oriented along the FFGS in the upper position, with its beam reaching close to the end of the FFGS (**Figure 3.6-27**). Between March 12 and 21, images show that with the FFGS On, the DIDSON viewed a greater portion of the FFGS than with the FFGS Off, because of the curvature of the FFGS when on (**Figure 3.6-32** and **Figure 3.6-33**; see also **Figure 3.6-27**). The unit also was used to assess predatory fish density beneath the barge, behind and near the end of the FFGS between March 21 and 22 (**Figure 3.6-34**). Between March 22 and 24, the unit was tilted into the lower position so that the river bed was visible for both the FFGS On and FFGS Off treatments (**Figure 3.6-35 and Figure 3.6-36**). Between March 24 and 27, the end-FFGS DIDSON was oriented perpendicular to the FFGS and observed the river channel (**Figure 3.6-37**). Between March 29 and 31, the DIDSON was oriented back along the barrier, with a slightly deeper upper position than previously. As occurred during other dates with the DIDSON oriented along the barrier, DIDSON images from these dates show that the slight curve near the end of the FFGS On treatment resulted in a greater extent of the FFGS being visible (e.g., flotation units; **Figure 3.6-39**). In contrast, with the FFGS Off, the FFGS was straighter, so that only a small portion of the FFGS was visible (**Figure 3.6-37**). Between March 31 and April 7, the end-FFGS DIDSON was oriented and tilted similar to the March 12 to 21 period (**Figure 3.6-33** and **Figure 3.6-34**). Between April 10 and 15, the DIDSON was pointed slightly closer to the surface than previously (**Figure 3.6-41** and **Figure 3.6-42**). Excessive noise and data processing issues necessitated data deletion between March 27 and 29 (the DIDSON tilted too close to the surface) and between April 4 and 10 (with the DIDSON oriented under the barge) (**Table 3.6-16**).

Acoustic processing of DIDSON data included a number of steps, which are described in detail in **Appendix A**. DIDSON fish tracks were exported as time-stamped variables for further analyses.

Table 3.6-16 Summary of Positions of End-FFGS DIDSON during the 2014 Study				
Start (PST/UTC)	**End (PST/UTC)**	**Orientation**	**Horizontal Tilt**	**Notes**
3/12/14 16:41 / 4/12/14 00:41	3/21/14 07:17/15:17	Along FFGS	Upper	Bottom of FFGS visible (**Figure 3.6-33** and **Figure 3.6-34**).
3/21/14 07:17/15:17	3/22/14 08:54/16:54	Behind FFGS	Upper	Underneath barge (**Figure 3.6-35**).
3/22/14 08:54/16:54	3/24/14 09:19/17:19	Along FFGS	Lower	River bed visible with FFGS On and Off (**Figure 3.6-36** and **Figure 3.6-37**).
3/24/14 09:19/17:19	3/27/14 08:44/16:44	River channel	Upper	Perpendicular to FFGS/buoy line, viewing open water (**Figure 3.6-38)**.
3/27/14 08:44/16:44	3/29/14 05:43/13:43	Along FFGS	Upper	Data deleted because of excessive noise (too close to surface)
3/29/14 05:43/13:43	3/31/14 13:19/21:19	Along FFGS	Upper	Similar to 3/12-3/21 but slightly deeper (**Figure 3.6-39** and **Figure 3.6-40**).
3/31/14 13:19/21:19	4/7/14 10:00/18:00	Along FFGS	Upper	Similar to 3/12-3/21 (**Figure 3.6-33** and **Figure 3.6-34**).
4/7/14 10:00/18:00	4/10/2014 17:20 / 4/11/2014 01:20	Along/behind FFGS	Upper	Data deleted because of processing issues and noise when oriented underneath the barge
4/10/2014 17:20 / 4/11/2014 01:20	4/15/2014 05:30/13:30	Along FFGS	Upper	Similar to 3/12-3/21 and 3/29-4/7, but oriented slightly closer to the surface (**Figure 3.6-41** and **Figure 3.6-42**).

Data Analysis

Split-Beam Transducers

Processed data were output in 10-minute files for each 5-m (16-ft) range ensonified by the Walnut and Dagmar's transducers. Data from both transducers were filtered to include only acoustic targets estimated to be 30 to 100-cm (12-39 in) TL, which were assumed to be potential predatory fish of most relevance to juvenile salmonids[25]. The density (number of predatory fish per 1,000 cubic m [35,315 cubic ft) in each 5-m (16-ft) range was calculated. Rejection of larger targets also reduced the difficulties associated with multiple closely associated fish (i.e., tightly swimming schools) being tracked by the software as single, very large fish.

Data from the Walnut transducer were used to test Hypothesis H7. The overall sampling period was divided into three periods of approximately equal length in order to assess whether any observed patterns were consistent over time: March 11 to 26, March 26 to April 9, and April 9 to 24. Each 10-minute sample was matched to the FFGS treatment that occurred during the sample (FFGS On or FFGS Off); transitional samples when the FFGS was being moved were excluded from analysis. A total of nearly 4,800 samples were available for analysis (**Table 3.6-17**), with each sample consisting of a predatory fish density estimate in each of the six 5-m (16-ft) ranges ensonified by the transducer. The location of the Walnut transducer in relation to the FFGS was such that it was reasoned with the FFGS Off, the 0-5-m (16-ft) and 5-10-m (16-33 ft) ranges could have been within the FFGS

[25] Fish greater than 100 cm would have had a greater chance of being non-predatory species, such as sturgeon, whereas fish less than 30 cm would have been less likely to have sufficiently wide gape to prey on juvenile salmonids.

footprint (**Figure 3.6-27**) (i.e., affected by changes in hydrodynamics caused by the FFGS being On or Off[26]); in contrast, with the FFGS On, all 5-m (16-ft) ranges from the Walnut transducer could have been within the FFGS footprint if downstream river flow and velocity were affected by the FFGS position.

As with other analyses of predatory fishes, Hypothesis H7 was tested by resampling (bootstrapping) to produce statistical summaries of the data. Hypothesis H7 was accepted if predatory fish density in the outermost ranges (i.e., 15 to 20 m [49-66 ft], 20 to 25 m [66-82 ft], and 25 to 30 m [82-98 ft]) was significantly greater with the FFGS On than with the FFGS Off (i.e., bootstrapped 95 percent confidence intervals did not overlap), and no significant difference occurred in density between treatments (FFGS On/Off) for the innermost ranges (0 to 5 m [0-16 ft] and 5 to 10 m [16-33 ft]). The data for the 10 to 15-m (33-49 ft) range were not included in the hypothesis test because this range was aligned directly with the FFGS's downstream end when the FFGS was Off.

Table 3.6-17 Number of Samples Included in Split-Beam Transducer Analyses

Hypothesis H7 (Walnut Only)			Hypothesis H10 (Walnut + Dagmar's)		
Dates	**Treatment**	**No. of Samples**	**Dates**	**Treatment**	**No. of Samples**
3/11/14–3/26/14	FFGS Off	608	3/11/14–3/26/14	FFGS Off	600
	FFGS On	565		FFGS On	560
3/26/14–4/9/14	FFGS Off	674	3/26/14–4/9/14	FFGS Off	635
	FFGS On	821		FFGS On	695
4/9/14–4/24/14	FFGS Off	1,079	4/9/14–4/16/14	FFGS Off	317
	FFGS On	1,039		FFGS On	400
Total		4,786	Total		3,207
Note: Each sample is 10 minutes and consists of data in each of six 5-m ranges.			Note: Each sample is 10 minutes and consists of data averaged across the 5-m ranges from each transducer.		

Data from the Walnut and Dagmar's transducers were used to test Hypothesis H10. The Walnut sampling data used to test H7 were averaged across the six 5-m (16-ft) ranges to give an overall mean density in each sample. These data were paired with the Dagmar's samples taken during the same 10-minute intervals, with the Dagmar's data also having been processed to give a mean density (across the eleven 5-m [16-ft] ranges from 0 to 55 m [0-180 ft] away from the transducer). An index of the relative predatory fish density in each paired sample was calculated as Walnut density ÷ (Walnut density + Dagmar's density). This index was taken to represent the proportion of predatory fishes in the vicinity of the FFGS footprint, under the assumption that the Walnut density represented the vicinity of the FFGS footprint because of its position downstream from the FFGS (and therefore potentially being influenced by hydrodynamic changes caused by the FFGS being On or Off), and the Dagmar's density was assumed to represent a reference proportion that was not influenced by the FFGS.

As with Hypothesis H7, resampling (bootstrapping) was used to produce statistical summaries of the data. Hypothesis H10 was accepted if the index of relative density was significantly greater (non-overlapping 95 percent confidence intervals) with the FFGS On than with the FFGS Off, which would indicate that the density at the Walnut transducer had increased relative to the density at the Dagmar's transducer. The same three sampling periods were used as for testing H7, except the third sampling period ended on April 16, coincident with the cessation of the Dagmar's sampling. This resulted in just over 3,200 samples for analysis (**Table 3.6-17**).

[26] This reasoning was made prior to the examination of the effects of the FFGS on velocity fields in the study area; see Section 3.3, "Hydrodynamics and Critical Streakline."

DIDSON

Processed DIDSON data were output in 30-minute files and were used to test Hypothesis H7. Consistent with the analysis of the split-beam transducers, data from both DIDSON units were filtered to include only acoustic targets estimated to be 30 to 100-cm (12-39 in) TL, which were assumed to be potential predatory fishes. Length was based on the maximum length estimated for the targets observed in each individual fish track. The approximate volume ensonified by the DIDSON units was calculated for two 5-m (16-ft) ranges near to and farther from the units. For the mid-FFGS DIDSON, the ranges were 2.5 to 7.5 m (8.2-24.6 ft) (near) and 7.5 to 12.5 m (24.6-41.0) (far), whereas for the end-FFGS, the ranges were 4.5 to 9.5 m (14.8-31.2 ft) and 9.5 to 14.5 m (31.2-47.6 ft). Sampling volumes within each range were estimated from the formula of Johnson et al. (2013):

$$\text{Volume} = (\frac{1}{3}\text{H})(\text{AB} + \sqrt{\text{ABCD}} + \text{CD}) ,$$

where H = range depth (range depth (i.e., 5 m [16 ft], the horizontal distance from the start of the range to the end of the range, aligned with the center of the DIDSON beam);
A = width at the near end of the range;
B = height at the near end of the range;
C = width at the far end of the range; and
D = height at the far end of the range.

Values for A, B, C, and D were calculated based on the known angles of isosceles triangles that estimated the horizontal and vertical spread of the DIDSON beams (i.e., for the vertical: 14°, 83°, and 83°; for the horizontal, 29°, 75.5°, and 75.5°) and the distances to the start and end points of the different ranges. Thus, it was estimated that the approximate volumes sampled ranged from 17.2 cubic m (607.4 cubic ft) (Mid-FFGS DIDSON, 2.5 to 7.5-m [8.2-24.6 ft] range) to 92.77 cubic m (3276.1 cubic ft) (End-FFGS DIDSON, 9.5 to 14.5-m [31.2-47.6 ft] range) (**Table 3.6-18**).

Table 3.6-18 Estimates of DIDSON Sampling Volume

DIDSON Location	Range (m)	A (m)	B (m)	C (m)	D (m)	Volume (m3)
Mid-FFGS	2.5–7.5	1.29	0.61	3.88	1.84	17.20
	7.5–12.5	3.88	1.84	6.50	3.07	64.83
End-FFGS	4.5–9.5	2.33	1.10	4.91	2.33	32.44
	9.5–14.5	4.91	2.33	7.50	3.56	92.77

The density (number of predatory fish per 10 cubic m [353 cubic ft]) in each 5-m (16-ft) range during each 30-minute period was calculated. In total, just over 1,700 samples were analyzed for the Mid-FFGS DIDSON and just over 1,000 for the End-FFGS DIDSON (**Table 3.6-19**). As with the split-beam transducer analyses, Hypothesis H7 was tested by resampling (bootstrapping) to produce statistical summaries of the data, with analyses conducted for each position of the DIDSON relative to the FFGS (see **Table 3.6-15**). When the DIDSON was oriented into the river channel or along the FFGS but not in the upper position, Hypothesis H7 was accepted if predatory fish density near the FFGS (i.e., in the 2.5 to 7.5-m (8.2-24.6 ft) range for the mid-FFGS DIDSON or in the 4.5 to 9.5-m (14.8-31.2 ft) range for the end-FFGS DIDSON) was significantly greater with the FFGS On than with the FFGS Off (i.e., bootstrapped 95 percent confidence intervals did not overlap), and no difference was observed in density farther from the DIDSON (i.e., in the 7.5 to 12.5-m [24.6-41.0] range for the mid-FFGS

DIDSON and 9.5 to 14.5-m [31.2-47.6 ft] range for the end-FFGS DIDSON). When the DIDSON was oriented along or behind the FFGS and in the upper position, Hypothesis H7 was accepted if predatory fish density was significantly greater with the FFGS On than with the FFGS Off.

Table 3.6-19 Number of Samples Included in DIDSON Analyses

Mid-FFGS			End-FFGS		
Dates	**Treatment**	**No. of Samples**	**Dates**	**Treatment**	**No. of Samples**
3/12/14–3/22/14	FFGS Off	191	3/12/14–3/21/14	FFGS Off	138
	FFGS On	164		FFGS On	130
3/22/14–3/24/14	FFGS Off	29	3/21/14–3/22/14	FFGS Off	18
	FFGS On	35		FFGS On	30
3/24/14–3/31/14	FFGS Off	177	3/22/14–3/24/14	FFGS Off	29
	FFGS On	157		FFGS On	22
3/31/14–4/3/14	FFGS Off	NA	3/24/14–3/27/14	FFGS Off	46
	FFGS On	80		FFGS On	44
4/3/14–4/8/14	FFGS Off	132	3/29/14–3/31/14	FFGS Off	49
	FFGS On	98		FFGS On	58
4/8/14–4/10/14	FFGS Off	56	3/31/14–4/7/14	FFGS Off	140
	FFGS On	49		FFGS On	139
4/10/14–4/22/14	FFGS Off	254	4/10/14–4/15/14	FFGS Off	96
	FFGS On	288		FFGS On	113
Total		1,710	Total		1,052

Note: Each sample is 30 minutes and consists of data in the 2.5 to 7.5-m and 7.5 to 12.5-m ranges (mid-FFGS DIDSON) or 4.5 to 9.5-m and 9.5 to 14.5-m ranges (end-FFGS DIDSON). NA indicates data not available because river bed was in close proximity to DIDSON beam and precluded clear images.

RESULTS

Split-Beam Transducers

The density of predatory fishes was greatest in the innermost 5-m (16 ft) ranges and generally decreased with distance from the Walnut transducer (**Figure 3.6-42**, **Figure 3.6-43**, and **Figure 3.6-44**). No significant difference

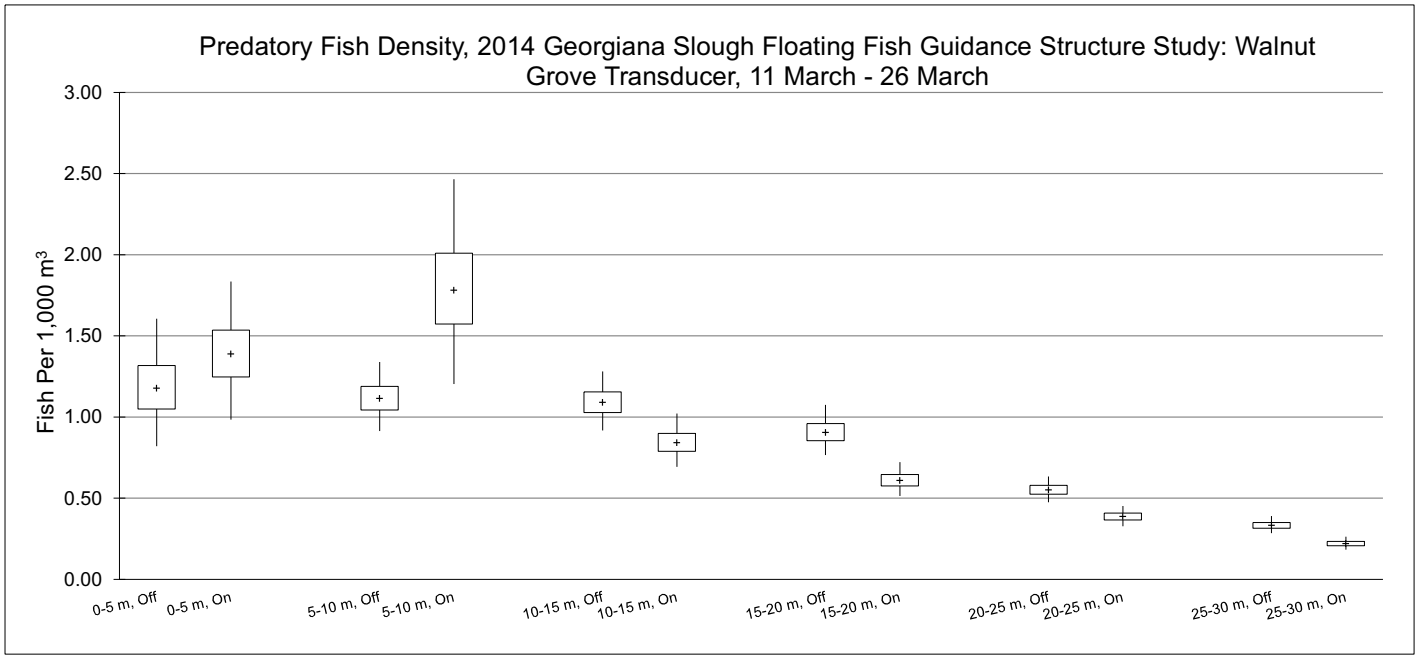

Note: Boxplots represent bootstrapped mean (+), interquartile range (box), and 95 percent confidence interval (whiskers). For each distance range, n = 608 samples with FFGS Off and 565 samples with FFGS On.

Figure 3.6-42 Predatory Fish Density Estimated by the Walnut Grove Split-Beam Transducer, March 11 to 26, 2014

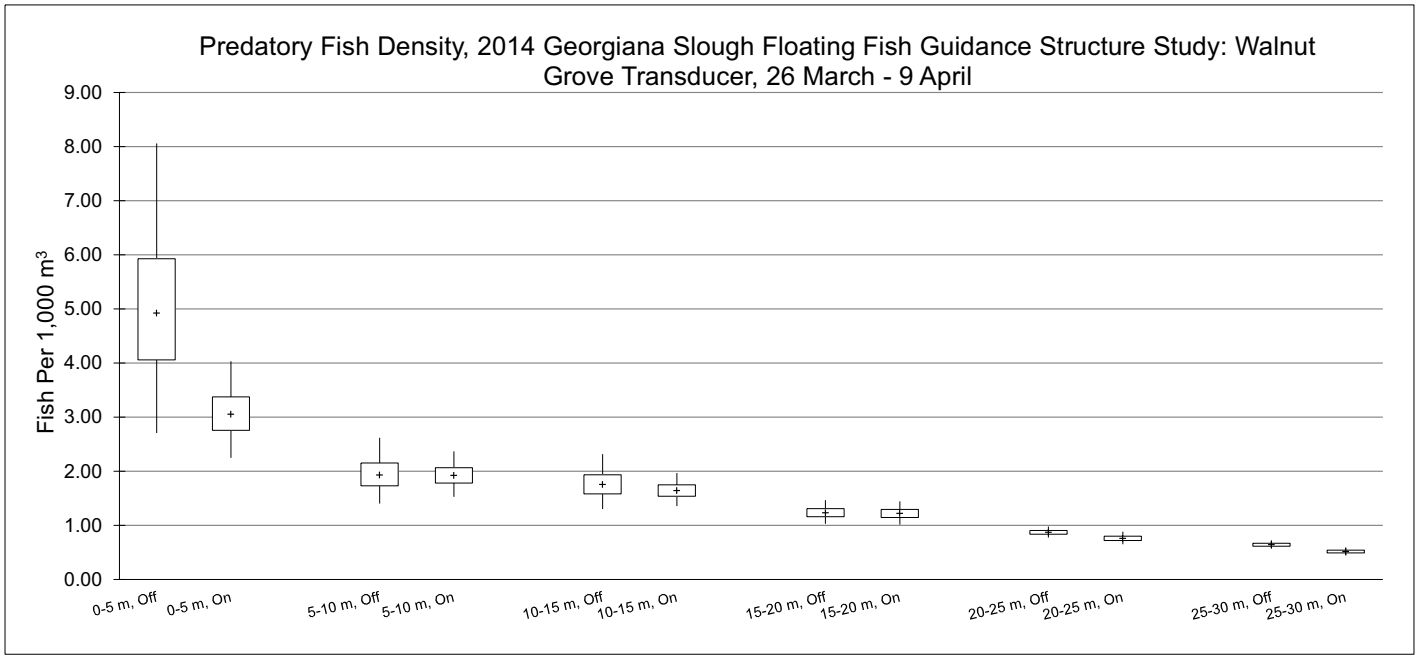

Note: Boxplots represent bootstrapped mean (+), interquartile range (box), and 95 percent confidence interval (whiskers). For each distance range, n = 674 samples with FFGS Off and 821 samples with FFGS On.

Figure 3.6-43 Predatory Fish Density Estimated by the Walnut Grove Split-Beam Transducer, March 26 to April 9, 2014

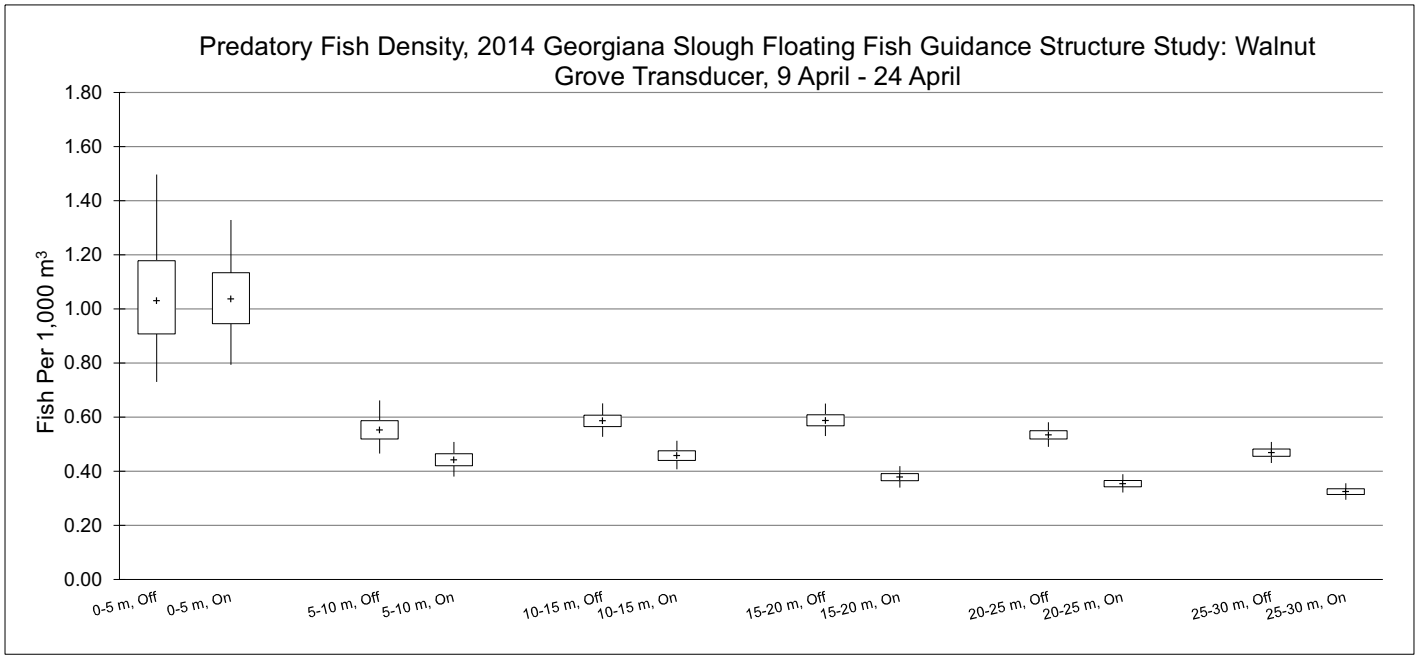

Note: Boxplots represent bootstrapped mean (+), interquartile range (box), and 95 percent confidence interval (whiskers). For each distance range, n = 1.079 samples with FFGS Off and 1,039 samples with FFGS On.

Figure 3.6-44 Predatory Fish Density Estimated by the Walnut Grove Split-Beam Transducer, April 9 to 24, 2014

occurred in density between the FFGS On and the FFGS Off in the innermost (0 to 5-m [0-16 ft] and 5 to 10-m [16-33 ft]) ranges during any of the three analysis periods. In contrast, and contrary to Hypothesis H7, density was significantly greater with the FFGS Off than with the FFGS On between March 11 and 26 and between April 9 and 24 in the outermost (15 to 20-m [49-66 ft], 20 to 25-m [66-82 ft], and 25 to 30-m [82-98 ft]) ranges; no significant differences occurred between March 26 and April 9 in these ranges. Therefore, Hypothesis H7 was rejected.

The index of the relative predatory fish density expressed as Walnut density ÷ (Walnut density + Dagmar's density) generally was in the range of 0.5 to 0.65 (**Figure 3.6-45**), indicating that the density estimated by the Walnut transducer generally was similar to or greater than the density estimated by the Dagmar's transducer. The index was not significantly different between the FFGS Off and the FFGS On between March 26 and April 9 and between April 9 and April 16, whereas between March 11 and March 26, the index was significantly greater with the FFGS Off (**Figure 3.6-45**), contrary to Hypothesis H10. Therefore, Hypothesis H10 was rejected.

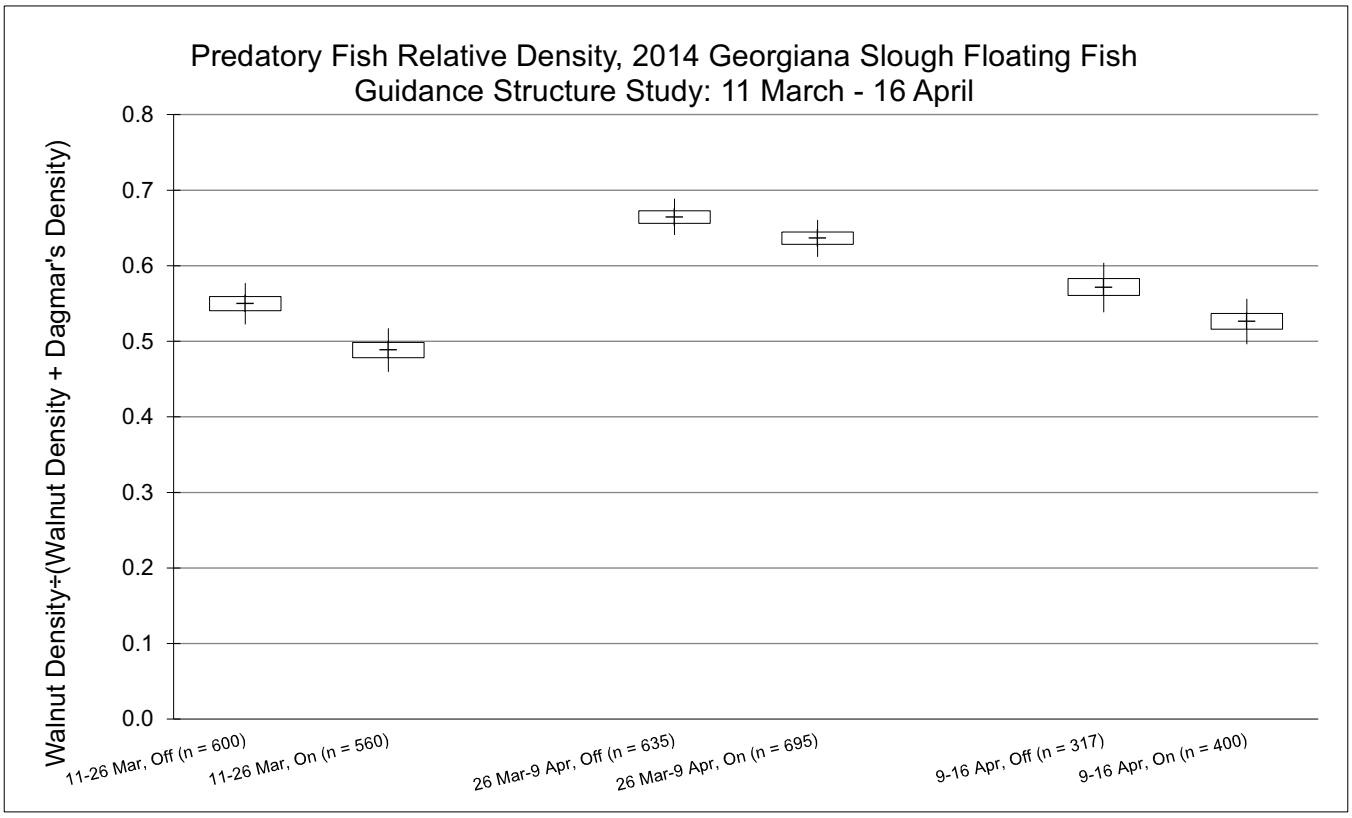

Note: Boxplots represent bootstrapped mean (+), interquartile range (box), and 95 percent confidence interval (whiskers).

Figure 3.6-45 Index of Relative Predatory Fish Density from Split-Beam Transducers, March 11 to April 16, 2014

DIDSON

Mid-FFGS

Just over 37,000 targets (potential predatory fishes 30 to 100-cm [12-39 in] TL) were detected with the mid-FFGS DIDSON between March 3 and April 22 (**Table 3.6-20**). The mean length by sampling date ranged from around 40 to 55 cm (15.7-21.6 in) TL.

Table 3.6-20 Summary of Targets (Fish) Detected with the Mid-FFGS DIDSON						
Date	FFGS Treatment	Range (m)	Number (n)	Min. Length (cm)	Max. Length (cm)	Mean Length (cm)
3-22 March	Off	2.5–7.5	892	30.1	98.4	44.5
		7.5–12.5	1,229	30.0	99.2	43.9
	On	2.5–7.5	887	30.0	99.9	48.8
		7.5–12.5	1,202	30.0	99.8	45.3
22-24 March	Off	2.5–7.5	22	31.1	76.9	44.8
		7.5–12.5	65	30.5	73.6	43.2
	On	2.5–7.5	24	32.0	67.6	44.5
		7.5–12.5	26	31.8	68.0	43.5
24-31 March	Off	2.5–7.5	4,524	30.0	100.0	55.1
		7.5–12.5	1,763	30.0	99.7	52.8
	On	2.5–7.5	598	30.1	99.5	50.9
		7.5–12.5	761	30.1	99.0	50.8
31 March-3 April*	On	2.5–7.5	328	30.0	97.2	47.6
		7.5–12.5	177	30.0	79.2	47.0
3-8 April	Off	2.5–7.5	657	30.0	96.0	42.3
		7.5–12.5	485	30.1	95.9	43.3
	On	2.5–7.5	284	30.1	93.0	44.1
		7.5–12.5	246	30.1	82.7	43.8
8-10 April	Off	2.5–7.5	57	30.0	65.1	41.2
		7.5–12.5	60	30.2	85.5	43.3
	On	2.5–7.5	38	31.5	84.5	41.9
		7.5–12.5	32	30.0	72.8	40.1
10-22 April	Off	2.5–7.5	4,400	30.0	100.0	49.4
		7.5–12.5	5,110	30.0	100.0	50.0
	On	2.5–7.5	6,079	30.0	100.0	47.7
		7.5–12.5	7,097	30.0	100.0	49.1

Notes: Data were filtered to include only targets of 30 to 100 cm (12-39 in) TL. Targets may include multiple detections of the same fish on different occasions.

*Data not available for FFGS Off treatment because river bed was in close proximity to DIDSON beam and precluded clear images.

In four of six time periods for which data were available for the FFGS On and the FFGS Off treatments, no significant difference was observed between the FFGS Off and the FFGS On in the density of predatory fishes near (2.5 to 7.5 m [8.2-24.6 ft]) the mid-FFGS; between March 24 and March 31 and between April 3 and April 8, density was significantly greater with the FFGS Off, contrary to Hypothesis H7 (**Figure 3.6-46**). Two significant differences in density occurred between the FFGS Off and the FFGS On farther from the DIDSON (7.5 to 12.5 m [24.6-41.0 ft]): between March 22 and March 24 and between March 24 and March 31, density again was

significantly greater with the FFGS Off than with the FFGS On (although not as pronounced as the difference observed in the 2.5 to 7.5-m [8.2-24.6 ft] range). Therefore, Hypothesis H7 was rejected for the mid-FFGS DIDSON. Estimates of density during periods when the DIDSON beams reached the river bed were likely to be biased low because the sampling volume was limited by the river bed.

Sampling volume was not limited by the river bed when the mid-FFGS DIDSON was in the upper position, so the observations made during times with the DIDSON in the upper position allowed assessment of differences in density of predatory fish near (2.5 to 7.5 m [8.2-24.6 ft]) and farther (7.5 to 12.5 m [24.6-41.0 ft]) from the FFGS. With the DIDSON pointing into the river channel, the density of predatory fish near (2.5 to 7.5 m [8.2-24.6 ft]) the DIDSON always was significantly greater than the density farther (7.5 to 12.5 m [24.6-41.0 ft]) from the DIDSON, regardless of whether the FFGS was On or Off (**Figure 3.6-46**). This same basic pattern generally was true when the DIDSON was pointing along the FFGS (except between March 22 and March 24 with the FFGS off), suggesting that relative differences in density between the 2.5 to 7.5-m (8.2-24.6 ft) and 7.5 to 12.5-m (24.6-41.0 ft) ranges could to some extent have been an artifact of the manner in which density was calculated (i.e., based on the volumetric approximation of Johnson et al. (2013)). To examine this possibility, density data were recalculated on the basis of the approximate areas represented by an isosceles triangle through the beam's midline; for the 2.5 to 7.5-m (8.2-24.6 ft) range, the area was 12.9 square m (138.8 square ft), and for the 7.5 to 12.5-m 24.6-41.0) range, the area was 24.2 square m (260.5 square ft). The area-based density estimates with the mid-FFGS DIDSON in the upper position resulted in fewer significant differences between the 2.5 to 7.5-m (8.2-24.6 ft) and 7.5 to 12.5-m (24.6-41.0 ft) ranges for a given FFGS treatment (**Figure 3.6-47**). With the DIDSON pointing into the river channel, significant differences no longer occurred in density between March 3 and March 22 (the with FFGS On) and between April 10 and April 22 (with the FFGS Off), and the magnitude of differences was lower in all cases. With the DIDSON pointing along the FFGS, no significant differences in density occurred between the 2.5 to 7.5-m (8.2-24.6 ft) and 7.5 to 12.5-m (24.6-41.0 ft) ranges. Overall, this suggested that the density of predatory fishes was somewhat greater nearer the FFGS than farther away from it.

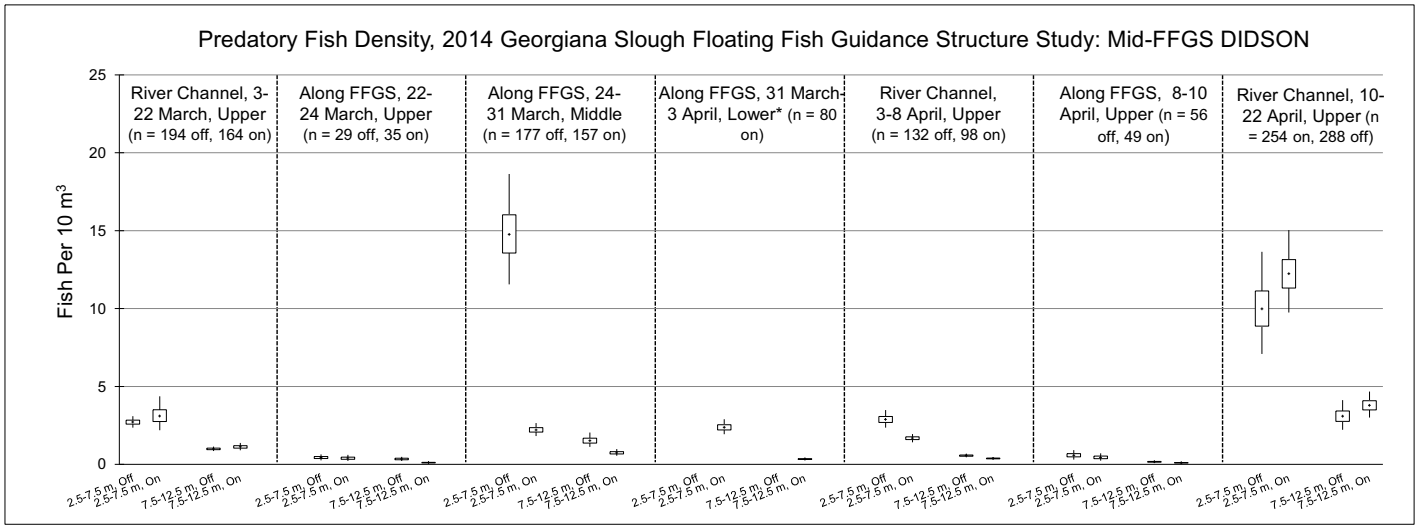

Note: Boxplots represent bootstrapped mean (+), interquartile range (box), and 95 percent confidence interval (whiskers) per 30 minutes of DIDSON sampling time. Labels indicate orientation of DIDSON (river channel = perpendicular to the FFGS; along the FFGS = parallel with the FFGS in downstream direction) and relative tilt of DIDSON unit (upper = sufficiently downward to avoid water surface reflection; middle = sufficiently downward to sample river bed with the FFGS Off; lower = sufficiently downward to sample river bed with the FFGS On and the FFGS Off).*Data not available for the FFGS Off treatment because the river bed was in close proximity to the DIDSON beam and precluded clear images.

Figure 3.6-46 Predatory Fish Volume-Based Density Estimated by Mid-FFGS DIDSON, March 3 to April 22, 2014

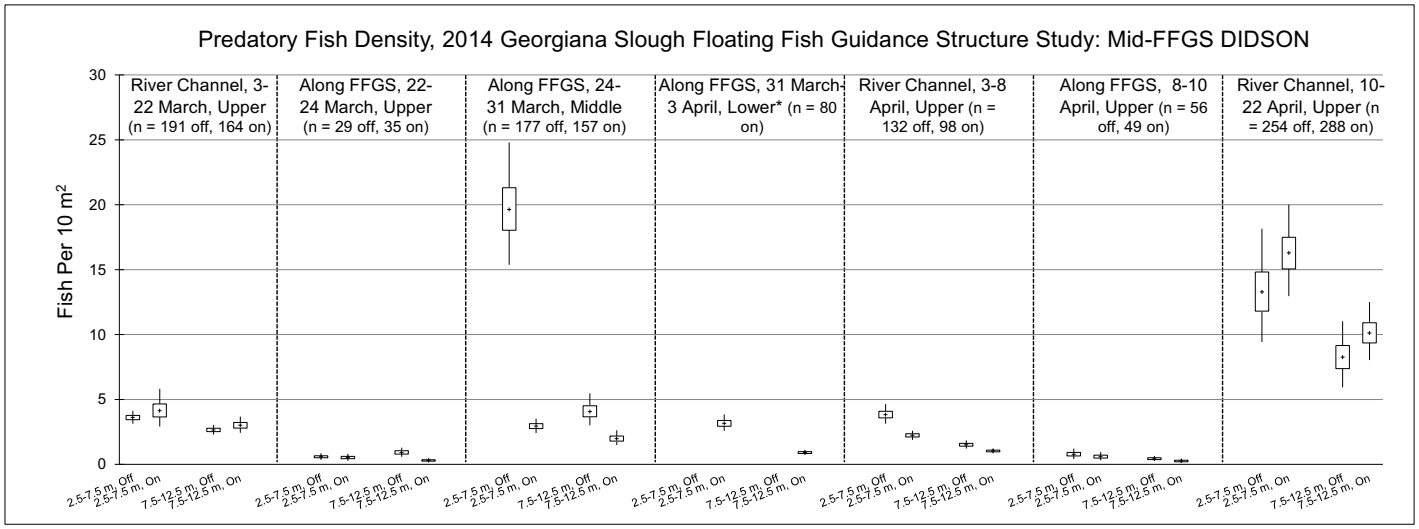

Note: Boxplots represent bootstrapped mean (+), interquartile range (box), and 95 percent confidence interval (whiskers) per 30 minutes of DIDSON sampling time. Labels indicate orientation of DIDSON (river channel = perpendicular to the FFGS; along the FFGS = parallel with the FFGS in downstream direction) and relative tilt of DIDSON unit (upper = sufficiently downward to avoid water surface reflection; middle = sufficiently downward to sample river bed with the FFGS Off; lower = sufficiently downward to sample river bed with the FFGS On and the FFGS Off). *Data not available for the FFGS Off treatment because the river bed was in close proximity to the DIDSON beam and precluded clear images.

Figure 3.6-47 Predatory Fish Area-Based Density Estimated by Mid-FFGS DIDSON, March 3 to April 22, 2014

End-FFGS

Almost 8,100 targets (potential predatory fish 30 to 100-cm [12-39 in] TL) were detected with the end-FFGS DIDSON between March 12 and April 15 (**Table 3.6-21**). The mean length by sampling date ranged from around 34 to 52 cm (13.4-20.5 in) TL.

Table 3.6-21 Summary of Targets (Fish) Detected with the End-FFGS DIDSON

Date	FFGS Treatment	Range (m)	Number (n)	Min. Length (cm)	Max. Length (cm)	Mean Length (cm)
12-21 March	Off	4.5–9.5	398	30.0	99.1	45.1
		9.5–14.5	216	30.1	85.5	44.6
	On	4.5–9.5	897	30.0	91.9	41.4
		9.5–14.5	373	30.0	97.9	43.0
21-22 March	Off	4.5–9.5	52	30.3	63.6	42.3
		9.5–14.5	10	32.4	52.5	40.8
	On	4.5–9.5	58	30.2	67.6	38.8
		9.5–14.5	3	32.2	35.4	33.6
22-24 March	Off	4.5–9.5	191	30.0	96.6	48.6
		9.5–14.5	23	30.2	53.0	40.6
	On	4.5–9.5	75	31.0	97.5	49.7
		9.5–14.5	51	30.4	96.3	51.6
24-27 March	Off	4.5–9.5	802	30.0	99.4	46.9
		9.5–14.5	436	30.0	98.9	44.3
	On	4.5–9.5	1,724	30.0	97.3	45.6
		9.5–14.5	835	30.0	99.6	46.0
29-31 March	Off	4.5–9.5	68	30.5	77.6	46.3
		9.5–14.5	28	30.9	83.9	43.4
	On	4.5–9.5	189	30.0	95.1	44.8
		9.5–14.5	134	30.0	95.1	43.5
31 March-7 April	Off	4.5–9.5	219	30.1	87.5	41.0
		9.5–14.5	49	30.0	69.1	41.9
	On	4.5–9.5	405	30.1	89.1	41.9
		9.5–14.5	104	30.5	81.3	39.2
10-15 April	Off	4.5–9.5	313	30.0	88.4	41.6
		9.5–14.5	20	30.3	46.5	34.3
	On	4.5–9.5	415	30.0	98.9	40.2
		9.5–14.5	6	30.7	87.0	48.0

Notes: Data were filtered to include only targets of 30 to 100 cm (12-39 in) TL. Targets may include multiple detections of the same fish on different occasions.

*Data not available for FFGS Off treatment because the river bed was in close proximity to the DIDSON beam and precluded clear images.

In contrast to the observations from the mid-FFGS DIDSON, the results from the analysis of the end-FFGS DIDSON provided some support for Hypothesis H7. Focusing on the dates with the DIDSON oriented along or behind the FFGS in the upper position, predatory fish density was significantly greater with the FFGS On than with the FFGS Off in five of ten comparisons (March 12 to March 21 and March 31 to April 7 in both the 4.5 to 9.5-m (31.2 ft) and 9.5 to 14.5-m (31.2-47.6 ft) ranges; and March 29 to March 31 in the 9.5 to 14.5-m (31.2-47.6 ft) range; **Figure 3.6-48**). No significant difference in density occurred between the FFGS On/Off near (4.5 to 9.5 m [14.8-31.2 ft]) the FFGS with the end-FFGS tilted into the lower position (March 22 to March 24), nor when the FFGS was oriented into the river channel (March 24 to March 27). Considering that with the FFGS On, more of the DIDSON's sampling volume was occupied by the FFGS (e.g., flotation units; compare **Figure 3.6-37** with the FFGS On to **Figure 3.6-38**with the FFGS Off), these results provided evidence that the density of predatory fishes was greater near the FFGS with the FFGS On than with the FFGS Off. Hypothesis H7 was tentatively accepted.

As with the mid-FFGS DIDSON, the data from the end-FFGS DIDSON during the period when the unit was oriented into the river channel and in the upper position (i.e., March 24 to March 27) were useful to assess differences in density between the ranges near (4.5 to 9.5 m [14.8-31.2 ft]) and farther (9.5 to 14.5 m [31.2-47.6 ft]) from the FFGS. The density near the FFGS was significantly greater than the density farther from the FFGS during both the FFGS On and FFGS Off treatments (**Figure 3.6-48**). As with the mid-FFGS DIDSON data, an alternative, area-based estimate of density was calculated to investigate whether the results from the volume-based density estimate could have reflected the sampling volume approximation. The area-based density estimate suggested that no significant difference existed between the 4.5 to 9.5-m (14.8-31.2 ft) and 9.5 to 14.5-m (31.2-47.6 ft) ranges with the FFGS Off; whereas with the FFGS On, the density near the FFGS still was significantly greater than the density farther from the FFGS (**Figure 3.6-47**). Taken together, the results from the mid-FFGS and end-FFGS DIDSON units suggested that the density of predatory fishes near the FFGS generally was greater than the density farther from the FFGS.

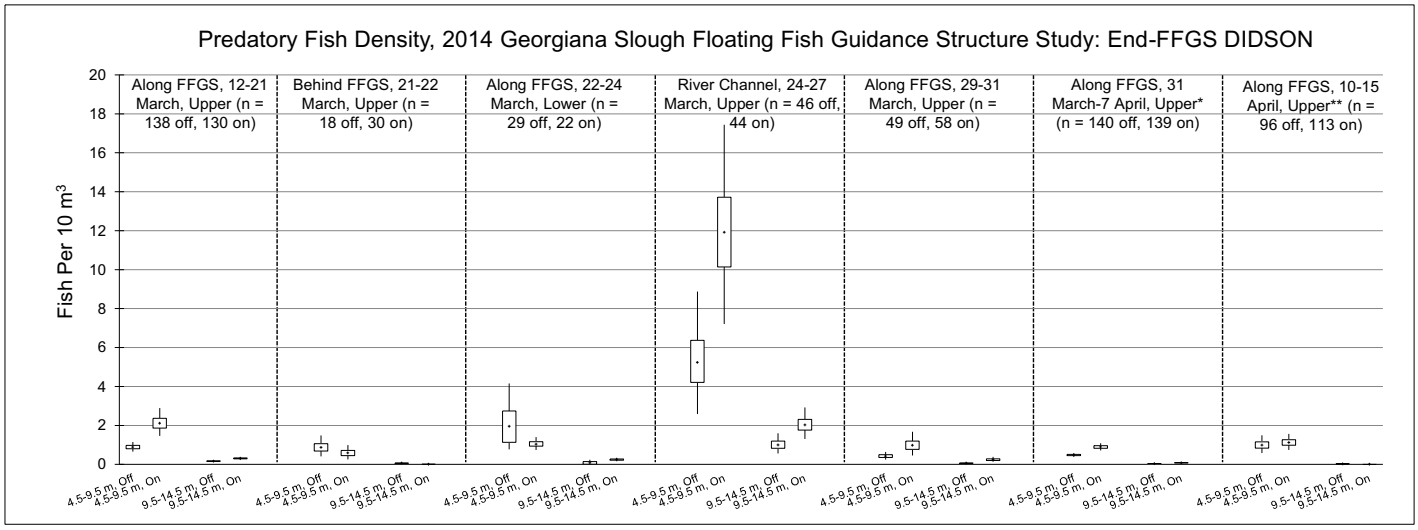

Note: Boxplots represent bootstrapped mean (+), interquartile range (box), and 95 percent confidence interval (whiskers) per 30 minutes of DIDSON sampling time. Labels indicate orientation of DIDSON (river channel = perpendicular to the FFGS; along the FFGS = parallel with the FFGS in the downstream direction; behind the FFGS = under the barge adjacent to the FFGS) and relative tilt of DIDSON unit (upper = sufficiently downward to avoid the water surface reflection; lower = sufficiently downward to sample the river bed with the FFGS On and Off).
*DIDSON oriented slightly closer to the FFGS than on other dates.
**DIDSON tilted slightly closer to the surface than on other dates.

Figure 3.6-47 Predatory Fish Area-Based Density Estimated by End-FFGS DIDSON, March 12 to April 15, 2014

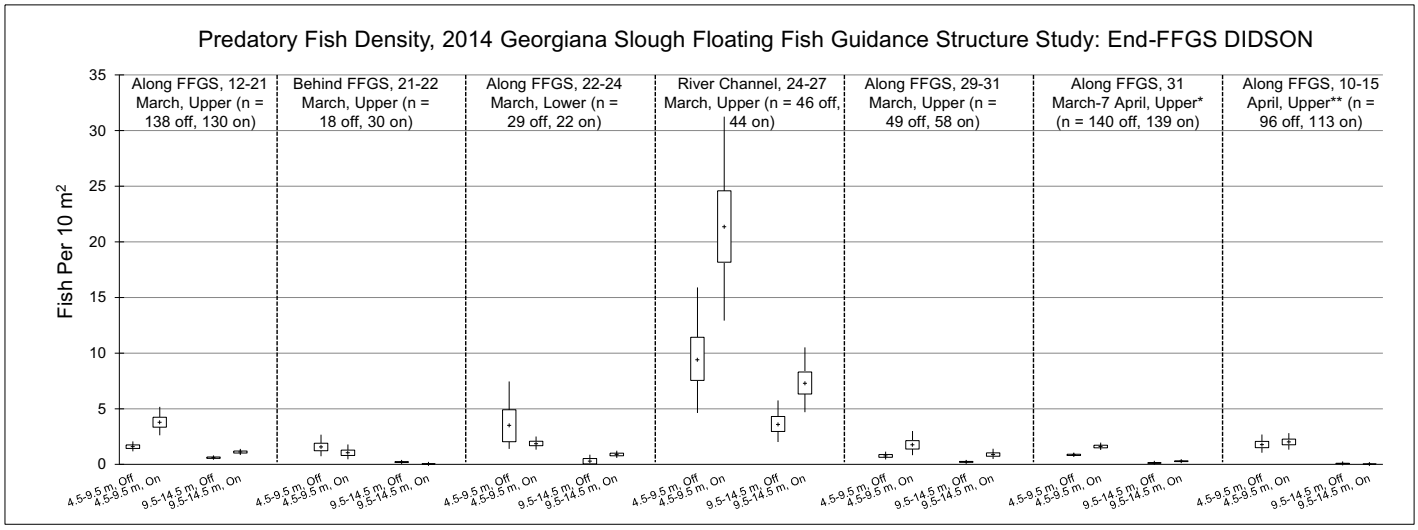

Note: Boxplots represent bootstrapped mean (+), interquartile range (box), and 95 percent confidence interval (whiskers) per 30 minutes of DIDSON sampling time. Labels indicate orientation of DIDSON (river channel = perpendicular to the FFGS; along the FFGS = parallel with the FFGS in the downstream direction; behind the FFGS = under the barge adjacent to the FFGS) and relative tilt of DIDSON unit (upper = sufficiently downward to avoid the water surface reflection; lower = sufficiently downward to sample the river bed with the FFGS On and Off).
*DIDSON oriented slightly closer to the FFGS than on other dates.
**DIDSON tilted slightly closer to the surface than on other dates.

Figure 3.6-48 Predatory Fish Volume-Based Density Estimated by End-FFGS DIDSON, March 12 to April 15, 2014

3.6.7 DISCUSSION

PREDATION

The data presented in this report suggest that the FFGS did not affect the probability of predation of acoustically tagged juvenile Chinook salmon in the study area. In addition, the probability of predation was not higher closer to the FFGS than further from the FFGS; Hypotheses H5 and H6 were rejected (**Table 3.6-22**). Lack of an apparent barrier effect on predation is consistent with the 2011 and 2012 BAFF studies (DWR 2012; DWR 2015b), whereas the 2009–2010 studies of a BAFF at the Head of Old River suggested higher predation with BAFF On (primarily reflecting guidance of juvenile salmon to the scour hole in the San Joaquin River just downstream from the Head of Old River) (DWR 2015a). Although the FFGS and BAFF technologies differ, both provide in-channel structure, and there was little evidence that either technology affected predation rates in the Sacramento River near the divergence with Georgiana Slough, at least with respect to operations (FFGS On versus FFGS Off; however, see "Conclusions" below regarding caveats for the comparison of FFGS On versus no FFGS). This difference between the Sacramento River at Georgiana Slough and the Head of Old River is probably related to the absence of a scour hole in the Sacramento River at Georgiana Slough.

Predation rates were greatest more than10 m (16 ft) from the FFGS buoy line, which is consistent with predation being greatest more than 80 m (262 ft) from the BAFF that was tested in 2011 and 2012 (DWR 2012; DWR 2015b). In contrast to the BAFF studies, this study expressed predation in relation to the proportion of fish passing within the different distance categories from the FFGS buoy line. This emphasized the appreciable extent of predation more than 10 m (16 ft) from the FFGS (see **Figure 3.6-2**). Relatively high predation rates > 10 m (> 16 ft) from the FFGS were particularly notable because relatively few juvenile Chinook salmon occurred in this area (most occurred within 10 m (16 ft) of the FFGS buoy line, which reflects the selection of tags that passed this close to the buoy line in order to assess barrier effectiveness). Although little predation was estimated to have occurred in the vicinity of the FFGS[27], a relatively high number of predation events were estimated to have occurred in the vicinity of the Offshore Downstream Dolphin to which the FFGS was attached (**Figure 3.6-1**). Several mechanisms, acting alone or synergistically, could explain the high number of predation events in the vicinity of the dolphin: 1) more juvenile Chinook salmon move through this area compared to other segments of the FFGS or near the FFGS (see **Figure 3.1-14**); 2) increased predator capture rate due to juvenile Chinook salmon disorientation from turbulent flows; 3) lower focal point velocity use by predators relative to other habitats (Facey and Grossman 1992); and 4) improved bioenergetic quality of microhabitat for predators because of greater differential between focal point velocity and adjacent feeding velocities nearby (Hayes and Jowett 1994; Bowen 1996).The end-FFGS DIDSON data suggested that predatory fish density near the end of the FFGS was relatively high at times in which data were available for analyses (see the following discussion of "Predatory Fish"), which would be consistent with the predation observations near the dolphin and would support the first two mechanisms suggested previously. The proportion of predation events within 10 m (16 ft) of the Offshore Downstream Dolphin with the FFGS on was 0.16 (i.e., 16% of predation events) and was double the proportion with FFGS Off, although the difference was not significant. As discussed in the "Results" section, a considerably greater sample size would be necessary to find a significant difference in these data, although the basic result would be consistent with the FFGS possibly guiding more juvenile Chinook salmon toward the dolphin when in the On position. In addition to the area near the Offshore Downstream Dolphin, a relatively high proportion of predation events were estimated to have occurred close to the Walnut Grove Bridge (**Figure 3.6-1**). Predation "hot spots" in association with bridge habitat have been noted for other locations in the Delta because of in-channel structures altering flow fields and providing predator habitat (Stevens 1963; Vogel 2011).

[27] As shown in Section 3.6.1 (**Table 3.6-1**), 5 of 431 fish (1.2%) were preyed on within 5 m (16 ft) of the buoy line, and 15 of 431 fish (3.5%) were preyed upon within 10 m (33 ft) of the buoy line.

Table 3.6-22 Summary of Objectives, Hypotheses, and Results Related to Predation and Predatory Fishes for the 2014 Study

Document Section	Method	Specific Objective	Hypothesis Number	Hypothesis	Result	Main Findings
3.6.1	Acoustic tagging (juvenile Chinook salmon)	Assess whether predation risk increases with FFGS on	H5	The probability of experimentally released Chinook salmon juveniles being eaten within the Georgiana Slough hydrophone array is greater with the FFGS On than with the FFGS Off	Reject hypothesis.	The probability of predation with FFGS On and FFGS Off was not significantly different. Probability of predation was negatively related to turbidity.
3.6.1	Acoustic tagging (juvenile Chinook salmon)	Assess whether predation risk of juvenile Chinook salmon changes in relation to the proximity to the FFGS (i.e., because the FFGS harbors predatory fishes or increases their predation effectiveness)	H6	The probability of experimentally released Chinook salmon juveniles being eaten within the Georgiana Slough hydrophone array increases with decreasing distance from the FFGS	Reject hypothesis.	The probability of predation was lowest less than 5 meters and 5 to 10 meters from the FFGS buoy line, and highest more than 10 meters from the buoy line.
3.6.6	Active hydroacoustics	Assess whether the physical structure of the FFGS and its effect on study area hydrodynamics results in changes in predatory fish density and the proportion of predatory fish density near the FFGS (e.g., by providing structure for ambushing prey or resting near the structure, or by changing the hydrodynamics of the study area so that changes in predator behavior are evident further from the FFGS)	H7	The density of predatory fish in the vicinity of the FFGS footprint is greater with the FFGS On than with the FFGS Off	Reject hypothesis for split-beam transducers and mid-FFGS DIDSON. Tentatively accept hypothesis for end-FFGS DIDSON.	Neither split-beam transducer nor mid-FFGS DIDSON found the density to be significantly greater near the FFGS with the FFGS On. However, the density generally was significantly higher with the FFGS On for the end-FFGS DIDSON. In addition, predatory fish density was significantly greater nearer the FFGS than farther away, for both DIDSON units (irrespective of the FFGS being On or Off).
3.6.3	Acoustic tagging (predatory fishes)	Assess whether the physical structure of the FFGS and its effect on study area hydrodynamics results in changes in the amount of time spent near the FFGS footprint by individual predatory fish (e.g., by providing more structure for ambushing prey or resting)	H8	Tagged predatory fish released in the vicinity of the FFGS footprint reside there longer when the FFGS is On than when the FFGS is Off	Reject hypothesis for striped bass and *Micropterus* spp.	No difference existed in residence time between FFGS On or Off treatments for either species.

Table 3.6-22 Summary of Objectives, Hypotheses, and Results Related to Predation and Predatory Fishes for the 2014 Study

Document Section	Method	Specific Objective	Hypothesis Number	Hypothesis	Result	Main Findings
3.6.4	Standardized angling	Assess whether predation risk of juvenile Chinook salmon changes with FFGS position (i.e., because the FFGS harbors predatory fishes or increases their predation effectiveness)	H9	The standardized angling catch rate of predatory fish in the vicinity of the FFGS footprint is greater when the FFGS is On compared to when the FFGS is Off.	Reject hypothesis for all predatory fish combined, striped bass, and *Micropterus* spp.	The difference in standardized angling catch rate between areas hypothesized to be affected by the FFGS and reference sites did not differ between the FFGS On and the FFGS Off treatments for any species.
3.6.6	Active hydroacoustics	Assess whether the physical structure of the FFGS and its effect on study area hydrodynamics results in changes in predatory fish density and the proportion of predatory fish density near the FFGS (e.g., by providing structure for ambushing prey or resting near the structure, or by changing the hydrodynamics of the study area so that changes in predator behavior are evident further from the FFGS)	H10	The proportion of predatory fish in the study area that is in the vicinity of the FFGS footprint is greater with the FFGS On than with the FFGS Off	Reject hypothesis.	No significant difference occurred in the index of relative predatory fish density (Walnut vs. Dagmar's) with the FFGS On versus the FFGS Off.
3.6.5	Acoustic tagging (predatory fishes)	Assess the use of different habitat types (e.g., open water, mud bank, riprap) by predatory fishes	H11	The percentage of time that predatory fish species spend within different habitat types in the study area is not equal	Accept hypothesis for striped bass and *Micropterus* spp.	Striped bass occupied the Open Water habitat significantly more than any other habitat zone; *Micropterus* spp. occupied zones near the release dock significantly more than many other zones. Striped bass spent little time near the FFGS (generally significantly less than expected based on zone area), whereas *Micropterus* spp. often were found in the nearshore FFGS Off zone, as well as other zones on the same bank as the release dock (and occurred in them significantly more than expected based on area). *Micropterus* behavior appeared partly related to homing.

Table 3.6-22 Summary of Objectives, Hypotheses, and Results Related to Predation and Predatory Fishes for the 2014 Study

Document Section	Method	Specific Objective	Hypothesis Number	Hypothesis	Result	Main Findings
3.6.5	Acoustic tagging (predatory fishes)	Assess the use of different water velocities by acoustically tagged predatory fishes in relation to those available	H12	The percentage of time that predatory fish species spend in different water velocities in the study area is not equal	Accept hypothesis for striped bass and *Micropterus* spp.	Across the 0 to 0.45 m/s range, striped bass were found at low velocity (0 to 0.05 m/s) significantly less than expected, based on available velocity; *Micropterus* spp. were found at the highest velocity (0.45 m/s) significantly less than expected, based on its availability.

The GLM analysis suggested that turbidity in the study area was a reliable predictor of predation probability for juvenile Chinook salmon. This is consistent with the results at the Head of Old River in 2011–2012 (DWR 2015a) and in the Sacramento River on a broader scale (Newman 2003), and presumably reflects reduced ability of visual predators to detect and prey on juvenile Chinook salmon. There was little support for any of the other hypothesized relationships between probability of predation and various potentially important predictors. For some predictors such as predator density, the lack of a relationship with predation probability may not be so surprising because of the inherent variability in predator density over short spatial and temporal scales as fish move around the study area.

No significant relationship was found between temperature and predation probability in this study (**Table 3.6-2**, **Table 3.6-3**). This was surprising because studies have found such relationships (Newman 2003; Zeug and Cavallo 2013; DWR 2015b) and there was some evidence for a positive relationship between catch rate of *Micropterus* spp. and water temperature (see Section 3.6.4). Acoustically tagged sub-adult striped bass inhabiting the San Francisco Bay estuary watershed, which includes the Delta, were detected most often and in the highest number in water temperatures between 16 and 20°C (LeDoux-Bloom 2012).This may indicate that prey species residing in or moving through habitat within this temperature range may experience greater potential predation rate by sub-adult striped bass. However, evidence for relationships between temperature and predation probability in part depends on the type of analysis utilized: GLM analysis of predation probability at the Head of Old River did not find strong support for this predictor (DWR 2015a). However, in the same study, the proportion of juvenile Chinook salmon eaten was significantly positively related to temperature when all four years of study (2009-2012) were combined and analyzed with a univariate correlation analysis (DWR 2015a: Figure 6-9). To some extent this reflects differences in the data used because the GLM analysis conducted two sets of analyses: the first was based on data for 2009, 2010, and 2011, including the effects of barriers, as well as other predictors such as temperature and flow; the second was based on data for 2011 and 2012, which included only the effects of non-barrier-related predictors because the effect of the barrier (no barrier in 2011, rock barrier in 2012) was confounded by markedly different flows in 2011 and 2012.

This study's results suggested that ambient light or day/night had no significant influence on predation probability. These results were in contrast to the Head of Old River study, where predation probability was strongly positively related to ambient light level (DWR 2015a: Tables 6-59 and 6-61).

This study was similar to previous studies in the Delta (e.g., DWR 2012; Buchanan et al. 2013; DWR 2015a) and elsewhere, in there being some uncertainty existing in the classification of predation events, with respect to whether a fish had been preyed on and, in particular, the location and timing of predation. Although recent advances in acoustic tagging technology allow predation to be determined (e.g., Predation Detection Acoustic Tags [PDAT; see http://www.htisonar.com/PDAT-predation-detection-acoustic-tag.html), the lag time between a predation event and the change in acoustic signal may limit the utility of such technology for addressing fine-scale questions[28], such as predation occurring in close proximity to the FFGS, given that fish such as striped bass often are moving rapidly and may leave the vicinity of the FFGS quite quickly; such technology has greater promise for broad-scale (through-Delta) survival questions. Possible future approaches to address predation of juvenile salmonids near the FFGS and other in-channel structures could include tethering studies (e.g., Grimaldo et al. 2000), as used near water diversions upstream from the study area (Michel et al. 2014). In addition, more recent

[28] Preliminary testing found a mean lag time of 59.3 hours (range: 22.3-140 hours); see http://www.slideshare.net/htisonar/efficacy-of-a-new-acoustic-tag-designed-to-indicate-occurrence-of-a-predation-event

research suggests that it may be possible to classify predation-related events from DIDSON data (Price et al. 2013), although the feasibility of using this method in the study area in the future would depend on the ability to observe smaller fish (which, along with other smaller objects, often are filtered out of acoustic data because of the acoustic noise) and would be relatively labor-intensive because of the manual data manipulation required. However, this method could be useful to assess predation in the vicinity of the dolphins to which any future FFGS is attached.

PREDATORY FISH

This study used several methods to investigate the potential influence of the FFGS on predatory fish behavior in the study area. Based on the weight of evidence from these various study elements (**Table 3.6-22**), little evidence exists to suggest a broad-scale effect of the FFGS on predatory fish behavior in the study area, although evidence indicated the possibility of a localized effect on fish occurring near the FFGS. Predatory fish did not reside in the study area longer with the FFGS On than with the FFGS Off (Hypothesis H8). No difference existed in the predatory fish standardized catch rate in areas hypothesized to be influenced by the FFGS relative to reference areas between the FFGS On and Off treatments (Hypothesis H9). The habitat zones near the FFGS were not occupied more frequently relative to other areas by striped bass, whereas the nearshore habitat in the vicinity of the FFGS was occupied more frequently by *Micropterus* spp. (Hypothesis H11); however, evidence existed for homing to initial capture areas near the FFGS, discussed further herein. Neither the density nor the proportion of predatory fish in the vicinity of the FFGS was greater with the FFGS On than with the FFGS Off when assessed by split-beam-transducer or mid-FFGS DIDSON active hydroacoustics (Hypotheses H7 and H10). However, the end-FFGS DIDSON data provided some support for Hypothesis H7 (i.e., that the density of predatory fish was greater with the FFGS On than with the FFGS Off. Both mid-FFGS and end-FFGS DIDSON data also suggested that predatory fish density was significantly higher near the FFGS than further away, regardless of whether the FFGS was On or Off.

Residence time in the study area was not related to FFGS operations for either striped bass or *Micropterus* spp. Patterns of residence time agreed with results from the 2012 BAFF study (DWR 2015b): striped bass left the study area much more rapidly than *Micropterus* spp., presumably reflecting migration to spawning or other areas. As discussed further herein, many *Micropterus* spp. may have been maintaining territories, possibly related to spawning. Species-specific differences in residence time have been reported for predatory fishes in other studies in the Delta. Miranda et al. (2010) described little fidelity of six tagged adult striped bass within the SWP's Horseshoe Bend fish-salvage release site because fish were detected on one to three dates after tagging.

In another study investigating residence time of predatory fishes, Gingras and McGee (1997) found that the flux of striped bass into or out of Clifton Court Forebay (CCF) was appreciable; 0 to 100 percent (mean 17 percent) of weekly fish movements at the CCF was through the radial gates as opposed to other parts of the CCF. Although turnover of striped bass may be appreciable, other predatory fishes also may reside in specific areas for relatively short periods. For example, Cavallo et al. (2013) conducted a predator removal effort on a 1.6-km (1 mi) reach of the North Fork Mokelumne River and collected just over 90 percent of around 160 predatory fishes that were vulnerable to electrofishing; 6 days later, a similar effort yielded 83 percent of around 600 predatory fishes at the same site. The most abundant of these fish were redear sunfish (*Lepomis microlophus*), largemouth bass, bluegill (*Lepomis macrochirus*), redeye bass, and spotted bass, with only 10 striped bass collected on both days, which indicates substantial turnover of species other than striped bass. Acoustically tagged striped bass (n = 32) near the outfall of the Sacramento Regional Wastewater Treatment Plant (SRWTP) were detected for an average of just

under 7 hours between March and May 2012, whereas smallmouth bass (n = 2) were detected for 1.4 hours and just under 72 hours (Robertson-Bryan, Inc. et al. 2013). In general, these observations from previous studies are consistent with the results of the present study.

Acoustically tagged striped bass occurred relatively infrequently in both the FFGS Off and FFGS On zones, generally less than expected because of the size of these zones. The FFGS On zone is offshore (and previously was designated mostly as part of the Open Water habitat zone by DWR 2015b during the 2012 BAFF study), yet the pattern of striped bass occurrence in that zone did not provide evidence of association with the FFGS and was essentially contrary to expectations: the zone was selected significantly less with the FFGS On than expected based on its area, whereas with the FFGS Off, the zone was selected based on its area. However, the DIDSON data suggested that predatory fishes (or at least larger fish that may have been predatory fishes) occurred in relatively high density near the FFGS compared to open water areas further away. Thus, the FFGS may provide habitat for a portion of the predatory fishes occurring in the study area, but the results for acoustically tagged striped bass emphasized that the presence of the FFGS does not result in widespread use of the near-FFGS area. As noted above in the discussion related to "Predation," a relatively high number of predation events occurred near the Offshore Downstream Dolphin to which the FFGS was attached. The dolphin actually was just outside the FFGS On zone, so that predatory fish including striped bass occurring close to it generally would be categorized as being in the Open Water habitat zone.

The potential for in-channel structures to affect predation and predatory fish behavior in the Delta was reviewed by Vogel (2011), who provided several examples of such structures that have been shown or are hypothesized to provide predatory fish habitat: the partially buried SRWTP outfall pipe on the river bed near Freeport, water diversion and drainage structures associated with agricultural irrigation, docks and marinas, and bridges. Predatory fishes also have been shown to associate with the in-channel pipes at the SWP/CVP salvage release sites (Miranda et al. 2010).

Of the various structures reviewed by Vogel (2011), one quantitative study exists related to predation and predatory fishes at the SRWTP outfall. In that study, standardized angling at the SRWTP outfall (diffuser) found catch rates of striped bass to be significantly greater than at one reference site with in-channel structure (i.e., Freeport Bridge) but not significantly different than catch rate at another reference site (Miller Park) or in the thermal plume 120 m (394 ft) downstream from the outfall (Robertson-Bryan, Inc. et al. 2013); no significant differences existed between sites for the other predatory fishes examined (i.e., Sacramento pikeminnow, smallmouth bass, spotted bass, and white catfish). Although striped bass occurred in relatively high density near the SRWTP outfall, no acoustically tagged juvenile Chinook salmon passing through the outfall area were preyed on, in contrast to extensive predation upstream and downstream from the outfall area; this illustrates that a relatively high density of predator fishes near in-channel structure need not result in high predation rates. Vogel (2011) noted for boat docks and marinas that surprisingly little is known of the importance of these structures for predation, in theory these structures should facilitate effective predation by the combination of vertical posts driven into the channel and supporting overhead structure (e.g., docks and shade canopies). He further suggested that predation problems associated with such structures would be heightened where the structures are positioned so that large quantities of flow (and therefore fish, such as juvenile salmonids) pass beneath them. Sabal et al. (2016), in their study of striped bass predation near Woodbridge Irrigation District Dam on the lower Mokelumne River, suggested that in-channel habitat alterations can cause aggregations of predatory fishes, which respond to enhanced feeding conditions (e.g., concentration and disorientation of prey).

In this study, little evidence from acoustic tagging indicated striped bass aggregate near the FFGS or at any of the other major in-channel structures (as represented by the habitat zones Dock 1, Dock 2 [Dagmar's Landing], Bridge Right, Bridge Left, Dock 3 [Boon Dox], or Dock 4), which generally were used at rates similar to or less than expected because of their area; the species was strongly associated with the Open Water habitat zone. This, in combination with results from the predation analyses, suggests limited evidence that the FFGS influences the behavior of striped bass on a broader scale in the study area.

However, as noted previously, the mid-FFGS and end-FFGS DIDSON results suggested that predatory fish can occur near the FFGS in relatively high density compared to adjacent open water areas, and thus the FFGS has the potential to exert a localized effect on predatory fishes occurring in its vicinity. Active hydroacoustics such as DIDSON surveys have been used to assess the presence of predatory fishes in relation to in-channel structures in the Delta and elsewhere. Using DIDSON, Michel et al. (2014) found the density of predatory fishes in the vicinity of the City of Sacramento's in-river intake was relatively low in comparison to adjacent bank and river channel habitats, whereas density near the on-bank Freeport Regional Water Authority intake was significantly greater than the adjacent river channel but similar to the adjacent river bank habitat. Williams et al. (2003) reported that large predatory fishes rarely were found in association with a Washington State Ferry terminal's in-channel structures when assessed by DIDSON, but SCUBA surveys found higher abundance of predatory fishes at the terminal than at a reference site. In another DIDSON study, Grothues and Able (2010) assessed association of fish greater than 250 mm (9.8 in) in association with piers and adjacent habitat in the lower Hudson River, and found them to be relatively uncommon and slightly more abundant in open water near piers or habitat adjacent to piers, at pier edges, and under piers. Large fish, such as striped bass, most often were oriented to structure as single individuals or in loose aggregations of a few individuals, whereas schools occurred in open water away from structures.

In this study, the fact that predatory fish density from the mid-FFGS DIDSON was not significantly greater with the FFGS On compared with the FFGS Off suggests, at least for the upstream portion of the FFGS (which is closer to shore; see **Figure 3.6-28**), that the FFGS's structure rather than its position may have been of greater importance to the predatory fishes occurring near it. In contrast, for the end-FFGS DIDSON, support was shown for predatory fish density being higher with the FFGS On than with the FFGS Off. This could be because the downstream portion of the FFGS offers more advantageous habitat for predatory fishes with the FFGS On, compared to FFGS Off, as described earlier (disorientation of juvenile salmonids coupled with bioenergetically advantageous velocity refugia for predators). Alternatively, with the FFGS On, the end-FFGS DIDSON simply may have detected larger numbers of fish occurring in the river channel, particularly because tagged striped bass generally occurred mostly in the Open Water habitat zone. Therefore, the detection by DIDSON would not necessarily have indicated association of these fish with the FFGS, rather the intersection of the FFGS with more frequently used habitat by this species. However, because of the relatively high number of predation events just downstream from the FFGS in the vicinity of the Offshore Downstream Dolphin to which the FFGS was attached, it is possible that the end-FFGS DIDSON sampled relatively high numbers of predatory fish with the FFGS On. The limited apparent spatial influence of the FFGS also was suggested by the density and proportion of predatory fish just downstream from the FFGS at the Walnut split-beam transducer not being significantly greater with the FFGS On than with the FFGS Off. This limited apparent influence of the FFGS on predatory fish farther from the FFGS could be attributed to the minor hydrodynamic influence of the FFGS, which is apparent in the virtual

absence of any discernible effect on velocity magnitude and variability (error) from ADCP measurements (see **Table 3.3-4**[29] in Section 3.3, "Hydrodynamics and Critical Streakline").

In contrast to striped bass, acoustically tagged *Micropterus* spp. were found mostly in nearshore habitat zones near the release site, including the FFGS Off zone. Release of predatory fish from Dock 3 (Boon Dox) following acoustic tagging (or in some cases following recapture) inevitably will have affected the patterns of habitat use by acoustically tagged fish, and also is likely to have affected catch rates during standardized angling, and possibly also density estimates from active hydroacoustics. This potential bias presumably would have increased the number of predatory fish near the FFGS, as many predatory fish were relocated to just upstream[30] of the FFGS by capture and release. With respect to the occurrence of *Micropterus* spp. in the FFGS Off zone, the nearshore habitat in this zone had a high catch rate for predatory fish during the 2012 BAFF study (S. Pagliughi, AECOM, unpublished data).

The primary nearshore habitat type in the FFGS Off zone is riprap, as designated by DWR 2015b. This zone may constitute suitable habitat for predatory fishes, particularly *Micropterus* spp., regardless of the FFGS presence, resulting in relatively high density. The analysis of homing to capture site illustrated that fish originally captured in the FFGS SAA returned there at a high rate. Fish captured in the other SAAs also tended to inhabit the SAA where they initially were captured in more than the FFGS SAA, suggesting that occupancy of the habitat zones near the FFGS to some extent reflected the origin of the fish. Homing behavior, as exemplified by *Micropterus* spp. tag code # 3947 (**Figure 3.6-27**), has been noted in *Micropterus* spp. at various locations. For example, Larimore (1952) found that smallmouth bass, which were experimentally relocated up to 1.3 km (0.8 mi) in Jordan Creek (Illinois), returned to home pools on more than 50 percent of occasions, with larger fish returning at greater rates. Homing may be associated with return to spawning sites. As reviewed by DWR 2015b, smallmouth bass (Robbins and MacCrimmon 1974; Edwards et al. 1983) and spotted bass (McMahon et al. 1984), spawning occurs on rocky or other hard substrates (e.g., riprap), with the timing of spawning related to water temperature and day length (see also **Appendix E**, "Focal Predatory Fish Species"). Therefore, territories such as that of *Micropterus* spp. tag code # 3947 may be spawning sites.

Similar to the general findings from acoustic tagging and active hydroacoustics, standardized angling did not suggest greater predation potential or differences in predatory fish behavior with the FFGS On compared to the FFGS Off. Standardized angling catches were variable, and only partial evidence supported increased water temperature for increased catch of *Micropterus* spp. This may reflect increased bioenergetic demand for prey as water temperature and metabolism increased (Hanson et al. 1997). A positive correlation between predatory fish density and water temperature was observed from active hydroacoustic data at the Head of Old River (DWR 2015a), which also may have reflected seasonal migration (e.g., of striped bass). Increased catch rates of predatory fishes also occurred with increasing water temperature during standardized angling associated with the study of the SRWTP (Robertson-Bryan, Inc. et al. 2013).

The near-surface water velocity occupied by predatory fishes was not uniform across the range of available water velocity in the study area. Striped bass occurred at the lowest velocities (0 to 0.05 m/s [0-0.16 ft/s]) significantly less than velocities that were available to them, reflecting the species' occurrence primarily in the Open Water

[29] This does not rule out the possibility of localized turbulence immediately adjacent to the FFGS.
[30] The distance between the midpoint of the dock where fish were released and the upstream end of the FFGS is approximately 50 m (164 ft).

habitat zone, which generally had higher velocity than the nearshore zones. At the Head of Old River, striped bass occurred broadly across the range of available water velocity (0 to 0.3 m/s [0-1.0 ft/s]); (Greenwood 2014; DWR 2015a). In this study, *Micropterus* spp. occurred across most of the range of available water velocity; the exception was the 0.45 m/s (1.48 ft/s) interval, at which occurrence was less than its availability within the study area. Published velocity criteria for *Micropterus* spp. suggest that optimum suitability occurs at a very low range (0 to 0.05 m/s [0-0.16 ft/s]) and steeply declines with increasing velocity, so that by 0.3 m/s (1.0 ft/s), suitability is on the order of 0.1 to 0.4 m/s (0.03-1.31 ft/s), and zero suitability exists at 0.6 to 0.9 m/s (2.00-2.95 ft/s) (Edwards et al. 1983; McMahon et al. 1984). Individual studies vary: whereas Todd and Rabeni (1989) found that smallmouth bass preferred velocities less than 0.2 m/s (0.66 ft/s), they noted that Larimore and Garrells (1982) found that velocities less than 0.53 m/s (1.74 ft/s) were preferred, more in keeping with the broader range found in this study. Those earlier studies generally reported distribution in relation to water velocity below the surface (e.g., at 60 percent of water column depth), whereas this study relied on the near-surface water velocity interpolation; consideration of water velocity closer to the substrate may be more appropriate for *Micropterus* spp.

CONCLUSIONS

Overall, this study found relatively little evidence of a connection between the FFGS and predation, with the evidence being limited to the relatively high proportion of predation events that were estimated to have occurred in the vicinity of the Offshore Downstream Dolphin to which the FFGS was attached. The FFGS appeared to have a localized effect on predatory fish behavior (i.e., density near the FFGS was greater than further away, based on DIDSON observations). However, conclusions regarding the effects of the FFGS on predation and predatory fish behavior must be qualified for two important reasons. First, the logistical challenges of manipulating the FFGS meant it was only possible to test FFGS On and FFGS Off. It is clearly of interest to be able to compare the FFGS On with a true control of no FFGS, for the presence of the FFGS in the water may influence predation and predatory fish behavior regardless of treatment. Second, the experimental protocol for testing effects on juvenile salmonid routing (i.e., switching the FFGS treatment every day) may have deterred predatory fish from inhabiting the vicinity of the FFGS as frequently as they may during constant FFGS On conditions. Therefore, any long-term deployment of the FFGS should be accompanied by appropriate monitoring, perhaps a scaled-down version of this study (e.g., with fewer hydrophones for the acoustic tagging elements), to re-evaluate the evidence for changes in behavior of predatory fishes (e.g., close association of predatory fish with the FFGS and greater predation risk for juvenile salmonids passing near the FFGS).

3.7 ANALYSIS OF DIEL ARRIVAL DISTRIBUTION

3.7.1 INTRODUCTION

Multiple analyses of the movement rates of acoustically tagged juvenile Chinook salmon in the lower Sacramento River and the Delta have shown that tagged fish were consistently detected moving downstream more frequently during dark and crepuscular periods than during daylight periods (Plumb et al. 2016; Burau et al. 2007; Zajanc et al. 2013). This finding has significant implications for our understanding of entrainment rates in tidal junctions where instantaneous entrainment risk varies throughout the tidal day, because the phasing between the 24.8 hour tidal day and the 24 hour diurnal day can result in sustained periods when either large flood tides or large ebb tides occur only during dark hours (**Figure 3.7-1**). If juvenile Chinook salmon are more likely to move downstream during dark and diurnal periods then this coupling between diurnal cycles - and tidal cycles will

affect the overall entrainment risk observed at the Georgiana Slough/Sacramento River junction during an acoustic telemetry study.

During the 2011 and 2012 BAFF studies fish were released in the Sacramento River just downstream of Steamboat Slough, about 9 km upstream of the Georgiana Slough junction. In 2011 many of the study fish reached Georgiana Slough several hours after being released, which raised the concern that fish released at Steamboat Slough might not exhibit the same outmigration behavior as fish which have spent several days moving downstream and, as a result, the overall entrainment risk for these study fish might not account for the effects of diurnal cycle - tidal cycle coupling. In order to address these concerns the release location for the 2014 FFGS study was moved upstream to the City of Sacramento to provide study fish with more time to acclimatize to outmigration before reaching the Georgiana Slough junction. This rationale for changing the release location was formalized to be tested in the 2014 FFGS study plan as Hypothesis H4 (**Table 2-1**):

"The diel distribution of juvenile Chinook salmon arriving at the Georgiana Slough hydrophone array released at Steamboat Slough is different from the fish released at the City of Sacramento."

In order to test Hypothesis H4, the diel movement bias of acoustically tagged juvenile Chinook salmon released at the City of Sacramento (2008 North Delta Study and 2014 FFGS Study), to the diel movement bias of acoustically tagged juvenile Chinook salmon released below Steamboat Slough (2011 and 2012 BAFF studies) were compared.

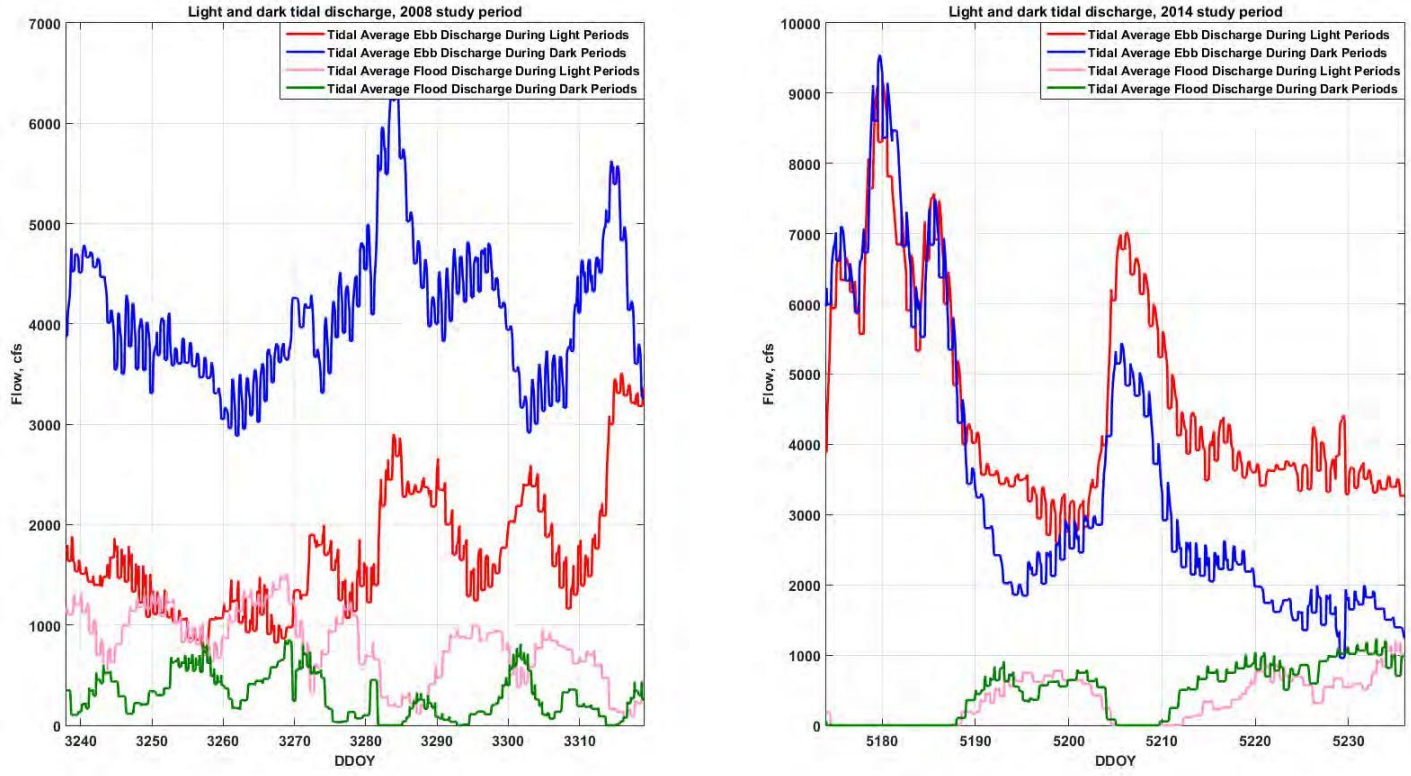

Note: Time series showing the effects of phasing between the 24 hour solar day and the 24.8 hour tidal day at the Georgiana Slough junction. During midwinter large ebb tides occurring during the night (left panel, blue line), while large flood tides occur during the day (left panel, purple line). Around the time of the spring equinox this phasing is reversed, with large ebb tides occurring during the day (right panel, red line), and larger floods occurring during the night (right panel, green line). This phasing is stable year-to-year, so that large ebb tides will occur at night at Georgiana Slough around midwinter in future years.

Figure 3.7-1 Tidal Flow through the Georgiana Slough Junction during Light and Dark Periods in Midwinter and Spring

3.7.2 METHODS

APPROACH

Quantifying the observed diel arrival distribution of acoustically tagged juvenile Chinook salmon for each of the study datasets is straightforward, but comparisons between these distributions are complicated by the fact that each study occurred over a different portion of the solar year, so that the total percentage of each study period that occurred during light, dark, and crepuscular periods varied. For example, **Figure 3.7-2** shows that 68 percent of the 2008 North Delta Study period occurred during dark and crepuscular periods, while 51 percent of the 2011 BAFF Study occurred during dark and crepuscular periods. As a result, if a greater proportion of fish from the North Delta Study (City of Sacramento release) arrived during dark periods than fish from the 2011 BAFF Study (Steamboat Slough release), the difference in diel arrival distribution between studies would not necessarily indicate a behavioral difference due to release location.

The difficulties in comparing diel distributions due to differing photoperiods between studies are compounded by the tidal cycle - diel cycle interactions illustrated in **Figure 3.7-1**, because this interaction results in different percentages of water entering the junction during dark and light periods during each study. In order to address these challenges a scalar transport approach was used to estimate what the flux of acoustically tagged fish into the Georgiana Slough junction would be for each study if fish displayed no behavior beyond random dispersion, and then subtracted the diel distribution of this no-behavior estimated arrival signal from the observed diel distribution for each study to derive an estimated diel movement bias. The estimated movement diel bias from each study was then compared to look for evidence of behavioral differences between fish released at the City of Sacramento and fish released at Steamboat Slough.

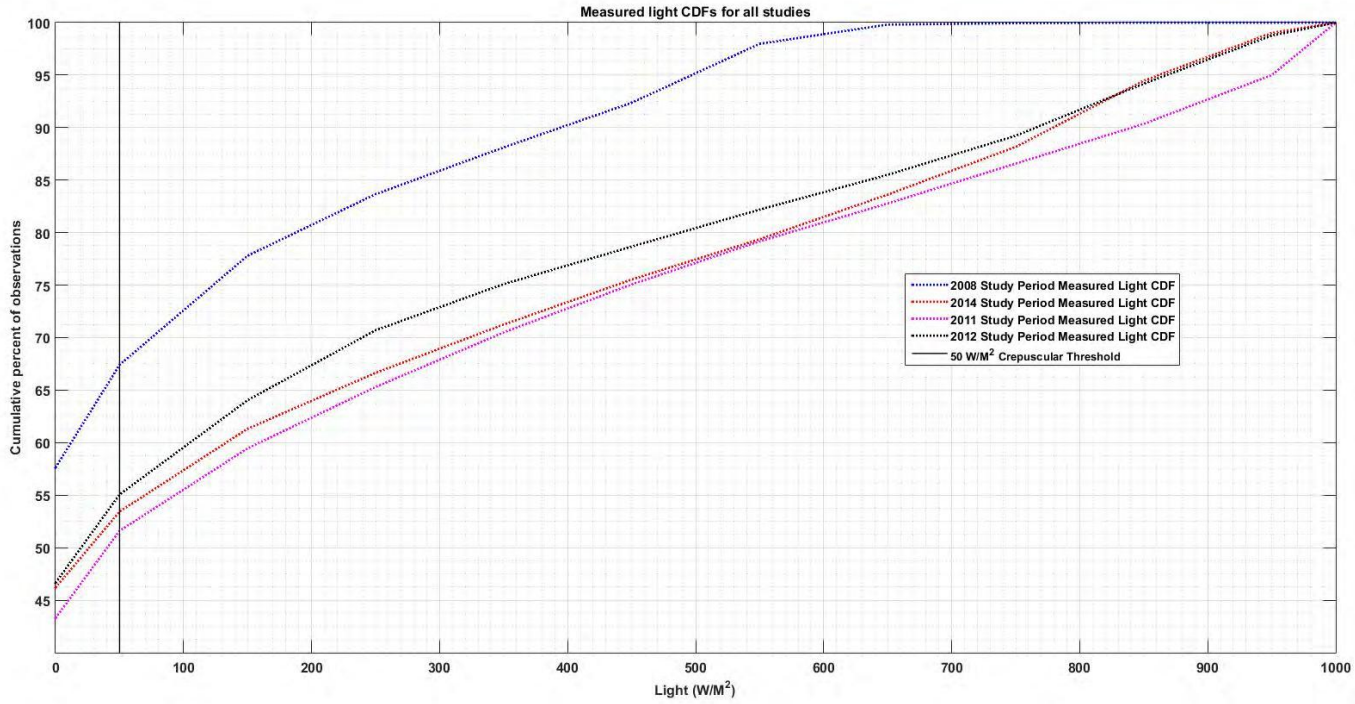

Note: Curve showing cumulative distribution functions (CDF) for the measured light during each study's fish arrival period. The vertical dark grey line shows the 50 Watts per square meter cut off for crepuscular periods. The 2008 North Delta Study (blue dotted line) took place midwinter and as a result a greater percentage of this study took place during dark or crepuscular periods

Figure 3.7-2 CDF Functions for the Measured Light during Each Study's Fish Arrival Period

ESTIMATING FISH ARRIVAL-LIGHT DISTRIBUTION FOR EACH SET OF FISH TRACKS

The first step in estimating the diel movement bias for each study was to estimate the light value when each fish track segment arrived in the Georgiana Slough/Sacramento River junction. Because the spatial scale of the acoustic tracking array varied between study years, the time of arrival was defined as the time when each track segment was closest to the center of the Georgiana Slough junction, and interpolated the observed light signal to estimate the amount of light in the junction at that time. In order to maintain a consistent data source across study years, light data from the California Department of Water Resources Rio Vista Gauging station was used to estimate light levels in Walnut Grove. This station supplied sensor light levels in Watts per square meter (W/m^2) in 15-minute increments. The interpolation of the light signal to the time when each fish track segment first reached the center of Georgiana Slough was performed during the covariate assignment step of the spatial analysis described in Section 3.5.1 herein.

The 2014 and 2008 study track sets contained a significant number of fish that transited the junction on ebb tides and then entered the junction again from downstream in the Sacramento River on flood tides. As discussed in Section 3.5.1 these tracks were broken into ebb tide and flood tide segments and for the purposes of this analysis each track segment was treated as an independent event with each segment contributing a light value to the study's population of light values at arrival. There were no light values recorded for flood tide tracks for Steamboat Slough releases because there were no flood tides during the 2011 BAFF Study, and because the manual predator classification process utilized for the 2012 BAFF Study removed these track segments from the analysis pool.

ESTIMATING THE NO-BEHAVIOR FLUX OF ACOUSTICALLY TAGGED SALMON FOR EACH STUDY

In order to account for the difference in the balance between light period water transport and dark period water transport during each study we estimated the distribution of light values when non-behaving study fish were likely to arrive at the Georgiana Slough/Sacramento River junction. This was accomplished in two steps: 1) the estimated flux of fish carrying water into the junction at 15-minute increments was calculated; and 2) the estimated the concentration of study fish in the water entering the junction for each 15-minute increment multiplied by the fish carrying water flux was multiplied by the fish concentration to arrive at an estimated fish flux.

The estimated flux of fish carrying water into the junction used the Walnut Grove Above (WGA), Walnut Grove Below (WGB), and Georgiana Slough (GS) gauges operated by the USGS and California Water Science Center. These three gauges form a control volume around the Georgiana Slough junction and provide discharge in each branch of the junction. WGA is located upstream of the junction and records positive values when upstream flow is entering the junction on ebb tides, and WGB is located downstream of the junction and records negative values when flow is entering the junction on flood tides. The flux of fish carrying water into the junction was estimated as the sum of water entering from upstream and downstream, using:

$$\text{Fish Carrying Water Flux} = (\text{WGA} \times \text{MaskWGA}) + (\text{WGB} \times \text{MaskWGB} \times \text{DensityCorrection})$$

where:

$\text{MaskWGA} = 0$ if $\text{WGA} < 0$, 1 if $\text{WGA} > 0$;

MaskWGB = 1 if WGB < 0, 0 if WGB > 0; and

DensityCorrection = 0.75 for the 2008 North Delta Study and 2014 FFGS studies and 0.0 for the 2011 and 2012 BAFF studies.

The density correction term multiplied by the flood tide flow is included to partially account for the fact that the water entering the junction on flood tides is mostly water that passed through the junction on ebb tides, and as a result, is likely to contain a lower density of tagged fish due to prior entrainment in Georgiana Slough. A correction factor of 0.75 was chosen because the entrainment rate during the ebb tide prior to converging and flood tides was often between 0.2 and 0.3 during prior studies at Georgiana Slough (**Figure 3.7-3**) (also see Section 3.5 and **Section 3.3**). A correction factor of 0.0 was used for the 2011 and 2012 BAFF studies because no flood tide track segments were included for these studies. It is important to note that this correction factor approach represents a vast oversimplification of the mechanics of tidal transport, but a mature analysis would require three dimensional hydrodynamic modeling and particle tracking that is beyond the scope of this analysis.

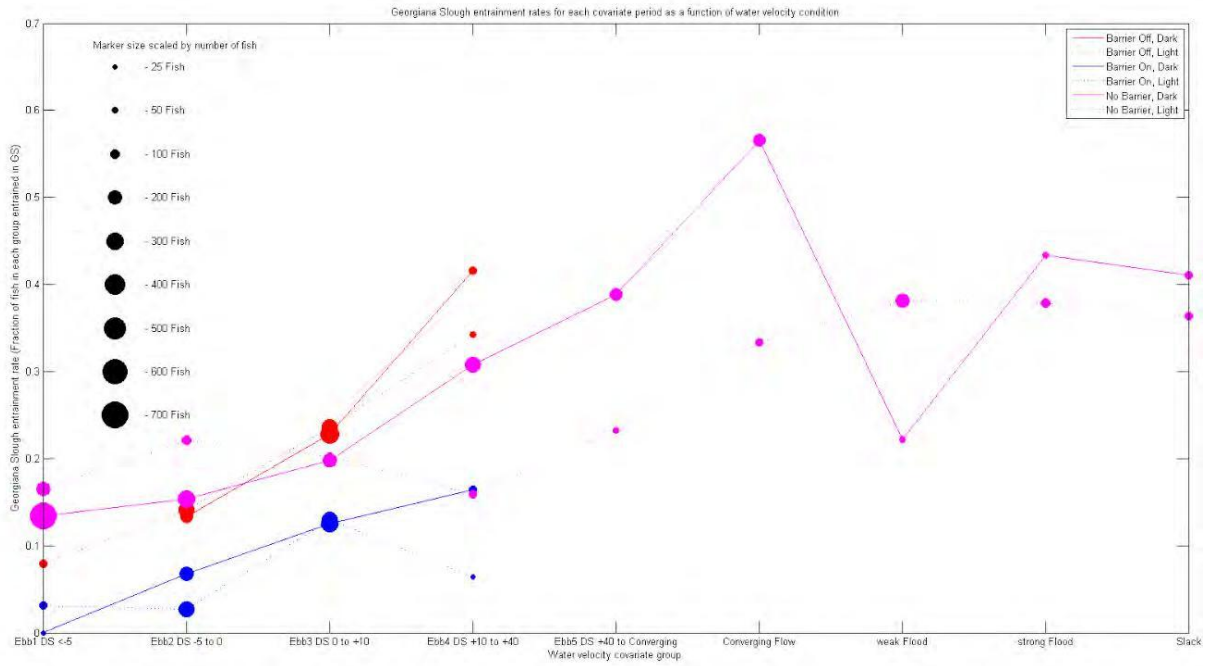

Note: Lines show entrainment rates measured at Georgiana Slough during the 2011 and 2012 BAFF studies and the 2008 North Delta Study for 9 covariate periods that summarize the full range of tidal forcing in the junction. Solid lines show entrainment rates during dark periods, dotted lines show entrainment rates during light periods. The size of the marker for each covariate period indicates the total number of fish contributing to that period's entrainment rate estimate. The red lines indicates periods when the BAFF was Off, the blue lines indicates periods when the BAFF was On, and the purple lines indicate periods with no BAFF. Note that entrainment in Georgiana Slough during periods when the BAFF as Off or not installed at the end of the ebb cycle is around 20% - 30%. More information on these tidal covariate periods can be found in Section 3.3 and Section 3.5.

Figure 3.7-3 Measured Entrainment Rates in Georgiana Slough as a Function of Critical Streakline Position

The 15-minute fish carrying water flux signal provides an estimate of the rate at which water containing fish was transported into the junction. In order to use this signal to estimate the arrival rate of non-behaving study fish, the fish carrying water flux needs to be corrected for the release concentration of study fish. During each of the studies contributing to this analysis acoustically tagged fish were continuously released upstream at a constant rate, but because the flow past the release sites was constantly changing, the constant-in-time release strategy

resulted in a time-varying ratio of tagged fish per unit discharge. To estimate the release concentration of fish it was assumed that fish became uniformly mixed within the bolus of water passing the release site over a tidal period, and then used the total volume of water that passed downstream of WGA during a 25-hour period to estimate the total volume of that bolus of water. This approach yields the following equation for estimating the concentration of no-behavior study fish per unit discharge for every 15-minute interval during each study:

$$\text{Concentration study fish}_{15\text{min}} = \frac{Release\ Rate\left(\frac{fish}{hr}\right) \times 25(hr)}{\sum_{-12.5\ hr}^{+12.5\ hr}(WGA)}$$

Using the concentration time series the no-behavior fish flux into the junction was then estimated as:

$$\text{Fish Flux}_{15\text{min}} = (\text{Fish Carrying Water Flux}_{15\text{min}}) \times (\text{Concentration study fish}_{15\text{min}})$$

For the purpose of this calculation a release rate of 1 fish per hour was assumed, but because the fish flux signal is used to calculate normalized probability mass functions (PMFs) and normalized cumulative distribution functions (CDFs) the actual release rate does not matter as long as it is sufficiently large to minimize rounding errors when these parameters are estimated.

It is important to note that this procedure does not account for the effects of entrainment in Steamboat Slough and Sutter Slough for fish released at the City of Sacramento (2008 North Delta Study and 2014 FFGS Study). Because the ultimate goal of this analysis is to try to correct each study's observed diel arrival distribution for the diel balance of water transport into the junction, not accounting for entrainment in Steamboat Slough and Sutter Slough will bias this correction if entrainment in Steamboat Slough and Sutter Slough creates a time-varying change in the concentration of study fish per unit discharge passing Steamboat Slough. Based on the fact that the location of the critical streakline is relatively static in the Steamboat Slough and Sutter Slough junctions over a range of Sacramento River flows (see Section 3.3.4), it was expected that the change in fish density of water passing Steamboat and Sutter sloughs to be relatively static as well, so it was anticipated that the bias caused by not accounting for upstream entrainment would be minimal.

ESTIMATING THE FISH ARRIVAL-LIGHT DISTRIBUTION FROM THE NO-BEHAVIOR FISH FLUX

Estimated 15 minute no-behavior fish flux time series was used for each study period to compute a sample of discrete light values corresponding to the light values when hypothetical non-behavior tagged fish arrived in the junction. This calculation resulted in a sample of discrete "observations" that represent the estimate of the effect of the diel distribution of water transport into the junction. This no-behavior light distribution was then used to correct the observed fish-arrival light distribution derived from each study's fish track segments for the diel distribution of water transport to estimate movement bias of each study's fish sample.

The sample of discrete no-behavior light values for each study was computed by taking the estimated no-behavior fish flux for each 15-minute period during each study's fish arrival period, multiplying this fish flux number by 100 and rounding to the nearest integer, and then adding this number of discrete samples of that 15-minute period's light value to the study's no-behavior light sample. This procedure is summarized in the following pseudo code:

```
for i=first fish arrival time : to : last fish arrival time
        nSamples = round( 100 * fishFlux(i) )
```

```
        lightValue = lightSignal(i)
        newDiscreteValues = ones(nSamples,1) * lightValue
        discreteLightArray = [discreteLightArray;newDiscreteValues]
    end
```

For each study this computation was performed using the light and fish flux 15-minute time series starting with the value closest in time to when the first study fish arrived in the center of the junction, and ending with the value closest in time to when the last study fish arrived in the center of the junction. Because there was an interruption in the continuous fish releases during the 2011 BAFF Study this process was carried out separately for each continuous release period and the resulting no-behavior samples were concatenated.

The multiplication factor of 100 was used to minimize the effects of rounding errors when using the continuous flux values to computing a discrete number of samples to add for every 15-minute increment. Because the no-behavior samples are used to compute normalized distributions the length of the no-behavior sample does not need to match that of the observed arrival-light sample.

A probability mass function and discrete cumulative distribution function for every study's observed fish arrival-light sample and estimated no-behavior arrival-light sample was calculated using standard techniques and consistent bin boundaries for every study. The first bin included all samples with light values ranging from 0 to 1 W/m^2 and includes all times when there was no measured light. The second bin included all periods from 1 W/m^2 to 50 W/m^2 which we classified as crepuscular periods, and subsequent bins progressed in 100 W/m^2 intervals. Fifty W/m^2 was chosen as the upper limit for crepuscular periods as this value usually corresponded with the amount of light present 1 hour after morning civil twilight, and 1 hour before evening civil twilight (**Figure 3.7-4**).

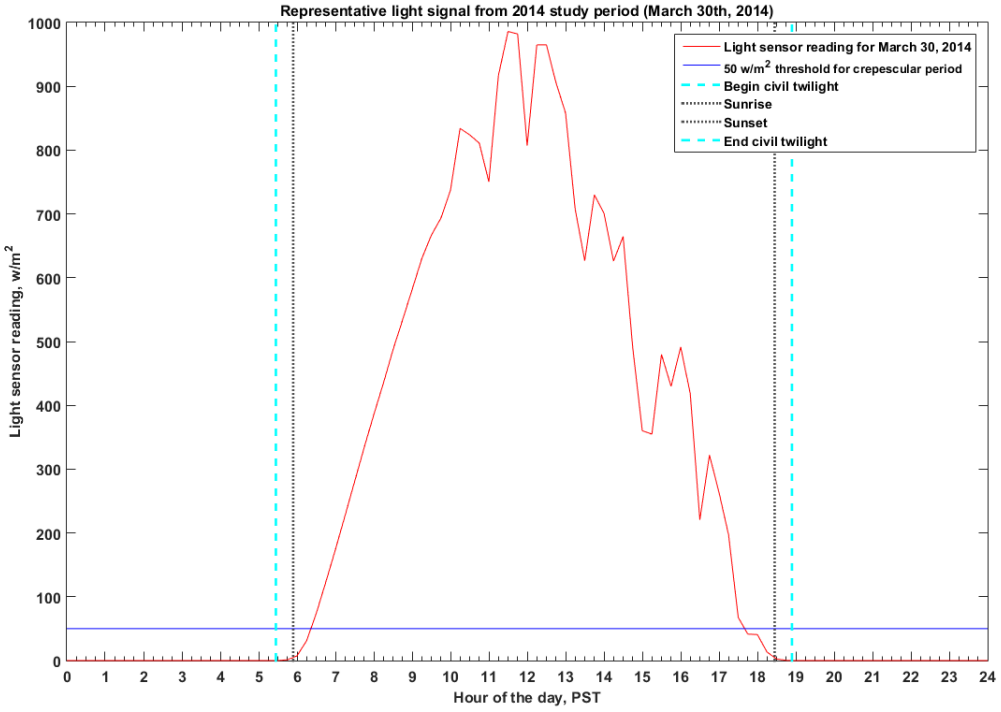

Note: Red line indicates the measured light during a single 24-hour period during the 2014 FFGS study. The vertical dashed blue lines indicate the start and end of civil twilight, the dotted black lines indicate sunrise and sunset, and the horizontal blue line indicates the 50 W/m^2 boundary for crepuscular periods.

Figure 3.7-4 Example Measured Light Signal from a 24-Hour Period during the 2014 FFGS Study

ESTIMATING THE DIEL MOVEMENT BIAS FOR EACH STUDY GROUP

For each study group the estimated no-behavior arrival-light PMF was subtracted from the observed fish arrival-light PMF to derive an estimate of the difference between the diel distribution of water transport into the junction and the diel distribution of fish arrival in the junction. This difference is referred to as the "diel movement bias" for each study group, which was used as an estimate of the study fish's bias towards moving or holding under each light condition. A diel movement bias was also calculated using the light signal PMF from each study period to illustrate the difference between estimates of diel movement bias based solely on photoperiod and estimates of diel movement bias that also account for water transport.

ESTIMATING RATIOS OF DARK TO LIGHT FLOW AND FLUX

In order to illustrate the differences between the ratio of light and dark water transport over the course of each study period a time series showing the ratio of dark-to-light water transport and the ratio of estimated dark-to-light no-behavior fish flux was computed for each study period. These ratios were computed for each quantity of interest by dividing the total dark period flux by the total light period flux occurring within a rolling 24-hour window. The results for each window were reported at the time step corresponding to the center of the window. This process is summarized as:

$$\text{Ratio}_{15\text{min}} = \frac{\sum_{-12hrs}^{+12\ hrs}(Dark\ Flux)}{\sum_{-12hrs}^{+12\ hrs}(Light\ Flux)}$$

3.7.3 RESULTS

PHOTOPERIOD AND DIEL WATER TRANSPORT DISTRIBUTION

There were significant differences between photoperiod and discharge conditions during each study period. The Georgiana Slough barrier studies occurred around the time of the spring equinox and had a more even balance between dark and light periods than the 2008 North Delta Study, which was conducted midwinter when there were more dark and crepuscular hours than daylight hours (**Table 3.7.1**, **Figure 3.7.1**). The differences between study photoperiods were compounded by differences in Sacramento River discharge during each study period; the 2011 and 2012 BAFF studies occurred during periods when the Sacramento River rarely or never reversed downstream of Georgiana Slough (**Figure 3.7-5**), while the 2008 North Delta Study and the 2014 FFGS Study occurred during low discharge periods when the Sacramento River regularly reversed downstream of Georgiana Slough (**Figure 3.7-1**).

Table 3.7-1 Percentage of Each Study Period Occurring during Dark and Crepuscular Periods

Study	Percent of Study Occurring during Dark Periods	Percent of Study Occurring during Dark or Crepuscular Periods
2008 North Delta Study	52	67
2011 BAFF Study	44	51
2012 BAFF Study	46	55
2014 FFGS Study	46	54

Because of the higher discharges during the BAFF studies, the balance of water transport between dark and light periods was predominantly determined by photoperiod, while this ratio was driven by tidal period-diurnal period phasing during the 2008 and 2014 studies. The 2008 North Delta Study occurred during one of the midwinter time periods when large ebb tides occurred at night and large flood tides occurred during the day (**Figure 3.7-1**, left panel), while the 2014 study took place as this phasing was reversing, with larger ebbs occurring during the day and larger floods taking place at night (**Figure 3.7-1**, right panel). As a result of these factors the 2011 and 2011 study periods began with an even ratio of dark to light transport that shifted in favor of daytime transport as photoperiod increased (**Figure 3.7-6**, bottom panels), the 2014 study started with an even ratio of dark to light transport that shifted in favor of daytime transport as tidal-diurnal phasing shifted (**Figure 3.7-6**, top-right panel), and the 2008 study occurred during a period when the majority of the water transport through the Georgiana Slough junction occurred at night (**Figure 3.7-6**, bottom-left panel).

These trends in dark/light water transport carried over to the estimated no-behavior fish flux time series computed for each study. The ratio of estimated dark fish flux to light fish flux for the 2011 and 2012 studies was almost identical to the ratio of water transport (**Figure 3.7-7**), while the effects of tidal period-diurnal period coupling observed during the 2008 study and 2014 study were enhanced by the correction factor that was used to account for reduced fish densities on flood tides (**Figure 3.7-8**). The effect of the correction factor is due to the fact that ebb tide water transport is generally much greater than flood tide water transport, so that adding a correction factor which reduces the magnitude of flood tide transport increased the effect of the dark or light bias of ebb tide transport for each period.

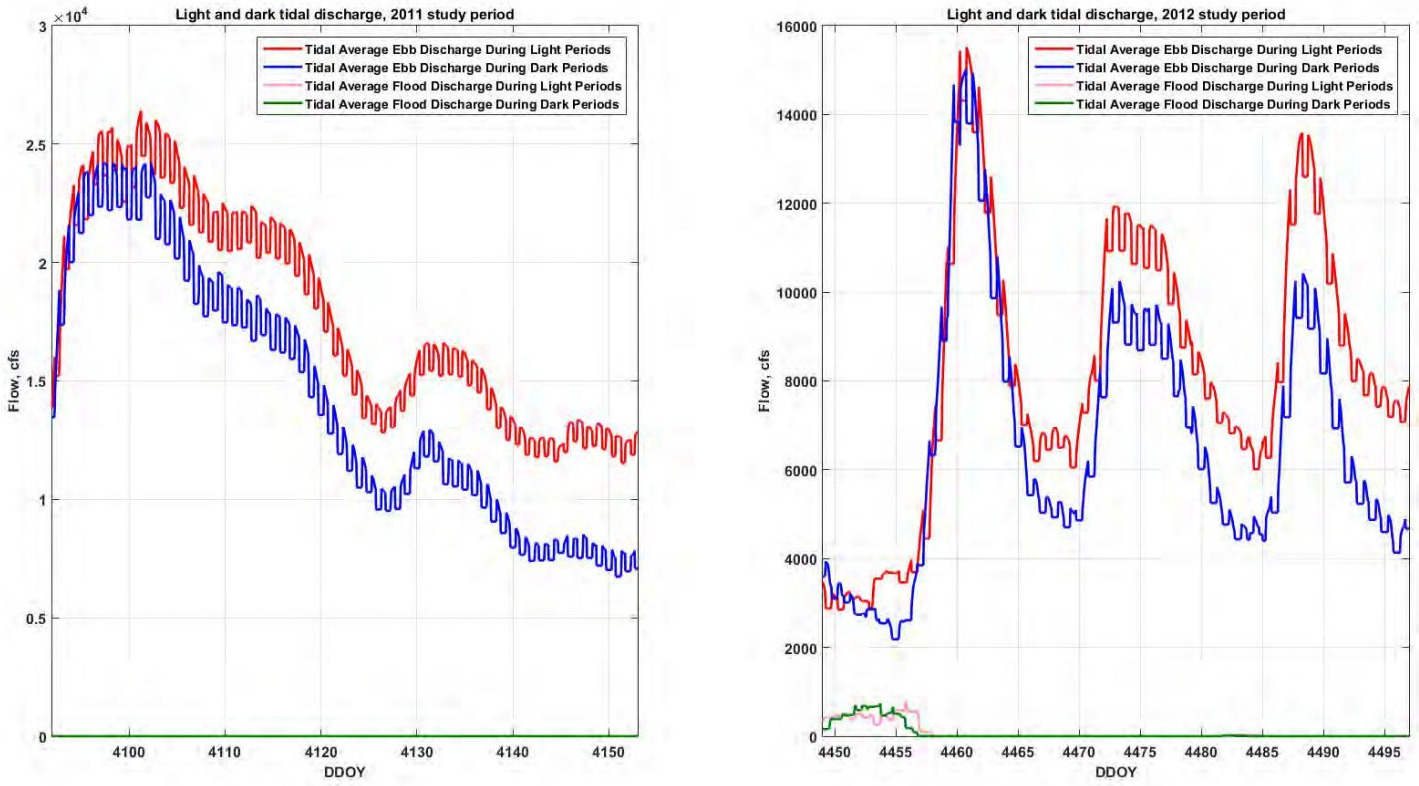

Note: Red lines indicate tidal average ebb tide flow during light periods, blue lines indicate tidal average ebb tide flow during dark periods, green lines purple lines indicate tidal average flood tide flow during light periods and green lines indicate tidal average flood tide flow during dark periods. Note that during the majority of these study periods Sacramento River discharge was high enough that reversing flow did not occur in the Georgiana Slough junction. The balance between light and dark flow was predominantly determined by photoperiod during these studies.

Figure 3.7-5 Time Series Showing Light and Dark Tidal Flow in the Georgiana Slough Junction for the 2011 and 2012 BAFF Studies

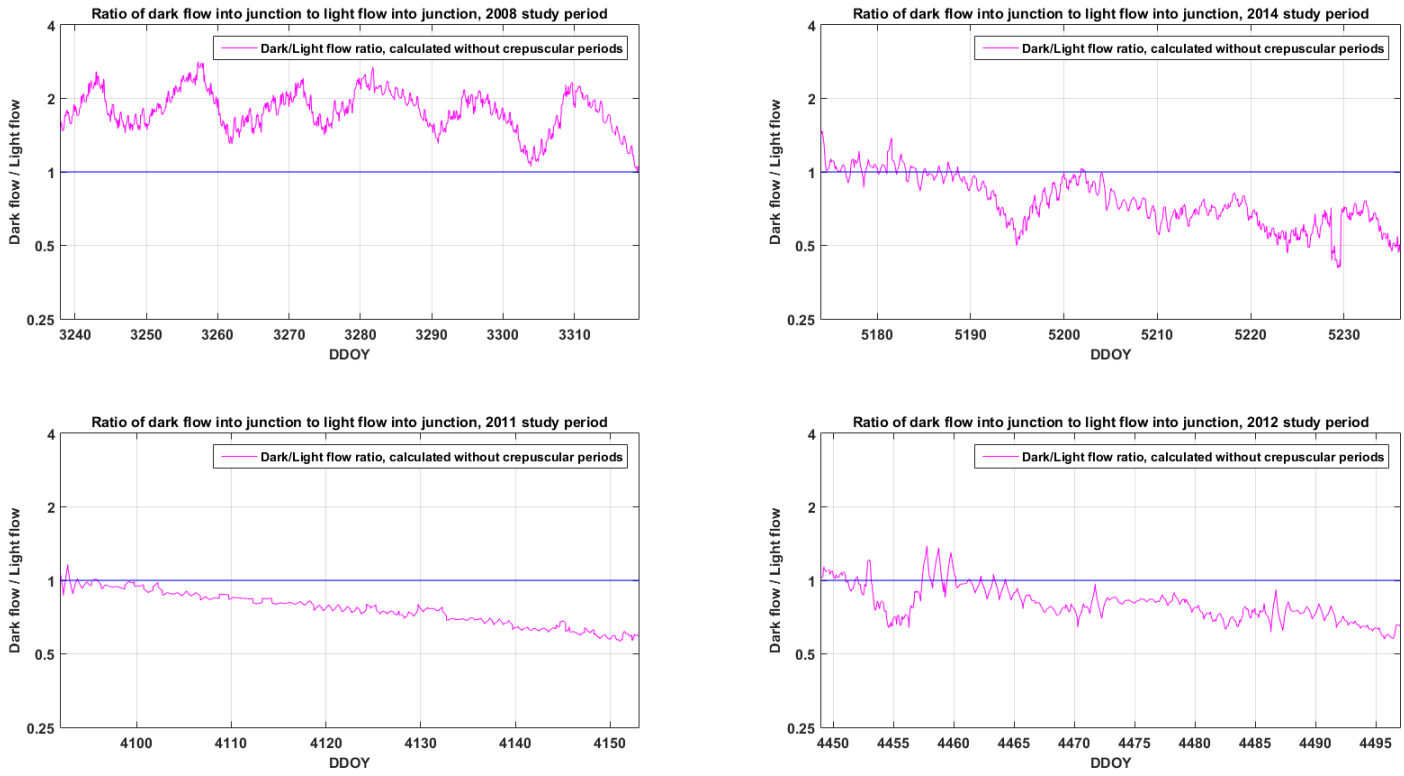

Figure 3.7-6 **24-hour Ratio of Dark Flow into the Georgiana Slough Junction to Light Flow into the Georgiana Slough Junction during each Study Period**

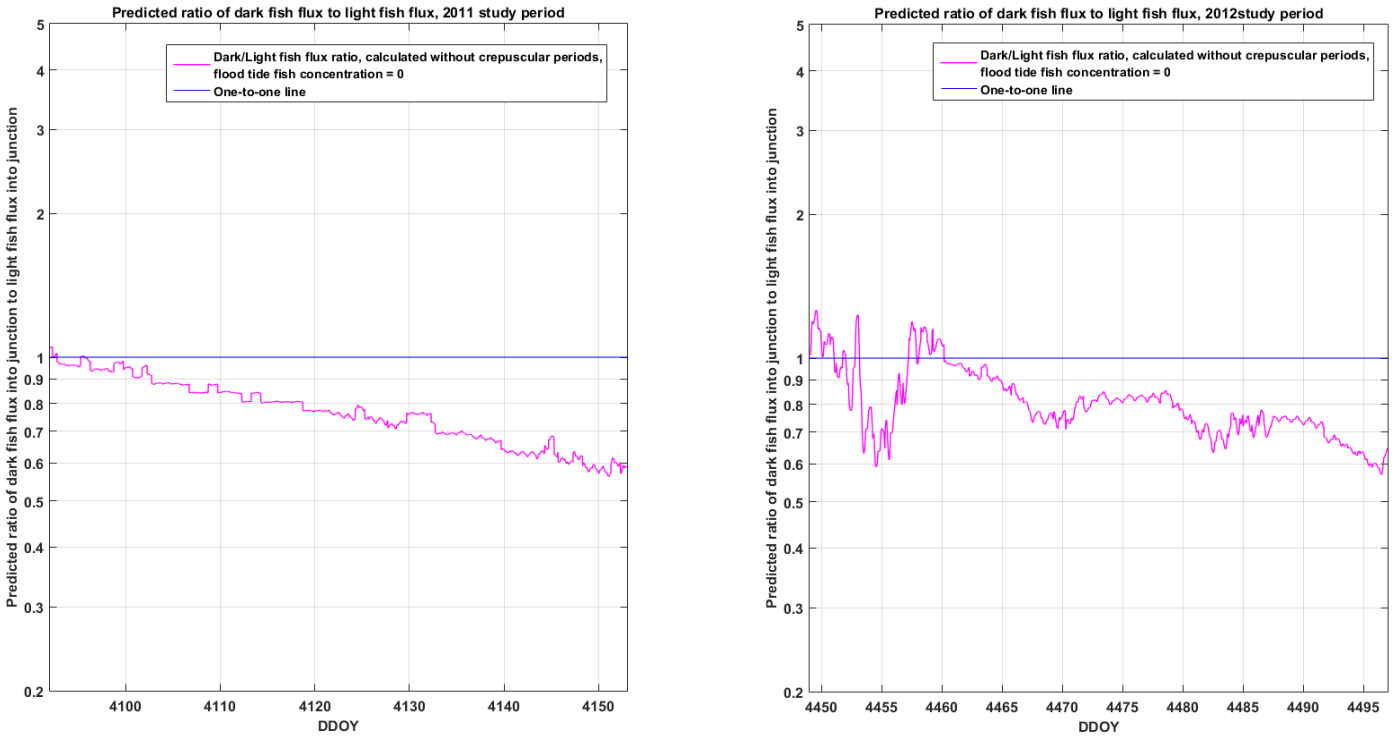

Note: Time series showing the predicted 24-hour ratio of no-behavior study fish flux into the Georgiana slough junction for fish released below Steamboat Slough (2011 and 2012 BAFF studies). Note that the predictions indicate that more fish should enter the junction during daylight periods than during dark periods.

Figure 3.7-7 Predicted Ratio of Dark to Light Fish Flux into the Georgiana Slough Junction for the 2011 and 2012 BAFF Studies

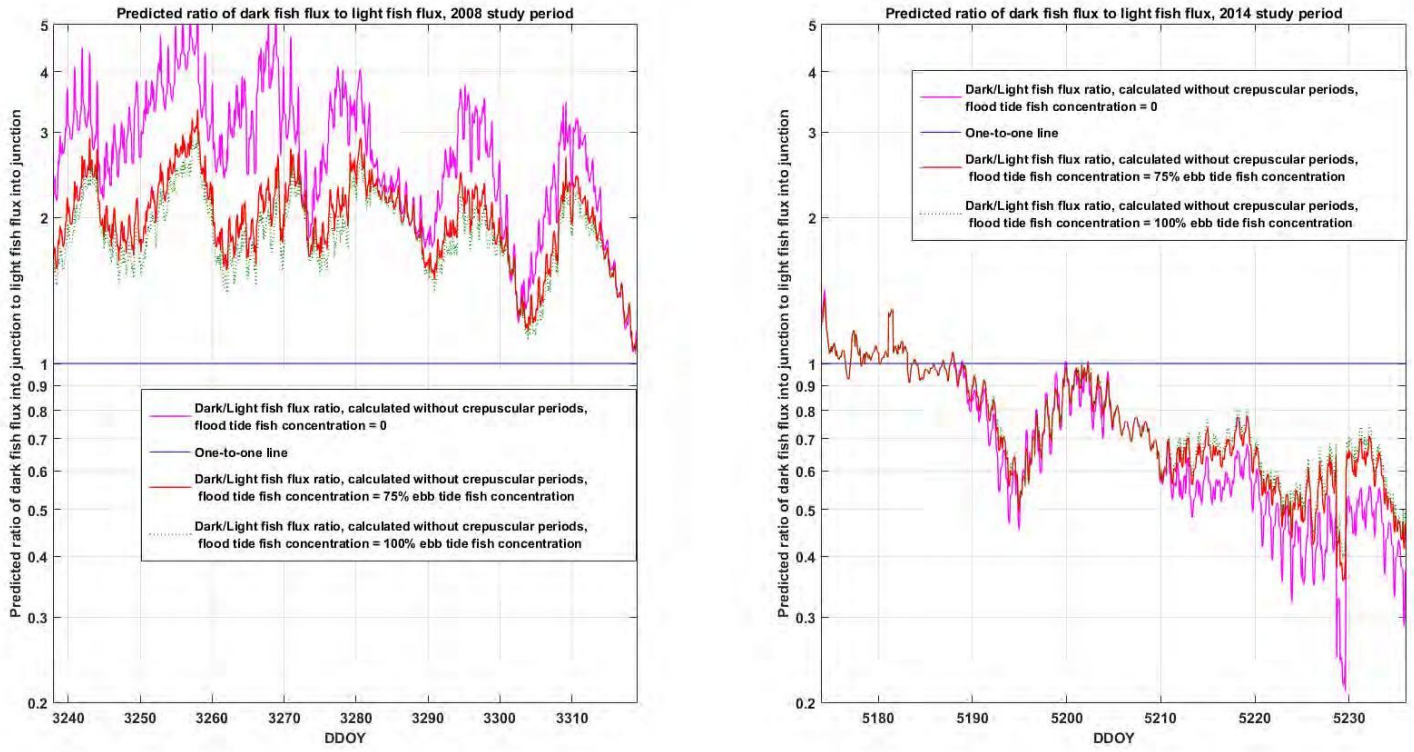

Note: Time series showing the predicted 24-hour ratio of no-behavior study fish flux into the Georgiana slough junction for fish released at the City of Sacramento (2008 North Delta Study and 2014 FFGS Study). The three time series show how the assumption about the density of tagged fish present in flood tides affects the predicted ratio of dark to light fish flux; because of the phasing between the solar day and tidal day the assumed flood tide fish density can affect predictions about how many study fish will arrive during dark and light periods. Note that because the tidal-solar phasing is reversed between the 2008 and 2014 study period these studies have opposite dark/light transport biases.

Figure 3.7-9 Predicted ratio of Dark to Light Fish Flux into the Georgiana Slough Junction for the 2008 North Delta Study and 2014 FFGS Study

FISH ARRIVAL-LIGHT DISTRIBUTIONS AND ESTIMATED DIEL MOVEMENT BIAS

Correcting the observed fish arrival light-distribution for the diel balance of water transport into the Georgiana Slough junction changed the interpretation of the diel movement bias for all study groups. When each study's fish arrival-light distribution was compared to the measured light distribution it appeared that fish from the 2008 study and the 2012 study were displaying a bias towards moving during fully dark periods while fish from the 2011 and 2014 study did not appear biased towards movement during dark periods (**Figure 3.7-9** and **Figure 3.7-10**, bottom panels). However, when the transport corrected diel movement bias using the estimated no-behavior fish arrival-light sample was calculated, the results indicated that fish from the 2008 study were negatively biased towards movement during fully dark periods, but positively biased towards moving during crepuscular periods (defined as < 50 W/m^2) and low light periods (50 W/m^2 – 150 W/m^2) (**Figure 3.7-9** and **3.7-10**, top left panel). Similarly, when increased daytime water transport during the 2011, 2012, and 2014 studies was corrected for the results indicated that fish from these studies were positively biased towards moving during fully dark periods, and fish from the 2014 BAFF Study were also positively biased towards moving during crepuscular periods (**Figure 3.7-9** and **3.7-10**, top panels).

COMPARISON BETWEEN SACRAMENTO RELEASES AND STEAMBOAT SLOUGH RELEASES

Fish released at the City of Sacramento arrived in the Georgiana Slough junction more frequently than water transport would predict during crepuscular and low light conditions during both the 2008 and 2014 studies, and less frequently than water transport would predict during full daylight conditions (**Figure 3.7-10**, upper left panel). While fish from the 2008 North Delta Study were not positively biased towards moving during fully dark periods, they did display a positive bias towards moving during the two lowest light periods (0-50 W/m^2 and 50-150 W/m^2), and fish from both studies consistently displayed a near-zero or negative bias during full daylight. In contrast, fish released at Steamboat Slough displayed a positive bias towards moving in fully dark conditions, but no bias towards moving during crepuscular or low light conditions, and an inconsistent response to daylight conditions (**Figure 3.7-10**, upper right panel).

These results indicate that fish from both release sites are positively biased towards moving in fully dark periods, but only fish from the City of Sacramento release site are positively biased towards moving during crepuscular and low light periods. Additionally, only fish released at the City of Sacramento are consistently negatively biased towards moving in full daylight conditions. Based on these results Hypothesis H4 was accepted.

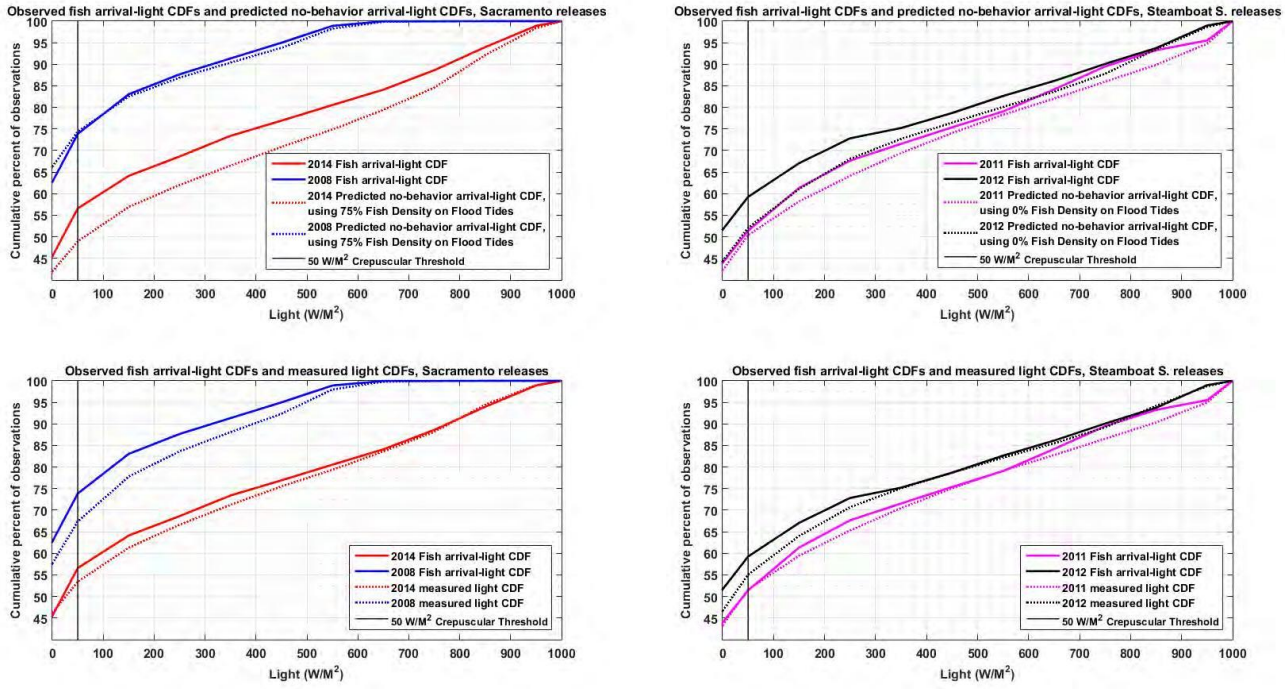

Note: Cumulative distribution functions comparing observed fish arrival-light distributions and predicted no-behavior fish arrival light-distributions (top panels) and comparing observed fish arrival-light distributions and measured light distributions (bottom panels). The distributions for fish released at the City of Sacramento are shown in the left panels, and the distributions for fish released below Steamboat Slough are shown in the right panels.

Figure 3.7-9 CDF Functions Comparing Observed Fish Arrival-Light Distributions, Measured Light Distributions, and Predicted No-Behavior Fish Arrival Light Distributions

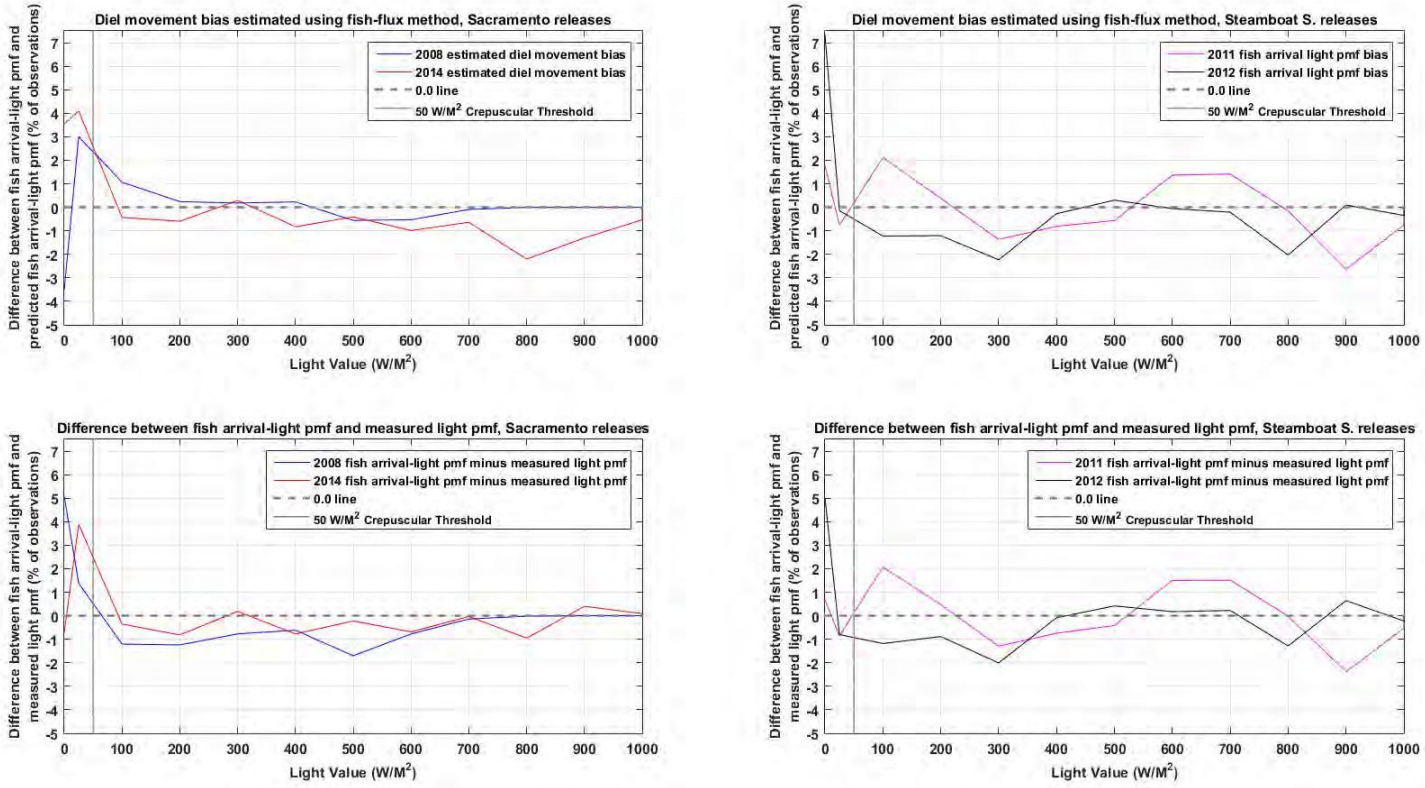

Note: Estimated diel movement bias calculated using the predicted no-behavior fish arrival light-distributions (top panels) and calculated using the measured light distributions (bottom panels). The distributions for fish released at the City of Sacramento are shown in the left panels, and the distributions for fish released downstream of Steamboat Slough are shown in the right panels.

Figure 3.7-10 Estimated Diel Movement Bias for Fish Released at the City of Sacramento and for Fish Released downstream of Steamboat Slough

4 INTEGRATION AND SYNTHESIS OF RESULTS

4.1 HYDRODYNAMICS AND CRITICAL STREAKLINE

The FFGS is expected to be most effective when the critical streakline is to the left of the downstream tip of the FFGS (when in the On position); in 2014, the downstream tip of the FFGS was 35 m (115 ft) from the left bank of the Sacramento River. The critical streakline generally was to the right of the downstream end of the FFGS in the On position at high flow > 364 m^3/s (> 12,850 cfs: 100% of time to the right) and mid-flow 288 to 364 m^3/s (10,170 – 12,850 cfs: 84% of time to the right). However, even during low river discharges 0 to 288 m^3/s (0 – 10,170 cfs), the critical streakline peak was to the right of the downstream end of the FFGS 69 percent of the time. For all river discharges combined, the critical streakline was to the left of the downstream end of the FFGS in the On position about 21percent of the study period; thus, it was expected that the actual effectiveness of the FFGS would produce protection efficiency of less than or equal to 21 percent.

For the low river discharges, the critical streakline is left of the FFGS in the On position 31percent of the time. In Section 3.2, it was shown that the juvenile Chinook salmon entrainment rate into Georgiana Slough ranged from 31.9 percent (Day, On) to 57.5 percent (Night, On) during low river discharges. However, Section 3.1 results showed that during high approach velocity (> 0.25 m/s [> 0.82 ft/s]) conditions, protection efficiency was significantly greater with FFGS On (79.0%) compared to FFGS Off (55.4%). These results suggest that the FFGS possibly protected fish even when the critical streakline was right of the FFGS downstream end and flow was in the downstream direction.

Under all flow conditions, the critical streakline was located to the right of the FFGS downstream end for a majority of the time. The most common FFGS segment that juvenile Chinook salmon crossed the FFGS line was in Segment 9 – the segment immediately past the FFGS' downstream end (see **Figure 3.1-14**). These results suggest that juvenile Chinook salmon may have been deterred or guided, but when passing the FFGS's downstream end a substantial proportion were entrained through Segment 9 into Georgiana Slough.

It appears that the FFGS may not have extended sufficiently into the Sacramento River channel to produce high juvenile Chinook salmon deterrence during many river discharges. For example, if the FFGS had extended to 50 m (164 ft) from the left bank, **Figure 3.3-27** suggests that more than 50 percent of the experimental period the critical streakline would not have been located to the right of the FFGS downstream end. Given the inverse relationship between critical streakline position and discharge, it is expected that the FFGS would have been more effective for the conditions encountered in 2011. Greater effectiveness for the 2014 observed conditions would have required an FFGS extending 110 m (361 ft) farther downstream to the shoal separating Georgiana Slough from the Sacramento River, virtually blocking the entire Georgiana Slough junction.

4.2 FFGS PERFORMANCE

GLM modelling found little difference between overall entrainment into Georgiana Slough with FFGS On compared to Off (see Section 3.4, "Generalized Linear Modeling of Fish Fates", **Table 3.4-1**). However, under intermediate flows (7,062-14,125 cfs) the FFGS reduced entrainment by 20 percent (or by five percentage points, from 19.1 percent entrainment with FFGS Off to 23.9 percent with FFGS On; Romine et al. 2016). Furthermore, 62 percent (1,013) of the fish that passed the FFGS (1613) did so during intermediate flows. These results contrast with that of the univariate Hypothesis H16 protection efficiency test that had a minimal sample size (**Table 3.2-2**)

which showed that there was a significant improvement in protection efficiency with the FFGS On compared to Off. For the univariate test of Hypothesis H16, only individuals that passed within 10 m (33 ft) of the FFGS were aggregated into samples (see DWR 2012: 2-6) by the conditions present when the juvenile Chinook salmon arrived. All juvenile Chinook salmon that were placed in a given sample were nearest the FFGS when the FFGS was in the same operating state (On or Off), light conditions, and the approach velocity (see definitions in Section 3.1.1) was the same.

GLM modelling showed that entrainment into Georgiana Slough was lowest at high flows (> 14,125 cfs) during the day, but that the FFGS actually increased entrainment probability at high flows (see Section 3.4, subsection "Entrainment Summary"). In contrast, the test for Hypothesis H16 conducted during higher flows showed that when the approach velocity was ≥ 0.25 m/s (≥ 0.82 ft/s) protection and overall efficiency were significantly greater with the FFGS On compared to Off (Section 3.1, "Floating Fish Guidance Structure Performance", **Table 3.1-7**). The univariate test results could be explained by juvenile Chinook salmon having insufficient time, or being reluctant, to swim under the FFGS at higher discharge, and that at higher flows water deceleration upstream of the FFGS caused by the FFGS structure, could have been detectable at a greater distance from the barrier compared to lower flows. Also, as previously discussed, greater discharge leads to the critical streakline being closer to the left bank of the Sacramento River, which would be expected to increase the performance of the FFGS. However, as suggested in Section 3.4.4 "Discussion" in relation to GLM results, the high discharge could have resulted in greater turbulence created by the downstream end of the FFGS, which would explain the pattern of increased entrainment with the FFGS in the On position. Such turbulence was not evident from the examination of ADCP data (see "Influence of FFGS on the Velocity Field" subsection in Section 3.3.3 "Results), but should be investigated further using thermal camera data collected during this study. Therefore, the results of the GLM and univariate analyses suggested that various hydrodynamic phenomena were of importance: at lower flows, flood tides were important and the high percentage of fish entering Georgiana Slough was facilitated by the critical streakline being to the right of the FFGS, reducing its effectiveness; at intermediate flows, FFGS performance improved, possibly because of the increased detection and lower ability to swim under the barrier as discussed previously, in addition to more favorable critical streakline position; at high flows, the critical streakline position was further improved relative to the FFGS, but possible turbulence increased entrainment into Georgiana Slough.

Visual cues from the FFGS and its associated equipment may have caused some of the observed patterns in entrainment. As described in Section 3.4.4 "Discussion" for GLM results, entrainment tended to be slightly greater by night than by day. This could have been partly the result of fish being guided by the buoy line, which would have been more visible by day than by night (and which did not change position, in contrast to the FFGS); in addition, the greater nighttime flood tides could have given a greater tendency for entrainment at night. Entrainment into Georgiana Slough was highest during low flows (< 7,062 cfs) at night when the FFGS was in the Off position (63.9%; **Table 3.4-1**) and, as previously discussed, was lowest during high flows (> 14,125 cfs) during the day when the FFGS was Off . Under intermediate flows and with the FFGS On: 1) entrainment was decreased by 3.4 percentage points at night, but 2) entrainment was decreased by 6.9 percentage points during the day. These results also suggest that a visual cue may assist juvenile Chinook salmon in detecting and avoiding the FFGS.

4.3 THROUGH-DELTA TRAVEL TIME AND SURVIVAL

As noted in Section 3.2 "Survival Model", entrainment into Georgiana Slough was similar between FFGS On and Off and because the FFGS likely did not alter reach-specific survival and did not appear to reduce overall entrainment consistently over the entire study, Delta-wide survival was unaffected by operation of the FFGS. Modes of release group-specific travel time distributions via Georgiana Slough and the interior Delta ranged from 4.59 to 7.44 days (Section 3.2. "Survival Model"). Travel times were similar for juvenile Chinook salmon travelling via the Sacramento River and Sutter or Steamboat sloughs (modes were 2.33 to 5.56 days). Consistent with other years (Perry et al. 2010; Perry et al. 2012), survival in the Georgiana Slough route was lower than that the Sacramento River, and Sutter or Steamboat sloughs (**Figure 3.2-11)**. At least two mechanisms may provide understanding for these findings: 1) the longer travel time through the Georgiana Slough route provided more time for predators to encounter a juvenile Chinook salmon and thus the total number of predator encounters was likely higher; and 2) the Georgiana Slough route is longer and therefore a juvenile Chinook salmon may pass more predators before reaching Chipps Island than a juvenile Chinook salmon outmigrating via the other routes. If more predators are passed along the out-migratory route this would hypothetically increase the number of encounters a juvenile Chinook salmon would experience. In addition, these two mechanisms could work synergistically: more predators to pass and a longer time for these predators to locate a juvenile Chinook salmon and thus the number of encounters could be additionally increased. Juvenile salmonids entering the interior Delta have relatively more alternative channels that they could enter as a result of entrainment on flood flows (e.g., Old River, Fisherman's Cut, and False River), which would also increase travel time and the potential for increased predation. There was evidence that higher discharge was positively related to higher survival (**Figure 3.2-13)** and this finding is consistent with those from previous north Delta studies (Newman 2003; Perry 2010) and from the San Joaquin River-Old River divergence: higher discharge in 2011 produced the lowest predation rate (10.1%) observed in the four years of study (DWR 2015a).

The average downstream velocity (V_{Down}) of juvenile Chinook salmon released near the City of Sacramento was 0.17 m/s (0.56 ft/s) in 2014 (**Figure 3.2-3A**). The V_{Down} was similar to the juvenile Chinook salmon transit speed for individuals traveling past the San Joaquin River-Old River divergence in 2009, 0.16 m/s (0.52 ft/s) (SD = 0.16 m/s [0.52 ft/s]; DWR 2015a). Both of these values are much smaller than the reported transit speed reported by DWR (2015a) for juvenile Chinook salmon traveling past the San Joaquin River-Old River divergence during other Spring seasons that were monitored in 2010, 2011, and 2012 (**Table 4-1**). The reason for this was attributed to the findings that Average Channel Velocity (ACV) was positively correlated with transit speed ($r = 0.583$, $P < 0.0001$, DWR 2015a: D-13). In addition, ACV is positively correlated with discharge (**Table 4-1**). So, one possible explanation for the value of V_{Down} observed from the juvenile Chinook salmon released in the Sacramento River is that the low flow in the 2014 study area (Section 3.3, **Figure 3.3-8** "Discharge Measured in the Sacramento River at Freeport during the Study Period") caused the low velocity reported, 0.17 m/s (0.56 ft/s). It is hypothesized that in years that exhibit significantly higher flows the V_{Down} will significantly increase. As noted in Section 3.2.3 "Discussion" for Section 3.2 "Survival Model", the through-Delta transit times of juvenile Chinook salmon during the spring 2014 FFGS study were actually considerably lower than transit times observed during studies undertaken at similar discharge in winter of other years (e.g., Perry 2010). This could reflect a greater tendency for the older smolts released in the spring during the FFGS study of 2014 to rapidly migrate, as they may be in a more advanced state of physiological preparedness for ocean entry.

Table 4-1 Juvenile Chinook Salmon Transit Speed for Tags Determined to Have Not Been Eaten during Experimental Fish Release Periods at the Head of Old River, 2009-2012					
Treatment – Year	Discharge Minimum (cfs)	Discharge Maximum (cfs)	Mean ACV (m/s) (SD)	Mean Transit Speed (m/s) (SD) Tags Not Eaten	Statistical Grouping of Transit Speed
BAFF – 2009	-1,300	2,070	0.186 (0.269)	0.162 (0.164)	a
BAFF – 2010	913	3660	0.510 (0.131)	0.290 (0.106)	b
No barrier – 2011	4,250	8,040	0.605 (0.034)	0.535 (0.153)	c
Rock barrier – 2012	210	2,620	0.371 (0.076)	0.261 (0.163)	b

Notes: ACV = average channel velocity; BAFF = bio-acoustic fish fence; cfs = cubic feet per second; m/s = m per second; SD = standard deviation

Source: Reprinted from DWR (2015a) Table D-13. Original data compiled by Turnpenny Horsfield Associates 2013.

4.4 COMPARISONS BETWEEN YEARS: BAFF AND FFGS

The FFGS study in 2014 marked the third year of study of engineering solutions to reduce juvenile salmonid entrainment into Georgiana Slough. In 2011, a "wet" water year occurred in the Sacramento River watershed, resulting in high river discharge (**Figure 4-2**). A BAFF was deployed at the Sacramento River-Georgiana Slough divergence, with test fish releases over 16 March–28 March and 15 April–15 May. The overall efficiency was high with the BAFF Off, 73.4 percent (DWR 2012), and the percentage of fish remaining in the Sacramento River was similarly high (77.7%; Perry et al. 2014). That result suggested juvenile Chinook salmon remained in the Sacramento River in very high numbers without the assistance of the BAFF. Nevertheless, when the BAFF was in operation the overall efficiency was 90.8 percent and the percentage entrained was 92.3 percent, with both of these improvements being significant (DWR 2012; Perry et al. 2014). The same was true for protection efficiency; E_P was 72.7 percent with the BAFF Off and 90.5 percent with the BAFF On and that improvement was statistically significant. The GLM analysis of 2011 results showed position on the cross-section of the river as a juvenile Chinook salmon approached the barrier was the most important determinant of entrainment into Georgiana Slough (Perry et al. 2014). In addition, the critical streakline was closer to the left bank of the Sacramento River than in any other year studied. Therefore a larger percentage of juvenile Chinook salmon than in any other year would have remained in the Sacramento River if they acted only as neutrally buoyant particles. So, when stimulated to move away from the entrance to Georgiana Slough by the BAFF there was significant improvement in protection and overall efficiency. This resulted in the GLM showing that after the cross-stream position, operation of the BAFF was the next most important variable in determining the probability of juvenile Chinook salmon being entrained into Georgiana Slough.

In 2012, a "below normal" water year occurred in the Sacramento River watershed. This resulted in an intermediate river discharge among the three years studied (DWR 2015b, **Figure 4-1**) and reversals of flows were recorded in the Sacramento River during that Spring's study period. A BAFF was deployed at the Sacramento River-Georgiana Slough divergence and, similar to 2011, juvenile Chinook salmon overall efficiency was high with the BAFF Off, 75.2 percent; 75.6 percent of fish remained in the Sacramento River (DWR 2015b). As with 2011, juvenile Chinook salmon thus remained in the Sacramento River in very high numbers without the assistance of the BAFF. However, when the BAFF was in operation the overall efficiency was 89.7 percent, 88.2 percent of fish remained in the Sacramento River, and these improvements were significant. The same was true

for protection efficiency; E_P was 74.6 percent with the BAFF Off and 87.9 percent with the BAFF On and that improvement was statistically significant. The GLM analysis again showed cross-stream position had the greatest influence on entrainment into Georgiana Slough followed by critical streakline position, and the BAFF status. This supported the hypothesis test that overall and protection efficiencies were significantly improved by BAFF operation. So, as with 2011, when stimulated to move away from the entrance to Georgiana Slough, juvenile Chinook salmon moved sufficiently that there was significant improvement in overall and protection efficiencies, and a reduction in the percentage of fish entering Georgiana Slough. Because cross-stream position and critical streakline position were identified as the two most important factors influencing probability of entrainment into Georgiana Slough, a lower cost barrier (the FFGS that is the subject of this report) was identified for evaluation as a structure to positively change fish cross-stream position relative to the critical streakline.

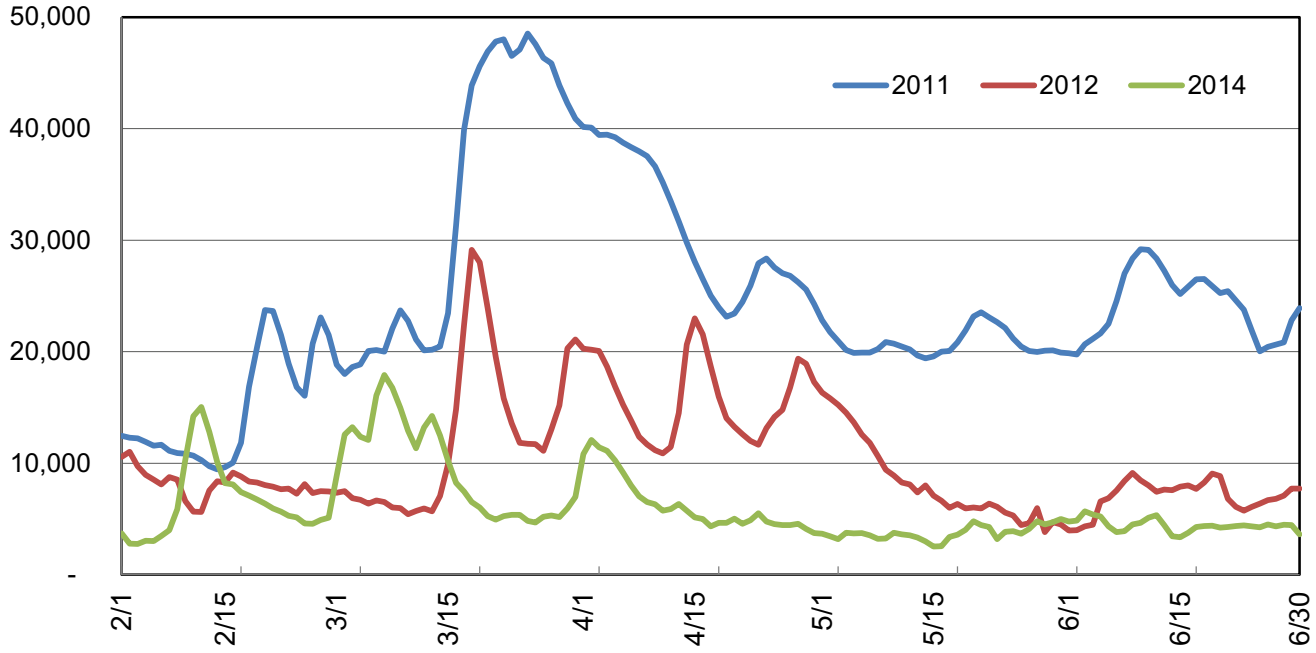

Figure 4-1. Mean Daily Discharge (cfs) in the Sacramento River Upstream of the Sacramento River-Georgiana Slough Divergence, 2011, 2012, and 2014

In 2014, a "critically dry" water year occurred in the Sacramento River watershed. This resulted in the lowest river discharges among the three years studied (**Figure 4-3**) and twice daily reversals of flow were seen in the Sacramento River during much of the Spring's study period (**Figure 3.4-2**). As described in Section 3.1 "Floating Fish Guidance Structure Performance," juvenile Chinook salmon overall efficiency with the FFGS Off was 73.8 percent; 77.3 percent of fish remained in the Sacramento River (Section 3.4 Generalized Linear Modeling of Fish Fates; Romine et al. 2016). When the FFGS was in operation the overall efficiency increased to 77.7 percent and this improvement produced a P-value of 0.0516; however, as previously discussed, the GLM analysis showed that the efficacy of the FFGS varied depending on discharge—suggesting that the FFGS overall efficiency and effectiveness may require further study. When the juvenile Chinook salmon that were determined to have been eaten by predatory fishes were removed from the dataset, protection efficiency (E_P) with the FFGS Off was 54.6 percent. This result showed a higher proportion of juvenile Chinook salmon were entrained into Georgiana Slough than in any other study year. The critical streakline was closer to the right bank of the Sacramento River during the 2014 Spring than in any other year studied; as previously discussed, this contributed substantially to

the high E_P and proportion of fish entrained into Georgiana Slough that was observed with the FFGS Off—the conditions encountered during the testing were outside of those for which the FFGS had been designed. The protection efficiency with the FFGS On was 72.8 percent and that improvement was statistically significant, showing (from the univariate analyses) that the FFGS was reducing entrainment into Georgiana Slough. The GLM analysis demonstrated that the entrainment reduction was limited to intermediate discharge conditions.

4.5 PREDATION AND PREDATORY FISHES

The FFGS did not increase predation when On compared to Off, which was also the case for the BAFF in 2011 (DWR 2012) and 2012 (DWR 2015b). The survival analysis for the 2011 BAFF study showed that in 2011, a high flow year, juvenile Chinook salmon moved through the Sacramento River-Georgiana Slough divergence area with high survival rates: 1) 0.979 - BAFF Off; and 2) 0.975 – BAFF On (DWR 2012: Table 3-17). These were the highest survival rates observed during the study. At least three mechanisms could explain the relatively high survival rate in 2011: 1) a high water volume made the search volume for predators much larger; 2) fast transit velocity by juvenile Chinook salmon reduced predator encounter rate; and 3) juvenile Chinook salmon were distributed away from the river margins and more toward the river center. Transit velocity and distance traveled are important elements affecting predation rate of juvenile salmonids (Anderson et al. 2005). Higher velocity areas near the river center would have had increased energetic costs for predatory fishes, which appeared to be reflected in predators spending less time nearer the river center than in lower river discharge habitats (DWR 2012). This last mechanism was also supported by the 2D tracks of juvenile Chinook salmon that were determined to have been eaten in 2011; very little time was spent away from river margins by predatory fishes that had ingested a juvenile Chinook salmon. Predation was low, probably as a result of high discharge, and the predation rate was not affected by BAFF operation in 2011.

The survival analysis for the 2012 BAFF showed that at the intermediate river discharge observed in 2012 (**Figure 4-2**), juvenile Chinook salmon moved through the Sacramento River study area with slightly lower survival rates than recorded in 2011: 1) 0.933 - BAFF Off; and 2) 0.929 – BAFF On (DWR 2015b: Table 3-17). At least two mechanisms could explain this higher predation rate: 1) lower flows than 2011 occurred in 2012 and thus turbidity was lower, allowing increased prey detection distances for visual predators; 2) predation rates were also greater upstream of the experimental area, suggesting higher predation rates throughout the Sacramento River and north Delta ecosystem compared to 2011 (which also could have been partly due to turbidity or other factors); and 3) lower discharges compared to 2011 allowed predators to spend more time away from the river margins and more time in open water habitats – this may have increased predator-prey encounter rates. This last mechanism was supported by the 2D tracks of juvenile Chinook salmon that were determined to have been eaten in 2012 and the tracks of tagged predatory fishes; more time was spent in open water by predatory fishes that had ingested juvenile Chinook salmon.

For the FFGS, in 2014, the predation rate on juvenile Chinook salmon was 0.15 (survival = 0.85) with the FFGS in the On position and 0.17 (survival = 0.83) in the Off position (Section 3.6.1, subsection “Hypotheses H5 and H6 (Resampling Analysis)”). As with the BAFF in 2011 and 2012, the operation of the FFGS did not appear to affect predation. Higher predation rates in 2014 than in 2011 and 2012 would have been expected on the basis of lower discharge resulting in longer travel time and greater distance traveled (both increasing the risk of predation through greater potential for predator encounter). As previously described in Section 4.3, the results for 2014 illustrated the apparent positive relationship between discharge and survival, as has been observed in other years in the north Delta (Newman 2003; Perry 2010). Longer travel time and distance could have increased predator-

prey encounter rates by providing less time in the area for predators to locate the juvenile Chinook salmon. In addition, turbidity was shown to be an important variable predicting predation probability in 2014, and could have explained differences between years as turbidity is typically positively related to discharge (e.g., Cloern et al. 2011); lower turbidity in 2014 would have increased predation risk to juvenile Chinook salmon from visual predators.

The results for Georgiana Slough contrast with the situation at the Head of Old River, where the BAFF appeared to increase the predation rate when On compared to Off in 2009 under low river discharges (DWR 2015a: Table 6-49 and Figure 3-1). It is hypothesized that the primary difference between the Sacramento River-Georgiana Slough and the San Joaquin River-Old River divergences was the configuration of the channel in the vicinity of the barriers. At the Head of Old River, the BAFF guided juvenile Chinook salmon toward an area of high predatory fish density (as shown by hydroacoustic monitoring), referred to as the "scour hole," which also exhibited eddies across a variety of river discharges; high rates of predation were inferred from a high concentration of stationary juvenile Chinook acoustic tags compared to other areas in the vicinity, presumably a result of defecation by predatory fishes. At Georgiana Slough, both the BAFF and the FFGS guided fish away from shore and into open water habitat in the center of the river. These results suggest that it is important to consider the site-specific channel configuration at each location where a behavioral guidance structure is proposed, particularly with respect to in-water structures with which predatory fishes could be associated. In this regard, there was evidence for a relatively high proportion of predation events occurring near the Offshore Downstream Dolphin to which the FFGS was tethered, suggesting that this structure could have provided advantageous habitat for predatory fishes (also suggested by DIDSON monitoring results, which showed density at the end-FFGS DIDSON was significantly greater with FFGS On compared to FFGS Off).

Standardized angling results showed some support for the hypothesis that increased water temperature is correlated with increased *Micropterus* spp. catch (Section 3.6.4, "Standardized Angling (Hypothesis H9)"). Also, a positive correlation between predatory fishes (> 30 cm [> 12 in] TL) density and water temperature was observed from active hydroacoustic data at the Head of Old River (DWR 2015a: 6-89), which may have reflected seasonal migration (e.g., of striped bass). In 2013, standardized angling at the San Joaquin River-Old River divergence showed a highly significant correlation (Spearman's rank coefficient = 0.5023; P-value = 0.0005) between temperature and catch per unit effort for predatory fishes in the vicinity of the Head of Old River (Kennedy et al. 2014: 20). Increased catch rates of predatory fishes also occurred with increasing water temperature during standardized angling associated with the study of the SRWTP (Robertson-Bryan, Inc. et al. 2013). These results from Georgiana Slough, the Head of Old River, and the area near the SRWTP all suggest that greater water temperature increases the likelihood of predation, possibly as result of increased bioenergetics requirements and seasonal migrations. This emphasizes the need to consider through-Delta or near-barrier survival in the context of ambient conditions, for comparisons across seasons (e.g., with-barrier conditions in Spring versus no-barrier control in Winter) are likely to be confounded by differing predation rates.

This page intentionally left blank.

5 RECOMMENDATIONS

5.1 TEST ADDITIONAL FFGS CONFIGURATIONS AND CONSIDER DYNAMIC DEPLOYMENT AS PART OF A COST-BENEFIT ANALYSIS

The principal finding of the present study was that the FFGS showed some potential to be effective, but only at intermediate discharges (7,062-14,125 cfs) (Romine et al. 2016). Only one configuration of the FFGS was tested, and it is recommended that additional study be made of different lengths, depths, and angles of FFGS, as undertaken for FFGS in other locations (Scruton et al. 2003). As described in Section 3.4.4 "Discussion of the GLM of Fish Fates," a different FFGS configuration might produce different results. Based on the analysis at three ranges of river discharges, the FFGS was not fully effective during the study because its design placement assumed critical streakline conditions that were essentially not present. Placement of a longer FFGS further into the Sacramento River and further downstream to deter fish with the observed Type 2 fish behavior described in Section 3.5 "Spatial Analysis of Fish Distribution and Behavior," could potentially increase barrier effectiveness, based on hydrodynamic entrainment alone. The importance of critical streaklines is a key advance in the knowledge of juvenile salmonid entrainment into Delta river junctions such as Georgiana Slough (Perry et al. 2016: Box 3). In addition, the observation that 41 of 173 (23.7%) juvenile Chinook salmon entrained into Georgiana Slough went under the FFGS suggests that a deeper FFGS (3 m instead of 1.5 m [10 ft instead of 5 ft]) is worthy of investigation (with 1.5 m- [5-ft] sections being included as necessary to accommodate shallow water depths near the river bank). An analysis is recommended to determine the optimal distance the FFGS should extend from the left bank versus the added cost that would be incurred for the benefit gained from a longer barrier. This recommended analysis should take into consideration the velocity fields present in the 2011, 2012, and 2014 as examples of a wide range of discharge regimes that can occur in the Winter/Spring at the Sacramento River-Georgiana Slough divergence. The recommended testing of various FFGS configurations described previously should also consider dynamic deployment of the FFGS, such as angling the FFGS closer to the bank at high flows in order to limit the potential for increased entrainment created by turbulence.

5.2 TEST A COMBINATION OF FFGS AND BAFF

Given that the FFGS showed limited potential to be effective for reducing entrainment of juvenile salmonids into Georgiana Slough, whereas the BAFF tested in 2011 and 2012 reduced entrainment by around 50-67 percent, an experiment to test the FFGS in combination with a BAFF is recommended at the Sacramento River-Georgiana Slough area. The FFGS was most successful at reducing entrainment into Georgiana Slough at intermediate river discharges (7,062 to 14,125 cfs). Section 3.1 showed the FFGS created a significant improvement in protection efficiency (mean with FFGS On = 79.0%), when approach velocities were high (≥ 0.25 m/s [≥ 0.82 ft/s]). The BAFF produced significant improvement in protection efficiency at both low and high velocities. However in 2011, the BAFF produced the highest protection efficiencies (mean = 97.5%; DWR 2012: Table 3.2-6) under low (<0.25 m/s [< 0.82 ft/s]) across-barrier velocity conditions. In addition, in 2012 the BAFF produced significantly higher protection efficiencies (mean = 94.2%; DWR 2015b: Table 3.2-10) in low approach-velocity conditions. Thus, a FFGS upstream of a BAFF may provide an effective combination to reduce entrainment under a wide range of river discharges. Furthermore, it is difficult to predict what the discharge magnitudes will be in the Sacramento River in Spring. A combination of barriers would have the potential advantage of protecting juvenile salmonids under a wide range of flows. As described in the previous section, dynamic deployment of the FFGS (e.g., changing the barrier angle with changing flow) is also recommended as part of such an evaluation.

5.3 USE CRITICAL STREAKLINE ANALYSIS TO ASSESS OPTIMAL ENGINEERING SOLUTIONS AT MULTIPLE JUNCTIONS

As described in detail in the "Junction Suitability for Non-Physical Barriers and Alternative Junctions" portion of Section 3.3.4 "Recommendations and Conclusions," preliminary analyses indicate that the critical streakline locations at the Sutter and Steamboat sloughs divergences from the Sacramento River are considerably more predictable than the critical streakline location at Georgiana Slough. This, in theory, should make barrier optimization at these junctions relatively more straightforward than at Georgiana Slough: given the goal of increased through-Delta survival, the upstream location of these barriers relative to Georgiana Slough leads to the recommendation that engineering solutions to increase entrainment into these junctions be studied. The combination of engineering solutions at these junctions together with an FFGS or BAFF at Georgiana Slough is recommended to be studied for potential effects on overall through-Delta survival.

5.4 ASSESS PREDATION AND PREDATORY FISHES WITH NO BARRIER AND OVER A LONG-TERM BARRIER DEPLOYMENT; LIMIT IN-WATER STRUCTURE SIZE

The present study's findings suggest three main recommendations related to predation and predatory fishes. First, the effects of an FFGS (or BAFF or other technology) on predation and predatory fish behavior are recommended to be compared to a true no-barrier control (i.e., no in-water structure), because the presence of the FFGS in the water may influence predation and predatory fish behavior regardless of treatment (FFGS On versus FFGS Off). Logistically, it is challenging to provide a true no-barrier control during the same year as a barrier is tested, because installation and removal generally cannot be done rapidly and would be expensive to do multiple times in one year. This suggests that it may be more fruitful to conduct a no-barrier control experiment in a different year, at the same time of the year, for purposes of comparison. Such data already exist, for the 2008 North Delta Study (Romine et al. 2013) and these data would serve as an initial point of comparison for predation analyses, given comparable flow conditions. Additional years of no-barrier studies are recommended. The second recommendation related to predation and predatory fishes is to conduct a study of predation and predatory fish behavior during long-term deployment because, as discussed in the "Conclusions" section of Section 3.6.7 "Discussion," the 2014 experimental protocol for testing effects on juvenile salmonid routing (i.e., switching the FFGS treatment every day) may have deterred predatory fish from inhabiting the vicinity of the FFGS as frequently as they may during constant FFGS On conditions. Lastly, it is recommended that, to the extent possible, future deployments of an FFGS avoid having large in-water structures such as the three-pile dolphin (Offshore Downstream Dolphin) to which the FFGS was tethered, as the results from the present study suggest that such structures may be associated with a relatively high proportion of predation events.

6 REFERENCES

Adams, N. S., D. W. Rondorf, S. D. Evans, and J. E. Kelly. 1998. Effects of Surgically and Gastrically Implanted Radio Transmitters on Growth and Feeding Behavior of Juvenile Chinook Salmon. *Transactions of the American Fisheries Society* 127:128–136.

Agresti, A., and B. A. Coull. 1998. Approximate is Better than 'Exact' for Interval Estimation of Binomial Proportions. *The American Statistician* 52:119–126.

Akaike, H. 1973. Information Theory as an Extension of the Maximum Likelihood Principle. In *Second International Symposium on Information Theory*, eds. B. N. Petrov and F. Csaki, 267–281. Budapest, Hungary: Akademiai Kiado.

Aksnes, D. L., and J. Giske. 1993. A Theoretical Model of Aquatic Visual Feeding. *Ecological Modeling* 67(2):233–250.

Anderson, J. J., E. Gurarie, and R. W. Zabel. 2005. Mean Free-Path Length Theory of Predator–Prey Interactions: Application to Juvenile Salmon Migration. *Ecological Modelling* 186(2):196–211.

Beakes, M., J. Moore, N. Retford, R. Brown, J. Merz, and S. Sogard. 2012. Evaluating Statistical Approaches to Quantifying Juvenile Chinook salmon Habitat in a Regulated California River. *River Research and Applications*. DOI: 10.1002/rra.2632.

Beamish, F. W. H. 1978. Swimming Capacity. In *Fish Physiology,* Vol. VII, *Locomotion,* ed. W. S. Hoar and D. J. Randall, 101–187. New York: Academic Press.

Bever, A. J., and M. L. MacWilliams. 2015 (in press). *Factors Influencing the Calculation of Periodic Secondary Circulation in a Tidal River*.

Blackman, S. 1986. Multiple Target Tracking with Radar Applications. Dedham, MA: Artech House.

Blake, A., and M. Horn. 2006. Acoustic Tracking of Juvenile Chinook Salmon Movement in the Vicinity of Georgiana Slough, Sacramento River, California—2003 Study Results. Draft report. Sacramento, CA: U.S. Geological Survey.

Blake, A. R., and J. R. Burau. 2015 (in press). *Acoustic Tracking of Juvenile Salmon in Clarksburg Bend, California*. Prepared for the U.S. Geological Survey.

Blake, A. R., and M. J. Horn. 2015a (in press). *Acoustic Tracking of Juvenile Chinook Salmon Movement in the Vicinity of the Delta Cross Channel, Sacramento River, California, 2001 Study Results*. Prepared for the U.S. Geological Survey.

———. 2015b (in press). *Acoustic Tracking of Juvenile Chinook Salmon Movement in the Vicinity of Georgiana Slough, Sacramento River, California, 2003 Study Results*. Prepared for the U.S. Geological Survey.

Bowen, M. D. 1996. Habitat Selection and Movement of a Stream-Resident Salmonid in a Regulated River and Tests of Four Bioenergetics Optimization Models. Ph.D. dissertation. Utah State University, Logan.

Bowen, M. D., and R. Bark. 2010. *2010 Effectiveness of a Non-Physical Fish Barrier at the Divergence of the Old and San Joaquin Rivers (CA).* Technical memorandum 86-68290-10-07. Denver, CO: U.S. Bureau of Reclamation.

Bowen, M. D., S. Hiebert, C. Hueth, and V. Maisonneuve. 2012. 2009 Effectiveness of a Non-Physical Fish Barrier at the Divergence of the Old and San Joaquin Rivers (CA). Technical Memorandum 86-68290-09-05. US Department of the Interior, Bureau of Reclamation, Technical Service Center, Denver, CO.

Brandes, P. L., and J. S. McLain. 2001. Juvenile Chinook Salmon Abundance, Distribution, and Survival in the Sacramento–San Joaquin Estuary. In *Contributions to the Biology of Central Valley Salmonids*, ed. R. L. Brown. *Fish Bulletin* 179(2):39–136. California Department of Fish and Game.

Brown, M. L., M. S. Allen, and T. D. Beard. 2012. Data Management and Statistical Techniques. In *Fisheries Techniques*, ed. A. V. Zale, D. L. Parrish, and T. M. Sutton, 15–77. Third edition. Bethesda, MD: American Fisheries Society.

Buchanan, R. A., J. R. Skalski, P. L. Brandes, and A. Fuller. 2013. Route Use and Survival of Juvenile Chinook Salmon through the San Joaquin River Delta. *North American Journal of Fisheries Management* 33(1):216–229.

Buckley, J. and B. Kynard. 1985. *Vertical Distribution of Juvenile American Shad and Blueback Herring During the Seaward Migration in the Connecticut River.* Massachusetts Cooperative Fishery Research Unit, Department of Forestry and Wildlife Management, Amherst, Massachusetts.

Burnham, K. P., and D. R. Anderson. 2002. Model Selection and Multimodal Inference: A Practical Information Theoretic Approach. Second edition. New York: Springer.

Burwen, D. L., S. J. Fleischman, and J. D. Miller. 2007. *Evaluation of Dual-Frequency Imaging Sonar for Estimating Fish Size in the Kenai River.* Alaska Department of Fish and Game, Fishery Data Series No. 07 44. Anchorage, AK.

Calcagno, V., and C. de Mazancourt. 2010. glmulti: An R Package for Easy Automated Model Selection with (Generalized) Linear Models. *Journal of Statistical Software* 34(12):29.

California Department of Fish and Wildlife. 2015. *State & Federally Listed Endangered & Threatened Animals of California.* Biogeographic Data Branch, California Natural Diversity Data Base, 14 p.

California Department of Water Resources. 2012. *2011 Georgiana Slough Non-Physical Barrier Performance Evaluation Project Report*. Sacramento, CA: Bay-Delta Office.

———. 2014 (February). Experimental Design and Study Plan for the 2014 Georgiana Slough Floating Fish Guidance Structure Performance Evaluation. Prepared by AECOM. Sacramento, CA: Bay-Delta Office, South Delta Branch.

———. 2015a (April). An Evaluation of Juvenile Salmonid Routing and Barrier Effectiveness, Predation, and Predatory Fishes at the Head of Old River, 2009–2012. Prepared by AECOM, ICF International, and Turnpenny Horsfield Associates. Sacramento, CA and Ashurst, UK.

———. 2015b (December). *2012 Georgiana Slough Non-Physical Barrier Performance Evaluation Project Report.* Prepared by AECOM. Sacramento, CA: Bay-Delta Office, South Delta Branch.

California Irrigation Management Information System. 2014. Statewide Integrated Pest Management Program. California Weather Data for CIMIS Station 140, Twitchell Island, University of California, Department of Agriculture and Natural Resources, Davis.

California State University, Chico, CA. 2015. Sacramento River. A Guide to Recreation and Public Access. Geographical Information Center. Accessed September 19, 2015. http://www.sacramentoriver.org/sac_river_atlas.php

Cash, K. M., N. S. Adams, T. W. Hatton, E. C. Jones, and D. W. Rondorf. 2002. Three-Dimensional Tracking to Evaluate the Operation of the Lower Granite Surface Bypass Collector and Behavioral Guidance Structure during 2000. Report by U. S. Geological Survey for U. S. Army Corps of Engineers, contract W68SBV00104592, Walla Walla, WA.

Cavallo, B., P. Gaskill, J. Melgo, and S. C. Zeug. 2015. Predicting Juvenile Chinook Salmon Routing in Riverine and Tidal Channels of a Freshwater Estuary. *Environmental Biology of Fishes*. DOI: 10.1007/s10641-015-0383-7.

Cavallo, B., J. Merz, and J. Setka. 2013. Effects of Predator and Flow Manipulation on Chinook Salmon (*Oncorhynchus tshawytscha*) Survival in an Imperiled Estuary. *Environmental Biology of Fishes* 96(2–3): 393–403.

Chapman, E. D., A. R. Hearn, C. J. Michel, A. J. Ammann, S. T. Lindley, M. J. Thomas, P. T. Sandstrom, G. P. Singer, M. L. Peterson, R. B. MacFarlane, and A. P. Klimley. 2013. Diel Movements of Out-migrating Chinook Salmon (*Oncorhynchus tshawytscha*) and Steelhead Trout (*Oncorhynchus mykiss*) Smolts in the Sacramento/San Joaquin Watershed. *Environmental Biology of Fishes* 96(2–3):273–286.

Childers, W. F. 1971. Hybridization of Fishes in North America (Family Centrarchidae). In *Seminar/Study Tour in the U.S.S.R. on Genetic Selection and Hybridization of Cultivated Fishes*. April 19–29 May 1968. Lectures Report of FAO/UNDP(TA), (2926): 360 p. Available: http://www.fao.org/docrep/005/b3310e/B3310E10.htm#ch10. Accessed April 9, 2015.

Chow, V. T. 1959. *Open-Channel Hydraulics*. New York: McGraw-Hill.

Cloern, J. E., N. Knowles, L. R. Brown, D. Cayan, M. D. Dettinger, T. L. Morgan, D. H. Schoellhamer, M. T. Stacey, M. van der Wegen, R. W. Wagner, and A. D. Jassby. 2011. Projected Evolution of California's San Francisco Bay-Delta River System in a Century of Climate Change. *PLoS One* 6(9).

Coyle, S., R. Durborow, and J. Tidwell. 2004. *Anesthetics in Aquaculture*. Available: http://www.aces.edu/dept/fisheries/aquaculture/documents/5864154-3900fs.pdf. Accessed January 2014.

Dauble, D. D., S. M. Anglea, and G. E. Johnson. 1999. *Surface Flow Bypass Development in the Columbia and Snake Rivers and Implications to Lower Granite Dam*. Final Report. Prepared for the U.S. Army Corps of Engineers, Washington, DC.

Deltaboating.com. 2014. Sacramento River Tide Tables. Available: http://www.deltaboating.com/tides/tidesac.html. Accessed January 2014.

DWR. *See* California Department of Water Resources.

Edwards, E. A., G. Gebhart, and O. E. Maughan. 1983. Habitat Suitability Index Information: Smallmouth Bass. U.S. Fish and Wildlife Service. FWS/OBS-82/10.36.

Ehrenberg, J. E., and T. W. Steig. 2003. Improved Techniques for Studying the Temporal and Spatial Behavior of Fish in a Fixed Location. *ICES Journal of Marine Science* 60:700–706.

Faber, D. M., J. Kim, G. R. Ploskey, R. L. Townsend, M. A. Weiland, T. Fu, D. Deng, J. R. Skalski, J. S. Hughes, E. S. Fischer, and R. L. McComas. 2010. *Evaluation of a Behavioral Guidance Structure at Bonneville Dam Second Powerhouse Including Passage Survival of Juvenile Salmon and Steelhead Using Acoustic Telemetry*. Prepared for the U.S. Army Corps of Engineers, under an Interagency Agreement with the U.S. Department of Energy, Contract DE-AC05-76RL01830. PNNL-18753, with Pacific Northwest National Laboratory and W. Richland (eds.), Richland, Washington.

Faber, D. M., G. R. Ploskey, M. A. Weiland, D. Deng, J. S. Huges, J. Kim, T. Fu, E. S. Fischer, T. J. Monter, and J. R. Skalski. 2011. *Evaluation of Behavioral Guidance Structure on Juvenile Salmonid Passage and Survival at Bonneville Dam in 2009.* Final Report (March). Prepared for the U.S. Army Corps of Engineers, under an Interagency Agreement with the U.S. Department of Energy, Contract DE-AC05-76RL01830. PNNL-20338, Pacific Northwest National Laboratory, Richland, Washington.

Ferrari, M. C. O., L. Ranåker, K. L. Weinersmith, M. J. Young, A. Sih, and J. L. Conrad. 2014. Effects of Turbidity and an Invasive Waterweed on Predation by Introduced Largemouth Bass. *Environmental Biology of Fishes* 97(1):79–90.

Fong, D. A., S. G. Monismith, M. T. Stacey, and J. R. Burau. 2009. Turbulent Stresses and Secondary Circulation in a Tidal-Forced Channel with Significant Curvature and Asymmetric Bedforms. *Journal of Hydraulic Engineering* 135:198–208.

Freeman, E. A., and G. Moisen. 2008. Presence-Absence: An R Package for Presence Absence Analysis. *Journal of Statistical Software* 23(11).

Gibson, A. J. F., E. A. Halfyard, R. G. Bradford, M. J. W. Stokesbury, and A. M. Redden. 2015. Effects of Predation on Telemetry-Based Survival Estimates: Insights from a Study on Endangered Atlantic Salmon Juvenile Chinook Salmons. *Canadian Journal of Fisheries and Aquatic Sciences* 72:1–13.

Gingras, M., and M. McGee. 1997 (January). *A Telemetry Study of Striped Bass Emigration from Clifton Court Forebay: Implications for Predator Enumeration and Control*. IEP Technical Report 54. Interagency Ecological Program for the San Francisco Bay/Delta Estuary.

Greenwood, M. F. D. 2014. *Combining Acoustic Tag and Hydrodynamic Data to Assess Velocity Habitat Suitability for Predatory Fishes in the Sacramento–San Joaquin Delta, California*. Poster presented at the 8th Biennial Bay-Delta Science Conference, Sacramento, CA. Available: http://www.eposters.net/pdfs/combining-acoustic-tag-and-hydrodynamic-data-to-assess-velocity-habitat-suitability-for-predatory.pdf. Accessed June 10, 2015.

Gregory, R. S. 1993. Effect of Turbidity on the Predator Avoidance Behaviour of Juvenile Chinook Salmon (*Oncorhynchus tshawytscha*). Can. J. Fish. Aquat. Sci., 50: 241-246.

Grimaldo, L. F., C. M. Peregrin, and R. E. Miller. 2000. Examining the Relative Predation Risks of Juvenile Chinook Salmon in Shallow Water Habitat: the Effect of Submerged Aquatic Vegetation. *IEP Newsletter* 13(1):55–59.

Gross, E. S., M. L. MacWilliams, and W. J. Kimmerer. 2009. Three-Dimensional Modeling of Tidal Hydrodynamics in the San Francisco Estuary. *San Francisco Estuary and Watershed Science* 7(2).jmie_sfews_11011. Available: http://escholarship.org/uc/item/9rv243mg.

Grothues, T. M., and K. W. Able. 2010. *Association of Adult Fishes with Piers in the Lower Hudson River: Hydroacoustic Surveys for an Undersampled Resource*. Final Report to the Hudson River Foundation Grant #003/07A. Tuckerton, NJ: Institute of Marine and Coastal Sciences, Rutgers University Marine Field Station.

Guthrie, D. M. and W. R. A. Muntz. 1993. Role of Vision in Behavior. In: Pitcher, T. J. (editor), Behavior of Teleost Fishes, Second Edition. Chapman and Hall, London, pp. 89-128.

Hanson, C. H. 2009 (October). Expert Report of Dr. Charles H. Hanson Per Rule 26(a)(2). *Coalition for a Sustainable Delta et al. v. McCamman et al.*, No. 1:08-CV-00397-OWW-GSA.

Hanson, P., T. Johnson, D. Schindler, and J. Kitchell. 1997. *Fish Bioenergetics 3.0*. Sea Grant Institute, Center for Limnology, University of Wisconsin, Madison.

Hayes, J. W., and I. G. Jowett. 1994. Microhabitat Models of Large Drift-Feeding Brown Trout in Three New Zealand Rivers. *North American Journal of Fisheries Management* 14:710–725.

Hoar, W. S. 1951. The Behaviour of Chum, Pink, and Coho Salmon in Relation to their Seaward Migration. *Journal of the Fisheries Research Board of Canada* 8b(4): 241-263.

Holbrook, C. M., R. W. Perry, P. L. Brandes, and N. S. Adams. 2013 Adjusting Survival Estimates for Premature Transmitter Failure: a Case Study from the Sacramento–San Joaquin Delta. *Environmental Biology of Fishes* 96:165–173.

Horn, M., and A. Blake. 2004 Acoustic Tracking of Juvenile Chinook Salmon Movement in the Vicinity of the Delta Cross Channel. 2001 Study Results. USBR Technical Memorandum No. 8220-04-04. Denver, CO: Technical Service Center.

Hosmer, D. W., and S. Lemeshow. 2000. *Applied Logistic Regression.* New York: John Wiley and Sons.

Itzawa, Y. and T. Takeda. 1982. Respiration of carp under anesthesia induced by mixed bubbling of carbon dioxide and oxygen. Bulletin of the Japanese Society of Science and Fisheries 48(4):489-493.

Iwama, G. K. and P. A. Ackerman. 1994. Anesthesia. In: Biochemistry and Molecular Biology of Fishes, vol. 3. (eds. P.W. Hochachka & T.P. Mommsen), pp. 1-15. Amsterdam: Elsevier Science B.V.

Johnson, E. L., T. S. Clabough, M. L. Keefer, C. C. Caudill, P. N. Johnson, M. A. Kirk, and M. A. Jepson. 2013. *Evaluation of Dual Frequency Identification Sonar (DIDSON) for Monitoring Pacific Lamprey Passage at Fishways of Bonneville and John Day Dams, 2012*. Technical Report 2013-5. Portland, OR: U.S. Army Corps of Engineers.

Johnson, G. E., A. E. Giorgi, and M. W. Erho. 1997. *Critical Assessment of Surface Flow Bypass Development in the Lower Columbia and Snake Rivers.* Completion Report for the U.S. Army Corps of Engineers, Portland and Walla Walla Districts, Washington.

Kennedy, T., M. Cane, M. D. Bowen, and C. LeDoux-Bloom. 2014. *The Temporary Barriers Project: Head of Old River Predatory Fish Study 2013.* Fishery Foundation of California and AECOM technical memorandum prepared for the California Department of Water Resources. Sacramento, CA.

King, R., B. J. T. Morgan, O. Gimenez, and S. P. Brooks. 2010. *Bayesian Analysis for Population Ecology*. Boca Raton, FL: Chapman and Hall.

Kock, T. J., T. L. Liedtke, B. K. Ekstrom, R. G. Tomka, and D. W. Rondorf. 2012. *Behavior and Passage of Juvenile Salmonids during the Evaluation of a Behavioral Guidance Structure at Cowlitz Falls Dam.* U.S. Geological Survey Open-File Report 2012-1030. Washington, DC.

Larimore, R. W. 1952. *Home Pools and Homing Behavior of Smallmouth Bass in Jordan Creek*. Illinois Natural History Survey Biological Notes 28. Illinois Natural History Survey, Urbana.

Larimore, R. W., and D. D. Garrels. 1982. *Seasonal and Daily Microhabitat Selection by Illinois Stream Fishes*. Final Report. Illinois Natural History Survey, Champaign.

Li, T., and J. J. Anderson. 2009. The Vitality Model: A Way to Understand Population Survival and Demographic Heterogeneity. *Theoretical Population Biology* 76:118–131.

Liedtke, T. L., and A. M. Wargo-Rub. 2012. Techniques for Telemetry Transmitter Attachment and Evaluation of Transmitter Effects on Fish Performance. In *Telemetry Techniques: A User Guide for Fisheries Research, ed. N. Adams, J. Beeson, and J. Eiler.* Bethesda, MD: American Fisheries Society.

Liedtke, T. L., J. W. Beeman, and L. P. Gee. 2012. *A Standard Operating Procedure for the Surgical Implantation of Transmitters in Juvenile Salmonids*. U.S. Geological Survey Open-File Report 2012-1267.

Link, W. A., and R. J. Barker. 2010. *Bayesian Inference with Ecological Applications.* London: Elsevier.

Maes, J., A. W. H. Turnpenny, D. R. Lambert, J. R. Nedwell, A. Parmentier, and F. Ollevier. 2004. Field Evaluation of a Sound System to Reduce Estuarine Fish Intake Rates at a Power Plant Cooling Water Inlet. *Journal of Fish Biology* 64:938–946.

Manel, S., H. C. Williams, and S. J. Ormerod. 2001. Evaluating Presence-Absence Models in Ecology: The Need to Account for Prevalence. *Journal of Applied Ecology* 38:921–931.

Martinelli, T. L., H. C. Hansel, and R. S. Shively. 1998. Growth and Physiological Responses to Surgical and Gastric Radio Transmitter Implantation Techniques in Subyearling Chinook Salmon (*Oncorhynchus tshawytscha*). *Hydrobiologia* 371/372:79–87.

Mazerolle, M. J. 2006. Improving Data Analysis in Herpetology: Using Akaike Information Criterion (AIC) to Assess the Strength of Biological Hypotheses. *Amphibia-Reptilia* 27(2):169–180.

McDonald, J. H. 2014. *Handbook of Biological Statistics*. Third edition. Baltimore, MD: Sparky House Publishing.

McMahon, T. E., G. Gebhart, O. E. Maughan, and P. C. Nelson. 1984. *Habitat Suitability Index Models and Instream Flow Suitability Curves: Spotted Bass*. U.S. Fish and Wildlife Service. FWS/OBS-82/10.72.

McQuivey, R.S. 1973. Summary of turbulence data from rivers, conveyance channels, and laboratory flumes. Geological Survey Professional Paper 802-B. U.S. Geological Survey, Washington DC. Available: http://pubs.usgs.gov/pp/0802b/report.pdf. Accessed July 10, 2015.

Michel, C., J. Notch, S. Hayes, and S. Lindley. 2014. *Predator Densities and Associated Salmonid Smolt Mortality around Water Diversions*. Paper presented at 8th Biennial Bay-Delta Science Conference, Sacramento, CA.

Miranda, J., R. Padilla, J. Morinaka, J. DuBois, and M. Horn. 2010. *Release Site Predation Study*. Sacramento: California Department of Water Resources.

Moffatt & Nichol. 2014 (January 6). *Georgiana Slough Floating Fish Guidance Structure Basis of Design*. Walnut Creek, CA. Prepared for the California Department of Water Resources, Bay-Delta Office, South Delta Management.

Moyle, P. B. 2002. *Inland Fishes of California*. Second edition. Berkeley: University of California Press.

Mulligan, K. 2014 (December). An Analysis of Partial-Depth, Floating, Impermeable Guidance Structures for Downstream Fish Passage at Hydroelectric Facilities. Hydro Research Foundation, Evergreen, Colorado. Final Report

Muthukumarana, S., C. J. Schwarz, and T. B. Swartz. 2008. Bayesian Analysis of Mark-Recapture Data with Travel Time-Dependent Survival Probabilities. *The Canadian Journal of Statistics* 36:5–28.

National Marine Fisheries Service. 2009 (June 4). Biological Opinion and Conference Opinion on the Long-Term Operations of the Central Valley Project and State Water Project. Southwest Regional Office, Long Beach, CA.

Newman, K. B. 2003. Modelling Paired Release-Recovery Data in the Presence of Survival and Capture Heterogeneity with Application to Marked Juvenile Salmon. *Statistical Modelling* 3:157–177.

Niiler, P. P., A. S. Sybrandy, K. Bi, P. Poulain and D. Bitterman. 1995. Measurements of the water-following capability of holey-sock and TRISTAR drifters. *Deep Sea Research Part I: Oceanographic Research Papers* 42(11):1951-1964.

Niiler, P., and J. D. Paduan. 1995. Wind-Driven Motions in the Northeast Pacific as Measured by Lagrangian Drifters. *Journal of Physical Oceanography* 25:2819–2830.

NMFS. *See* National Marine Fisheries Service.

Nobriga, M. L., and F. Feyrer. 2007. Shallow-Water Piscivore-Prey Dynamics in California's Sacramento–San Joaquin Delta. *San Francisco Estuary and Watershed Science* 5. Available: http://repositories.cdlib.org/jmie/sfews/vol5/iss2/art4.

Ohlmann, J. C., P. F. White, A. L. Sybrandy, and P. P. Niiler. 2005. GPS-Cellular Drifter Technology for Coastal Ocean Observing Systems. *Journal of Atmospheric and Oceanic Technology* 22:1,381–1,388.

Perry, R. W. 2010. *Survival and Migration Dynamics of Juvenile Chinook Salmon (*Oncorhynchus tshawytscha*) in the Sacramento–San Joaquin River Delta*. Doctor of Philosophy dissertation, University of Washington, Seattle.

Perry, R. W., P. L. Brandes, J. R. Burau, A. P. Klimley, B. MacFarlane, C. Michel, and J. R. Skalski. 2013. Sensitivity of Survival to Migration Routes Used by Juvenile Chinook Salmon to Negotiate the Sacramento–San Joaquin River Delta. *Environmental Biology of Fishes* 96:381–392.

Perry, R. W., P. L. Brandes, J. R. Burau, P. T. Sandstrom, and J. R. Skalski. 2015. Effect of Tides, River Flow, and Gate Operations on Entrainment of Juvenile Salmon into the Interior Sacramento–San Joaquin River Delta. *Transactions of the American Fisheries Society* 144(3):445-455.

Perry, R. W., J. G. Romine, N. S. Adams, A. R. Blake, J. R. Burau, S. V. Johnston, and T. L. Liedtke. 2014. Using a Non-physical Behavioural Barrier to Alter Migration Routing of Juvenile Chinook Salmon in the Sacramento–San Joaquin River Delta. *River Research and Applications* 30(2):192–203.

Perry, R. W., J. G. Romine, S. J. Brewer, P. E. LaCivita, W. N. Brostoff, and E. D. Chapman. 2012. *Survival and Migration Route Probabilities of Juvenile Chinook Salmon in the Sacramento–San Joaquin River Delta during the Winter of 2009–10.* U.S. Geological Survey Open-File Report 2012-1200. U.S. Geological Survey, Reston, VA.

Perry, R. W., J. R. Skalski, P. L. Brandes, P. T. Sandstrom, A. P. Klimley, A. Ammann, and B. MacFarlane. 2010. Estimating Survival and Migration Route Probabilities of Juvenile Chinook Salmon in the Sacramento–San Joaquin River Delta. *North American Journal of Fisheries Management* 30(1):142–156.

Perry, R. W., R. A. Buchanan, P. L. Brandes, J. R. Burau, and J. A. Israel. 2016. Anadromous Salmonids in the Delta: New Science 2006–2016. *San Francisco Estuary and Watershed Science* 14(2).

Piper, R. G., I. B. McElwain, L. E. Orme, J. P. McCraren, L. G. Fowler, and J. R. Leonard. 1982. *Fish Hatchery Management*. Reprinted by the American Fisheries Society in cooperation with the U.S. Fish and Wildlife Service, Bethesda, MD. 517 p.

Plumb, J. M., N. S. Adams, R. W. Perry, C. M. Holbrook, J. G. Romine, A. R. Blake, and J. R. Burau. 2015 (in press). *Diel Activity of Patterns of Juvenile Late-Fall Chinook Salmon with Implications for Operation of a Gated Water Diversion in the Sacramento–San Joaquin River Delta*. River Research and Applications.

Price, V. E., P. J. Auster, and L. Kracker. 2013. Use of High-Resolution DIDSON Sonar to Quantify Attributes of Predation at Ecologically Relevant Space and Time Scales. *Marine Technology Society Journal* 47(1):33–46.

R Core Team. 2014. R: A Language and Environment for Statistical Computing. R Foundation for Statistical Computing, Vienna, Austria. Available: http://www.R-project.org/. Accessed July 9, 2014.

Rainey, W. S. 1985. *Considerations in the Design of Juvenile Bypass Systems.* Paper presented at the Symposium on Small Hydropower and Fisheries. Denver, CO.

Richter, B. 2011. Nextera Energy Annual Report.

Robbins, W. H., and H. R. MacCrimmon. 1974. *The Black Basses in America and Overseas.* Sault Ste. Marie, Ontario, Canada: Biomanagement and Research Enterprises. As cited in Edwards et al. 1983.

Robertson-Bryan, Inc., Hydroacoustic Technology, Inc., Flow Science, and Larry Walker Associates. 2013 (March). *Temperature Study to Assess the Thermal Impacts of the Sacramento Regional Wastewater Treatment Plant Discharge on Aquatic Life of the Lower Sacramento River*. Prepared for the Central Valley Regional Water Quality Control Board on behalf of the Sacramento Regional County Sanitation District.

Romine, J., R. Perry, S. Johnston, C. Fitzer, S. Pagliughi, and A. Blake. 2014. Identifying when Tagged Fishes Have Been Consumed by Piscivorous Predators: Application of Multivariate Mixture Models to Movement Parameters of Telemetered Fishes. *Animal Biotelemetry* 2:3.

Romine, J. G., R. W. Perry, S. J. Brewer, N. S. Adams, T. L. Liedtke, A. R. Blake, and J. R. Burau. 2013. The Regional Salmon Outmigration Study—Survival and Migration Routing of Juvenile Chinook Salmon in the Sacramento–San Joaquin River Delta during the Winter of 2008–09. U.S. Geological Survey Open-File Report 2013-1142.

Romine, J. G., R. W. Perry, A. C. Pope, P. Stumpner, T. L. Liedtke, K. K. Kumagai, and R. L. Reeves. 2016. Evaluation of a floating fish guidance structure at a hydrodynamically complex river junction in the Sacramento–San Joaquin River Delta, California, USA. *Marine and Freshwater Research*. http://dx.doi.org/10.1071/MF15285

Ruebush, B. C., G. G. Sass, J. H. Chick, and J. D. Stafford. 2012. *In-situ* Tests of Sound-Bubble-Strobe Light Barrier Technologies to Prevent Range Expansions of Asian Carp. *Aquatic Invasions* 7(1):37–48.

Sabal, M., S. Hayes, J. Merz, and J. Setka. 2016. Habitat Alterations and a Nonnative Predator, the Striped Bass, Increase Native Chinook Salmon Mortality in the Central Valley, California. *North American Journal of Fisheries Management* 36(2):309-320.

San Luis & Delta-Mendota Water Authority and Charles H. Hanson. 1996 (May). *Georgiana Slough Acoustic Barrier Applied Research Project: Results of 1994 Phase II Field Tests*. Technical Report 44. Interagency Ecological Program for the San Francisco Bay/Delta Estuary. Prepared for California Department of Water Resources and U.S. Bureau of Reclamation.

Scott, S. 2011. *A Positive Barrier Guidance System Designed to Improve Safe Downstream Passage of Anadromous Fish*. Paper presented at Fish Passage 2011. The National Conference on Engineering & Ecohydrology for Fish Passage. University of Massachusetts, Amherst, Tuesday, June 28, 2011. Available: https://bdo-portal.water.ca.gov/documents/92073/148337/Updated+FGS+Paper+2011.pdf.

Scruton, D. A., L. M. N. Ollerhead, K. D. Clarke, C. Pennell, K. Alfredsen, A. Harby, and D. Kelley. 2003. The Behavioral Response of Juvenile Atlantic Salmon (*Salmo salar*) and Brook Trout (*Salvelinus fontinalis*) to Experimental Hydropeaking on a Newfoundland (Canada) River. *River Research and Applications* 19:577–587.

Singer, G. P., A. R. Hearn, E. D. Chapman, M. L. Peterson, P. E. LaCivita, W. N. Brostoff, A. Bremner, and A. Klimley. 2013. Interannual Variation of Reach Specific Migratory Success for Sacramento River Hatchery Yearling Late-Fall Run Chinook Salmon (*Oncorhynchus tshawytscha*) and Steelhead Trout (*Oncorhynchus mykiss*). *Environmental Biology of Fishes* 96(2–3):363–379.

Sladky, K. K., C. R. Swanson, M. K. Stoskopf, M. R. Loomis, and G. A. Lewbart. 2001. Comparative Efficacy of Tricaine Methanesulfonate and Clove Oil for Use as Anesthetics in Red Pacu (*Piaractus brachypomus*). *American Journal of Veterinary Research* 62(3):337–342.

Smith, D.L., E.L. Brannon, and M. Odeh. 2005. Response of Juvenile Rainbow Trout to Turbulence Produced by Prismatoidal Shapes. *Transactions of the American Fisheries Society* 134:741-753.

Sokal, R. R. and F. J. Rohlf. 1995. *Biometry*. Third edition. New York: W. H. Freeman and Company.

Steel, A. E., P. T. Sandstrom, P. L. Brandes, and A. P. Klimley. 2013. Migration Route Selection of Juvenile Chinook Salmon at the Delta Cross Channel, and the Role of Water Velocity and Individual Movement Patterns. *Environmental Biology of Fishes* 96(2–3):215–224.

Stevens, D. E. 1963. *Food Habits of Striped Bass, Roccus saxatilis (Walbaum), in the Sacramento–Rio 14 Vista Area of the Sacramento River*. University of California, Berkeley.

Swanson, C., P. S. Young, and J. J. Cech. 2004. Swimming in Two-Vector Flows: Performance and Behavior of Juvenile Chinook Salmon near a Simulated Screened Water Diversion. *Transactions of the American Fisheries Society* 133(2):265–278.

Taylor, E. B. 1988. Adaptive Variation in Rheotactic and Agonistic Behavior in Newly Emerged Fry of Chinook Salmon, *Oncorhynchus tshawytscha*, from Ocean- and Stream-Type Populations. *Canadian Journal of Fisheries and Aquatic Sciences* 45(2): 237-243.

Thorpe, J. E. and A. Moore. 1997. The Migratory Behaviour of Juvenile Atlantic Salmon. In: Ueda, H. and H. A. Bern (editors), Physiology and Ecology of Fish Migration. Proceedings of the International Symposium on Fish Migration. Lake Toya, Hokkaido, Japan. Memoirs of the Faculty of Fisheries Hokkaido University 44(1): 39-46.

Todd, B. L., and C. F. Rabeni. 1989. Movement and Habitat Use by Stream-Dwelling Smallmouth Bass. *Transactions of the American Fisheries Society* 118(3):229–242.

Townsend, R. L., J. R. Skalski, P. Dillingham, and T. W. Steig. 2006. Correcting Bias in Survival Estimation Resulting from Tag Failure in Acoustic and Radiotelemetry Studies. *Journal of Agricultural, Biological, and Environmental Sciences* 11:183–196.

Turnpenny, A. W. H., and N. O'Keeffe. 2005. *Screening for Intake: A Best Practice Guide.* Science Report SC03231. Bristol, England: Environment Agency, Rio House.

Vogel, D. 2011 (April). *Insights into the Problems, Progress, and Potential Solutions for Sacramento River Basin Native Anadromous Fish Restoration*. Prepared for Northern California Water Association and Sacramento Valley Water Users. Red Bluff, CA: Natural Resource Scientists, Inc.

Vogel, D. A., and K. R. Marine. 1991 (July). *Guide to Upper Sacramento River Chinook Salmon Life History*. Prepared for the U.S. Bureau of Reclamation, Central Valley Project. Redding, CA: CH2M Hill.

Ward, J. H. 1963. Hierarchical Grouping to Optimize an Objective Function. *Journal of the American Statistical Association* 58:236–244.

West, J. L., and F. E. Hester. 1966. Intergenetic Hybridization of Centrarchids. *Transactions of the American Fisheries Society* 95:280–288.

Whitney, R., L. Calvin, M. Erho, and C. Coutant. 1997. Downstream Passage for Salmon at Hydroelectric Projects in the Columbia River Basin: Development, Installation, and Evaluation. Northwest Power Planning Council, Portland, Oregon.

Williams, G. D., R. M. Thom, D. K. Shreffler, J. A. Southard, L. K. O'Rourke, S. L. Sargeant, V. I. Cullinan, R. Moursand, and M. Stamey. 2003 (September). *Assessing Overwater Structure-Related Predation Risk on Juvenile Salmon: Field Observations and Recommended Protocols*. Sequim, WA: Pacific Northwest National Laboratory.

Zeug, S. C., and B. J. Cavallo. 2013. Influence of Estuary Conditions on the Recovery Rate of Coded-Wire-Tagged Chinook Salmon (*Oncorhynchus tshawytscha*) in an Ocean Fishery. *Ecology of Freshwater Fish* 22(1):157–168.

———. 2014. Controls on the Entrainment of Juvenile Chinook Salmon (Oncorhynchus tshawytscha) into Large Water Diversions and Estimates of Population-Level Loss. PLoS One 9(7):e101479.

This page intentionally left blank.

APPENDIX A

2014 GEORGIANA SLOUGH FFGS STUDY
STUDY FISH SUMMARY STATISTICS

Table A – 1
Mean and range weight (g) and fork length (mm) of juvenile Chinook salmon released by date, at Georgiana Slough

		Weight (g)		Fork length (mm)	
Date	**N**	**Mean**	**Range**	**Mean**	**Range**
1-Mar	9	41.5	25.6 - 61.3	156	135 - 177
2-Mar	12	39.9	19.2 - 53.0	156	123 - 168
3-Mar	12	40.3	22.1 - 61.5	157	139 - 178
4-Mar	12	42.1	25.4 - 75.4	160	140 - 197
5-Mar	12	40.4	23.4 - 53.1	155	134 - 172
6-Mar	12	41.1	20.5 - 70.2	155	125 - 188
7-Mar	12	34.7	22.4 - 58.7	148	131 - 172
8-Mar	12	35.7	16.3 - 59.5	149	117 - 178
9-Mar	13	40.7	26.5 - 51.0	157	137 - 169
10-Mar	18	39.8	17.1 - 69.2	155	118 - 185
11-Mar	19	40.5	18.0 - 69.2	155	117 - 187
12-Mar	19	38.3	22.3 - 57.4	152	127 - 180
13-Mar	20	38.4	17.0 - 65.3	154	121 - 184
14-Mar	20	36.9	21.3 - 51.7	153	127 - 170
15-Mar	18	37.4	20.5 - 52.9	153	125 - 172
16-Mar	20	37.6	14.2 - 60.1	153	113 - 184
17-Mar	19	43.5	27.1 - 62.3	161	138 - 184
18-Mar	20	36.8	17.6 - 57.8	153	125 - 173
19-Mar	19	40.5	20.1 - 80.1	156	124 - 193
20-Mar	20	36.3	20.8 - 64.0	152	123 - 181
21-Mar	22	41.7	19.3 - 63.0	157	127 - 181
22-Mar	22	42.3	21.1 - 72.4	159	129 - 195
23-Mar	20	46.5	16.2 - 92.2	162	115 - 204
24-Mar	19	37.9	18.3 - 49.6	153	118 - 167
25-Mar	19	41.4	23.1 - 77.5	159	135 - 199
26-Mar	20	39.0	18.0 - 79.7	154	123 - 194
27-Mar	19	41.8	15.1 - 71.3	158	116 - 187
28-Mar	20	37.8	18.3 - 74.5	152	125 - 189
29-Mar	17	42.4	30.2 - 56.3	158	144 - 171
30-Mar	21	45.9	17.2 - 73.6	160	116 - 190
31-Mar	18	49.2	21.5 - 75.6	165	127 - 192
1-Apr	19	44.9	22.5 - 66.9	161	130 - 182
2-Apr	19	44.4	21.3 -71.8	159	126 - 188
3-Apr	20	42.6	19.5 - 83.0	159	121 - 200

4-Apr	18	43.2	27.1 - 71.4	160	137 - 186
5-Apr	22	41.6	17.7 - 91.2	156	118 - 202
6-Apr	19	40.3	18.9 - 76.3	156	124 - 192
7-Apr	19	46.5	20.8 - 68.0	162	127 - 186
8-Apr	21	42.3	18.9 - 66.4	158	128 - 184
9-Apr	21	46.1	26.6 - 93.1	162	137 - 204
10-Apr	18	47.4	21.4 - 76.4	164	129 - 193
11-Apr	22	43.8	29.7 - 63.7	159	142 - 178
12-Apr	22	51.1	29.2 - 83.5	168	142 - 198
13-Apr	20	48.8	25.9 - 86.6	163	133 - 198
14-Apr	24	43.4	19.3 - 73.0	158	125 - 184
15-Apr	7	43.4	23.1 - 54.1	160	132 - 174
Overall	**826**	**41.7**	**14.2 - 93.1**	**157**	**113 - 204**

Table A – 2
Mean and range weight (g) and fork length (mm) of juvenile Chinook salmon released by date, at Sacramento

		Weight (g)		Fork length (mm)	
Date	**N**	**Mean**	**Range**	**Mean**	**Range**
1-Mar	75	42.7	13.3 - 79.9	157	109 - 195
2-Mar	120	40.2	13.7 -80.1	155	112 - 197
3-Mar	120	39.7	16.1 -82.5	155	115 - 194
4-Mar	120	40.3	19.5 - 69.7	156	122 - 187
5-Mar	120	39.4	15.6 - 78.6	154	116 - 188
6-Mar	120	41.0	15.1 - 81.5	156	113 - 196
7-Mar	120	39.5	14.7 - 75.2	155	110 - 190
8-Mar	120	40.3	17.1 - 72.4	155	123 - 193
9-Mar	111	41.3	17.0 - 87.0	157	115 - 196
10-Mar	100	37.6	16.4 - 72.7	153	113 - 189
11-Mar	97	37.0	16.3 - 88.5	150	116 - 203
12-Mar	98	40.3	17.1 - 75.3	155	120 - 187
13-Mar	97	38.9	18.1 - 83.0	155	122 - 204
14-Mar	96	39.6	16.3 - 78.5	155	121 - 197
15-Mar	98	37.9	15.1 - 73.6	155	115 - 191
16-Mar	97	39.1	18.0 - 86.5	154	122 - 198
17-Mar	98	40.8	14.8 - 85.9	157	117 - 198
18-Mar	98	39.2	14.4 - 77.9	155	110 - 193
19-Mar	97	42.5	15.2 - 67.3	159	116 - 184

Table A – 2
Mean and range weight (g) and fork length (mm) of juvenile Chinook salmon released by date, at Sacramento

20-Mar	97	39.4	21.7 - 83.2	156	124 - 201
21-Mar	102	41.7	17.9 - 81.6	156	123 - 196
22-Mar	101	43.0	20.6 - 82.6	159	123 - 197
23-Mar	101	41.6	15.0 - 83.6	158	115 - 197
24-Mar	99	43.7	18.9 - 97.0	160	125 - 203
25-Mar	97	42.4	15.3 - 84.4	160	116 - 200
26-Mar	97	40.3	16.2 - 97.1	157	117 - 206
27-Mar	96	39.9	18.6 - 66.4	156	125 - 187
28-Mar	96	42.0	15.1 - 82.2	157	111 - 193
29-Mar	99	42.3	21.4 - 82.7	158	128 - 197
30-Mar	98	43.3	14.5 - 93.0	157	108 - 205
31-Mar	99	44.2	19.4 - 98.6	159	121 - 206
1-Apr	94	43.7	21.2 - 88.1	159	125 - 198
2-Apr	100	43.6	18.3 - 112.0	158	118 - 206
3-Apr	96	37.9	15.3 - 88.7	153	116 - 200
4-Apr	101	41.6	15.7 - 63.3	157	115 - 182
5-Apr	100	42.9	16.9 - 96.2	158	122 - 206
6-Apr	103	43.7	18.0 - 95.3	160	121 - 206
7-Apr	104	44.5	14.2 - 89.5	160	112 - 200
8-Apr	102	46.6	24.9 - 82.3	164	135 - 198
9-Apr	103	45.3	20.5 - 86.9	161	122 - 198
10-Apr	99	45.5	21.2 - 91.9	161	124 - 203
11-Apr	103	45.2	15.6 - 107.2	160	120 - 213
12-Apr	98	46.3	16.5 - 86.7	162	116 - 199
13-Apr	101	46.6	16.9 - 93.3	162	119 - 202
14-Apr	105	47.4	18.6 - 103.7	163	122 - 212
15-Apr	42	41.7	23.7 - 93.4	156	134 - 199
Overall	**4635**	**41.8**	**13.3 - 112.0**	**157**	**109 - 213**

This page intentionally left blank.

APPENDIX B

2014 GEORGIANA SLOUGH FFGS STUDY
SUMMARY OF STANDARD OPERATING PROCEDURES

QUALITY ASSURANCE/QUALITY CONTROL PLAN

2014 Georgiana Slough Floating Fish Guidance Structure Performance Evaluation

Focus Area: Effectiveness of a floating fish guidance structure at guiding/deterring juvenile fish from entering Georgiana Slough on the Sacramento River

Prepared for:

California Department of Water Resources
Jacob McQuirk and Ryan Reeves
1416 9th Street
Sacramento, CA, 94236-001
Phone: 916-653-6868
Email: jacobmc@water.ca.gov/ rreeves@water.ca.gov

Prepared by:

US Geological Survey
Noah Adams
Columbia River Research Laboratory
5501A Cook-Underwood Road
Cook, WA, 98650
Phone: 509-538-2299
Email: nadams@usgs.gov

The purpose of the Quality Assurance/Quality Control (QA\QC) plan for the 2014 Georgiana Slough Floating Fish Guidance Structure Performance Evaluation was to ensure that the data were collected, analyzed, and reported in a standardized manner in close accordance with good laboratory practices procedures. Many investigators from multiple federal, state, and local agencies as well as the private sector were involved in this project. Each of these organizations has their own procedures and guidelines for ensuring QA/QC. This plan attempted to take the information from different organizations and present it in a standardized format.

Due to the length of the final project report, DWR decided not to include the QA/QC plan in its entirety in the report. Instead, the table of content for the QA/QC plan as well as a list of the Standard Operating Procedures (SOPs) included in the plan are provided below. The QA/QC plan in its entirety is on file with DWR and is available upon request.

Table of Contents for QA/QC Plan

The Standard Operating Procedures Appended to QA/QC Plan

Standard Operating Procedure (SOP)

Pre-Deployment Testing of Cables and Hydrophones for 3D Acoustic Array
Tag-Drag Tests of the 3D Acoustic Array
Remote Access for Georgiana 3D Array
Raw Data Transfer
General Operation of the FFGS
Obtaining Underwater Light Level Data
Obtaining Climate and Weather Data
Obtaining Water Quality Data
Equipment Cleaning, Inspection and Treatment for Invasive Aquatic Organisms
Tag Coding of Acoustic Transmitters
Tag Programming of Acoustic Transmitters
Incorporating Tags into Drifter Releases
Keeping Instrument Logs
Completing Field Over Site Checklist
Recording Data in Laboratory Notebooks
Daily QA/QC Checks on Remote Acoustic Nodes
Daily On-Site-Checks of the 3D Acoustic Array
Daily QA/Q Checks on ATR at 3D Acoustic Array
Fish Transport Procedures
Surgical Tag Implantation
Tag Assistant and Curator
Installation and Maintenance of Fixed Hydroacoustic Monitoring Equipment
Drifter Study Plan
Hydrodynamic Monitor

This page intentionally left blank.

APPENDIX C

2014 GEORGIANA SLOUGH FFGS STUDY
FISH TAGGING EFFECTS STUDY

Survival, wound healing, transmitter loss, and growth in juvenile Chinook salmon surgically implanted with acoustic transmitters

Introduction

In support of the 2014 Georgiana Slough Floating Fish Guidance Structure (GSFFGS) Study, a controlled laboratory study was completed to evaluate the condition of juvenile Chinook salmon surgically implanted with acoustic telemetry transmitters and to document the risk of transmitter loss. The objectives of the study were to evaluate: 1) risk of mortality due to tagging, 2) the healing of the surgical wounds through time, 3) the risk of transmitter loss, and 4) differences between taggers.

Telemetry studies make the assumption that fish equipped with transmitters will behave and perform comparably to untagged fish. More explicitly stated, the assumption is that the collection, handling, and tagging of the fish, combined with the act of carrying the transmitter, will have minimal impact on the fish. When transmitters are implanted using invasive procedures such as surgery there is more likely to be a "transmitter effect". Testing this assumption by measuring potential transmitter effects is critical to making valid inferences to the untagged population. Evaluating transmitter effects can be difficult in field settings due to the limited opportunity to recapture and examine tagged fish and the often limited information available on the "normal" behavior of untagged fish with which comparisons could be made. For the 2014 GSFFGS study, the assumption was evaluated under controlled laboratory conditions where tagged fish could be closely monitored and there was opportunity to examine fish following tagging. This study (hereafter referred to as "the tag effects study") was conducted at the U.S. Fish and Wildlife Service's California and Nevada Fish Health Center in Anderson, California (co-located with the Coleman National Fish Hatchery) with the assistance of Scott Foott (Center Director) and his staff.

Methods

Study Design

The ideal study design for an evaluation of transmitter effects is to replicate the exact conditions used in the primary telemetry study. For example, the ideal study design for this tag effects study would involve the same fish, the same tagging procedures, the same personnel, and the same water source and temperatures as the GSFFGS study, which it was designed to support. Logistical considerations unfortunately prevented us from meeting that ideal. Nonetheless every effort was made to match the GSFFGS study whenever possible. As will be outlined in the methods, the tag effects study procedures matched the GSFFGS study on several details including: fish source, transport procedures, tagging procedures, taggers, and post-tagging recovery and holding (Figure 1). Differences between the two studies included: an additional transport for the tag effects study fish when GSFFGS fish were released

into the Sacramento River, and different water sources and thermal regimes during the holding period (Figure 1). Although the tag effects study design was less than ideal, any evaluation of transmitter effects is a worthwhile effort considering the value of the data generated for the GSFFGS study, and the potential implications of the study findings.

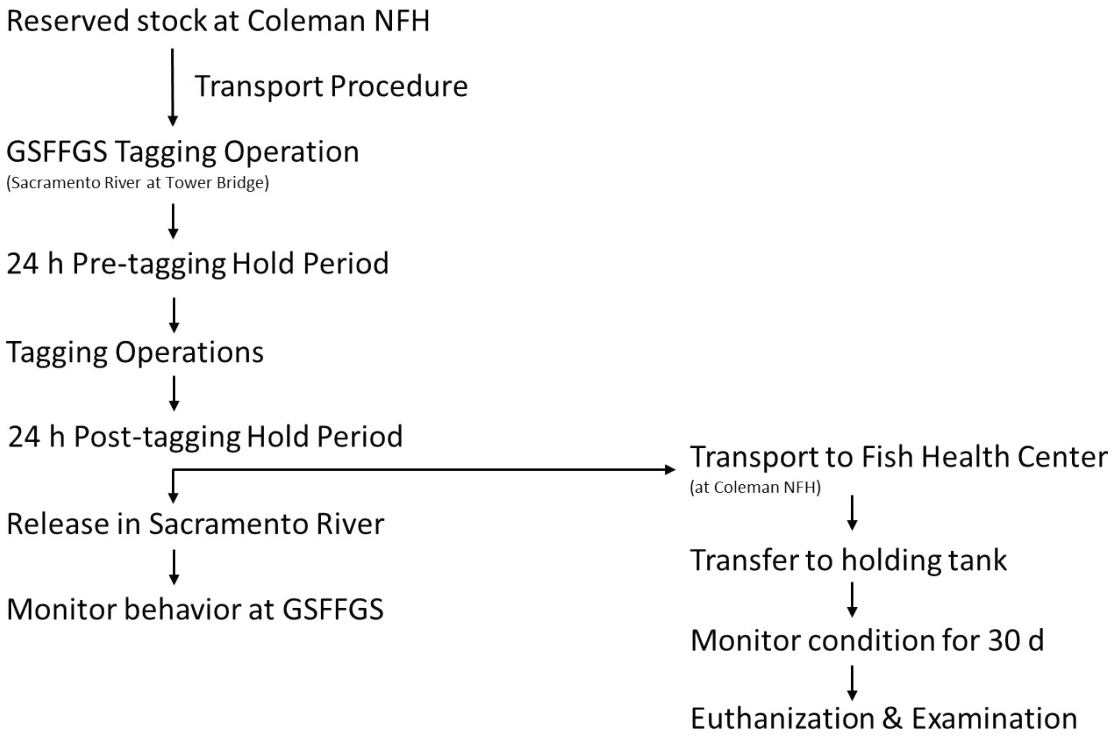

Figure B-1. — Flow chart showing the procedures used for the GSFFGS study (left column) and the tag effects study conducted at the Fish Health Center (left column, then right column).

A 30 d monitoring period was used for the tag effects study based on the anticipated life of the transmitters used for the GSFFGS study. Two acoustic transmitter models were used for the GSFFGS study: one manufactured by HTI (Hydroacoustic Technology, Inc.) and one manufactured by Vemco Acoustic Telemetry (Figure 2). Dummy transmitters (with no working components) that simulated the transmitters used for the GSFFGS study were used for the tag effects study. A transmitter (one model or the other) was surgically implanted into the abdominal cavity of a study fish, along with a 12.5 mm passive integrated transponder (PIT) tag. The PIT tag was required to individually identify fish in the tag effect study because, unlike the GSFFGS study, the fish could not be identified by the unique acoustic signal emitted from the transmitter. The dummy acoustic transmitters had weights of 1.12 g (HTI acoustic tag) and 0.65 g (Vemco V5 acoustic tag). The PIT tag mean weight was 0.09 g. The combined transmitter weights were 1.21 g for HTI/PIT and 0.74 g for Vemco/PIT.

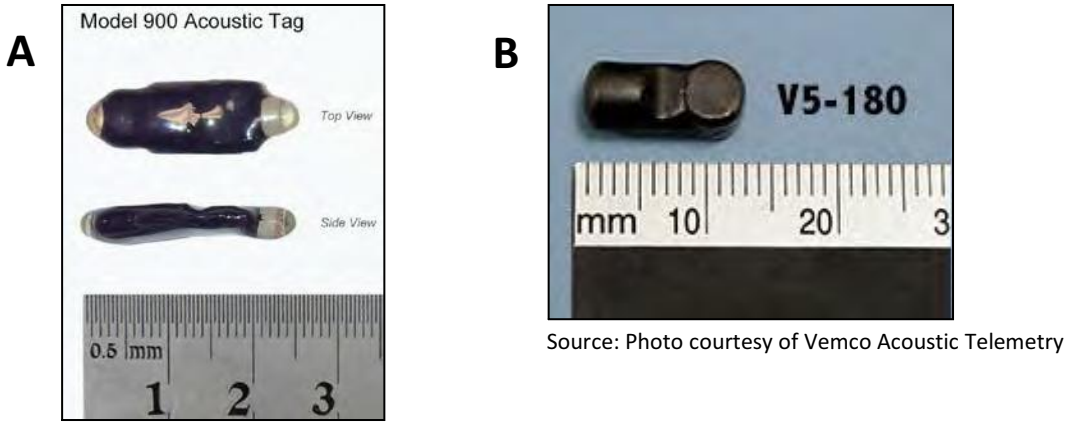

Source: Photo courtesy of Vemco Acoustic Telemetry

Source: Photo courtesy of Hydroacoustic Technology, Inc.

Figure B-2. — Acoustic transmitter models used for the GSFFGS study: A) Model 900-LD manufactured by HTI (Hydroacoustic Technology, Inc.) and B) Model V5 manufactured by Vemco Acoustic Telemetry.

Two experiments were conducted to represent the early season and late season influences of the taggers and fish condition. Three taggers were used for the GSFFGS study and their potential influence was evaluated in the tag effects study. Two dates were selected (one early in the GSFFGS study period and one later in the period) when all taggers were present. On these dates, each tagger tagged 17 – 18 fish with dummy tags and PIT tags to be used in an experiment. On each of the dates each tagger also handled 6 –10 control fish which were minimally handled and held using the same procedures as the tagged groups of fish. The control fish were included to allow detection of large-scale effects such as poor conditions during transport or a disease outbreak that could have influenced the tagged fish and confounded our interpretation of the survival or condition of the experimental groups. A summary of the tagging dates and sample sizes by tagger and transmitter type is presented in Table 1.

The California and Nevada Fish Health Center was selected as the study site based both on logistical ease and on the capability of staff. The logistical consideration involved executing the transport of fish. A transport was established for the GSFFGS study and it moved fish daily from Coleman National Fish Hatchery to the tagging location. This system was used, in reverse, for the tag effects study. The study fish were tagged at the GSFFGS study tagging location on the Sacramento River at the Tower Bridge, held for a 24 h post-tagging recovery period, and then transported to the Fish Health Center at Coleman. The fish transport protocols put in place for the GSFFGS study were used when dummy-tagged fish were transported. The second rationale for using the Fish Health Center as the study site was based on the availability and capability of Center staff. Following delivery, fish were put into tanks at the Fish Health Center. Center staff has experience in fish culture and monitoring, and their assistance was requested to feed the fish and regularly monitor the tank for dead, dying, or sick fish and for any transmitters that might have been shed. They were prepared to do diagnostic testing for disease on fish

that died or became sick during the experiment. This regular care and monitoring was critical to the full evaluation of transmitter effects and would not have been possible without the support of Scott Foott and his staff at the Fish Health Center.

Table B-1. — Summary of the tag date, the numbers of fish tagged by transmitter type, the number of control fish, and the tagger for the two experiments that comprised the tag effects study, 2014.

Experiment	Tag date	Tagger	Number of fish tagged with HTI	Number of fish tagged with Vemco	Number of controls	Number of fish in experiment
1	3/11	1	8	10	10	28
		2	8	10	10	28
		3	8	10	10	28
						84
2	4/1	1	7	10	7	24
		2	8	10	7	25
		3	8	10	6	24
						73
TOTAL			47	60	50	157

FISH SOURCE

Juvenile late fall-run Chinook salmon used for the tag effects study were from the same source as those used for the GSFFGS study and were treated identically. Fish were removed from a dedicated raceway at the Coleman National Fish Hatchery and transported in insulated containers to the GSFFGS tagging operation on the Sacramento River. Fish for the tag effects study were transported concurrently with GSFFGS study fish on selected dates (see Table 1).

TAGGING AND RECOVERY PROCEDURES

The standard operating procedures (SOP) and taggers used for the GSFFGS study were used for the tag effects study. As part of the tagging SOP, fish fork length (FL) and weight information were collected. These data were used as the initial size for the growth calculations. On dates when an experiment was started, one tagger was randomly selected to start tagging. That tagger continued until they completed tagging their study fish and then the second and third taggers completed their allotted fish.

Following the SOP for the GSFFGS study, tagged fish were held in perforated 76 L containers in the Sacramento River for 24 h after tagging to recover from handling and tagging. Control fish were minimally handled: netted out of the holding container and transferred to perforated 76 L containers for holding. Following this holding period the containers were removed from the river and the fish were transferred to an insulated 265 L tote for transport to the Fish Health Center.

FISH HOLDING AND MONITORING AT THE FISH HEALTH CENTER

Dummy-tagged fish and controls arrived at the Fish Health Center approximately 3 h after their departure from the GSFFGS tagging operation in Sacramento. Upon arrival fish were removed from the 265 L container and placed into a single tank (approximate volume 1700 L) for the 30 d monitoring period. The tank was monitored daily for dead or compromised fish and for shed PIT or acoustic tags. Temperature monitors were placed into the tank and recorded water temperature approximately every 10 min for the duration of the holding period. Fish were fed commercial pellets based on a maintenance ration and were held under natural photoperiod conditions.

EVALUATION PROCEDURES

At the completion of each experiment fish were euthanized, weighed, measured, photographed, and necropsied using the unique PIT tag to individually identify fish. Photographs were taken to show both the internal and external view of the incision. Wound healing and fish condition were assessed using a rubric developed by USGS to establish criteria for consistent grading of fish. During the necropsy procedure scores were assigned for six categorical variables from the USGS rubric, which were designed to document the condition of the fish, the progress of wound healing, and the potential for transmitter loss. Two variables were binomial, using presence and absence as the two possible states. The binomial variables included suture retention/loss, and presence/absence of fungus. The four additional variables were categorical with 3-5 possible states (Table 2) and included suture effectiveness, incision apposition, incision healing, and signs of tag expulsion. In all cases, the best outcome for a variable was zero so that low scores predict better fish condition or wound healing.

Table B-2. — Variables from the USGS rubric used to assess fish condition and wound healing and the definitions of their categorical scores. The best outcome for all variables is a score of zero, and condition decreases with higher scores.

Variable	Score 0	Score 1	Score 2	Score 3	Score 4
Suture effectiveness	Intact	Not fully intact	Not intact		
Incision apposition	0% open	25% open	50% open	75% open	100% open
Incision healing	100% Healed	75% healed	50% healed	25% healed	Not healed
Tag expulsion	No signs of expulsion	Some pressure or bulging	Expulsion process active		

ANALYSIS

Mean initial and final (30 d) fish size data and summaries of the wound healing variables are presented. The percentage weight increase was calculated as (final weight-initial weight)/initial weight *100, adjusted for transmitter weight. Findings for each tagger are presented, along with a combined total.

Results

Two 30 d experiments were initiated during the GSFFGS tagging operation to represent the potential changes throughout the season in tagger proficiency and fish condition (Table 3). Mean water temperature in the holding tanks at the Fish Health Center ranged from 12.3 to 13.1 °C during the two experiments (Table 3). A total of 107 tagged fish and 50 control fish were used for the experiments (157 total fish). There were no mortalities in the experimental groups or control groups, in either of the experiments. Based on observations of fish in the tanks, Fish Health Center staff did not observe any gross signs of disease or distress during either of the experiments.

The mean initial FL of Chinook salmon (both experiments combined) was 156 mm, and the initial mean weight was 40.9 g (Table 4). Using the combined mass of the dummy HTI acoustic transmitter and the PIT tag, the tag burden (tag weight to body weight ratio) range was 1.3% - 5.3% at the time of tagging. The combined tag burden range was 0.8% - 3.2% for the Vemco transmitter at the time fish were tagged. The mean combined tag burden was 3.2% for fish tagged with HTI transmitters (Table 5) and 1.9% for those tagged with Vemco transmitters (Table 5). The initial size (FL and weight) of the juvenile Chinook salmon were very similar for all taggers. The fish had a mean weight increase of 48.9% over the approximately 30 d holding periods. In experiment 1, fish had a mean percent weight increase of 42.0%, as compared to 56.3% mean percent weight increase in experiment 2. The percent weight increase was similar among taggers within each of the experiments.

The control fish were minimally handled, so initial weight and length measurements were not taken for those groups. Considering that all the treatment and control fish were removed from the same cohort of hatchery fish that was used for the GSFFGS study, it is reasonable to assume that the size distribution of the control fish was similar to the treatment fish. Control fish were included in the experiments to assess general transport and holding conditions for the tagged fish, and to monitor for disease processes that could have influenced our evaluation of healing in the tagged fish. Necropsies were not conducted for control fish at 30 d post-holding because there were no disease outbreaks or mortalities observed.

Table B-3. — Tagging date, sampling date, and mean water temperatures for the two experiments conducted at the Fish Health Center in 2014.

	Experiment 1	Experiment 2
Tagging date	March 11	April 1
Sampling date	April 14	May 8
Mean water temperature (ºC)	12.3	13.1

Table B-4. — Mean initial and final fork length (FL; mm), weight (g), and mean percent weight increase for fish used in the tag effects study, 2014, by tagger and overall.

	N	Initial mean FL	Initial mean weight	Final mean FL	Final mean weight	Mean % weight increase
Tagger 1	35	156	39.8	167	59.6	48.9%
Tagger 2	36	157	41.7	167	61.9	47.8%
Tagger 3	36	156	41.3	167	62.1	50.1%
Total	**107**	**156**	**40.9**	**167**	**61.2**	**48.9%**

Table B-5. — Mean combined tag burden (%) of HTI and Vemco transmitters and PIT tags for fish used in the tag effects study, 2014, by tagger and overall.

	Mean tag burden (Vemco)	Mean tag burden (HTI)
Tagger 1	2.0%	3.2%
Tagger 2	1.9%	3.1%
Tagger 3	1.9%	3.2%
Total	**1.9%**	**3.2%**

Necropsies conducted 30 d after tagging revealed that fish were in good general condition. There were no mortalities, and no gross external or internal signs of disease. Over half of the fish examined did however have some fungal growth on or near the incision or sutures (61.6% overall). There were only minor differences between the taggers related to the presence of fungus: Tagger 1 handled 29% of the fish that had fungus present, tagger 2 handled 35% of the affected fish and 36% was handled by tagger 3.

Across the two experiments, one acoustic tag was shed from a tagged fish. The shed tag was from a fish in the first experiment, implanted with an HTI transmitter, which had a tag burden of 2.9% at the time of tagging. No tags were shed during the second experiment. Fish exams revealed that 11 additional fish (10.4%) showed some signs of lateral pressure on the incision that could have, through time, led to some transmitter loss. The remaining 95 tagged fish (89.6%) had a tag expulsion score of zero, meaning that there were no signs of transmitter expulsion. The risk of tag expulsion did not appear to be related to differences in taggers. Most of the fish that showed some signs of tag expulsion were not significantly impacted: 10 of the 11 fish (90.9%) had scores of 1 using the USGS rubric, meaning that the tag was putting some pressure on the incision or the lateral body wall. The remaining fish (9.1%) had an expulsion score of 2, suggesting an active expulsion process. In both experiments, fish implanted with Vemco transmitters more commonly showed signs of tag expulsion than fish implanted with HTI transmitters (Table 6). In experiment 1, Vemco transmitters made up 80% of the fish that showed some signs of expulsion and in experiment 2 Vemco transmitters made up 67% of the affected fish (Table 6).

Table B-6. — Mean expulsion scores for fish with scores greater than zero, by transmitter type, for each experiment.

	Mean expulsion score	Number of fish that showed signs of expulsion	Vemco	HTI
Experiment 1	0.11	5	80%	20%
Experiment 2	0.11	6	67%	33%
Total	**0.11**	**11**	**73%**	**27%**

Most (95.8%) of the sutures used to close the incisions were still in place at 30 d post-tagging, with slightly higher suture retention for tagger 2 (98.6%) compared to tagger 1 (92.9%) and tagger 3 (95.8%; Table 7).

Sutures that were in place at the time of necropsy were still generally effective. The majority of the fish (73.9%) had a suture effectiveness score of zero, indicating that the suture pattern was intact and effective. The overall mean suture effectiveness score was 0.28 (Table 7). A value closer to zero represents more effective suture patterns. The mean suture effectiveness scores showed only minor differences among taggers, and all taggers had mean scores close to zero (Table 7).

The incisions made to insert transmitters were healing well at 30 d post-tagging. The overall mean incision apposition score (0.44) and incision healing score (0.66) indicated that a large proportion of fish showed good apposition of the edges of the incision and incision healing (Table 7). Tagger 1 had a higher proportion of individual fish with scores above zero for these variables, resulting in higher mean scores (Table 7).

Table B-7. — Mean suture retention (%) and wound healing scores for Chinook salmon used in the tag effects study, 2014 by tagger and overall. Wound healing scores of zero represent the most advanced wound healing.

	N	% Suture retention	Suture effectiveness score	Incision apposition score	Incision healing score
Tagger 1	35	92.9%	0.23	0.69	0.91
Tagger 2	36	98.6%	0.28	0.36	0.64
Tagger 3	36	95.8%	0.33	0.28	0.44
Total	**107**	**95.8%**	**0.28**	**0.44**	**0.66**

The tag effects study was designed with two experiments so that fish condition and tagger competency could be evaluated early and later in the study period. There were some differences in fish size and healing between the experiments. The fish were somewhat larger at the time of tagging for the second

experiment (Table 8). The percent weight increase for the juvenile salmon was also largest for experiment 2, as was the mean water temperature (Table 3). The scores for suture effectiveness were low across both experiments (Table 8). Considering the scale for suture effectiveness scores ranged from 0 (sutures fully intact and functional) to 2 (suture pattern not intact), the mean scores for each experiment show consistently effective sutures. The healing scores were highest for the first experiment and then showed a decrease for the second experiment. The mean incision healing score for tagger 1 was 1.22 in experiment 1 and decreased to 0.59 in experiment 2. Tagger 2 also had improved healing, from 0.72 in experiment 1 to 0.56 in experiment 2. Tagger 3 had the same healing score of 0.44 in both experiments. Again, considering the scale used for healing where zero represents complete healing and four represents less than 25% of the length of the incision being healed, the mean scores show that the average condition in all experiments was significantly healed incisions (75-100% of the incision length) on average.

Table B-8. — Mean initial weight (g), weight increase (%), suture effectiveness score, and incision healing score for the two experiments used in the tag effects study 2014.

	Experiment 1	Experiment 2
Initial Weight (g)	38.1	43.7
% Weight Increase	42.0%	56.0%
Suture Effectiveness	0.16	0.41
Incision Healing	0.81	0.53

Discussion

The objectives of the study were to evaluate: 1) risk of mortality due to tagging, 2) the healing of the surgical wounds through time, 3) the risk of transmitter loss, and 4) differences between taggers.

There were no mortalities among the 157 experimental and control fish for the experiments, so the risk of mortality due to tagging was minimal. This finding is further supported in that the fish for the experiments were handled more than the fish for the GSFFGS study in that they underwent several additional water source transfers and a 3-4 h transport. Fish implanted with acoustic transmitters and PIT tags performed well during the 30 d holding period following tagging, as they ate well and showed positive weight gain. There were no signs of gross disease or distress while the fish were held for 30 d in tanks, and there was no evidence of disease processes when fish were euthanized and necropsied following 30 d of holding. The most significant finding, from the perspective of observations of fish in the holding tanks, was the presence of fungus on more than half of the study fish. Although a high proportion of fish had some fungus present, the area of impact to each fish was small, with fungus detected on or near the sutures or incision area, but not covering large areas of the fish. The presence of fungus on fish is not surprising considering that fish were held in tanks where water temperatures were relatively high, water velocities were nominal, and the presence of residual commercial fish food can

encourage fungal growth. Future evaluations could potentially limit fungal growth with increased flow in tanks, increased rigor in tank cleaning, and reduced water temperatures.

The surgical wounds showed progressive healing through time, with the mean condition showing that incisions were 75-100% healed 30 d after tagging. There are several related drivers that lead to incision healing such as effective sutures and incision apposition. The USGS rubric used to score tagged fish evaluated six variables to capture the influence of these drivers. Each of the variables had positive outcomes. We found that suture effectiveness was high, meaning that the suture patterns were well executed initially, and were effective at creating enough tension across the incision to maintain the edges of the incision in contact (apposition) to enable healing. The apposition scores support this finding, showing that the incision edges were well approximated 30 d after tagging. There was a high proportion (61.6%) of fungus for experimental fish, and the fungus was most commonly noted to be on or near the incision area of the fish. Although the fungal load may have delayed healing in individual fish, leading to increased variability in healing scores, it did not have a significant effect on overall healing, as evidenced by the low mean scores for wound healing.

One acoustic transmitter (0.9%) was expelled during the tests. The tag was not recovered in the tank, so the timing of the tag loss could not be determined. At the time of tagging the tag burden for the fish was 2.9%, well below the SOP maximum of 5% tag burden. The weight of the tag, relative to the weight of the fish was not likely, therefore, to be the strongest driver of the tag loss. There was some evidence of tag loss risk as evidenced by the mean tag expulsion score of 0.11. With the USGS rubric, a score of zero represents no sign of transmitter loss and the mean score is close to zero, however 11 tagged fish (10.4%) showed some signs of lateral pressure during the 30 d exams. Of the 11 fish that had tag expulsions scores above zero, only one fish had a score of 2. The rubric score of 1 suggests that the tag is exerting some pressure on the incision or lateral body wall, but does not imply that the tag is likely to be shed. The rubric score of 2, however, is evidence that the pressure is significant and the tissue (incision or lateral body wall) is affected enough that the tag will likely eventually be lost. The expulsion risk score for fish implanted with Vemco transmitters was higher than for fish implanted with HTI transmitters in both experiments. The single tag that was expelled was an HTI tag, and the fish with the score of 2 was implanted with a Vemco transmitter. The processes that results in tags being expelled are complex and not completely understood, so the explanation for the difference in tag expulsion risk between the two transmitter types is not clear. The HTI transmitter was longer, and more tapered at one end, and taggers noted that the insertion process was easy and efficient for these tags. The Vemco tags, on the other hand, were shorter, with a larger diameter that required more manipulation to get into the body cavity through the incision. One hypothesis that may explain the higher tag loss risk for Vemco transmitters is that those tags could apply more pressure over a small area of the incision or body wall due to their shape. The longer HTI tags, which were heavier, had their mass distributed over a larger area which may have reduced the impact to a single area. Overall, the risk of transmitter loss was very

low in these experiments, so differences in risk between the transmitter models were not a significant source of risk.

Tagger performance was found to be high and generally similar. The taggers all had 100% survival of their tagged fish and showed similar incidence of fungus on tagged fish. There were some minor differences in the scores for the variables in the USGS rubric, for example tagger 1 had a higher mean incision apposition and healing score compared to the other taggers. Alternately, tagger 3 had a slightly higher suture effectiveness score than the other taggers. Overall the differences between the scores for the taggers were small, and there were no clear trends that one tagger had greater proficiency than the other taggers. Some differences noted in the rubric scores for the taggers could be the result of variability in scoring using the USGS rubric. We have found in other studies that it takes a considerate amount of effort and training to standardize the scoring of fish. Although the scoring done for this study is reliable for distinguishing major surgical or healing outcomes such as poorly healed incisions or gross inflammation or infection, the minor differences noted between taggers could be attributed to the subjective nature of the scoring system and lack of rigorous standardization. Several different project personnel were used to necropsy and score the fish from these experiments, and although training was provided, it was brief. The trends in fish survival, fish growth, and tag retention, which are less subjective, suggest that the three taggers had very similar outcomes for the fish examined. Another potential source of variability between taggers was experience. Although all of the taggers had undergone rigorous training and testing, tagger 1 started tagging for the GSFFGS with less experience than the other taggers. There is evidence of increased proficiency in experiment 2 where the mean healing scores were closer to zero.

In conclusion, the results of the tag effects study suggest that juvenile Chinook salmon surgically implanted with acoustic transmitters for the GSFFGS study were not likely to lose their transmitters or suffer negative effects from the tagging process or the presence of the transmitter. We found a low risk of transmitter loss for the tag effects study, and predict an even lower risk for the GSFFGS study because those fish had less handling and they did not carry a PIT tag along with their acoustic tag. Additionally, the three taggers that contributed to the GSFFGS study demonstrated high proficiency and equivalent competency during the tag effects study and should therefore not introduce any bias into the evaluation of the GSFFGS.

This page intentionally left blank.

APPENDIX D

2014 GEORGIANA SLOUGH FFGS STUDY
CONFERENCE ON FATES – PREDATION AND GUIDANCE RULES

2014 Georgiana Slough Floating Fish Guidance Structure Conference on Fates – Predation and Guidance Rules

November 17 – 19, 2014

Rules for Determining Predation

Objective: Determine if a juvenile Chinook salmon, implanted with a tag, was eaten, and if so, where and when

1. Eight people (Four teams of 2 people) evaluate all tracks from tags inserted in juvenile Chinook salmon

    a) At the beginning of the Conference on Fate (COF), all participants will review the predation rules set out here

    b) Any changes to the rules must be agreed to before making predation determinations

2. Once the track has been reviewed, the COF participants will assign a predation fate to the predation event in the fate spreadsheet

3. Fate assignment

    a) Eaten

        i. Predation location

        ii. Date and time of predation

    b) Not Eaten

    c) Unknown (The proportion of tracks receiving an "Unknown" classification varies with the discharge regime. There are often more Unknowns when discharges are small and thus velocity is quite low or negative – producing less downstream forcing operating on smolts at a microscale).

4. Rules for determining predation

    a) Juvenile Chinook salmon behavior is evidenced by purposeful, directed movement downstream. It is important to note that some data suggest that juvenile Chinook salmon in 2014 may have held at unknown locations during slack and flood tides then moved during ebb tides.

b) Predator behavior is evident when the tagged juvenile Chinook salmon executes patrolling loops in the area, and/or changes speed or direction often, and/or holds position for extended time periods. However, as discussed above, a Chinook salmon might move into the experimental area, stop and hold - waiting for the next ebb tide, and then continue its migration. Carefully compare the movement patterns of a tagged Chinook salmon to the velocity field if and when it holds position to determine if the tide may be influencing the movement.

    i. A single 90 degree turn is not definitive proof that a tag is in a predator; three or more turns greater than 30 degrees would be important information (and one piece of evidence) used to establish a salmon may have been eaten.

    ii. Low or negative water velocity in the area of a smolt may make large turns (greater than 30 degrees) more likely. If there are large turns, and the water velocity is low (< 2 Body Lengths per second (BLS)) or negative then 5 or more turns of a ≥ 30 degree angle are required before these turns are considered evidence of predation. A turn under the WG bridge would not count toward the 5 turn rule because smolts can often make turn as they pass under shadows.

c) The following metrics can be used to quantitatively distinguish between juvenile Chinook salmon and predator behavior:

    i. Tortuosity

    ii. Movement rate (within array and/or transit time to downstream node), e.g. movement rate of smolts was significantly faster than predators at the Head of Old River.

    iii. Residence time in the experimental area

    iv. Detection at downstream node (note: this is considered the weakest form of evidence)

        - If a tag never reached a downstream node, this is suggestive evidence that the tag was eaten.

        - If a tag reached a downstream node in less than 3 hours and velocity in the hydrophone array was > +0.25 m/s then this is evidence that the tag was not eaten and passed the downstream node in an uneaten smolt.

d) If predation is determined the research team should follow the track back in time. The echo in which the first predator-like behavior is noted by the team should be recorded as the location of the predation event. It is probable that there will be a marked change in direction or speed when the predation event occurred.

    i. If the location of the predation event was outside the array, then code the predation event as "arrive as a predator" (upstream) or "return as predator" (return from downstream).

e) If a track stops in the center of the array, or is otherwise incomplete it may be necessary to re-track the file to add additional data and get both longer tracks and longer trailing ends of tag detections.

f) 2D track positions that are outside of the array are less reliable and should not be solely used to determine predation.

g) If, using the above rules, it is not clear in which category a track belongs, use Unknown.

h) Use the preponderance of evidence to make the determination of predation or not.

i) If, after 2 minutes of review, there is a question on whether or not the smolt has been eaten, code as Unknown and move on.

Rules for Determining Guidance

Objective: Obtain guidance efficiency for 2D tracks of juvenile Chinook salmon that were not eaten upstream of the FFGS

1. Eight people (Four teams of 2 people) evaluate all tracks from tags inserted in juvenile Chinook salmon

    a) At the beginning of the COF, all participants will review the guidance rules set out here

    b) Any changes to the rules must be agreed to before making guidance determinations

2. Once the track has been reviewed, the COF participants will assign a guidance fate to the response event in the fate spreadsheet

3. Rules for determining guidance/deterrence

a) Establish a line of approach (LOA) for the tag of interest. This line should be immediately upstream of the approach to the FFGS. The last point on the LOA line shall be referred to as the Start Point.

b) Establish a point downstream (Endpoint) that represents the end of the course change you wish to analyze. The point can be any distance but should not exceed 100 meters from the Start Point.

c) Draw imaginary lines on the LOA and the line between the Start Point and End Point. The line between the Start Point and the End Point shall be referred to as the Changed Course Line (CCL).

d) Look for a marked change in direction that may indicate that the track has been guided and/or deterred by the FFGS. Look at the velocity vectors when reviewing the CCL.

e) The following approach and metrics can be used to quantitatively distinguish guidance or deterrence:

   ii. Measure the angle (Angle A) between LOA and the CCL.

   iii. If Angle A is greater than 25 degrees, then it is likely that the fish was guided/deterred.

   iv. If Angle A is between 21 and 25 degrees then the CCL does not provide strong evidence for guidance/deterrence or no guidance/deterrence.

   v. If Angle A is less than 21 degrees then it was likely that the fish was not guided/deterred.

   vi. Enter guidance/deterrence determination in the fates spreadsheet.

   vii. Record the angle of change in the fates spreadsheet (if guidance is determined to have occurred, you must enter an angle of change).

   viii. Record the start and stop times for the guidance/deterrence CCL (distance that the track guided along the FFGS). If the track was deterred away from the FFGS without being guided along FFGS (e.g., the track pivoted away from the FFGS), record the start and stop with the same time.

APPENDIX E

2014 GEORGIANA SLOUGH FFGS STUDY
TRANSITION CLASSIFICATIONS USED TO
IDENTIFY CONSUMED SMOLT TAGS

Table E-1 Transition Classifications used to Identify Consumed Smolt Tags	
Transition	**Transition Type**
FPT-FPT	Unknown
FPT-GEO	Unknown
FPT-LPS	Unknown
FPT-MAL_E	Unknown
FPT-MIN_Downstream	Unknown
FPT-MOK	Unknown
FPT-SAC_Downstream	Unknown
FPT-SAC_Upstream	Unknown
FPT-STM_Downstream	Unknown
FPT-STM_Upstream	Unknown
FPT-SUT_Upstream	Unknown
FPT-WGB	Unknown
GEO-FPT	Predator
GEO-GEO	Unknown
GEO-LPS	Unknown
GEO-MAL_E	Unknown
GEO-MAL_W	Unknown
GEO-MIN_Downstream	Unknown
GEO-MOK	Unknown
GEO-SAC_Downstream	Predator
GEO-SAC_Upstream	Predator
GEO-STM_Upstream	Predator
GEO-WGB	Predator
LPS-GEO	Predator
LPS-LPS	Unknown
LPS-MAL_E	Unknown
LPS-MAL_W	Unknown
LPS-MOK	Unknown
LPS-SAC_Upstream	Predator
LPS-WGB	Predator
MAL_E-GEO	Predator
MAL_E-MAL_E	Unknown
MAL_E-MAL_W	Unknown
MAL_E-MIN_Downstream	Unknown
MAL_E-MOK	Predator
MAL_E-SAC_Downstream	Unknown
MAL_E-STM_Downstream	Unknown
MAL_W-FPT	Predator
MAL_W-GEO	Predator
MAL_W-MAL_E	Unknown

Table E-1
Transition Classifications used to Identify Consumed Smolt Tags

Transition	Transition Type
MAL_W-MAL_W	Unknown
MAL_W-MIN_Downstream	Unknown
MAL_W-MOK	Predator
MAL_W-SAC_Downstream	Unknown
MAL_W-WGB	Predator
MIN_Downstream-FPT	Predator
MIN_Downstream-GEO	Unknown
MIN_Downstream-MAL_E	Unknown
MIN_Downstream-MAL_W	Unknown
MIN_Downstream-MIN_Downstream	Unknown
MIN_Downstream-MOK	Predator
MIN_Downstream-SAC_Downstream	Unknown
MIN_Downstream-STM_Downstream	Unknown
MIN_Downstream-STM_Upstream	Predator
MIN_Downstream-SUT_Upstream	Predator
MOK-GEO	Predator
MOK-LPS	Unknown
MOK-MAL_E	Unknown
MOK-MAL_W	Unknown
MOK-MIN_Downstream	Unknown
MOK-MOK	Unknown
MOK-SAC_Downstream	Predator
MOK-SAC_Upstream	Predator
MOK-STM_Downstream	Predator
MOK-WGB	Predator
ReleaseBD-GEO	Predator
ReleaseBD-LPS	Predator
ReleaseBD-MAL_E	Predator
ReleaseBD-MAL_W	Predator
ReleaseBD-MIN_Downstream	Predator
ReleaseBD-MOK	Predator
ReleaseBD-SAC_Downstream	Predator
ReleaseBD-SAC_Upstream	Predator
ReleaseBD-WGB	Predator
ReleaseGeo-GEO	Unknown
ReleaseGeo-LPS	Unknown
ReleaseGeo-MAL_E	Unknown
ReleaseGeo-MAL_W	Unknown
ReleaseGeo-MOK	Unknown
ReleaseGeo-SAC_Downstream	Unknown

Table E-1 Transition Classifications used to Identify Consumed Smolt Tags	
Transition	**Transition Type**
ReleaseGeo-SAC_Upstream	Predator
ReleaseGeo-WGB	Predator
ReleaseSac-FPT	Unknown
ReleaseSac-GEO	Unknown
ReleaseSac-MIN_Downstream	Unknown
ReleaseSac-MOK	Unknown
ReleaseSac-SAC_Downstream	Unknown
ReleaseSac-SAC_Upstream	Unknown
ReleaseSac-STM_Downstream	Unknown
ReleaseSac-STM_Upstream	Unknown
ReleaseSac-SUT_Upstream	Unknown
ReleaseSac-WGB	Unknown
SAC_Downstream-GEO	Unknown
SAC_Downstream-LPS	Unknown
SAC_Downstream-MAL_E	Unknown
SAC_Downstream-MAL_W	Unknown
SAC_Downstream-MIN_Downstream	Predator
SAC_Downstream-MOK	Predator
SAC_Downstream-SAC_Downstream	Unknown
SAC_Downstream-SAC_Upstream	Predator
SAC_Downstream-STM_Downstream	Unknown
SAC_Downstream-SUT_Upstream	Predator
SAC_Downstream-WGB	Unknown
SAC_Upstream-FPT	Predator
SAC_Upstream-GEO	Unknown
SAC_Upstream-LPS	Unknown
SAC_Upstream-MAL_E	Unknown
SAC_Upstream-MAL_W	Unknown
SAC_Upstream-MOK	Unknown
SAC_Upstream-SAC_Downstream	Unknown
SAC_Upstream-SAC_Upstream	Unknown
SAC_Upstream-STM_Downstream	Unknown
SAC_Upstream-STM_Upstream	Unknown
SAC_Upstream-SUT_Upstream	Unknown
SAC_Upstream-WGB	Unknown
STM_Downstream-FPT	Predator
STM_Downstream-GEO	Unknown
STM_Downstream-LPS	Unknown
STM_Downstream-MAL_E	Unknown
STM_Downstream-MAL_W	Unknown

Table E-1 Transition Classifications used to Identify Consumed Smolt Tags	
Transition	**Transition Type**
STM_Downstream-MIN_Downstream	Predator
STM_Downstream-MOK	Predator
STM_Downstream-SAC_Downstream	Unknown
STM_Downstream-STM_Downstream	Unknown
STM_Downstream-STM_Upstream	Predator
STM_Downstream-SUT_Upstream	Predator
STM_Upstream-FPT	Predator
STM_Upstream-MAL_E	Unknown
STM_Upstream-MIN_Downstream	Unknown
STM_Upstream-SAC_Upstream	Unknown
STM_Upstream-STM_Downstream	Unknown
STM_Upstream-STM_Upstream	Unknown
STM_Upstream-SUT_Upstream	Unknown
STM_Upstream-WGB	Unknown
SUT_Upstream-FPT	Predator
SUT_Upstream-GEO	Unknown
SUT_Upstream-MAL_E	Unknown
SUT_Upstream-MAL_W	Unknown
SUT_Upstream-MIN_Downstream	Unknown
SUT_Upstream-SAC_Upstream	Unknown
SUT_Upstream-STM_Downstream	Unknown
SUT_Upstream-STM_Upstream	Unknown
SUT_Upstream-SUT_Upstream	Unknown
SUT_Upstream-WGB	Unknown
WGB-FPT	Predator
WGB-GEO	Unknown
WGB-MAL_E	Unknown
WGB-MAL_W	Unknown
WGB-MOK	Unknown
WGB-SAC_Downstream	Unknown
WGB-SAC_Upstream	Predator
WGB-STM_Downstream	Unknown
WGB-WGB	Unknown

APPENDIX F

FOCAL PREDATORY FISH SPECIES

This appendix describes the focal predatory fish species from the 2014 Georgiana Slough Floating Fish Guidance Structure (GSFFGS) study. The brief accounts below mostly rely on information provided by Moyle (2002) and references therein, with other sources as noted. As described in the main body of this report, the focal predatory fishes for study based on high abundance in previous years at the same location were striped bass, smallmouth bass, and spotted bass. However, there was difficulty identifying the black basses, and that redeye bass and potential hybrids of spotted, smallmouth, and redeye bass may have been present, so the characteristics of all three black basses are described below.

1.1 Striped Bass

Striped bass (*Morone saxatilis*) is native to the eastern United States (St. Lawrence River to Louisiana) and was introduced to the San Francisco estuary in 1879 (Dill and Cordone 1997). A commercial fishery for striped bass was established within 10 years of introduction and continued until the fishery was prohibited in 1935, with annual catches averaging nearly 660,000 pounds in the fishery's final decade (Skinner 1962, as cited by Dill and Cordone 1997). The sport fishery developed more slowly than the commercial fishery; by the late 1960s, it constituted approximately 60% of the angling dependent on the San Francisco estuary, including the ocean and river Pacific salmon fisheries (Chadwick 1968, as cited by Dill and Cordone 1997).

The adult striped bass population (males age 2 and older and females age 4 and older) was estimated at between 2.3 and 3 million fish in the early 1960s (Dill and Cordone 1997). Adult abundance generally declined from the 1960s to the late 1980s/early 1990s, at which point female abundance was approximately 500,000 fish and male abundance was 300,000 to 400,000 fish (Loboschefsky et al. 2012). Subsequent abundance from the mid-1990s to mid-2000s was higher. The abundance of subadult striped bass (males younger than age 2 and females younger than age 4) was estimated to be variable (4 to 15 million fish) between 1981 and 2003; age 2 abundance doubled in the mid- to late 1990s (Loboschefsky et al. 2012).

Striped bass are epipelagic opportunistic feeders, and prey changes with life stage. Juvenile and older striped bass prey upon fish and invertebrates. Striped bass have not been studied in the Pacific Ocean. Modeling has estimated, however, that the total annual consumption of prey fish by striped bass adults (age 3 and older) between 1969 and 2004 in the San Francisco Bay-Delta watershed ranged between approximately 8,200 metric tons in 1994 and approximately 30,500 metric tons in 1972 (Loboschefsky et al. 2012). Annual total consumption of prey fish by subadult striped bass (those ages 1 and 2) between 1981 and 2003 was estimated to have varied between approximately 2,000 metric tons in 1988 and approximately 19,000 metric tons in 1999/2000 (Loboschefsky et al. 2012).

The abundance of young-of-the-year striped bass that was collected in the Fall Midwater Trawl survey conducted by the California Department of Fish and Wildlife has declined considerably over time. It is unknown why this has occurred, based on the lack of a similar decline in adult abundance (Baxter et al.

2010). Factors related to the decline in young-of-the-year abundance may include changes in summer food availability, fall Delta outflow, water clarity, and low adult abundance (Mac Nally et al. 2010; Thomson et al. 2010).

A long-term shift in striped bass distribution into shallower areas apparently also has occurred, which has lowered the number of the species able to be caught in survey trawls (Sommer et al. 2011). Telemetry studies of subadult striped bass have shown seasonal shifts in habitat use in winter and spring associated with water temperature and schooling behavior based on salinity and possibly sex (LeDoux-Bloom 2012). Seasonal habitat use may influence predation rates and create seasonal predation hotspots. Of particular relevance at the GSFFGS is the overlap of adult upstream migration periods with the downstream migration period of juvenile salmonids.

Based on catch composition from angling in this and other studies (e.g., DWR 2012), striped bass appears to be the main predatory fish species at the GSFFGS study site and elsewhere in the Delta, at least during the main months of interest for outmigrating juvenile salmonids (winter through spring). The effects on trends in the populations of native fish species from striped bass predation have received some study. Using a modeling approach, Lindley and Mohr (2003) suggested that increases in the abundance of adult striped bass could appreciably increase the probability of extinction of winter-run Chinook salmon. No support exists for abundance of adult striped bass (combined with water clarity) as a factor influencing trends in delta smelt abundance (Maunder and Deriso 2011; Miller et al. 2012). The main biological and ecological characteristics of striped bass are summarized in Table 1.

1.2 Smallmouth Bass

Smallmouth bass (*Micropterus dolomieu*) is native to the central and eastern United States north to southern Quebec. The species apparently was the first black bass species introduced into California (in 1874), and stocking was emphasized in the San Joaquin basin in the late 1800s (Dill and Cordone 1997). Larger prey such as crayfish and fish become more important above 50-mm TL (Moyle 2002). The species has hybridized with other *Micropterus* species such as spotted bass and smallmouth bass (Moyle 2002). Moyle (2002) noted that the effect of smallmouth bass on native fishes is poorly understood, but that the species coexists with native fishes when smallmouth bass density is low. A summary of the biology and ecology of smallmouth bass is presented in Table 2.

1.3 Spotted Bass

Spotted bass (*Micropterus punctulatus*) is native to the central and lower Mississippi basin from southern Illinois south and in Gulf Coast drainages from northwestern Florida to western Texas (see references cited by Moyle 2002). The northern subspecies was brought to hatcheries at Friant and Elk Grove in the 1930s and may have escaped to the San Joaquin River in 1936, before intentional introduction into various Central Valley rivers (Tuolumne, Cosumnes) and other water bodies in the late 1930s/early 1940s (Dill and Cordone 1997). The Alabama subspecies was subsequently introduced in

the 1970s, primarily to provide fishing opportunity in reservoirs with fluctuating lake levels; it is unknown to what extent the northern or Alabama subspecies or their hybrids are the main subspecies in different areas (Moyle 2002). Spotted bass of 150-mm TL and greater prey mostly on crayfish and fish, whereas smaller individuals (75-150-mm TL) consume a variety of prey including fish (see references cited by Moyle 2002). Moyle (2002) suggested that the impact of spotted bass on native fishes may be low because the species primarily occupies reservoirs and the rivers upstream of such reservoirs. A summary of spotted bass biology and ecology is presented in Table 3.

1.4 Redeye Bass

The native range of redeye bass (*Micropterus coosae*) is fairly restricted (streams in Alabama, Georgia, Tennessee, Florida, North Carolina, and South Carolina; Dill and Cordone 1997). Originally introduced into some Central Valley streams in the 1960s, the species' range has increased and Moyle (2002: 407) noted "small numbers are apparently further spread downstream in the Delta" and "they are abundant in the foothill reaches of the [Cosumnes River] and its forks". Hybridization with smallmouth and spotted bass has been found (Moyle 2002). Moyle (2002) described redeye bass as voracious predators, with small individuals taking aquatic insects and small fish; the diet of larger individuals includes fish and other prey (e.g., crayfish). Redeye bass have been found to dominate the fish fauna of some reaches of Central Valley rivers (e.g., the Cosumnes), which Moyle (2002) attributed to small adult size, aggressive behavior, and generalized habitat and feeding requirements. A summary of redeye bass biology and ecology is provided in Table 4.

Table F-1
Main Biological and Ecological Characteristics of Striped Bass

Maximum Size and Age	Size By Age	Diet and Other Feeding Characteristics	Primary Habitat and Environmental Conditions	Migratory Behavior	Intraspecific Associations	Reproduction
125 cm FL (41 kg), >30 years (Moyle 2002)	First year: 9–11 cm FL Second year: 23–30 cm FL Third year: 28–40 cm FL Fourth year: 44–54 cm FL Growth of 5–10 cm/year thereafter (Moyle 2002) Assumed sizes at age in bioenergetics modeling by Loboschefsky et al. (2012): 1: 172 mm FL 2: 254 mm FL 3: 448 mm FL 4: 537 mm FL 5: 611 mm FL 6: 680 mm FL (Loboschefsky, pers. comm., 2013)	Age 1: 12% fish, 88% other (by volume) Age 2: 82% fish, 18% other (by volume) Age 3+: 99% fish, 1% other (by volume) (values assumed by Loboschefsky et al. 2012) Opportunistic feeders that consume most possible prey types, including fish such as threadfin shad, juvenile striped bass, and juvenile salmonids (Moyle 2002; Tucker et al. 1998)	Pelagic (Moyle 2002); temperature tolerance 7.2° to 27°C, salinity 0–33.7 ppt, current velocity tolerance 0–500 cm/s and optimum 0–100 cm/s (Hassler 1988)	Subadults (~230–420 mm FL) in the Bay-Delta watershed have three main residency patterns: riverine (freshwater), low-salinity zone (0.5 to 10 ppt), and bay (10–30 ppt) (LeDoux-Bloom 2012). Riverine residents from the Sacramento/American Rivers move to the south Delta (Clifton Court Forebay) in fall, and then return upstream to the rivers in spring. Subadults emigrate to the ocean in winter and return to the bays and rivers in late spring (LeDoux-Bloom 2012). Adults generally move into freshwater from San Pablo and San Francisco Bays in fall, and many overwinter in the Delta before a spring upstream spawning migration and return to the bays thereafter (Moyle 2002).	Gregarious (Moyle 2002)	Spawn in freshwater mostly from mid-April to mid-June (Hassler 1988). No spawning occurs below 14°C, optimum temperature is 15° to 20°C, and spawning ceases at >21°C (Moyle 2002). Most spawning in the Sacramento River, principally between Feather River mouth (river km 125) and Colusa (river km 195), although spawning may occur in the Delta during wetter years (Moyle 2002). Females typically first spawn at 4–6 years (45 cm FL), and males mostly first spawn at 2–3 years (25 cm FL) (Moyle 2002). Spawning consists of up to 30 fish (of which 1-2 are female) leaving a main group of thousands of adults aggregated inshore; spawning in the main current near the surface.

Notes: °C = degrees Celsius; Bay-Delta = San Francisco Bay/Sacramento–San Joaquin Delta; cm = centimeters; FL = fork length; kg = kilograms; cm/s = centimeters per second; mm = millimeters; ppt = parts per thousand

TableF-2
Main Biological and Ecological Characteristics of Smallmouth Bass

Maximum Size and Age	Size By Age	Diet and Other Feeding Characteristics	Primary Habitat and Environmental Conditions	Migratory Behavior	Intraspecific Associations	Reproduction
Maximum reported length: 69-cm TL; maximum reported weight: 5.4 kg; maximum reported age: 26 years (see references in Froese and Pauly 2011). In California: 4.1 kg, fish older than 4 years and 40 cm are not uncommon (Moyle 2002).	In streams (with Deer Creek as an example), size at end of first year: 80 mm; end of second year: 138 mm; end of third year: 187 mm; end of fourth year: 223 mm; and end of fifth year: 275 mm (Moyle 2002).	Feed largely on crustaceans and aquatic insects until 3-5-cm TL; crayfish and fish dominate diet of smallmouth bass 10-15-cm TL and greater; frequently cannibalistic at all sizes (Moyle 2002). Most active in evening and early morning, although feeding may occur any time of day or night depending on conditions (Moyle 2002).	Most populations occur where summer temperatures are 20°-27°C; most abundant in moderate-gradient streams with pools, riffles, and runs with rocky bottoms and overhanging trees, typically at 100-1,000 m elevation in the Central Valley; rarely found in upper reaches of estuaries in California (Moyle 2002). Adult instream flow criteria include optimal suitability at 0 ft/s velocity (decreasing to zero suitability at 2 ft/s), optimal depth of 4 feet and greater (zero-low suitability at 2 feet or less depth), and a preference for cobbles/boulder habitat (Edwards et al. 1983).	Small home ranges and return to home areas if displaced (references in Moyle 2002). Move into shallow water (<1.5 m) in lakes or quiet areas of streams to spawn (Moyle 2002).	Rarely school (Moyle 2002).	Nests are created by solitary males near cover (e.g., submerged logs and boulders) in rubble, gravel, or sand bottoms at depths of around 1 m, but may also be found from 0.5 to 5 m (Moyle 2002). Males may use favorable nesting sites in successive years (references in Moyle 2002). Most reservoir spawning is in May/June but may extend into July in streams, with male nest building beginning at 13°-16°C (Moyle 2002). Sexual maturity is usually reached at the end of the third or fourth year (Moyle 2002).

Notes: °C = degrees Celsius; cm = centimeters; FL = fork length; kg = kilograms; cm/s = centimeters per second; mm = millimeters; ppt = parts per thousand; TL = total length; SL = standard length

Table F-3
Main Biological and Ecological Characteristics of Spotted Bass

Maximum Size and Age	Size By Age	Diet and Other Feeding Characteristics	Primary Habitat and Environmental Conditions	Migratory Behavior	Intraspecific Associations	Reproduction
Maximum reported length: 63.5-cm TL; maximum reported weight: 4.7 kg; maximum reported age: 7 years (see references in Froese and Pauly 2011). In California: 4.3 kg, 45-cm TL (Moyle 2002).	Growth rates are greater in newer reservoirs, and slower in cool streams (few fish live longer than 4-5 years). Size ranges for native populations: First year: 65-170-mm TL Second year: 150-325-mm TL Third year: 205-405-mm TL Fourth year: 245-435-mm TL Fifth year: 315-505-mm TL Sixth year: 280-565-mm TL Seventh year: 315-610-mm TL (Moyle 2002)	Diet for individuals < 75-mm TL is mostly aquatic insects and crustaceans; for individuals 75-150-mm TL, diet consists of aquatic insects, fish, crayfish, and terrestrial insects; larger individuals primarily eat crayfish and fish, including the young of their own species and other black basses (Moyle 2002 and references therein).	Prefer slower, more turbid water than smallmouth bass and faster water than largemouth bass, and tend to reside in pools in streams (Moyle 2002). Optimal instream criteria for adult spotted bass are velocity < 0.2 ft/s (with no suitability above nearly 3 ft/s), depth of around 5-10 ft (with no suitability of waters around 18 feet and deeper), and a variety of substrates (ranging from silt to bedrock) that are coarser than plant detritus/organic material and mud/soft clay (McMahon et al. 1983).Prefer summer water temperatures of 24°-31°C and may be found in brackish water to 10 ppt, although there generally is low tolerance for brackish water (references in Moyle 2002).	Adults generally occupy a limited area for most of the year but spring spawning migrations are common (references in Moyle 2002).	Larger fish tend to be solitary, whereas juveniles occur in small schools (Moyle 2002).	Stream-dwelling males create nests in low-current areas substrates ranging from debris to gravel (Moyle 2002). Late spring spawning at 15°–18°C, continues until late May/early June (22°–23°C), preceded by male nest building in late March/early April (14°–15°C; references in Moyle 2002). Sexual maturity begins in second or third year (Moyle 2002).

Notes: °C = degrees Celsius; cm = centimeters; kg = kilograms; ppt = parts per thousand; TL = total length

Table F-4
Main Biological and Ecological Characteristics of Redeye Bass

Maximum Size and Age	Size By Age	Diet and Other Feeding Characteristics	Primary Habitat and Environmental Conditions	Migratory Behavior	Intraspecific Associations	Reproduction
Maximum reported length: 47-cm TL; maximum reported weight: 3.7 kg; maximum reported age: 10 years (see references in Froese and Pauly 2011). In California: 41-cm TL, although fish >35-cm TL may be hybrids with smallmouth bass (Moyle 2002).	Extremely slow growth in streams, with size in first year 4.5-6.5-cm TL, and only growing 2-3 cm/yr to reach 25-cm TL after 9-10 years (references in Moyle 2002).	Opportunistic (surface, water column, and bottom), with diet frequently consisting of terrestrial insects, aquatic insects, fish, crayfish, and salamanders (Moyle 2002).	Typically occur in clear and warm streams (summer temperatures 26°–28°C), in pools, water pockets near boulders, and undercut banks (Moyle 2002). Some segregation by size class evident: small individuals in riffles, medium individuals in runs, and large individuals in pools (Crain, pers. comm., 2014).	Spring spawning migration up small tributary streams or to pool heads in larger streams (Moyle 2002).	Variable by habitat: in lower (tidal) Mokelumne River, low abundance and solitary adults; in Cosumnes River, small and medium individuals often formed loose schools (Crain, pers. comm., 2014).	Males construct nests in beds of gravel within upper reaches of streams, with late spring spawning at temperatures of 17°–21°C (Moyle 2002).

Notes: °C = degrees Celsius; cm = centimeters; FL = fork length; kg = kilograms; mm = millimeters; ppt = parts per thousand; TL = total length

1.5 References

Baxter, R., R. Breuer, L. Brown, L. Conrad, F. Feyrer, S. Fong, K. Gehrts, L. Grimaldo, B. Herbold, P. Hrodey, A. Mueller-Solger, T. Sommer, and K. Souza. 2010. *2010 Pelagic Organism Decline Work Plan and Synthesis of Results*. Sacramento, CA: Interagency Ecological Program.

California Department of Water Resources. 2012. *2011 Georgiana Slough Non-Physical Barrier Performance Project Report*. Sacramento, CA.

Chadwick, H. 1968. Striped Bass Fishing: How Good Will It Be in 1991? *Outdoor California* 29(6):1–3.

Crain, Patrick. Fish Biologist. ICF International, Sacramento, CA. May 28, 2014—e-mail to Marin Greenwood, Aquatic Ecologist, ICF International, Sacramento, CA.

Dill, W. A., and A. J. Cordone. 1997. History and Status of Introduced Fishes in California, 1871–1996. *California Department of Fish and Game Fish Bulletin* 178:1–414.

DWR. *See* California Department of Water Resources.

Edwards, E. A., G. Gebhart, and O. E. Maughan. 1983. *Habitat suitability index models: smallmouth bass*. U.S. Fish and Wildlife Service. FWS/OBS-82/10.36.

Froese, R. and D. Pauly. Editors. 2011.FishBase. World Wide Web electronic publication. 04/2014. Available: www.fishbase.org. Accessed: May 27, 2014.

Hassler, T. J. 1988. *Species Profiles: Life Histories and Environmental Requirements of Coastal Fishes and Invertebrates (Pacific Southwest): Striped Bass*. U.S. Fish and Wildlife Service Biological Report 82 (11.82). U.S. Army Corps of Engineers, TR EL-82-4.

LeDoux-Bloom, C. M. 2012. Distribution, Habitat Use, and Movement Patterns of Sub-Adult Striped Bass *Morone saxatilis* in the San Francisco Estuary Watershed, California. Dissertation. University of California, Davis.

Lindley, S. T., and M. S. Mohr. 2003. Modeling the Effect of Striped Bass (*Morone saxatilis*) on the Population Viability of Sacramento River Winter-Run Chinook Salmon (*Oncorhynchus tshawytscha*). *Fishery Bulletin* 101(2):321–331.

Loboschefsky, E. Division of Environmental Services, California Department of Water Resources, West Sacramento, CA. April 19, 2013—e-mail to Marin Greenwood, Aquatic Ecologist, ICF International, Sacramento, CA.

Loboschefsky, E., G. Benigno, T. Sommer, K. Rose, T. Ginn, A. Massoudieh, and F. Loge. 2012. Individual-Level and Population-Level Historical Prey Demand of San Francisco Estuary Striped Bass Using a Bioenergetics Model. *San Francisco Estuary and Watershed Science* 10(1).

Mac Nally, R., J. R. Thomson, W. J. Kimmerer, F. Feyrer, K. B. Newman, A. Sih, W. A. Bennett, L. Brown, E. Fleishman, S. D. Culberson, and G. Castillo. 2010. Analysis of Pelagic Species Decline in the Upper San Francisco Estuary Using Multivariate Autoregressive Modeling (MAR). *Ecological Applications* 20:1417–1430.

Maunder, M. N., and R. B. Deriso. 2011. A State-Space Multistage Life Cycle Model to Evaluate Population Impacts in the Presence of Density Dependence: Illustrated with Application to Delta Smelt (*Hypomesus transpacificus*). *Canadian Journal of Fisheries and Aquatic Sciences* 68:1285–1306.

McMahon, T. E., G. Gebhart, O. E. Maughan, and P. C. Nelson. 1984. *Habitat suitability index models and instream flow suitability curves: spotted bass*. U.S. Fish and Wildlife Service. FWS/OBS-82/10.72.

Miller, W. J., B. F. J. Manly, D. D. Murphy, D. Fullerton, and R. R. Ramey. 2012. An Investigation of Factors Affecting the Decline of Delta Smelt (*Hypomesus transpacificus*) in the Sacramento-San Joaquin Estuary. *Reviews in Fisheries Science* 20(1):1–19.

Moyle, P. B. 2002. *Inland Fishes of California.* Berkeley, CA: University of California Press.

Skinner, J. E. 1962. *An Historical Review of the Fish and Wildlife Resources of the San Francisco Bay Area*. California Department of Fish and Game, Water Projects Branch Rep. 1.

Sommer, T., F. Mejia, K. Hieb, R. Baxter, E. Loboschefsky, and F. Loge. 2011. Long-Term Shifts in the Lateral Distribution of Age-0 Striped Bass in the San Francisco Estuary. *Transactions of the American Fisheries Society* 140(6):1451–1459.

Thomson, J. R., W. J. Kimmerer, L. R. Brown, K. B. Newman, R. Mac Nally, W. A. Bennett, F. Feyrer, and E. Fleishman. 2010. Bayesian Change Point Analysis of Abundance Trends for Pelagic Fishes in the Upper San Francisco Estuary. *Ecological Applications* 20:1431–1448.

Tucker, M. E., C. M. Williams, and R. R. Johnson. 1998. *Abundance, Food Habits, and Life History Aspects of Sacramento Squawfish and Striped Bass at the Red Bluff Diversion Complex, Including the Research Pumping Plant, Sacramento River, California, 1994–1996: Annual Report*. Red Bluff, CA: U.S. Fish and Wildlife Service.

This page intentionally left blank.

APPENDIX G

FURTHER DETAILS OF SPLIT-BEAM TRANSDUCER AND DIDSON FIELD METHODS AND DATA PROCESSING

FURTHER DETAILS OF SPLIT-BEAM TRANSDUCER AND DIDSON FIELD METHODS AND DATA PROCESSING

Split-Beam Transducers

The locations of the transducers were georeferenced. Echoview's® Sonar Data version 6.2 was used for data analysis. After the files were imported into Echoview, calibration consisted of entering data on water temperature (used for calculating the speed of sound) and acoustic system information, including beam angle, frequency, and range gates for analysis. As a first step before analysis, files were visualized by "play-back" in Echoview, providing a high-resolution color echogram of the file. Comments were recorded on presence of fish targets, as well as on regions overshadowed by acoustic interference. The primary source of acoustic interference was volume reverberation from bubbles introduced by boat traffic, rain, or high wind events. During this preparatory phase before analysis, file sets were selected for exclusion from further analysis, either through deletion of the whole file for long-term events such as wind, or by exclusion of specific areas of the file via Echoview's region editing tools. Although fish targets often were seen in the echograms that ultimately were excluded, the overshadowing noise prevented effective analysis of the traces. In a few rare cases, file sets were excluded (e.g., if the sonar head was bumped and shifted out of position).

Two techniques were used to limit the effects of unwanted background noise or reverberation. On clear, calm days, most of the volume reverberation was likely to be observed at a relatively low level. With collection of data files at a -75 dB threshold, which is considerably lower than the acoustic size of the cutoff for fish targets of 16 cm (-40 dB), the threshold eliminating data between the collection threshold and the lower cutoff for 16-cm fish removed most data that would have interfered with data analysis. However, on days with higher turbidity attributable to runoff-related increases in discharge, and when winds were present, a subtraction echogram was employed along with thresholding, to minimize the unwanted effects of background interference. Even with the increased threshold and background subtraction, some regions were masked by high noise events, and no fish data were recoverable from these regions; such files were removed and excluded from further analysis.

Background noise subtraction was done before any thresholding (identifying target thresholds) of the data during the analysis phase because thresholding ignores targets smaller than a certain size. Background noise removal reduces the signal strength of the entire echogram, essentially subtracting the gain in signal strength on a target imposed by other scatterers in the water column within that ping. Thus, background noise removal reduces target size to an extent. The effect, although small, can have an impact at the threshold level.

The background noise echogram is artificial and is designed to mirror the noise signal being returned. In Echoview, this background signal is then subtracted from the SV echogram. Visual observation was used to determine what appeared to be the most effective noise removal level. The next step was to convert the noise-subtracted echogram back to a target strength echogram, from which a single-targets (ST) echogram was created and on which all data used for analyses were exported.

The ST echogram essentially functioned as a secondary filter, placed on the raw target strength echogram, removing unwanted signals. First, the signal was thresholded to the -40 dB level, which was the minimum cutoff for fish of 16 cm or larger. Pulse width was used as a primary filter, to test the returning wave shape. Echoes from reverberation should have corrupted wave shapes in comparison to point-source target echoes (fish). The pulse width was measured at the half amplitude (endpoint criterion equal to -6 dB). The pulse width measurement was compared with the nominal transmitted shape (0.4 ms). Echoes with pulse width measurements less than 0.3 times the nominal or greater than 1.5 times the nominal were rejected.

The next filter was the maximum allowable beam compensation. This filter put a limit on how far off the center axis of the transducer beam a target could be. For these analyses, the level was set at 10 dB. A target could be 10 dB off peak and still could be included in the analysis. The further off the center axis that a target was, the less reliable were the estimates of size and position.

The final filter involved examining the standard deviation of the angles of the samples in both the X and Y range. Samples that fell outside the above-specified ranges were rejected. A line of maximum range also was included. This was a line beyond which echoes were not analyzed. This range was set to exclude the first contact from the FFGS that the computer would interpret as a fish trace. The last stage of establishing this filter involved laying grid lines over the echogram. The range grid (5-meter spacing) and time component (10 minutes) were what Echoview used to create cells of data (layers) during the export phase, as shown in Figure 3.6-28 for the Walnut transducer.

The last step in Echoview, before data were exported for analysis, was to generate fish tracks. The human eye can easily see what constitutes a candidate fish track and what does not, but a computer must be programmed to accomplish this task. This process is called trace formation. Trace formation may be either two-dimensional, using range and time, or four-dimensional, using time and X/Y/Z position produced by a split-beam system.

Echoview's α−β Fish Tracker implements a fixed coefficient filtering method as presented by Blackman (1986). The filtering process selects out single targets as candidates for a track. The

algorithm is applied to a single target detection data point. The sensitivity of the tracker to unpredicted changes in the position and velocity of a fish is controlled by the alpha and beta gains, respectively. Each fish echo that has passed echo extraction tests is characterized by a ping number (time) and range. These provide X and Y coordinates. When a candidate echo is received, it "opens" a new trace. The range of this first seed echo is projected horizontally. A "tracking window" is centered about this position to provide a range window in the following ping. Any echo inside this range window by definition must be correlated to the seed echo. If multiple echoes fall inside the window, a best fit is calculated, and that echo is linked to the original seed echo, providing a fish trace containing two echoes. Again, the echo that is closest to the center of the window is selected to be linked to the growing fish trace. A maximum range can be specified, outside of which echoes will not be included. This is useful when fish are close together, to avoid the track jumping from fish to fish.

Fish tracks were used to provide single targets, for density calculations. Because of the number of tracks involved and the time necessary to review all the tracks, the movement of one fish could be shown as several tracks. Fish tracking parameters were adjusted to result in the greatest number of acceptable tracks without causing inclusion of traces formed by the track jumping from fish to fish. Therefore, at high densities, the number of fish is likely to be underestimated because single targets are excluded from tracks.

The analytical strategy for processing this data set was to minimize Type 2 errors. A Type 1 error is defined as missing a valid fish, and a Type 2 error is defined as including a false fish or one created from reverberation or interference. On the basis of the noise levels observed during data collection in previous years (DWR in press), it was concluded that the Type 2 errors could overwhelm the data set and provide a greater source of bias than could Type 1 errors. Consequently, echo-selection criteria and trace-formation criteria were used to minimize the formation of false fish traces. The high noise levels combined with this strategy may result in the loss of some smaller fish targets.

Exporting the trace formation process produced a data file with a line (record) for each fish trace. Traces were coded by date and time, and contained information such as mean target strength, range, off-axis distance, velocity, direction of travel, and the number of single target pings included. Exporting data by 5-meter layers provided a density spreadsheet for every 10-minute block of data, which gave the average density of fish per unit volume of water and standardized the effects of changing beam volume with distance away from the transducer.

Data files produced by the trace formation process were imported into Excel spreadsheets. The range and angular position columns were selected in each file and were plotted as a scatter plot.

The scatter plot then was evaluated for data groupings to search for anomalous distributions of targets. The largest issue was determining whether fish traces were indeed fish and not debris; or apparent large fish created from multiple echoes of small fish close to each other, resulting in the acoustic signal of a large individual. This latter problem was particularly evident in 2014, for which many schools with 3 to 4 fish were apparent towards the end of the collection period. Several methods were employed to look at overall data quality. First, fish tracks were classified as debris or fish. This step was done visually in Echoview. Large fish typically exhibited certain behavior as they moved through the transducer beam. For this reason, the fish traces did not appear as a straight line but instead displayed movement right and left in the channel as the fish passed. Furthermore, during high-flow events, most debris was present near the surface as it floated by. An X/Y plot of candidate fish traces often revealed the presence of debris (DWR 2015, in press). Some of the deeper traces may be less clear, but typically subsurface debris target strengths were lower than the threshold used to delineate large fish. By restricting analyses to exclude certain portions of the water column, much of the debris was removed from the data used for analysis.

Fish orientation, and to an extent species, can play a substantial role in estimation of target size. The decibel scale used to measure fish size is logarithmic and referenced in negative numbers (i.e., where the larger the negative number, the smaller the fish). Fish size was estimated from echo target strength using the following equation:

$$\text{Fish total length (cm)} = 1529 * e^{(-0.1142 * |\text{Target Strength (dB)}|)}$$

Thus, for example, an echo intensity of -30 dB was estimated to be a fish of nearly 50 cm, whereas an echo intensity of -40 dB was estimated to be a fish just under 16 cm. These sizes assumed parallel orientation of a fish to the transducer, as typically is the case when looking down on a fish. When looking from the side, however, fish may not be perfectly oriented parallel to the transducer. When this occurs, a fish target appears smaller than it actually is because of the reduced cross sectional area of the target. Little can be done to rectify this problem, and so fish size is likely to be somewhat underestimated in these cases, which results in lower density estimates if minimum size thresholds are being used, as was done in this study for predatory fish.

DIDSON

Typical images from the DIDSON that are discussed in Section 3.6.6 are presented here in Figures G-1 to G-14. Acoustic processing of DIDSON data included the following series of steps, resulting in a final output:

1. Raw data examination

2. Excess noise and background data removal

3. Smoothing and beam dilation

4. Multibeam Target Detection improvement

5. Target filtering

6. Target conversion

7. Fish track detection

8. Track spreadsheet summary creation

Raw data examination determined where potential processing problems may arise and which techniques may prove most useful for analysis. Based on previous experience (DWR 2015, in press), files had to be deleted from analysis when partial shading of the image occurred because of movement of debris or incorrect aiming of the DIDSON sonar and when excessive background interference limited the utility of the data.

Excess noise removal for the most part was the same as removing background interference and consisted of removing a portion of the DIDSON image that was not relevant to the analysis, typically the bottom or structure images. The standard background noise removal technique available in the DIDSON software was used for the study. This technique does not assume a static background and allows for some slow movement of the background. The software takes a mean image of a previous number of specified pings that are subtracted from the current ping. Thus, slow-moving objects (e.g., sand waves) would not be detected as motion because the previous pings are only fractions of a second apart. Although this technique is effective and can be used directly in Echoview, processing time can be slow because of the large file sizes (DWR 2015, in press). It was more efficient to allow the DIDSON Control and Display software to perform background subtraction and data reduction (i.e., removal of frames where no motion was detected) and create its own Convolved Samples Over Threshold (CSOT) files, which then were imported to Echoview for analysis. The DIDSON CSOT files were created in batch mode, and after a file directory was specified, the data reduction proceeded autonomously. During this phase, not only was the background removed, but frames empty of detected movement were deleted that, when few fish were present, reduced file size by more than 90 percent in some cases, greatly speeding up further analyses. To determine the best settings for noise removal, sample files were selected, run through the process, and examined so that fish targets were not being dropped inappropriately. This was accomplished by adjusting the cluster area size and the threshold above the background under the record options tab of the Image Capture dialog menu

in the DIDSON software. Attempting to reduce the filters enough to select smaller fish occasionally resulted in arcing of larger targets at close range, but overall this was assessed to have a minimal effect on the results.

After the background was removed from the multibeam echogram, several steps were employed in Echoview to improve target detection. Data threshold settings ensured that the proper targets were included for analyses. Two additional data operators in Echoview were used to further increase the visibility of targets. The first step was use of a median operator, which helped smooth the image without imparting any serious changes to future analyses. Adjusting this smoothing variable allowed for greater or less target definition. For smaller fish in particular, proper operation of target recognition may be troublesome (DWR in press), so a dilation filter was applied to the smoothed image. This procedure made targets easier to select but artificially increased the target size by one beam width on either side of the target. The effects of this increase in size were subtracted manually from the Excel spreadsheets of fish length data.

The next phase was to detect multibeam targets and to filter targets according to length criteria. Again, a series of target criteria were tried until it visually appeared that the software was correctly identifying most fish targets. This was only a minor consideration for larger targets; changes in parameters primarily affected small targets. To filter targets, the minimum acceptable fish length was identified (15 cm), and all targets below that threshold were excluded.

To allow Echoview to identify fish traces and to provide data suitable for analyses, multibeam data then were converted to a single-target echogram, and at this point, further analyses were identical to those used for the split-beam data; the only difference was that instead of describing fish size as a function of target strength, the actual length of the fish as detected by the multibeam target selection criteria was used.

Selecting and creating fish tracks involved the same algorithms and selection parameters described previously for the split-beam transducer. The only difference when fish tracking with DIDSON data was the loss of the minor axis component (used to calculate depth of fish in the water column). Because multiple beams are used to reference the target, the result is usually accurate positioning—much more so than with split-beam data, which can have a relatively high degree of position inaccuracy under some conditions. With better positioning data, fish tracks also are likely to be better defined because the position accuracy allows the tracking algorithm to perform better. For the DIDSON sonar data, the down- and cross-field resolutions are restricted to 512 by 96 pixels; thus, targets at closer ranges are better resolved because of pixel size. Measurement accuracy decreases at further ranges because the beam widens with distance. Furthermore, if the DIDSON sonar is operated in low-frequency mode, this error is compounded

because the beams are wider. Another potential source of measurement error is a target's aspect angle relative to the beam. As noted by DWR 2015 (in press), previous studies using a side-aspect deployment have shown that fish aspects close to 0 (perpendicular to the beam) yield the most accurate lengths (Burwen et al. 2007).

DIDSON fish tracks were exported as time-stamped variables for further analyses.

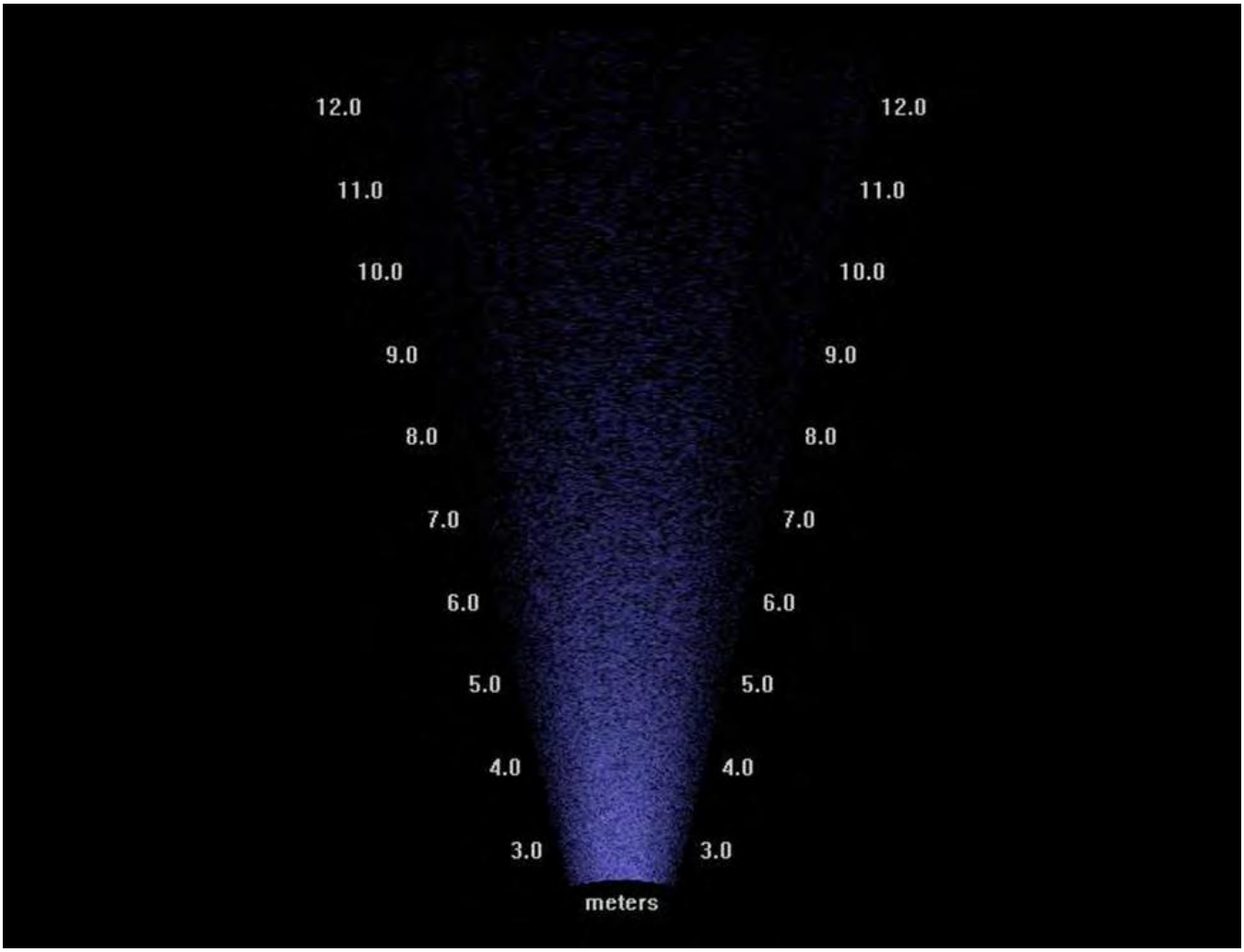

Note: Numbers along the sides of the image represent distance (meter) from the DIDSON unit. The image is of open water.

Figure G-1 Typical Image from Mid-FFGS DIDSON when Oriented toward the River Channel (Perpendicular to the FFGS) in the Upper Position

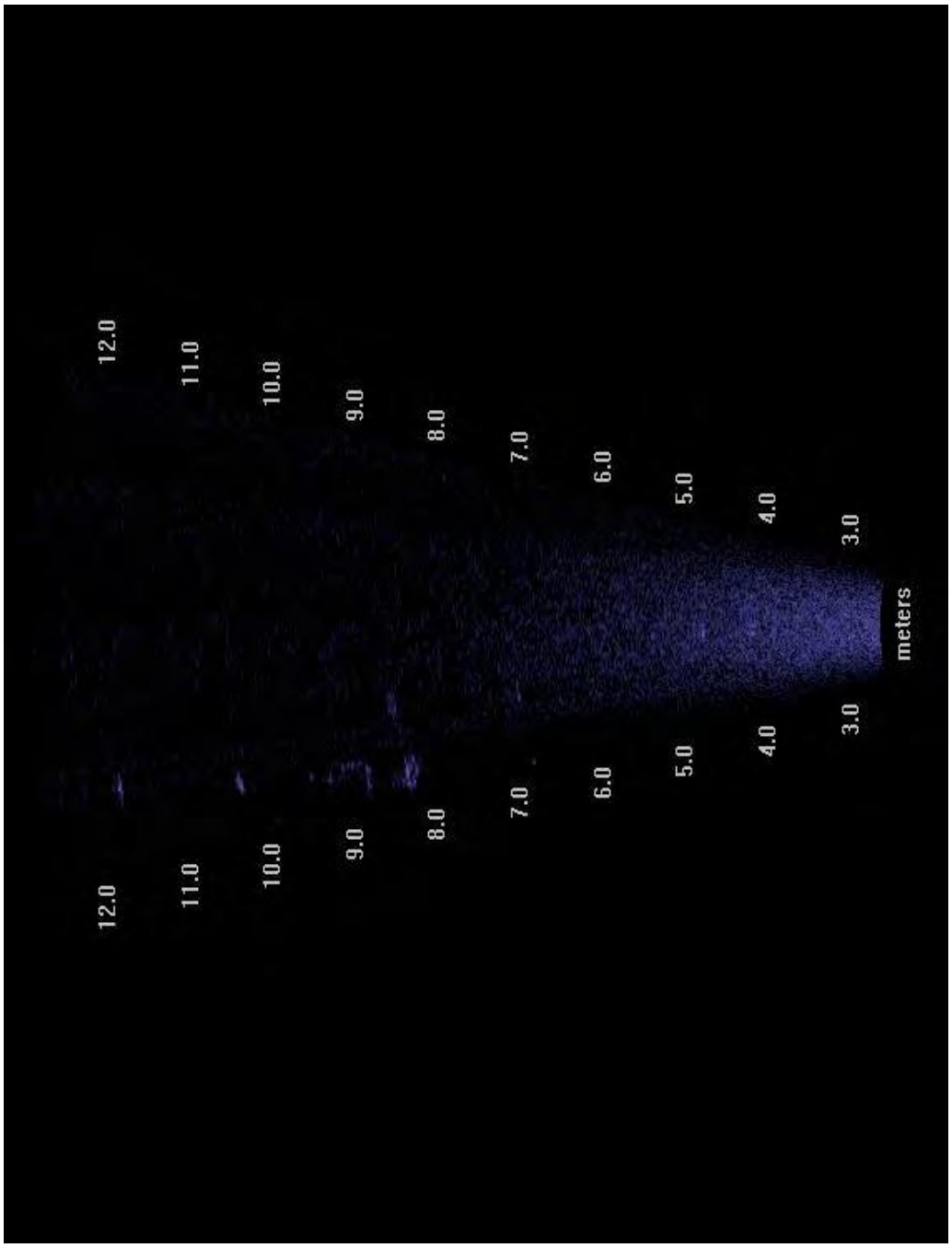

Note: Numbers along the sides of the image represent distance (m) from the DIDSON unit. The image is rotated to better represent downstream orientation of the DIDSON. The underside of the FFGS is visible from 8.0 to 12.0 meters on the lower edge of the image.

Figure G-2 Typical Image from Mid-FFGS DIDSON when Oriented along the FFGS in the Upper Position

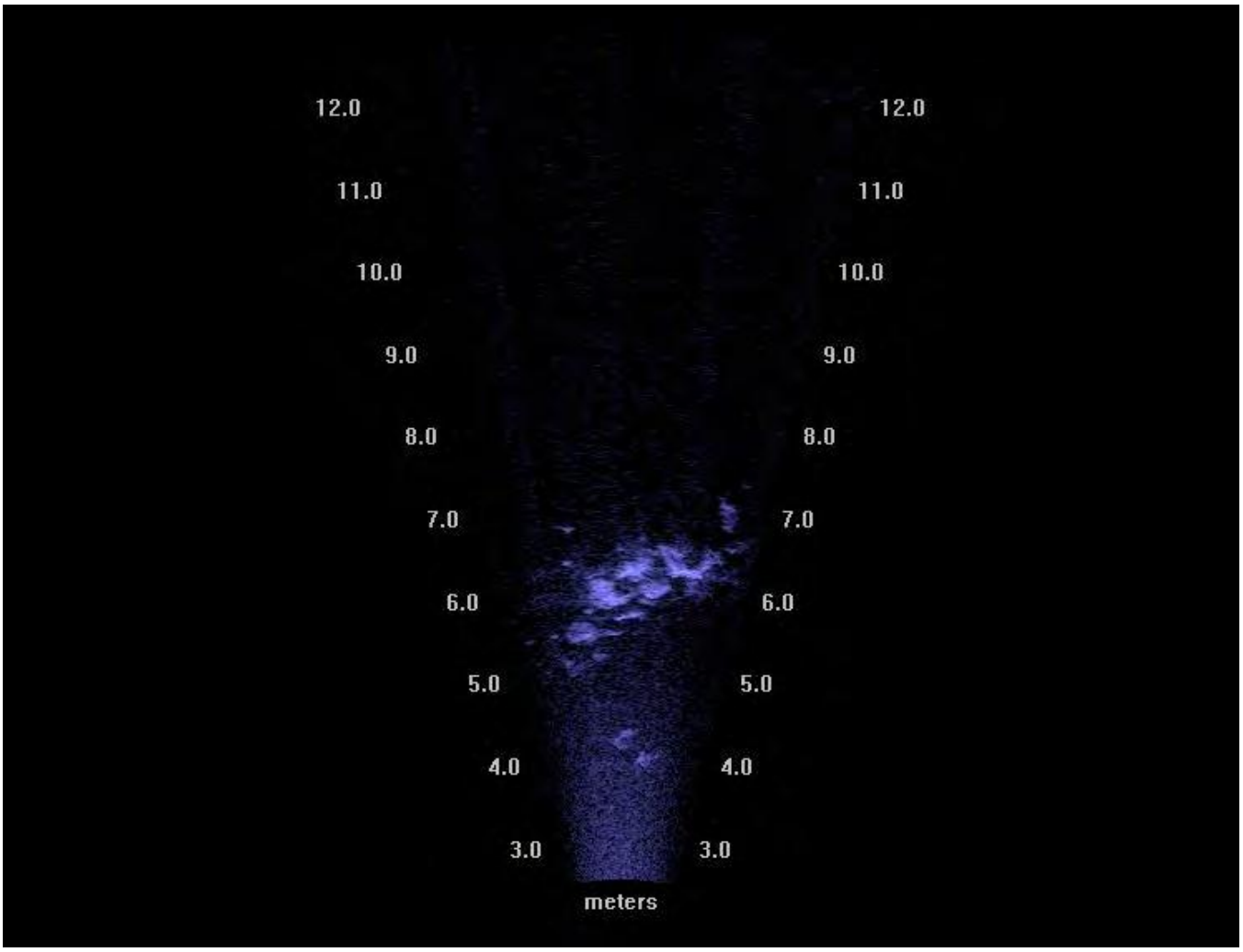

Note: Numbers along the sides of the image represent distance (meter) from the DIDSON unit. The rocks visible at around 6.0 to 7.0 meters are the edge of the nearshore riprap. Beyond the riprap is the open water of the river channel.

Figure G-3 Typical Image from Mid-FFGS DIDSON when Oriented toward the River Channel (Perpendicular to the FFGS) in the Middle Position with FFGS Off

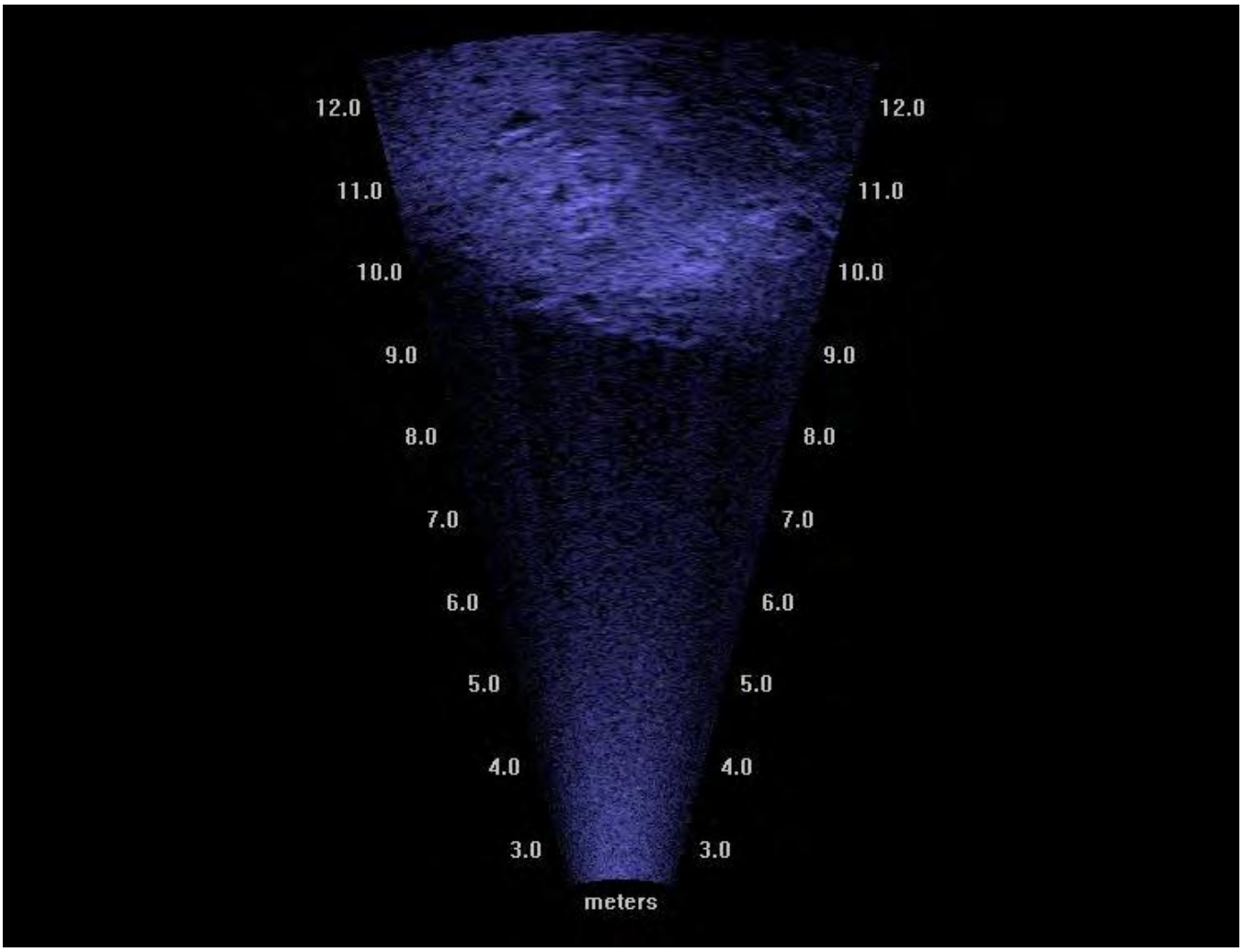

Note: Numbers along the sides of the image represent distance (meter) from the DIDSON unit. The river bed is visible at around 9.0 to 12.5 meters.

Figure G-4 Typical Image from Mid-FFGS DIDSON when Oriented toward the River Channel (Perpendicular to the FFGS) in the Lower Position with FFGS On

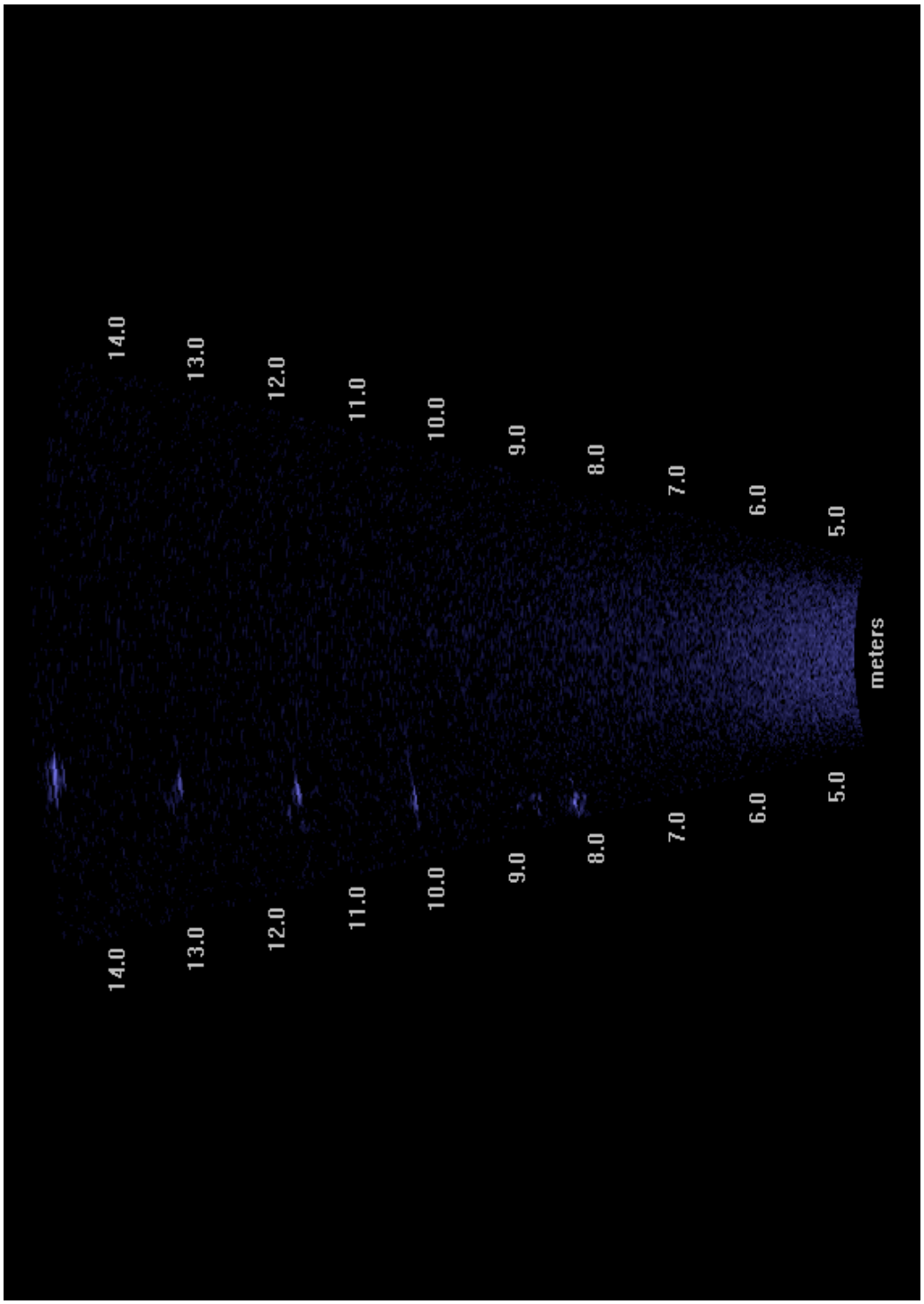

Note: Numbers along the sides of the image represent distance (meter) from the DIDSON unit. The image is rotated to better represent downstream orientation of the DIDSON. Poles extending from the underside of the FFGS near its end are visible from 8 to 14.5 meters on the lower edge of the image.

Figure G-5 Typical Image from End-FFGS DIDSON when Oriented along the FFGS in the Upper Position with the FFGS Off

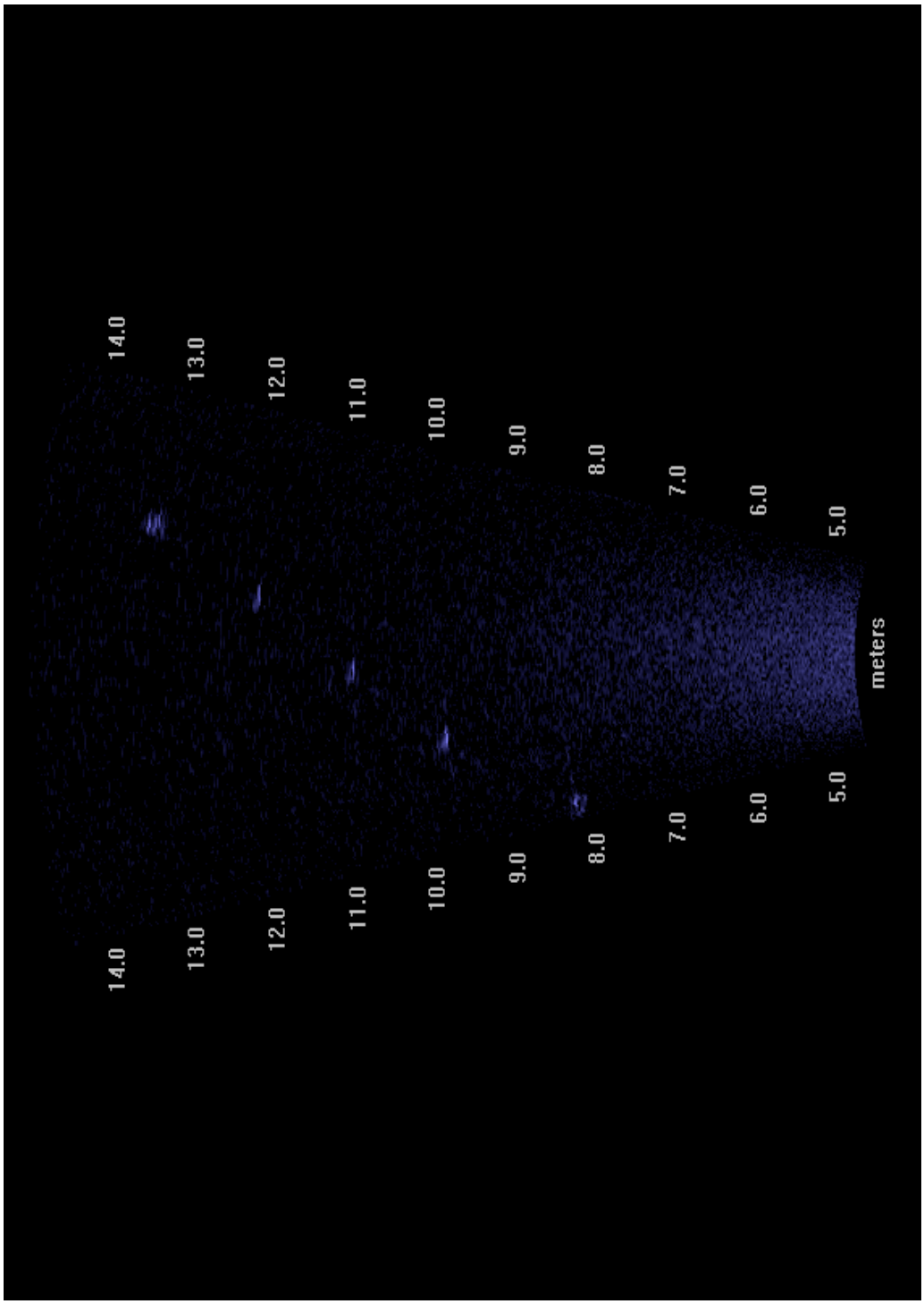

Note: Numbers along the sides of the image represent distance (meter) from the DIDSON unit. The image is rotated to better represent downstream orientation of the DIDSON. Poles extending from the underside of the FFGS near its end are visible from 8 to 13.5 meters on the lower edge of the image. Note angle of poles in comparison to the FFGS off (see **Figure 3.6-30**), caused by the curving of the FFGS near its downstream end when on.

Figure G-6 Typical Image from End-FFGS DIDSON when Oriented along the FFGS in the Upper Position with the FFGS On

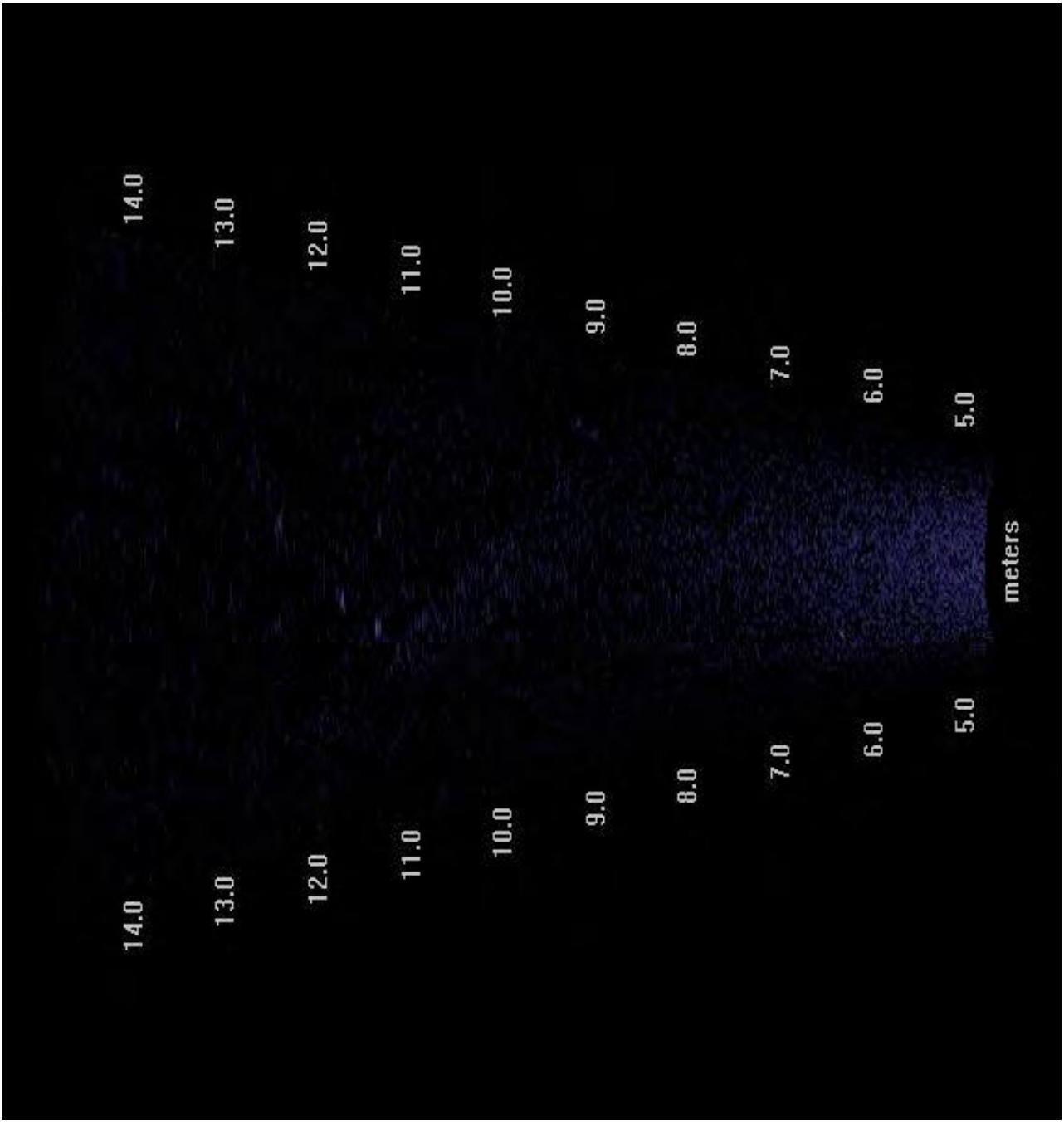

Note: Numbers along the sides of the image represent distance (meter) from the DIDSON unit. The image is rotated to better represent downstream orientation of the DIDSON. Image shows the underside of the barge behind the FFGS, faintly visible in the middle at about 9 to 12.5 meters.

Figure G-7 Typical Image from End-FFGS DIDSON when Oriented behind the FFGS in the Upper Position

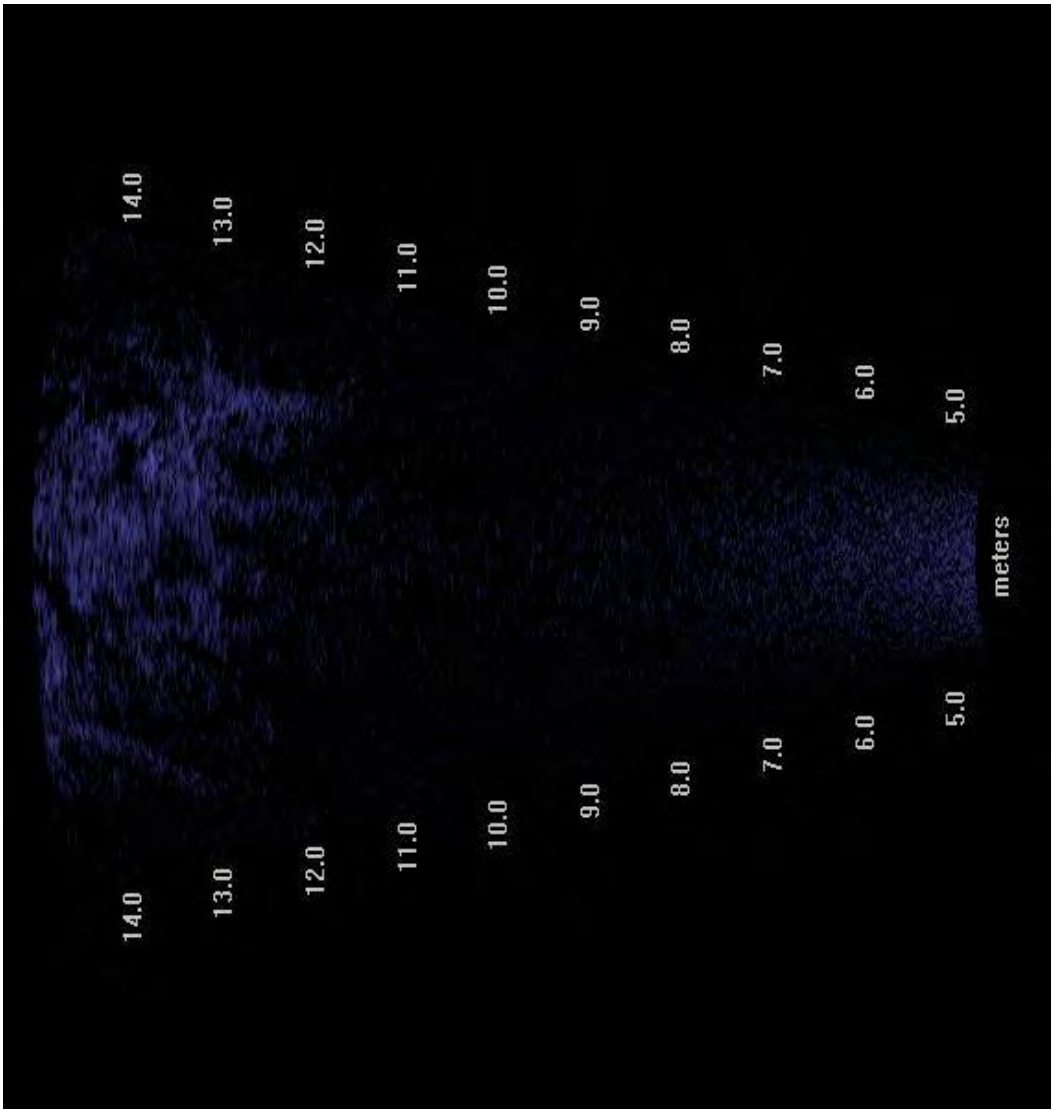

Notes: Numbers along the sides of the image represent distance (meter) from the DIDSON unit. The image is rotated to better represent downstream orientation of the DIDSON. The river bed is visible at around 12.0 to 14.5 meters.

Figure G-8 Typical Image from End-FFGS DIDSON when Oriented along the FFGS in the Lower Position with the FFGS On

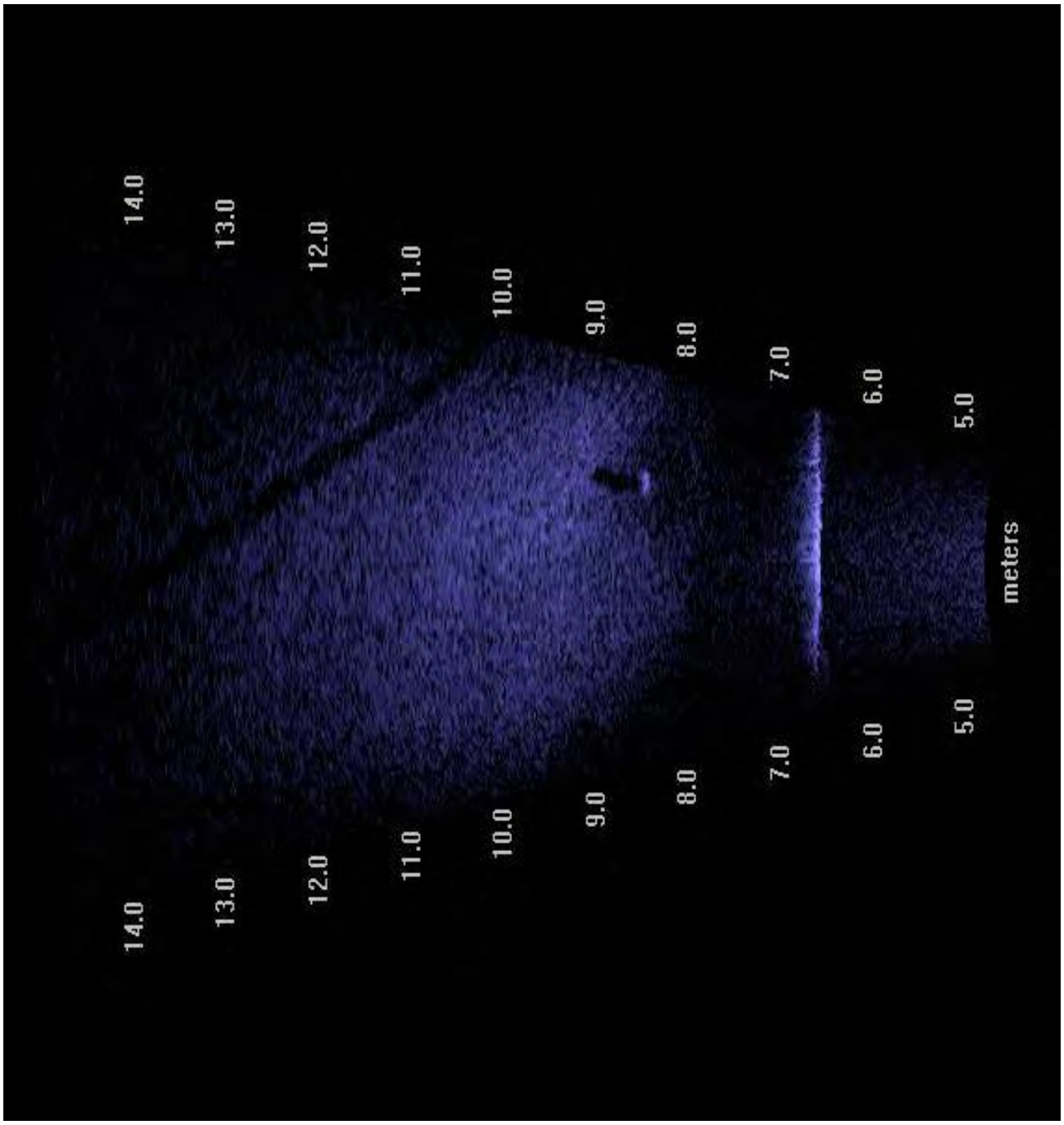

Note: Numbers along the sides of the image represent distance (meter) from the DIDSON unit. The image is rotated to better represent downstream orientation of the DIDSON. The river bed is visible at around 6.5 to 14.5 meters. The bright line at 6.5 meters likely is part of an anchor cable associated with the FFGS.

Figure G-9 Typical Image from End-FFGS DIDSON when Oriented along the FFGS in the Lower Position with the FFGS Off

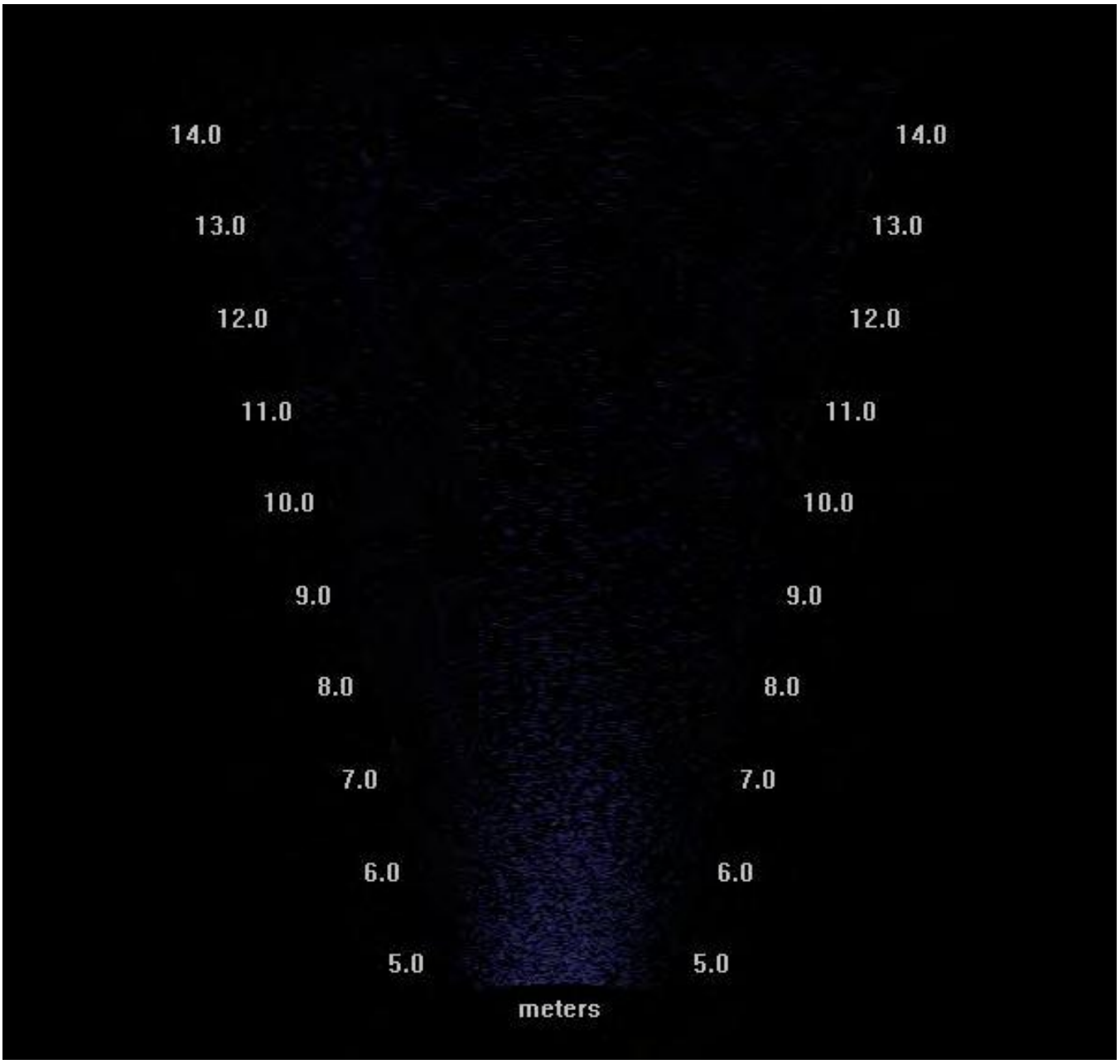

Note: Numbers along the sides of the image represent distance (meter) from the DIDSON unit. The image is of open water.

Figure G-10 **Typical Image from End-FFGS DIDSON when Oriented toward the River Channel (Perpendicular to the FFGS) in the Upper Position**

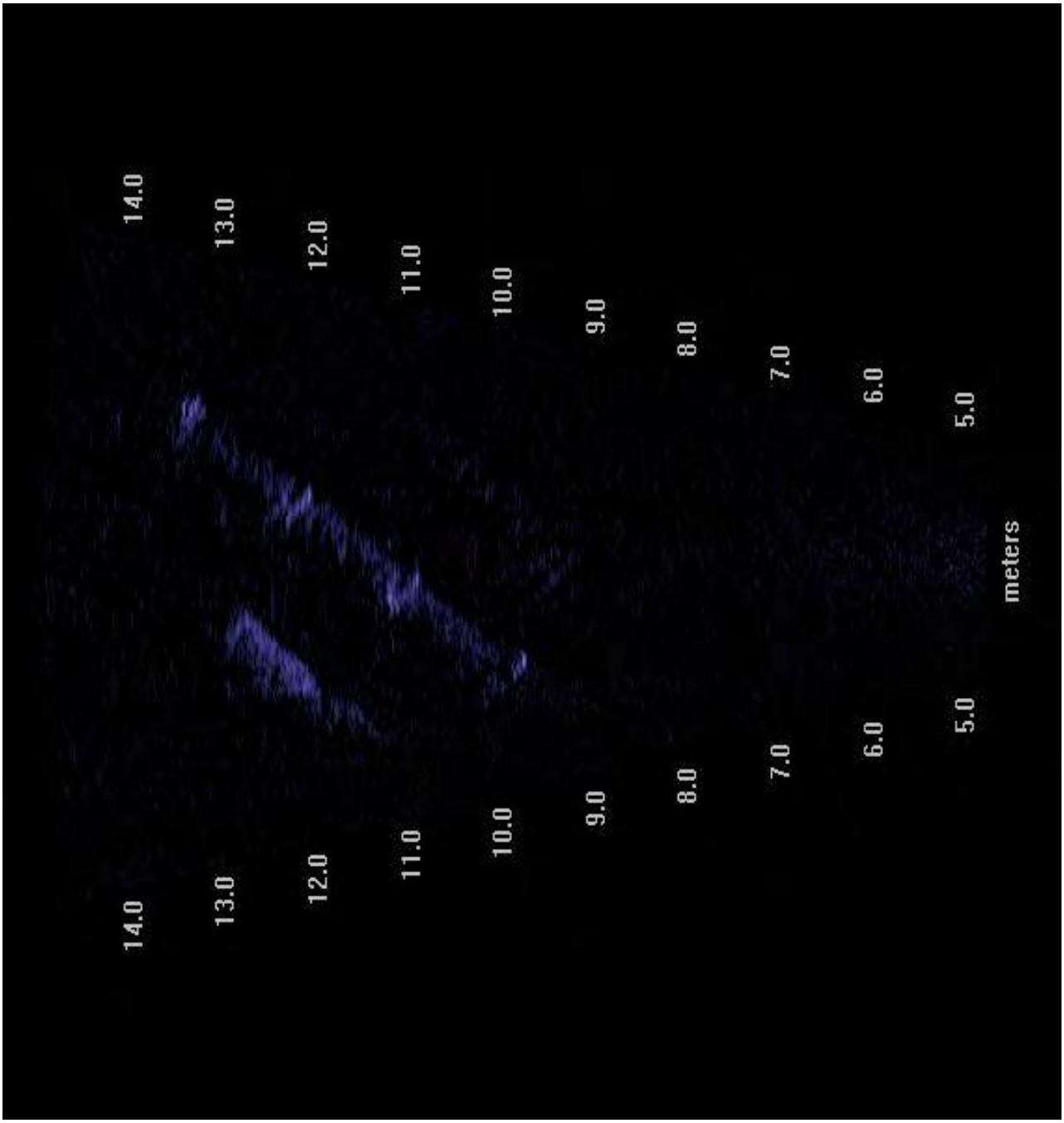

Notes: Numbers along the sides of the image represent distance (meter) from the DIDSON unit. The image is rotated to better represent downstream orientation of the DIDSON. A flotation unit is visible from 10 to 13.5 meters, a result of the curving of the end of the FFGS in the on treatment.

Figure G-11 Typical Image from End-FFGS DIDSON when Oriented along the FFGS in the Upper Position (Slightly Deeper Tilt) with the FFGS On

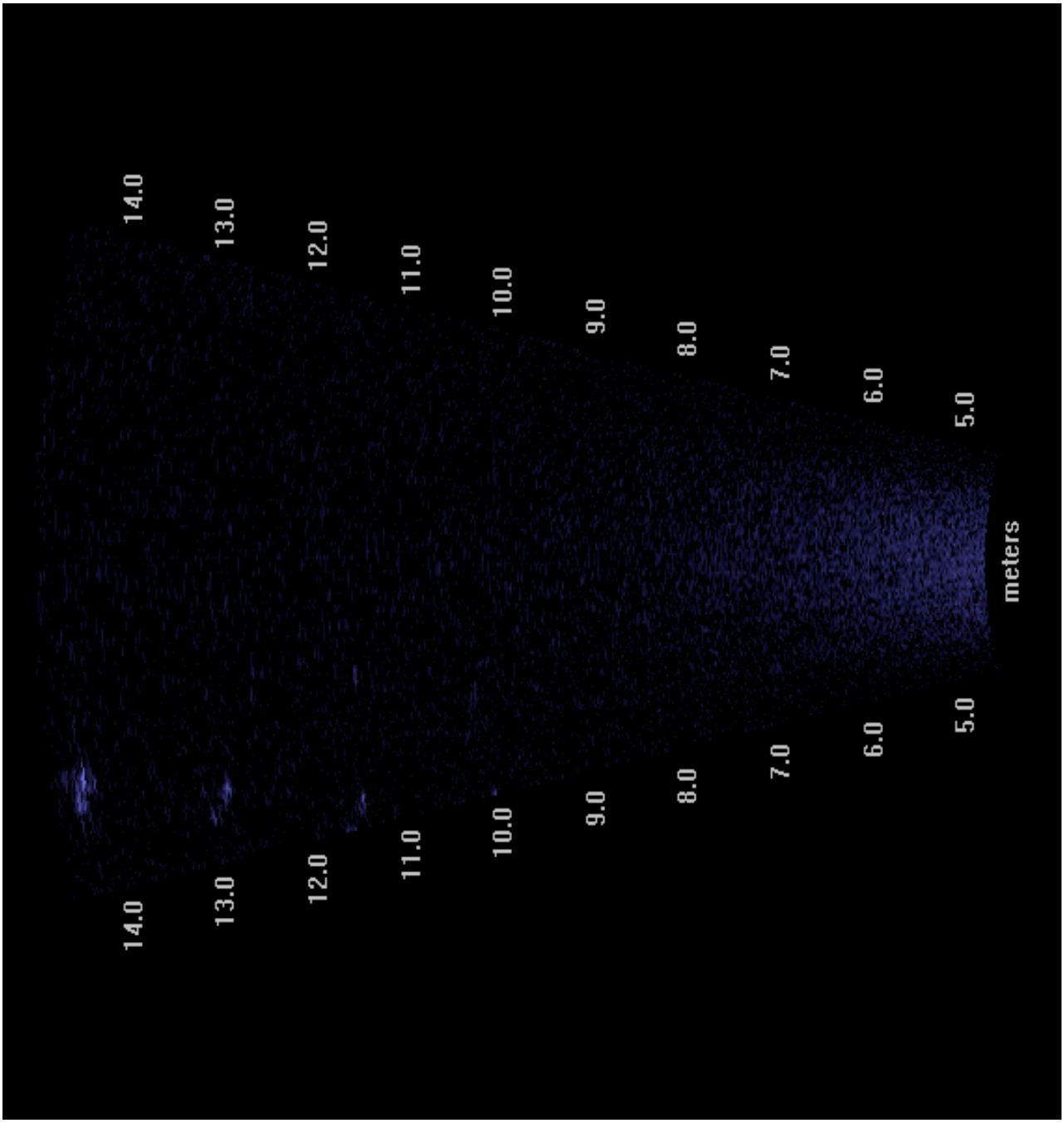

Note: Numbers along the sides of the image represent distance (meter) from the DIDSON unit. The image is rotated to better represent downstream orientation of the DIDSON. Poles extending from the underside of the FFGS near its end are visible at about 12.5 to 14.5 meters, as a result of the relatively straight alignment of the FFGS in the off treatment (contrast with **Figure 3.6-39**).

Figure G-12 **Typical Image from End-FFGS DIDSON when Oriented along the FFGS in the Upper Position (Slightly Deeper Tilt) with FFGS Off**

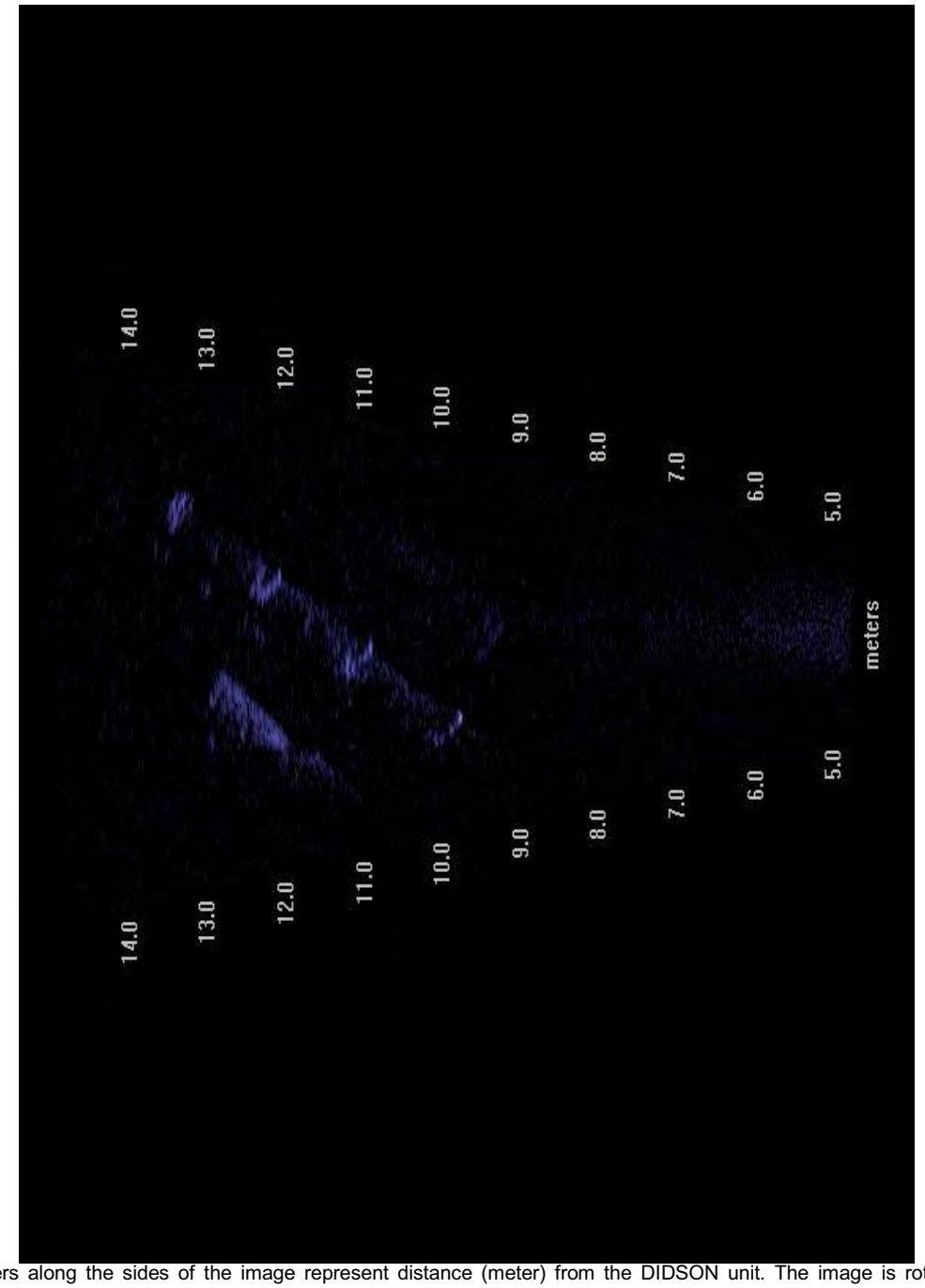

Note: Numbers along the sides of the image represent distance (meter) from the DIDSON unit. The image is rotated to better represent downstream orientation of the DIDSON. A flotation unit is visible from 10 to 13.5 meters, a result of the curving of the end of the FFGS in the on treatment.

Figure G-13 Typical Image from End-FFGS DIDSON when Oriented along the FFGS in the Upper Position (Shallow Tilt) with the FFGS On

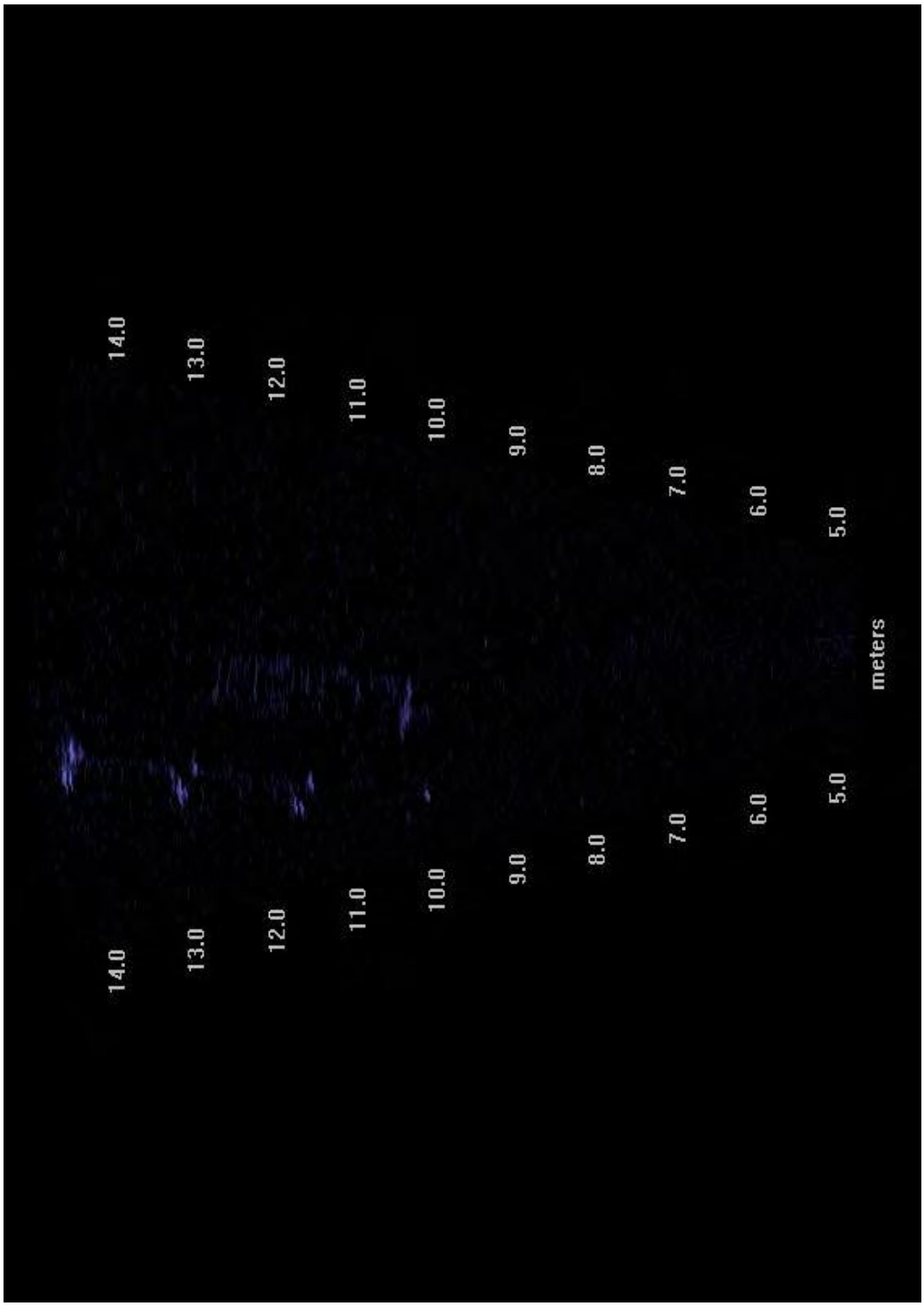

Note: Numbers along the sides of the image represent distance (meter) from the DIDSON unit. The image is rotated to better represent downstream orientation of the DIDSON. A flotation unit is visible from 10 to 14.5 meters; note its relatively parallel alignment to the DIDSON center line, reflecting the FFGS off.

Figure G-14 Typical Image from End-FFGS DIDSON when Oriented along the FFGS in the Upper Position (Shallow Tilt) with the FFGS Off